GEOLOGICAL SURVEY OF CANADA
PAPER 89-2

RADIOGENIC AGE AND ISOTOPIC STUDIES: REPORT 3

1990

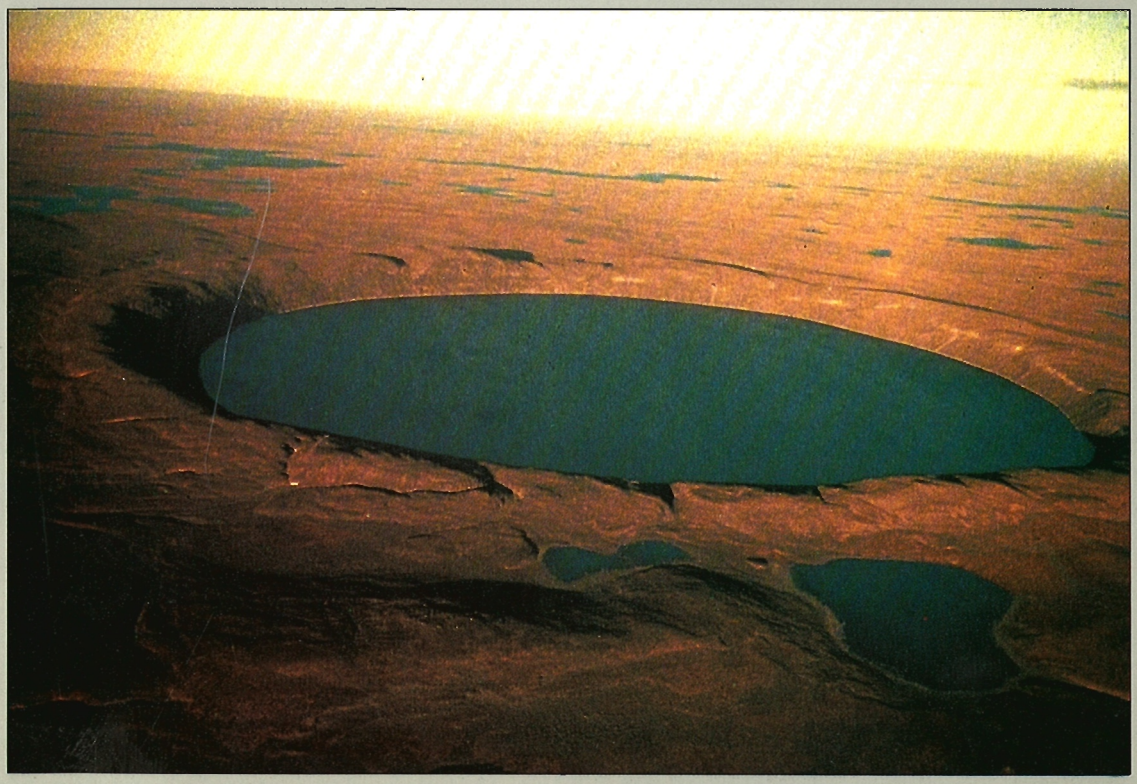

Energy, Mines and Resources Canada
Énergie, Mines et Ressources Canada

Canada

THE ENERGY OF OUR RESOURCES

THE POWER OF OUR IDEAS

STAFF, GEOCHRONOLOGY SECTION: GEOLOGICAL SURVEY OF CANADA

Research Scientists:	Otto van Breemen J. Chris Roddick Randall R. Parrish James K. Mortensen
Post-Doctoral Fellows:	Francis Ö. Dudás Ernst Hegner
Visiting Scientist:	Mary Lou Bevier
Professional Scientists:	W. Dale Loveridge Robert W. Sullivan Patricia A. Hunt Reginald J. Theriault Jack L. Macrae
Technical Staff:	Klaus Santowski Jean-Claude Bisson Dianne Bellerive Fred B. Quigg Rejean J.G. Segun

Sample crushing and preliminary mineral separation are done by the Mineralogy Section

GEOLOGICAL SURVEY OF CANADA
PAPER 89-2

RADIOGENIC AGE AND ISOTOPIC STUDIES: REPORT 3

1990

Available in Canada through

authorized bookstore agents and other bookstores

or by mail from

Canadian Government Publishing Centre
Supply and Services Canada
Ottawa, Canada K1A 0S9

and from

Geological Survey of Canada offices:

601 Booth Street
Ottawa, Canada K1A 0E8

3303-33rd Street N.W.,
Calgary, Alberta T2L 2A7

100 West Pender Street
Vancouver, B.C. V6B 1R8

A deposit copy of this publication is also available for reference
in public libraries across Canada

Cat. No. M44-89/2E
ISBN 0-660-13699-6

Price subject to change without notice

Cover Description:

Aerial photograph of the New Quebec Crater, a meteorite impact structure in northern Ungava Peninsula, Quebec, taken in 1985 by P.B. Robertson (GSC 204955 B-1). The diameter of the lake is about 3.4km and the view is towards the east-southeast. As outlined in a paper by J.C. Roddick in this publication, the age of the structure has been determined to be less than one million years old. This is the youngest impact structure known in Canada.

CONTENTS

ERRATUM

Paper 88-2, Radiogenic Age and Isotopic Studies: Report 2

Page 37, The correct citation of this paper is:

van Staal, C.R., Langton, J.P., and Sullivan, R.W., A U-Pb zircon age for the ophiolitic Deveraux Formation, Elmtree Terrane, northeastern New Brunswick; in Radiogenic Age and Isotopic Studies: Report 2, Geological Survey of Canada, Paper 88-2, p. 37-40, 1988.

INTRODUCTION

"Radiogenic Age and Isotopic Studies" is an annual collection of reports presenting data from the Geochronology Section of the Continental Geoscience Division. The main purpose of this collection is to make geochronological and other radiogenic isotope data produced by the section available promptly to the geological community. Reports make full presentation of the data, relate these to field settings, and make comparatively short interpretations. Readers are cautioned that some data reported here are part of work in progress, and more extensive publications may follow at a later date. Other geochronological and isotope data produced in the laboratory but published in outside journals or separate GSC publications are summarized at the end of this report.

The first report describes Rb-Sr and Sm-Nd procedures currently in use at the laboratory in a manner similar to previous presentations for U-Pb, K-Ar, and Sm-Nd using high performance liquid chromatography (HPLC) methods. $^{40}Ar/^{39}Ar$ analyses have become well established, and three papers contain these types of data, including that on the age of the New Quebec Crater, shown as the cover photograph for this volume. Several contributions summarize work in New Brunswick stemming from studies in part funded by Mineral Development Agreements. Other papers dealing with studies in the northwest Canadian Shield, Baffin Island, Ontario, and Yukon Territory complement mapping programs of the division.

The Geochronology Section depends not only on the financial resources and scientific expertise of Continental Geoscience Division of which it is part, but also on other groups within the Geological Survey. The Mineralogy Section of the Mineral Resources Division in particular provides us with mineral separations and rock powders, which are carefully and tediously prepared from generally large (10-30 kg) rock samples. For this we thank G. Gagnon, B. Machin, R. Christie, and R. Delabio. D. Walker and M. Villeneuve provide us with very high quality scanning electron photomicrographs of mineral grains for morphological studies. Some of these have been prominently displayed on previous covers of this publication series. They, in addition to A. Roberts, help us identify problematic minerals using microprobe and X-ray diffraction patterns, respectively. Finally, the Analytical Chemistry Section of the Mineral Resources Division allows us access to an atomic absorption spectrometer for potassium analyses for K-Ar dating. We are thankful for all of this collective assistance.

INTRODUCTION

«Âge radiométrique et études isotopiques» est une collection annuelle de rapports qui présentent des données provenant de la Section de la géochronologie de la Division géoscientifique du continent. Le but principal de la collection est de rendre les données géochronologiques et les autres données sur les isotopes radiogéniques produites par la section facilement accessibles à la collectivité du domaine géologique. On trouve dans ces rapports une présentation complète des données, le lien qui existe entre ces dernières et la situation sur le terrain ainsi que des interprétations comparativement courtes. Le lecteur doit toutefois savoir que certaines données reproduites dans le présent document originent de travaux en cours et que des publications plus détaillées pourraient suivre. D'autres données géochronologiques et isotopiques produites au laboratoire, mais publiées dans des revues extérieures ou dans d'autres publications de la CGC, sont résumées à la fin du présent rapport.

Le premier rapport traite des méthodes Rb-Sr et Sm-Nd actuellement utilisées au laboratoire, d'une façon similaire aux présentations antérieures des méthodes U-Pb, K-Ar et Sm-Nd par chromatographie liquide à haute pression. Les analyses $^{40}Ar/^{39}$ sont maintenant bien établies et trois documents renferment des données en découlant, y compris les données sur l'âge du cratère du Nouveau-Québec montré en page couverture. Plusieurs communications résument les travaux effectués au Nouveau-Brunswick et qui résultent des études financées en partie par les ententes d'exploitation minérale. D'autres, consacrées à des études menées dans le nord-ouest du Bouclier canadien, dans l'île de Baffin, en Ontario et dans le territoire du Yukon complètent les programmes de cartographie de la division.

La Section de la géochronologie dépend non seulement des ressources financières et des compétences scientifiques de la Division géoscientifique du continent, dont elle fait partie, mais aussi d'autres groupes de la Commission géologique. La Section de la minéralogie de la Division des ressources minérales, en particulier, lui fournit des séparations de minéraux et des poudres de roches qui sont soigneusement et fastidieusement préparées à partir d'échantillons généralement grands (de 10 à 30 kg). Les membres de la Section de la géochronologie tiennent à en remercier MM. G. Gagnon, B. Machin, R. Christie et R. Delabio. MM. D. Walker et M. Villeneuve ont fournis d'excellentes microphotographies à balayage électronique de grains de minéraux destinées à des études morphologiques. Certaines de ces photographies ont été avantageusement représentées en page couverture d'anciens numéros de la série. Ils ont en outre, avec la participation de M. A. Roberts, aidé les chercheurs de la Section à identifier des minéraux douteux en utilisant respectivement des méthodes de microsonde et de diffraction de rayons X. Enfin, la Section de la chimie analytique de la Division des ressources minérales a permis à ces mêmes chercheurs d'accéder au spectromètre d'absorption atomique en vue d'y effectuer des analyses de potassium aux fins de datation à l'aide de la méthode K-Ar. La Section de la géochronologie exprime de vifs remerciements à tous ces collaborateurs.

R.R. Parrish

Methods for Rb-Sr and Sm-Nd isotopic analyses at the geochronology laboratory, Geological Survey of Canada

R.J. Theriault[1]

Theriault, R.J., Methods for Rb-Sr and Sm-Nd isotopic analyses at the geochronology laboratory, Geological Survey of Canada; in Radiogenic Age and Isotopic Studies: Report 3, Geological Survey of Canada, Paper 89-2, p. 3-6, 1990.

Abstract

Chemical and mass spectrometry procedures for Rb-Sr and Sm-Nd isotopic analyses at the Geological Survey of Canada's geochronology laboratory are described. The chemistry is performed in a clean air environment and reagents are either redistilled or purchased as ultrapure products. Chemical procedures consist of weighing and total spiking of samples with ^{87}Rb-^{84}Sr or ^{149}Sm-^{148}Nd tracer solution; HF and HNO_3 dissolution, including high-pressure dissolution for Sm-Nd analyses; and two stages of ion exchange column chemistry. Mass spectrometry is carried out on a Finnigan-MAT 261 mass spectrometer equipped with a variable multicollector. Sr, Nd and Sm, are analyzed in static multicollector mode, whereas Rb is analyzed in single-peak jumping mode.

Résumé

Le présent document décrit les méthodes chimiques et de spectrométrie de masse des analyses isotopiques des systèmes Rb-Sr et Sm-Nd effectuées au laboratoire de géochronologie de la Commission géologique du Canada. Les manipulations chimiques se font en salle blanche et les réactifs sont soit redistillés soit achetés comme produits ultra purs. Les méthodes chimiques comprennent la pesée des échantillons et l'addition de solutions dosées de $^{87}Rb-^{84}Sr$ ou de $^{149}Sm-^{148}Nd$ agissant comme traceurs; la dissolution avec du HF et du HNO_3, y compris la dissolution sous haute pression pour les analyses de Sm-Nd; et deux étapes de séparation sur colonne échangeuse d'ions. La spectrométrie de masse se fait à l'aide d'un spectromètre de masse Finnigan-MAT 261 équipé d'un multicollecteur variable. On analyse le Sr, le Nd et le Sm en mode multicollecteur statique, alors que l'analyse du Rb se fait en mode pic par pic.

INTRODUCTION

The ^{147}Sm-^{143}Nd decay scheme is ideal as a tracer for studying the long term evolution of the lithosphere. The similar geochemical behaviour of light rare earth elements (LREE) makes the Sm-Nd pair relatively undisturbed by most crustal processes thus allowing the Sm-Nd isotopic system to record the evolution of rocks since their time of extraction from the depleted mantle. Although more prone to resetting than the Sm-Nd system, and less precise a geochronometer than the U-Pb system in zircon and monazite, the Rb-Sr isotopic system is widely used in ^{87}Sr - ^{86}Sr tracer studies - and often complements the K-Ar or ^{40}Ar - ^{39}Ar systems - in mica cooling ages.

The chemical procedures employed for Rb-Sr and Sm-Nd analyses are similar in many respects. The similarity in analytical methods warrants treatment of the two isotopic systems under one title. The procedures for extraction and separation of LREE are a variant of those of Richard et al. (1976). They have been recently introduced to the laboratory by postdoctoral fellow E. Hegner.

The chemical treatment for Sm-Nd analysis described in this paper is distinct from the high performance liquid chromatography (HPLC) method of LREE separation discussed by Sullivan (1988).

1 Geological Survey of Canada, 601 Booth Street, Ottawa, Ontario, K1A 0E8

This paper outlines the reagents and materials employed in chemistry, weighing, spiking, and sample dissolution, column exchange chemistry, and mass spectrometry. The object of this paper is two-fold. Firstly, it completes the description of analytical methods (Hunt and Roddick, 1987; Parrish et al., 1987; Sullivan, 1988; Roddick, 1990) utilized at the Geological Survey of Canada's geochronology laboratory. Secondly, it serves as reference for studies making use of isotopic data generated at the geochronology laboratory by the procedures described below.

MATERIALS AND REAGENTS

The chemical reagents are distilled in quartz (HCl) or teflon two-bottle(HF) (Mattinson, 1972) stills, or purchased as ultrapure reagents (HNO_3). De-ionized, ultrapure H_2O is produced by a Millipore-^{TM} water purification system consisting of reverse osmosis, organic scavenging, and ion exchange cartridges. Rb-Sr and Sm-Nd chemistry makes use of Savillex^{TM} PFA teflon screwtop dissolution vessels. TFE teflon bombs are additionally employed for Sm-Nd analysis. The chemistry is carried out in laminar flow, class 100 air work cabinets and fumehoods.

WEIGHING AND SPIKING

The amount of rock powder or mineral separate weighed is such that about 200 ng Nd and 1 µg Sr are provided for mass analysis. The samples are weighed in PFA teflon screwtop vials (Fig. 1) and moistened with approximately 1/2 ml of 16M HNO_3, which is an oxidant during dissolution. Samples are immediately spiked with mixed tracers enriched in ^{87}Rb-^{84}Sr or ^{149}Sm-^{148}Nd. The spike solutions are highly enriched in these isotopes, and their isotopic compositions have been accurately measured (J.C. Roddick, pers. comm., 1989), thus permitting determination of isotopic composition and concentration on the same sample solution. The amount of spike isotope added to the sample is such that error magnification is minimal. Because Rb – Sr ratios can vary greatly in mica and whole-rock samples, two specially calibrated spike solutions, differing in their Rb – Sr ratios, are used.

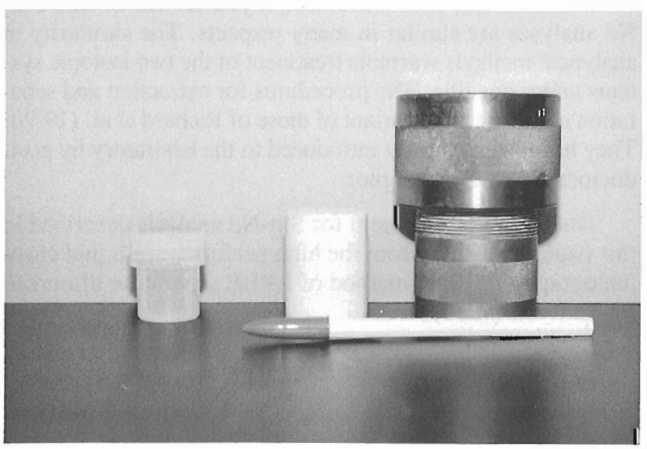

Figure 1. Sample dissolution apparatus. From left to right: PFA Savillex^{TM} teflon screwtop vial, TFE teflon bomb, and pressure resistant steel jacket.

SAMPLE DISSOLUTION

Sm-Nd

The dissolution process typically consists of a first dissolution in PFA teflon screwtop vessels and a second, high-pressure dissolution in TFE teflon bombs in steel jackets.

The first step consists of adding about 3 ml of 48% HF to the PFA teflon vessels and placing them on a hot plate for at least 12 h at 150°C. This allows decomposition of major silicate phases and formation of SiF_4. Samples are then dried at 150°C.

The second dissolution step involves taking the dried residues up in 3 ml of HF and 1/2 ml of HNO_3 and transferring them into TFE teflon bombs. These bombs are placed in pressure-resistant steel jackets (Fig. 1) and left to decompose under high pressure at 200°C for 5 days. This procedure ensures complete dissolution of all refractory phases and equilibration of sample and spike. Sample solutions are then dried and fluorides are converted to soluble chlorides by adding up to 20 ml of 6N HCl and heating them at about 80°C for up to 2 h. Finally, samples are dried, redissolved in 1 ml of 2.5N HCl, centrifuged to remove potentially undissolved fluorides, and loaded on cation exchange columns.

Rb-Sr

The dissolution process for Rb-Sr analysis consists of two HF-HNO_3 treatments similar to the first dissolution described above for Sm-Nd analyses. The samples are brought to complete dryness between acid treatments. The dual dissolution on a hot plate is adequate for breakdown of Rb- and Sr-bearing phases and sample-spike equilibration. Dissolution under high pressure is not required for Rb-Sr analyses as refractory phases contain negligible amounts of Rb and Sr. Samples are finally transformed into chlorides by adding approximately 10 ml of 6N HCl, dried, centrifuged, and redissolved in 1 ml of 2.5N HCl prior to cation exchange chromatography.

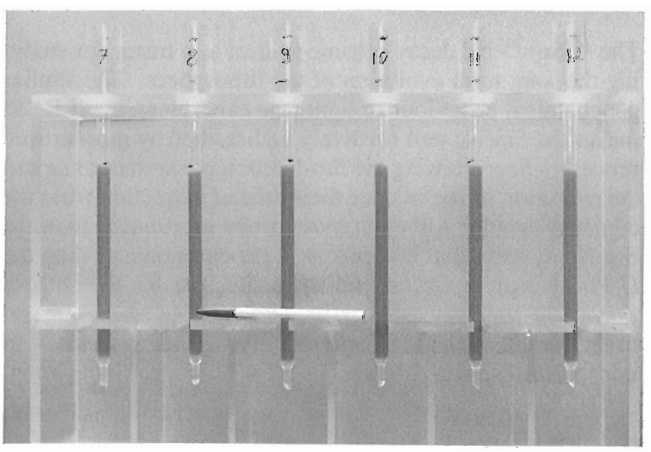

Figure 2. First-stage cation exchange columns made of 10 mm bore quartz glass and a volume of 15 ml of resin for extraction of Rb, Sr, and LREE.

CATION EXCHANGE COLUMN CHEMISTRY

Separation and purification of Rb, Sr, Sm, and Nd is done by elution through two stages of cation exchange columns. The first stage is common to both Rb-Sr and Sm-Nd analysis and serves as a preliminary method of extraction of Rb, Sr, and LREE. Second-stage column chemistry serves to individually purify Rb and Sr and separate Nd from Sm. The elution schemes are calibrated by atomic absorption spectrometry for Rb and Sr and with Eriochrome Black T for LREE.

Extraction of Rb, Sr and LREE

Sample solutions in 1 ml of 2.5N HCl are loaded onto quartz columns packed with 15 ml of AG50W-X8 200-400 mesh cation exchange resin (Fig. 2). After eluting 32 ml of 2.5N HCl, Rb, accompanied by traces of K, Ca, Fe, Al, etc., is collected as 20 ml of 2.5N HCl (32-52 ml cut). An additional 40 ml of 2.5N HCl are discarded before Sr, along with elution tailings of Ca and Mg, is collected as a subsequent 25 ml fraction (92-117 ml cut). For obtaining LREE, 15 ml of 6.2N HCl are eluted after Sr has been collected. The LREE are then collected in 30 ml of 6.2N HCl (132-162 ml cut). Once collected, all separates are brought to dryness. Rb and Sr are redissolved in 1 ml of 0.6N HCl and LREE in 0.2 ml of 0.18N HCl prior to loading on second stage columns.

Purification of Rb and Sr

The second-stage column chemistry for Rb and Sr makes use of low-normality HCl and resin with close cross-linkage to individually purify the Rb and Sr separates obtained from the first-stage columns. Purification is done on quartz columns packed with 3 ml of AG50W-X12 200-400 mesh cation exchange resin (Fig. 3). Clean Sr separates are obtained by loading 1 ml of 0.6N HCl Sr solutions on the second-stage columns and eluting with 84 ml of 0.6N HCl followed by 20 ml 2.5N HCl and collecting the Sr in 15 ml of 2.5N HCl (104-119 ml cut). Once the clean Sr separates have been collected, Rb from the first-stage columns is dissolved in 1 ml of 0.6N HCl. This solution is loaded onto the second-stage columns and purified by eluting 64 ml 0.6N HCl and collecting Rb in the following 20 ml cut of 0.6N HCl (64-84 ml cut).

The blanks for the dissolution and the two-stage cation exchange process are typically 1 ng for Sr and 50 pg for Rb.

Separation of Sm and Nd

Sm and Nd are separated on quartz columns packed with 2 ml of 100-200 mesh teflon powder coated with a HDEHP (Di-2-ethylhexyl orthophosphoric acid) cation exchange resin (Fig. 4). The active teflon powder is prepared by evaporation of a 1:10:100 (by weight) solution of HDEHP, teflon powder, and acetone. The dried LREE cuts from the first-stage columns are dissolved in 0.2 ml of 0.18N HCl, centrifuged in order to remove possible resin beads from the first-stage columns, loaded on the second stage columns, and washed into the resin bed with four successive additions of 0.2 ml of 0.18N HCl. After eluting 12 ml of 0.18N of HCl, Nd is collected in 6 ml of 0.18N HCl (12-18 ml cut). The collection of Nd is followed by the elution of 4 ml of 0.4N HCl and the collection of Sm in 5 ml of 0.4N HCl (22-27 ml cut). This method provides Nd free of Sm, but tailings of elution peaks result in significant amounts of Ce, Pr, and Nd in Sm. Dissolution and cation-exchange chemistry blanks range from 100 to 300 pg for Nd and 30 to 100 pg for Sm.

MASS SPECTROMETRY

Isotopic measurements are made on a Finnigan MAT 261 mass spectrometer equipped with six variable Faraday cups and one fixed collector. The instrument is used in static mode to measure Sr, Nd, and Sm isotopic compositions and in single collector peak jumping mode for Rb, using a collector reserved for alkalis. The analyzer of the mass spectrometer is pumped down to a vacuum better than 10^{-7} torr (1.333×10^{-9} Pa) prior to analysis. Samples are loaded on Re and Ta filaments that have been outgassed at 2000°C

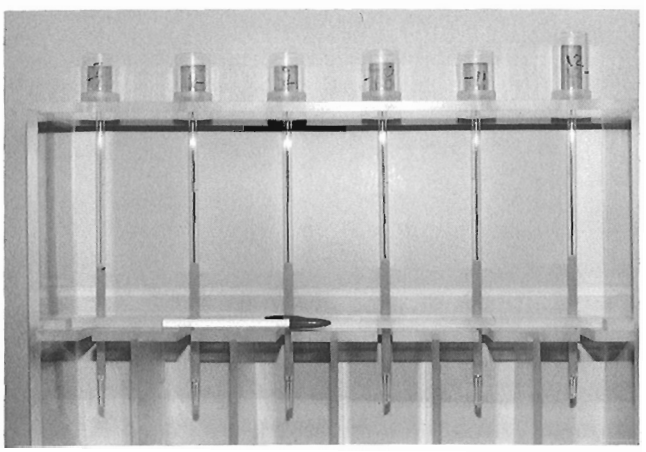

Figure 3. Quartz columns (6 mm bore) packed with 3 ml resin used for purification of Rb and Sr.

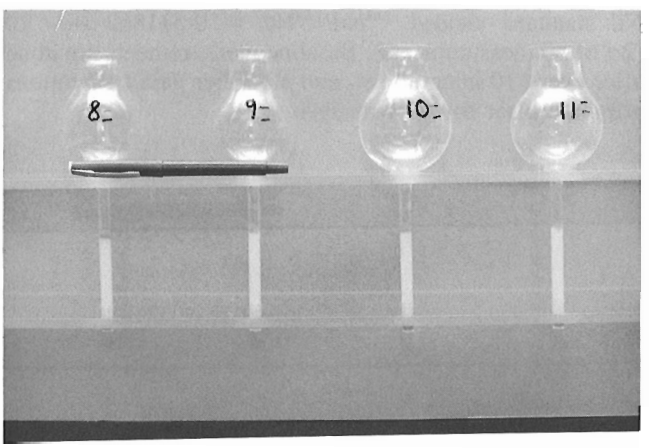

Figure 4. Quartz columns (6 mm bore) filled with 2 ml teflon-HDEHP resin bed for separation of Nd and Sm.

for 10 min. Loading of samples onto filaments is carried out in a clean air cabinet prior to loading in the mass spectrometer. Sr, Nd, and Sm are loaded on filaments in 2 µl 0.5M H_3PO_4, whereas Rb is dissolved in water and loaded as a chloride. Rb, Nd, and Sm samples are loaded on the evaporation filament of a double Re filament assembly. Sr is loaded on a single Ta filament.

Measurement of Sr and Rb

Sr is measured at filament temperatures of 1200 to 1300°C, corresponding to ^{88}Sr intensities in the order of 3 to 5 x 10^{-5} A. Atomic masses 84, 85, 86, 87, and 88 are collected in separate Faraday cups. Atomic mass 85 is monitored for the presence of Rb, which interferes isobarically with ^{87}Sr. Typically, 80 to 120 8-s mass integrations are sufficient to yield an internal precision of $^{87}Sr/^{86}Sr$ better than 5 x 10^{-5}. The external precision determined on 80 measurements of NBS SRM 987 standard is estimated to be better than 3 x 10^{-5} yielding $^{87}Sr/^{86}Sr = 0.710252 +/- 30$ (2σ of the population; normalized to $^{86}Sr/^{88}Sr = 0.1194$). Amplifier gain calibrations are performed before every analysis, and baseline measurements are done after every 20 mass integrations.

Rb is ionized by heating the sample-free ionization filament up to 800°C, corresponding to a ^{87}Rb signal of 3 to 5 x 10^{-6} A. An analysis typically consists of 40 10-s mass integrations. The $^{85}Rb - ^{87}Rb$ is corrected for 0.07% fractionation per atomic mass unit during analysis. This fractionation has been determined from analysis of normal Rb.

Measurement of Nd and Sm

During analysis of Nd, the ionization filament is kept at approximately 1900°C and the evaporation filament at 800 to 1000°C, resulting in a ^{144}Nd signal of 1.5 to 3 x 10^{-12} A. Atomic masses 143, 144, 145, 146, 147, and 148 are collected. Mass 147 is monitored to detect and correct for the presence of Sm, one of the isotopes of which is an isobar of ^{144}Nd. The ratios are corrected for mass fractionation by normalization to $^{146}Nd/^{144}Nd = 0.7219$. In static mode, 80 to 100 8-s mass integrations yield an internal precision for $^{143}Nd/^{144}Nd$ equal or better than 10^{-5}. The external precision is estimated to be better than 2.5 x 10^{-5}. The La Jolla Nd standard yielded $^{143}Nd/^{144}Nd = 0.511862 +/- 20$ (2σ of 80 measurements). Baseline measurements are done after every 10 integrations, and amplifier gain calibrations are done prior to every analysis.

For analysis of Sm, the ionization and evaporation filaments are brought to temperatures similar to those for Nd. Data are collected when ^{149}Sm is emitting a signal of approximately 4 x 10^{-12} A. Atomic masses 147, 149, 152, and 156 are collected, the latter to monitor CeO, which interferes isobarically with ^{152}Sm. The 147/149 ratio is normalized to 147/152 = 0.56081. An analysis typically consists of 48 8-s mass integrations. Amplifier gain calibrations are done after every three analyses.

REFERENCES

Hunt, P.A. and Roddick, J.C.
1987: A compilation of K-Ar ages; in Radiogenic Age and Isotopic Studies: Report 1, Geological Survey of Canada, Paper 87-2, p. 143-205.

Mattinson, J.M.
1972: Preparation of hydrofluoric, hydrochloric, and nitric acids at ultralow lead levels; Analytical Chemistry, v.44, p. 1715-1716.

Parrish, R.R, Roddick, J.C, Loveridge, W.D., and Sullivan, R.W.
1987: Uranium-lead analytical techniques at the geochronology laboratory, Geological Survey of Canada; in Radiogenic Age and Isotopic Studies: Report 1, Geological Survey of Canada, Paper 87-2, p. 3-7.

Richard, P., Shimuzu, N., and Allegre, C.J.
1976: $^{143}Nd/^{146}Nd$, a natural tracer: an application to oceanic basalts; Earth and Planetary Science Letters, v.31, p. 269-278.

Roddick, J.C.
1990: $^{40}Ar - ^{39}Ar$ evidence for the age of the New Quebec Crater, northern Québec; in Radiogenic Age and Isotopic Studies: Report 3, Geological Survey of Canada, Paper 89-2 (this publication).

Sullivan, R.W.
1988: Samarium-neodymium and rare-earth element liquid chromatography (HPLC) techniques at the geochronology laboratory, Geological Survey of Canada; in Radiogenic Age and Isotopic Studies: Report 2, Geological Survey of Canada, Paper 88-2, p. 9-20.

^{40}Ar-^{39}Ar evidence for the age of the New Quebec Crater, northern Quebec

J.C. Roddick[1]

Roddick, J.C., ^{40}Ar – ^{39}Ar evidence for the age of the New Quebec Crater, Northern Quebec in Radiogenic Age and Isotopic Studies: Report 3, Geological Survey of Canada, Paper 89-2, p. 7-16 1990.

Abstract

$^{40}Ar/^{39}Ar$ analysis of an impactite from the New Quebec Crater indicates an age of 0.47+ 0.52 / −0.47 Ma. The Ar systematics of the impactite sample are complex. Inclusions in the sample have old apparent ages due to the presence of significant amounts of residual radiogenic Ar generated in the target Archean gneisses prior to the impact event. The melt matrix also shows the effects of the degassing of this old radiogenic Ar from the inclusions. Rapid cooling of the melt after impact caused some of the residual radiogenic Ar to be absorbed and trapped in the melt. Conventional age-spectrum ages are variable, but an isotope correlation plot successfully reveals the anomalous trapped Ar composition and indicates the age of the impact event. The trapped Ar is shown to be correlated with anion sites containing Cl. Glaciations were common in North America at the time of impact and some geological features suggest that the impact may have taken place on glacial ice. The Ar systematics of this impactite are similar to those of previous analyses of Mistastin Lake Crater samples and suggest that the Mistastin impact event may be 10 Ma younger than previously supposed.

Résumé

L'analyse par la méthode $^{40}Ar/^{39}Ar$ d'une impactite provenant du cratère du Nouveau-Québec indique un âge de 0,47 ± 0,52/− 0,47 Ma. La classification et la taxonomie de l'Ar de l'échantillon d'impactite sont complexes. Les inclusions de l'échantillon sont apparemment vieilles en raison de la présence d'importantes quantités d'Ar radiogénique résiduel produit dans les gneiss cibles de l'Archéen avant l'impact. La gangue fondue montre également les effets du dégazage de cet ancien Ar radiogénique des inclusions. Le refroidissement rapide de la gangue fondue après l'impact a été à l'origine de l'absorption et du piégeage d'une certaine quantité d'Ar radiogénique résiduel. Les âges classiques obtenus par le spectre des âges sont variables mais une courbe de corrélation isotopique montre bien la composition anormale de l'Ar piégé et indique l'âge de l'impact. On démontre que l'Ar piégé correspond à des sites d'anions renfermant du Cl. Des glaciations étaient courantes en Amérique du Nord au moment de l'impact et certaines caractéristiques géologiques semblent indiquer que l'impact aurait pu se produire sur de la glace de glacier. La classification et taxonomie de l'Ar de cette impactite ressemblent à celles des premières analyses des échantillons du cratère du Lac Mistastin et portent à croire que l'impact de Mistastin pourrait être 10 Ma plus jeune qu'on ne le croyait auparavant.

1 Geological Survey of Canada, 601 Booth Street, Ottawa, Ontario, K1A 0E8

INTRODUCTION

Meteorite impact cratering is an infrequent but common phenomenon erratically recorded on the earth. The record is generally confined to land areas, which occupy only 30% of the total earth surface, though there is one exception of a known underwater impact (Jansa and Pe-Piper, 1987). Geological processes of uplift and erosion also generally limit the terrestrial record to surfaces a few hundred million years old (Grieve, 1984). The establishment of the frequency of cratering is important to a number of fields of research. Firstly, crater counts are used to estimate the age of planetary surfaces, such as Mars, where direct sampling is not available. Here, a crater production rate is required to relate observed numbers of craters to age. With this information a better understanding of planetary geological processes is obtained. The correct cratering rate for the earth has yet to be determined as there is some uncertainty in comparison of recent terrestrial crater rates (0-120 Ma events) with estimates from older crater rates (200-360 Ma events) and with astronomical observations of earth-crossing asteroids (Grieve, 1984). Secondly, attempts have been made to assess the possibility of a periodicity in the recent cratering record (Alvarez and Muller, 1984), but as yet the record is too incomplete (Grieve et al., 1986). Finally the possibility of correlation of impacts with major extinction events (Weissman, 1985) and geomagnetic reversals (Muller and Morris, 1986) has been discussed.

Critical to the definition of a more precise terrestrial cratering rate, and any variations in such a rate as might be produced by periodic cometary showers, is the determination of the ages of impact craters. Owing to the complex nature of impact rocks the $^{40}Ar - ^{39}Ar$ technique is the most suitable method of dating these events, though even this method may have limitations depending on the suitability of the sample material. In Canada, a number of impact craters have been dated, several by $^{40}Ar/^{39}Ar$ methods. (see Grieve, 1982 and Grieve et al., 1986). The following presents new results of $^{40}Ar/^{39}Ar$ analyses on a sample from the New Quebec Crater, a small structure in northern Quebec. It is the youngest and best preserved of known craters in Canada (Innes, 1964) and though it has not been dated radiometrically, it is estimated to be less than 5 Ma old (Grieve, 1982).

PREVIOUS STUDIES OF THE NEW QUEBEC CRATER

The New Quebec Crater is a circular, lake-filled depression, about 3.4 km in diameter and 267 m deep located in the Archean tonalitic gneiss terrane of northern Quebec, just south of the Cape Smith Belt. The bedrock rim rises 100 m above the surrounding tundra (Fig. 1). It was first noted on oblique aerial photographs taken in 1943, and scientific investigations soon led to the speculation that it was a meteorite impact crater (Meen, 1951). Interestingly, the discovery and speculation on the origins of the New Quebec Crater led to the establishment in 1951 of the meteorite crater program of the Dominion Observatory (Innes, 1964). Subsequent research was devoted to testing the impact hypothesis by examining the topographic form (Millman, 1956), structure of the rim (Shoemaker, 1961; Currie and Dence, 1963; Currie, 1966), and gravity profile of the crater (Innes, 1964). Harrison (1954) showed that the crater rim had been glaciated. While all these studies supported a meteorite impact origin, clear petrographic evidence of an impact was not found.

Detailed geological mapping of the crater and its surrounds by Currie (1966) did not resolve the uncertainty. Currie found no evidence of the expected ejecta blanket associated with impacts but did document structural deformation consistent with impact (Currie and Dence, 1963) or a volcanic origin. The lack of definitive evidence for impact led Currie (1966) to propose an origin by "up-doming of country rock by hot fluids or possibly by a fluid-charged magma." He supported this mechanism with the discovery of a single vesicular glassy rock inside the crater, which he concluded was of volcanic origin, though additional study of the sample supported a meteorite impact origin, as a fragment of impact melt rock with shocked mineral clasts (Robertson et al., 1968).

Despite several expeditions to the crater in the interval 1963 to 1986 in search of additional impact material, it was not until 1986 that another small glassy impactite sample was found about 3 km to the north-northwest of the crater (Marvin et al., 1988). More recently, a 1988 expedition discovered 20 impactite fragments (total weight 1.5 kg) in an apparent outwash channel, which originates on the eastern crater rim and curves northward to Lac Laflamme, located 3 km north-northwest of the crater rim (R.A.F. Grieve, pers. comm., 1989).

SAMPLE DESCRIPTION

The $^{40}Ar/^{39}Ar$ analyses were carried out on a portion of the original fist-sized sample of impact melt rock collected by Currie (1966) and denoted DNQ-62-FI. The following is a summary of Currie's description of the sample: On a fresh surface the rock is dull grey, with 15 to 20% white to pale buff inclusions. The matrix is highly vesicular, with vesicles ranging in size from microscopic to 5 mm. The inclusions

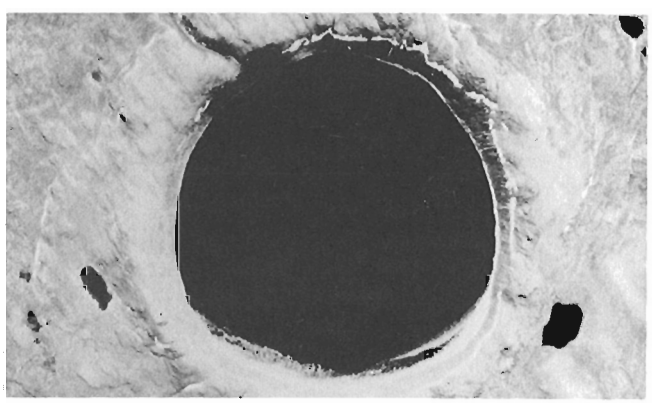

Figure 1. Aerial view of the New Quebec Crater. Diameter of the lake is about 3.4 km. Photo by P.B. Robertson (GSC 204955C-2.

range in size from 0.5 to 5 mm and are round to lensoid, with some being elongate. In thin section, the matrix is a brownish, glassy or cryptocrystalline material charged with plagioclase microlites (An_{33}) and lesser amounts of magnetite and opaque dust. The microlites comprise one third to one half of the matrix, the opaque minerals 5 to 10%. The remainder of the matrix is translucent to transparent, brownish or greenish brown isotropic material. The inclusions range from fresh single crystals of plagioclase to blobs of clear glass. The crystals are partly recrystallized, with some showing sinuous lamellae of clear glass. The contact of crystal and matrix is diffuse, with some formation of microlites at the boundary. Most inclusions are clear glass with minor amounts of partly melted fragments and usually an unfilled vesicle in the centre. Around the inclusions the plagioclase microlites are well orientated, bending around the inclusions in flow textures.

Additional thin section examination reveals that the groundmass also contains a quench texture of long needles of a dark greenish fibrous mineral, presumed to be pyroxene pseudomorphed by chlorite. The feldspar microlites are typically 50 to 100 μm long and 5 to 10 μm in diameter (Fig. 2).

Marvin et al. (1988) provide petrographic detail for another small (5 g) vesicular fragment found on the shore of Lac Laflamme. Their description is similar to that of DNQ-62-FI but has additional information from electron microprobe analysis. Within this fragment, both feldspar (300 μm long) and pyroxene crystallites are present with glass of siliceous peraluminous composition. The feldspar laths have a higher An content than those in DNQ-62-FI ($An_{40}Ab_{54}Or_6$). The inclusions are quartz, irregular masses of silica, and rare apatite. The quartz displays two or three intersecting sets of shock-produced planar features. Similar planar features were described in the quartz of DNQ-62-FI by Robertson et al. (1968).

ANALYTICAL TECHNIQUES

Sample preparation and neutron irradiation

A small 2 cm cube of DNQ-62-FI was crushed in an agate mortar, sieved to -160 +149 μm size, ultrasonically washed in water, and magnetically separated into two fractions on a Frantz™ LB-1 separator. The magnetic fraction consists of grey homogeneous grains representative of the melt matrix with fine feldspar microlites. It was carefully handpicked to eliminate any white feldspar or clear quartz/glass inclusions. The non-magnetic fraction was handpicked to concentrate the clear and white inclusions in the sample. A selection of grains from both fractions were mounted, but not polished, for electron microprobe determinations of their approximate compositions. Five grains of the melt matrix yielded approximate feldspar compositions with iron present as well, while three of six grains of the inclusions had a quartz/silica composition and three were feldspar.

The two samples were wrapped in aluminium foil packets (0.49 g melt matrix; 0.086 g inclusions) for neutron irradiation. They were arranged along with several other unrelated samples in an aluminium can 40 mm x 19 mm diameter, along with one CaF_2 sample and eight packets of FCT-3 biotite, a new $^{40}Ar/^{39}Ar$ flux monitor prepared by the United States Geological Survey, Reston, Virginia, from the Fish Canyon Tuff. Its age is 27.68 ± 0.03 Ma (M.J. Kunk, pers. comm. 1988). The can was irradiated for 45 min. in position 5C of the enriched uranium research reactor at McMaster University, Hamilton, Ontario. It received an approximate fast neutron fluence of 3×10^{16} neutrons/cm^2, which results in a J factor of 2.1×10^{-4}. Flux variation over the irradiation can had a range of 3.0% and is mainly along the axis of the can. The errors quoted on the integrated ages take account of this uncertainty, though the individual step ages do not.

The procedures for $^{40}Ar/^{39}Ar$ analysis are detailed in Appendix 1, since they have not been presented previously for this laboratory. Data in isotope correlation plots have been regressed using the two-error treatment of York (1969) with data-point errors and correlation coefficients on the errors calculated according to Roddick (1988). Regressions that scatter beyond experimental limits (MSWD > 2.5) have been multiplied by the square root of MSWD to provide realistic error estimates. All errors are quoted at the 2σ level, unless otherwise stated.

ARGON SYSTEMATICS AND DATA PRESENTATION

The dating of impact melt rocks by the $^{40}Ar/^{39}Ar$ technique presents a number of problems not encountered in the analyses of other terrestrial rocks and minerals. While most geological processes take place at rates consistent with a close approach to chemical and thermal equilibrium, at least on a local scale, a meteorite impact is a catastrophic event in which equilibrium is the exception. Thus, an impactite or

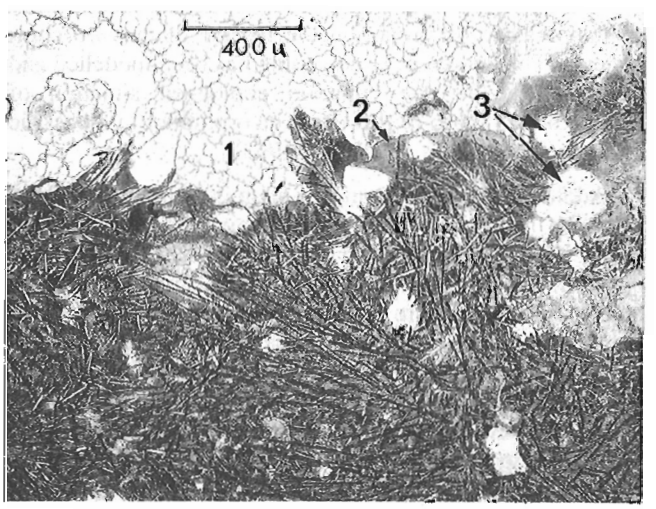

Figure 2. Photomicrograph of melt matrix texture of DNQ-62-FI from the New Quebec Crater. Melt matrix is feldspar laths, long needles of pyroxene pseudomorphed by chlorite and opaques set in a glassy or cryptocrystalline base. Ballan quartz is present in the upper third (1); brown glass or cryptocrystalline melt is visible at (2); two vesicles are located at (3).

impact melt rock is often an amalgamation of melted target material with shocked and unmelted clasts or inclusions of the target country rock. The effects on the K – Ar system can be complicated enough to prevent the determination of even an approximation to the time of the impact event.

In the ideal case, melt material would have been well above the closure temperature for Ar and then quickly cooled. It would then be completely degassed, and the measurement of radiogenic Ar subsequently generated (denoted $^{40}Ar^*$) would precisely date the impact event. This is often the case and conventional K – Ar dating of the Ries crater in Germany, for example, has successfully determined the time of impact (Gentner et al., 1963). In other cases, the ages obtained may be anomalous. Mak et al. (1976) showed that some impactites with inclusions from the Mistastin Lake crater yielded realistic ^{40}Ar – ^{39}Ar spectra ages, whereas others were clearly too old. This problem is related to the incomplete degassing of radiogenic Ar generated in the unmelted inclusions prior to the impact event (here denoted as $^{40}Ar_o^*$). The presence of inclusions is common in impactites, and if small enough they may go undetected in a dating sample or prove impossible to separate.

In these cases, with incompletely degassed inclusions, $^{40}Ar/^{36}Ar$ step heating analysis may be able to resolve the $^{40}Ar^*$ from the residual $^{40}Ar_o^*$. This residual $^{40}Ar_o^*$ is located in the most retentive sites in the inclusions, as it was retained during exposure to melt temperatures. During laboratory heating this residual $^{40}Ar_o^*$ may not be released until relatively high temperatures. If much of the $^{40}Ar^*$ generated since the impact is released at lower temperatures, there will be a separation of the two Ar components. In an age spectrum, in which the apparent age of each heating step is plotted against the cumulative amount of ^{39}Ar released, the initial Ar release would have an age plateau reflecting the time of impact. With further heating, ages would increase with degassing of $^{40}Ar_o^*$ in the retentive sites of the inclusions. The successful separation of the components is dependent on the degree of degassing of the inclusions and a marked temperature difference in the release of the two components. This mode of Ar degassing has been modelled and demonstrated for the common geological situation of xenocrysts (granitic in this case) incorporated in a basaltic magma (Gillespie et al., 1982, 1983).

Additional complications can arise if the residual $^{40}Ar_o^*$ diffusing from the inclusions is retained within the melt phase. Rapid cooling after an impact will prevent this $^{40}Ar_o^*$ from escaping from the impactite and will impose a high Ar partial pressure on the melt component. In this case, the melt absorbs some of this $^{40}Ar_o^*$ and subsequent analysis of the melt will yield ages that are too old. The anomalous ages arise because the standard age calculation assumes that any Ar trapped in a sample at the time of its crystallization has the composition of present-day atmospheric Ar with a $^{40}Ar/^{36}Ar$ value of 295.5. Measurement of ^{36}Ar in a sample thus permits correction for the trapped ^{40}Ar component. Numerous analyses of terrestrial rocks demonstrate that atmospheric $^{40}Ar/^{36}Ar$ is an appropriate correction, presumably because of interaction during crystallization with fluids containing atmospheric Ar. In the case of the absorption of residual $^{40}Ar_o^*$, the trapped component will no longer have an atmospheric $^{40}Ar/^{36}Ar$, and a different composition greater than 295.5 should be used. In previous studies, this residual $^{40}Ar_o^*$ has been termed excess Ar (Lanphere and Dalrymple, 1976).

The trapped Ar component is apparently located in sites with diffusional characteristics that are different from the sites of $^{40}Ar^*$ generated by radioactive decay. Roddick and Rex (1980), in analyzing plagioclase separates, first suggested a correlation of this trapped Ar component with Cl and Br in the mineral. This supported a theoretical assessment of Harrison and McDougall (1981) that trapped Ar was associated with anion vacancies. They also correlated the anion vacancies with Ar released at high temperatures. This anion dependence was subsequently documented by Claesson and Roddick (1983), who showed a good correlation of trapped Ar (high in $^{40}Ar/^{36}Ar$) in plagioclase with Cl and Br anion sites. They also showed that there were two trapped components of different $^{40}Ar/^{36}Ar$ compositions, one released at low temperature and one at high temperature. Since the trapped and radiogenic components may have different diffusional mechanisms, step heating analysis may be used to separate these two types of Ar and permit the determination of the correct trapped $^{40}Ar/^{36}Ar$.

The usual method of resolving the different Ar components is by three isotope correlation plots of ^{40}Ar, ^{39}Ar, ^{36}Ar (Turner, 1971; Roddick et al., 1980; Claesson and Roddick, 1983). ^{40}Ar is used as the reference isotope as it is the most abundant and, therefore, can be measured precisely, thereby minimizing correlations between errors in the two ratios. On this plot, the X-intercept (inverse $^{40}Ar/^{39}Ar$, comprising K-derived radiogenic ^{40}Ar and neutron-induced ^{39}Ar) defines the age of a sample, while the Y-intercept (inverse $^{40}Ar/^{36}Ar$) represents the trapped Ar composition. Binary mixing between the two end members defines a linear array with negative slope. Roddick et al. (1980) used this plot to discuss mixing relatioships of more than one trapped component in metamorphic biotites. Recently, Heizler and Harrison (1988) have successfully used this plot to demonstrate that a variety of minerals may contain several trapped, thermally distinct components, each with different $^{40}Ar/^{36}Ar$ values. During laboratory heating, one component may dominate the Ar released in a particular temperature range. By applying the appropriate trapped $^{40}Ar/^{36}Ar$ corrections, they were able to resolve several apparently complex age spectra and recover meaningful ages.

The preceding discussion suggests that several techniques should be used to assess the results of ^{40}Ar – ^{39}Ar dating of impact rocks. Age spectra of both melt material and inclusions may permit a rapid assessment of the presence of residual $^{40}Ar_o^*$, but correlation plots have the advantage of independently assessing the composition of the trapped $^{40}Ar/^{36}Ar$ component. Finally, comparison of release patterns of ^{36}Ar with those of Cl and Br may distinguish different diffusional mechanisms for trapped Ar components

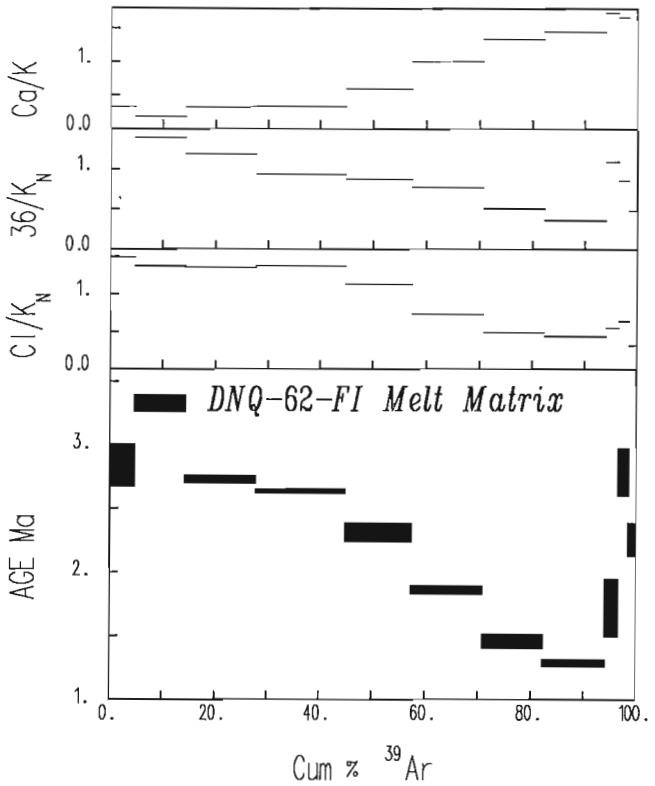

in the sample and help reveal if more than one site is involved. The Cl and Br can be traced in step heating experiments via reactions during neutron irradiation which produce ^{38}Ar from Cl and ^{80}Kr from Br. This is analogous to the use of ^{37}Ar to trace gas evolution from Ca sites in a sample. All these gas isotopes may be ratioed to K-derived ^{39}Ar and plotted against the cumulative amount of ^{39}Ar released to provide element variation plots comparable to the age spectra, where the radiogenic $^{40}Ar^*$ is also ratioed to K-derived ^{39}Ar. For the present impact sample, no Br.derived ^{80}Kr was detected.

Figure 3. Age spectrum plot of data from DNQ-62-FI melt matrix and element variation plots for each heating step. The Ca and Cl variations have been determined from measurements of neutron derived ^{37}Ar and ^{38}Ar respectively. The ratios in the variation plots refer to the amounts of gases released in each step and are thus comparable to the age spectra, where the apparent ages correspond to ratios of $^{40}Ar^*$ to K-derived ^{39}Ar. The subscript N indicates ratios normalized to the integrated ratio for the sample.

Table 1. Argon step heating data for the New-Quebec impactite.

TEMP. (°C)	$^{36}Ar_{tr}$	$^{37}Ar_{Ca}$ (X 10^{-9} cm^3 STP)[a]	$^{38}Ar_{Cl}$	$^{39}Ar_K$	^{40}Ar	% Atmos. ^{40}Ar	Apparent age Ma	$\pm 2\sigma$[b]	^{39}Ar (%)
DNQ-62-FI Melt Matrix (490.75 mg)									
450	0.001	0.016	0.001	0.006	0.30	54.8	8.69	11.47	0.0
500	0.102	0.175	0.019	1.017	37.73	79.7	2.84	0.17	4.7
550	0.084	0.195	0.035	2.078	43.12	57.5	3.32	0.07	9.6
600	0.100	0.492	0.048	2.900	50.49	58.4	2.73	0.03	13.4
650	0.100	0.647	0.063	3.705	55.57	53.3	2.64	0.02	17.1
700	0.068	0.836	0.038	2.697	36.63	54.8	2.31	0.07	12.5
750	0.065	1.515	0.026	2.889	33.38	57.3	1.86	0.04	13.4
800	0.037	1.735	0.015	2.488	20.50	53.0	1.46	0.05	11.5
900	0.027	1.933	0.014	2.569	16.69	47.5	1.29	0.03	11.9
1000	0.017	0.484	0.004	0.537	7.48	67.3	1.72	0.23	2.5
1100	0.010	0.354	0.003	0.049	6.03	49.8	2.79	0.19	1.9
1200	0.004	0.971	0.001	0.284	2.87	40.7	2.26	0.13	1.3
1500	0.014	0.362	0.000	0.051	6.09	69.9	13.5	10.0	0.2
Total[c]	0.63	0.27	9.72	21.63	316.9	58.6	2.29	0.0	
Conc.(/g)	1.3	19.80	0.54	44.08	645.7				
DNQ-62-FI Inclusions (85.92 mg)									
500	0.068	0.287	0.014	0.104	24.58	81.3	16.6	4.3	8.3
600	0.014	0.034	0.004	0.106	24.63	17.2	71.3	2.4	8.4
650	0.005	0.011	0.002	0.097	15.88	8.9	55.1	1.9	7.8
750	0.002	0.057	0.001	0.157	35.70	2.1	81.7	1.8	12.6
850	0.005	0.112	0.002	0.184	45.13	3.4	86.9	1.3	14.7
950	0.010	0.054	0.002	0.144	58.25	5.1	139.2	1.5	11.5
1050	0.011	0.068	0.000	0.136	89.10	3.7	222.8	2.9	10.9
1150	0.017	0.120	0.003	0.175	160.77	3.1	306.7	3.3	14.0
1250	0.018	0.086	0.001	0.080	261.92	2.0	921.1	33.1	6.4
1350	0.037	0.071	0.000	0.045	177.94	6.2	1026.8	34.7	3.6
1450	0.010	0.021	0.000	0.015	39.48	7.5	729.4	34.8	1.2
1550	0.009	0.035	0.002	0.007	31.50	8.4	1162.1	125.0	0.5
Total[c]	0.21	0.03	0.96	1.25	964.9	6.3	253.2	5.5	
Conc.(/g)	2.4	11.13	0.35	14.56	11230.0				

[a] All gas quantities have been corrected for decay, isotopes derived from minor interfering neutron reactions, and blanks. tr denotes trapped Ar and Ca, Cl and K denote Ar derived from these elements. ^{40}Ar denotes trapped plus radiogenic Ar. Atmos. ^{40}Ar assumes a trapped Ar component of atmospheric composition.
[b] Errors from steps are analytical only and do not include the error in the irradiation parameter J.
[c] Includes the integrated age. The uncertainty in J (0.5%) is included in the error.

RESULTS

Table 1 presents the analytical data and Figure 3 the age spectra and element variation plots for the melt matrix of sample DNQ-62-FI. The age spectrum, except for the initial 5% ^{39}Ar release at 2.8 Ma, is smoothly varying from a low temperature Ar release at a maximum of 3.3 Ma decreasing to 1.3 Ma at 94% of ^{39}Ar release. It then rises abruptly for the last 6% of gas evolved. The spectra is reminiscent of the saddle-shaped patterns seen in samples known to contain excess ^{40}Ar (Lanphere and Dalrymple, 1976). In those cases, the minima in the saddle-shaped spectra approached the crystallization ages of the samples. Thus, this age spectra indicates a maximum age of 1.3 Ma for the impact melt matrix.

In the context of the processes outlined in the last section, it appears that this melt matrix contains a trapped Ar component with a $^{40}Ar/^{36}Ar$ greater than 295.5. The vesicular nature of the sample demonstrates that a significant fluid pressure was present during cooling, while the quench texture seen in thin section (Fig. 2) suggests that cooling was rapid. Thus, the absorption of some Ar from the fluid would be expected. The element variation patterns (Fig. 3) show that there is an excellent positive correlation of trapped ^{36}Ar and Cl-derived Ar with the age spectra pattern. The oldest ages are associated with the trapped Ar in anion sites. In contrast, the Ca/K ratio has a continuous increase with Ar release (Fig. 3). The patterns are similar to those described by Claesson and Roddick (1983) in plagioclase with excess ^{40}Ar.

Figure 4 presents an isotope correlation plot for the melt matrix data. A good linear array with increasing $^{39}Ar/^{40}Ar$ with release temperature is defined for the data from 550°C to 900°C. These temperature steps correlate with the smoothly decreasing age steps for 5 to 94% of the gas release in Figure 3. A regression line fitted through these seven steps (Fig. 4) defines an age of 0.47 +0.52 / -0.47 Ma from intersection with the X-axis and a trapped $^{40}Ar/^{36}Ar$ value of 489 ± 53. There is a significant scatter of the data beyond the experimental error (MSWD = 48), suggesting that the trapped component may be of a slightly variable composition. This is to be expected in a rapidly quenched melt that is interacting with unmelted inclusions. This scatter contributes to the high uncertainty in the age of the melt matrix. The age is younger than the maximum of 1.3 Ma indicated by the 900°C minimum in the age spectrum (Fig. 3) and indicates that there is still a significant trapped component in the 900°C step. The three steps at 1000°C and higher are also disposed around the regression line. This suggests that the trapped component in these fractions is of a similar composition to that in the lower temperature release, despite the fact that the element variation plots (Figure 3) suggest another anion reservoir is releasing trapped Ar.

An age spectrum using the $^{40}Ar/^{36}Ar$ determined by the correlation plot for correction of trapped Ar results in a more uniform and younger age for the melt matrix (Fig. 5). Two steps (500 and 1000°C) have negative ages because their trapped $^{40}Ar/^{36}Ar$ components appear to be less than 489. Excluding these two steps the integrated age of the 550 to 1200°C steps, which represent 94% of the gas, is 0.33 ± 0.08 Ma, an age similar to the correlation plot age. The error is unrealistically low because no error has been assigned to the trapped composition.

Figure 6 presents the age spectrum and Ca/K variation for the concentrate of inclusions in DNQ-62-FI. The initial gas release indicates an age of 17 Ma and then exponentially rises to a maximum age of about 1200 Ma. All heating steps in the inclusions analysis record ages that are much older than the melt matrix and indicate that they have not lost all their previously generated radiogenic $^{40}Ar^*$ during

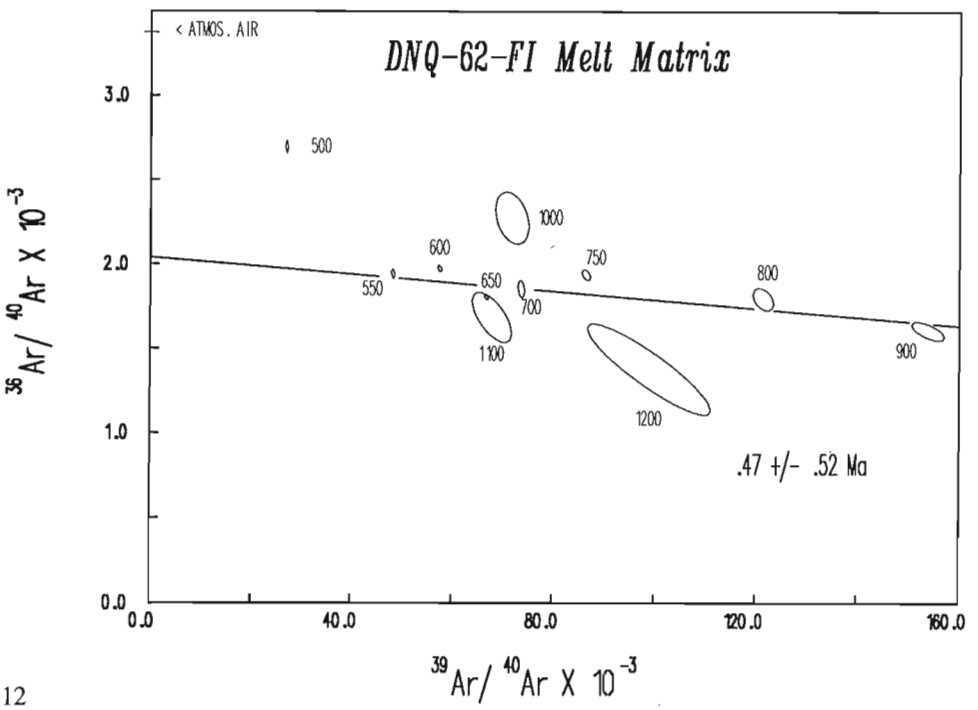

Figure 4. An isotope correlation plot for DNQ-62-FI melt matrix. The regression line was fitted through heating steps 550-900°C and represents about 90% of the total ^{39}Ar released. The intersection with the X-axis corresponds to an age of 0.47 +0.52/ −0.47 Ma (MSWD = 48) and the Y-axis intercept to a trapped Ar component with a $^{40}Ar/^{36}Ar$ of 489 ±53. Steps 450 and 1500°C, with high errors and less than 0.25% of ^{39}Ar have been omitted from the plot. A chord from atmospheric $^{36}Ar/^{40}Ar$ through any data point will intersect the X-axis at a $^{39}Ar/^{40}Ar$ value representative of the conventional $^{40}Ar/^{39}Ar$ age, calculated assuming atmospheric composition for the trapped $^{40}Ar/^{36}Ar$.

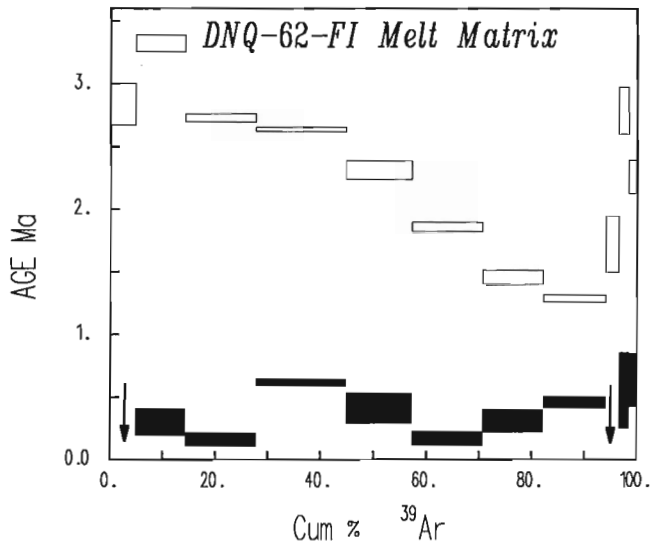

Figure 5. Age spectrum plot of data from DNQ-62-FI melt matrix as in Figure 3 with an atmospheric composition assumed for trapped Ar (open boxes) and the same data using the trapped $^{40}Ar/^{36}Ar$ of 489 determined from the correlation plot (filled boxes). The arrows designate two fractions with negative apparent ages.

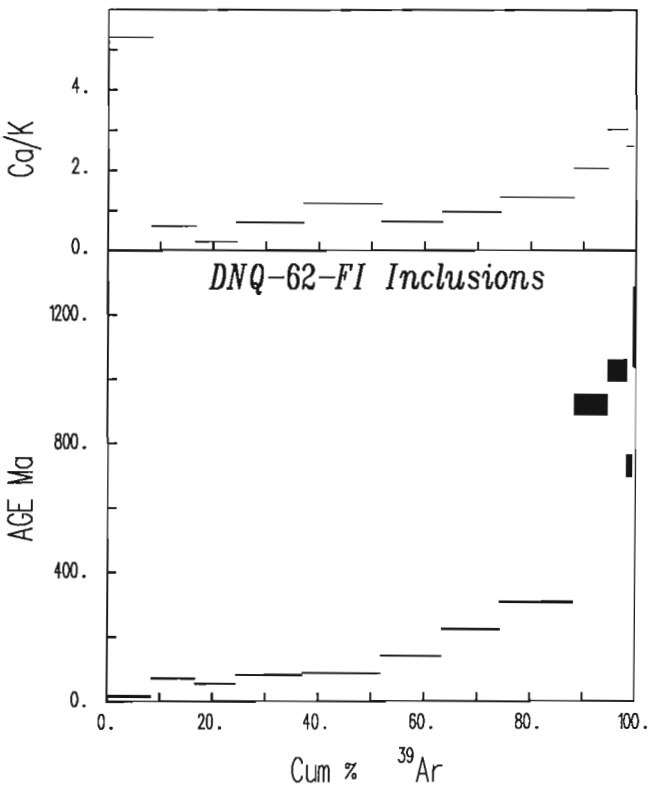

Figure 6. Age spectrum plot of data from DNQ-62-FI inclusions and Ca/K element variation for each heating step.

the impact event. Even the lowest temperature release contains large amounts of residual $^{40}Ar_o*$. A correlation plot (not shown) shows no separation of trapped and radiogenic $^{40}Ar*$ components. The excessive amounts of residual $^{40}Ar_o*$ dominate all gas steps. It is clear that these inclusions are the source of the trapped Ar with the anomalous $^{40}Ar/^{36}Ar$ in the melt matrix. The Ca/K variation follows approximately the age spectrum pattern and indicates that sites high in Ca have retained the greatest proportion of residual $^{40}Ar_o*$. The Cl content of the inclusions is low and precision on individual steps inadequate to define any clear parterns of trapped Ar reservoirs.

DISCUSSION AND CONCLUSIONS

$^{40}Ar/^{39}Ar$ dating of an impact melt rock from the New Quebec Crater has shown that the Ar systematics of impactites may be complex, but with careful analysis the age of the cratering event can be revealed. The inclusions in the impactite still contain significant amounts of radiogenic ^{40}Ar generated in the target Archean gneisses prior to the impact event, precluding their use in defining the time of the event. Even the melt matrix shows the effects of the degassing of this old radiogenic Ar from the inclusions. Owing to high fluid pressures and the rapid cooling of the melt after impact some of the residual radiogenic ^{40}Ar was absorbed and trapped in the melt. Conventional age spectrum calculations, assuming an atmospheric $^{40}Ar/^{36}Ar$ trapped component, yield ages that are too old. An isotope correlation plot successfully reveals the anomalous trapped Ar composition and indicates the best estimate of the age of the impact event is 0.47 +0.52 / -0.47 Ma. The trapped Ar is shown to be correlated with anion sites containing Cl. Even the highest temperature fractions, when corrected for trapped Ar, have ages indistinguishable from the bulk of the sample Ar gas. This indicates that all inclusions have been removed from the melt concentrate and that the trapped Ar in all fractions is of a similar composition.

The age of the New Quebec Crater at 0.47 +0.52 / -0.47 Ma, while younger than the previous estimate of less than 5 Ma, is within the known geological constraints. Previous work has shown that the rocks outside the crater rim have been glaciated at least twice (Currie, 1966). The latest glacial striations define a northeast direction of ice movement. The effects of this glaciation are see in the scouring of northeast-trending valleys crossing the crater rim (Currie, 1966). This is the known direction of advance of the Laurentide Ice Sheet in the region from 24 Ka to 7 Ka, when the last ice retreated from the area of the New Quebec Crater (Dyke and Prest, 1987). Another set of striations indicate ice movement with a S70°E trend, but valleys cutting the crater rim in this direction do not appear to be glaciated. This suggests that the impact event took place between two periods of different ice movement. The timing and movement of glaciations prior to the Laurentide is more uncertain as any record of glaciations in the area is lacking. The sediments in the New Quebec Crater may provide the best record of earlier glaciations (Bouchard, 1989), though they cannot extend the record back beyond about 1 Ma, the upper error limit of the present $^{40}Ar/^{39}Ar$ age. The lower age limit for the time of impact is thus poorly constrained but probably 25 Ka or older.

One of the anomalous features of this crater is the lack of an ejecta impact blanket. This has resulted in some uncertainty as to the cause of the circular structure and to suggestions that it is not a meteorite impact feature but one of terrestrial origin (Currie, 1966). While recent finds of additional impactites have resolved the uncertainty on the origin, the lack of significant ejecta remains a puzzle. Since the recent glaciations have only modified the crater rim structure and not removed it, it is unlikely that they could have removed significant ejecta material. In addition, the crater site is close to a centre of glaciation (Dyke and Prest, 1987), thus minimizing the effects of glacial erosion. One possible explanation for this apparently missing ejecta is that the impact took place during a glaciation and that ejecta consisted of both ice and rock material. In that case the ejecta would be deposited on glacial ice to be subsequently transported away from the impact site. Budd and Smith (1987) have modelled ice thicknesses during the Laurentide Ice Sheet and suggest that up to 3 km of ice may accumulate, more than enough to provide a surface to remove ejecta from the region. Glaciations in North America extend back to late Pliocene time, and may have developed similar ice thicknesses. The current estimate of the time of impact (up to 1 Ma) is within this window of glaciations. Future models of the impact event at the New Quebec Crater should perhaps consider that the surface layer of the target may have been glacial ice.

Another feature observed by Currie (1966) also suggests the presence of ice during the impact. He observed that all the country rocks of the region out to 3 km from the crater centre contained significant amounts of a distinctive bright green epidote. In the outer 2-3 km zone the epidote was confined to major fractures. Beyond this halo of alteration the epidote was absent or of a different character. He concluded that the epidote grew under almost static conditions at low pressure (120 bars). This feature was consistent with his model of an explosive fluidized dome. However, if the impact took place on an ice layer, significant melting and penetration of the rock by water would take place. Subsequent alteration and the formation of epidote under near static conditions could occur.

The age spectra pattern of the DNQ-62-FI melt matrix is similar to that determined for the Type 1 samples of Mak et al. (1976) for the Mistastin Lake impact crater. While it was concluded that the age of the Mistastin impact was 38 $\pm$ 4 Ma, the age spectra of those samples rose rapidly to about 41 to 38 Ma and then decreased monotonically to minima near 29 Ma at 85-97% gas release. The authors commented on the remarkable coincidence of the minima ages of four samples, all between 28.3 and 30.6 Ma. If the New Quebec Crater melt matrix were to be analyzed in about 30 Ma, the age spectra pattern would mimic those of the Mistastin Lake crater samples. Mak et al. (1976) did not present isotope correlation plots, nor did they discuss the possibility of excess argon in the samples. They did, however, analyze inclusions of maskelynite and other samples with significant inclusions. These samples yielded spectra with ages of 200 to 700 Ma and rising age patterns similar to DNQ-62-FI inclusions (Fig. 6), thus documenting the incomplete degassing of the impactites. On the basis of the interpretation of the New Quebec Crater melt matrix spectrum it is likely that the Type 1 samples from Mistastin also contain anomalous trapped Ar and that the correct age of the Mistastin Lake impact crater is 29 Ma or slightly younger. Further analyses, as suggested by Mak et al. (1976), but using the detailed approach of correlation plots to defining trapped argon composition should resolve this uncertainty.

ACKNOWLEDGEMENTS

I would like to thank L. Adamitz, G. LeCheminant, and F. Quigg for technical assistance. T.M Harrison provided advice on the Ar furnace design. R.A.F Grieve, W.D. Loveridge, and R.R. Parrish are thanked for critically reading the manuscript.

REFERENCES

Alvarez, W. and Muller, R.A.
1984: Evidence from crater ages for periodic impacts on the Earth; Nature, v. 308, p. 718-720.

Baksi, A.K.
1973: Quantitative unspiked argon runs in K-Ar dating; Canadian Journal of Earth Sciences, v. 10, p. 1415-1419.

Bouchard, M.A.
1989: The Nouveau-Québec (Nunavik) crater: a possible site for a long range Cenozoic stratigraphic record beneath continental ice sheets; Geological Association of Canada, Program with Abstracts, v. 14, p. A61.

Budd, W.F. and Smith, N.
1987: Conditions for growth and retreat of the Laurentide Ice Sheet; Géographie physique et Quaternaire, v. XLI, p. 279-290.

Claesson, S. and Roddick, J.C.
1983: $^{40}Ar/^{39}Ar$ data on the age and metamorphism of the Ottfjället dolerites, Särv Nappe, Swedish Caledonides; Lithos, v. 16, p. 61-73.

Currie, K.L.
1966: Geology of the New Quebec Crater; Geological Survey of Canada, Bulletin 150, 36 p.

Currie, K.L. and Dence, M.R.
1963: Rock deformation in the rim of the New Quebec Crater, Canada; Nature v. 198, p.80.

Dyke, A.S. and Prest, V.K.
1987: Late Wisconsinan and Holocene history of the Laurentide Ice Sheet; Géographie physique et Quaternaire, v. XLI, p. 237-263.

Gentner, H.U., Lippolt, H.J., and Schaeffer, O.A.
1963: Argonbestimmungen an Kaliummineralien - XI Die Kalium - Argon - Alter der Gläser des Nördlinger Rieses und der böhmisch-mährischen Tektite; Geochimica Cosmochimica Acta, v. 27, p. 191-200.

Gillespie, A.R., Huneke, J.C., and Wasserburg, G.J.
1982: An assessment of ^{40}Ar-^{39}Ar dating of incompletely degassed xenoliths; Journal of Geophysical Research, v. 87, B11, p. 9247-9257.

1983: Eruption age of a Pleistocene basalt from ^{40}Ar-^{39}Ar analysis of partially degassed xenoliths; Journal of Geophysical Research, v. 88, B6, p. 4997-5008.

Grieve, R.A.F.
1982: The record of impact on Earth: implications for a major Cretaceous/Tertiary impact event; Geological Society of America, Special Paper 190, p. 25-38.

1984: The impact cratering rate in recent time; Journal of Geophysical Research, v. 89, p. B403-B408.

Grieve, R.A.F., Sharpton, V.L., Goodacre, A.K., and Garvin, J.B.
1986: A perspective on the evidence for periodic cometary impacts on Earth; Earth and Planetary Science Letters, v. 76, p. 1-9.

Harrison, J.M.
1954: Ungava (Chubb) Crater and glaciation; Journal of the Royal Astronomical Society of Canada, v. 48, p. 16-20.

Harrison, T.M. and McDougall, I.
1981: Excess ^{40}Ar in metamorphic rocks from Broken Hill, New South Wales: implications for $^{40}Ar/^{39}Ar$ age spectra and the thermal history of the region; Earth and Planetary Science Letters, v. 55, p. 123-149.

Heizler, M.T. and Harrison, T.M.
1988: Multiple trapped argon isotope components revealed by $^{40}Ar/^{39}Ar$ isochron analysis; Geochimica et Cosmochimica Acta, v. 52, p. 1295-1303.

Innes, M.J.S.
1964: Recent advances in meteorite crater research at the Dominion Observatory, Ottawa, Canada; Meteoritics, v. 2, p. 219-241.

Jansa, L.F. and Pe-Piper, G.
1987: Identification of an underwater extraterrestrial impact crater; Nature, v. 327, p. 612-614.

Lanphere, M.A. and Dalrymple, G.B.
1976: Identification of excess ^{40}Ar by the $^{40}Ar/^{39}Ar$ age spectrum technique; Earth and Planetary Science Letters, v. 32, p. 141-148.

Mak, E.K., York, D., Grieve, R.A.F., and Dence, M.R.
1976: The age of the Mistastin Lake crater, Labrador, Canada; Earth and Planetary Science Letters, v. 31, p. 345-357.

Marvin, U.B., Kring, D.A., and Boulger, J.D.
1988: Petrography of impactite from the New Quebec Crater (abstract); Meteoritics, v. 23, p. 287-288.

Meen, V.B.
1951: Chubb Crater, Ungava, Quebec; Proceedings of the Geological Association of Canada, v. 4, p. 49-59.

Millman, P.M.
1956: A profile study of the New Quebec Crater; Publication of Dominion Observatory, Ottawa, v. 18, No. 4, p. 59-82.

Muller, R.A. and Morris, D.E.
1986: Geomagnetic reversals from impacts on the earth; Geophysical Research Letters, v. 13, p. 1177-1180.

Robertson, P.B., Dence, M.R., and Vos, M.A.
1968: Deformation in rock-forming minerals from Canadian craters; in Shock Metamorphism of Natural Materials, ed. B.M. French and N.M. Short; Mono Book Corp., Baltimore, p. 433-452.

Roddick, J.C.
1983: High precision intercalibration of ^{40}Ar-^{39}Ar standards; Geochimica et Cosmochimica Acta, v. 47, p. 887-898.

1988: The assessment of errors in $^{40}Ar/^{39}Ar$ dating; in Radiogenic Age and Isotopic Studies: Report 2, Geological Survey of Canada, Paper 88-2, p. 3-8.

Roddick J.C. and Rex, D.C.
1980: Low-grade metamorphic effects on plagioclase as detected by $^{40}Ar/^{39}Ar$ analyses (abstract); EOS, v. 61, p. 398.

Roddick, J.C., Cliff, R.A., and Rex, D.C.
1980: The evolution of excess argon in Alpine biotites – a ^{40}Ar-^{39}Ar analysis; Earth and Planetary Science Letters, v. 48, p. 185-208.

Shoemaker, E.M.
1961: Geological reconnaissance of the New Quebec Crater, Canada; U.S. Geological Survey Branch of Astrogeologic Studies Semiannual Progress Report, Feb.-Aug., p. 74-78.

Staudacher, Th., Jessberger, E.K., Dorflinger, D., and Kiko, J.
1978: A refined ultrahigh-vacuum furnace for rare gas analysis; Journal Physics, E: Scientific Instruments, v. 11, p. 781-789.

Turner, G.
1971: ^{40}Ar-^{39}Ar ages from the Lunar Maria; Earth and Planetary Science Letters, v. 11, p. 169-191.

Weissman, P.R.
1985: Terrestrial impactors at geological boundary events: comets or asteroids?; Nature, v. 314, p. 517-519.

York, D.
1969: Least squares fitting of a straight line with correlated errors; Earth and Planetary Science Letters, v. 5, p. 320-324.

APPENDIX 1.

$^{40}Ar/^{39}Ar$ ANALYSIS

Argon extractions were performed in a double-vacuum resistance-heated tantalum furnace, similar in design to that described by Staudacher et al. (1978). The furnace temperature was measured with a 3%-25% Re-W thermocouple in the base of the tantalum furnace tube and maintained by a Eurotherm™ three term electronic controller capable of ± 0.5°C stability. Samples were loaded into a glass Christmas tree flanged to the top of the furnace tube and the entire system baked to about 150°C under vacuum for 16 hours. Following further degassing of the furnace (to 1600°C) and getters (described below), a sample was dropped into the crucible and step heating commenced. The furnace was allowed to cool between 20-min heating steps and the evolved gas purified in three stages of gettering. A getter in the furnace section, consisting of SAES™-ST707 pellets at 25°C, absorbed H_2 during sample heating. Gas was then transferred to a second stage, using liquid nitrogen cooled activated charcoal, where ST707 pellets maintained at 250°C removed active gases. A final getter section of SAES™-ST707 getter at 450°C ensured complete cleanup of all active gases. Charcoal traps were heated to 150°C during gas purification to desorb hydrocarbons (Roddick et al., 1980) and ensure 100% absorption of Ar on the traps when cooled with liquid nitrogen. Total extraction and purification blanks are $\approx 7 \times 10^{-10}$ cm^3 ^{40}Ar below 1200 °C and 6×10^{-9} at 1550°C and have an uncertainty of $\pm 50\%$.

A modified MS 10 mass spectrometer with a 0.4 Testa permanent magnet and solid state electronics was used to analyze the argon. Sensitivity was 1.5×10^{-6} A/Pascal (or 7×10^{-8} cm^3 STP/V) and additional collector slit plates resulted in an abundance sensitivity of 15 ppm at 10^{-8} Pascals. Data collection involved computer — controlled voltage peak switching to scan the five Ar masses and baselines on either side of ^{36}Ar. Twelve scans of the ion beams were recorded by a Keithley™ 642 electrometer with a 10^{11} ohm resistor, feeding a Solartron™ DVM with output to a HP 9826 computer for data reduction. The peak switching interval of 5 s delay and 4 s integration resulted in a detection limit of 1×10^{-12} cm^3 STP of argon. Intensities at masses 28, 43, and 80 were also monitored.

Measured mass spectrometer peak intensities were processed and corrected in the following order:

(1) A dynamic memory (or zero) correction, caused by the response of the electrometer to varying beam intensities.

(2) Linear extrapolation of Ar isotope peak heights or isotopic ratios $^{i}Ar/^{39}Ar$ (i = 40, 38, 37, 36) to the time at which the mass spectrometer was equilibrated with the inlet section.

(3) Tailing effects under ^{39}Ar, ^{38}Ar, and ^{37}Ar peaks (zero levels taken on either side of the ^{36}Ar peak).

(4) Isobaric interference of doubly charged ^{80}Kr on ^{40}Ar. Kr is produced by neutron reaction with Br in a sample.

(5) Spectrometer mass discrimination.

(6) Atmospheric Ar extraction blanks (listed above).

(7) Radioactive decay of ^{39} ($\lambda = 7.05 \times 10^{-6}$ day^{-1}) and ^{37}Ar ($\lambda = 0.01975$ day^{-1}).

(8) Minor products of neutron reactions on K, Ca, and Cl: $(^{40}Ar/^{39}Ar)_K = 0.025$, $(^{38}Ar/^{39}Ar)_K = 0.0107$, $(^{40}Ar/^{39}Ar)_{Ca} = 3.00$, $(^{38}Ar/^{39}Ar)_{Ca} = 0.050$, $(^{37}Ar/^{39}Ar)_{Ca} = 1480$. Cl corrections to ^{36}Ar were determined using a ^{36}Cl half life of 3.0×10^5 years (Roddick, 1983).

Data Table 1 lists the Ar isotope quantities after the above corrections. Mass spectrometer discrimination and sensitivity were monitored with each sample by analyzing atmospheric argon from a pipette system. Close monitoring of the sensitivity and careful gas clean-up procedures allow the MS 10 to be used as a precise manometer (Baksi, 1973). Using monitors with known amounts of K, Ca, and Cl the concentrations in unknowns may be determined.

The ^{40}Ar – ^{39}Ar ratio, age, and errors for each gas fraction (Table 1) were calculated using formulae detailed in Roddick (1988). Duplicate analyses of sample gas fractions indicate a precision of 0.2% (2σ) in measured $^{40}Ar/^{39}Ar$ ratios for ^{39}Ar beams greater than 0.8×10^{-9} cm^3 STP. Isotopic ratios for correlation plots may be derived from the gas quantities of Table 1. Errors in these ratios were evaluated as detailed in Roddick (1988).

Miocene $^{40}Ar-^{39}Ar$ and K-Ar ages for basaltic volcanic rocks in southwestern Dawson map area, western Yukon Territory

J.K. Mortensen[1] and J.C. Roddick[1]

Mortensen, J.K. and Roddick, J.C., Miocene $^{40}Ar-^{39}Ar$ and K-Ar Ages for Basaltic Volcanic Rocks in southwestern Dawson map area, western Yukon Territory; in Radiogenic Age and Isotopic Studies: Report 3, Geological Survey of Canada, Paper 89-2, p. 17-22, 1989.

Abstract

Several small occurrences of fresh olivine basalt were identified during geological mapping of southwestern Dawson map area in western Yukon Territory. These occurrences consist mainly of alkali olivine basalt containing abundant peridotite nodules and xenoliths of underlying rock units, and typically form small cinder cones and valley-filling flows. They closely resemble the Selkirk Lavas of western Yukon, the Stikine Volcanic Belt of southern Yukon and northern British Columbia, and Prindle Volcano and other centres in eastern Alaska. A whole-rock sample from one of the occurrences yielded $^{40}Ar-^{39}Ar$ and K-Ar ages of 19.5 and 19.9 Ma, and a K-Ar whole-rock age of 17.2 Ma was determined for a sample from a second occurrence. These ages are considerably older than any previously reported from other young volcanic centres in this region, and their significance is uncertain. They appear to indicate that basaltic volcanism in the northern Canadian Cordillera extended back at least to the Early Miocene Epoch. The ages may, however, also reflect the effects of excess Ar derived from assimilated radiogenic xenoliths. Further work is planned to test these hypotheses.

Résumé

On a observé plusieurs petites manifestations de basalte à olivine frais au cours de travaux de cartographie géologique du secteur sud-ouest de la feuille de Dawson, dans l'ouest du Yukon. Ces manifestations sont principalement constituées de basaltes à olivine alcalins renfermant d'abondants nodules de péridotite et des xénolites des unités de roches sous-jacentes, et forment typiquement de petits cônes de scories et des coulées de remplissage de vallée. Elles ressemblent étroitement aux laves de Selkirk de l'ouest du Yukon, à la zone volcanique de Stikine du sud du Yukon et du nord de la Colombie-Britannique, ainsi qu'au volcan de Prindle et autres centres de l'est de l'Alaska. Un échantillon de roche totale provenant de l'une de ces manifestations a donné des âges de 19,5 Ma et 19,9 Ma par les méthodes $^{40}Ar-^{39}Ar$ et K-Ar et un âge de roche totale de 17,2 Ma a été déterminé par la méthode K-Ar pour un échantillon provenant d'une autre manifestation. Ces âges sont beaucoup plus anciens que tous ceux qu'on avait signalés auparavant pour d'autres centres volcaniques plus jeunes de cette région; leur signification demeure toutefois incertaine. Ils semblent indiquer que le volcanisme basaltique du nord de la Cordillère canadienne remonte au moins au Miocène inférieur. Les âges peuvent cependant aussi refléter les effets d'un excès d'Ar provenant de xénolites radiogéniques assimilés. On prévoit d'autres travaux pour vérifier ces hypothèses.

INTRODUCTION

Isolated occurrences of olivine basalt of Late Tertiary and Quaternary age have been identified in several areas of southern and western Yukon Territory and eastern Alaska (Mitchell, 1987). These centres typically comprise small cinder cones, massive flows and/or pillow basalt. Some of the better known localities include the Miles Canyon-Alligator Lake area south of Whitehorse, the Watson Lake area and the Fort Selkirk area in Yukon, and Prindle Volcano in eastern Alaska (Fig. 1). In western Yukon these volcanic rocks have been informally referred to as the "Selkirk lavas," based on a correlation with basalts of the Selkirk Volcanics near Fort Selkirk (Bostock, 1936; Sinclair et al,

1 Geological Survey of Canada, 601 Booth Street, Ottawa, Ontario K1A 0E8

1978; equivalent to the Selkirk Series of Tempelman-Kluit, 1974). Some of the centres in southern Yukon have been included in the Stikine volcanic belt (e.g. Alligator Lake, Eiche et al., 1987). Relatively few of the centres have been mapped in detail or studied petrologically. Reliable ages for volcanism are also limited; in a few cases isotopic ages are available (reviewed by Hickson, in press), but the timing of volcanism has generally been inferred from one of the following: a) state of preservation of constructional volcanic landforms; b) observed relationships between extrusive rock units and reasonably well dated Pleistocene glacial features; c) relationships with such regionally developed stratigraphic markers as the White River Ash; or d) historical records. Taken together, the data suggest that most volcanic activity ranged in age from Late Pliocene (about 2.4 Ma) to Recent.

Four small accumulations of fresh basaltic volcanic rocks were identified during regional mapping in the southwestern Dawson map area in western Yukon (Mortensen, 1988a, b). In this paper we briefly describe the four occurrences and report and discuss new K-Ar and $^{40}Ar-^{39}Ar$ whole-rock ages from two of the localities.

REGIONAL SETTING

Southwestern Dawson map area is mainly underlain by polydeformed metamorphic rocks of the Yukon-Tanana Terrane, considered to be largely of middle and late Paleozoic age (Mortensen, 1988a, b, unpublished data). Undeformed upper Cretaceous andesitic volcanic rocks and clastic sediments, and related hypabyssal intrusions locally overlie and intrude the metamorphic assemblage. Bimodal mid-Eocene dykes and small plugs occur in a narrow band adjacent to the Tintina Fault Zone (Fig. 1), and Lower to mid-Eocene clastic sediments fill an elongate graben structure that marks the Tintina Fault Zone itself (Mortensen, 1988b).

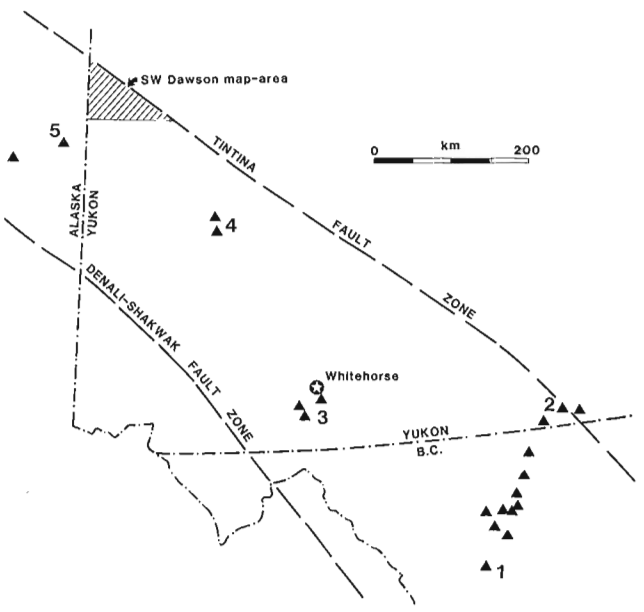

Figure 1. Distribution of Late Tertiary and Quaternary volcanic centres in northern British Columbia, Yukon Territory, and eastern Alaska. Individual centres include: 1) Mt. Edziza; 2) Watson Lake area; 3) Alligator Lake-Miles Canyon; 4) Fort Selkirk; 5) Prindle Volcano. Study area is hatchured.

The study area was not affected by Pleistocene glaciation and is heavily vegetated; hence outcrop is generally restricted to stream valleys and road cuts. Although unglaciated, the present land surface reflects substantial modification by periglacial and permafrost-related processes (e.g., cryoplanation, *see* Hughes et al., 1972); thus distinctive volcanic landforms may not be preserved.

A prominent raised-terrace system is developed along Yukon and Fortymile rivers in the study area (Fig. 2), and can be traced more than 50 km up the Fortymile River from the Yukon-Alaska border (Foster, 1976). The age of these terraces is not well constrained.

Occurrences of Young Basaltic Rocks

Fortymile Occurrence

The best exposure of young mafic volcanic rocks in the study area is located at the edge of a raised river terrace on the west side of the Yukon River, 5.5 km upstream from the mouth of Fortymile River (Fig. 2, 3). It was briefly described by Green (1972, p. 104). Volcanic rocks at this locality appear to fill a valley cut into underlying carbonaceous quartz-muscovite schist (Fig. 3). A section of volcanic rocks approximately 125 m thick is exposed. The lower 100 m consists of massive, lithic-rich debris flow deposits passing upwards into crudely stratified scoriaceous basaltic agglomerate

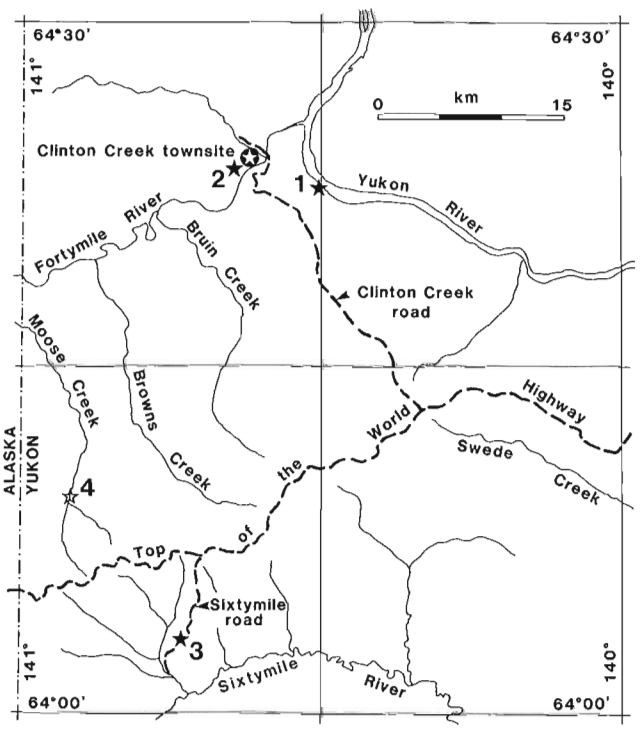

Figure 2. Location map for basalt occurrences discussed in this paper. Solid stars represent outcrop occurrences; open stars represent float occurrences. Locality numbers are: 1) Fortymile River; 2) Clinton Creek townsite; 3) Sixtymile road; 4) Moose Creek.

and breccia. The upper 25 m of section consists of a single massive flow displaying spectacular columnar jointing (Fig. 3). The basalt is fresh and unaltered, dark grey, and weathers to a medium chocolate brown. Euhedral to anhedral olivine and pyroxene phenocrysts (and possible xenocrysts) to 0.8 cm in diameter locally comprise up to 3% of the rock by volume. Rounded coarse-grained peridotite nodules to 3 cm in diameter are also common. Many of these nodules have weathered out, leaving round cavities lined by olivine and pyroxene grains. It is uncertain what proportion (if any) of the isolated olivine and pyroxene phenocrysts in the rock were derived by disaggregation of peridotite nodules.

The massive jointed flow is truncated by a raised river-terrace surface and is covered by thick terrace gravel deposits. Terrace gravels in this area locally contain significant amounts of placer gold, and it was hoped that an age for the volcanic unit would provide a maximum age for both terrace development and for deposition of the gold-bearing gravels.

Sixtymile Occurrence

Fresh basaltic rocks are exposed in a small area of bulldozed trenching about 100 m west of the Sixtymile Road, approximately 8.4 km from the junction with the Top-of-the-World Highway (Fig. 2). The volcanic rocks overlie older sandstones, siltstones, and mudstones of Late Cretaceous age (Mortensen, 1988b), and consist mainly of scoriaceous basalt and agglomerate that probably originally formed a small cinder cone. Olivine phenocrysts to 2 mm and plagioclase phenocrysts to 1 mm in diameter make up less than 2% of the rock by volume. The basalt is unaltered except for minor chloritization of olivine phenocrysts. Some vesicules are partly filled with carbonate and/or zeolites.

The basaltic rocks are observed both overlying and cross-cutting baked and bleached Cretaceous sediments, and sedimentary xenoliths and less commonly xenoliths of the underlying metamorphic rocks are abundant. Ultramafic nodules were not observed at this locality, although many of the olivine phenocrysts display corroded outlines and may be in part xenocrysts derived from disaggregated peridotite nodules. Glasmacher (1984) reports a single geochemical analysis of basalt from this occurrence, which falls in the alkali olivine basalt field.

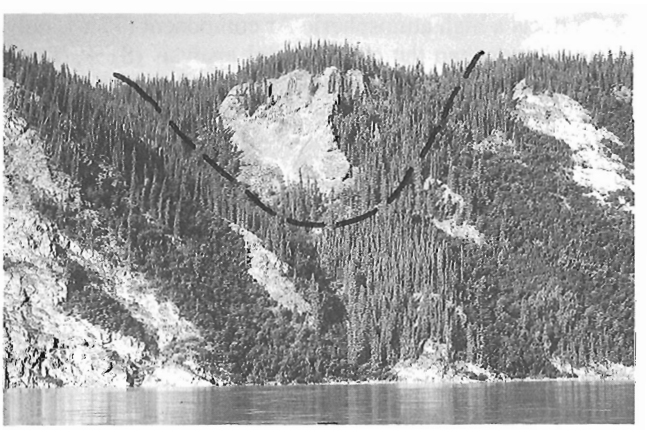

Figure 3. View looking west-southwest towards the Fortymile basalt occurrence. The heavy dashed line shows the contact between basaltic rocks and underlying schists. Exposed basalt section is approximately 125 m thick.

Clinton Creek Townsite Occurrence

A third exposure of fresh, olivine-phyric basalt occurs 1.5 km west of the abandoned Clinton Creek townsite (Fig. 2) (Htoon, 1979). Htoon mapped two small areas of basalt in this area, each less than 150 m in maximum dimension, situated about 200 m apart. The exposures have now been much disrupted by road construction in the area, and original contact relationships are difficult to decipher. When examined by the first author in 1987, much of the exposed basalt consisted of variably scoriaceous material that may have been derived from either flows or agglomerate. Htoon (1979) described the occurrences as "undeformed columnar jointed flows lying unconformably on metamorphic rocks."

The basalt in this occurrence consists of a fine-grained groundmass of plagioclase, olivine, pyroxene, magnetite, and glass surrounding scattered euhedral to irregular olivine phenocrysts to 1.5 cm in diameter. Much of the glass is altered to palagonite. Rounded medium-grained peridotite nodules to 8 cm diameter as well as xenoliths of the underlying metamorphic rocks are locally abundant.

Moose Creek Occurrence

Large angular boulders (to 1 m in diameter) of fresh and unaltered, massive, olivine-phyric basalt are abundant in the headwaters of Moose Creek (Fig. 2), and occur with decreasing frequency for at least 5 km downstream. The basalt contains abundant xenoliths of locally derived metamorphic rocks. Although the source of the boulders was not located, their distribution constrains the vent position to approximately that shown in Figure 2.

Other Occurrences

Clasts of locally derived, unaltered, olivine-phyric basalt occur in stream gravels in a number of other localities in the study area, suggesting that additional volcanic centres were present. One such example is about 7 km above the mouth of Bruin Creek (Fig. 2), where boulders of vesicular basalt containing olivine phenocrysts to 0.8 cm diameter make up a small proportion of creek gravels.

In the area immediately adjacent to the Tintina Fault Zone, basalts of the bimodal Eocene suite may be mistaken for the younger olivine basalt suite. The Eocene rocks, however, are typically less vesicular and more highly altered than the younger basalts, and are plagioclase- rather than olivine-phyric.

SAMPLING AND ANALYTICAL TECHNIQUES

Two samples were selected for dating in this study, one from the massive jointed flow at the Fortymile occurrence (M-1077), and the other from massive, non-vesicular basalt from the Sixtymile occurrence (M-263). In both cases

xenoliths were avoided and the samples checked during crushing to select only massive basalt. The samples were sieved to -50+80 mesh and washed in cold 10% reagent grade HCl for 5 min in an ultrasonic bath and then repeatedly washed with water (Souther et al., 1984).

The conventional K-Ar analyses were performed using procedures detailed in Roddick and Souther (1987). The sample selected for $^{40}Ar-^{39}Ar$ dating was wrapped in an aluminium foil packet and irradiated along with several other samples and aliquots of FCT-3 biotite. This biotite is a new $^{40}Ar-^{39}Ar$ flux monitor prepared by the United States Geological Survey, Reston, Virginia, from the Fish Canyon Tuff. Its age is 27.68 ± .03 Ma (M.J. Kunk, pers. comm., 1988). The can was irradiated for 45 min in position 5C of the enriched uranium research reactor at McMaster University, Hamilton, Ontario. It received an approximate fast neutron fluence of 3×10^{16} neutrons/cm^2, which results in a J factor of 2.1×10^4. Flux variation over the irradiation can had a range of 3.0% and is mainly along the axis of the can. The errors quoted on the integrated age take account of this uncertainty, though the individual step ages do not. The procedures for $^{40}Ar-^{39}Ar$ analysis are detailed in Roddick (1990).

RESULTS AND DISCUSSION

Table 1 presents the two conventional K–Ar results. The 17.2 ± 0.5 and 19.9 ± 0.5 Ma are both Early Miocene ages and though similar are distinct from each other when the error limits are considered. In addition the ages are considerably older than expected. Although closely similar in lithology, geochemistry, and nature of included xenoliths to many other young volcanic centres in southern and western Yukon, the oldest age previously obtained for any of these centres is only 2.4 Ma. Prindle Volcano, which lies less than 50 km west of the Sixtymile Road and Moose Creek occurrences described in this paper, consists of xenolith-rich alkali olivine basalt (Foster et al., 1966). It is also considered to be very young (probably Quaternary, Foster et al., 1987; and H.L. Foster, pers. comm., 1989) because of its well preserved cinder cone. The only direct age constraint for Prindle Volcano is provided by the presence of White River Ash dated at 1880 years BP (Lerbekmo et al., 1975; Downes, 1985), which mantles both the cone and a related lava flow (Foster, 1981). Volcanic rocks in the Fort Selkirk area, 200 km southeast of the study area, range in age from about 1.6 Ma to Recent (Hickson, in press; Jackson, 1989, pers. comm., 1989).

The above indirect evidence suggests that the two K-Ar ages reported on Table 1 may be too old. Souther et al. (1984) obtained anomalously old K-Ar ages (up to 22 Ma) for whole-rock samples from Mount Edziza in northern British Columbia, a volcanic complex known to be no older than 8 Ma. They attributed anomalously old ages to two possible factors: 1) the presence of excess argon in xenolith-rich or rapidly cooled basaltic magmas from ice-contact or subaqueous environments; and 2) isotopic fractionation of atmospheric Ar during vacuum bakeout of a sample prior to Ar analysis as originally proposed by Baksi (1974).

Table 1. K-Ar data for volcanic rocks, Dawson map area, Yukon Territory.

Field No.	Lab. no.	Material	K wt% ± 1σ %	Rad ^{40}Ar cm^3/g 10^{-7}	% Atmos. $^{40}Ar^{\alpha}$	Age ± 2σ Ma
M-263	3942	Whole rock	1.033 ± 0.	6.953	37.5	17.2 ± 0.3
M-1077	3994	Whole rock	1.315 ± 0.	10.22	81.3	19.9 ± 0.5

σ = standard error; cm^3/g is determined at standard temperature and pressure.
α = corrected of a line blank of 2 X 10^{-7} cm^3 atmospheric Ar.

For the two samples in the present study it appears that both factors may be responsible for producing anomalously old ages. Country-rock xenoliths are present at both of the localities sampled in the present study, and it is also possible that excess Ar has been incorporated. However, the two ages are very similar and would require the absorption of excess argon proportional to K content. Furthermore, Pb isotopic analyses of basalt samples from each of the localities yield non-radiogenic compositions (M.L. Bevier, pers. comm., 1989) suggesting minimal amounts of crustal contamination.

The second factor, atmospheric Ar fractionation, may have occurred in sample M-1077 during Ar analysis, as it has a much higher atmospheric Ar content than the other sample (Table 1). When compared to the amount of atmospheric Ar expected in basaltic rocks (Roddick, 1978), M-263 has a typical amount whereas M-1077 has ten times as much. This is usually a good indicator of secondary alteration (Roddick, 1978) and suggests that, despite the apparent freshness of the sample in thin section, it must have some incipient alteration. Baksi (1974) first showed that loosely held atmospheric Ar can fractionate during vacuum bakeout of basalts prior to analysis and that this results in K-Ar ages that are older than if no fractionation took place. Souther et al. (1984), noting a correlation of anomalously old ages with high atmospheric Ar suggested that isotopic fractionation of atmospheric Ar had produced the old ages.

In order to investigate the effects of isotopic fractionation in M-1077 and to attempt to determine if excess argon is present in this sample, $^{40}Ar-^{39}Ar$ analysis was undertaken. Table 2 and Figure 4 present the results of the age spectrum analysis of M-1077. Table 2 shows that this analysis also reflects a high atmospheric Ar component (77%), only slightly lower than the conventional analysis (81%, Table 1) but that it is concentrated in the initial heating steps. Calculations show that 90% of the atmospheric Ar in the analysis is released in the first three heating steps and that the remaining atmospheric Ar is of an amount similar to that in sample M-263. Previously a similar pattern was demonstrated in basalts containing devitrified glass (Roddick, 1978).

The age spectrum (Fig. 4) has significant variation in the ages of the steps. The initial 30% of ^{39}Ar released has an age of about 22 to 21 Ma and then a plateau is defined at 19.5 Ma for up to 77% of ^{39}Ar released. The remaining gas defines a U-shaped pattern with a minimum age of 18 Ma and then rises to a maximum of 66 Ma.

The possible effects of isotopic fractionation of atmospheric Ar may be reflected in the first 30% gas release. The ages are 1.5 Ma older than the subsequent plateau and are consistent with the fractionation of atmospheric Ar as

originally proposed by Baksi (1974). The effects are minor in this sample because the amount of radiogenic Ar is a significant proportion (≈25%) of the total Ar. If the sample had a small fraction of radiogenic Ar (2-3%) and were only 1 or 2 Ma old, as some samples were in the study of Souther et al. (1984), the increase of 1.5 Ma would almost double the age of a conventional K-Ar analysis. Since this large amount of atmospheric Ar, associated with alteration, is degassed in the first three steps, the effects of isotopic fractionation are considered to not affect subsequent gas release. The excellent agreement with the conventional K-Ar age also indicates that, if present, the effects of isotopic fractionation are minor in the conventional analysis.

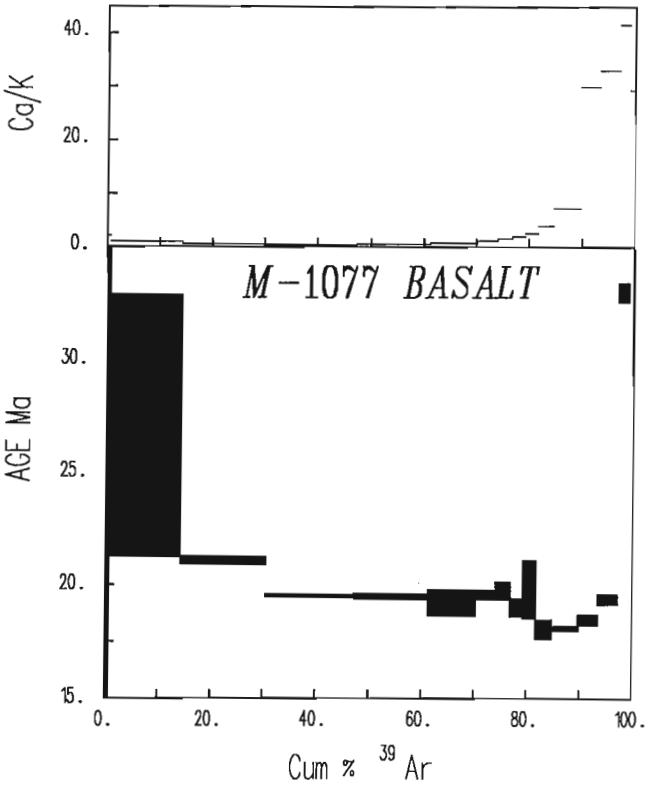

Figure 4. $^{40}Ar/^{39}Ar$ spectrum plot and Ca/K variation of data from basalt sample M-1077, Fortymile locality. The Ca was determined from neutron derived ^{37}Ar.

A small amount of excess Ar is present in the high-temperature release of this sample with apparent ages of 62 Ma. This excess correlates with release from Ca-rich sites in the sample, presumably pyroxene (Fig. 4). It is unclear if there is any excess Ar present in the rest of the gas fractions between 30 and 80% gas release, but the well defined plateau suggests that it is minor or that it must be proportional to the radiogenic Ar in the sample. Only the small trough at 85% gas release suggests that there may be an excess component that is minimized in the release at this temperature. Thus the present interpretation is that the correct age of this sample may be represented by the plateau at 19.5 Ma. This age is only slightly younger than the conventional K-Ar age and is in better agreement with the age of the other sample.

CONCLUSIONS

Two basalt samples from southwestern Dawson map area in western Yukon Territory yield ages of 17 to 20 Ma. These ages are much older than expected and their significance is unclear. Three different explanations are possible: 1) extrusion of alkali olivine basalt in southern and western Yukon and eastern Alaska occurred over a period of at least 20 Ma; 2) the basalts dated in this study represent an older and unrelated volcanic event; or 3) the samples analysed contained enough excess ^{40}Ar to produce ages that are considerably

Table 2. Argon step heating data for Dawson map area sample.

TEMP. (°C)	$^{36}Ar_{tr}$	$^{37}Ar_{Ca}$ (X 10^{-9} cm^3 STP)[a]	$^{38}Ar_{Cl}$	$^{39}Ar_K$	^{40}Ar	% Atmos. ^{40}Ar	Apparent age Ma	$\pm 2\sigma$[b]	^{39}Ar (%)
BASALT M-1077 (497.86 mg)									
450	1.145	0.058	0.012	0.052	343.80	98.4	39.7	205.8	0.6
600	3.611	0.630	0.108	1.218	1155.06	92.4	27.1	5.8	13.7
650	0.524	0.457	0.056	1.445	236.13	65.6	21.1	0.2	16.3
700	0.173	0.336	0.044	1.477	127.92	39.9	19.5	0.1	16.6
750	0.105	0.365	0.031	1.241	95.62	32.5	19.5	0.1	14.0
800	0.067	0.333	0.015	0.800	60.86	32.6	19.2	0.6	9.0
850	0.032	0.215	0.012	0.342	27.41	34.7	19.6	0.2	3.9
900	0.021	0.207	0.013	0.245	19.07	32.4	19.7	0.4	2.8
950	0.011	0.229	0.013	0.216	14.30	23.5	19.0	0.4	2.4
1000	0.006	0.295	0.016	0.217	13.20	13.1	19.8	1.3	2.4
1050	0.007	0.536	0.024	0.258	14.39	13.8	18.0	0.4	2.9
1100	0.024	1.699	0.044	0.448	28.69	24.6	18.1	0.1	5.1
1150	0.009	5.034	0.049	0.323	18.46	13.7	18.5	0.2	3.6
1200	0.012	5.735	0.055	0.334	20.78	16.9	19.4	0.2	3.8
1300	0.016	3.582	0.027	0.165	19.44	24.8	33.0	0.4	1.9
1400	0.030	1.131	0.013	0.074	21.45	41.9	62.2	2.4	0.8
1500	0.026	0.244	0.003	0.016	10.23	75.1	59.9	148.7	0.2
Total[c]	5.82	0.54	21.08	8.87	2226.8	77.2	21.4	1.5	
Conc.(/g)	11.7	42.35	1.08	17.82	4472.8				

[a] All gas quantities have been corrected for decay, isotopes derived from minor interfering neutron reactions, and blanks. $_{tr}$ denotes trapped Ar and Ca, Cl and K denote Ar derived from these elements. ^{40}Ar denotes trapped plus radiogenic Ar. Atmos. ^{40}Ar assumes a trapped Ar component of atmospheric composition.

[b] Errors from steps are analytical only and do not include the error in the irradiation parameter J.

[c] Includes the integrated age. The uncertainty in J (0.5%) is included in the error.

older than the true emplacement age. The first two possibilities cannot be tested as yet because of the very limited age data base for Upper Tertiary and Quaternary volcanic rocks in this region. The third possibility appears unlikely in view of 1) the similarity in ages obtained from widely separated localities; 2) the apparent absence of crustal contamination as indicated by measured Pb isotope compositions for the basalts; and 3) the apparently well defined plateau observed in a $^{40}Ar-^{39}Ar$ age spectrum.

Further examination and sampling of young basalt occurrences in western Yukon for petrological and geochronological study will be carried out during the 1989 field season.

ACKNOWLEDGMENTS

We thank H.L. Foster, L.E. Jackson, C. Hickson, and M.L. Bevier for useful discussions. The paper benefitted from critical reviews by M.L. Bevier and R. Parrish.

REFERENCES

Baksi, A.K.
1974: Isotopic fractionation of a loosely held atmospheric argon component in the Picture Gorge basalts; Earth and Planetary Science Letters, v. 21, p. 431-438.

Bostock, H.S.
1936: Carmacks District, Yukon; Geological Survey of Canada, Memoir 189, 67p.

Downes, H.
1985: Evidence for magma heterogeneity in the White River Ash (Yukon Territory); Canadian Journal of Earth Sciences, v. 22, p. 929-934.

Eiche, G.E., Francis, D.M., and Ludden, J.N.
1987: Primary alkaline magmas associated with the Quaternary Alligator Lake volcanic complex, Yukon Territory, Canada; Contributions to Mineralogy and Petrology, v. 95, p. 191-201.

Foster, H.L.
1976: Geologic map of the Eagle quadrangle, Alaska; U.S. Geological Survey, Miscellaneous Geologic Investigations Map I-922.

1981: A minimum age for Prindle Volcano, Yukon-Tanana Upland; in The United States Geological Survey in Alaska: Accomplishments During 1979, eds. N.R.D. Albert and T. Hudson; U.S. Geological Survey, Circular 823-B, p. B37-B38.

Foster, H.L., Forbes, R.B., and Ragan, D.L.
1966: Granulite and peridotite inclusions from Prindle Volcano, Yukon-Tanana Upland, Alaska; U.S. Geological Survey, Professional Paper 550-B, p. B115-B119.

Foster, H.L., Keith, T.E.C. and Menzie, W.D.
1987: Geology of east-central Alaska; U.S. Geological Survey, Open-File Report 87-188.

Glasmacher, U.
1984: Geology, petrography and mineralization in the Sixty Mile River area, Yukon Territory, Canada (translated from German); unpublished diploma thesis, Technical University Aachen, Federal Republic of Germany.

Hickson, C.A.
Volcanic vent map, Canadian Cordillera compilation; in Volcanos of North America, ed. C.A. Wood; Cambridge University Press (in press).

Htoon, M.
1979: Geology of the Clinton Creek asbestos deposit, Yukon Territory; unpublished M.Sc. thesis, University of British Columbia, Vancouver.

Hughes, O.L., Rampton, V.N., and Rutter, N.W.
1972: Quaternary geology and geomorphology, southern and central Yukon; in 24th International Geological Congress, Guide Book A-11, p. 59.

Jackson, L.E., Jr.
1989: Pleistocene subglacial volcanism near Fort Selkirk, Yukon Territory; in Current Research, Part E, Geological Survey of Canada Paper 89-1E, p. 251-256.

Lerbekmo, J.F., Westgate, J.A., Smith, D.G.W., and Denton, G.H.
1975: New data on the character and history of the White River Ash volcanic eruption, Alaska; in Quaternary Studies, ed. R.P. Suggate and M.M. Cresswell; Royal Society of New Zealand, Wellington.

Mitchell, R.H.
1987: Mantle-derived xenoliths in Canada; in Mantle Xenoliths, ed. P.H. Nixon; John Wiley and Sons, New York.

Mortensen, J.K.
1988a: Geology of southwestern Dawson map area, Yukon Territory; in Current Research, Part E, Geological Survey of Canada Paper 88-1E, p. 73-78.

1988b: Geology, southwestern Dawson map area (scale 1:250,000); Geological Survey of Canada, Open File 1927.

Roddick, J.C.
1978: The application of isochron diagrams in $^{40}Ar-^{39}Ar$ dating: a discussion; Earth and Planetary Science Letters, v. 41, p. 233-244.

1988: The assessment of errors in $^{40}Ar/^{39}Ar$ dating; in Radiogenic Age and Isotopic Studies: Report 2, Geological Survey of Canda, Paper 88-2, p. 3-8.

1989: $^{40}Ar/^{39}Ar$ evidence for the age of the New Quebec Crater, northern Québec; in Radiogenic Age and Isotopic Studies: Report 3, Geological Survey of Canada, Paper 89-2 (p. 5).

Roddick, J.C. and Souther, J.G.
1987: Geochronology of Neogene volcanic rocks in the northern Garibaldi Belt, British Columbia; in Radiogenic Age and Isotopic Studies: Report 1, Geological Survey of Canada, Paper 87-2, p. 21-24.

Sinclair, P.D., Tempelman-Kluit, D.J., and Medaris, L.G. Jr.
1978: Lherzolite nodules from a Pleistocene cinder cone in central Yukon; Canadian Journal of Earth Sciences, v. 15, p. 220-226.

Souther, J.G., Armstrong, R.L., and Harakal, J.
1984: Chronology of the peralkaline, late Cenozoic Mount Edziza Volcanic Complex, northern British Columbia, Canada; Geological Society of America Bulletin, v. 95, p. 337-349.

Tempelman-Kluit, D.J.
1974: Carmacks map area; Geological Survey of Canada, Open File 200.

A U-Pb zircon-baddeleyite age for a differentiated mafic sill in the Ogilvie Mountains, west-central Yukon Territory

J.K. Mortensen[1] and R.I. Thompson[2]

Mortensen, J.K. and Thompson, R.I., A U-Pb zircon-baddeleyite age for a differentiated mafic sill in the Ogilvie Mountains, west-central Yukon Territory; in Radiogenic Age and Isotopic Studies: Report 3, Geological Survey of Canada, Paper 89-2, p. 23-28, 1990.

Abstract

Abundant gabbroic to dioritic sills occur within Mississippian and Jurassic strata of the North American Cordilleran miogeocline along a strike length of over 200 km in west-central Yukon Territory. These sills had previously been assigned an Early Cretaceous age. Zircon and baddeleyite recovered from a granophyric differentiate near the top of one sill in southern Ogilvie Mountains, however, yielded a U-Pb age of 232.2 +1.5/-1.2 Ma (latest Middle Triassic). The sills are clearly intrusive into Mississippian sedimentary units; however, if all sills are of Triassic age, contacts between the sills and Jurassic units must be entirely tectonic. Although the sills were intruded at shallow depths, sill emplacement does not appear to have affected the style of concomitant Triassic sedimentation. Evidence for Triassic magmatism elsewhere in the miogeocline of the Canadian Cordillera is extremely limited, and the tectonic significance of the sills in west-central Yukon remains enigmatic.

Résumé

Les auteurs ont découvert de nombreux filons-couches dont la nature varie de grabbroïque à dioritique à l'intérieur de couches du Mississippien et du Jurassique du miogéosynclinal de la Cordillère de l'Amérique du Nord, répartis sur une longueur suivant la direction de plus de 200 km dans le centre-ouest du Yukon. On avait auparavant fait remonter ces filons-couches au Crétacé inférieur. Toutefois, du zircon et de la baddéléyite provenant d'une roche granophyrique formée par différentiation magmatique et située près du sommet des filons-couches dans le sud des monts Ogilvie, ont donné un âge U-Pb de 232,2 + 1,5/− 1,2 Ma (partie supérieure du Trias moyen). Les filons-couches sont nettement intrusifs dans des unités sédimentaires du Mississippien; toutefois, si tous les filons-couches sont triasiques, leurs contacts avec des unités jurassiques doivent être de nature entièrement tectonique. Bien que les filons-couches se soient introduits à de faibles profondeurs, leur mise en place ne semble pas avoir perturbé le style de la sédimentation concommittante qui s'est produite au Trias. Les indices du magmatisme triasique, dans le miogéosynclinal de la Cordillère canadienne, sont extrêmement limités ailleurs, et l'importance tectonique des filons-couches du centre-ouest du Yukon reste énigmatique.

[1] Geological Survey of Canada, 601 Booth Street, Ottawa, Ontario K1A E8
[2] Geological Survey of Canada, 100 West Pender Street, Vancouver, B.C. V6B R8

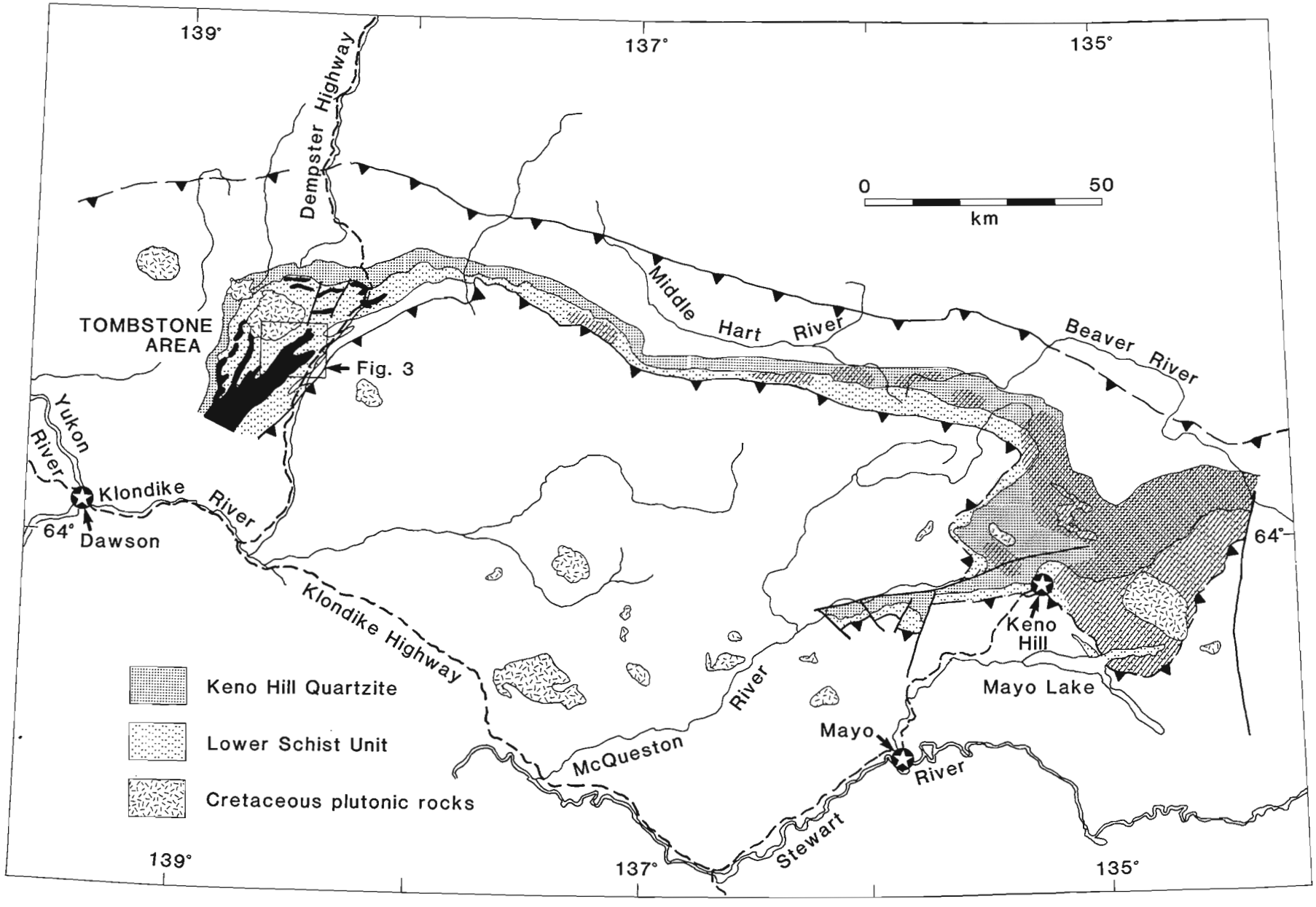

Figure 1. Distribution of Keno Hill Quartzite and Lower Schist Division in west-central Yukon (after Tempelman-Kluit, 1970). Mafic sill occurrences are shown in solid black where they have been mapped in detail in the Tombstone Range, and areas where isolated exposures of mafic sills are known to occur farther east are shown in hatchure.

INTRODUCTION

Thick mafic sills intrude Phanerozoic sedimentary strata of the North American Cordilleran miogeocline in a narrow band that extends from the Tombstone Range in eastern part of Dawson map area (116B, C) to the Keno Hill District in southern Nash Creek (106D) and northern Mayo (105M) map areas (Fig. 1), a strike length of over 200 km. In the Keno Hill District the sills form an important host to Ag-rich vein ores (Boyle, 1965; Lynch, 1986). The sills are associated with only two stratigraphic units, the Keno Hill Quartzite and the Lower Schist Division (Green, 1972). Whereas the Lower Schist Division is known to be of Jurassic age from macrofossil collections from several widely separated localities (Poulton and Tempelman-Kluit, 1982), the age of the Keno Hill Quartzite has been in dispute for many years. Tempelman-Kluit (1970; *see also* Poulton and Tempelman-Kluit, 1982) argued for an Early Cretaceous depositional age for this unit based on a presumed conformable contact with the underlying Lower Schist Division. Blusson (1978), on the other hand, suggested a probable late Paleozoic depositional age. This controversy was recently resolved when mid-Mississippian conodonts were recovered from a sample of Keno Hill Quartzite from the Ogilvie Mountains (M.J. Orchard, pers. comm., 1986). Contacts between Keno Hill Quartzite and the Lower Schist Division are now considered to be faults.

In view of the clearly intrusive relationships of the mafic sills into Keno Hill Quartzite, Tempelman-Kluit (1970) and Green (1972) assigned them an Early Cretaceous age.

Samples for U-Pb geochronology were collected from two mafic sills in the Tombstone Range in 1986. In this paper we report a U-Pb zircon-baddeleyite age for one of these samples, and discuss some of the implications of this age for the evolution of the North American continental margin.

REGIONAL SETTING

The Ogilvie Mountains in west-central Yukon Territory are underlain by a stratigraphic sequence ranging from mid-Proterozoic through Jurassic in age (Tempelman-Kluit, 1970; Green, 1972; R.I. Thompson and C.F. Roots, unpublished mapping). This sequence has been greatly foreshortened by northward-directed thrust faults, which produce multiple structural repetitions of individual lithological units. A composite stratigraphic section for mid-Paleozoic and younger units in the area is shown in Figure 2. In this area, mafic sills are observed intruding only the Keno Hill Quartzite. Farther east, in the Nash Creek and Mayo map areas, similar thrust complications exist, and the sills occur within both the Keno Hill Quartzite and Lower Schist Division (Green, 1972; Boyle, 1965).

The mafic sills range from less than 1 m to more than 240 m in thickness, and individual sills can be traced up to 40 km along strike. They are typically fine to coarse grained, equigranular, and dioritic to gabbroic in composition. Some thicker sills are weakly differentiated from base to top (Tempelman-Kluit, 1970). Quartz commonly occurs as an interstitial phase and comprises up to 15% by volume in the upper parts of some thick sill exposures. Narrow chill zones are developed along sill margins, and adjacent sedimentary wall rocks are strongly bleached and hornfelsed. Tempelman-Kluit (1970) estimated that the total volume of mafic sill material present in the Tombstone Range alone is in excess of 250 km^3.

Although generally massive and unfoliated, the sills have been folded and faulted together with the enclosing strata.

SAMPLE SELECTION AND PROCESSING

Samples weighing approximately 25 kg were collected from two sites near the tops of two separate sill exposures (Fig. 3). In each case the samples consisted of coarse-grained hornblende-clinopyroxene gabbro containing 4-5% interstitial quartz. Heavy mineral concentrates were prepared using standard Wilfley table and heavy-liquid techniques, and zircon and baddeleyite were further concentrated by magnetic separation. Final mineral fractions for isotopic analysis were selected based on magnetic susceptibility and grain size, morphology, and clarity. Techniques for sample dissolution, U and Pb separation, mass spectrometry and data reduction are described by Parrish et al. (1987). Errors for Pb-U and Pb-Pb ages of individual analyses, and for calculated concordia intercept ages, are given at the 2σ level.

ANALYTICAL RESULTS

Only one of the two samples collected (sample TW-87-158, Fig. 3) yielded sufficient zircon and baddeleyite for dating. Zircon recovered from the rock ranges from euhedral, highly fractured grains with abundant mafic inclusions to clear, colourless, irregular grains and shards. Baddeleyite occurs as pale to dark brown and reddish brown, transparent cleavage fragments. A total of six fractions of zircon and one fraction of baddeleyite were analyzed. Analytical data are given in Table 1 and are plotted in Figure 3. Uranium concentrations in the zircons range from moderate to high, and the degree of discordance is generally proportional to uranium concentration.

The seven analyses fall on a discordia line with calculated upper and lower intercept ages of 232.5 +2.3/ -1.7 Ma and 40.3 +37.3/ -37.6 Ma, respectively. One analysis (fraction C) is relatively imprecise and falls slightly above this regression line. Omitting this analysis from the regression yields upper and lower intercept ages of 232.2 +1.5/ -1.2 Ma and 27.8 +28.7/ -28.8 Ma, with a MSWD = 0.77. The upper intercept age is interpreted to be the emplacement age for the sill, and the lower intercept age is considered to reflect mainly recent lead loss. The dated sill was therefore intruded in latest Middle Triassic time.

DISCUSSION

A late Middle Triassic crystallization age for mafic sills in the Tombstone Range is consistent with the Mississippian conodont age determined for Keno Hill Quartzite, which the sills intrude. It poses a problem farther east, however, where lithologically identical sills occur within both Keno Hill

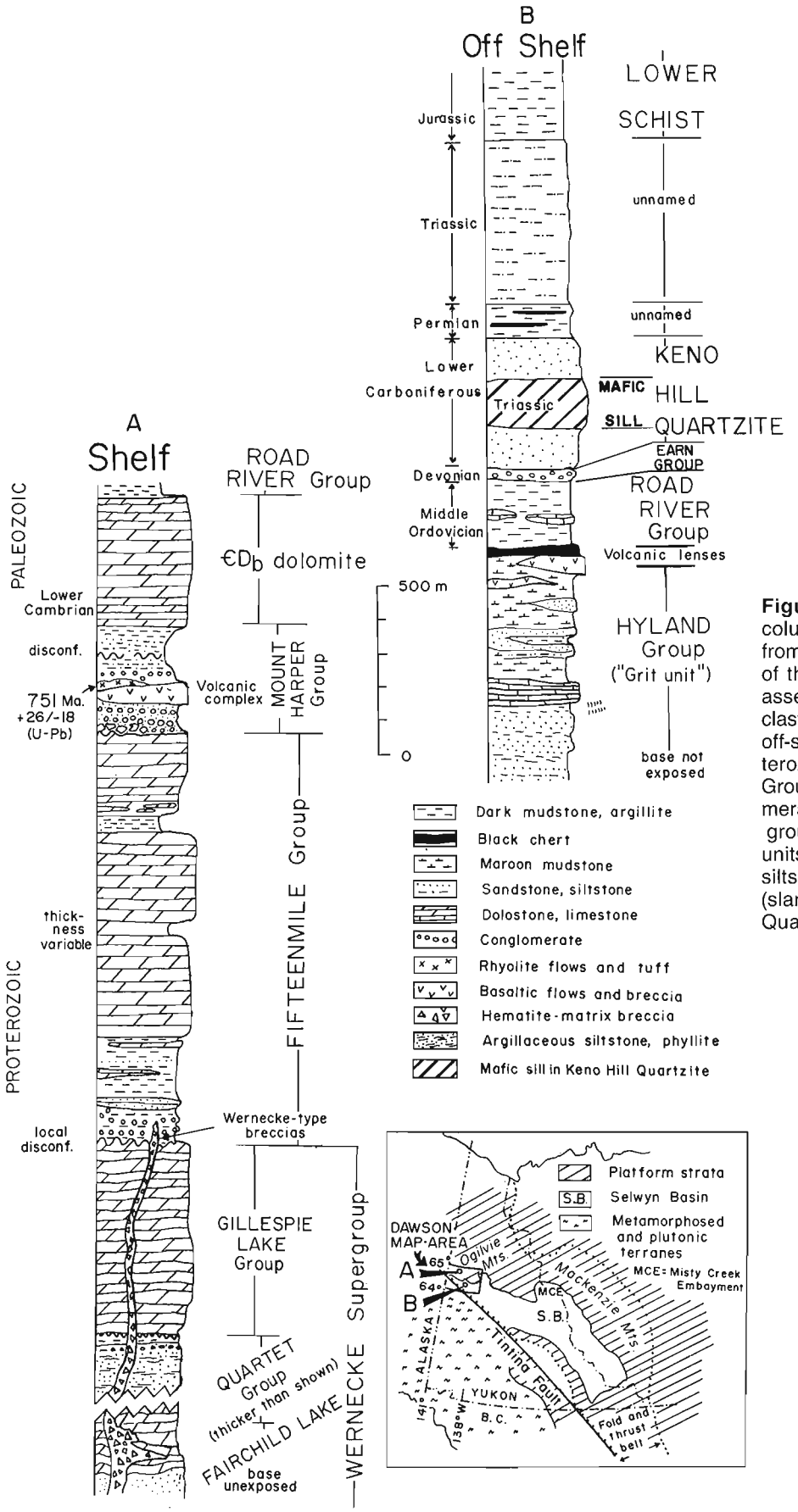

Figure 2. Generalized stratigraphic columns for Dawson map area (adapted from Roots and Thompson, in press), north of the Tintina Fault. Column A, the shelf assemblage, consists of Proterozoic shelf clastic and carbonate rocks. Column B, the off-shelf assemblage, consists of Late Proterozoic sandstone and shale (Hyland Group), Paleozoic shale, volcanics, conglomerate and quartzite (Road River and Earn groups; Keno Hill Quartzite and unnamed units), and unnamed Triassic and Jurassic siltstone and shale units. The mafic sill(s) (slanted line pattern) intrude the Keno Hill Quartzite in the Dawson map area.

Table 1. U-Pb zircon results.

Fraction,[1] Size	Weight (mg)	U (ppm)	Pb^{2} (ppm)	$^{206}Pb/^{204}Pb$[3]	Pb_c[4] (pg)	^{208}Pb[2] (%)	$^{206}Pb/^{238}U \pm$SEM%[5]	$^{207}Pb/^{235}U \pm$SEM%[5]	$^{207}Pb/^{206}Pb \pm$SEM%[5]	$^{207}Pb/^{206}$ age, error (Ma)[6]
Sample TW-87-158 (64 21.0'N; 138 29.8'W)										
A +149,M2,clr	0.316	1731	81.6	4313	275	54.4	0.03429 (.06)	0.23989 (.10)	0.05075 (.05)	229.3 (2.2)
B +149,M2,cldy	0.366	1675	77.6	2759	469	56.1	0.03337 (.07)	0.23341 (.11)	0.05078 (.06)	230.8 (2.6)
C +62-74,M2,clr	0.062	1645	77.9	973	224	59.6	0.03335 (.08)	0.23260 (.16)	0.05059 (.12)	222.2 (5.4)
E +74,N1,clr	0.110	217	8.4	5967	9	19.0	0.03616 (.12)	0.25337 (.13)	0.05082 (.08)	232.8 (3.5)
F +74,N1,clr,a	0.207	213	8.1	13200	8	17.4	0.03626 (.09)	0.25405 (.10)	0.05082 (.03)	232.2 (1.5)
G +74,M2,clr,a	0.061	1268	57.5	14800	12	40.4	0.03620 (.09)	0.25356 (.10)	0.05080 (.03)	231.7 (1.5)
H baddeleyite	0.033	418	13.9	1994	16	2.3	0.03593 (.09)	0.25150 (.12)	0.05077 (.07)	230.4 (3.1)

Notes: [1]sizes (-74+62) refer to length aspect of zircons in microns (i.e., through 74 micron sieve but not the 62 micron sieve); cl=clear; cldy=cloudy; NM1=non-magnetic cut with frantz at 1 degree side slope, Mag0=magnetic cut with frantz at 0 degree side slope; [2]radiogenic Pb; [3]measured ratio, corrected for spike and fractionation; [4]total common Pb in analysis corrected for fractionation and spike; [5]corrected for blank Pb and U, common Pb, errors quoted are one sigma in percent; [6]corrected for blank and common Pb, initial common Pb compositions are from Stacey and Kramers (1975), errors are two sigma in Ma; decay constants used are those of Steiger and Jäger (1977); for analytical details see Parrish et al. (1987).

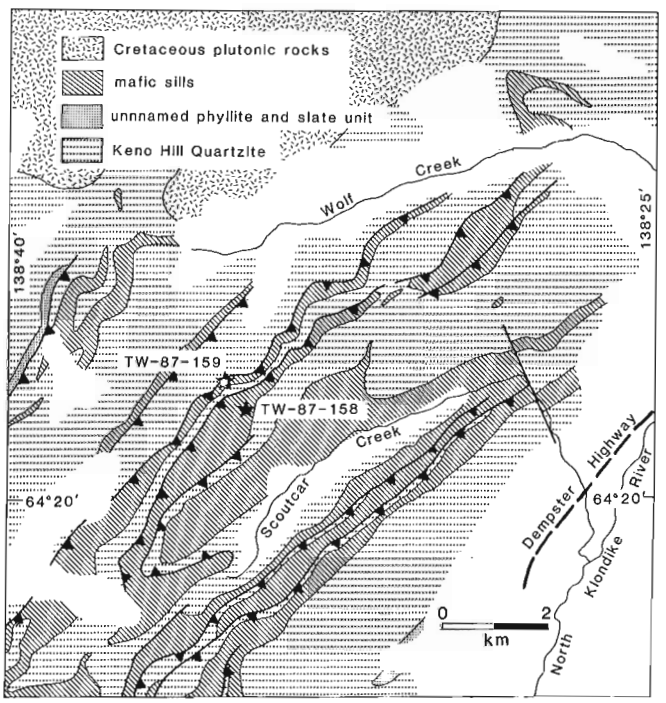

Figure 3. Detailed geological map of part of the southern Tombstone Range (modified from Tempelman-Kluit, 1970). Two localities sampled for U-Pb geochronology are shown as solid stars.

Quartzite and the Lower Schist Division, which has yielded a Jurassic fossil age. Three possible explanations exist: 1) mafic sills of more than one age are present; 2) the Lower Schist Division includes both fossiliferous Jurassic strata and older (pre-Middle Triassic) components; or 3) contacts between the sills and the Lower Schist Division are all faulted. Isotopic dating of other mafic sills is required to test the first possibility. Complex thrust imbrication has been documented in this area (J.G. Abbott, pers. comm., 1989), hence the third possiblity is presently favoured by the authors.

Triassic magmatism is well documented in accreted terranes outboard of the North American continental margin (Wheeler and McFeely, 1987; Woodsworth et al., in press), but is extremely rare within the miogeocline itself. Host strata for the mafic sills described here, however, can unquestionably be tied stratigraphically to cratonic North America. Only two other Triassic intrusions have been recognized within the miogeocline of the Canadian Cordillera. One is a small foliated granitoid intrusion that cuts Middle Kaza Group stratigraphy in east-central British Columbia, and yields a preliminary Early or Middle Triassic U-Pb zircon age (D.C. Murphy and R. Parrish, pers. comm., 1989). The other is the Cross kimberlite in the southern Rocky Mountains near Elkford, which has yielded Early Triassic Rb-Sr mica ages (Pell, 1987).

The volume and extent of the Triassic intrusive event in western Yukon, and the fact that virtually all of the magma was apparently emplaced as sills rather than dykes, may have important implications for the tectonic evolution of the continental margin in Triassic time. Feeder dykes for the sills have not been recognized. This is probably because, in the Ogilvie Mountains at least, the sills intruded only the relatively thin Keno Hill Quartzite, and the base of this unit is invariably a thrust fault; thus the sills have been decoupled from their feeder dyke systems, which now presumably lie in lower thrust units farther to the southwest. Intrusion as sills rather than dyke swarms reflects emplacement at very shallow depths, where deviatoric stresses favour flat-lying rather than dyke-like magma chambers. Observed thicknesses of the Upper Mississippian through Triassic section overlying the Keno Hill Quartzite (Fig. 2) confirms this, and suggests that the sills were likely emplaced at a depth no greater than 1-2 km. The overall regional stress regime during sill emplacement, therefore, cannot be constrained by their horizontal orientation. It is likely that the sills were fed by a dyke system at depth, which itself may have been intruded into extensional fractures.

More puzzling is the apparent absence of any significant perturbation in the style of sedimentation during sill emplacement. Triassic sediments in the Ogilvie Mountains comprise a condensed section of carbonaceous, wavy laminated siltstones, fine sandstones and limestone that thins to the north and is considered to represent a starved basin deposit. These units yield conodont ages spanning the entire Triassic Period (M.J. Orchard, pers. comm., 1987). Although the sedimentology of the Triassic strata has not been studied in detail, there is no evidence for a significant change in the nature or style of sedimentation, coincident with sill emplacement.

The Triassic sills in western Yukon, therefore, remain something of an enigma in the evolution of the continental margin. Further work is required on their field relationships and petrology in order to better understand the significance of this major magmatic event.

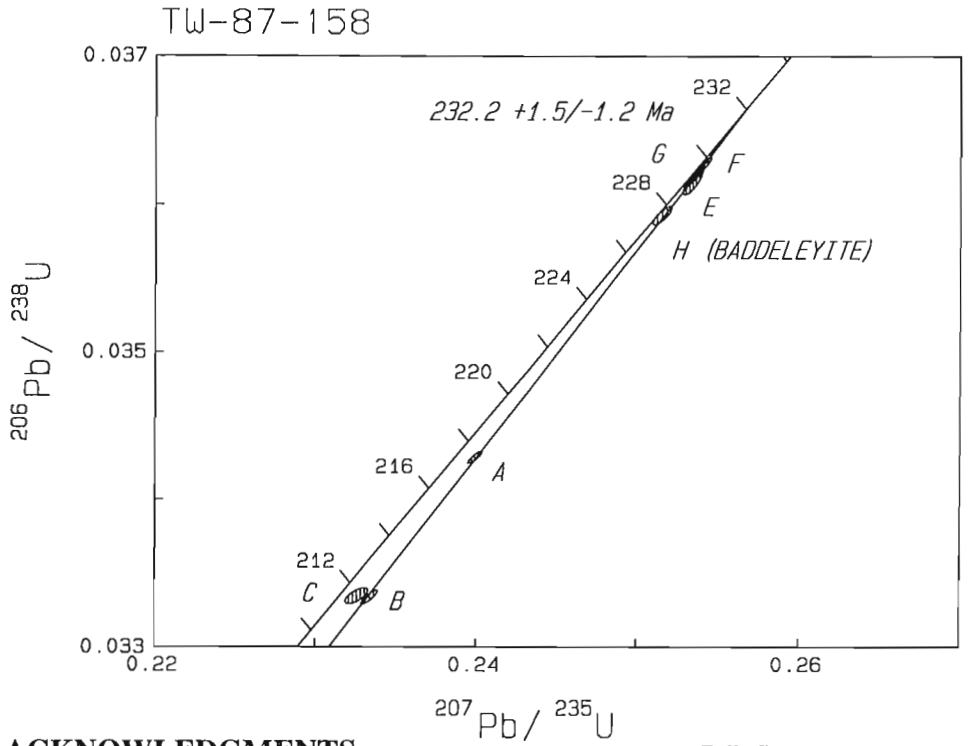

Figure 4. U-Pb concordia plot for sample TW-87-158. Fraction C is excluded from the regression.

ACKNOWLEDGMENTS

D.C. Murphy and R. Parrish are thanked for providing discussions and preliminary geochronological results. We gratefully acknowledge the assistance of the Geochronology Section staff for carrying out the analyses reported here.

REFERENCES

Blusson, S.L.
1978: Regional geologic setting of lead-zinc deposits in Selwyn Basin, Yukon; in Current Research, Part A, Geological Survey of Canada, Paper 78-1A, p. 77-80.

Boyle, R.W.
1965: Geology, geochemistry and origin of lead-zinc-silver deposits of the Keno Hill-Galena Hill area, Yukon Territory; Geological Survey of Canada, Bulletin 111, 302p.

Green, L.H.
1972: Geology of Nash Creek, Larsen Creek, and Dawson map-areas, Operation Ogilvie; Geological Survey of Canada, Memoir 364, 157p.

Lynch, G.
1986: Mineral zoning in the Keno Hill silver-lead mining district, Yukon; in Yukon Geology, v. 1, Exploration and Geological Services Division, Yukon; Indian and Northern Affairs Canada, p. 89-97.

Parrish, R., Roddick, J.C., Loveridge, W.D., and Sullivan, R.W.
1987: Uranium-lead analytical techniques at the geochronology Laboratory, Geological Survey of Canada; in Radiogenic Age and Isotopic Studies, Report 1, Geological Survey of Canada, Paper 87-2, p. 3-7.

Pell, J.
1987: Alkaline ultrabasic rocks in British Columbia; British Columbia Ministry of Energy, Mines and Petroleum Resources, Open File 1987-7, 109p.

Poulton, T.P. and Tempelman-Kluit, D.J.
1982: Recent discoveries of Jurassic fossils in the Lower Schist Division of central Yukon; in Current Research, Part C, Geological Survey of Canada Paper 82-1C, p. 91-94.

Roots, C.F. and Thompson, R.I.
Long-lived basement weak zones and their role in extensional magmatism in the Ogilvie Mountains; in Proceedings Volume for the Eighth International Conference on Basement Tectonics, ed. M.J. Bartholomew (in press).

Stacey, J.S. and Kramers, J.D.
1975: Approximation of terrestrial lead isotope evolution by a two-stage model; Earth and Planetary Science Letters, v. 26, p. 207-221.

Steiger, R.H. and Jäger, E.
1977: Subcommission on Geochronology: Convention on the use of decay constants in geochronology and Cosmochronology; Earth and Planetary Science Letters, v. 36, p. 359-362.

Tempelman-Kluit, D.J.
1970: Stratigraphy and structure of the «Keno Hill Quartzite» in Tombstone River-Upper Klondike River map areas; Geological Survey of Canada, Bulletin 180, 102p.

Wheeler, J.O. and McFeely, P.
1987: Tectonic assemblage map of the Canadian Cordillera and adjacent parts of the United States of America; Geological Survey of Canada, Open File 1565.

Woodsworth, G.J., Anderson, R.G. and Armstrong, R.L.
in press Plutonic regimes; in Cordilleran Orogen. ed. H. Gabrielse and C.J. Yorath; (Geology of Canada, No. 4). Geological Survey of Canada.

U-Pb zircon and monazite ages from plutonic rocks in the Contwoyto-Nose lakes map area, central Slave Province, District of Mackenzie, Northwest Territories

O. van Breemen[1], J.E. King[1], and W.J. Davis[2]

van Breemen, O., King, J.E., and Davis, W.J., U-Pb zircon and monazite ages from plutonic rocks in the Contwoyto-Nose lakes map area, central Slave Province, District of Mackenzie, Northwest Territories; in Radiogenic Age and Isotopic Studies: Report 3, Geological Survey of Canada, Paper 89-2, p. 29-37, 1990

Abstract

U-Pb zircon and monazite ages are reported for samples from five of six groups of plutonic rocks in the map area. A synvolcanic quartz porphyry (C2) has yielded a U-Pb zircon age of 2660.4 +0.9/-0.5 Ma, whereas a biotite tonalite (C3) that predates D2 has yielded an age of 2649 ± 2 Ma. About 40 Ma separates this earlier plutonic phase from syn-D2 (C4) diorite and tonalite units dated at 2608.0 ± 1.0 Ma and 2608 +5/-3 Ma. A leucotonalite of the C5 group is of similar age. Four syn-D3 (C6) two-mica granites and monzogranites have yielded a cluster of ages close to 2583 Ma.

Résumé

On donne les âges obtenus par la méthode U-Pb appliquée au zircon et à la monazite pour des échantillons de cinq des six groupes de roches plutoniques de la région cartographiée. L'âge obtenu par la méthode U-Pb appliquée au zircon d'un porphyre à quartz synvolcanique (C2) est de 2660,4 + 0,9 − 0,5 Ma alors que celui d'une tonalite à biotite (C3) antérieure à D2 a donné un âge de 2649 +/− 2 Ma. Environ 40 Ma séparent cette première phase plutonique des unités de diorite et de tonalite contemporaines à D2 (C4) pour lesquelles on a obtenu des âges de 2608 ± 1 Ma et de 2608 + 5/− 3 Ma. Une leucotonalite du groupe C5 a un âge similaire. Quatre échantillons de granites à deux micas et de monzogranites contemporains à D3 (C6) ont donné une série d'âges proches de 2583 Ma.

INTRODUCTION

This study reports ages from nine plutonic units in the western Contwoyto Lake area of the central Slave Province, District of Mackenzie, Northwest Territories (Fig. 1). Precise ages on the plutonic units are important not only to date individual ages of crystallization, but also to 1) evaluate the time span and possible diachroneity of each of the groups; 2) to bracket or date the time of sedimentation and deformation events; and 3) to integrate the tectonic evolution of the Contwoyto Lake area with that of the Slave Province in general. The study is part of ongoing geochronological research investigating plutonic rocks in the Slave Province by van Breemen (van Breemen et al., 1987; Henderson et al., 1987; van Breemen and Henderson, 1988). In the Contwoyto Lake area, the geochronological research is closely intergrated with 1:100 000 scale mapping of the Contwoyto Lake map sheet (NTS 76E) by J.E. King and coworkers (King et al., 1988, 1989), a project partly funded by the Canada-NWT MDA agreement (Project C1.1.1). U-Pb ages of volcanic units from the region are reported by Mortensen et al. (1988).

1 Geological Survey of Canada, 601 Booth Street, Ottawa, Ontario K1A 0E8
2 184 University Ave., St. John's, Newfoundland, A1B 1Z7
Department of Earth Sciences, Memorial University of Newfoundland, St. John's Newfoundland, A1B 3X5

GENERAL GEOLOGY

The western Contwoyto Lake area is underlain by turbidites of the Contwoyto and Itchen Formation, basaltic to felsic volcanic rocks of the Central Volcanic Belt, and numerous plutons of variable composition and age (Tremblay, 1976; Bostock, 1980; King et al., 1988,1989). The area has undergone high-T/low-P metamorphism and at least three phases of regional Archean deformation (D1-D3) (King et al., 1988, 1989; Relf, 1989). Iron formation in the turbidites of the Contwoyto Formation hosts the Lupin gold deposit (Bullis, 1988,; Kerswill, 1986), and the Central Volcanic Belt hosts the Condor massive sulphide (Zn-Ag-Pb-Cu) deposit (Bubar and Heslop, 1985).

Plutonic rocks in the area have been subdivided into six groups on the basis of cross-cutting relations, modal composition, relative strain state, and geochemistry (King et al., 1988, 1989; Davis and King, 1988; Davis, 1989). These groups are identified by the nomenclature C1,C2,...C6, which denotes their geographic location ('C' for Contwoyto) and their interpreted age of emplacement. Relative time relations are based on field observations as reported in King et al. (1988, 1989). The salient features of each of the groups are as follows.

C1- Synvolcanic

Strongly metamorphosed gabbro bodies within the Central Volcanic belt.

Table 1. U-Pb zircon and monazite data.

Fraction,[1] Size	Weight (mg)	U (ppm)	Pb^{2} (ppm)	$^{206}Pb/^{204}Pb$[3]	Pb_c[4] (pg)	$^{208}Pb/^{206}Pb$[2]	$^{206}Pb/^{238}U \pm$ SEM%[5]	$^{207}Pb/^{235}U \pm$ SEM%[5]	R	$^{207}Pb/^{206}Pb$ age, error[6] (Ma)[6]		SEM%
1. Quartz-porphyritic granodiorite (KGA-D221-87)												
a, -74+62	0.009	109.6	65.02	1284	26	0.174	0.50853 (.16)	12.682 (.17)	0.97	2660.8	(1.3)	0.038
b, -62+44	0.014	220.8	131.2	1757	56	0.178	0.50792 (.10)	12.665 (.12)	0.94	2660.6	(1.4)	0.042
c, -62+44	0.014	190.5	113.4	3052	28	0.177	0.50914 (.093)	12.689 (.11)	0.96	2659.8	(1.0)	0.031
d, -62+44	0.021	136.4	81.84	10140	9	0.181	0.51171 (.090)	12.759 (.10)	0.96	2660.6	(0.9)	0.028
2A. Olga biotite tonalite, melanocratic (KGA-D72b-87, D172-88)												
a, -74+62 NM3	0.029	109.6	59.97	1278	77	0.127	0.48669 (.089)	12.035 (.12)	0.87	2646.9	(2.0)	0.060
b, -74+62 NM3	0.021	190.2	99.85	3678	32	0.103	0.47599 (.086)	11.733 (.10)	0.95	2641.6	(1.1)	0.033
c, -62+44 NM3	0.008	76.60	44.07	1005	20	0.151	0.50233 (.20)	12.430 (.21)	0.98	2647.9	(1.5)	0.045
d, 74 NM3	0.007	104.7	59.74	904	26	0.134	0.50504 (.20)	12.502 (.20)	0.98	2648.6	(1.4)	0.041
2B. Olga biotite tonalite (KGA-D72a-87)												
a, +74	0.017	103.2	52.54	1773	28	0.141	0.44842 (.093)	11.048 (.11)	0.94	2640.7	(1.3)	0.039
b, +74	0.006	87.5	98.98	2187	15	0.136	0.46663 (.098)	11.519 (.11)	0.95	2643.9	(1.2)	0.035
3. Southern diorite (KGA-D218-87)												
a, +149 NM0	0.051	82.53	48.84	5707	23	0.243	0.48463 (.086)	11.695 (.098)	0.96	2606.3	(1.0)	0.029
b, -149+74 NM0	0.051	90.39	55.51	3207	45	0.261	0.49645 (.088)	11.992 (.10)	0.95	2607.9	(1.1)	0.033
c, -149+74 NM0	0.059	95.64	59.01	2266	79	0.266	0.49702 (.10)	12.003 (.12)	0.94	2607.5	(1.4)	0.041
4. Chunky tonalite (D110-88)												
a, +74 NM0	0.012	130.07	75.17	4175	12	0.178	0.49608 (.096)	11.971 (.11)	0.96	2606.1	(1.1)	0.032
b, +74 NM0	0.011	242.4	133.8	5683	14	0.134	0.49047 (.087)	11.813 (.099)	0.96	2603.1	(0.9)	0.029
c, +74 NM0	0.003	408.4	222.3	3148	12	0.164	0.47345 (.10)	11.249 (.11)	0.96	2580.3	(1.1)	0.033
d, -74+62 NM0	0.009	96.80	56.24	2097	12	0.189	0.49496 (.13)	11.927 (.14)	0.97	2603.8	(1.1)	0.034
5. Siege leucotonalite (KGA-D217-87)												
a, -149+74 NM2	0.009	158.0	81.35	1350	32	0.063	0.48313 (.10)	11.720 (.12)	0.92	2614.9	(1.7)	0.050
b, -149+74 NM2	0.012	85.97	48.41	5203	6	0.130	0.50035 (.11)	12.259 (.12)	0.97	2631.5	(1.0)	0.030
c, -149+74 NM2	0.106	179.4	93.46	3785	15	0.109	0.47146 (.21)	11.419 (.21)	0.99	2612.4	(1.0)	0.030
d, -149+44 NM2	0.012	93.37	51.12	2961	16	0.098	0.49950 (.11)	12.150 (.12)	0.96	2619.5	(1.1)	0.034
e, -74+44 NM2	0.014	132.0	70.35	2594	22	0.074	0.49568 (.095)	12.026 (.11)	0.95	2615.2	(1.2)	0.035
6. Biotite-muscovite monzogranite (KGA-D216-87)												
a, monazite	0.007	5598	14070	1792	62	4.806	0.48555 (.089)	11.485 (.10)	0.97	2572.9	(0.9)	0.028
b, monazite	0.004	3451	9473	8836	51	5.303	0.48961 (.094)	11.601 (.11)	0.97	2575.8	(1.0)	0.028
c, monazite	0.002	2185	14080	3233	32	13.85	0.49476 (.14)	11.770 (.15)	0.98	2582.4	(1.1)	0.032
d, monazite	0.002	5560	16120	8724	42	5.584	0.49544 (.090)	11.758 (.10)	0.96	2578.4	(1.0)	0.028
7. Pegmatitic granite dyke (KGA-K308)												
a, monazite	0.005	15099	11040	11560	19	0.551	0.49206 (.10)	11.712 (.11)	0.97	2583.3	(0.9)	0.028
b, monazite	0.006	25418	18790	24820	20	0.593	0.48567 (.11)	11.522 (.12)	0.98	2577.9	(0.9)	0.028
c, monazite	0.002	16331	11840	13950	65	0.543	0.49016 (.084)	11.647 (.096)	0.96	2580.5	(0.9)	0.028
d, monazite	0.003	7018	4549	12020	50	0.339	0.49723 (.084)	11.928 (.096)	0.96	2596.3	(0.9)	0.028
8. Biotite-muscovite monzogranite (KGA-K193)												
a, monazite	0.003	3284	3414	12550	24	1.268	0.49301 (.089)	11.782 (.098)	0.96	2590.0	(0.9)	0.028
b, monazite	0.004	3294	2931	17700	20	0.918	0.49284 (.084)	11.771 (.096)	0.96	2589.1	(0.9)	0.028
c, monazite	0.005	5234	4333	14940	49	0.791	0.48886 (.083)	11.607 (.096)	0.96	2579.2	(0.9)	0.028
9. Wolverine monzogranite (KGA-D78-88)												
a, monazite	0.002	1645	10310	3966	23	13.52	0.49211 (.094)	11.722 (.106)	0.96	2584.6	(1.1)	0.032
b, monazite	0.001	1789	12250	2306	24	14.84	0.49306 (.115)	11.722 (.106)	0.97	2581.3	(1.1)	0.034
c, monazite	0.002	2523	5912	6840	24	4.326	0.49219 (.090)	11.698 (.102)	0.96	2580.9	(1.0)	0.029
d, monazite	0.001	6978	12980	2209	93	3.441	0.46592 (.085)	11.022 (.104)	0.92	2573.1	(1.4)	0.042

Notes: [1] fraction sizes are in microns; samples are zircon unless indicated otherwise, NM1=non-magnetic cut with frantz at 1 degree side slope; [2] radiogenic Pb; [3] measured ratio, corrected for spike and fractionation; [4] total common Pb in analysis corrected for fractionation and spike; [5] corrected for blank Pb and U, common Pb, errors quoted are one sigma in percent; R, correlation of isotope ratio errors; [6] corrected for blank and common Pb, errors are two sigma in Ma; [7] error for corresponding isotope ratio at 1 sigma.

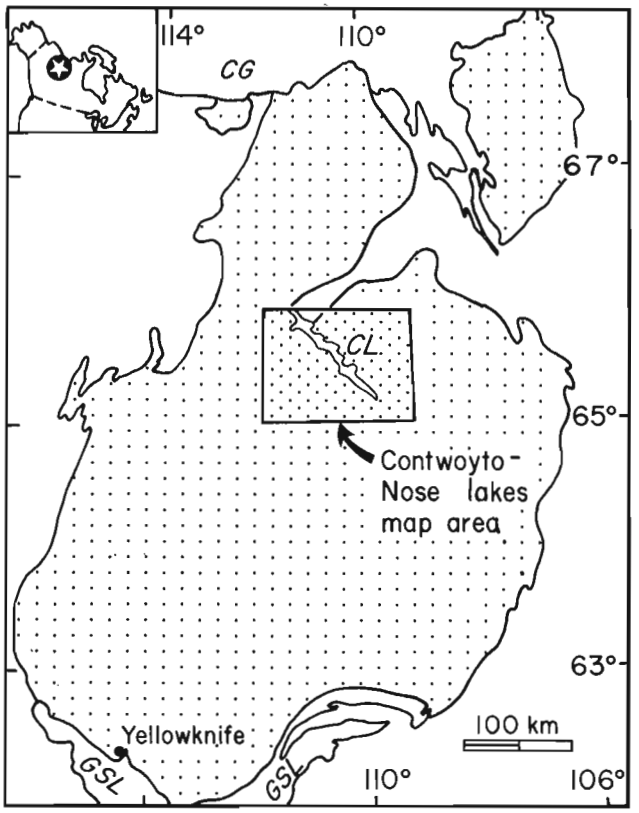

Figure 1. Sketch map showing Contwoyto-Nose lakes map area within the Slave Province (stippled).

C2- Synvolcanic

Quartz-porphyritic biotite granodiorite that forms veins and irregular plutons within the Central Volcanic Belt.

C3- Predates D2 (relationship to D1 not known; predates C4 diorites and tonalites and was probably broadly coeval with volcanics of the Central volcanic belt.)
Composite body (Olga tonalite) of biotite quartz diorite to tonalite that forms numerous texturally and mineralogically distinct tabular intrusive units.

C4- Syn D2

Medium-grained biotite-hornblende gabbro to quartz diorite and biotite tonalite to granodiorite with accessory magnetite.

C5- Late D2

Fine- to medium-grained biotite leucotonalite to granodiorite with accessory apatite, magnetite, and muscovite. Contains abundant xenoliths of host rocks and is ubiquitously intruded by leucocratic veins.

C6b- Pre- to post D3

Fine- to very coarse-grained biotite-muscovite granodiorite to syenogranite with accessory apatite, tourmaline, and magnetite. It is intimately associated with pegmatites and contains abundant xenoliths of host rocks.

C6b- Pre- to post D3 (relative time relationship between C6a and C6b not known from field relations).
Medium grained, commonly K-feldspar porphyritic granodiorite to syenogranite with accessory biotite and muscovite.

GEOCHRONOLOGY

Analytical techniques for U-Pb zircon and monazite analyses have been described in Parrish et al. (1987), who also described a modified form of the regression analysis technique of York (1969). In this method, the degree of fit is indicated by the mean square of weighted deviates (MSWD), which if greater than 2.5 is taken to indicate that there is significant geological scatter beyond analytical uncertainty. For the more concordant data sets, the regression techniques of Davis (1982) are used. In this case a probability of fit less than 10% indicates significant geological scatter. References to York (1969) and Davis (1982) are indicated by "Y" and "D". Isotopic data are presented in Table 1 and displayed in isotope ratio plots Figures 2, 3 and 4. Treatment of analytical errors has been described by Roddick (1987). Uncertainties for ages are quoted at the 2 sigma level. Zircons have been strongly and monazites lightly abraded (Krogh, 1982).

The samples collected are described below (field numbers are as indicated in Table 1).

C2 – quartz porpyritic granodiorite (sample 1; KGA-D221-87; 65° 34′N, 111° 47′W)

Zircons in this sample of porphyritic granodiorite are not abundant and are small (< 74 microns). Crystals are clear, euhedral, and simple prismatic (with square cross sections) and have length (L) to breadth (B) ratios of approximately 2:1. Continuous euhedral zoning is seen in some, and there is no evidence of cores. Cracks and inclusions are not abundant. Uranium concentrations range between 110 and 220 ppm. On a concordia diagram (Fig. 3) the data points are within 0.5% of the concordia. These data fit a chord (D) yielding an upper intercept age of 2660.4 +0.9/ -0.5 Ma and lower intercept of 50 Ma with a probability of fit of data points to the chord of 38%.

C3 – Olga biotite tonalite, melanocratic (sample 2A; KGA-D72b-87; 65° 27′30″N, 111° 46′W)

Zircons are not abundant and are generally clear to light brown. Zircons are prismatic with L:B of 2:1 to 5:1. Both (201) and (011) prism faces are prominently developed and facets on pyramids are multiple. Some round fluid inclusions are present and transverse cracks are common. No cores were recognized.

U concentrations range from 190 to 80 ppm. U-Pb data points are from 1 to 7% discordant. Regression analysis (D) yields an upper intercept age of 2649 ± 2 Ma and a lower intercept of about 220 Ma with a 7% probability of fit.

C3 – Olga biotite tonalite (sample 2B; KGA-D72a; 65° 27″30′N, 111° 46″W)

Zircons are scarce and generally fine grained. They are simple prisms with L:B of 2.1 to 5:1. The zircons are in general clear and colourless, although some, fluid inclusions and finer dark inclusions and fine cracks are present. Some grains that appear to have cores were avoided in the selection for analysis.

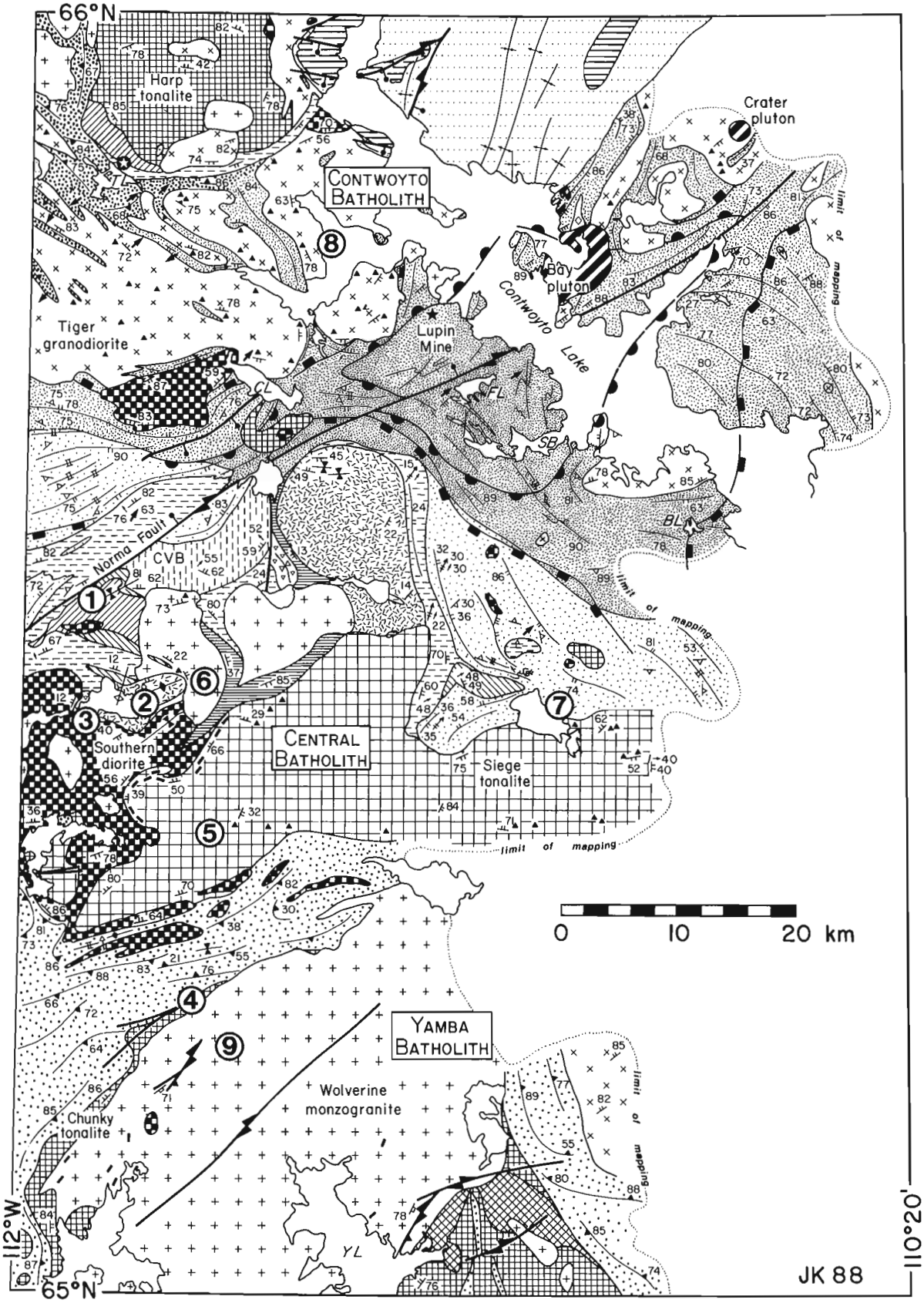
66°N
65°N
112°W
110°20'
Harp tonalite
Crater pluton
CONTWOYTO BATHOLITH
Bay pluton
Contwoyto Lake
Lupin Mine
Tiger granodiorite
Norma Fault
CVB
CENTRAL BATHOLITH
Southern diorite
Siege tonalite
YAMBA BATHOLITH
Wolverine monzogranite
Chunky tonalite
limit of mapping
CL
FL
SB
BL
YL
0 10 20 km
JK 88

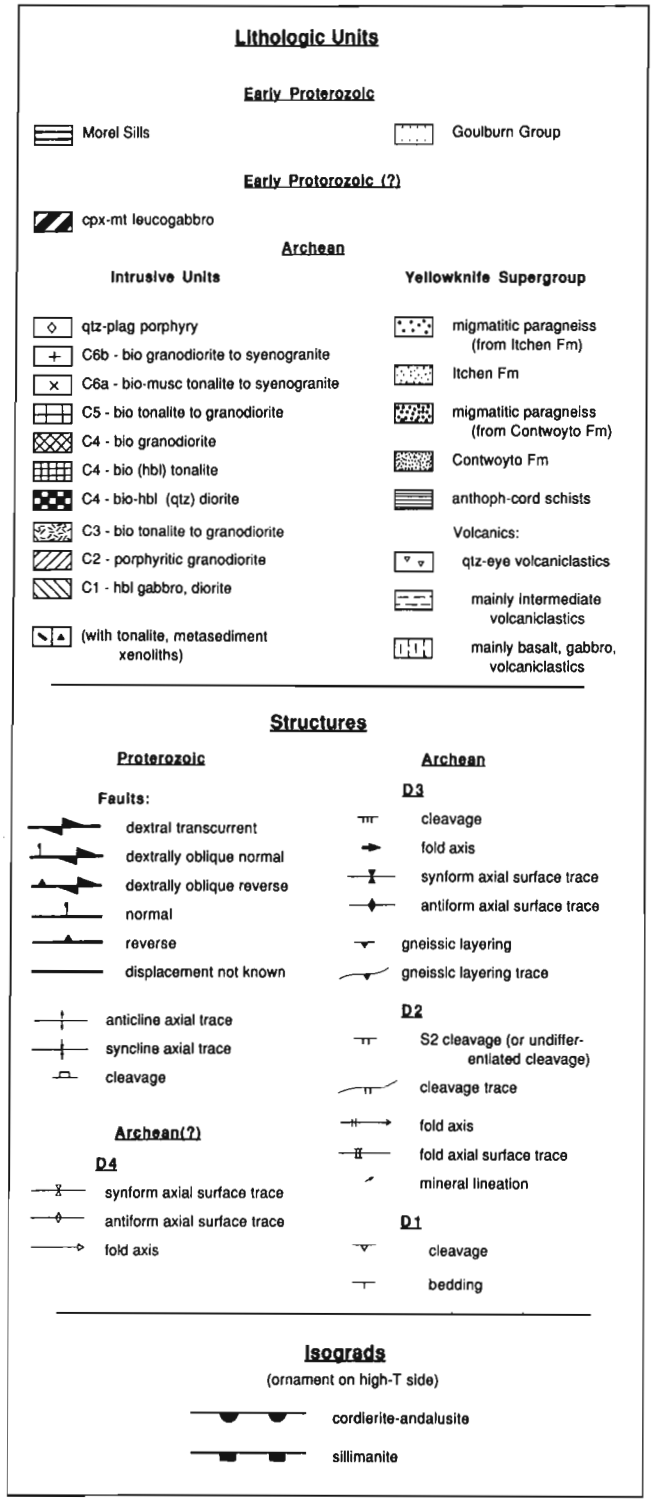

Figure 2. General geology of Contwoyto Lake and region to south of it. Sample locations are shown by large numbered red circles.

Only two fractions were of sufficient quality for analysis. Their discordance of 9 and 14% is remarkable in view of the low U content of 90-100 ppm. A line through these two points (Y) yields an upper intercept age of 2650 ± 5 Ma and a lower intercept of ca. 180 Ma. The age is identical to that of sample 2. However, the error on the upper intercept age is purely analytical and does not include a possible component of data-point scatter beyond that of analytical error.

C4 – Southern diorite (sample 3; KGA-D218-87; 65° 27′N, 111° 53′W)

Zircons range from fine to coarse and from equidimensional to simple prismatic, L:B of 4:1. Crystals are clear and light brown. There are some fluid inclusions, few cracks, and no observable cores. In polished and etched sections internal zoning is seen to be commonly discordant, especially near the outer margins, which imparts a rounded appearance to many crystals. Such features suggest changing interference to zircon growth during crystallization of a magma (van Breemen and Hanmer, 1986).

U concentrations are low, ca. 90 ppm, and range from virtually concordant to 3% discordant. Regression analysis (D) yields an upper intercept age of 2608.0 ± 1.0 Ma and a lower intercept of ca. 150 Ma with a 62% probability of fit.

C4 – Chunky tonalite (sample 4; KGA-D110-88; 65° 13′44″N, 111° 40′38″W)

Zircons are subhedral prismatic with L:B ratios of 2:1 to 6:1. Terminations are generally rounded. The colour is clear to light brown. Many grains have inclusions and cracks, but evidence for cores is rare.

U concentrations range from ca. 100 ppm to 400 ppm. Data points range from one to 8% discordant. Regression analysis for all four data points (D) yields a line with an upper intercept age of 2608 +5/ -3 Ma, a lower intercept age of 950 Ma and a probability of fit of 43%. The upper intercept age is interpreted as the time of intrusion.

C5 – Siege leucotonalite (sample 5; KGA-D217-87; 65° 22′N, 111° 40′W)

Zircons range from equidimensional crystals to prisms with L:B ratios of 2:1 to 4:1. Prism cross sections are mostly square. Crystals are generally colourless and clear with some fluid and some fine dark inclusions. Some crystals contain cores. Cracks occur most commonly in the fraction of flat crystals (5c). In such flat crystals, cores can be more easily recognized and avoided. Cores could also be avoided in fractions 5a and 5e, which consisted of prisms (L:B < 2) with regular zoning parallel to the prism faces clearly visible in transmitted light. Fraction 5b consisted of stubby crystals (L:B < 2) without clearly visible zoning in which cores would be more difficult to recognize. Fraction 5d consisted of both stubby and prismatic types.

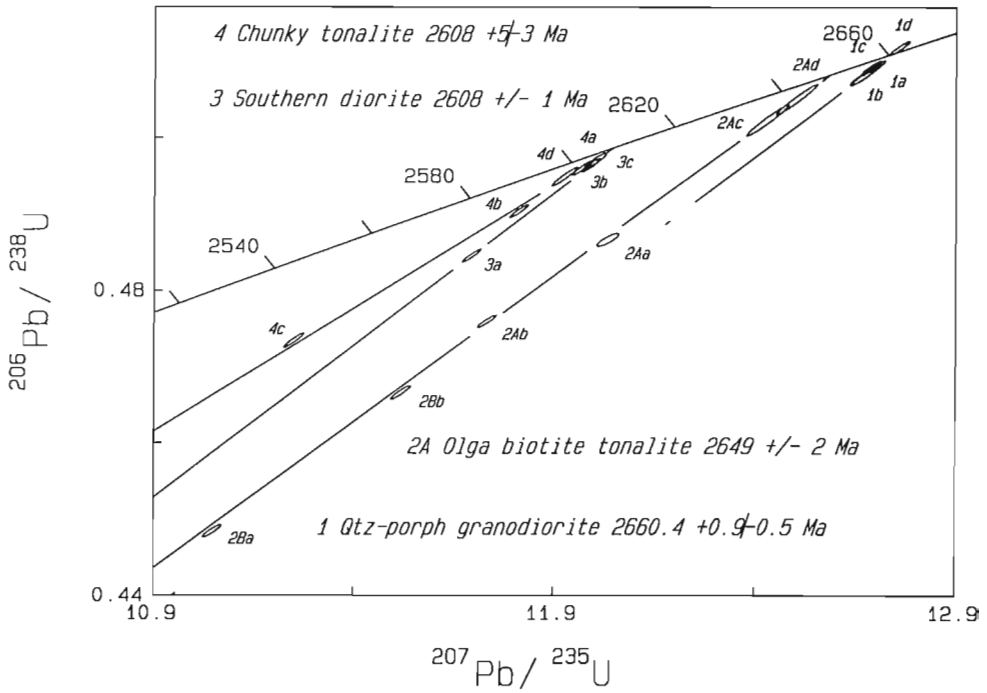

Figure 3. U-Pb isotope ratio plot showing zircon data points with error envelopes for samples 1, Synvolcanic porphyry (C2); 2A,B Olga plutonic suite (C3); 3, Southern diorite (C4); and 4, Chunky tonalite (C4). Note age gap between plutonic-rocks groups C3 and C4. Numbers and letters with data points correspond to those of Table 1.

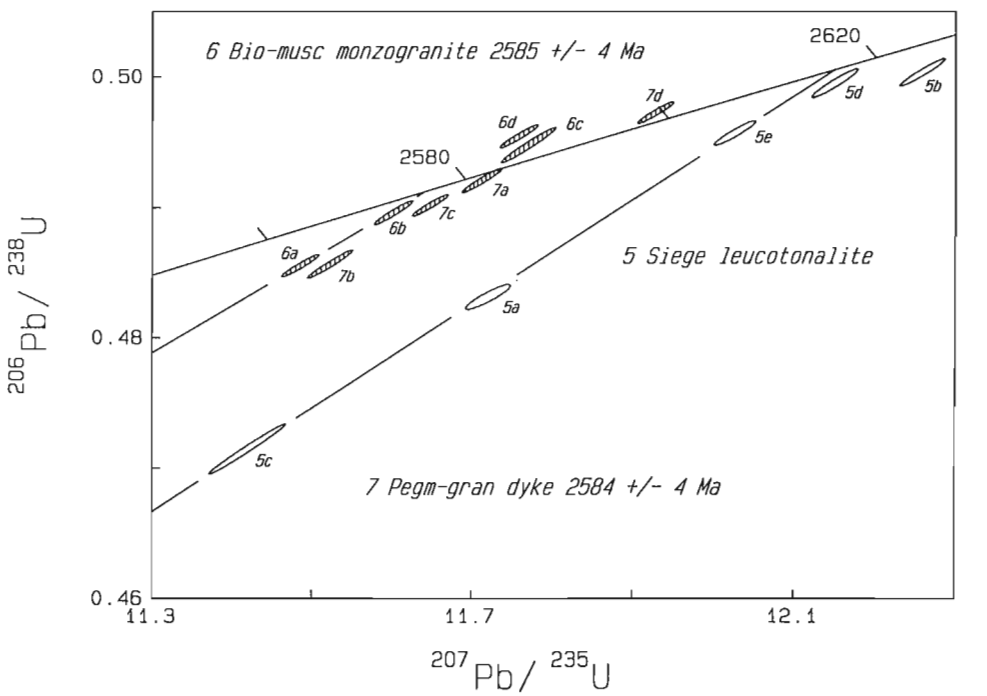

Figure 4. U-Pb isotope ratio plot showing zircon data points (closed error envelopes) for sample 5, the Siege leucotonalite (C5), and monazite data points (open error envelopes) for samples 6, biotite-muscovite monzogranite (C6), and 7, Pegmatite granitic dyke (C6). Regression line through samples 5a, 5c, and 5e has upper and lower intercepts at 2616 ± 2 Ma and 140 Ma. This upper intercept age may be too old owing to an inherited radiogenic Pb component as seen in samples 5b and 5d. Numbers and letters with data points correspond to those of Table 1.

Uranium concentrations range from 90 to 180 ppm. Data points vary from 0.5 to 7% discordant with the more discordant points corresponding to fractions higher in U. Points 5a, 5c, and 5e fit a chord with a probability of 21% with an upper intercept age of 2616 ± 2 Ma and a lower intercept of 137 Ma (Fig. 4). Low U fractions 5b and 5d consisting entirely or partly of stubby crystals correspond to ^{207}Pb – ^{206}Pb ages of 2632 Ma and 2620 Ma.

Field evidence (King et al., 1988) indicates that the Siege pluton cuts the Southern diorite and it should, therefore, yield an age younger than that diorite, which is dated at 2608 ± 1 Ma. The siege leucotonalite, however, contains an abundance of xenoliths of country rock. Older ^{207}Pb – ^{206}Pb ages for the nearly concordant fractions 5d and 5b are thus interpreted to reflect undetected cores. Although, in spite of the microscopic evidence, a small component of inherited radiogenic lead cannot be ruled out for fractions 5a, 5c, and 5e, such inheritance is likely to be small in view of the alignment of data points. One cannot, in fact, rule out the possibility that parts of the Siege leucotonalite crystallized before the Southern diorite. Finally it is considered unlikely that the Siege tonalite is more than several million years younger than the Southern diorite.

C6 – Biotite-muscovite monzogranite (sample 6; KGA-D216-87; 65° 28′30″N, 111° 40′W)

Zircons are translucent, strongly magnetic, and contain abundant cores. Only monazite was analyzed, i.e., four single grains. Data points 6b and 6a are normally discordant where 6d and 6c lie above the concordia with reverse discordances of 0.8% and 0.4%. Points 6a, 6b, and 6d fit a regression line (Y) with upper and lower intercept ages of 2576 Ma and 601 Ma and a MSWD of 1.08. This line is interpreted in terms of a lead loss line for isotopic systems that started above the concordia as a result of an excess of thorogenic ^{206}Pb (Scharer, 1984). According to this interpretation, the ^{207}Pb – ^{235}U age of the highest point, 6d, i.e., 2585 Ma, is slightly younger than the age of crystallization of the magmatic monazite. Fraction 6c has an older ^{207}Pb – ^{206}Pb age, even though it is more Th-rich than fraction 6d, which would suggest an inherited component of monazite in 6c (Copeland et al., 1988). The age of intrusion and uncertainties are assigned at 2585 ± 4 Ma.

C6 – Pegmatitic granite dyke (sample 7; KGA-K308; 65° 27′30″N, 111° W)

Zircons from this sample are metamict. Four single monazite grains were analyzed. Data points 7a, 7b, and 7c are concordant to slightly discordant and are close to a regression line (Y) with upper and lower intercept ages of 2583.5 Ma and 832 Ma and a MSWD of 3.4 (Fig. 4). Again it is possible that a Pb loss line was generated from points initially slightly above the concordia so that the age of intrusion was slightly older. The upper intercept age and uncertainty of 2584 ± 4 Ma is taken as the age of igneous crystallization. Sample 7d is slightly reverse discordant with a ^{207}Pb – ^{235}U age of 2599 ± 2 Ma; it may contain an inherited Pb component.

C6a – biotite-muscovite monzogranite (sample 8; KGA-K193-88; 65° 49′30″N, 111° 25′W)

Zircons are highly variable and of poor quality. Three single monazite grains were analyzed. Two data points 8a and 8b are almost concordant with an average ^{207}Pb – ^{206}Pb age of 2589.5 Ma, whereas a third point 8c is 0.7% discordant with a ^{207}Pb – ^{206}Pb age of 2579.2 Ma (Fig. 5). If a Pb loss line similar to that of sample 6 is taken (lower intercept of 600 Ma) and passed through point 8c, an upper intercept age of

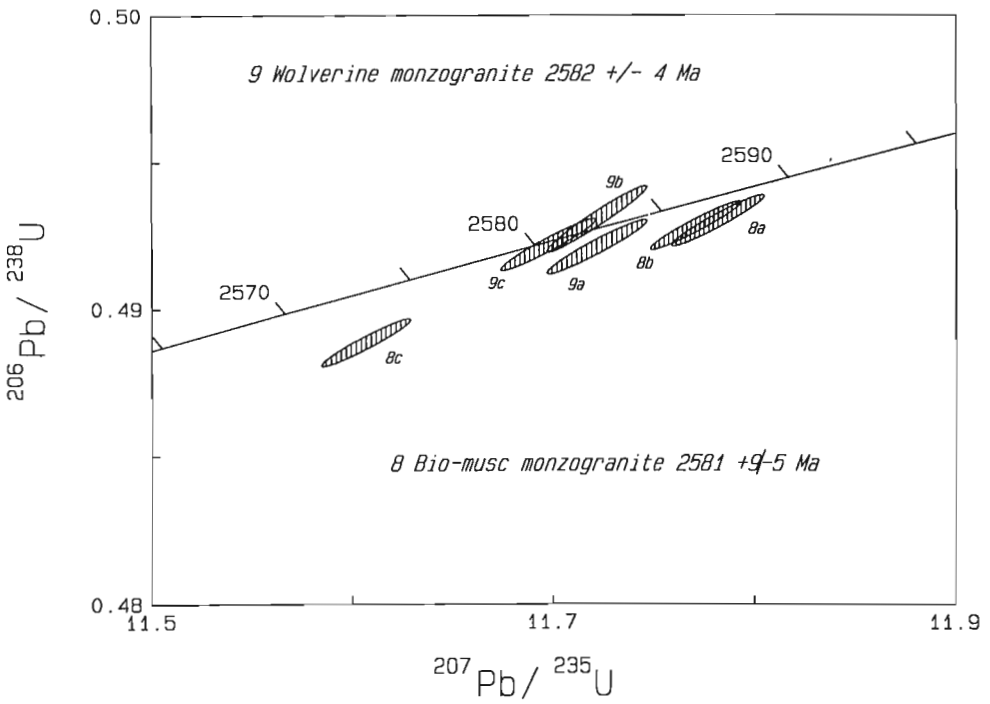

Figure 5. U-Pb isotope ratio plot showing zircon data points for samples 8, a biotite-muscovite monzogranite from the Contwoyto Batholith (C6), and 9, a monzogranite from the Wolverine plutonic suite, Yamba Batholith (C6). Numbers and letters with data points correspond to those of Table 1.

2581 Ma is obtained. As the original isotopic system may have started above the concordia and as we lack duplicate analyses, an inherited component cannot be ruled out. In view of this, we assign a larger uncertainty with the age at 2581 +/ 9-5 Ma. This sample requires more work.

C6 – Wolverine monzogranite (sample 9; KGA-D78-88; 65° 12′N, 111° 37′W)

Zircons are of poor quality. Three single monazite grains were analyzed. One, 9d, is strongly discordant and is not on the isotope ratio plot (Fig. 5). Three of the analyses yield concordant data points with similar ^{207}Pb – ^{206}Pb ages (Table 1) and overlapping ^{207}Pb – ^{235}U age uncertainties. The average of the former model Pb ages is 2582.3 Ma and of the latter 2581.8 Ma, from these we infer the age of granite emplacement at 2582 ± 4 Ma.

DISCUSSION

All of the lower intercepts for chords are less than 300 Ma from the origin and there is therefore no evidence for a Proterozoic lead loss effect. Upper intercept ages interpreted as ages of crystallization of zircon in a magma support the relative times of emplacement as determined in the field. The oldest plutonic ages, for the C2 porphyritic granodiorite, is 2660.4 +0.9/ -0.5 Ma. This age is slightly younger than the 2667.6 +3.0/ -1.6 Ma age (Mortensen et al., 1988) of an intermediate volcanic tuff in the Central Volcanic Belt with which it is spatially associated (King et al., 1988). The ca. 2649 ± 2 Ma age for the melanocratic phase of the Olga plutonic suite is 10-20 Ma younger than the Central Volcanic Belt and porphyry magmatism but is 40 Ma older than the next known age of magmatism, the C4 tonalite-diorite episode (see below). Like the volcanics and porphyry, the Olga plutonic suite is thought to have experienced both D1 and D2, whereas the C4 bodies are interpreted to have been emplaced syn-D2. The C3 Olga tonalite is therefore considered to be more closely related in tectonic context to the earlier, C1-C2 phases of magmatism than to the later, C4 phase.

The age of 2608 ± 1.0 Ma for the C4 Southern diorite and 2608 +5/ -3 Ma for the C4 Chunky tonalite provide ages for ongoing D2 regional deformation, although the time of initiation and absolute duration of D2 has not yet been established. A porphyritic sill at Concesssion Lake (see discussion in Mortensen et al., 1988), contains the D2 cleavage (S2) and has been dated at 2603.9 +0.9/ -0.8 Ma (Mortensen et al., 1988). This indicates a minimum time span of 3 Ma for the D2 event. The C5 Siege Tonalite has also been interpreted to be emplaced syn-D2. Although a precise crystallization age has not been determined, the constraints imposed by the radiometric data suggest emplacement was consistent with the timing of D2 indicated by the Southern diorite and Chunky tonalite.

Ages obtained for the final, C6 plutonic episode cluster at 2583 ± 5 Ma. These ages establish a time during the D3 phase of deformation associated with the C6 plutonic episode.

The ages reported in this paper suggest that there were two plutonic episodes in the Contwoyto Lake area. The first (2660-2650 Ma), including the C2-C3 groups, associated in time and space with volcanism in the Central Volcanic Belt. The second (2610-2580), including the C4-C6 groups comprises the bulk of the granitoids presently exposed in the area. Major element geochemistry of the C4 group of the second magmatic episode is similar to that of recent continental margin arc magmatism (Davis, 1989).

The present geochronologic data base from the Contwoyto Lake area allows preliminary comparison with data from elsewhere in the Slave Province. The lithology, structural setting, and close temporal relation (slightly younger) to volcanism of the Olga plutonic suite are similar to those of the Hackett River granodiorite, 140 km to the east of the present area, which has yielded a U-Pb zircon age of 2666 + 20/ -28 Ma (Frith and Loveridge, 1982). Given the large age uncertainties, these two bodies may be products of temporally related magmatism. The ages for the C4 magmatism are apparently younger than magmatism of similar composition in the Artillery Lake area dated at 2622 +1.4/ -1.2 Ma and 2717 ± 7 (van Breemen and Henderson, 1988). Circa 2.62 Ga ages have also been reported from the Yellowknife area, although in that case uncertainties were considerably greater (Henderson et al., 1988).

In the Contwoyto Lake map area, the ages obtained from the C6 bodies do not overlap with C4 to C5 plutonic ages. However, a temporal break is not likely in light of data for other late-tectonic, granites in the Slave Province. In addition to ca. 2685 Ma ages for two-mica granites reported from the Slave Province northeast of the Bathurst Fault (van Breemen et al.,1987), a two-mica granite in the Artillery Lake area to the southeast has yielded a U-Pb monazite age of 2606 ± 5 Ma and a large megacrystic granite, from the same area, an age of 2596 +3/ -6 Ma (van Breemen and Henderson, 1988). The presently available data are, therefore, compatible with a continuum of C4- to C6-type magmatism across the Slave Province. The data set is small, however, and more geochronological information, intergrated with careful mapping, is necessary to separate more detailed spatial-temporal relationships.

ACKNOWLEDGEMENTS

The manuscript has benefitted from critical reviews by J.B. Henderson and R.R. Parrish. We thank W.D. Loveridge, K. Santowski, J. MacRae, and J.C. Bisson for their contributions in generating the age determinations.

REFERENCES

Bostock, H.H.
1980: Geology of the Itchen Lake area, District of Mackenzie; Geological Survey of Canada, Memoir 391, 101 p.

Bubar, D.S. and Heslop, L.B.
1985: Geology of the Gondor volcanogenic massive sulphide deposit, Slave Province, N.W.T.; Canadian Insitute of Mining and Metallurgy Bulletin, v. 78, p. 52-60.

Bullis, H.R.
1988: Lupin mine – an update; gold deposit: an update; in Exploration Overview, Northwest Territories 1988; Geology Division, Indian and Northern Affairs Canada, Yellowknife, N.W.T., p. 27.

Copeland, P., Parrish, R.R., and Harrison, T.M.
1988: Identification of inherited radiogenic Pb in monazite and implications for U-Pb systematics; Nature, v. 333, p. 760-763.

Davis, D.
1982: Optimum linear regression and error estimation applies to U-Pb data; Canadian Journal of Earth Sciences, v. 19, p. 2141-2149.

Davis, W.J.
1989: Geochemistry of ca. 2.6 Ga calc-alkaline plutonism in the central Slave Province; Geological Association of Canada, Mineralogical Association of Canada, Program with Abstracts, v. 14, p. A24.

Davis, W.J. and King, J.E.
1988: Geochemical evolution of plutonism in the central Slave Province; Geological Association of Canada, Mineralogical Association of Canada, Program with Abstracts, v. 13, p. A30.

Frith, R.A. and Loveridge, W.D.
1982: Ages of Yellowknife Supergroup volcanic rocks, granitoid intrusive rocks and regional metamorphism in the northeastern Slave Structural Province; in Current Research Part A, Geological Survey of Canada, Paper 82-1A, p. 225-237.

Henderson, J.B., van Breemen, O., and Loveridge, W.D.
1987: Some U-Pb zircon ages from Archean basement, supracrustal and intrusive rocks, Yellowknife-Hearne Lake area, District of Mackenzie; in Radiogenic Age and Isotopic Studies: Report 1, Geological Survey of Canada, Paper 87-2, p. 111-121.

Hill, J.D. and Frith, R.A.
1982: Petrology of the Regan Intrusive Suite in the Nose Lake-Beechey Lake map area, District of Mackenzie, N.W.T.; Geological Survey of Canada, Paper 82-8, 26 p.

Kerswill, J.A.
1986: Gold deposits hosted by iron formation in the Contwoyto Lake area, Northwest Territories; in An international Symposium on Geology of Gold Deposits, Gold '86, ed. A.M. Chatter; Poster volume, Toronto, Ontario, p. 82-85.

King, J.E., Davis, W.J., Relf, C., and Avery, R.W.
1988: Deformation and plutonism in the western Contwoyto Lake map area, central Slave Province, District of Mackenzie, N.W.T.; in Current Research, Part C, Geological Survey of Canada, Paper 88-1C, p. 161-176.

King, J.E., Davis, W.J., van Nostrand, T., and Relf, C.
1989: Geology of the western Contwoyto Lake map area, central Slave Province, District of Mackenzie, N.W.T.: Archean to Proterozoic deformation and plutonism; in Current Research, Part C, Geological Survey of Canada, Paper 89-9C, p. 81-94.

Krogh, T.E.
1982: Improved accuracy of U-Pb ages by the creation of more concordant systems using an air abrasion technique; Geochimica et Cosmochimica Acta, v. 46, p. 637-649.

Mortensen, J.K., Thorpe, R.I., Padgham, W.A., King, J.E., and Davis, W.J.
1988: U-Pb zircon ages for felsic volcanism in Slave Province, N.W.T.; in Radiogenic and Isotopic Studies: Report 2, Geological Survey of Canada, Paper 88-2, p. 85-95.

Parrish, R.R., Roddick, J.C., Loveridge, W.D., and Sullivan, R.W.
1987: Uranium-lead analytical procedures at the geochronology laboratory, Geological Survey of Canada; in Radiogenic Age and Isotopic Studies: Report 1, Geological Survey of Canada, Paper 87-2, p. 3-7.

Relf, C.
1989: Archean deformation of the Contwoyto Formation metasediments, western Contwoyto Lake area, N.W.T.; in Current Research, Part C, Geological Survey of Canada, Paper 89-1C, p. 95-105.

Roddick, J.C.
1987: Generalized numerical error analysis with application to geochronology and thermodynamics; Geochimica et Cosmochimica Acta, v. 51, p. 2129-2135.

Schärer, U.
1984: The effect of initial ^{230}Th disequilibrium on young U-Pb ages: the Makalu case, Himalaya; Earth and Planetary Science Letters, v. 67, p.191-204.

Tremblay, L.P.
1976: Geology of northern Contwoyto Lake area, District of Mackenzie; Geological Survey of Canada, Memoir 381, p. 56.

van Breemen, O. and Hanmer, S.
1986: Zircon morphology and U-Pb geochronology in active shear zones: studies on syntectonic intrusions along the northwest boundary of the Central Metasedimentary Belt, Grenville Province, Ontario; in Current Research, Part B, Geological Survey of Canada, Paper 86-1B, p. 775-784.

van Breemen, O. and Henderson, D.B.
1988: U-Pb zircon and monazite ages from the eastern Slave Province and Thelon Tectonic Zone, Artillery Lake area, N.W.T.; in Radiogenic Age and Isotopic Studies: Report 2, Geological Survey of Canada, Paper 88-2, p. 73-83.

van Breemen, O., Henderson, J.B., Sullivan, R.W., and Thompson, P.H.
1987: U-Pb zircon and monazite ages from the eastern Slave Province, Healey Lake area, N.W.T.; in Radiogenic Age and Isotopic Studies: Report 1, Geological Survey of Canada, Paper 87-2, p. 101-110.

U-Pb ages of zircons from the Anton Complex, southern Slave Province, Northwest Territories

F. Ö. Dudás[1], J. B. Henderson[1] and J. K. Mortensen[1]

Dudás, F.Ö., Henderson, J.B., and Mortensen, J.K., U-Pb ages of zircons from the Anton Complex, southern Slave Province, Northwest Territories; in Radiogenic Age and Isotopic Studies: Report 3, Geological Survey of Canada, Paper 89-2, p. 39-44, 1990.

ABSTRACT

U-Pb analyses of zircon from two samples of the Anton Complex metatonalite indicate crystallization ages of approximately 2642 ± 15 Ma for each. The Anton Complex is therefore significantly younger than the Sleepy Dragon Complex, which is considered to be a basement unit. It is also younger than most of the volcanics in the Yellowknife Supergroup, indicating that the Anton Complex cannot be basement to the supracrustal sequence in the western part of Slave Province. The age of the Anton Complex overlaps, within uncertainty, with the age of the western granodiorite phase of the Defeat Plutonic Suite, and it is possible that the Anton Complex is a slightly older, more deformed member of the Defeat Suite.

Résumé

La méthode U-Pb appliquée aux zircons provenant de deux échantillons de la métatonalite du complexe d'Anton indique des âges de cristallisation d'environ 2642 ± 15 Ma pour chaque échantillon. Le complexe d'Anton est par conséquent beaucoup plus jeune que le complexe de Sleepy Dragon qu'on supposait être une unité du socle. Il est également plus jeune que la plupart des roches volcaniques du supergroupe de Yellowknife, indiquant qu'il ne peut donc pas constituer le socle de la séquence supracrustale de la partie ouest de la province des Esclaves. L'âge du complexe d'Anton une certaines incertitude, concorde, avec certaines limites d'incertitude, avec celui de la phase granodioritique occidentale de la série plutonique de Defeat, et il est possible que le complexe d'Anton soit un membre légèrement plus vieux et plus déformé de la série de Defeat.

INTRODUCTION

The southern part of the Slave Structural Province consists of four Archaean lithologic or litho-tectonic units: foliated granitoids and gneisses (the Anton and Sleepy Dragon complexes), granitoid intrusions, volcanic rocks (the Yellowknife, Cameron River and Beaulieu River greenstone belts), and sedimentary rocks. The predominantly basaltic volcanic and sedimentary rocks that make up the Yellowknife Supergroup have been interpreted as overlying basement represented by the Anton and Sleepy Dragon complexes. Continuing field mapping (Henderson, 1985; Helmstaedt and Padgham, 1986; Lambert, 1988; James, 1989) and geochronological studies (Henderson et al., 1987; Mortensen et al., 1988) have revealed an increasingly complex picture of the relationships between these units, and have made it possible to propose and to test regional tectonic models for the evolution of the Slave craton (McGlynn and Henderson, 1970; Henderson, 1985; Easton, 1985; Padgham, 1985; Helmstaedt et al., 1986; Hoffman, 1986; Fyson and Helmstaedt, 1988; Kusky, 1989). In this paper, we report U-Pb analyses of zircons from two samples of the Anton Complex and interpret the results in light of recent tectonic models for the Slave Province.

The Anton Complex (Henderson, 1985) is a 30 × 15 km body that lies north-northwest of Yellowknife (Fig. 1). Although it has not been mapped in detail, the Anton Complex is known to consist mainly of foliated granodioritic and granitic intrusions with some granitoid gneisses. The complex is older than the plutonic rocks adjacent to it (the western phase of the Defeat Plutonic Suite, the Awry Plutonic Suite, the Prosperous Granite, and the Duckfish Granite), although it has gradational contacts with the Awry, Defeat, and Prosperous granitoids (Henderson, 1985). There is no evidence that rocks of the Anton Complex intrude supracrustal rocks of the Yellowknife Supergroup.

1 Geological Survey of Canada, 601 Booth Street, Ottawa, Ontario K1A 0E8

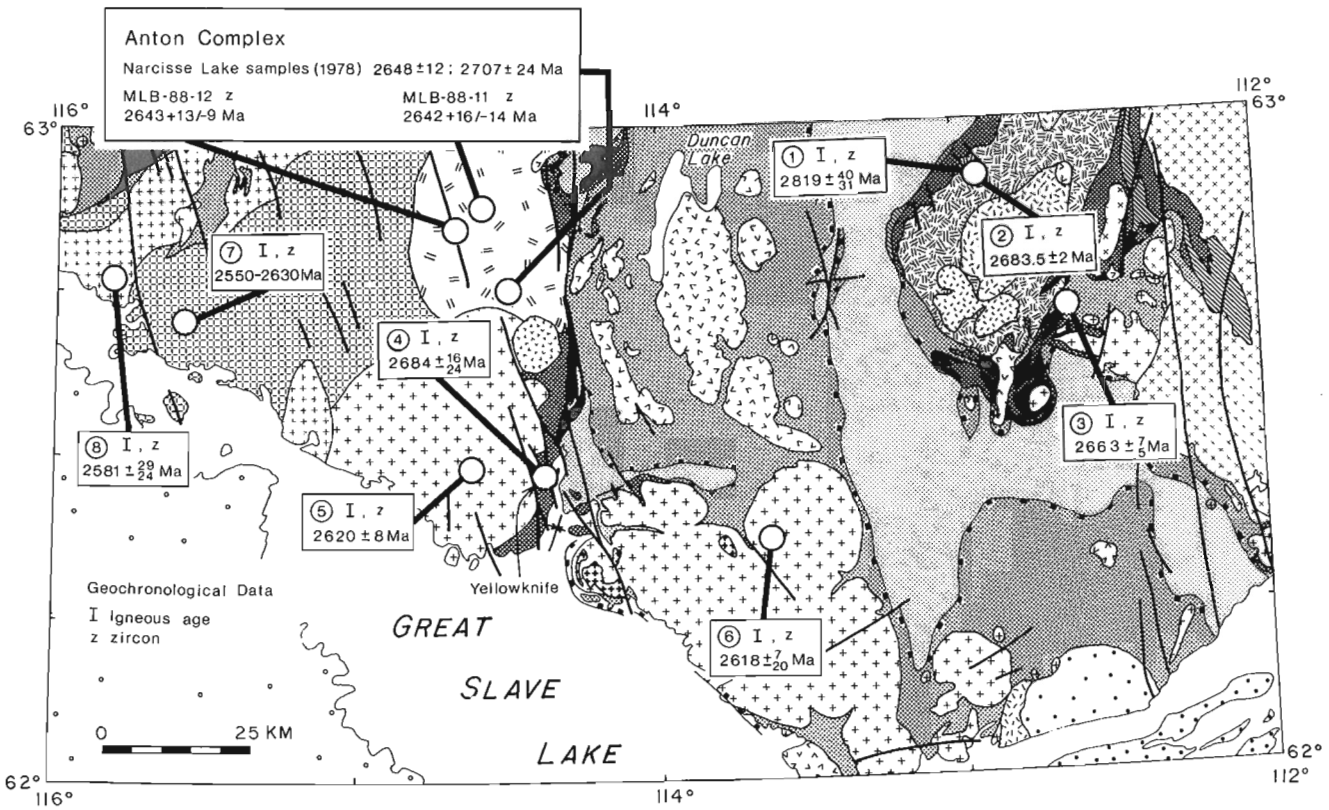

PALEOZOIC ROCKS.

PROTEROZOIC ROCKS.

DUCKFISH GRANITE: granite, massive, mafic-poor.

MOROSE GRANITE: granite, massive, biotite-muscovite.

REDOUT GRANITE: granite, biotite-muscovite.

PROSPEROUS GRANITE: granite, massive, biotite-muscovite.

MEANDER LAKE PLUTONIC SUITE: granite, granodiorite, undivided, massive, biotite, locally muscovite.

AWRY PLUTONIC SUITE: granite, granodiorite, undivided, massive to locally weakly foliated, biotite-poor.

STAGG PLUTONIC SUITE: granite, granodiorite, tonalite, undivided, massive to weakly layered or foliated, biotite, locally hornblende.

DEFEAT PLUTONIC SUITE: granodiorite, tonalite, granite, undivided, massive to weakly foliated, biotite, rarely hornblende.

WOOL BAY QUARTZ DIORITE: quartz diorite, diorite, massive to locally weakly layered, hornblende.

AMACHER GRANITE: granite, massive, biotite in aggregates.

YELLOWKNIFE SUPERGROUP:
Greywacke, siltstone, mudstone, interbedded, greenschist grade.
Schist, psammitic to pelitic, interlayered, amphibolite grade.

Felsic volcanic rocks, mainly dacitic to rhyolitic, includes massive, structureless domes to thick massive volcaniclastic units to thin bedded sediments, minor more mafic volcanic units locally present.

Andesitic pillow lavas, pillowed breccias, minor massive flows, volcaniclastic sediments.

Basalt, minor andesite, massive and pillowed flows, minor fragmental units, locally minor more felsic units, includes contemporaneous intrusions of gabbroic dykes, sills and irregular bodies.

ANTON COMPLEX: granodiorite, tonalite, granite, undivided, weakly to moderately foliated, may be in part older than Yellowknife Supergroup but also includes younger intrusive phases.

SLEEPY DRAGON COMPLEX: granodiorite, tonalite, granite, undivided, mylonitic gneisses to massive bodies, in part older than Yellowknife Supergroup, may include some post-Yellowknife intrusions.

Figure 1. Geologic sketch map of part of the southern Slave Province showing the location of samples collected from the Anton Complex and reported in this paper. In addition, the location of previously analyzed Anton Complex samples are also indicated. Locations 1 through 8 are previously reported geochronological data: 1 and 2 - Sleepy Dragon Complex; 3 and 4 - Yellowknife volcanics; 5 and 6 - Defeat Plutonic Suite; 7 - Awry Plutonic Suite; 8 - Stagg Plutonic Suite (Henderson et al., 1987).

The Anton Complex has been compared in its structural setting to the Sleepy Dragon Complex, a somewhat similar granitoid terrane to the east (Fig. 1) that has been shown on both geological and geochronological grounds to represent basement to the Yellowknife Supergroup (Henderson, 1985; Henderson et al., 1987). Because the Sleepy Dragon complex is somewhat similar to the Anton Complex in its geological setting and lithology, the Anton Complex may also represent basement to the Yellowknife Supergroup (Henderson, 1985).

In a recently proposed tectonic model, a large structural basement block in the western part of Slave Province was christened the "Anton Terrane" (Kusky, 1989). If the Anton Complex is to represent the "type location" for the "Anton Terrane," an accurate age determination for the Anton Complex is required. Kusky (1989) suggested that the "Anton Terrane" and the "Sleepy Dragon Terrane" are fragments of a once-contiguous pre-Yellowknife Supergroup cratonic block.

This model is testable, to some degree, by determining whether the two complexes are of similar age. Previous geochronologic studies (K-Ar and U-Pb on zircons) suggest that the Anton Complex is broadly contemporaneous with the adjacent Yellowknife greenstone belt. We initiated this study of the geochronology of the Anton Complex to address these concerns.

SAMPLE DESCRIPTIONS AND ANALYTICAL PROCEDURES

Two samples of metatonalite were collected from two of the more mafic and gneissic localities known in the complex (Fig. 1). They are quite similar given the known lithological variability of the Anton Complex. Both outcrop areas are fairly heterogeneous, everywhere foliated, locally discontinuously layered, and consist of dark, pinkish grey, medium-grained, weakly inequigranular metatonalite. The metatonalite in both areas is cut by a few dykes and veins of purple-pink leucocratic granite to pegmatite, presumably related to the lithologically similar Awry Plutonic Suite to the west (Fig. 1).

The two rocks analyzed are altered to varied degrees, but originally consisted of quartz-plagioclase-hornblende-biotite metatonalite with trace amounts of opaque minerals, zircon, and apatite. Sample MLB-88-12, the more mafic of the two rocks, contains about 30% mafic minerals; it is also the least altered, with plagioclase about 10 to 50% saussuritized and about half of the mafic minerals altered to chlorite. Sample MLB-88-11, on the other hand, contains only about 15% mafic minerals, but these have all been altered to chlorite. The plagioclase is between 50 and 70% saussuritized. Both samples have an annealed protomylonitic aspect with a moderate to strongly developed fabric, due primarily to the elongate quartz lenticles but also to the orientation of the mafic mineral aggregates and plagioclase porphyroclasts. Any original igneous textures have been obliterated during subsequent metamorphism and deformation, which was followed by a static retrograde event expressed by the pseudomorphing of the mafic minerals by chlorite and the saussuritization of plagioclase.

Approximately 30 kg of each sample were processed using standard Wilfley table and heavy liquid techniques. Zircon was the only mineral recovered that was datable by U-Pb analyses. Most of the zircons in both samples were strongly magnetic. Analytical techniques employed are as described by Parrish et al. (1987).

RESULTS

Sample MLB-88-11

Polished and etched grain mounts of zircon from this sample display well developed igneous zoning with no evidence for metamorphic overgrowths. Coarse zircon grains (>200 μm length; fractions A, B, and E on Table 1) were pinkish

Table 1. U-Pb zircon results.

Fraction,[1] Size	Weight (mg)	U (ppm)	Pb^2 (ppm)	$^{206}Pb/^{204}Pb$[3]	Pb_c[4] (pg)	^{208}Pb[2] (%)	$^{206}Pb/^{238}U$ ±SEM%[5]	$^{207}Pb/^{235}U$ ±SEM%[5]	$^{207}Pb/^{206}Pb$ ±SEM%[5]	$^{207}Pb/^{206}Pb$ age, error (Ma)[6]
Sample MLB-88-11										
A +200,N2,a	0.0108	191	105.2	2793	23	9.9	0.49004 (.09)	12.0415 (.11)	0.17882 (.04)	2636.3 (1.1)
B +250,N2,a	0.0150	385	199.1	11290	15	11.5	0.46638 (.08)	11.2154 (.10)	0.17441 (.03)	2600.4 (0.9)
C -150,N2	0.0101	662	297.9	11250	16	9.5	0.41391 (.09)	9.6894 (.10)	0.16978 (.03)	2555.5 (1.0)
D -150,N2,a	0.0074	491	238.5	893	115	11.1	0.43949 (.09)	10.5152 (.14)	0.17353 (.08)	2592.0 (2.8)
E +150,N2,a	0.0053	39.5	21.9	1012	7	10.3	0.50209 (.21)	12.2929 (.22)	0.17757 (.09)	2630.3 (3.0)
F -150,N2,a	0.0063	303	164.9	1836	32	14.6	0.47714 (.09)	11.6850 (.11)	0.17761 (.04)	2630.7 (1.5)
Sample MLB-88-12										
A +250,N1,a,s	0.0275	698	357.0	29870	20	4.9	0.48518 (.08)	11.8490 (.09)	0.17713 (.03)	2626.1 (0.9)
B +250,N1,a,s	0.0303	635	325.7	22500	26	5.2	0.48500 (.09)	11.8804 (.10)	0.17766 (.03)	2631.1 (0.9)
C +250,N1,a,s	0.0361	751	381.6	39590	21	4.4	0.48370 (.09)	11.8313 (.10)	0.17740 (.03)	2628.7 (0.9)
D -200,N1,a	0.0367	731	379.9	28590	29	7.7	0.48218 (.08)	11.6839 (.10)	0.17574 (.03)	2613.1 (0.9)
E -100,M5,a	0.0050	609	322.8	4566	20	15.1	0.46501 (.09)	11.2026 (.10)	0.17473 (.03)	2603.4 (1.0)
F +150,N1,a	0.0113	747	393.4	9737	27	7.3	0.49022 (.08)	11.9450 (.10)	0.17672 (.03)	2622.4 (0.9)
G +150,M1,a	0.0169	693	374.7	15490	24	7.9	0.50042 (.08)	12.2810 (.10)	0.17800 (.03)	2634.3 (0.9)
H +150,M1,a,s	0.0091	525	293.6	19200	8	11.5	0.50225 (.08)	12.3563 (.09)	0.17843 (.03)	2638.3 (0.9)

Notes: [1]sizes (+150) refer to sieve size of zircons in microns (i.e., through 200 micron sieve but not the 150 micron sieve);
a=abraded, s=single grain analysis, N1=non-magnetic cut with frantz at 1 degree side slope, M1=magnetic cut with frantz at 1 degree side slope; [2]radiogenic Pb; [3]measured ratio, corrected for spike and fractionation; [4]total common Pb in analysis corrected for fractionation and spike; [5]corrected for blank Pb and U, common Pb, errors quoted are one sigma in percent; [6]corrected for blank and common Pb, initial common Pb compositions are from Cumming and Richards (1975), errors are two sigma in Ma; decay constants used are those of Steiger and Jäger (1977); for analytical details see Parrish et al. (1987).

to reddish, rust-stained, and intensely fractured. The grains were mostly subhedral and broken prisms, with length-to-width ratios between 2 and 4. Although fractures and iron stains obscured much internal detail, several of these grains appeared to have rounded cores 50 - 150 μm in length. These grains were strongly abraded prior to analysis; the fractions analyzed averaged less than 50 μm in diameter, and included only colourless, fracture-free, non-magnetic grains. A finer zircon population (≤ 200 μm in length, averaging near 150 μm; fractions C, D and F on Table 1) consisted of clear, colourless to faintly pinkish, subhedral prisms with length-to-width ratios between 4 and 10 (averaging between 6 and 7). These grains showed no cores, few fractures, and few inclusions.

Six zircon analyses from this sample range from 0.4 to 15.1% discordant (Fig. 2), with the degree of discordance correlating closely with measured U-content (Table 1). The data form a roughly linear array, and a best-fit regression line through the data (MSWD = 188) yields upper and lower concordia intercept ages of 2642 +16/ -14 Ma and 844 Ma, respectively. One fraction (E) is nearly concordant, and yields a ^{207}Pb–^{206}Pb age of 2630 Ma. None of the grains analyzed contained visible cores, hence we interpret the data array mainly to reflect post-crystallization Pb-loss from a single igneous population. The ^{207}Pb–^{206}Pb age of the most concordant analysis (2630 Ma) should, therefore, be a minimum age for the sample. Fraction A is 3.0% discordant but yields a slightly older ^{207}Pb–^{206}Pb age (2636 Ma). It is uncertain whether this indicates the presence of an optically undetected, minor inherited zircon component in this fraction, or whether the scatter in the data is due to complex, multi-stage Pb-loss from the zircon population. If some or all of the zircon fractions contain inherited zircon, our age estimate may be slightly too old. We consider the calculated upper intercept age and associated error, however, to be a reasonable and conservative estimate of the crystallization age for the sample.

Sample MLB-88-12

Zircons in the least magnetic fraction of this sample were predominantly dark brown, anhedral, prismatic to equant fragments. Most grains were coarse (> 200 μm, some exceeding 500μm) and intensely fractured, with hydrous iron oxide coatings along the fractures. Several of these grains appeared to be aggregates of smaller zoned zircons cemented by complexly zoned igneous zircon. As in the previous sample, there is no evidence for metamorphic overgrowths on the grains. Even after severe abrasion to grain sizes below 100 μm, clear, unfractured zones within the zircons remained dark brown. Fractions A, B, C, and F of Table 1 represent this group of zircons. Smaller grains of the same population (fraction D of Table 1) were subhedral, rounded prism fragments, only 50% of which showed terminations. These dark brown zircons were also intensely fractured. Relatively fracture-free and colourless zircons (fraction E of Table 1) occurred only in the more magnetic zircon fractions. The colourless zircons were mostly subhedral, rounded prisms with length-to-width ratios exceeding 3, and were much smaller than the dark brown zircons that make up the bulk of the zircon concentrate. Fractions G and H of Table 1 were taken from an intermediate magnetic fraction, but have morphological features similar to fractions A, B, C, and F.

Eight zircon fractions, four of which were single crystals, range from 0.7 to 7.6% discordant (Fig. 3). A best-fit regression line through the data (MSWD = 138) yields upper and lower concordia intercept ages of 2641 +5/ -4 Ma and 862 Ma (Fig. 3), respectively. The most concordant fraction (H, 0.7% discordant), yields a ^{207}Pb–^{206}Pb age of 2638 Ma (Table 1). As with the previous sample, we consider the data to reflect post-crystallization Pb-loss in a single igneous zircon population. We therefore interpret 2638 Ma to be a minimum age for the sample, and the calculated upper intercept age to be the best estimate for original crystallization age of the gneiss.

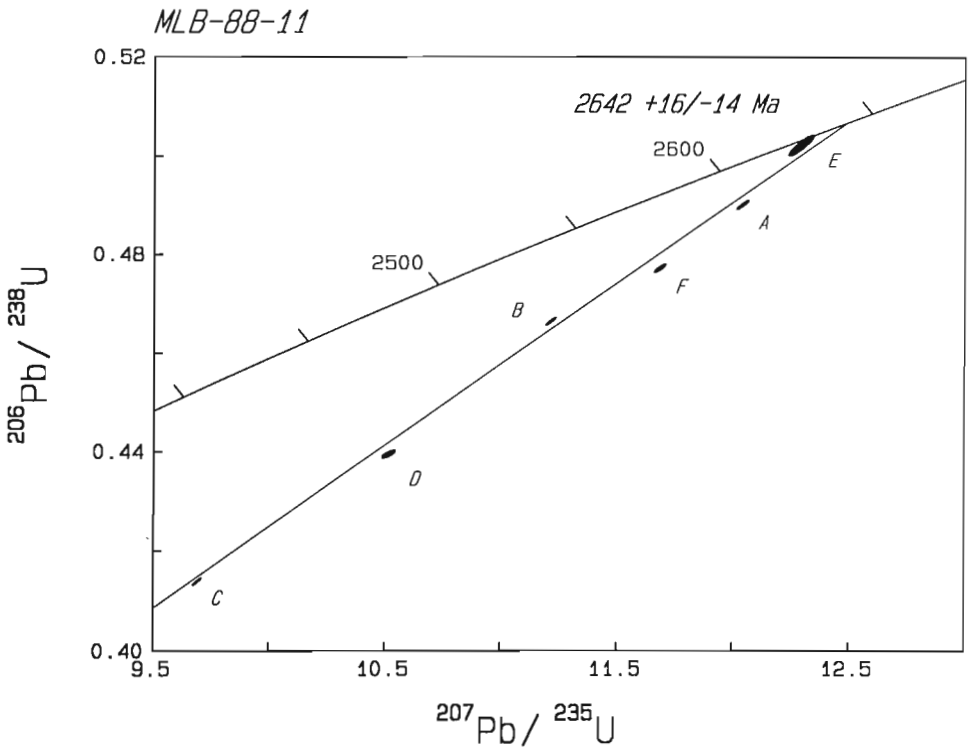

Figure 2. Concordia plot of U-Pb zircon data for sample MLB-88-11.

DISCUSSION

The U-Pb data suggest that the age of the two samples is 2.64 Ga. Assuming no inherited zircon was present, sample MLB-88-11 has a minimum age of 2630 Ma, and sample MLB-88-12 a minimum age of 2638 Ma. The degree of scatter of individual analyses about best-fit regression lines may either reflect complex, multi-stage Pb-loss from the zircons, or the presence of a very minor inherited zircon component, or both. If inherited zircon cores were present in some or all of the fractions analyzed, the actual crystallization may be slightly younger than 2.64 Ga.

Four U-Pb analyses of unabraded, multi-grain zircon fractions were carried out in 1978 on samples of Anton Complex gneisses (Henderson, 1985; W.D.Loveridge, pers. comm., 1989). These analyses range from 12 to 22% discordant, and lie within the general array of data generated in this study.

Several units surrounding the Anton Complex have previously been dated (Henderson et al., 1987). Among these, the Townsite flows in the central part of the Yellowknife Supergroup at Yellowknife are significantly older (2684 + 16/ -24 Ma) than the Anton Complex, and suggest that what we have sampled of the Anton Complex was not basement to the Yellowknife Supergroup. Based on observed contact relationships the western granodiorite phase of the Defeat Plutonic Suite (2620 ± 8 Ma) and the Awry Plutonic Suite (2550 - 2630 Ma) are clearly younger than the Anton Complex, although their ages overlap within the uncertainty of the analyses. The Anton Complex could be an older, more strongly deformed unit of the Defeat Plutonic Suite.

U-Pb zircon ages for two units of the Sleepy Dragon Complex (2683 and 2819 Ma; Henderson et al., 1987) are significantly older than those determined for the Anton Complex samples. The relatively young age of the Anton Complex suggests that the term "Anton Terrane" may be an inappropriate name for basement exposures in the western part of Slave Province, some of which have yielded U-Pb zircon ages as old as 3480 Ma (Bowring and Van Schmus, 1984), and in which the world's oldest rocks, the 3962 Ma Acasta gneisses (Bowring et al., 1989) also occur.

The zircon age of the Anton Complex places it in an apparent hiatus in igneous activity in the Slave Province. Well-dated Yellowknife Supergroup volcanic rocks in the Slave Province fall within the age ranges 2698 - 2687 Ma and 2675 - 2663 Ma, whereas plutonic units fall mainly in the age range 2625 - 2580 Ma (Henderson et al., 1987; Mortensen et al., 1988; van Breemen et al., 1987, 1990; van Breemen and Henderson, 1988). With the exception of the Olga plutonic suite in Contwoyto Lake map area, dated at 2649 ± 2 Ma (van Breemen et al., 1990), rocks with ages between 2625 and 2660 Ma are conspicuously absent. It is possible that other as yet undated plutonic units of similar age to the Anton Complex may occur elsewhere in the western part of Slave Province.

ACKNOWLEDGMENTS

We greatly appreciate the use of the Indian and Northern Affairs Beaver aircraft kindly provided by W.A.Padgham, Northern Affairs Program. We thank the Mineral Separation Laboratory staff for preparing the bulk zircon separates, J.L.Macrae, J.C.Bisson, and K.Santowski for performing the zircon analyses, and W.D.Loveridge for preliminary data reduction and for discussion and interpretation of earlier GSC analytical results. A review of the manuscript by Otto van Breemen was very helpful.

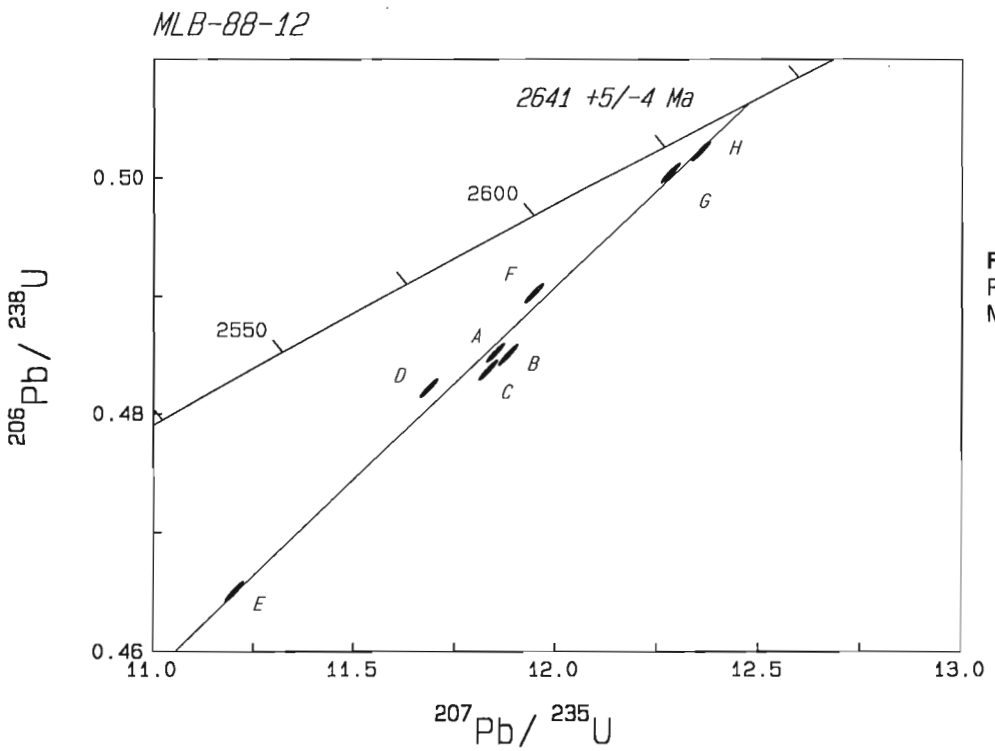

Figure 3. Concordia plot of U-Pb zircon data for sample MLB-88-12.

REFERENCES

Bowring, S. A. and Van Schmus, W. R.
1984: U-Pb zircon constraints on evolution of Wopmay Orogen, N.W.T.; Geological Association of Canada - Mineralogical Association of Canada, Program with Abstracts, v. 9, p. 47.

Bowring, S.A., Williams, I.S., and Compston, W.
1989: 3.96 Ga gneisses from the Slave province, Northwest Territories, Canada; Geology, v. 17, p. 971-975.

Cumming, G.L. and Richards, J.R.
1975: Ore lead ratios in a continually changing earth; Earth and Planetary Science Letters, v. 28, p. 155-171.

Easton, R.M.
1985: The nature and significance of pre-Yellowknife Supergroup basement in the Point Lake area, Slave Structural Province, Canada; in Evolution of Archean Supracrustal Sequences, ed. L.D. Ayres, P.C. Thurston, K.D. Card, and W. Weber; Geological Association of Canada, Special Paper 28, p. 153-167.

Fyson, W. K. and Helmstaedt, H.
1988: Structural patterns and tectonic evolution of supracrustal domains in the Archean Slave province, Canada; Canadian Journal of Earth Sciences, v. 25, p. 301-315.

Helmstaedt, H. and Padgham, W.A.
1986: A new look at the stratigraphy of the Yellowknife Supergroup at Yellowknife, N.W.T. - Implications for the age of gold-bearing shear zones and Archean basin evolution; Canadian Journal of Earth Sciences, v.23, p. 454-475.

Helmstaedt, H., Padgham, W.A., and Brophy, J.
1986: Multiple dikes in the lower Kam Group, Yellowknife greenstone belt: evidence for Archean sea floor spreading?; Geology, v. 14, p. 562-566.

Henderson, J.B.
1985: Geology of the Yellowknife-Hearne Lake area, District of Mackenzie: a segment across an Archean basin; Geological Survey of Canada, Memoir 414, p. 135.

Henderson, J.B., van Breemen, O., and Loveridge, W.D.
1987: Some U-Pb zircon ages from Archean basement, supracrustal and intrusive rocks, Yellowknife-Hearne Lake area, District of Mackenzie; in Radiogenic Age and Isotopic Studies Report 1; Geological Survey of Canada, Paper 87-2, p. 111-121.

Hoffman, P.F.
1986: Crustal accretion in a 2.7-2.5 Ga "granite - greenstone" terrane, the Slave Province, N.W.T.: a prograding trench-arc system?; in Workshop on the Tectonic Evolution of Greenstone Belts, ed. M.J. de Wit and L. Ashwal; Lunar and Planetary Institute Technical Report 86-10, 120 p..

James, D.T.
1989: Basement-cover relations between the Archean Yellowknife Supergroup and the Sleepy Dragon Complex north of Fenton Lake, District of Mackenzie, N.W.T.; in Current Research, Part C; Geological Survey of Canada, Paper 89-1C, p. 29-36.

King, J.E., Davis, W.J., Relf, C., and Avery, R.W.
1988: Deformation and plutonism in the western Contwoyto Lake map area, central Slave Province, District of Mackenzie, N.W.T.; in Current Research, Part C; Geological Survey of Canada, Paper 88-1C, p. 161-176.

Kusky, T.M.
1989: Accretion of the Archean Slave province; Geology, v. 17, p. 63-67.

Lambert, M.B.
1988: Cameron River and Beaulieu River volcanic belts of the Archean Yellowknife Supergroup, District of Mackenzie, Northwest Territories; Geological Survey of Canada, Bulletin 382, 145 p.

McGlynn J.C. and Henderson, J.B.
1970: Archean volcanism and sedimentation in the Slave Structural Province; in Symposium on Basins and Geosynclines of the Canadian Shield, ed. A. Baer; Geological Survey of Canada, Paper 70-40, p. 31-44.

Mortensen, J.K., Thorpe, R.I., Padgham, W.A., King, J.E., and Davis, W.J.
1988: U-Pb zircon ages for felsic volcanism in Slave Province, N.W.T.; in Radiogenic Age and Isotopic Studies: Report 2; Geological Survey of Canada, Paper 88-2, p. 85-95.

Padgham, W.A.
1985: Observations and speculations on supracrustal successions in the Slave Structural Province; in Evolution of Archean Supracrustal Sequences, ed. L.D. Ayres, P.C. Thurston, K.D. Card, and W. Weber; Geological Association of Canada, Special Paper 28, p. 133-151.

Parrish, R.R., Roddick, J.C., Loveridge, W.D., and Sullivan, R.W.
1987: Uranium-lead analytical procedures at the geochronology laboratory, Geological Survey of Canada; in Radiogenic Age and Isotopic Studies: Report 1; Geological Survey of Canada, Paper 87-2, p. 3-7.

Steiger, R.H. and Jäger, E.
1977: Subcommission on geochronology: convention on the use of decay constants in geo- and cosmochronology; Earth and Planetary Science Letters, v. 36, p. 359-362.

van Breemen, O. and Henderson, J.B.
1988: U-Pb zircon and monazite ages from the eastern Slave Province and Thelon Tectonic Zone, Artillery Lake area, N.W.T.; in Radiogenic Age and Isotopic Studies: Report 2; Geological Survey of Canada, Paper 88-2, p. 73-83.

van Breemen, O., Henderson, J.B., Sullivan, R.W., and Thompson, P.H.
1987: U-Pb zircon and monazite ages from the eastern Slave Province, Healey Lake area, N.W.T.; in Radiogenic Age and Isotopic Studies: Report 1; Geological Survey of Canada, Paper 87-2, p. 101-110.

van Breemen, O., King, J.E., and Davis, W.J.
1990: U-Pb zircon and monazite ages from plutonic rocks in Contwoyto - Nose Lakes map area, central Slave Province, District of Mackenzie; in Radiogenic Age and Isotopic Studies: Report 3, Geological Survey of Canada, Paper 89-2 (this publication).

Late Archean U-Pb zircon age for the Clinton-Colden gabbro-anorthosite intrusion, eastern Slave Province, District of Mackenzie, Northwest Territories

R.I. Macfie[1], O. van Breemen[2], and W.D. Loveridge[2]

Macfie, R.I., van Breemen, O., and Loveridge, W.D., Late Archean U-Pb zircon age for the Clinton-Colden gabbro-anorthosite intrusion, Eastern Slave Province, District of Mackenzie Northwest Territories; in Radiogenic Age and Isotopic Studies: Report 3, Geological Survey of Canada, Paper 89-2, p. 45-48, 1990.

Abstract

A gabbro anorthosite intrusion in the eastern part of Slave Structural Province has yielded a U-Pb zircon age of 2686 ± 3 Ma. This age provides a minimum for basic-to-intermediate volcanic rocks cut by the intrusion. In addition, the age is within the range of published ages for volcanic rocks in the eastern part of Slave Structural Province, suggesting that this basic intrusion is associated with the volcanism.

Résumé

L'âge obtenu par la méthode U-Pb appliquée au zircon d'une intrusion d'anorthosite à gabbro située dans la partie est de la province des Esclaves est de 2686 ± 3 Ma. Cet âge fournit un âge minimum pour des roches volcaniques de nature basique à neutre traversées par l'intrusion. De plus, il se situe à l'intérieur de la fourchette des âges publiés pour des roches volcaniques se trouvant dans la partie est de la province des Esclaves, phénomène qui semble indiquer que cette intrusion basique est associée au volcanisme.

INTRODUCTION

The Clinton-Colden gabbro-anorthosite intrusion underlies an area of approximately 20 km^2 at the southeast end of Clinton-Colden Lake in the eastern part of the Slave Province (Fig. 1). The area lies within Artillery Lake map area (NTS 750) (Henderson et al., 1987), and the intrusion was discovered during the course of mapping in 1984 (Henderson and Macfie, 1985).

The gabbro-anorthosite body intrudes tholeiitic mafic, calcalkaline intermediate, and minor felsic meta-volcanic rocks (Wodicka, 1987) of the Yellowknife Supergroup at the southern end of the greenstone belt at Clinton-Colden Lake (Fig. 2). The intrusion contains inclusions of mafic to felsic meta-volcanic rock, and anorthosite plagioclase-phyric dykes are observed to cut adjacent meta-volcanic rocks. The body consists of meta-gabbro to meta-anorthosite, the composition varying in an irregular manner depending upon the closeness of packing of magmatic plagioclase, the most abundant mineral in the intrusion. Layering such as characterizes most Archean anorthositic intrusions is absent. Local geology and the macroscopic appearance of the intrusion have been described by Macfie (1987).

The intrusion has been partly hydrated during deuteric or subsequent metamorphism. The magmatic mineral assemblage consisted predominantly of medium- to coarse-grained plagioclase (An_{65-85}), coarse oikocrystic clinopyroxene, and an opaque oxide, probably titanomagnetite. Clinopyroxene has been almost completely replaced by pseudomorphic actinolite to tschermakite, the latter occurring as rims adjacent to plagioclase that supplied Al, not one for further growth of the fine tschermakite grains. The opaque-oxide phase was altered to open trellis networks of ilmenite and rutile, interstices being filled by fine chlorite and amphibole. Apart from marginal overgrowth of some

1 Department of Geology, University of Ottawa and Ottawa-Carleton Geoscience Centre, Ottawa, Ontario K1N 6N5
2 Geological Survey of Canada, 601 Booth Street, Ottawa, Ontario K1A 0E8

plagioclase grains by amphibole and fine epidote adjacent to epidote-calcite fractures, the plagioclase appears unaltered and grains retain near-magmatic calcic compositions. The only other magmatic phase preserved is minor zircon in fine euhedral grains occurring with amphibole pseudomorphs of clinopyroxene that are interstitial to magmatic plagioclase in some rocks. These grains appear to be of primary origin, for they show no evidence of metamorphic overgrowth.

The intrusion is undeformed apart from a sub-rectilinear set of fine fractures, along which plagioclase is strongly altered to fine epidote, and minor high-strain zones trending N15°E, which are approximately parallel to shear zones in adjacent younger granitoid rocks. These high-strain zones are related to Proterozoic movement along the Thelon Tectonic Zone, which lies approximately 30 km to the east. Outside of such zones, which rarely exceed 1 m in width, the intrusion is unfoliated.

Rare Earth Element (REE) evidence suggests that the gabbro-anorthosite intrusion is petrogenetically related to rocks of the volcanic pile that it intrudes (Macfie, 1989). It may be the largest syn-volcanic mafic intrusion known in the Slave Structural Province.

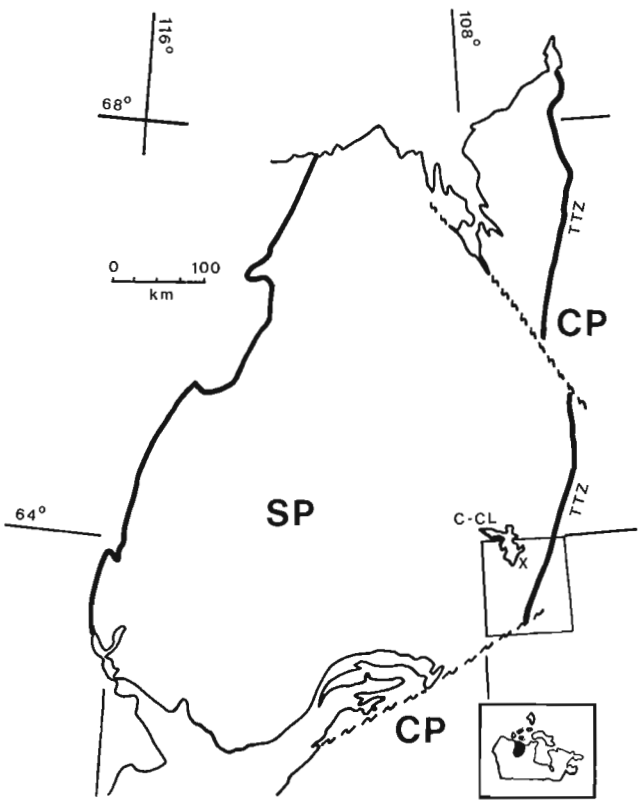

Figure 1. Location of the Clinton-Colden gabbro-anorthosite intrusion (X), at Clinton-Colden Lake (C-CL) in the eastern Slave Province (SP). Artillery Lake map area, enclosed in box, includes a portion of the Thelon Tectonic Zone (TTZ) at the margin of the Churchill Province (CP).

SAMPLE DESCRIPTION AND ANALYTICAL RESULTS

The sample was collected near the southeastern margin of the intrusion (Fig. 2). It is a coarse-grained gabbro with euhedral to subhedral, well preserved, little-epidotized, calcic plagioclase grains enclosed in coarse-grained Ca-amphibole pseudomorphs of oikocrystic clinopyroxene. Zircon occurs as microscopic euhedral to anhedral grains in coarse amphibole. In a zircon separate most of the grains showed the characteristic irregularities of crystals formed in basic magmas at a late stage (Poldervaart, 1956), although there are also simple dipyramidal shapes. Most grains contain cracks, are of poor quality, and range from colourless to brown.

Analytical techniques for U-Pb zircon analysis have been described in Parrish et al. (1987). U-Pb analytical data are presented in Table 1 and an isotope ratio plot in Figure 3. Analytical uncertainties are calculated according to the methods of Roddick (1987). Uncertainties for ages are given at the two sigma level.

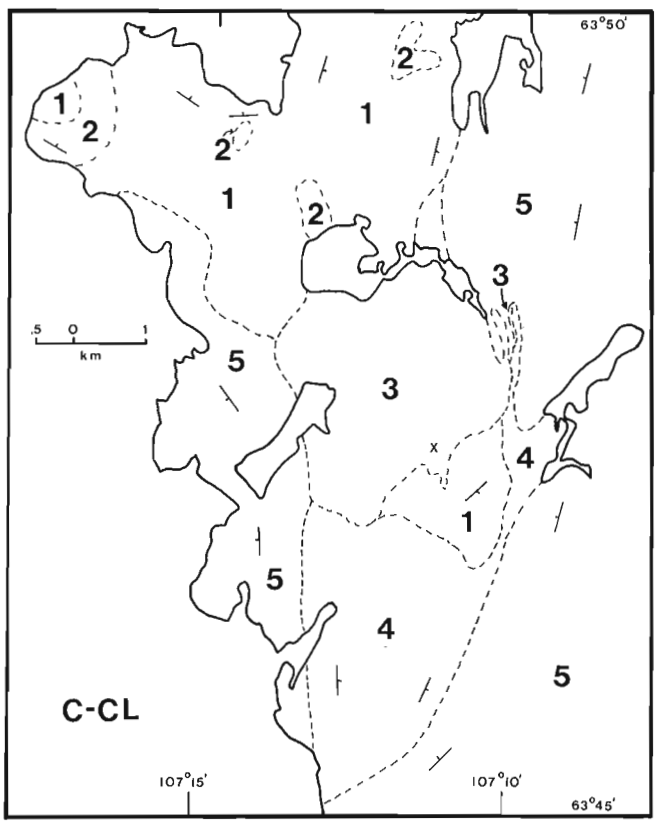

Figure 2. Local geology and sample location (X). Mafic and intermediate volcanic rocks (1) and felsic volcanic rocks (2) are intruded by the Clinton-Colden gabbro-anorthosite intrusion (3) having an age of 2686 ± 3 Ma; both are cut by a diorite-quartz diorite intrusion (4) and by a voluminous granodiorite-tonalite intrusive complex (5). Unit 5 is a pluton of the Tarantula plutonic suite dated elsewhere in the Artillery Lake and Healey Lake map areas at 2622 +1.4/-1.2 Ma and 2616 +7/-6 Ma (van Breemen and Henderson, 1988; van Breemen et al., 1987). C-CL = Clinton-Colden Lake.

Table 1. U-Pb zircon data.

Fraction,[1] Size	Weight (mg)	U (ppm)	Pb[2] (ppm)	$^{206}Pb/^{204}Pb$[3]	Pb_c[4] (pg)	$^{208}Pb/^{206}Pb$[2]	$^{206}Pb/^{238}U$	±SEM%[5]	$^{207}Pb/^{235}U$	±SEM%[5]	R	$^{207}Pb/^{206}Pb$ age, error[6] (Ma)	SEM%[7]
Clinton Colden anorthosite (HBA-G95A)													
a, +149,n= 6	0.030	59.87	35.51	3860	15	0.156	0.51441 (.093)		13.0235 (.11)		0.96	2685.8 (1.0)	0.031
b, +105,n=12	0.008	122.4	78.70	3243	10	0.269	0.51420 (.099)		13.0137 (.11)		0.95	2685.3 (1.1)	0.035
c, +105,n=13	0.015	373.2	238.4	26070	7	0.259	0.51360 (.083)		13.0051 (.095)		0.96	2684.2 (0.9)	0.028
d, +149,n= 1	0.007	533.1	423.6	14080	8	0.611	0.51360 (.084)		12.9975 (.097)		0.96	2685.1 (0.9)	0.028

Notes: [1]fraction sizes are in microns; n=number of cystals; [2]radiogenic Pb; [3]measured ratio, corrected for spike and fractionation; [4]total common Pb in analysis corrected for fractionation and spike; [5]corrected for blank Pb and U, common Pb, errors quoted are one sigma in percent; R correlation of errors in isotope ratios; [6]corrected for blank and common Pb, errors are two sigma in Ma; [7]error for corresponding isotope ratio at one sigma.

Uranium concentrations in the four fractions vary greatly, from 60 ppm to 530 ppm. In view of this, it is remarkable that all four data points are clustered at about 0.5 % discordant. The average ^{207}Pb-^{206}Pb model age is 2685.1 Ma. A regression line drawn through the four data points and a postulated lower intercept of 500 Ma yields an upper intercept age of 2686.2 ± 0.7 Ma (York, 1969). A similar regression using a maximum likely lower intercept age of 1000 Ma yields an upper intercept age of 2688.2 ± 0.9 Ma. The age of igneous emplacement is assigned at 2686 ± 3 Ma.

DISCUSSION

Volcanic activity resulting in the Clinton-Colden greenstone belt must have begun before 2683 Ma, the minimum U-Pb date obtained for intrusion of the cross-cutting gabbro-anorthosite. Thus volcanism in the area had begun at least 8 million years before a rhyolite from the central part of the belt crystallized at 2671 ± 4 Ma (van Breemen and Henderson, 1988). On the basis of accumulated geochronological data for the Slave Structural Province, Mortensen et al. (1988) have suggested that two periods of volcanic activity occurred, one from 2698 to 2687 Ma and the other from 2675 to 2663 Ma, with an apparent concentration of the older ages in the east. The date obtained for the Clinton-Colden intrusion (providing a minimum age for the onset of volcanism in the area) falls near the end of the older volcanic episode, whereas the date obtained for the rhyolite falls within the younger. The date obtained by van Breemen and Henderson (1988) from the rhyolite suggested that the Clinton-Colden belt was anomalously young relative to other volcanic belts in the eastern part of Slave Province, but our date for the gabbro-anorthosite demonstrates that volcanism was occurring in the Clinton-Colden volcanic belt at approximately the same time as in other belts in the eastern part of Slave Province.

ACKNOWLEDGEMENTS

This paper has been critically read by J.B. Henderson.

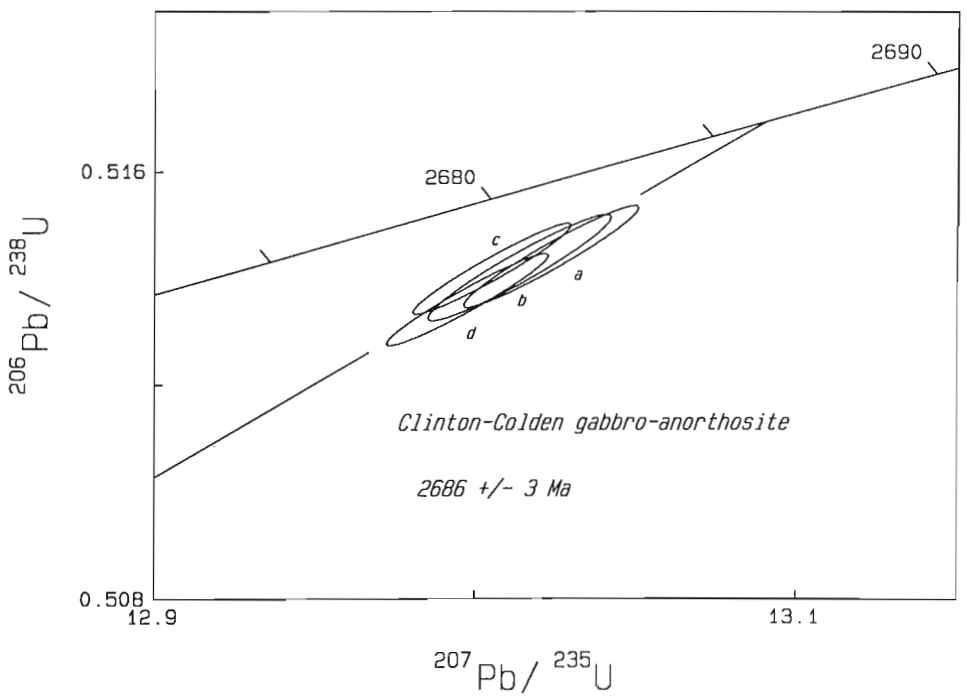

Figure 3. Isotope ratio plot. Letters identifying data points correspond to those of Table 1.

REFERENCES

Henderson, J.B. and Macfie, R.I.
1985: The northern Artillery Lake map area: a transect across the Thelon Front, District of Mackenzie; in Current Research, Part A; Geological Survey of Canada, Paper 85-1A, p. 411-416.

Henderson, J.B., McGrath, P.H., James, D.T., and Macfie, R.I.
1987: The Artillery Lake map area and the Thelon Tectonic Zone - an integrated study; in Current Research, Part A; Geological Survey of Canada, Paper 86-1A, p. 411-416.

Macfie, R.I.
1987: The Clinton-Colden hornblende gabbro-anorthosite intrusion, Artillery Lake map area, District of Mackenzie; in Current Research, Part A; Geological Survey of Canada, Paper 87-1A, p. 681-687.

1989: The petrology and mineralogy of the Clinton-Colden gabbro- anorthosite intrusion, Slave province, N.W.T.; unpublished M.Sc. thesis, University of Ottawa, 126 p.

Mortensen, J.K., Thorpe, R.I., Padgham, W.A., King, J.E., and Davis, W.J.
1988: U-Pb zircon ages for felsic volcanism in Slave Province, N.W.T.; in Radiogenic Age and Isotopic Studies: Report 2; Geological Survey of Canada, Paper 88-2, p. 85-95.

Parrish, R.R., Roddick, J.C., Loveridge, W.D., and Sullivan, R.W.
1987: Uranium-lead analytical techniques at the geochronology laboratory, Geological Survey of Canada; in Radiogenic Age and Isotopic Studies: Report 1; Geological Survey of Canada, Paper 87-2, p. 3-7.

Roddick, J.C.
1987: Generalized numerical error analysis with applications to geochronology and thermodynamics; Geochimica et Cosmochimica Acta, v. 51, p. 2129-2135.

Poldervaart, A.
1956: Zircons in rocks, 2. Igneous rocks; American Journal of Science, v. 254, p. 521-554.

van Breemen, O. and Henderson, J.B.
1988: U-Pb zircon and monazite ages fom the eastern Slave Province and Thelon Tectonic Zone, Artillery Lake area, N.W.T.; in Radiogenic Age and Isotopic Studies: Report 2; Geological Survey of Canda, Paper 88-2, p. 73-83.

Wodicka, N.
1987: Geology and geochemistry of part of the Clinton-Colden greenstone belt, N.W.T.; unpublished B.Sc. thesis, University of Ottawa, 82p.

York, D.
1969: Least squares fitting of a straight line with correlated errors; Earth and Planetary Science Letters, v. 5, p. 320.

U-Pb zircon age from the Himag plutonic suite, Thelon Tectonic Zone, Churchill Structural Province, Northwest Territories

R. A. Frith[1] and O. van Breemen[1]

Frith, R.A. and van Breemen, O., U-Pb age from the Himag Plutonic suite, Thelon Tectonic Zone, Churchill Structural Province, Northwest Territories; in Radiogenic Age and Isotopic Studies: Report 3, Geological Survey of Canada, Paper 89-2, p. 49-54, 1990.

Abstract

A 1994 +6/ -4 Ma U-Pb zircon age has been obtained from the central part of the Trys megacrystic granodiorite, Himag plutonic suite. This age falls within the 2.0 - 1.9 Ga range of ages for plutons within the Thelon Tectonic Zone.

Résumé

Un âge de 1994 + 6/ -4 Ma a été obtenu par la méthode U-Pb appliquée au zircon de la partie centrale de la granodiorite à mégacristaux de Trys, de la série plutonique de Himag. Cet âge se situe dans la fourchette des âges (2,0 à 1,9 Ga) des plutons se manifestant à l'intérieur de la zone tectonique de Thelon.

INTRODUCTION

This paper reports on the dating of the Trys megacrystic granodiorite, which forms part of an extensive body of megacrystic granodiorite and granodiorite orthogneiss, informally referred to here as the "Himag plutonic suite." These granitoids form the principal rock types of a batholithic-scale intrusion that underlies an anomalously high aeromagnetic pattern dominating the eastern half of the Ellice River map area. The same aeromagnetic high is hosted by a variety of rock types outside the Ellice River map area and it may be traced within the Thelon Tectonic Zone (TTZ; Fig. 1; Thompson and Henderson, 1983). South of the MacDonald Fault, Bostock et al. (1987) have termed this zone the Taltson Magmatic Zone in order to emphasize the occurrence of large relatively undeformed plutons, in contrast to the much greater degree of deformation and abundance of gneiss in the TTZ to the north.

GEOLOGICAL SETTING

The Ellice River map area (Frith, 1982), at the southeastern end of the the Bathurst Fault System (Fig. 1, 2), straddles the boundary between the eastern Slave Structural Province and the Thelon Tectonic Zone, a Proterozoic feature separating the Archean Slave Province from the Archaean Queen Maud Block to the east. The western boundary of the TTZ, or Thelon Front, has been left-laterally faulted along the Bathurst Fault System (BFS; Fig. 2). In the Ellice River area, rocks in the northwest half of the system show brittle failure with displacement along one or two major fault planes. Along the southeast part of the fault system the major fault planes splay into multiple branches, and movement takes place, with decreasing throw, along increasingly wide, ductile shear zones.

The eastern part of the Slave Structural Province south of the Bathurst Fault System comprises of supracrustal rocks of the Yellowknife Supergroup made up of metasedimentary turbidites of granodioritic composition (Frith, 1987) and mafic to intermediate volcanic flows and pyroclastic rocks (Frith and Roscoe, 1980) intruded by late Archean (ca. 2.6 Ga) granodiorites and tonalites (Hill and Frith, 1982; Frith and Fryer, 1985). In the southern part of the Ellice River map area, beyond the migmatite line, round pluton shapes typical of the eastern Slave Structural Province, become elongated (Frith, 1982; Henderson et al., 1987). The rocks west of the Thelon Front, but north of the Bathurst Fault System (i.e., in the Tinney Hills-Overby Lake area; Thompson et al., 1986;1985) are similar to those of the Slave Structural Province near the southern margin of the Ellice River map area. However, they have been folded or uplifted into elongated crests and troughs that parallel the regional NNE-SSE trends of the Thelon Tectonic Zone.

1 Geological Survey of Canada, 601 Booth Street, Ottawa, Ontario K1A 0E8

The Thelon Front lies near the peak of a gradual eastward prograding sequence of regional Late Archean metamorphism at the eastern margin of the Slave Structural Province (Fig. 1; Frith, 1982; Frith and Loveridge, 1982). Both Proterozoic retrograde metamophism and north-south deformation, as shear zones, extend into the Slave Structural Province. Archean cordierite porphyroblasts near the Thelon Front have been completely retrograded and locally sheared out parallel to the Thelon Front.

Thelon Tectonic Zone

The Thelon Tectonic Zone in the Ellice River (Frith, 1982) and Tinney Hills-Overby Lake (Thompson et al., 1985) map areas has been divided into two subzones (A and B on Fig. 2) as in Thompson et al. (1985; Fig. 1).

Subzone A:

The rocks east of the Thelon Front are highly deformed and stretched in a northerly orientation along sub-vertical planes, which may be referred to as a "straight zone." Amphibolite derived from basic volcanic rocks and diabase dykes is abundant, particularly adjacent to the Thelon Front. Elsewhere in the subzone, rusty-coloured paragneiss and migmatite are most prevalent, commonly with remnant textures that suggest a derivation from Slave-like supracrustal rocks. U-Pb zircon analyses from a granodiorite migmatite complex in the northern part of subzone A provide an approximate age of 2.6 Ga. (van Breemen et al., 1987). As this age is close to the peak of magmatic activity within the Slave Structural Province, zone A may represent a deeper level of the same Archaean craton (van Breemen and Henderson, 1988).

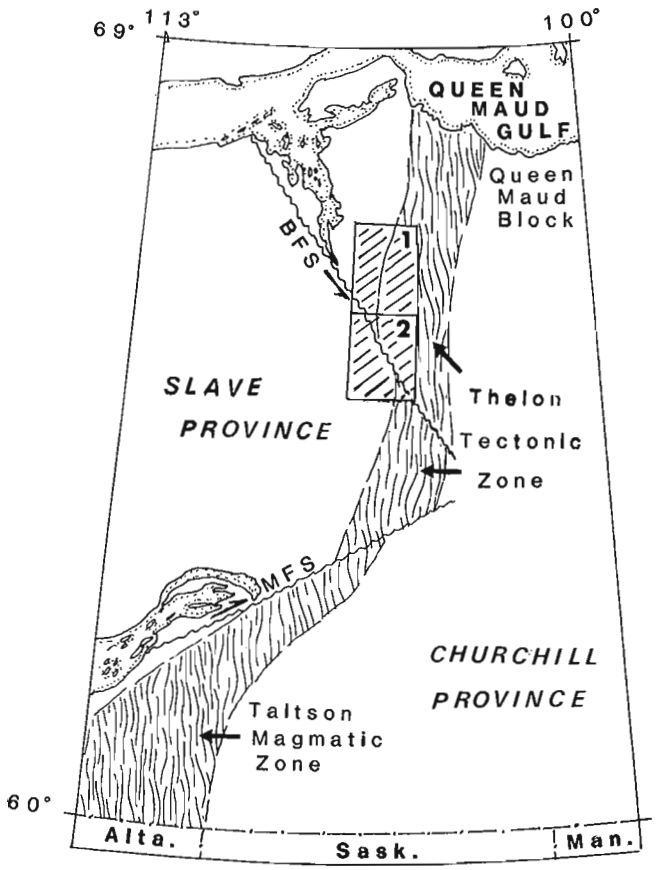

Figure 1. Thelon Tectonic Zone (Thompson and Henderson, 1983), and Taltson Magmatic Zone (Bostock et al., 1987) showing the location of the Tinney Hills-Overby Lake (west half) (1) and Ellice River (2) map areas. BFS = Bathurst Fault System; MFS = MacDonald Fault System.

Subzone B:

There are two principal rock groups in the subzone; various igneous intrusions (Fig. 2) and host rocks. The host rocks are similar to those of subzone A but have a higher proportion of migmatite, whereas paragneiss is locally of higher metamorphic grade (granulite facies). There is also a significant increase in the presence of K-feldspar augen in both the leucosome and within the paleosome of the host rocks. Some narrow mafic to intermediate volcanic belts are present on both sides of the subzone. Generally, the metamorphism is higher than subzone A, commonly at granulite facies. The margins of the Himag plutonic suite are locally gradational with augen textured paragneiss and migmatite. Rocks of the Himag plutonic suite are described in more detail below. In the eastern part of the zone garnet leucogranites or tonalites intruded granulite-facies (orthopyroxene-bearing) paragneiss and migmatite. These and various other igneous intrusive rocks, one of which is a megacrystic K-feldspar granodiorite of the Himag plutonic suite, have yielded Early Proterozoic ages (Fig. 2).

Himag intrusive suite

The suite is 25-30 km wide in the Ellice River map area and tapers toward the north-adjacent Tinney Hills-Overby Lake map areas (Fig. 2). The single mappable unit in the Ellice River area is named the Trys megacrystic granodiorite. Small related intrusions, which may connect at depth, extend along strike to the north. The suite consists of massive to heterogenous granodiorite, diorite, and granite, commonly with biotite, plagioclase, quartz, and characterized by K-feldspar megacrysts. It is the ubiquitous presence of these K-feldspar megacrysts that unifies this heterogeneous suite of rocks. The megacrysts are variable in size, shape, and abundance. They most commonly have a rounded, anhedral shape, are white to buff coloured, and are 2-4 cm across. In some thin-sections, perthitic and rapakivi textures may be observed. Where ductile conditions prevailed, quartz occurs as elongate lenticles, and the megacrysts occur as augen in a matrix of biotite schist or gneiss. Secondary deformed simple alaskite pegmatites are also present (Fig. 3). Locally these deformed pegmatites give the rocks a migmatitic appearance. The degree of augen development is highly variable, but the granites are most attenuated near major shear zones that cut the intrusion in a northerly direction parallel to the Thelon Front or parallel to the ductile deformation that forms part of the Bathurst Fault Zone.

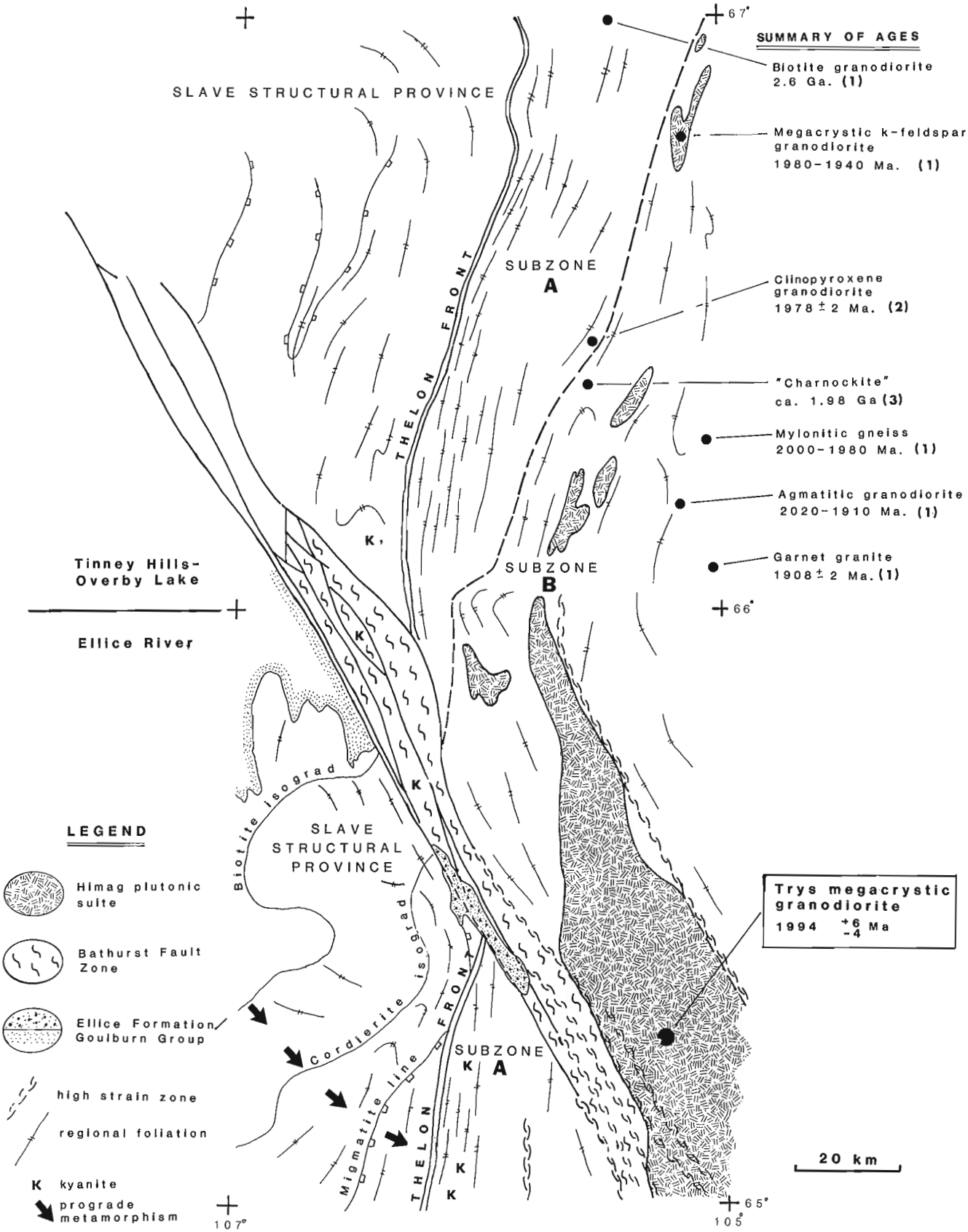

Figure 2. Geological sketch map showing the important tectonic elements, metamorphic isograds, and geochronology along the central sub-zone of the Thelon Tectonic Zone and the distribution of the northern part of the Himag intrusive suite. Ages are from the following sources: 1) van Breemen et al. (1987); 2) conventional U-Pb single crystal analyses (O. van Breemen); and 3) U-Pb ion probe analyses (J.C. Roddick). Geology is after Thompson et al. (1986) for the Tinney Hills-Overby Lake (west half) map area and Frith (1982) for the Ellice River map area.

Table 1. U-Pb zircon data.

Fraction,[1] Size	Weight (mg)	U (ppm)	Pb^{2} (ppm)	$^{206}Pb/^{204}Pb$[3]	Pb_c[4] (pg)	$^{208}Pb/^{206}Pb$[2]	$^{206}Pb/^{238}U$	±SEM%[5]	$^{207}Pb/^{235}U$	±SEM%[5]	R	$^{207}Pb/^{206}Pb$ age, error[6] (Ma)	SEM%[7]
1. Trys megacrystic granite													
a, +149,NM1,n=1	0.003	190.4	72.80	976	12	0.113	0.35985 (.22)		6.0838 (.25)		0.93	1994.7 (3.3)	0.093
b, +149,NM1,n=1	0.006	349.1	133.7	3190	15	0.118	0.35866 (.099)		6.0559 (.11)		0.93	1992.4 (1.4)	0.040
c, +149,NM1,n=1	0.019	418.6	160.5	8563	21	0.118	0.35949 (.084)		6.0672 (.096)		0.96	1991.6 (1.0)	0.029
d, +149,NM1,n=1	0.006	196.8	77.21	2027	13	0.152	0.35795 (.13)		6.0166 (.14)		0.94	1984.3 (1.7)	0.047

Notes: [1]fraction sizes are in microns); NM1=non-magnetic cut with frantz at 1 degree side slope, n=number of cystals; [2]radiogenic Pb; [3]measured ratio, corrected for spike and fractionation; [4]total common Pb in analysis corrected for fractionation and spike; [5]corrected for blank Pb and U, common Pb, errors quoted are one sigma in percent; R correlation of errors in isotope ratios; [6]corrected for blank and common Pb, errors are two sigma in Ma; [7]error for corresponding isotope ratio at one sigma.

Paragneiss enclaves of rusty quartzofeldspathic-biotite gneiss, with or without hornblende, garnet, aluminosilicate, and aplite segregation veins, occur within the suite, particularly at the margins. Like the megacrystic orthogneiss, the inclusions are commonly sheared and mylonitized where close to the principal northerly trending shear zones.

SAMPLE DESCRIPTIONS AND ANALYTICAL RESULTS

The sample of Trys megacrystic granodiorite collected for zircon extraction was typical of the coarser variety of the Himag plutonic suite. The rocks contain the characteristic K-feldspar megacrysts, which make up from 30 to 60% of the rock in a matrix of biotite, grey quartz, and white to light buff plagioclase or K-feldspar. The megacrysts are 2-6 cm long and were both rounded and euhedral. The degree of augen development can be related to the degree of strain. In thin section, augens are sheared and show aggregate textures owing to grain diminution and polygonization, a feature most prevalent around the margins of larger grains (Fig 3). The mafic minerals commonly form schlieren-like wisps of biotite and retrograded hornblende, which looks drawn out by strain. Quartz is concentrated along leucocratic layers, with granulated plagioclase (andesine?) and K-feldspar. Magnetite is the most prominent accessory mineral and is present along with apatite, sphene, and zircon.

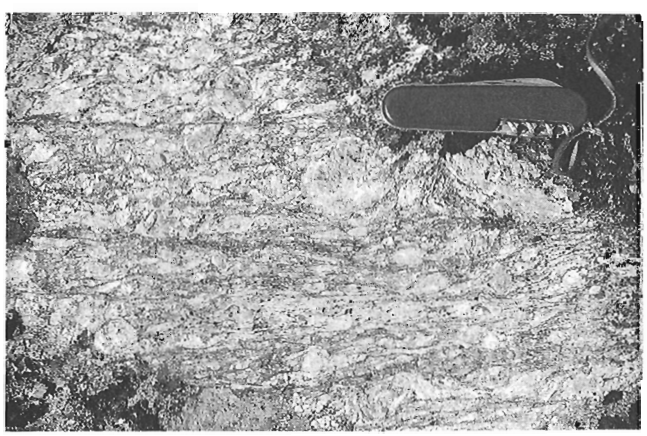

Figure 3. Augen granodiorite orthogneiss from the central part of the Trys megacrystic granodiorite, showing the variation of megacryst/augens, the attenuation, and grain reduction along shear surfaces owing to regional strain related to the Bathurst Fault System.

Zircons range from subhedral prismatic (length to breadth ratios up to 4:1) to ovoid and irregular forms. Cracks are common. There is little evidence of cores. Four single crystals of the coarse prismatic variety (ca. 160 microns long by 80 microns wide) were selected and strongly abraded. Analytical techniques have been described by Parrish et al. (1987). Isotopic data are presented in Table 1 and displayed in isotope ratio plot Fig. 3. Treatment of analytical errors has been described by Roddick (1987). Errors for ages are quoted at the 2 sigma level.

U concentrations range between 190 ppm and 420 ppm. Data points a,b, and c are clustered, ca. 0.7 % discordant and with a range of ^{207}Pb–^{206}Pb model ages from 1991.6 Ma to 1994.7 Ma. The fourth slightly discordant point (d) corresponds to a ^{207}Pb–^{206}Pb age of 1984.3 Ma. Given the absence of cores, the fact that all of the analyses were from single crystals and the agreement within analytical errors of analyses a,b, and c, their average age is related to the time of granite crystallization. The younger age for analysis d is attributed to renewed zircon growth during the protracted metamorphic and tectonic history of the region (van Breemen et al., 1987). Such an interpretation is consistent with both the texture of the rock and the morphology of the zircons.

A minimum age for magmatic crystallization of 1990 Ma is based on the the ^{207}Pb–^{206}Pb ages and uncertainties for points a, b, and c. A maximum magmatic crystallization age of 2000 Ma is obtained by calculating a regression line from points a,b, and c and a maximum likely lower intercept at 1000 Ma. A more probable lower intercept is taken to be 400 Ma, which with the same three data points yields a crystallization age with estimated uncertainties of 1994 +6/ -4 Ma.

DISCUSSION

Collision along the Thelon Tectonic Zone in the range 1.97 to 1.92 Ga has been inferred from tuff beds in the Bear Creek foredeep straddling the Bathurst Fault to the Northwest (Grotzinger et al., 1989; S.A. Bowring in Hoffman, 1989). In the Moraine Lake area south of the Bathurst fault, emplacement of a clinopyroxene granite sheet during shearing was dated at 1957 +9/ -5 Ma. Farther south, in the Daisy Lakes area of the Great Slave Shear zone, vertically and horizontally lineated granites dated at 1976 ± 5 Ma and 1978 ± 5 Ma indicate convergent movement at 1977 Ma (van Breemen et al., 1990). More recent U-Pb dating of the clinopyroxene granodiorite and charnockite first dated by van Breemen et al. (1987) have yielded primary magmatic ages of 1978 ± 2

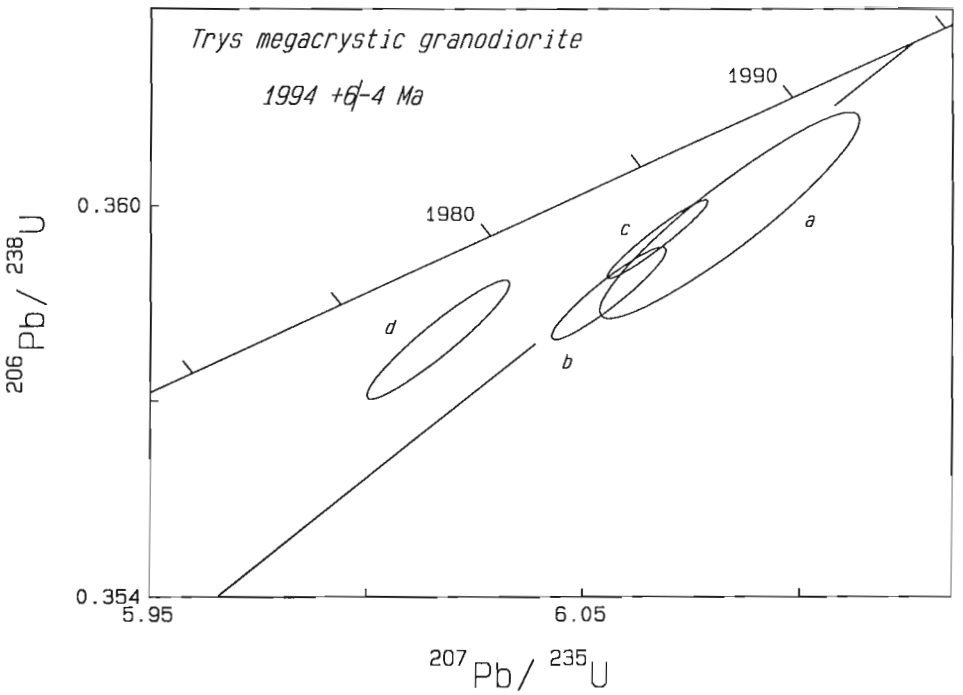

Figure 4. Isotope ratio plot. Letters identifying data points correspond to Table 1.

Ma and ca. 1.98 Ga respectively (Fig.2). In both instances regularly zoned magmatic zircon was overgrown by irregularly zoned zircon, which can be attributed to subsequent syntectonic melting during dynamic conditions.

Given these data, it is likely that the Himag Plutonic suite, which is dated reliably at 1994 +6/ -4 Ma was emplaced prior to the major tectonism along the Thelon Tectonic Zone. Similar megacrystic granites have been dated in the Artillery Lake map area (Critchell granite) and the Moraine Lake transect, both in the TTZ between the Bathurst and MacDonald faults (van Breemen and Henderson, 1988; James et al., 1988). Neither of these igneous intrusions was dated with confidence because of the intense subsequent high-temperature deformation involving renewed zircon growth. However, in both instances, the maximum ages obtained with single, strongly abraded crystals were ca. 1.98 Ga. The increasing grouping of ages at this time suggests that these maximum ages reflect not inheritance but emplacement along the TTZ of the Himag plutonic suite as well as plutons of more intermediate composition in the 2.00 - 1.96 Ga interval, and that only rocks of more aluminous composition, such as the 1908 $\pm$ 2 Ma syntectonic garnet granite of the Overby Lake area (van Breemen et al., 1987), are significantly younger. Further work is clearly required to substantiate this hypothesis.

ACKNOWLEDGEMENTS

This paper has greatly benefitted from critical review by J.B. Henderson.

REFERENCES

Bostock, H.H., van Breemen, O., and Loveridge, W.D.
1987: Proterozoic geochronology in the Taltson Magmatic Zone, N.W.T.; in Radiogenic Age and Isotopic Studies: Report 1; Geological Survey of Canada, Paper 87-2, p. 73-80.

Frith, R.A.
1982: Second preliminary report on the geology of the Beechey Lake-Duggan Lakes map areas, District of Mackenzie; in Current Research, Part A; Geological Survey of Canada, Paper 82-1A, p. 203-211.

1987: Precambrian geology of the Hackett River Area, District of Mackenzie, N.W.T.; Geological Survey of Canada, Memoir 417, 61p.

Frith, R.A. and Fryer, B.J.
1985: Geochemistry and origin of the Regan Intrusive Suite and other granitoids in the northeastern Slave Province, northwest Canadian Shield; Canadian Journal of Earth Sciences, v. 22, pp. 1048-1065.

Frith, R.A. and Loveridge, W.D.
1982: Ages of Yellowknife Supergroup volcanic rocks and regional metamorphism in the northeastern Slave Province; in Current Research, Part A; Geological Survey of Canada, Paper 82-1A, p. 225-237.

Frith, R.A. and Roscoe, S.M.
1980: Tectonic setting and sulphide deposits of the Hackett River belt, Slave Province; Canadian Mining and Metallurgical Bulletin, v. 73, no. 815, p. 143-153.

Henderson, J.B., Thompson, P.H, and James, D.T.
1987: The Healey Lake map area and the Thelon Front problem, District of Mackenzie; in Current Research, Part A; Geological Survey of Canada, Paper 82-1A, p. 191-195.

Hill, J.D. and Frith, R.A.
1982: Petrology of the Regan Intrusive Suite, in the Nose Lake-Beechey Lake map area, District of Mackenzie, N.W.T.; Geological Survey of Canada, Paper 82-8, 26p.

Hoffman, P.F.
1989: Precambrian geology and tectonic history of North America; in ed. A.W. Bally and A.R. Palmer. The Geology of North America–An Overview; Geological Society of America, The Geology of North America, v. A., p. 447-512.

Grotzinger, J.P., Adams, R.D., McCormick, D.S., and Myrow, P.
1989: Sequence stratigraphy, correlation between Wopmay orogen and Kilohigok basin, and further investigations of the Bear Creek Group (Goulburn Supergroup), District of Mackenzie; in Current Research Part C.; Geological Survey of Canada Paper 89-1C, p. 107-119.

James, D.T., van Breemen, O., and Loveridge, W.D.
1988: Early Proterozoic U-Pb zircon ages for granitoid rocks from the Moraine Lake transect, Thelon Tectonic Zone, District of Mackenzie; in Radiogenic Age and Isotopic Studies: Report 2; Geological Survey of Canada, Paper 88-2, p. 67-72.

Parrish, R.R., Roddick, J.C, Loveridge, W.D., and Sullivan, R.W.
1987: Uranium-lead analytical techniques at the geochronology laboratory, Geological Survey of Canada; in Radiogenic Age and Isotopic Studies: Report 1; Geological Survey of Canada, Paper 87-2, p. 3-7.

Roddick, J.C.
1987: Generalized numerical error analysis with applications to geochronology and thermodynamics; Geochimica et Cosmochimica Acta, v. 51, p. 2129-2135.

Thompson, P.H. and Henderson, J.B.
1983: Polymetamorphism in the Healey Lake area – implications for the Thelon Tectonic Zone; in Current Activities Forum 1983, Program with Abstracts; Geological Survey of Canada, Paper 83-8, p. 2.

Thompson, P.H., Culshaw, N., Buchanan, J.R., and Manojlovic, P.
1986: Geology of the Slave Province and the Thelon Tectonic Zone in the Tinney Hills-Overby Lake (west half) map area, District of Mackenzie; in Current Research, Part A; Geological Survey of Canada, Paper 86-1A, p. 275-289.

Thompson, P.H., Culshaw, N., Thompson, D.L. and Buchanan, B.R.
1985: Geology across the western boundary of the Thelon Tectonic Zone in the Tinney Hills-Overby Lake (west half) map area, District of Mackenzie; in Current Research, part A; Geological Survey of Canada, Paper 85-1A, p. 555-572.

van Breemen, O. and Henderson, J.B.
1988: U-Pb and monazite ages from the eastern Slave Province, and Thelon Tectonic Zone, Artillery Lake area, N.W.T.; in Radiogenic Age and Isotopic Studies: Report 2; Geological Survey of Canada Paper 88-2, p. 73-83.

van Breemen, O., Thompson, P.H., Hunt, P.A. and Culshaw, N.
1987: U-Pb zircon and monazite geochronology from the northern Thelon Tectonic Zone, District of Mackenzie; in Radiogenic Age and Isotopic Studies: Report 1; Geological Survey of Canada, Paper 87-2, p. 81-93.

van Breemen, O., Hanmer, S.K., and Parrish, R.R.
1990: Archaean and Proterozoic mylonites along the southeastern margin of the Slave Province; in Radiogenic Age and Isotopic Studies: Report 3; Geological Survey of Canada, Paper 89-2 (this publication).

Archean and Proterozoic mylonites along the southeastern margin of the Slave Structural Province, Northwest Territories

O. van Breemen[2], S.K. Hanmer[2], and R.R. Parrish[1]

van Breemen, O., Hanmer, S.K., and Parrish, R.R., Archean and Proterozoic mylonites along the southeastern margin of the Slave Structural Province, Northwest Territories; in Radiogenic Age and Isotopic Studies: Report 3, Geological Survey of Canada, Paper 89-3, p. 55-62, 1990.

Abstract

Within the Great Slave Shear zone, mylonites of the Schist Lakes Belt are cut by granite that has yielded a U-Pb zircon age of 2562 ± 20 Ma, demonstrating the existence of Archean mylonites in the shear zone. To the southeast of this belt, a 1976 ± 5 Ma granite age provides a maximum for dip-lineated protomylonite, while a 1978 ± 5 Ma granite age provides a maximum for strike-lineated mylonite and a minimum for dip-lineated mylonite. The ages indicate that at least some of the vertical, or convergent, movement occurred during the 1981-1973 Ma interval.

Résumé

À l'intérieur de la zone de cisaillement de Great Slave, des mylonites de la zone de Schist Lakes sont traversées par des granites qui ont donné au moyen de la méthode U-Pb appliquée au zircon un âge de 2562 ± 20 Ma, prouvant ainsi l'existence de mylonites archéennes dans la zone de cisaillement. Au sud-est de cette zone, un granite âgé de 1976 ± 5 Ma fournit un âge maximum pour une protomylonite à linéation suivant le pendage, alors qu'un granite âgé de 1978 ± 5 Ma fournit un âge maximum pour une mylonite à linéation suivant la direction et un âge minimum pour une mylonite à linéation suivant le pendage. Les âges indiquent qu'au moins un certain nombre de mouvements verticaux ou convergents se sont produits au cours de l'intervalle de 1981 à 1973 Ma.

INTRODUCTION

Great Slave Lake shear zone (Hanmer, 1988a), a predominantly Early Proterozoic dextral transcurrent structure of crustal proportions, lies along the southeast margin of Slave Craton. It extends northeastwards from the 25 km wide Laloche segment (Hanmer and Lucas, 1985; Hanmer and Connelly, 1986), into the Schist Lakes-Daisy Lakes area, where it is 13 km wide (Hanmer and Needham, 1988; Fig. 1). The mylonites of the Schist-Daisy segment form three distinct northeast-trending belts, which decrease in metamorphic grade from southeast to northwest; these are termed the Daisy Lakes, Schist Lakes, and Hornby Channel belts.

The Hornby Channel belt is a 0.5-1.5 km wide belt of strike-lineated, dextrally sheared, chlorite-bearing mylonites and ultramylonites. The upper amphibolite, strike-lineated protomylonites of the Schist Lakes belt are older than the granulite - amphibolite facies, dip-lineated mylonites of the Daisy Lakes belt. The Schist Lakes belt is intruded by the 'Sandwich' granite, which in turn is tectonically incorporated into the Daisy Lakes belt. The trend of the upper amphibolite and granulite-facies mylonites changes from 060° in the southwest to 030° in the northeast. To the northeast the greenschist facies mylonites trend 060°, thereby cutting across the older tectonites. Since the Hornby Channel ultramylonite belt truncates the other mylonites and granites of the Schist-Daisy segment, it is the youngest mylonite belt.

GEOLOGY

Schist Lakes Belt

A 7 km wide belt of strike-lineated, dextrally sheared, finely homoclastic (Hanmer, 1988b) ribbon protomylonites borders the southeastern flank of, and is reworked by, the Hornby Channel belt (Fig. 1, 2). Inclusions and large map

[1] Geological Survey of Canada, 601 Booth Street, Ottawa, Ontario K1A 0E8

pable screens of paragneiss, including layered graphitic sillimanite-garnet meta-pelite (metatexite and diatexite), occur throughout the belt (Hanmer and Needham, 1988). Whereas only minor quantities of quartz-rich metasediments occur in the Laloche segment (Hanmer and Lucas, 1985; Hanmer and Connelly, 1986), subfeldspathic meta-arenites are a significant component of the paragneisses of the Schist-Daisy segment. Mylonitization took place at upper amphibolite facies conditions in the southwestern part of the belt. To the northeast, the belt narrows progressively. There is also a textural transition within the granitic tectonites from finely homoclastic protomylonite to finely homoclastic mylonite. Furthermore, the metapelites are reduced to garnet-biotite schists, locally with fine feldspar porphyroclasts. A similar transition occurs across strike towards the northwest within the sector bounded by the North-South fault (Fig. 2) and Schist Lakes where the upper amphibolite assemblages are visibly re-worked by the Hornby Channel belt.

Daisy Lakes Belt

A 5 km wide belt of mixed dip-lineated tectonites forms a corridor through Daisy Lakes and Dion Lake (Fig. 2). The belt comprises two sub-belts. The 2 km wide northwestern sub-belt occupies the ground to the northwest of and within Daisy Lakes. It is composed mainly of finely homoclastic ribbon mylonites, demonstrably formed under upper amphibolite facies conditions from a coarse-grained biotite megacrystic granite, and associated inclusions of mylonitic clinopyroxene meta-tonalite and migmatized metasediment. The 3 km wide southeastern sub-belt occupies the ground between Daisy Lakes and part of Dion Lake. It is an intimate mixture of homoclastic garnet-orthopyroxene ribbon mylonite derived from garnet-orthopyroxene-biotite megacrystic granite, sillimanite-garnet-biotite-K feldspar quartz graphitic metapelite, marble, calc silicate, and coarsely foliated to platy clinopyroxene meta-tonalite. Clearly the

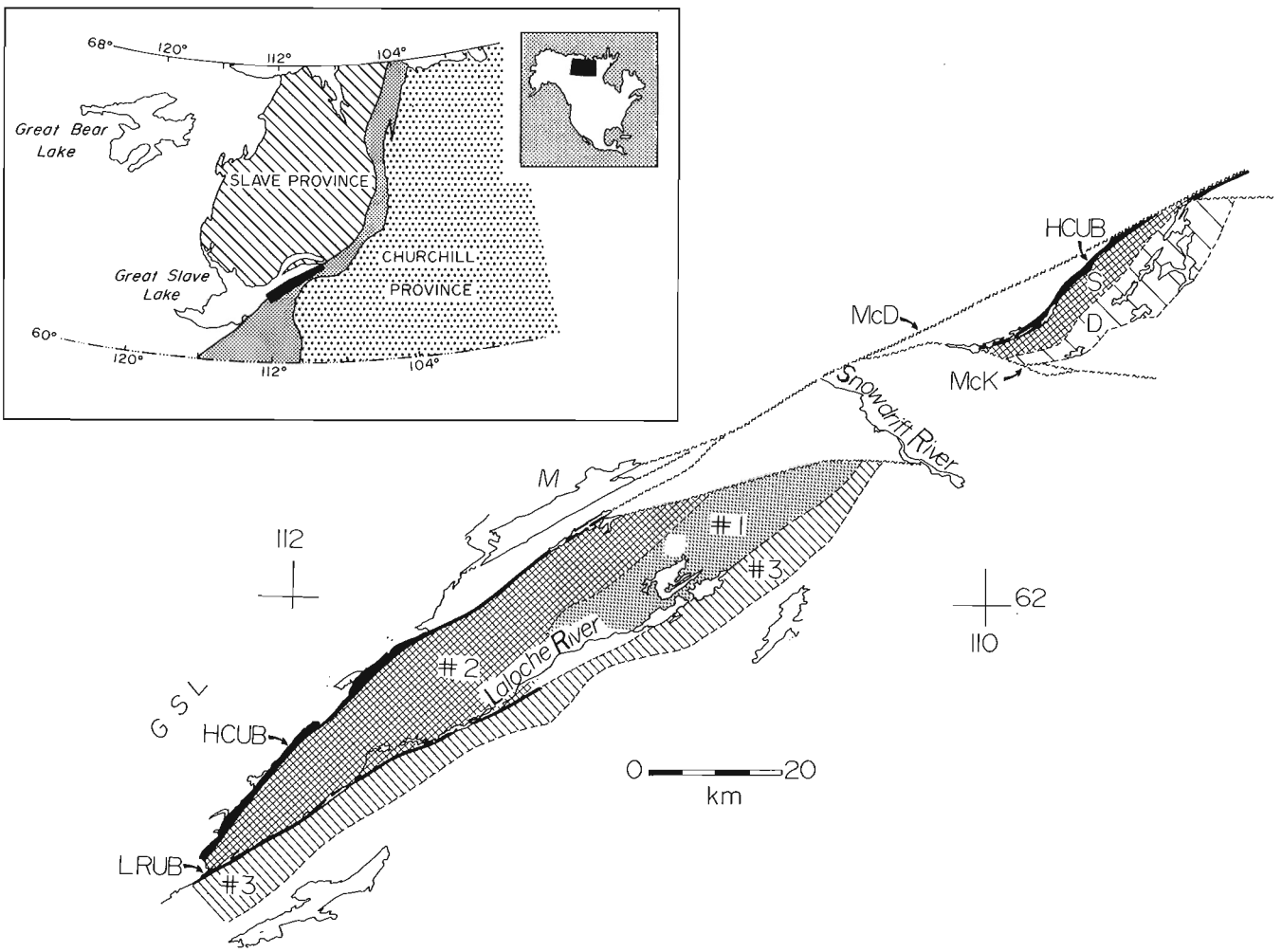

Figure 1. Distribution of mylonite belts nos. 1,2,3, Laloche River ultramylonite belt (LRUB), Hornby Channel ultramylonite belt (HCUB), Schist Lakes (S), and Daisy Lakes (D) within Great Slave Lake shear zone. McDonald-Wilson (McD) and McKee (McK) faults are shown. Abbreviated locations are Great Slave Lake (GSL), and McDonald Lake (M). Segments of Great Slave Lake shear zone are Laloche (southwest of Laroche lakes), Schist-Daisy (northeast of McKee fault), and Snowdrift segment.

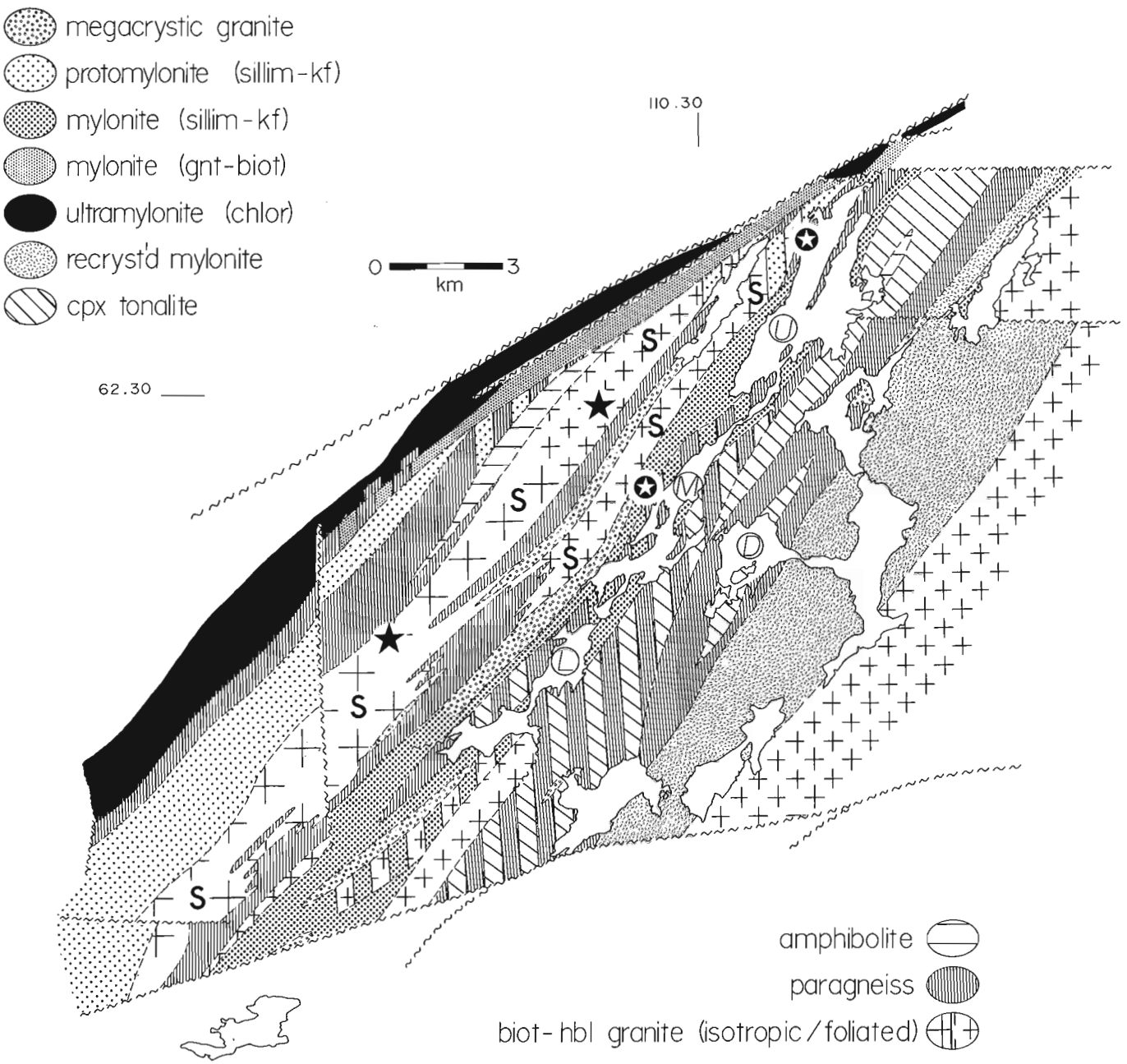

Figure 2. Detail of the geology of the northeast Schist Lakes belt, the isotropic to foliated hornblende-biotite granitoid 'Sandwich' granite, and the Daisy Lakes belt. Bar shading indicates map units of mixed lithologies. Note that the fingering out of the pargneiss is schematically illustrated. The meridional fault to the west is referred to as the North-South fault. S is 'Sandwich' granite. Abbreviations are Dion (D) and Daisy (U,M,L) Lakes. Black stars are sample 1 (HVA-CAM.1) in the southwest and sample 2 (HVA-CAM.2) in the northeast. White stars are sample 3 (HVA-VERT) at Middle Daisy Lake and sample 4 (HVA-HOR) at Upper Daisy Lake.
CPX = clinopyroxene.

Table 1. U-Pb zircon data.

Fraction,[1] Size	Weight (mg)	U (ppm)	Pb^{2} (ppm)	$^{208}Pb/^{204}Pb$[3]	Pb_c[4] (pg)	$^{208}Pb_c/^{206}Pb$[2]	$^{206}Pb/^{238}U$	±SEM%[5]	$^{207}Pb/^{235}U$	±SEM%[5]	R	$^{207}Pb/^{206}Pb$ age, error[6] (Ma)	SEM%[7]
1. 'Sandwich' granite, marginal													
a, −105+74	0.003	137.2	113.3	256	54	0.217	0.48014 (.67)		11.241 (.72)		0.95	2555.7 (7.5)	0.23
b, −105+74	0.006	151.2	85.18	223	131	0.255	0.45979 (.33)		10.601 (.51)		0.75	2530.0 (11)	0.34
c, −105+74	0.008	141.9	72.41	1264	26	0.154	0.45045 (.13)		10.080 (.13)		0.90	2479.7 (2.0)	0.059
2. 'Sandwich' granite, main													
a, +149 n=1	0.052	696.2	301.5	1440	658	0.057	0.41339 (.087)		9.198 (.12)		0.85	2470.2 (2.2)	0.065
b, −149+105 n=3	0.024	328.4	153.4	1665	130	0.100	0.42906 (.085)		9.805 (.11)		0.88	2515.0 (1.9)	0.055
c, −149+105 n=3	0.019	460.0	212.0	1988	121	0.062	0.43637 (.096)		9.941 (.12)		0.91	2509.8 (1.7)	0.049
d, −149+105 n=1	0.018	334.4	163.1	9467	18	0.083	0.45401 (.085)		10.387 (.10)		0.96	2517.0 (1.0)	0.029
e, tips n=1	0.002	1436	645.3	1196	60	0.026	0.43830 (.089)		10.074 (.12)		0.86	2524.8 (2.1)	0.064
3. Granite, vertical lineation													
a, −74+62, NM0	0.012	133.0	51.65	940	38	0.142	0.35739 (.094)		5.9727 (.14)		0.81	1974.1 (3.0)	0.084
b, −74+62, NM0	0.019	159.4	61.12	1455	47	0.137	0.35442 (.093)		5.9076 (.12)		0.86	1969.4 (2.3)	0.064
c, −62, NM0	0.015	124.4	49.15	2124	18	0.149	0.35545 (.096)		5.9474 (.11)		0.94	1976.2 (1.3)	0.037
d, −62, NM0	0.011	157.1	60.93	2147	19	0.170	0.35484 (.089)		5.9232 (.11)		0.94	1972.0 (1.3)	0.037
4. Granite, horizontal lineation													
a, 100, NM2	0.024	188.5	73.62	4478	110	0.157	0.35826 (.11)		6.0021 (.12)		0.96	1978.5 (1.2)	0.032
b, 75, NM2	0.015	214.8	84.73	675	23	0.146	0.35868 (.13)		6.0044 (.12)		0.77	1977.0 (4.6)	0.129

Notes: [1]fraction sizes are in micrometers; NM1=non-magnetic cut with frantz at 1 degree side slope, n=number of crystals; [2]radiogenic Pb; [3]measured ratio, corrected for spike and fractionation; [4]total common Pb in analysis corrected for fractionation and spike; [5]corrected for blank Pb and U, common Pb, errors quoted are one sigma in percent; R correlation of errors in isotope ratios; [6]corrected for blank and common Pb, errors are two sigma in Ma; [7]error for corresponding isotope ratio at one sigma.

southeastern shear-belt contains granulite-facies protoliths and mylonites. Hanmer and Needham (1988) suggested that the mylonites of the Daisy Lakes belt were formed during southeast-side-up movement associated with a strong component of shortening across the steeply dipping shear plane. However, dextral 'C and S' fabrics, asymmetrical extensional crenulation cleavage, rotated winged porphyroclasts, and obliquely intruded boudined (climbing) pegmatites indicative of local dextral transcurrent shear are also observed in the horizontal plane. In view of the rectilinear nature of the dip-parallel extension lineation, Hanmer and Needham (1988) suggested that the transcurrent component is relatively weak and relatively late compared to the dip-slip movement. The transcurrent component is particularly well developed in a 50 m wide strike-lineated, dextrally sheared mylonite, which forms much of the northwestern shore of Upper Daisy Lake (Fig. 2). At its northeastern end, this mylonite grades into a very poorly foliated megacrystic biotite granite. Although contact relations with the surrounding dip-lineated mylonities are nowhere exposed, we suggest that the granite protolith to the strike-lineated mylonites was intruded into already developed dip-lineated mylonites.

'Sandwich' granite

The strike-lineated protomylonites of the Schist Lakes belt are separated from the dip-lineated mylonites of the Daisy Lakes belt by a 2-3 km wide belt of equigranular, medium-grained, mildly foliated to isotropic biotite granite (Fig. 2), whose informal name derives from its location between the two mylonites belts. The 'Sandwich' granite is intrusive with respect to the Schist Lakes belt protomylonites, large recrystallized (annealed) xenoliths and rafts of which are included within the granite close to the contact. Smaller xenoliths of the same are scattered throughout the granite and are often 'assimilated' to the extent that only the biotite mafic bands of the misoriented and folded granitic xenoliths permit their distinction from the enclosing homogeneous granite. The Schist Lakes belt protomylonites are intruded, disrupted (broken apart, misoriented, and folded) and recrystallized (annealed within a corridor 500 m wide adjacent to the 'Sandwich' granite. On its southeastern side, the 'Sandwich' granite is heterogeneously sheared, with the local development of narrow (×100 m) mylonite zones. These mylonites are dip lineated and pass imperceptibly into the upper amphibolite facies mylonites of the northwestern subbelt of the Daisy Lakes belt. Clearly the 'Sandwich' granite separates the flanking mylonite belts in time as well as in space.

While the foregoing is applicable to 90% of the strike length of the 'Sandwich' granite, time relations at its northeastern end at the latitude of Upper Daisy Lake are somewhat more complex. Garnet-biotite mylonites at the northeastern end of the Schist Lakes belt clearly cross-cut the contacts between the Schist Lakes belt upper amphibolite facies protomylonites and the 'Sandwich' granite. Furthermore, the northeastern end of the 'Sandwich' granite is a biotite-bearing finely homoclastic protomylonite, demonstrably developed at the expense of the granite. Mylonitization that post-dated the 'Sandwich' granite (and probably post-Daisy Lakes belt) was concentrated on the northwestern side of the Schist-Daisy segment, even before the formation of chlorite-bearing mylonites in Hornby Channel belt. The garnet-biotite mylonites appear to represent local preservation of an upper greenschist precursor to the Hornby Channel belt.

SAMPLES

Samples were taken in order to address the following questions:

'Sandwich' granite: Two samples of the 'Sandwich' granite have been analyzed in order to determine the minimum age of the strike-lineated mylonites of the Schist Lakes belt. Sample 1 was taken from a metre-wide isotropic vein cutting annealed wallrock mylonites within the granite body. Sample 2 was taken from the interior of the granite.

Vertically lineated granite: A strongly foliated dip-lineated protomylonite derived from a megacrystic biotite granite that visibly grades into dip-lineated mylonites. This specimen was analyzed in order to determine the maximum age of the dip-lineated mylonites of the Daisy Lakes belt.

Horizontally lineated granite: Poorly foliated megacrystic biotite granite protolith to the narrow band of strike-lineated mylonite along the northwest shore of Upper Daisy Lake. This sample was analyzed to determine the maximum age of the minor transcurrent component within the Daisy Lakes belt, as well as the minimum age of the dip-lineated mylonites.

GEOCHRONOLOGY

Analytical techniques for U-Pb zircon analysis have been described in Parrish et al. (1987). U-Pb analytical data are presented in Table 1 and isotope ratio plots on Figures 3 and 4. Analytical uncertainties are calculated according to the methods of Roddick (1987). Uncertainties for isotope ratios are given at the 1 sigma and for ages at the 2 sigma level.

Sandwich granite (samples 1 and 2)

Zircons are subhedral, with L:B ratios of 2:1 to 5:1, and range from clear to translucent with many cracks. Terminations are generally rounded. In sample 1, both the (100) and the (101) faces are well developed. In sample 2, internal zoning contains some discordances and irregularities. Some zircons have apparent cores with less well zoned outer mantles.

U concentrations from sample 1 are close to 145 ppm. Data point 1a is concordant with a ^{207}Pb-^{206}Pb model age of 2556 ± 8 Ma; points 1b and 1c are ca. 15% discordant. A Davis (1982) regression line yields upper and lower intercept ages of ca. 2580 Ma and 1560 Ma, but with a probability of fit of only 3%.

U concentrations of sample 2 are high, ranging from 330-700 ppm with a single tip showing a U concentration of 1440 ppm. Data points are more discordant than for sample 1. Although showing considerable scatter, four out of the five points, including the single zircon crystal tip, 1e, are generally aligned. These four points are also aligned with the points for sample 1, and all seven yield a York (1969) regression line with upper and lower intercept ages of 2562 ± 20 Ma and ca. 890 Ma. Although the mean square of weighted deviates of 167 indicates excessive scatter, this age is accepted for the time of granite emplacement as it agrees with the ^{207}Pb-^{206}Pb model age of the concordant data point.

Vertically lineated granite (sample 3)

Zircons from this granite are subhedral, with rounded terminations and with L:B ratios of 2:1 to 5:1. Cracks are common and there are fluid inclusions as well as cores. U concentrations range from 120 to 160 ppm.

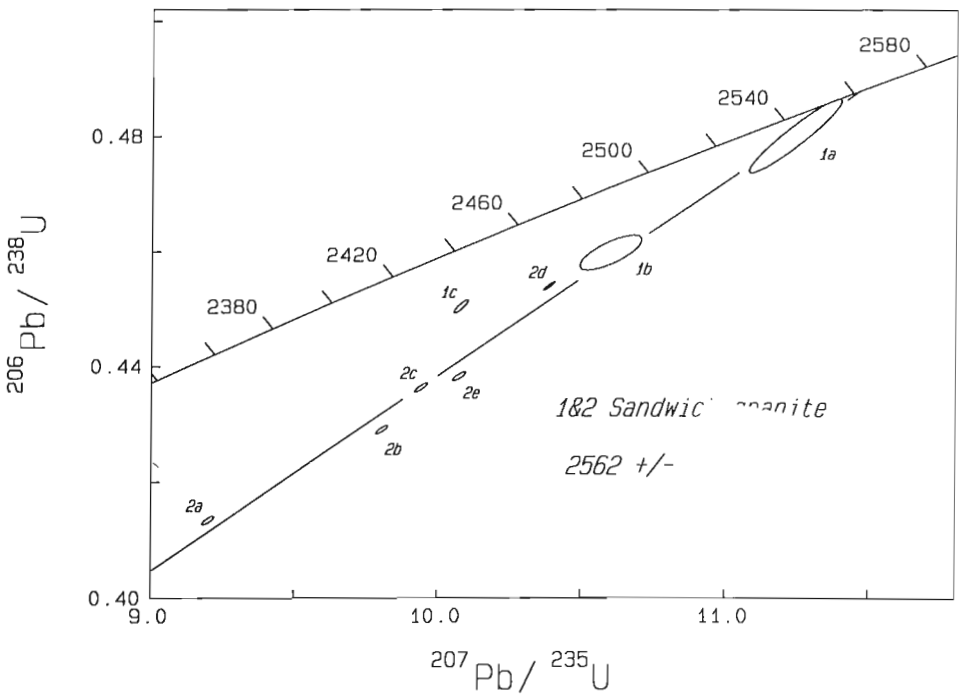

Figure 3. Isotope ratio plot for zircons from the 'Sandwich' granite (samples 1 and 2). Numbers and letters identifying data points correspond to those of Table 1.

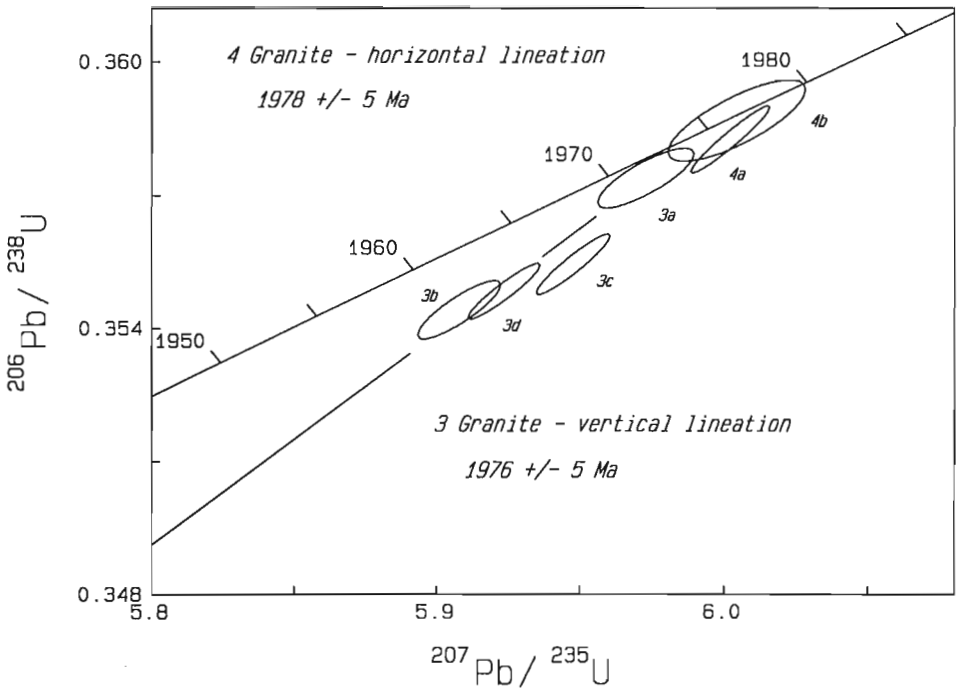

Figure 4. Isotope ratio plot for zircons from granites showing vertical (sample 3) and horizontal (sample 4) lineation.

While data point 3a is concordant, the other three points are ca. 1% discordant. Point 3c plots to the right of the general alignment of the other three points and may reflect memory in the zircon. A York (1969) regression line through the other three data points yields upper and lower intercept ages of 1976 +41/ -5 Ma and 770 Ma with a MSWD of 2.6. In view of the fact that data point 3a is concordant, the upper uncertainty limit is estimated by a regression line through this point and a maximum likely lower intercept age of 1000 Ma. This line corresponds to an upper intercept age of 1976.6 ± 4.6 Ma. The age and uncertainty of granite emplacement are therefore assigned at 1976 ± 5 Ma.

Horizontally lineated granite (sample 4)

Zircons range in shape from ovoid to prismatic with rounded terminations. L:B ranges from 1:1 to 4:1. The grains range from clear to translucent. Apparent cores are common, as are cracks.

U concentrations are close to 200 ppm. Only two fractions have been analyzed, both of which yield concordant or essentially concordant results. The age of crystallization is inferred to be the average ^{207}Pb-^{206}Pb age of 1978 ± 5 Ma.

DISCUSSION

The 2562 ± 20 Ma age for the Sandwich granite indicates that the northwestern zone of the northeast-trending dextral Great Slave shear in the Schist Lakes-Daisy Lakes area is of Archean age. The relation of this shear zone (for which the above is a minimum age) to Archean events in the Slave Structural Province to the north is not known. The granite age is not significantly different, however, from the second of two plutonic events in the Slave Province in the 2620 Ma to 2580 Ma interval (van Breemen and Henderson, 1988; van Breemen et al., 1990).

The vertically and horizontally lineated granites dated at 1976 ± 5 Ma and 1978 ± 5 Ma respectively are not significantly different in age. The latter age provides a maximum for transcurrent movement. As the horizontally lineated granite postdates the dip-lineated mylonites, at least some of the vertical movement has to have occurred within the interval 1981-1973 Ma. These granite ages are within the range of plutonism in the contiguous Taltson Magmatic Zone to the south and the Thelon Tectonic Zone to the the north (Bostock et al., 1987; Frith and van Breemen, 1990). In the Moraine Lake transect of the Thelon Tectonic zone, granite intrusion directly associated with shear movement of unspecified direction has been documented at 1957 +9/ -7 Ma (James et al., 1988).

REFERENCES

Davis, D.
1982: Optimum linear regression and error estimation applied to U-Pb data; Canadian Journal of Earth Sciences, v. 19, p. 2141-2149.

Bostock, H.H., van Breemen, O., and Loveridge, W.D.
1987: Proterozoic geochronology in the Taltson Magmatic Zone, N.W.T.; in Radiogenic Age and Isotopic Studies: Report 1; Geological Survey of Canada Paper 87-2, p. 73-80.

Frith, R.A., and van Breemen, O.
1989: U-Pb zircon age from the Himag plutonic suite, Thelon Tectonic zone, Churchill Structural Province, Northwest Territories; in Radiogenic Age and Isotopic Studies: Report 3; Geological Survey of Canada Paper 89-3 (this publication).

Hanmer, S.

1988a: Great Slave Shear Zone, Canadian Shield: reconstructed vertical profile of a crustal-scale fault zone; Tectonophysics, v. 149, p. 245-264.

1988b: Geology, Great Slave Lake Shear Zone; parts of Fort Resolution, Snowdrift and Fort Reliance map areas, District of Mackenzie, N.W.T.; Geological Survey of Canada, Open File 1783; 1:100 000.

Hanmer, S. and Connelly, J.N.

1986: Mechanical role of the syntectonic Laloche Batholith in the Great Slave Shear Zone, District of Mackenzie, N.W.T.; in Current Research, Part B; Geological Survey of Canada, Paper 86-1B, p. 811- 826.

Hanmer, S. and Lucas, S.B.

1985: Anatomy of a ductile transcurrent shear: the Great Slave Lake Shear Zone, District of Mackenzie, N.W.T.; (preliminary report); in Current Research Part B; Geological Survey of Canada, Paper 85-1B, p. 7-22.

Hanmer, S. and Needham, T.

1988: Great Slave Lake shear zone meets Thelon Tectonic Zone, District of Mackenzie, N.W.T.' in Current Research, Part A; Geological Survey of Canada, Paper 88-1A, p.33-49.

James, D.D., van Breemen, O., and Loveridge, W.D.

1988: Early Proterozoic U-Pb zircon ages for granitoid rocks from the Moraine Lake transect, Thelon Tectonic Zone, District of Mackenzie; in Rodiogenic Age and Isotopic Studies: Report 2; Géological Survey of Canada, Paper 88-2, p. 67-72.

Parrish, R.R., Roddick, J.C., Loveridge, W.D., and Sullivan, R.W.

1987: Uranium-lead analytical techniques at the geochronology laboratory, Geological Survey of Canada; in Radiogenic Age and Isotopic Studies: Report 1; Geological Survey of Canada, Paper 87-2, p. 3-7.

Roddick, J.C.

1987: Generalized numerical error analysis with applications to geochronology and thermodynomics; Geochimica et Cosmochimica Acta, v. 51, p. 2129-2135.

van Breemen, O. and Henderson, J.B.

1988: U-Pb zircon and monazite ages from the eastern Slave Province and Thelon Tectonic Zone, Artillery Lake area, N.W.T.; in Radiogenic Age and Isotopic Studies: Report 2; Geological Survey of Canada, Paper 88-2, p. 73-83.

van Breemen, O., King, J.E., and Davis, B.

1990: U-Pb zircon and monazite ages from plutonic rocks in the Contwoyto-Nose Lakes area, central Slave Province, District of Mackenzie; in Radiogenic Age and Isotopic Studies: Report 3; Geological Survey of Canada, Paper 89-2 (this publication).

York, D.

1969: Least squares fitting of a straight line with correlated errors; Earth and Planetary Science Letters, v. 5, p. 320.

Inherited Archean zircon in the Proterozoic Thelon Tectonic Zone: U-Pb geochronology of the Campbell granite, south of McDonald fault, District of Mackenzie, Northwest Territories

J.B. Henderson[1] and W.D.Loveridge[1]

Henderson, J.B. and Loveridge, W.D., Inherited Archean zircon in the Proterozoic Thelon Tectonic Zone: U-Pb geochronology of the Campbell granite, south of McDonald fault, District of Mackenzie, Northwest Territories; in Radiogenic Age and Isotopic Studies: Report 3, Geological Survey of Canada, Paper 89-2, p. 63-70, 1990.

Abstract

The Campbell granite is a large, lithologically homogeneous, heterogeneously deformed plutonic body within the Thelon Tectonic Zone. Zircon, which contains varied, finely zoned, internal cores with overgrowths that are not zoned, is present in both K-feldspar megacrysts and the matrix of both the moderately deformed and mylonitic granite samples that were analyzed. Separate U-Pb analyses of abraded zircon cores and tips from the mylonitic sample provide the end members of a four-point chord, which defines concordia intercept ages of 2545 +14/-13 and 1929 ± 14 Ma. The presence of zircon with overgrowths within the megacrystals suggests that the 1929 ± 14 Ma overgrowths represent a Proterozoic magmatic stage in the history of the granite, whereas the cores are xenocrysts with a complicated igneous history derived from Archean sources. U-Pb measurements on zircon from the moderately deformed sample confirm that the 1929 ± 14 Ma intercept defines the age of intrusion of the pluton. A $^{207}Pb/^{206}Pb$ age of about 3300 Ma on a metamict zircon core from the moderately deformed granite sample indicates the existence of an extremely old component in the Campbell granite. Two analyses on monazite provide inconclusive age results that are compatible with a 1903 to 1929 Ma age range.

Résumé

Le granite de Campbell est un grand massif plutonique, à lithologie homogène et à déformation hétérogène, qui se trouve à l'intérieur de la zone tectonique de Thelon. On trouve du zircon qui renferme des noyaux internes finement zonés accompagnés d'accroissements secondaires non zonés, dans des mégacristaux de feldspath potassique et dans la gangue des échantillons de granite modérément déformé et de granite mylonitique que l'on a analysés. Des analyses séparées par la méthode U-Pb des noyaux et des pointes abrasés de zircon provenant de l'échantillon mylonitique fournissent les membres extrêmes d'une corde à quatre points qui définit des âges d'intersection de 2545 + 14/−13 et de 1929 ± 14 Ma sur la courbe concordia. La présence du zircon avec des accroissements secondaires dans les mégacristaux semble indiquer que ces accroissements, âgés de 1929 ± 14 Ma représentent une phase magmatique du Protézoroïque dans l'histoire du granite, alors que les noyaux sont des xénocristaux à processus igné complexe remontant à l'Archéen. Des âges obtenus par la méthode U-Pb appliquée aux zircons provenant de l'échantillon de la zone modérément déformée confirment que l'intersection de 1929 ± 14 Ma définit l'âge de l'intrusion du pluton. L'âge $^{207}Pb/^{206}Pb$ d'environ 3300 millions d'années sur un noyau de zircon métamicte provenant de l'échantillon d'un granite modérément déformé indique l'existence d'un composant extrêmement vieux dans le granite de Campbell. Deux analyses de monazite fournissent des âges non concluants qui correspondent à la fourchette d'âge de 1903 à 1929 Ma.

1 Geological Survey of Canada, 601 Booth Street, Ottawa, Ontario K1A 0E8

INTRODUCTION

The Campbell granite is a major plutonic unit within the Thelon Tectonic Zone, the northwestern boundary zone of the Churchill Structural Province adjacent to the eastern part of the Slave Structural Province (Fig. 1). The Campbell granite has been mapped in the Artillery Lake area (Henderson et al., 1987; Henderson, 1989) as a major deformed plutonic body south of the McDonald fault (Fig. 2). Although only the northern part of the granite occurs within the area mapped, it forms a lensoid body 20 km wide and about 130 km long on the basis of its prominent positive magnetic expression and earlier regional reconnaissance mapping (Wright, 1967) (Fig. 1). Its faulted extension may correlate at least in part with the as yet unmapped, prominent, northerly trending, magnetic anomaly in the central part of the Thelon Tectonic Zone, north of the McDonald fault but east of the Artillery Lake area (Thomas et al.,1976; Henderson and Macfie, 1985; Fig. 1). The Campbell granite, therefore, is one of the larger plutonic bodies of the Thelon Tectonic Zone, comparable in scale to some of the large plutonic units of the somewhat similarly aged Taltson Magmatic Zone (Bostock et al., 1987, 1988) to the southwest (Fig. 1). Other recent geochronological data in the region from the Thelon Tectonic Zone and adjacent Slave Province are reported in van Breemen et al. (1987a,b), van Breemen and Henderson (1988), and James et al. (1988).

CAMPBELL GRANITE

The Campbell granite is a lithologically homogeneous plutonic body and contrasts strongly with the heterogeneous, dominantly granitoid gneisses with lesser supracrustal gneisses that occur to the east and west. Its eastern contact with these gneisses is a major ultramylonite zone; its western contact has not been observed. The biotite-poor granite is typically a moderately to sparsely megacrystic, dark pinkish grey to dark grey rock that weathers light pink to tan to grey. Locally minor veins of a pink younger granite may also be present. Rare inclusions of supracrustal gneisses may also be present as well. The mylonitic to weakly foliated granite is heterogeneously, but everywhere, deformed. The foliation is in general north-northeasterly trending, similar to most of the Thelon Tectonic Zone. Dips to either east or west are moderate to steep. In places the only structural element is a flat to gently plunging, northerly trending, mineral lineation. This structural grain is cross cut locally by cataclastic veins and epidote-filled fractures nearMcDonald-generation faults. The rock in the immediate vicinity of these faults is commonly extensively hematite stained, chloritized, and epidotized. Where best preserved, the rock is a metamorphosed megacrystic granite to granodiorite.

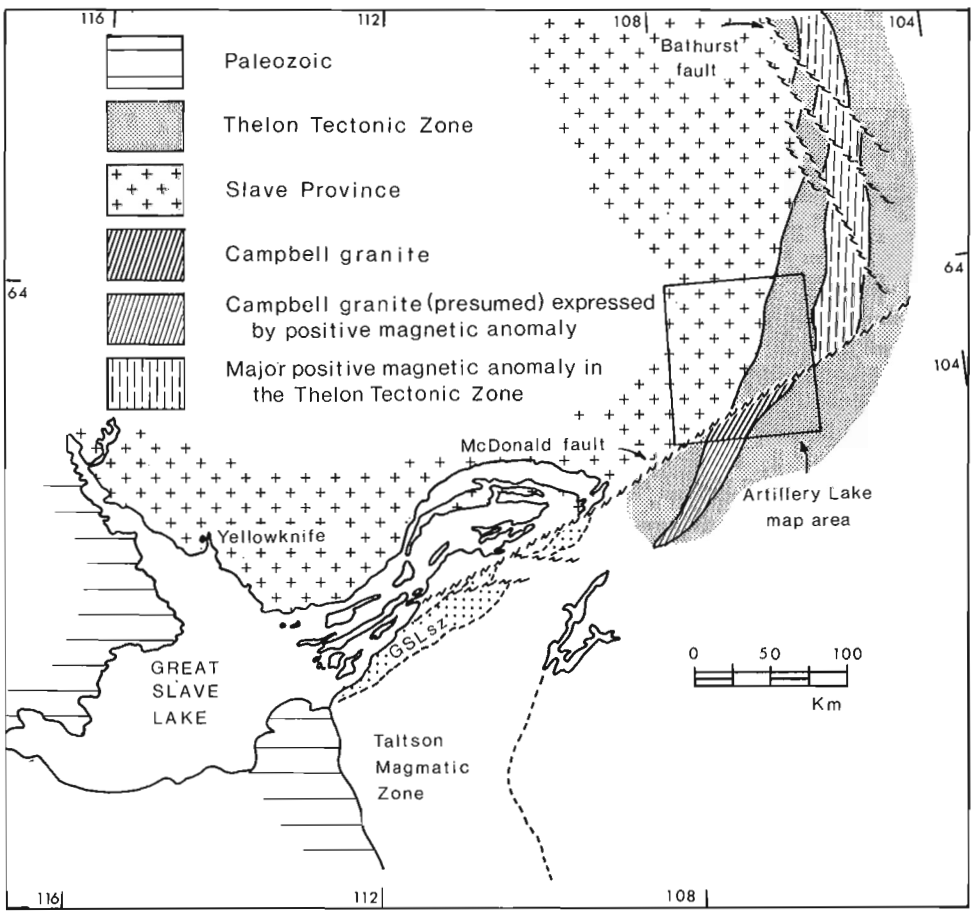

Figure 1. Location map showing the relative positions of the Slave Structural Province, Thelon Tectonic Zone, and Taltson Magmatic Zone with respect to the Campbell granite in the Artillery Lake area. GSLsz represents the Great Slave Lake shear zone.

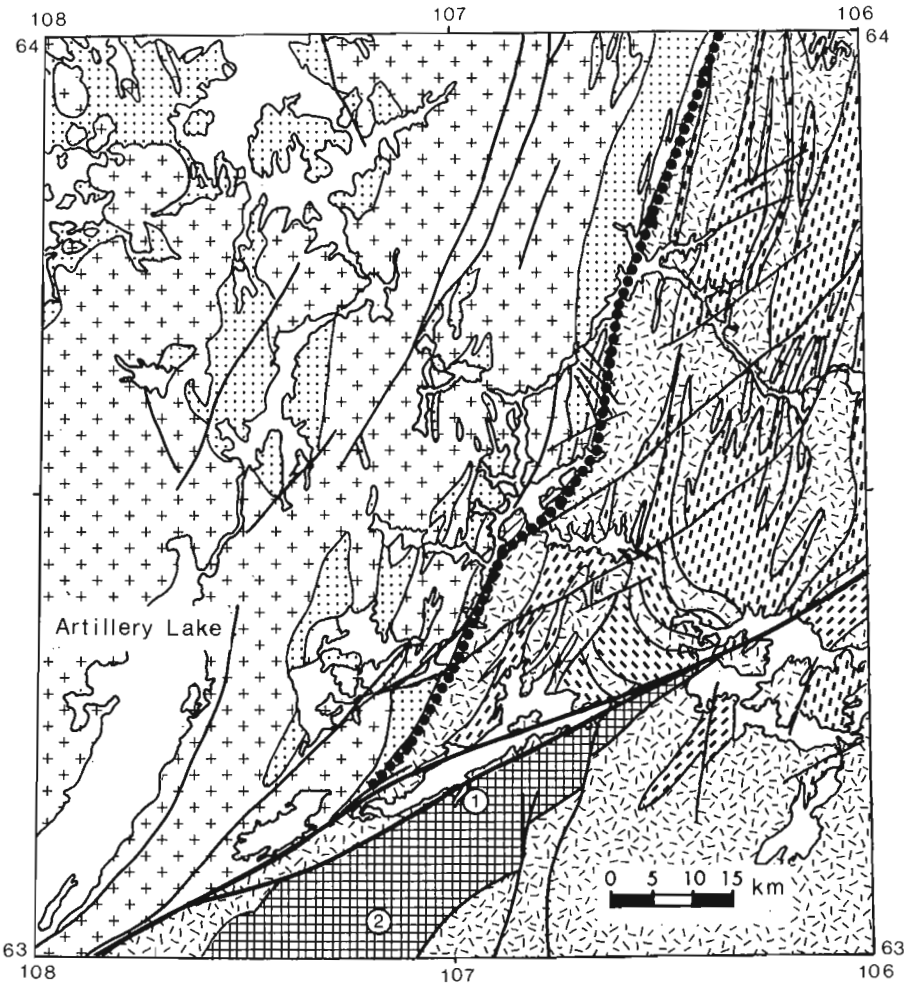

THELON TECTONIC ZONE

Campbell granite

Proterozoic dominantly granitoid gneisses

Proterozoic dominantly supracrustal gneisses

SLAVE PROVINCE

Archean granitoid rocks

Archean Yellowknife supracrustal rocks

Slave Province – Thelon Tectonic Zone boundary

McDonald fault

Figure 2. Generalized geology of the Artillery Lake area on the boundary between the Slave Structural Province and the Thelon Tectonic Zone. The locations of the two sample localities in the Campbell granite are indicated.

Sample 1 was collected in 1986 from the northern part of the pluton, immediately south of the McDonald fault (Fig. 2). It is a dark grey, lineated but unfoliated mylonite with some vaguely defined pinkish altered zones in which the biotite is almost entirely pseudomorphed by chlorite. Zircon was extracted only from the fresh, dark grey phase. In contrast to sample 2, which is less deformed, sample 1 consists of angular broken porphyroclasts of highly strained and fractured orthoclase up to 1 cm in size (Fig. 3) which, in other respects, are similar to the megacrysts in the less deformed rock. These porphyroclasts grade down into a fine-grained, intimately sutured, quartzofeldspathic matrix in which monomineralic polycrystalline quartz lamellae, forming approximately a quarter of the rock, give it a prominent planar aspect. Fine to extremely fine grained biotite occurs as elongate, wispy patches within the matrix. Accessory and secondary minerals include magnetite, apatite, zircon, monazite, epidote, and white mica.

In order to confirm the interpretation of the results on sample 1, a second sample of moderately deformed granite was collected in 1988 for analysis from the south-central part of the pluton within the Artillery Lake area (Fig. 2). It consists of anhedral to rounded megacrysts up to several centimetres in size, of both plagioclase and microcline with granulated boundaries. The microcline megacrysts contain inclusions of euhedral to subhedral plagioclase, less commonly subhedral biotite and anhedral quartz that are typically smaller than coarser anhedral plagioclase and biotite of the matrix. The inclusions are commonly oriented parallel to crystallographic directions within the K-feldspar. Also present are irregular coarse masses of polycrystalline quartz. These coarser phases grade down to the fine inequigranular matrix composed of intimately sutured quartz, plagioclase, and microcline, with irregularly distributed aggregates of dark, greenish brown, locally slightly chloritized biotite, which defines the weak foliation in the rock. Except for monazite, the analyzed rock contains a similar assemblage of accessory and secondary minerals.

GEOCHRONOLOGY

Zircon is abundant in both samples of the granite whereas monazite was recovered only from the first sample. Both phases were analyzed during this study.

Zircon occurs within the feldspar megacrysts and the matrix of the rock in both moderately deformed and mylonitic samples. Most of the zircons examined in the two samples have a generally similar morphology, consisting of a more strongly zoned inner core and a variably developed overgrowth of clear, unzoned, uranium-poor zircon, typically with radial fractures that can be seen in the zircon included in the megacrysts as well as in the matrix zircon (Fig. 3, 4). In general the cores of sample 1 zircons show greater range in U variation among the zones whereas in many of the cores of sample 2 zircons the zonation is much more subtle. A narrow, finely zoned layer that is relatively high in U between the core and the unzoned outer rim is particularly evident in the zircons of sample 2.

Analytical procedures are as presented in Bostock et al. (1988), except that regression calculations are according to Davis (1982).

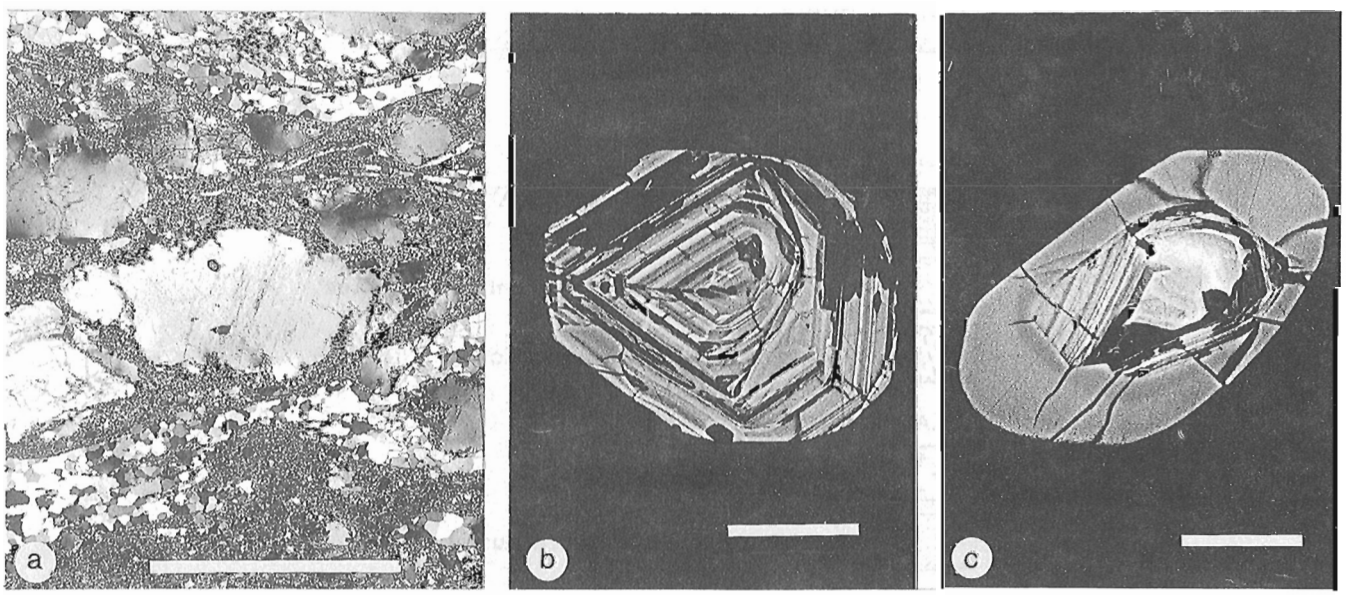

Figure 3. Campbell granite and its zircons. (a) Photomicrograph of the mylonitic Campbell granite (sample 1), showing coarse orthoclase porphyroclasts in a fine-grained quartzofeldspathic matrix and bands of finely polygonized quartz. The two dark spots in the central porphyroclast are zircons, which are also seen in (b) and (c). The scale bar is 1 mm. GSC 203884-X. (b) SEM image of lower zircon in (a). The grain is dominated by strongly zoned core material, although a poorly developed, very thin, clear, uranium-poor overgrowth as seen in (c) is present that partly truncates the core zonation. The scale bar is 20 m. GSC 203884-S. (c) SEM image of upper zircon in (a). Note the relatively thick, clear uranium-poor overgrowth on the strongly zoned core. The scale bar is 20 m. GSC 203884-R.

Sample 1

Three size fractions from the least magnetic zircon were analyzed, resulting in a poorly defined linear trend of data points (points 1-2, 1-3 and 1-5; Table 1, Fig. 5). In order to define more clearly the zircon systematics, tips and cores of zircon grains in the +74 micrometre, second least magnetic fraction were then separated by breaking individual grains with a sharp knife. The tips were moderately abraded and the cores extensively abraded (7 h) in order to remove as much as possible of the younger overgrowths. The resultant data points, 1-1 and 1-4 (Fig. 5), were collinear with the previously obtained points 1-2 and 1-3 (75% probability of fit), yielding concordia intercept ages of 2545 +14/-13 and 1929 ± 14 Ma. Fraction 1-5 falls below the chord thus defined. This may be due to secondary Pb loss, although its intermediate U content (298 ppm) does not distinguish it from the other fractions.

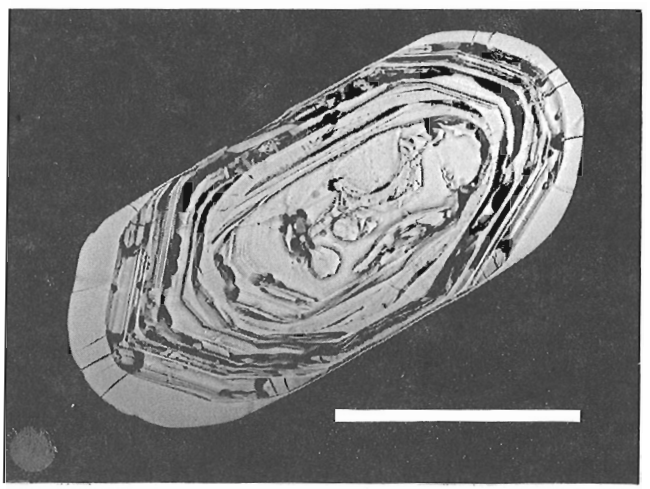

Figure 4. SEM image of a representative zircon from sample 1. The zircons are characterized by strongly zoned cores, which in some cases show periods of resorption subsequently followed by further deposition of zircon of varied uranium content. All have a final overgrowth of clear, uranium-poor zircon although its thickness is highly varied. The scale bar 100 m. GSC 203884-U.

Sample 2

Five zircon fractions were selected and analyzed from sample 2 (Table 1); two of these were cores and tips manually broken off and abraded in a similar fashion to those from sample 1. A third fraction (2-1) consisted of whole zircon grains from the most non-magnetic fraction, selected to visually exclude grains with cores.

The results of these three analyses are plotted on Figure 5. All fall in a linear array directly below the lower intercept of the chord defined by data from sample 1. The $^{207}Pb/^{206}Pb$ ages of fractions 2-1 and 2-2 (cores) agree with the 1929 Ma lower intercept age within analytical uncertainty, while that of fraction 2-3 (tips) is marginally lower at 1904.5 ± 3.7 Ma.

The two other fractions analyzed, 2-4 and 2-5, consisted of metamict cores that were probably broken from their attached tips during crushing of the rock. Results from these analyses are presented in Table 1 but fall outside the boundaries of Figure 5. Both are highly discordant and have $^{207}Pb/^{206}Pb$ ages greater than that of the sample 1 lower intercept age. Of particular interest is the $^{207}Pb/^{206}Pb$ age of fraction 2-5, 3302 Ma. Even though the common Pb content of this single zircon grain (core) is relatively high, no reasonable estimate of common Pb composition will change this $^{207}Pb/^{206}Pb$ age by more than 15 Ma.

Table 1. U-Pb isotopic data on zircon and monazite.

Sample Fraction	Weigth mg	U ppm	Pb* ppm	Measured $^{206}Pb/^{204}Pb$	Isotopic abundances ^{206}Pb = 100			Isotopic ratios		Age, Ma $^{207}Pb/^{206}Pb$
					^{204}Pb	^{207}PB	^{208}Pb	$^{206}Pb/^{238}U$	$^{207}Pb/^{235}U$	
Sample 1	63°10.6'		106°58.0'							
1.1 + 74 mo° CA	0.0276	540.6	257.6	6135	0.0114	15.55	12.17	0.43536	9.2496	2392
1.2 – 105 + 74 no°	0.0160	363.7	160.8	2434	0.0245	14.76	12.33	0.40793	8.1242	2281
1.3 – 62 no°	0.0080	181.3	75.99	997	0.0352	14.24	12.03	0.39087	7.4263	2200
1.4 + 74 mo° T	0.0221	353.1	143.6	4850	0.0100	13.50	10.78	0.38171	7.0354	2147
1.5 – 74 + 62 no°	0.0295	297.6	117.5	1433	0.0579	13.86	12.68	0.37035	6.6878	2111
1. monazite	0.0255	493.5	8001	5727	0.0017	11.67	5316	0.34435	5.5311	1903
1. monazite	0.0268	442.8	7194	3928	0.0088	11.78	5325	0.34415	5.5311	1904
Sample 2	63°02.1'		107°11.6'							
2.1 – 74 no°	0.0090	179.1	63.93	1736	0.0115	12.02	11.80	0.33660	5.5088	1937
2.2 + 74 mo° CA	0.0048	315.8	112.5	1774	0.0066	11.88	13.23	0.33184	5.3960	1925
2.3 + 74 mo° T	0.0174	275.7	94.54	907	0.0950	12.94	12.33	0.32997	5.3041	1904
2.4 – 74 mm C	0.0049	352.7	68.85	153	0.5190	19.82	42.34	0.16212	2.9136	2103
2.5 + 74 mm C	0.0249	355.8	185.2	268	0.3612	30.70	27.98	0.41915	15.565	3302

Numbered fractions are zircon
Fraction sizes are in micrometres
All zircon fractions are abraded, A = strong abrasion
no°, nonmagnetic at 0° slope
mo°, magnetic at 0° but nonmagnetic at 1° slope
mm, very magnetic
C = cores T = tips
Pb* radiogenic Pb
ppm

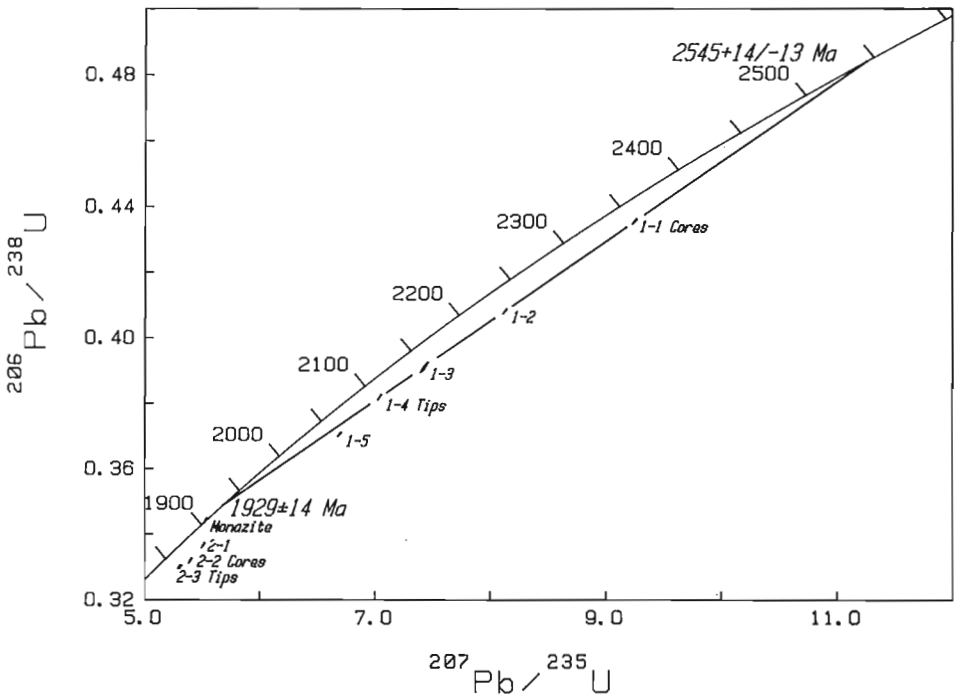

Figure 5. Concordia plot of zircon and monazite data from the two samples of the Campbell granite. The two sample 1 monazite data points are superimposed.

These results, when compared with those from fraction 2-2, indicate that there is more than one age of zircon core in sample 2. Fraction 2-2 was selected from the second most non-magnetic split; fractions 2-4 and 2-5 were selected from a much more magnetic portion. The cores concentrated in fractions 2-2 are not demonstrably different in age from the tips of fractions 2-3 or 1-4. The core of fraction 2-5, however, indicates an extremely old component (greater than 3300 Ma, possibly 3500 Ma?) in the Campbell granite at the location of sample 2.

Results from sample 1 suggest a single age of cores (2545 +14/-13 Ma), but these are also from a highly non-magnetic phase of zircon. Older cores may also be present in the more magnetic phases of this zircon concentrate as well.

Two monazite grains from sample 1 were also analyzed (Table 1, Fig. 2). The monazite results are marginally reversely discordant. Schärer (1984) has shown that the U decay series are not always in equilibrium in zircon, xenotime, and monazite at the time of formation of these minerals. ^{230}Th, a member of the ^{238}U/^{206}Pb decay chain, may be preferentially concentrated in monazite crystal lattices at the time of formation, owing to the affinity of monazite for Th. The decay of this excess ^{230}Th produces excess ^{206}Pb, which distorts the measured U-Pb age pattern, causing ^{238}U/^{206}Pb ages to be anomalously high and ^{207}Pb/^{206}Pb ages to be correspondingly low.

The relative differences between measured ^{207}Pb/^{206}Pb and ^{207}Pb/^{235}U ages (the latter unaffected by excess ^{206}Pb) are greatest in rocks that: (a) are young, (b) have high Th/U in the monazite, and (c) have low Th/U in the rock at the time of formation. The amount of ^{208}Pb expressed as a percentage of the total radiogenic monazite Pb may be used as an index of the monazite Th/U. For ages about 1900 Ma and for rocks with Th/U of 0.4 to 0.5, R.R. Parrish (pers. comm., 1988) has determined that the effect of ^{230}Th incorporation on ^{207}Pb/^{206}Pb age is likely to be less than 3 Ma for ^{208}Pb at about 80% but can be much greater than this for ^{208}Pb greater than 90%. In the two monazite grains measured, the ^{208}Pb is 98% of the radiogenic Pb; accordingly the true age of the monazite is not well defined. The two ^{207}Pb/^{235}U ages, 1905.4 ± 2.0 and 1905.4 ± 2.5 Ma, therefore provide a minimum age of 1903 Ma, but if recent Pb loss has occurred, the time of monazite closure may be as old as the zircon lower intercept age of 1929 ± 14 Ma.

DISCUSSION

The geochronological data from the first sample dated indicate that parts of a long history are recorded in the zircons of the granite. The position of the core data point (1-1) towards the upper intercept and the tip result (1-4) towards the lower intercept relative to the whole zircon analyses (1-2, 1-3) implies that Archean cores were overgrown by Proterozoic rims. Is the Campbell granite then an Archean pluton that has been metamorphosed to the extent that new zircon was grown at about 1929 Ma or are the older zircons mainly Archean xenocrysts caught up in an early Proterozoic pluton? Most of the zircons examined in the two samples analyzed, as well as those seen in thin section of other samples of the unit, have a generally similar morphology, consisting of a more strongly zoned inner core and a variably developed overgrowth of clear, unzoned, uranium-poor zircon. In particular, the occurrence of zircons with this clear overgrowth within the K-spar megacrysts (Fig. 3) would indicate that the overgrowth either predated or was synchronous with the growth of the megacrysts.

Whether or not the megacrysts are primary igneous phenocrysts or porphyroblasts due to later metasomatic or metamorphic events is critical as far as understanding the history of the granite is concerned. Vernon (1986) has presented several arguments favouring the interpretation of megacrysts in granitic rocks as igneous phenocrysts. Those applicable to the deformed Campbell granite include the presence within the megacryst of euhedral to subhedral inclusions of other minerals, typically smaller than the matrix of the least deformed granite, that are oriented parallel to crystallographic directions within the K-spar megacryst. It seems less likely that megacrysts containing inclusions of this size, morphology, and orientation could form metasomatically or metamorphically as porphyroblasts within a previously crystallized rock. Thus we suggest that the Campbell granite was more probably derived from a melt that initially crystallized during early Proterozoic time and which contained Archean zircon xenocrysts.

The fact that the first sample analyzed is essentially a mylonite is of some concern. It is conceivable that the zircons in sample 1 (cores and rims) were entirely of Archean age, but that during the course of subsequent mylonitization and the passage through the shear zone of fluids of moderate temperature, the zircons, or at least their outer margins, could have became open systems as far as U and Pb were concerned (in the sense of Gebauer and Grünenfelder, 1976). Given the degree of fracturing of the porphyoclasts these fluids could affect both the zircon within the feldspar as well as that in the matrix. The lower intercept age could then represent the age of deformation.

In order to test this possibility the second sample was analyzed, a sample that although deformed had not been exposed to as severe deformational conditions as the mylonite. The lower intercept age of 1929 $\pm$ 14 Ma from sample 1 is supported by the $^{207}Pb/^{206}Pb$ ages of several zircon fractions from sample 2 and is interpreted as dating the emplacement of the Campbell granite. $^{207}Pb/^{206}Pb$ ages of zircon cores range from 1925 to 3302 Ma (Table 1), supplementing the sample 1 intercept (i.e., zircon core) age of 2545 +14/-13 Ma. These results indicate that some strongly zoned, igneous zircon cores consist of inherited zircon of variable age, even as old as early Archean, whereas other, albeit on the whole less strongly zoned, igneous cores (fraction 2.2) appear to have formed essentially contemporaneously with the zircon tips.

This latter result confirms the interpretation of the sample 1 lower intercept (i.e., zircon tip) age as the age of plutonic emplacement. Deformation either followed the intrusion of the body so closely in time that any effects of the deformation on the zircon systematics are not resolvable or, if the deformation was significantly later, took place under conditions of temperature and fluid composition such that the influence on zircon was minimal.

Taken at face value, the 1929 Ma Campbell granite is towards the young end of the spectrum of Proterozoic granitoid ages identified in the Thelon Tectonic Zone to date; the other granites north of the McDonald fault are in the range 1910 - 2000 Ma (van Breemen et al., 1987a,c; van Breemen and Henderson, 1988; James et al., 1988; Frith and van Breemen, 1990). It is possible, however, that zircon fractions 1-2 to 1-4 have suffered minor secondary Pb loss, in which case the lower intercept age would be marginally lower than the true age of emplacement.

The Campbell granite is the first Proterozoic Thelon Tectonic Zone granite in which the zircons show a clearly expressed Archean memory. Zircon from some other granitoid units to the north of the fault may have an older component, but there is no indication that this component, as expressed by the U-Pb systematics, is as old as Archean (van Breemen et al., 1987a,c, 1988; James et al., 1988). On the other hand, south of the McDonald fault there is accumulating evidence indicating the presence of an ancient component near the Campbell granite. E. Hegner (pers. comm., 1989) has determined Nd model ages of 3.45 Ga and 3.6 Ga for granitoid gneisses 30 km east-southeast of the Campbell granite sample localities, which may represent the southern extension of the Archean Queen Maude Block across the McDonald fault. Van Breemen et al. (1990) report an Archean granite in the Great Slave Lake shear zone (Fig. 1) 130 km to the west-southwest of the sampled localities of the Campbell granite.

ACKNOWLEDGMENTS

J.K. Mortensen is thanked for his help in collecting sample 2, and M. Villeneuve and D. Walker are thanked for their help in the SEM photomicrography. An earlier version of this paper was critically reviewed by R.R. Parrish, Mikkel Schau, and O. van Breemen; the current one was reviewed by R.R. Parrish and O. van Breemen.

REFERENCES

Bostock, H.H. and Loveridge, W.D.
1988: Geochronology of the Taltson Magmatic Zone and its eastern cratonic margin, District of Mackenzie; in Radiogenic Age and Isotopic Studies: Report 2; Geological Survey of Canada, Paper 88-2, p. 59-65.

Bostock, H.H., Van Breemen, O., and Loveridge, W.D.
1987: Proterozoic geochronology in the Taltson Magmatic Zone, N.W.T.; in Radiogenic Age and Isotopic Studies: Report 1; Geological Survey of Canada, Paper 87-2, p. 73-80.

Davis, D.
1982: Optimum linear regression and error estimation applied to U-Pb data; Canadian Journal of Earth Sciences, v. 19, p. 2141-2149.

Frith, R.A. and van Breemen, O.
1990: U-Pb zircon age of the Himag plutonic suite, Thelon Tectonic Zone, Churchill Structural Province, Northwest Territories; in Radiogenic Age and Isotopic Studies: Report 3; Geological Survey of Canada, Paper 89-2 (this publication).

Gebauer, D. and Grünenfelder, M.
1976: U-Pb zircon and Rb-Sr whole-rock dating of low-grade metasediments. Example: Montagne Noire (southern France); Contributions to Mineralogy and Petrology, v. 59, p. 13-32.

Henderson, J.B.
1989: Geology, Artillery Lake, District of Mackenzie, N.W.T.; Geological Survey of Canada, Open File 2010.

Henderson, J.B., McGrath, P.H., James, D.T., and Macfie, R.I.
1987: An integrated geological, gravity and magnetic study of the Artillery Lake Area and the Thelon Tectonic Zone, District of Mackenzie; in Current Research, Part A; Geological Survey of Canada, Paper 87-1A, p. 803-814.

Henderson J.B. and Macfie, R.I.
1985: The northern Artillery Lake map area: a transect across the Thelon Front, District of Mackenzie; in Current Research, Part A; Geological Survey of Canada, Paper 85-1A, p. 441-448.

James, D.T., van Breemen, O., and Loveridge, W.D.
988: Early Proterozoic U-Pb zircon ages for granitoid rocks from the Moraine Lake transect, Thelon Tectonic Zone, District of Mackenzie; in Radiogenic Age and Isotopic Studies: Report 2; Geological Survey of Canada, Paper 88-2, p. 67-72.

Schärer, U.
1984: The effect of initial ^{230}Th equilibrium on young U-Pb ages: the Makalu case, Himalayas; Earth and Planetary Science Letters, v. 67, p. 191-204.

Thomas, M.D., Gibb, R.A., and Quince, J.R.
1976: New evidence from offset aeromagnetic anomalies for transcurrent faulting associated with the Bathurst and McDonald faults, Northwest Territories; Canadian Journal of Earth Sciences, v. 13, p.1244-1250.

van Breemen, O., Hanmer, S.K. and; Parrish, R.R.
1990: Archean and Proterozoic mylonites along the southeastern margin of the Slave Structural Province, N.W.T.; in Radiogenic Age and Isotopic Studies: Report 3; Geological Survey of Canada, Paper 89-2, (this publication)

van Breemen, O., Henderson, J.B., Loveridge, W.D., and Thompson, P.H.
1987a: U-Pb zircon and monazite geochronology and zircon morphology of granulites and granite from the Thelon Tectonic Zone, Healey Lake and Artillery Lake map areas, N.W.T.; in Current Research, Part A; Geological Survey of Canada, Paper 87-1A, p. 873-801.

van Breemen, O., Henderson, J.B., Sullivan, R.W., and Thompson, P.H.
1987b: U-Pb, zircon and monazite ages from the eastern Slave Province, Healey Lake area, N.W.T.; in Radiogenic Age and Isotopic Studies: Report 1; Geological Survey of Canada, Paper 87-2, p. 101-110.

van Breemen, O., Thompson, P.H., Hunt, P.A., Culshaw, N.
1987c: U-Pb zircon and monazite geochronology from the northern Thelon Tectonic Zone, District of Mackenzie; in Radiogenic Age and Isotopic Studies: Report 1; Geological Survey of Canada, Paper 87-2, p. 81-93.

van Breemen, O. and Henderson, J.B.
1988: U-Pb zircon and monazite ages from the eastern Slave Province and Thelon Tectonic Zone, Artillery lake area, N.W.T.; in Radiogenic Age and Isotopic Studies: Report 2; Geological Survey of Canada, Paper 88-2, p.73-83.

Vernon, R.H.
1986: K-feldspar megacrysts in granites — phenocrysts, not porphyroblasts; Earth-Science Reviews, v. 23, p. 1-63.

Wright, G.M.
1967: Geology of the southeastern barren grounds, parts of Mackenzie and Keewatin; Geological Survey of Canada, Memoir 350, 91p.

Pre-Missi granitoid domes in the Puffy Lake area, Kisseynew gneiss belt, Manitoba

P.A. Hunt[1] and H.V. Zwanzig[2]

Hunt, P.A. and Zwanzig, H.V., Pre-Missi granitoid domes in the Puffy Lake area, Kisseynew gneiss belt, Manitoba; in Radiogenic Age and Isotopic Studies: Report 3, Geological Survey of Canada, Paper 89-2, p. 71-75 1990.

Abstract

Foliated and gneissic granitoid rocks in the Kisseynew gneiss belt near Puffy Lake, Manitoba, intrude high-grade mafic to felsic rocks tentatively correlated with the 1.86 Ga Amisk Group of the Flin Flon metavolcanic belt. The intrusive granite gneiss and its country rocks are interpreted to be unconformably overlain by metasedimentary and metavolcanic rocks correlated with the 1.83 Ga Missi Group.

Highly deformed tonalite and granite gneisses yield U-Pb zircon concordia upper intercept ages of 1892 +66/-25 Ma and 1873 ± 4 Ma respectively. These ages are consistent with the proposed lithological correlations and support the existence of the proposed unconformity.

Résumé

Des roches granitoïdes fenilletées et gneissiques de la zone de gneiss de Kisseynew, située à proximité du lac Puffy, au Manitoba, pénétrent des roches de nature fortement mafique à felsique qu'on a corrélées, de façon expérimentale, avec le groupe d'Amisk âgé de 1,86 Ga de la zone métavolcanique de Flin Flon. D'après les auteurs, les roches métasédimentaires et métavolcaniques, corrélées avec le groupe de Missi vieux de 1,83 Ga, recouvrent en discordance le gneiss granitique intrusif et ses roches encaissantes.

Les gneiss à tonalite et les gneiss granitiques, fortement déformés, ont donné au moyen de la méthode U-Pb appliquée au zircon, des âges supérieurs de 1892 + 66/−25 Ma et de 1873 ± 4 Ma sur la courbe concordia. Ces âges correspondent aux corrélations lithologiques proposées et corroborent l'existence de la discordance proposée.

INTRODUCTION

During remapping of Early Proterozoic rocks along the boundary between the Kisseynew gneiss belt and the Flin Flon volcanic belt near Puffy Lake, in northern Manitoba, the contact between sedimentary gneisses of the Missi Suite and granitoid gneisses was interpreted as an unconformity; however, an intrusive relationship could not be ruled out because the contact is sheared (Zwanzig, 1984, 1988). The country rocks of the gneisses were tentatively correlated with the Amisk Group. Previous U-Pb geochronology has yielded ages of 1890 +6/-8 Ma for similar granitiod gneisses in the Herblet Lake dome, 70 km east of Puffy Lake, 1886 ± 2 Ma for Amisk Group metarhyolite from the Flin Flon area, and 1832 ± 2 Ma for rhyolitic meta-ignimbrite within the Missi Group at Wekusko Lake (Gordon et al., 1987, and in press). The high-grade Missi Suite at Puffy Lake has been correlated with the dated, lower grade Missi Group, but the age of the granitoid gneisses and their country rocks are uncertain.

GRANITOID ROCKS

The granitoid rocks comprise a tonalitic phase west of Puffy Lake Mine and a granitic phase to the northeast (Fig.1). These phases are respectively in the foot-wall and the hanging wall of the gold deposit, because the contacts dip to the northeast at moderate angles.

1 Geological Survey of Canada, 601 Booth Street, Ottawa, Ontario, K1A 0E8
2 Manitoba Energy and Mines, 535-330 Graham Avenue, Winnipeg, Manitoba R3C4E3

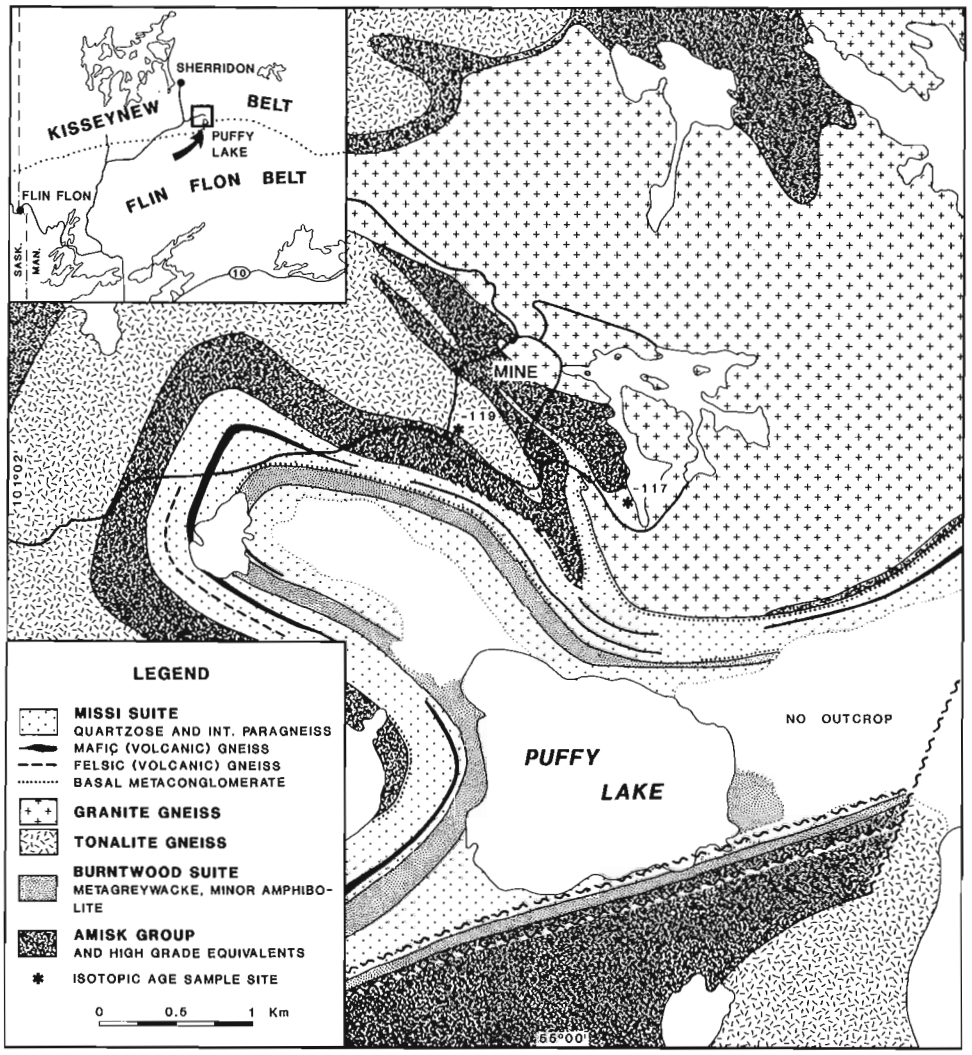

Figure 1. U-Pb zircon sample locations and simplified geology of the Puffy Lake area, Manitoba.

Table 1. U-Pb zircon results.

Fraction,[1] Size	Weight (mg)	U (ppm)	pb[2] (ppm)	$^{206}Pb/^{204}Pb$[3]	Pb_c[4] (pg)	^{208}Pb[2] (%)	$^{206}Pb/^{238}U$ ±SEM%[5]	$^{207}Pb/^{235}U$ ±SEM%[5]	$^{207}Pb/^{206}U$ ±SEM%[5]	$^{207}Pb/^{206}Pb$ age, error (Ma)[6]
Tonalite Gneiss (FQ-86-SH-119) (5502'N, 10059'W)										
A -74+62 NM1 abr	0.0123	134.5	44.1	3041	11	7.3	0.31782 (.10)	4.9439 (.12)	0.11282 (.04)	1845.4 (1.5)
B -105+74 NM1 abr	0.0173	363.7	121.3	10040	13	7.8	0.32122 (.09)	5.0168 (.10)	0.11327 (.03)	1852.5 (1.1)
C -149+105 NM1 abr	0.0207	442.5	144.7	10470	18	6.7	0.31883 (.08)	4.9776 (.10)	0.11322 (.03)	1851.9 (1.1)
D -149+105 NM0 abr	0.0091	360.8	122.0	8606	8	10.0	0.31754 (.09)	4.9961 (.10)	0.11411 (.03)	1865.9 (1.1)
E -149+105 NM0 abr	0.0155	373.0	129.8	1041	116	9.7	0.32807 (.09)	5.1678 (.15)	0.11425 (.10)	1868.1 (3.5)
Granite Gneiss (FQ-86-SH-117) (55°2'N, 10°58'W)										
A +74 NM1 abr	0.0193	736.3	242.7	7493	37	8.6	0.31450 (.09)	4.8986 (.10)	0.11296 (.03)	1847.7 (1.1)
B -62 NM1 abr	0.0108	800.5	277.1	5893	30	9.6	0.32639 (.09)	5.1179 (.10)	0.11372 (.03)	1859.8 (1.1)
C -74+62 NM1 abr	0.0150	694.9	240.4	6366	34	9.4	0.32711 (.09)	5.1424 (.10)	0.11402 (.03)	1864.4 (1.1)
D -74+62 NM1 abr	0.0095	374.5	127.0	585	126	10.0	0.31874 (.12)	4.9886 (.22)	0.11351 (.16)	1856.4 (5.7)
E -74 NM0 abr	0.0128	980.0	345.6	9796	27	10.5	0.32919 (.08)	5.1742 (.10)	0.11400 (.03)	1864.1 (1.1)
F +74 NM0 abr	0.0099	954.2	333.6	15880	12	9.4	0.33055 (.08)	5.2013 (.10)	0.11412 (.03)	1866.1 (1.0)

Notes: [1]sizes (-74+62) refer to length aspect of zircons in microns (i.e., through 74 micron sieve but not the 62 micron sieve); abr=abraded, NM1=non-magnetic cut with frantz at 1 degree side slope, Mag0=magnetic cut with frantz at 0 degree side slope; [2]radiogenic Pb;[3]measured ratio, corrected for spike and fractionation; [4]total common Pb in analysis corrected for fractionation and spike; [5]orrected for blank Pb and U, common Pb, errors quoted are one sigma in percent; [6]corrected for blank and common Pb, errors are two sigma in Ma; decay constants used are those of Steiger and Jager (1977); initial common Pb composition from Stacey and Kramers (1975); for analytical details see Parrish et al. (1987).

The tonalite gneiss is uniformly grey or weakly layered; a strong planar and linear fabric is common, especially at the margins of the body. An average mode consists of plagioclase (53%), quartz (27%), biotite plus minor hornblende (16%), potash-feldspar (4%), traces of apatite and magnetite, and secondary muscovite and calcite. The average grain size is 1-10 mm, with grains forming elongate aggregates that obliterate most primary igneous textures.

The granite gneiss forms large pink-weathering outcrops. The average mineral content is quartz (39%), plagioclase (30%), potash-feldspar (24%), and biotite (7%). It is slightly coarser grained than the tonalite gneiss. The quartz grains are flattened and the plagioclase is partly altered to white mica.

COUNTRY ROCKS OF THE GNEISSES

Both phases of gneiss intrude fine-grained amphibolite and minor felsic gneiss, which are interpreted as volcanic rocks, and mafic to felsic gneiss interpreted as sedimentary rocks (Zwanzig, 1984, 1988). These older rocks are tentatively correlated with the Amisk Group, which outcrops south of Puffy Lake. The contact between the two metaplutonic phases is not known for a screen of country rock generally separates them.

BURNTWOOD SUITE

Adjacent to Puffy Lake, undated graphitic garnet-biotite gneiss, derived from greywacke-mudstone turbidite (Bailes, 1980), and minor amphibolite occupy a narrow core of an early anticline, which has been refolded into a prominent S-shaped structure. These rocks have been assigned to the Burntwood Suite, which is probably equivalent to the Amisk Group, but their relationship to the granitoid gneiss is unknown.

MISSI SUITE

The Missi Suite contains mainly quartzofeldspathic gneisses, which are derived from sandstones with subordinate metabasalt and possible metarhyolite. A basal metaconglomerate is preserved north and west of Puffy Lake, but elsewhere conglomerate is generally absent or was deformed to ribbon gneiss. The conglomerate is in contact with the Amisk Group, the Burntwood Suite, and the granite gneiss. Consequently, the contact was interpreted as an unconformity (Zwanzig, 1984, 1988). This contact is folded; it is structurally upright in some localities within two sets of major folds, and is inverted in others.

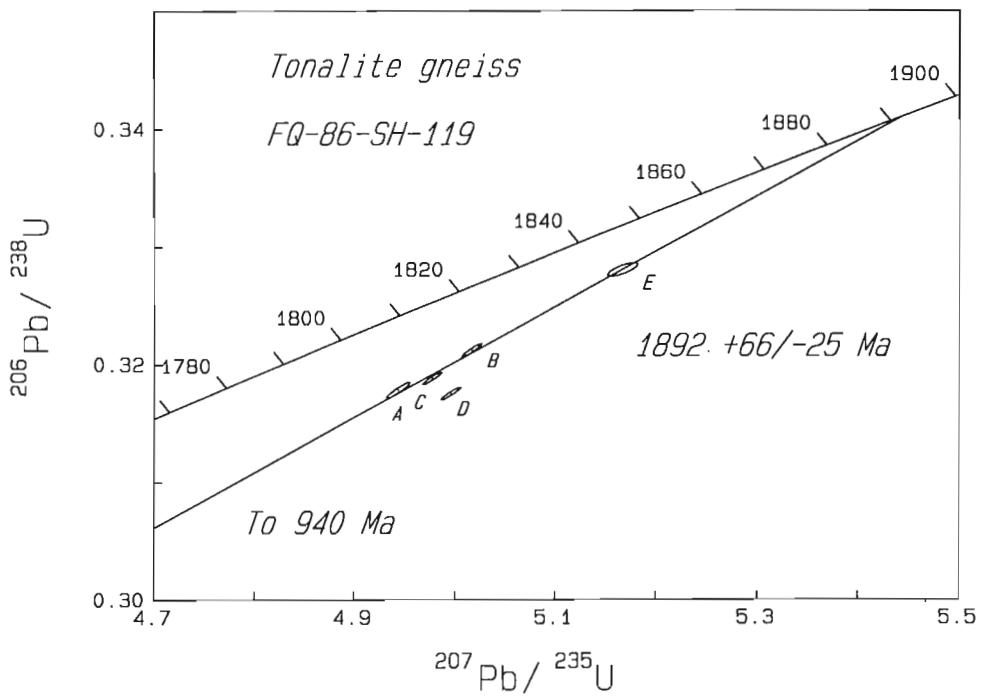

Figure 2. Concordia diagram showing the results of U-Pb analyses of zircon fractions from the tonalite gneiss (FQ-86-SH-119). Note that fraction D is not included in the regression.

U-Pb ZIRCON GEOCHRONOLOGY

Analytical methods followed those outlined by Parrish et al. (1987). U and Pb blanks during this study varied from 3 to 8 pg for U and 8 to 18 pg for Pb. Analytical results are given in Table 1.

Zircons separated from the tonalite gneiss were generally colourless, fractured, with 30% inclusions. Distinct igneous zoning is evident in plain polarized light in most grains. The diameter of individual grains ranges from 40 to 150 microns. The zircons are generally euhedral with well defined but slightly rounded terminations. The L:B ratio varied from 2:1 to 3:1, and the uranium contents of the zircons ranged from 130-400 ppm. All zircon fractions were abraded (Krogh, 1982).

Five zircon analyses range from 7 to 13% discordant (Fig. 2). A modified York (1969) regression (Parrish et al., 1987) on fractions A,B,C, and E yielded an upper intercept of 1892 +66/-25 Ma, a lower intercept of 940 Ma and a MSWD of 12 (Fig. 2). Fraction D was not included in the regression. It falls below the line owing to possible slight inheritance.

The upper intercept of 1.89 Ga is interpreted as the age of igneous crystallization of the tonalite gneiss.

Zircons separated from granite gneiss were colourless to light brown; clarity is poor because of zoning, internal fractures, and abundant inclusions. Cores are visible in some grains and these were avoided in the final selection. The crystals were euhedral and prismatic, with slighty rounded terminations. The L:B ratio was generally 2:1. Etched grains mounts reveal strong igneous zoning. Uranium content is high and ranges from 400 to 1000 ppm.

A modified York regression of fractions A,B,C,E, and F yields an upper intercept of 1873 $\pm$ 4 Ma and a lower intercept of 602 Ma, with a MSWD of 9 (Fig. 3). The analysis of fraction D is relatively imprecise owing to a high common lead content and was not included in the regression.

The upper intercept of 1873 Ma is interpreted as the age of igneous crystallization of the granite gneiss.

DISCUSSION

The pre-Missi ages of the granitoid gneisses support the unconformable relationship between the granite gneiss and the Missi Suite. The ages are also consistent with the interpretation that the fine-grained amphibolite and related rocks, intruded by the gneisses, are equivalent to the Amisk Group, although they could also be older. The age of the granitoid gneisses is close to that of the Amisk Group. This implies that the protolith may have been a synvolcanic intrusion into its own cover, a hypothesis that is consistent with the general absence of older rocks in the Flin Flon and Kisseynew belts, but which needs further testing.

The granitoid gneisses at Puffy Lake are part of a suite of orthogneisses that occur throughout the southern part of the Kisseynew belt. Individual bodies are, on average, 15 km long and occupy closed domal structures and recumbent sheath folds. They are complexes of highly deformed, metamorphosed intrusions, similar in age and composition to less deformed, composite intrusions in the Flin Flon belt. The bodies at Puffy Lake and Herblet Lake predate the Missi Suite, but some bodies (magnetite-biotite monzogranite of Schledewitz, 1987) appear to be younger and to have inclusions of Missi Suite rocks.

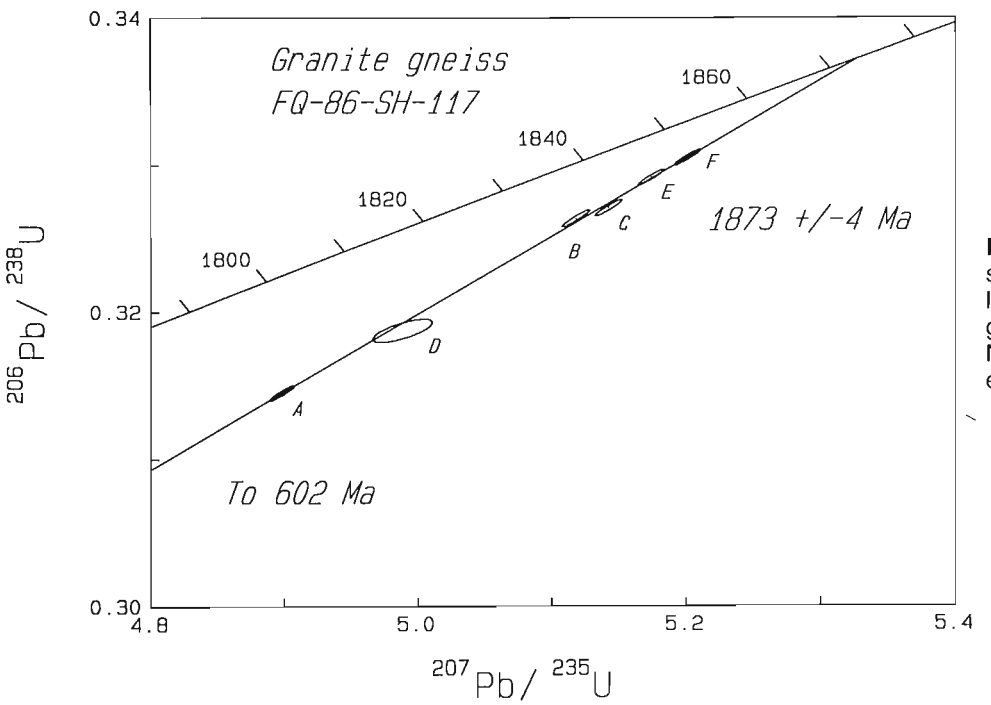

Figure 3. Concordia diagram showing the results of U-Pb analyses of zircon fractions from the granite gneiss (FQ-86-SH-117). Note that fraction D is not included in regression.

ACKNOWLEDGMENTS

Samples of the tonalite gneiss (FQ-86-SH-119) and granite gneiss (FQ-86-SH-117) were provided by S. Blussom of Pioneer Metals after discussion with E. Froese (Geological Survey of Canada) and T.M. Gordon (University of Calgary); their contribution is gratefully acknowledged.

REFERENCES

Bailes, A.H.
1980: Geology of the File Lake area; Manitoba Department of Energy and Mines, Mineral Resources Division, Geological Report GR78-1, 134p.

Gordon, T.M., Hunt, P.A., Bailes, A.H. and Syme, E.C.
In press: U-Pb ages from the Flin Flon and Kisseynew belts, Manitoba: Chronology of Early Proterozoic crust formation; in Geological Association of Canada, Special Paper J.F. Lewry and M.R. Stauffer; The Early Proterozoic Trans-Hudson Orogened.

Gordon, T.M., Hunt, P.A., Loveridge, W.D., Bailes, A.H. and Syme, E.C.
1987: U-Pb zircon ages from the Flin Flon and Kisseynew belts, Manitoba: chronology of early Proterozoic crust formation; Geologic Association of Canada - Mineralogical Association of Canada Joint Annual Meeting, Program with Abstracts, v. 12, p. 48.

Krogh, T.E.
1982: Improved accuracy of U-Pb zircon ages by the creation of more concordant systems using an air abrasion technique; Geochimica et Cosmochimica Acta, v. 96, p. 673-649.

Parrish, R.R., Roddick, J.C., Loveridge, W.D., and Sullivan, R.W.
1987: Uranium-lead analytical techniques at the Geochronology Laboratory, Geological Survey of Canada; in Radiogenic Age and Isotopic Studies: Report 1; Geological Survey of Canada, Paper 87-2, p. 3-7.

Schledewitz, D.C.P.
1987: Kisseynew Project: Kississing Lake; in Report of Field Activities 1987; Manitoba Energy and Mines, Minerals Division, p. 51-54.

Stacey, J.S. and Kramers, J.D.
1975: Approximation of terrestrial lead isotope evolution by a two stage model; Earth and Planetary Science letters, v. 26, p. 207-221.

Steiger, R.H. and Jäger, E.
1977: Submission on geochronology: Convention on the use of decay constants in geochronology and cosmochronology; Earth and Planetary Science Letters, v. 36, p. 359-362.

York, D.
1969: Least squares fitting of a straight line with correlated errors; Earth and Planetary Science Letters, v. 5, p. 320-324.

Zwanzig, H.V.
1984: Kisseynew Project: Lobstick Narrows-Cleunion Lake, Puffy Lake and Nokomis Lake areas; in Report of Field Activities 1984; Manitoba Energy and Mines, Mineral Resources, Minerals Division, p. 38-45.
1988: Kisseynew Project: Batty Lake Region; in Report of Field Activities 1988; Manitoba Energy and Mines, Minerals Division, p. 49-52.

A Rb-Sr study of granitic rocks associated with the Fostung scheelite deposit, Espanola, Ontario

W.D. Sinclair[1] and R.J. Theriault[1]

Sinclair, W.D. and Theriault, R.J., A Rb-Sr study of granitic rocks associated with the Fostung scheelite deposit, Espanola, Ontario; in Radiogenic Age and Isotopic Studies: Report 3, Geological Survey of Canada, Paper 89-2, p. 77-84, 1989.

Abstract

A Rb-Sr study of granitic rocks from the Fostung tungsten skarn deposit near Espanola, Ontario, has yielded an errorchron age of 1390 ± 26 Ma, initial Sr ratio of 0.71448 ± 0.00271, and MSWD of 6.15. The age of the granitic rocks and the associated tungsten deposit supports their correlation with anorogenic magmatism that was widespread throughout the mid-continent of North America about 1300 to 1500 Ma ago.

Résumé

Une étude du rapport Rb-Sr de roches granitiques provenant du gisement de skarn à tungstène de Fostung situé près d'Espanola, en Ontario, a donné un âge errochrone de 1390 ± 26 Ma, avec un rapport de strontium originel de 0,71448 ± 0,00271 et une (déviation moyenne du poids normal) de 6,15. L'âge des roches granitiques et du gisement de tungstène associé vient à l'appui de leur corrélation avec un magmatisme anorogénique qui était répandu dans toute la partie centrale du continent nord-américain il y a 1300 Ma à 1500 Ma.

INTRODUCTION

The Fostung deposit southeast of Espanola, Ontario, consists of scheelite-bearing skarn developed in calcareous sedimentary rocks of the Espanola Formation. It is unique in that it is perhaps the only significant tungsten-bearing skarn deposit in Proterozoic rocks in the Canadian Shield. The skarn and associated tungsten mineralization have been attributed to nearby intrusions of Nipissing diabase (e.g., Card, 1976). However, they are more likely related to granitic rocks that underlie the skarn deposit and which have been intersected locally as dykes in drill holes. K-Ar dating of muscovite from these granitic rocks yielded a Mid-Proterozoic age of 1427 ± 26 Ma (GSC 88-77; Hunt and Roddick, 1988). The Rb-Sr isotopic analysis of the granitic rocks associated with the skarn confirms the Mid-Proterozoic age of these rocks and supports their correlation with an episode of widespread anorogenic granite plutonism that occurred in the mid-continent of North America about 1300 to 1500 Ma ago.

REGIONAL GEOLOGY

The Fostung deposit is hosted by metasedimentary rocks of the Huronian Supergroup within the Southern Structural Province of the Canadian Shield (Fig. 1). These rocks, lie unconformably on Archean rocks, which are exposed to the northwest, and are bounded by the Grenville Front Tectonic Zone to the southeast. The Huronian strata are folded and faulted and have been intruded by a variety of igneous rocks. The oldest intrusive rocks are the Nipissing Diabase dykes and sills, a sample of which was recently dated at 2219.4 +3.6/-3.5 Ma by U-Pb isotopic analysis of baddeleyite (Corfu and Andrews, 1986; Krogh et al., 1988). A younger diabase dyke, belonging to the Sudbury dyke swarm, was dated at 1238±4 Ma by similar methods (Krogh et al., 1988). Felsic and mafic-felsic intrusions dated by Rb-Sr isotopic analysis include the Cutler granite (about 1750 Ma old, Wetherill et al., 1960), felsic plutons along the Grenville Front Tectonic Zone (about 1500-1800 Ma old, Fairbairn et al., 1969; Krogh and Davis, 1969), the Mongowin

1 Geological Survey of Canada, 601 Booth Street, Ottawa, Ontario K1A 0E8

ultramafic-trondjhemitic plutonic complex (1770 ± 75 Ma old, Van Schmus, 1971), the Croker Island Complex (1475 ± 50 Ma old, Van Schmus, 1965), and buried plutons on Manitoulin Island (1500 ± 20 Ma old, Van Schmus et al., 1975). These intrusive rocks represent stages of mid- to late-Proterozoic anorogenic magmatic activity that extended throughout much of the midcontinent of North America (Anderson, 1983).

TUNGSTEN-BEARING SKARN AND ASSOCIATED GRANITIC ROCKS

The general geology of the Fostung property is outlined on Figure 2. Tungsten-bearing skarn zones occur within a calcareous siltstone member of the Espanola Formation (Ginn and Beecham, 1986). The mineralogy of the skarns, described by Wilson (1982), is similar to that of tungsten-bearing skarns worldwide (Einaudi et al., 1981). Three types of skarn are present: 1) *pale green skarn* consists of quartz and feldspar with lesser amounts of tremolite, clinopyroxene, epidote, and clinozoisite; 2) *dark green skarn* is characterized mainly by actinolite with various mounts of quartz, feldspar, and chlorite; and 3) *garnet-bearing skarn* contains garnet (predominantly grossularitic), epidote, clinopyroxene, quartz, feldspar, and, in places, vesuvianite. Biotite hornfels separates and surrounds the skarn types.

Scheelite and molybdoscheelite are the principal tungsten minerals. They are most abundant in the garnet-bearing skarn and are commonly accompanied by pyrrhotite and minor chalcopyrite. Molybdenite also occurs in the skarn zones, but its distribution is erratic and does not correlate with that of tungsten. Other minerals that occur locally in the skarns include pyrite, sphalerite, bismuth, bismuthinite, arsenopyrite, stannite, fluorite, rutile, gold, and silver.

Intrusive rocks exposed at surface on the Fostung property include a sill of Nipissing Diabase, porphyritic diabase dykes related to the Sudbury dyke swarm, and an unusual unit of albitite and associated albitic breccias (Fig. 2). Adjacent to skarn, the Nipissing Diabase locally contains disseminated pyrrhotite and minor amounts of chalcopyrite and scheelite, and thus predates or is at least as old as the skarn. The porphyritic diabase dykes crosscut the skarn and

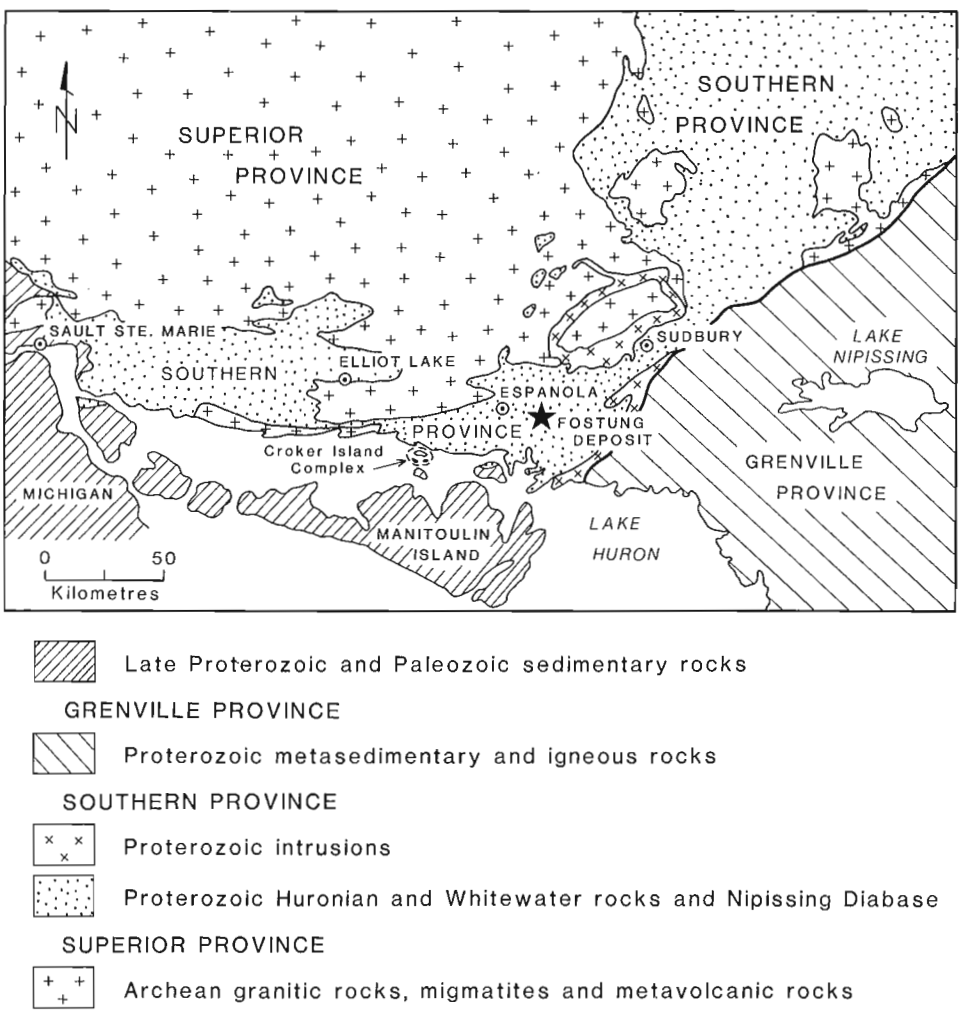

Figure 1. Regional setting of the Fostung deposit (modified after Card, 1978).

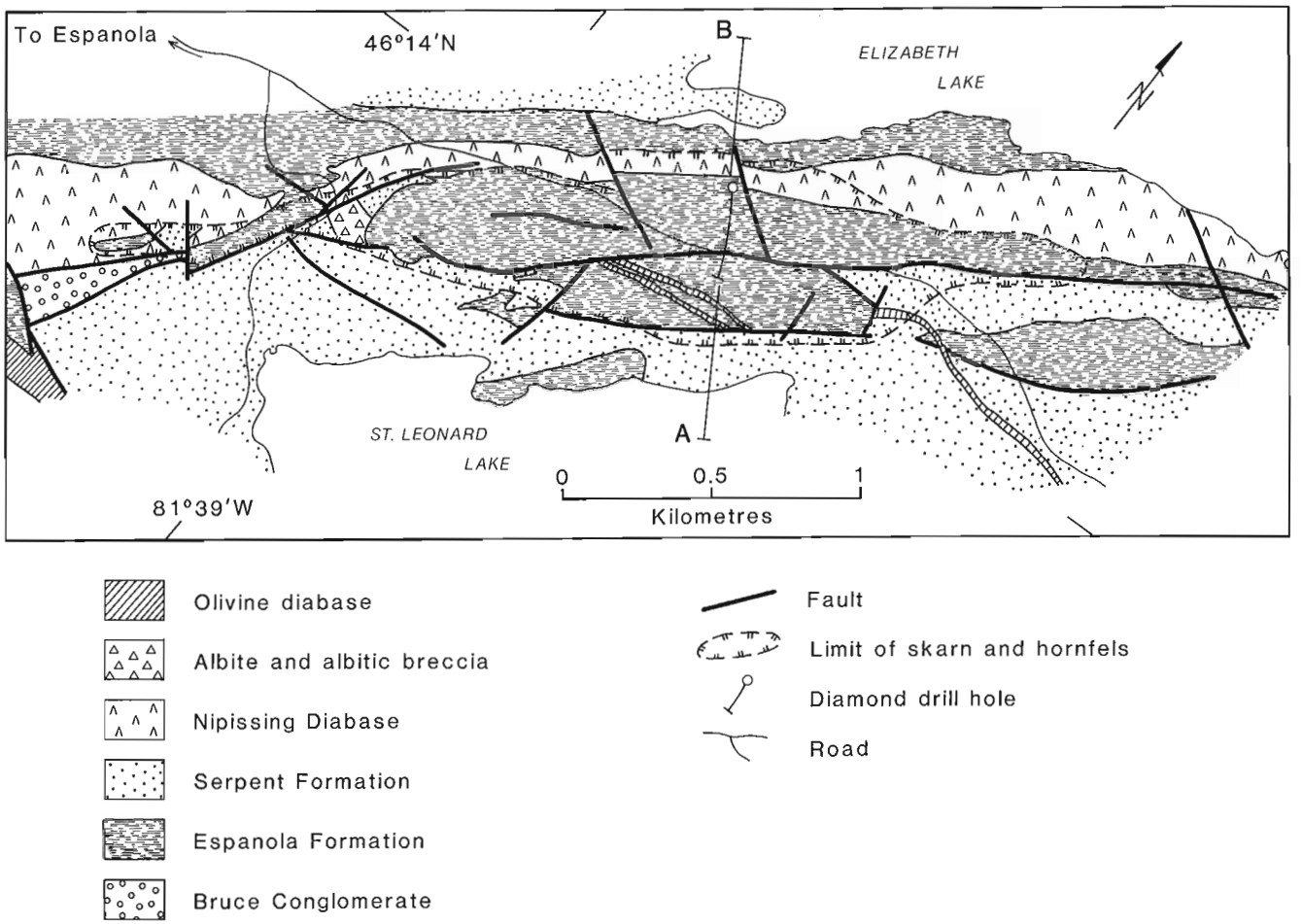

Figure 2. General geology of the Fostung deposit (modified after Ginn and Beecham, 1986).

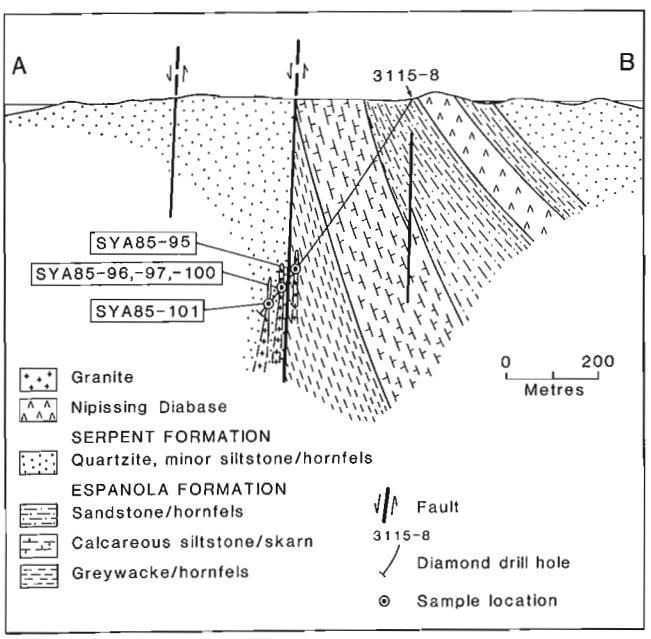

Figure 3. Cross-section A-B through the Fostung deposit showing the location of the samples analyzed in this study (modified after Ginn and Beecham, 1986).

are unmineralized; they thus appear to postdate formation of the skarn. Fragments of scheelite-bearing skarn in the albitic breccias suggest that the albitite also postdates formation of the tungsten-bearing skarn (Wilson, 1982). The absolute age of the albitite unit, however, is unknown.

Granitic rocks have not been found exposed at surface on the Fostung property but narrow dykes of felsic granitic rocks have been intersected in drill holes. Three such dykes, ranging from 0.5 to 4 m in width, were encountered in Sulpetro Minerals Ltd. drill hole 3115-8 (Fig. 3). One of the dykes consists of quartz-feldspar porphyry, the others are of fine-grained, equigranular granite. All of the granitic rocks are similar mineralogically, consisting of 35 to 40% quartz, 35 to 40% K-feldspar, 15 to 20% albite, and 2 to 5% muscovite.

The granitic rocks are altered in places, evident mainly by the replacement of albite, and to a lesser extent K-feldspar, by fine-grained sericite and carbonate. In other places, as much as 20% of the granite is replaced by clusters of medium-grained muscovite. Altered granite contains disseminated pyrite and locally trace amounts of molybdenite and sphalerite. One narrow granitic dyke contains 0.5% WO3 (Ginn and Beecham, 1986). The granitic dykes are, therefore, at least as old as the tungsten-bearing skarn zones and are probably genetically related. The dykes are too small,

however, to have been directly responsible for skarn formation; larger, related plutons at depth are more likely responsible for the formation of the skarns and associated mineralization.

The four whole-rock samples and one muscovite separate used in this study were collected from the only available drill hole that intersected the granitic rocks (Fig. 3). Detailed descriptions of these samples are given in the Appendix. Three of the four whole-rock samples analyzed appeared relatively unaltered in hand specimen, but in thin section feldspar grains in these three samples are seen to be weakly altered to sericite. This alteration represents weak hydrothermal alteration and may be deuteric in origin. Sample 85-101, on the other hand, is a more intensely altered rock in which sericite and carbonate have pervasively replaced albite; K-feldspar is slightly sericitized, and primary muscovite has been partly replaced by sericite around grain boundaries. Trace amounts of disseminated pyrite and molybdenite are also present. This stronger hydrothermal alteration is likely related to the tungsten mineralization.

Table 1. Chemical composition of granitic rocks associated with the Fostung skarn tungsten deposit and other selected granitic rocks in the region.

	SYA85-95	SYA85-96	SYA85-100	SYA85-101	B	E
Major elements (wt %)						
SiO_2	76.4	76.8	78.0	68.4	64.9	72.9
TiO_2	0.04	0.04	0.03	0.20	0.93	0.21
Al_2O_3	12.5	12.5	12.2	14.7	16.3	14.9
Fe_2O_3	0.2	0.0	0.0	0.2	2.41	0.89
FeO	0.3	1.1	0.5	1.4	2.87	0.65
MnO	0.02	0.01	0.01	0.08	0.07	0.01
MgO	0.17	0.22	0.12	0.70	1.20	0.33
CaO	0.93	0.16	0.08	2.17	2.99	0.66
Na_2O	2.16	1.94	2.57	2.87	3.06	2.95
K_2O	6.90	6.12	5.96	5.08	4.11	5.83
H_2OT	0.3	1.0	0.3	0.9	0.67	0.37
CO_2T	0.2	0.0	0.0	2.3	0.21	0.42
P_2O_5	0.42	0.04	0.03	0.12	0.29	0.03
S_T	0.06	0.46	0.13	0.30	0.07	≤0.01
F	0.06	0.05	0.03	0.13	-	-
$-0=F^2+S$	0.06	0.05	0.08	0.20	0.04	0.00
Total	100.6	100.2	99.9	99.4	100.1	100.2
Trace elements (ppm)						
Ba	1100	850	810	1700	1650	-
Rb	366	374	326	362	116	-
Sr	39	18	21	112	320	-
Be	5.2	5.1	2.3	6.3	-	-
Li	20	27	21	57	-	-
Nb	7	27	27	18	-	-
Y	75	51	50	7	43	-
Zr	49	58	51	130	425	-
La	16	9	7	50	-	-
Ga	10.3	14.3	11.8	17.5	28	-
Cu	8	240	55	110	9	-
Pb	28	12	6	23	20	-
Zn	19	120	10	100	88	-
Mo	290	6	28	68	-	-
Sn	≤3	3	≤3	5	-	-
W	4	7	4	8	-	-
D.I.*	96.9	97.1	98.7	91.4	77.0	95.9
A.S.I.**	0.99	1.24	1.13	1.04	1.09	1.21

Samples SYA85-95, -96, -100, and -101 were analyzed as follows: Major elements, Ba, Rb, Sr, Nb, Y, Zr, and Mo by XRF analysis; FeO by wet chemical analysis; H_2O_T, CO_{2T}, and ST by infrared spectrometric analysis; Be, Ga, La, Cu, Pb, Zn, and W by ICP emission spectrometric analysis; and F by pyrohydrolysis and ion chromatography; Analytical Chemistry Section, Geological Survey of Canada, Ottawa. Sn analyses by emission spectrometric analysis and Li by atomic absorption spectrometric analysis; X-Ray Assay Laboratories, Don Mills.

* Differentiation Index

** Alumina Saturation Index (mol% $Al_2O_3/(CaO + Na_2O + K_2O)$)

B: Average of four representative porphyritic quartz monzonite samples from Drill Hole No. 1, Manitoulin Island (Van Schmus et al., 1975).,
E: Coarse-grained quartz monzonite, Croker Island Complex (Van Schmus et al., 1975).

Chemical compositions of the four whole-rock samples are given in Table 1. With the exception of sample SYA85-101, the rocks are metaluminous to peraluminous, high-silica (>76% SiO_2), low-calcium (≤1% CaO) granites. They are similar in composition to a low-calcium granite of Turekian and Wedepohl (1961), except for higher contents of K_2O and Rb, and lower contents of Sr and TiO_2. They are distinctly more felsic than granitic rocks of the Croker Island Complex or the Manitoulin Island plutons (Table 1).

Sample SYA85-101 may be an altered granodiorite. It has, for example, higher TiO_2, MgO, and Zr contents than the other whole-rock samples. Ti, Mg, and Zr are generally relatively immobile during hydrothermal alteration, except in more extreme cases, and probably reflect a more granodioritic composition of this sample. The higher contents of CO_2 and F, however, are probably related to hydrothermal alteration.

The muscovite sample (SYA85-97) is from a part of one of the granitic dykes that contained about 20% medium-grained muscovite along with 1% disseminated pyrite and traces of sphalerite. It is the same granitic dyke from which two of the whole-rock samples (SYA85-96 and -100) were collected. The muscovite sample is also the same one that yielded a K-Ar age of 1427 ± 26 Ma (GSC 88-77; Hunt and Roddick, 1988).

DISCUSSION

Analytical procedures for the Rb-Sr isotopic analyses of the samples are described elsewhere in this volume (Theriault, 1990). The results of the analyses are given in Table 2 and are plotted on Figures 4 and 5.

The four whole-rock compositions (Fig. 4) yielded an errorchron age of 1390 ± 26 Ma, initial Sr ratio of 0.71448 ± 0.00271, and MSWD of 6.15. Omitting the more highly altered sample SYA85-101 resulted in an errorchron age of 1383 ± 14 Ma, initial Sr ratio of 0.71662 ± 0.00302, and a slightly lower MSWD of 3.47. Considering the overlap in error limits of both the ages and the initial ratios, no significant difference between the two sets of data is apparent.

The high initial $^{87}Sr/^{86}Sr$ ratio of the Fostung granitic rocks is probably due to a significant contribution of radiogenic Sr from older crustal rocks; the addition of radiogenic Sr may have occurred by contamination of the magma or possibly later, during hydrothermal alteration of the granitic rocks. The buried plutons on Manitoulin Island, in contrast, have an initial Sr ratio of 0.7078 ± 0.0010 (Van Schmus et al., 1975), and the Croker Island Complex has an initial Sr composition of about 0.705 (Van Schmus, 1965). The initial Sr ratio for the Mongowin plutonic complex, however, is higher than these two at 0.7113 ± 0.0001 and, as for the Fostung granitic rocks, has been attributed to contamination by older crustal material (Van Schmus, 1971).

The failure of the Rb-Sr data to fit within experimental errors is not surprising considering the nature of the samples analyzed. All of the samples were altered to some degree and at least one of the samples was significantly altered. Also, the granitic rocks are highly evolved, with high Rb/Sr and high initial $^{87}Sr/^{86}Sr$, indicating a significant component of added radiogenic Sr. Such rocks commonly have disturbed Rb-Sr systematics, for example S-type granites (Chappell and White, 1974).

Table 2. Results of Rb-Sr isotopic analyses on four-whole rock powders and one muscovite concentrate in duplicate.

Sample No.	Rb	Sr	$^{87}Rb/^{86}Sr$	$^{87}Sr/^{86}Sr$ (2σ)
SYA85-95	366.1	38.6	28.9755	1.292680(21)
SYA85-96	373.6	18.4	66.6414	2.057840(104)
SYA85-100	325.8	20.6	50.1300	1.700370(48)
SYA85-101	362.3	112.0	9.53835	0.904698(99)
SYA85-97*	1293.3	15.6	567.61	14.68010(132)
SYA85-97*	1294.6	15.3	583.83	14.85730(92)

* muscovite

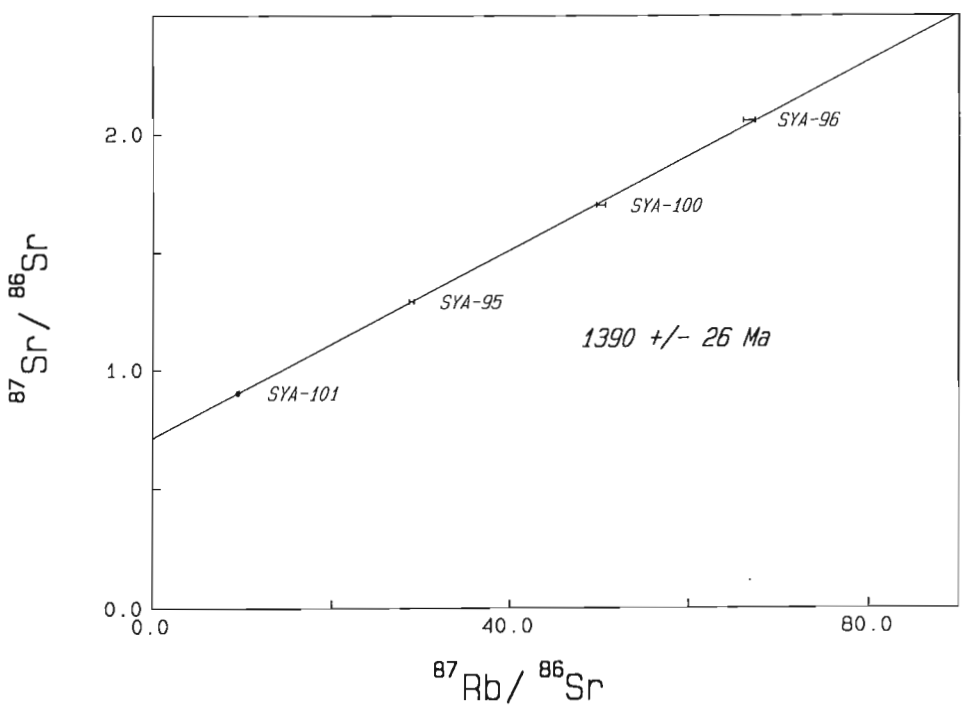

Figure 4. Rb-Sr errorchron plot, Fostung granitic rocks, Espanola area, Ontario.

The four whole-rock compositions together with the muscovite composition are shown in Fig. 5. Considering that the muscovite is from the same dyke as two of the whole-rock samples, and is thus an integral part of the whole-rock suite defining the 1390 Ma errorchron, the Rb-Sr isotopic composition of the muscovite should fall on the errorchron. Instead, the composition is discordant and a three-point errorchron through the muscovite data, and an initial Sr ratio of 0.7145 yielded an age of 1699 ± 12 Ma. The errorchron age through the muscovite data is not significantly affected by assuming a lower initial ratio of 0.705, which results in an age of 1700 ± 12 Ma.

Discordant whole-rock and mineral Rb-Sr ages have been widely reported since early investigations by Compston and Jeffrey (1959) and Fairbairn et al. (1961). Rb-Sr ages can serve as geochronometers for metamorphic events, providing that the whole-rock-mineral Rb-Sr system has been completely homogenized. However, partial disturbance of the Rb-Sr system in minerals can occur at temperatures of no more than a few hundred degrees because of the mobility of Rb and Sr (Dodson, 1973).

The 1699 Ma age indicated by the muscovite data possibly represents the age of emplacement of the granitic dykes, with a later resetting of the whole-rock Rb-Sr system during hydrothermal alteration at 1390 Ma. This possibility seems reasonable considering that other granitic plutons in the region such as the Cutler granite and the Mongowin plutonic complex are between 1700 and 1800 Ma old. In this scenario, the presence of another granitic intrusion, related to the alteration and mineralization at 1390 Ma and as yet undetected, cannot be ruled out.

An alternative and more likely explanation for the muscovite data is that they are due to either an excess of radiogenic Sr or a depletion of Rb, or possibly a combination of both. Considering the high ratio of ^{87}Rb to ^{86}Sr in the muscovite (the two analyses averaged 575), only a small amount of excess ^{87}Sr would be required to cause the observed displacement, in this case probably no more than 1 to 2 ppm. An excess of radiogenic Sr is also consistent with the high initial Sr ratio indicated by the whole-rock data, which we attribute to contamination by older crustal material. The muscovite-rich part of the dyke may, in fact, represent remnants of incompletely digested crustal material. To produce the same amount of displacement by removal of Rb would require removal of a much larger amount of Rb, which we think is less likely to have occurred. In either case, however, the result makes a meaningful interpretation of the Rb-Sr age of the muscovite impossible.

The Rb-Sr whole-rock errorchron ages are approximately the same as the K-Ar age of 1427 ± 26 Ma reported in Hunt and Roddick (1988), within error limits. Although the errorchron ages must be viewed as imprecise, they nevertheless support a Mid-Proterozoic age for the mineralization and alteration of the granitic dykes associated with the Fostung deposit. A similar age of emplacement for the granitic dykes is inferred because of the likely genetic relationship between the granitic rocks and tungsten mineralization.

The age of the granitic rocks supports their correlation with anorogenic magmatism that was widespread throughout the midcontinent of North America during Mid-Proterozoic time. According to Anderson (1983), this anorogenic granite magmatism occurred during at least three separate episodes: 1.41 to 1.49, 1.34 to 1.41, and 1.03 to 1.08 Ga ago. The Rb-Sr data for the Fostung granitic dykes suggest that they belong to the second of these magmatic periods.

Compositional similarities of the Fostung granitic rocks with other Mid-Proterozoic anorogenic granites include their slightly peraluminous and potassic nature. The high initial Sr ratio of 0.71448, however, is in contrast to the average of 0.7051 ± 0.0025 indicated by Anderson (1983). The high

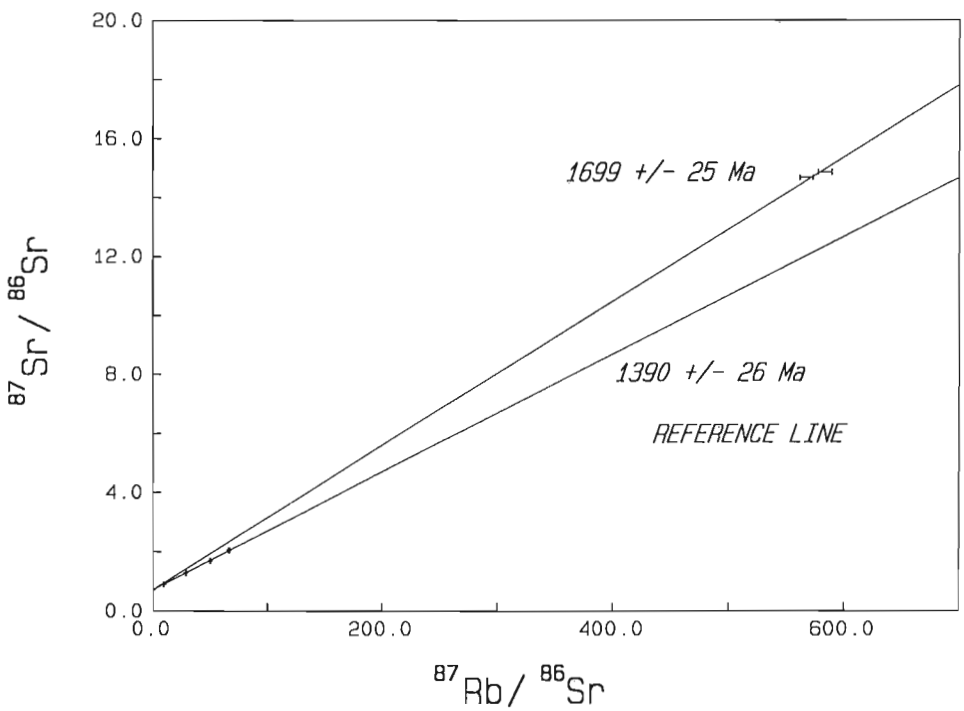

Figure 5. Rb-Sr errorchron plot for the muscovite data assuming an initial Sr ratio of 0.7145. The 1390 Ma errorchron determined from the four whole-rock samples is shown for reference.

initial Sr ratio of the Fostung granitic rocks suggests that either a significant portion of the parent magma was derived by melting of much older crustal rocks or else radiogenic Sr was added to the granitic rocks later during hydrothermal alteration.

The association of tungsten with Mid-Proterozoic granite, although not common, does occur elsewhere. In the St. Francois Mountains, Missouri, for example, wolframite-bearing veins are associated with the Silver Mine granite (Tolmin, 1933; Lowell, 1975). The occurrence of tungsten-bearing skarn associated with Mid-Proterozoic granite at Fostung, however, appears to be unique in the mid-continent of North America.

ACKNOWLEDGMENTS

J.C. Roddick critically reviewed this paper, and R.R. Parrish and B.E. Taylor also provided helpful comments. K.K. Nguyen drafted some of the figures.

REFERENCES

Anderson, J.L.
1983: Proterozoic anorogenic granite plutonism of North America; in Proterozoic Geology; Selected Papers from an International Proterozoic Symposium, ed. L.G. Medaris, Jr., C.W. Byers, D.M. Mickelson, and W.C. Shanks; Geological Society of America, Memoir 161, p. 133-154.

Card, K.D.
1976: Geology of the Espanola-Whitefish Falls area, District of Sudbury, Ontario; Ontario Division of Mines, Geoscience Report 131, 70p.

1978: Geology of the Sudbury-Manitoulin area, districts of Sudbury and Manitoulin; Ontario Geological Survey, Geoscience Report 166, 238p.

Chappell, B.W. and White A.J.R.
1974: Two contrasting granite types; Pacific Geology, v. 8, p. 173-174.

Compston, W. and Jeffrey, P.M.
1959: Anomalous common strontium in granite; Nature, v. 184, p. 1792.

Corfu, F. and Andrews, A.J.
1986: A U-Pb age for mineralized Nipissing diabase, Gowganda, Ontario; Canadian Journal of Earth Sciences, v. 23, p. 107-109.

Dodson, M.H.
1973: Closing temperature in cooling geochronological and petrological systems; Contributions to Mineralogy and Petrology, v. 40, p. 259-274.

Einaudi, M.T., Meinert, L.D. and Newberry, R.J.
1981: Skarn deposits; Economic Geology, 75th Anniversary Volume, p. 317-391.

Fairbairn, H.W., Hurley, P.M., and Pinson, W.H.
1961: The relation of discordant Rb-Sr mineral and whole rock ages in an igneous rock to its time of crystallization and to the time of subsequent $^{87}Sr/^{86}Sr$ metamorphism; Geochimica et Cosmochimica Acta, v. 23, p. 135-144.

Fairbairn, H.W., Hurley, P.M., Card, K.D., and Knight, C.J.
1969: Correlation of radiometric ages of Nipissing Diabase and Huronian metasediments with Proterozoic orogenic events in Ontario; Canadian Journal of Earth Sciences, v. 6, p. 489-497.

Ginn, R.M. and Beecham, A.W.
1986: The Fostung scheelite deposit, Espanola, Ontario; Canadian Geology Journal of CIM, v. 1, no. 1, p. 46-54.

Hunt, P.A. and Roddick, J.C.
1988: A compilation of K-Ar ages, Report 18; in Radiogenic Age and Isotopic Studies: Report 2; Geological Survey of Canada, Paper 88-2, p. 127-153.

Krogh, T.E. and Davis, D.W.
1969: Old isotopic ages in the northwestern Grenville Province, Ontario; Geological Association of Canada, Special Paper No. 5, p. 189-192.

Krogh, T.E., Corfu, F., Davis, D.W., Dunning, G.R., Heaman, L.M., Kamo, S.L., Machado, N., Greenough, J.D., and Nakamura, E.
1988: Precise U-Pb isotopic ages of diabase dykes and mafic to ultramafic rocks using trace amounts of baddeleyite and zircon; in Mafic Dyke Swarms, ed. H.C. Halls, and W.F. Fahrig; Geological Association of Canada, Special Paper 34, p. 147-152.

Lowell, G.R.
1975: Precambrian geology and ore deposits of the Silver Mine area, southeast Missouri: a review; in A Fieldguide to the Precambrian Geology of the St. Francois Mountains, Missouri, ed. G.R. Lowell; Southeast Missouri State University, Cape Girardeau, Missouri, p. 81-88.

Theriault, R.J.
1989: Methods for Rb-Sr and Sm-Nd isotopic analyses at the geochronology laboratory, Geological Survey of Canada; in Radiogenic and Isotopic Studies: Report 3; Geological Survey of Canada, Paper 89-2, p. 3-6.

Tolmin, C.
1933: The geology of the Silver Mine area, Madison County, Missouri; Missouri Bureau of Geology and Mines, 57th Biennial Report of the State Geologist, 1931-1932, Appendix 1, 39p.

Turekian, K.K. and Wedepohl, K.H.
1961: Distribution of the elements in some major suites of the Earth's crust; Geological Society of America Bulletin, v. 72, p. 175-192.

Van Schmus, W.R.
1965: The geochronology of the Blind River-Bruce Mines area, Ontario, Canada; Journal of Geology, v. 73, p. 755-780.

1971: Ages of lamprophyre dikes and of the Mongowin pluton, north shore of Lake Huron, Ontario, Canada; Canadian Journal of Earth Sciences, v. 8, p. 1203-1209.

Van Schmus, W.R., Card, K.D., and Harrower, K.L.
1975: Geology and ages of buried Precambrian basement rocks, Manitoulin Island, Ontario; Canadian Journal of Earth Sciences, v. 12, p. 1175-1189.

Wetherill, G.W., Davis, G.L., and Tilton, G.R.
1960: Age measurements of minerals from the Cutler batholith, Cutler, Ontario; Journal of Geophysical Research, v. 65, p. 2461-2466.

Wilson, B.S.
1982: The Fostung tungsten deposit; unpub. B.Sc. thesis, Queen's University, Kingston, Ontario, 80p.

APPENDIX

Description of samples analyzed:

SYA85-95

Quartz-feldspar porphyry; contains phenocrysts of quartz (15% by volume), plagioclase (15%), K-feldspar (5%), and biotite (1 to 2%), all about 0.5 to 1 mm in size, in a fine-grained matrix of quartz and K-feldspar grains 0.05 to 0.1 mm in size. Plagioclase phenocrysts have been replaced by sericite and trace amounts of carbonate. K-feldspar phenocrysts are turbid and slightly sericitized. Biotite phenocrysts are completely altered to sericite and carbonate. Trace amounts of disseminated pyrite and rutile are also present. The sample was collected from Sulpetro Minerals Ltd. drill hole 3115-8 at 450.6-450.7 m.

SYA85-96

Fine-grained granite; consists mainly of quartz (40%), K-feldspar (40%), albite (15%), and muscovite (5%). Grain size is typically about 0.5 mm, but a few grains range up to 1 mm. Muscovite occurs as radiating clusters and as inclusions in K-feldspar. Traces of chlorite occur as anhedral shreds, probably replacing biotite. Minor amounts of sericite (1 to 2%) have replaced albite and K-feldspar. Trace amounts of disseminated pyrite, apatite, rutile, and epidote are also present. Sample was collected from Sulpetro drill hole 3115-8 at 480.4-480.6 m.

SYA85-97

Muscovite-rich zone in granite; consists of 15 to 20% muscovite as clusters of medium-sized grains (2 mm across) that are clear and colourless except for inclusions of rutile. The muscovite is associated with quartz (50%), K-feldspar (20%), and albite (5%). About 1% pyrite and trace amounts of sphalerite occur as disseminated grains. Sample was collected from Sulpetro drill hole 3115-8 at 479.8-480.0 m and is from the same dyke as samples SYA85-96 and -100.

SYA85-100

Fine-grained granite; consists mainly of quartz (35%), K-feldspar (40%), albite (20%), and muscovite (5%), as 0.5 to 1 mm sized grains. Albite grains are partly sericitized. Disseminated pyrite, rutile, and apatite occur in accessory amounts. Trace amounts of disseminated molybdenite and chalcopyrite are also present. Sample was collected from Sulpetro drill hole 3115-8 at 482.5-482.6 m.

SYA85-101

Fine-grained granite/granodiorite; consists mainly of quartz (30%), K-feldspar (25%), albite (15%), muscovite/sericite (25%), and carbonate (5%). Muscovite (5%) occurs as discrete grains 0.5 to 1 mm in size and fine-grained muscovite/sericite (15 to 20%) replaces albite and, to a lesser extent, K-feldspar. Carbonate occurs as very fine-grained aggregates associated with the muscovite/sericite and as scattered interstitial grains. Trace amounts of disseminated pyrite, rutile, apatite, and molybdenite are also present. Sample was collected from Sulpetro drill hole 3115-8 at 530.9-531.0 m.

U-Pb zircon and baddeleyite ages from the Central Gneiss Belt, Ontario

O. van Breemen[1] and A. Davidson[1]

van Breemen, O. and Davidson, A., U-Pb zircon and baddeleyite ages from the central gneiss belt, Ontario; in Radiogenic Age and Isotopic Studies: Report 3, Geological Survey of Canada, Paper 89-2, p. 85-92, 1990

Abstract

A granulite-facies orthogneiss from eastern Algonquin domain has yielded a concordant array of zircon data points with upper and lower intercept ages of 1375 ± 13 and 1043 ± 23 Ma, interpreted respectively in terms of a primary igneous age and a late stage of metamorphism. A mildly deformed syntectonic pegmatite dating a late stage of a compressive regime of overthrusting of Muskoka domain over Parry Sound domain has yielded an age of 1103 +6/ -4 Ma. A clinopyroxene syenite dyke cutting coronitic olivine metagabbro in the southwestern part of Rosseau subdomain has yielded a U-Pb zircon age of 1058 +8/ -4 Ma, which provides a lower age limit for granulite-facies metamorphism in this subdomain. Additional U-Pb analyses of previously dated coronitic metagabbros in Muskoka and Algonquin domains suggest that fine-grained zircon aggregates replacing ca. 1170 Ma igneous baddeleyite continued to recrystallize into coarse zircon during the interval 1060 to 1030 Ma.

Résumé

Un orthogneiss à faciès des granulites provenant de la partie est du domaine d'Algonquin a fourni une série concordante de données obtenues à l'aide de méthodes appliquées au zircon avec des âges d'intersection supérieur et inférieur de 1375 ± 13 Ma et 1043 ± 3 Ma, qui ont été interprétés respectivement comme une phase ignée primaire et une phase tardive de métamorphisme. Une pegmatite syntectonique, moyennement déformée, ayant servi à déterminer l'âge d'une phase tardive d'un régime de compression de nappes de charriage, où le domaine de Muskoka a été charrié sur le domaine de Parry Sound, a fourni un âge de 1103 + 6/ -4 Ma. Un dyke de syénite à clinopyroxène traversant un métagabbro à olivine coronotisé dans la partie SO du sous-domaine de Rousseau, a donné un âge de 1058 + 8/ -4 Ma, grâce à la méthode U-Pb appliquée au zircon; cet âge établit une limite inférieure pour l'âge d'un métamorphisme à faciès des granulites dans ce sous-domaine. D'autres analyses du rapport U-Pb de métagabbros coronotisés datés antérieurement dans les domaines de Muskoka et d'Algonquin, semblent indiquer que des agrégats de zircon à grain fin remplaçant la baddéléyite éruptive âgée d'environ 1170 Ma ont poursuivi leur cristallisation pour donner des zircons à grain grossier entre 1060 Ma et 1030 Ma.

INTRODUCTION

This paper reports ages from different localities in Parry Sound, Muskoka, and Algonquin domains of the Grenville Structural Province in Ontario (Fig. 1). The samples were collected mostly to provide geochronological support for a textural and U-Pb geochronological study on igneous baddeleyite and metamorphic zircon in metagabbro (Davidson and van Breemen, 1988). It was found that igneous baddeleyite crystals have replacement rims of fine-grained columnar zircon in the same form as other silicate coronas around primary olivine and Fe-Ti oxide. Corona formation was thus interpreted to have been dated by zircon ages of ca. 1045 Ma. Baddeleyite U-Pb isotopic ratios pointing back to an age of ca. 1170 Ma were interpreted to date igneous crystallization. In the same region, other U-Pb zircon geochronological data suggested primary country rock igneous ages in the 1500-1340 Ma age range (van Breemen et al., 1986).

1 Geological Survey of Canada, 601 Booth Street, Ottawa, Ontario K1A 0E8

Data are presented from a coronite near the base of the Parry Sound shear zone along the northwestern boundary of Parry Sound domain but within Britt domain (sample 1, 87DM-50), as well as some new data from two coronites already dated (85DM-165 and 85DMSH-101c; here called samples 2 and 3, as in Davidson and van Breemen, 1988). Three other samples were collected to help interpretation of the U-Pb data from the coronites. Sample 4 (85DM-115-1) is a metamonzonite in granulite facies from the eastern part of Algonquin domain close to coronite samples 2 and 3; it provides geochronological information on the host rocks to the coronites. Samples 5 (85DMSD-62h) and 6 (86DM-10b) were collected from dykes which cut coronitic olivine metagabbros and, therefore, provide minimum ages for both primary igneous intrusion and metamorphism. Sample 5 is from a hypersthene granodiorite dyke that cuts across metamorphic foliation in coronite in Huntsville subdomain of Algonquin domain. Sample 6 is from a non-deformed pyroxene syenite pegmatite dyke cutting coronite within the disrupted gneissic tectonites of Seguin subdomain (structural level 3) close to the southwestern margin of Rosseau subdomain (level 1). It provides a minimum age for the emplacement of the upper deck of Muskoka domain (Culshaw et al., 1983; Davidson, 1984). Finally, sample 7 was collected from a syntectonic pegmatite in the boundary zone between Moon River subdomain (level 3) and Parry Sound domain (level 2), both of which tectonically overlie level 1 of Muskoka subdomain; this should date a late stage of the emplacement of level 3 against 2.

GEOCHRONOLOGY

U-Pb zircon isotopic data (Table 1) were obtained using techniques described by Parrish et al. (1987). A modified form of York's (1969) least squares fitting was used to calculate regression lines (Fig. 2, 3, and 4). Error envelopes at 2 sigma were obtained by the methods of Roddick (1987). Uncertainties for ages are given at the 2 sigma level.

Coronitic metagabbros (samples 1, 2, and 3)

We begin by relating new analyses from samples 2 and 3 to previously published data from these samples (Davidson and van Breemen, 1988). From sample 3 (85DMSH-101c), another strongly abraded fraction of baddeleyite was analyzed (Table 1). The corresponding data point (3a) plots on the previous alignment of six baddeleyite data points from

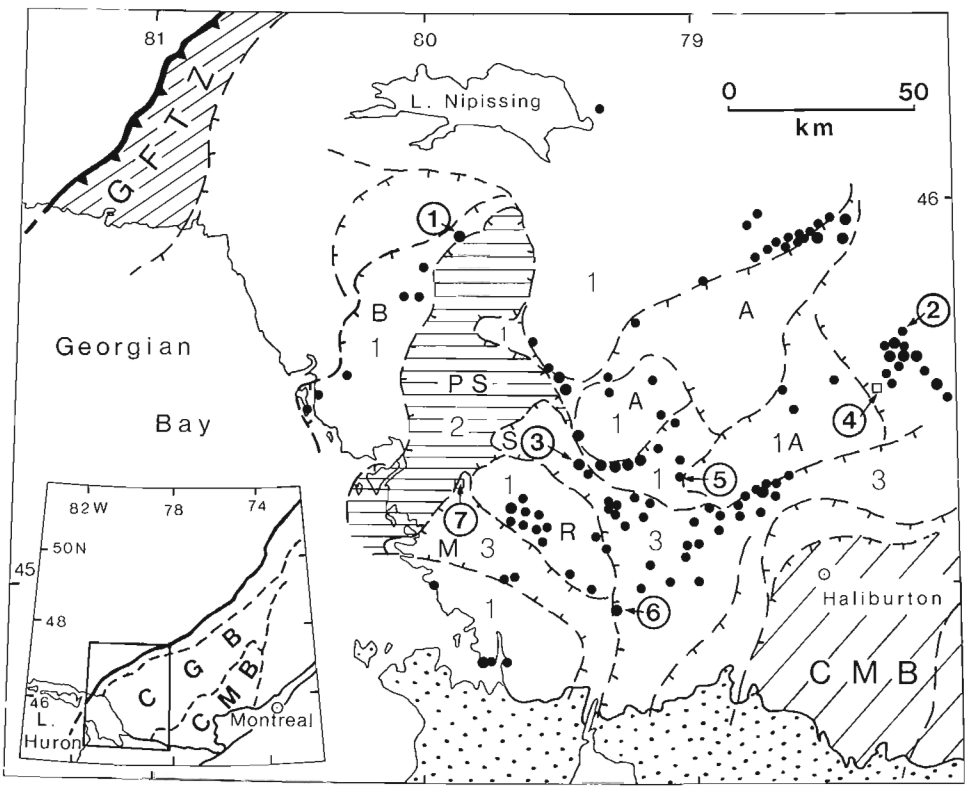

Figure 1. Regional structural framework of part of the Central Gneiss Belt northeast of Georgian Bay, Ontario, with sample locations (circled numbers). Heavy toothed line in upper left is Grenville Front; GFTZ = Grenville Front Tectonic Zone; CGB = Central Gneiss Belt; CMB = Central Metasedimentary Belt (terminology of Wynne-Edwards, 1972). Dashed lines are major shear zones, dip direction indicated. Black dots indicate distribution of coronitic olivine metagabbro. 1,2,3 indicate sequence of deck emplacemnt (after Culshaw et al., 1983). From deck 1, A = Algonquin domain, B = Britt domain, R = Rosseau subdomain. From deck 2, PS = Parry Sound domain. From deck 3, M = Moon River subdomain, S = Seguin subdomain. M, R, and S are part of the Muskoka domain. Stippled area is Paleozoic cover.

Table 1. U-Pb zircon data.

Fraction,[1] Size	Weight (mg)	U (ppm)	Pb[2] (ppm)	$^{206}Pb/^{204}Pb$[3]	Pb_c[4] (pg)	$^{208}Pb/^{206}Pb$[2]	$^{206}Pb/^{238}U$ ±SEM%[5]	$^{207}Pb/^{235}U$ ±SEM%[5]	R	$^{207}Pb/^{206}Pb$ age, error[6] (Ma)	SEM%[7]
1. Coronitic metagabbro, Parry Sound domain (87-DM-50)											
a, baddeleyite	0.027	602.6	108.9	4775	41	0.0085	0.19362 (.084)	2.0823 (.099)	0.95	1146.9 (1.3)	0.033
b, baddeleyite	0.053	608.1	112.3	22280	17	0.047	0.19098 (.086)	2.0426 (.098)	0.96	1135.9 (1.1)	0.028
c, baddeleyite	0.022	303.3	54.67	1935	43	0.0117	0.19252 (.085)	2.0636 (.11)	0.88	1140.2 (2.2)	0.056
d, zircon, aggregate	0.037	273.6	49.11	3008	39	0.045	0.18618 (.086)	1.9685 (.10)	0.90	1113.0 (1.8)	0.045
e, zircon, aggregate	0.039	264.0	47.76	4149	30	0.038	0.18865 (.172)	2.0044 (.18)	0.98	1122.8 (1.6)	0.040
2. Coronitic metagabbro, Algonquin domain (85DM-165)											
a, zircon	0.046	71.38	13.55	3893	9	0.198	0.17349 (.090)	1.7642 (.11)	0.93	1034.6 (1.6)	0.039
b, zircon	0.046	86.73	17.23	3122	15	0.223	0.17786 (.096)	1.8313 (.11)	0.93	1059.7 (1.6)	0.040
3. Coronitic metagabbro, Seguin subdomain (85DMSH-101c)											
a, baddeleyite	0.048	452.0	80.89	18150	15	0.005	0.19239 (.083)	2.0611 (.095)	0.96	1139.2 (1.1)	0.028
b, zircon	0.015	78.76	14.49	910	14	0.143	0.17570 (.14)	1.7902 (.16)	0.88	1038.7 (3.0)	0.074
c, zircon	0.025	38.52	6.99	915	12	0.113	0.17784 (.24)	1.8193 (.28)	0.70	1046.9 (8.0)	0.205
4. Metamonzonite in granulite facies, Algonquin domain (85DM-115)											
a, +105 NM0	0.28	79.17	18.57	2838	110	0.147	0.21879 (.058)	2.5441 (.097)	0.90	1300.2 (1.0)	0.051
b, +105 NM1	0.30	85.80	20.49	3643	100	0.161	0.22088 (.059)	2.5790 (.093)	0.89	1308.3 (0.9)	0.049
c, -105+74 NM0	0.16	95.75	20.57	3263	61	0.126	0.20560 (.065)	2.3139 (.099)	0.91	1236.5 (0.9)	0.048
d, -105+74 NM1	0.37	87.44	19.97	3992	110	0.144	0.21442 (.064)	2.4695 (.097)	0.91	1281.6 (0.9)	0.047
5. Hyperthene bearing granodiorite dyke, Algonquin domain (85DMSD-62h)											
a, +149 NM0 P	0.027	172.4	35.55	1009	56	0.125	0.19370 (.47)	2.1350 (.49)	0.97	1195.5 (2.4)	0.119
b, -105+74 NM0 P	0.075	178.5	39.43	3575	37	0.115	0.21265 (.21)	2.4887 (.23)	0.98	1312.8 (1.0)	0.049
c, -105+74 NM-1	0.043	149.4	33.99	1514	59	0.117	0.21991 (.10)	2.6087 (.14)	0.83	1339.0 (3.0)	0.078
d, -105+74 NM-1 R	0.036	200.7	48.22	1442	73	0.089	0.23153 (0.32)	2.8407 (.34)	0.96	1403.8 (1.7)	0.089
e, -62 NM-1	0.028	167.5	37.56	1825	35	0.101	0.21952 (.099)	2.6145 (.13)	0.92	1346.7 (2.1)	0.053
6. Clinopyroxene syenite dyke, boundary Seguin and Rosseau subdomains (86-DM-10b)											
a, +105 Mag3	0.093	1276	214.3	10056	1218	0.057	0.17189 (.15)	1.7604 (.16)	0.97	1049.0 (0.8)	0.042
b, -105+74 Mag3	0.088	1146	196.9	8966	123	0.067	0.17406 (.15)	1.7857 (.16)	0.97	1052.6 (0.8)	0.042
c, -105+62 Mag3	0.082	918.1	160.3	8356	99	0.080	0.17521 (.15)	1.7993 (.17)	0.97	1054.5 (0.8)	0.041
d, -74+62 Mag3	0.085	1136	193.1	7370	141	0.071	0.17167 (.15)	1.7604 (.16)	0.97	1051.6 (0.9)	0.043
7. Syntectonic pegmatite, Moon River/Parry Sound shear zone											
a, +149 Mag1	0.042	5441	356.4	5441	185	0.005	0.18169 (.15)	1.9016 (.17)	0.96	1092.6 (0.9)	0.047
b, +149 Mag1 NMCo	0.033	1513	262.0	5042	114	0.006	0.18465 (.15)	1.9388 (.17)	0.96	1099.0 (0.9)	0.047
c, +149 Mag1 NMCo	0.034	1628	280.0	8187	79	0.005	0.18431 (.15)	1.9342 (.17)	0.97	1098.1 (0.8)	0.042
d, -149+105 Mag1	0.051	1647	281.7	12305	78	0.006	0.18345 (.15)	1.9236 (.16)	0.97	1096.4 (0.8)	0.040

Notes: [1]sizes are in microns; NM1=non-magnetic cut with Frantz at 1 degree side slope, Mag0=magnetic cut with Frantz at 0 degree side slope, samples are zircon unless indicted otherwise; [2]radiogenic Pb;[3]measured ratio, corrected for spike and fractionation; [4]total common Pb in analysis corrected for fractionation and spike; [5]corrected for blank Pb and U, common Pb, errors quoted are one sigma in percent; R correlation of errors of isotope ratios; [6]corrected for blank and common Pb, errors are two sigma in Ma; [7]error at one sigma.

four coronitic metagabbros from Algonquin and Muskoka domains, consistent with an upper intercept age of ca. 1170 Ma (Fig. 2). A fraction of ovoid zircons previously analyzed from this coronitic metagabbro (point 3, Fig. 2) yielded a ^{207}Pb-^{206}Pb age of 1080 ± 4 Ma and was interpreted in terms of a mixture of igneous zircon of similar age to the baddeleyites and metamorphic zircon of ca. 1.05 Ga age. Two further fractions of ovoid zircon analyzed are concordant and yield younger ^{207}Pb-^{206}Pb ages of 1039 Ma (3b) and 1047 (3c) Ma (Table 1).

From sample 2 (85DM-165) in eastern Algonquin domain two additional zircon fractions were analyzed (Table 1). Selected crystals are oval-shaped and of metamorphic appearance, but distinct from the finer zircons of the polycrystalline rims surrounding the baddeleyite grains. Whereas in the nearby coronitic metagabbro (84DMSA-11d, sample 1 of Davidson and van Breemen, 1988) both previously analyzed zircon clusters and ovoid-shaped zircons agreed at an age of ca. 1045 Ma (Fig. 2), in sample 2 there appeared to be a discrepancy with the possibility that the ovoid zircon grains recrystallized later at 1031 Ma. Data points for the two new analyses are nearly concordant with ^{207}Pb-^{206}Pb model ages of 1035 Ma (2a) and 1060 Ma (2b, Fig. 2).

Baddeleyite data from sample 1 (87DM-50) yield an array of data points (1a, 1b, 1c) identical to that of the coronites from Algonquin and Muskoka domains (Fig. 2). Fraction 1a yields a ^{207}Pb-^{206}Pb age of 1147 Ma, which is taken as a minimum age for igneous crystallization. These data are consistent with a primary igneous age of ca. 1170 Ma for this coronitic metagabbro in Britt domain near the base of the Parry Sound shear zone, the same primary age as for coronites in Algonquin and Muskoka domains to the southeast.

In the same sample, zircon after baddeleyite consists of extremely fine crystals. Moreover, in the two fractions analyzed it was not possible to obtain aggregates in which baddeleyite was completely converted to zircon. However, aggregates with observable baddeleyite cores were avoided, and it is unlikely that baddeleyite constituted more than 10% of the material analyzed. The two fractions (1d, 1e) of zircon clusters are slightly more discordant than the baddeleyite fractions (Fig. 2) and yield ^{207}Pb-^{206}Pb ages of 1113 Ma and 1123 Ma as compared with 1146 Ma to 1136 Ma for the baddeleyites. Given that the baddeleyites contain 610-300 ppm U compared with 270 ppm for the zircons, it is possible to interpret the data in terms of a mixed age between igneous baddeleyite at 1170 Ma and a younger metamorphic age.

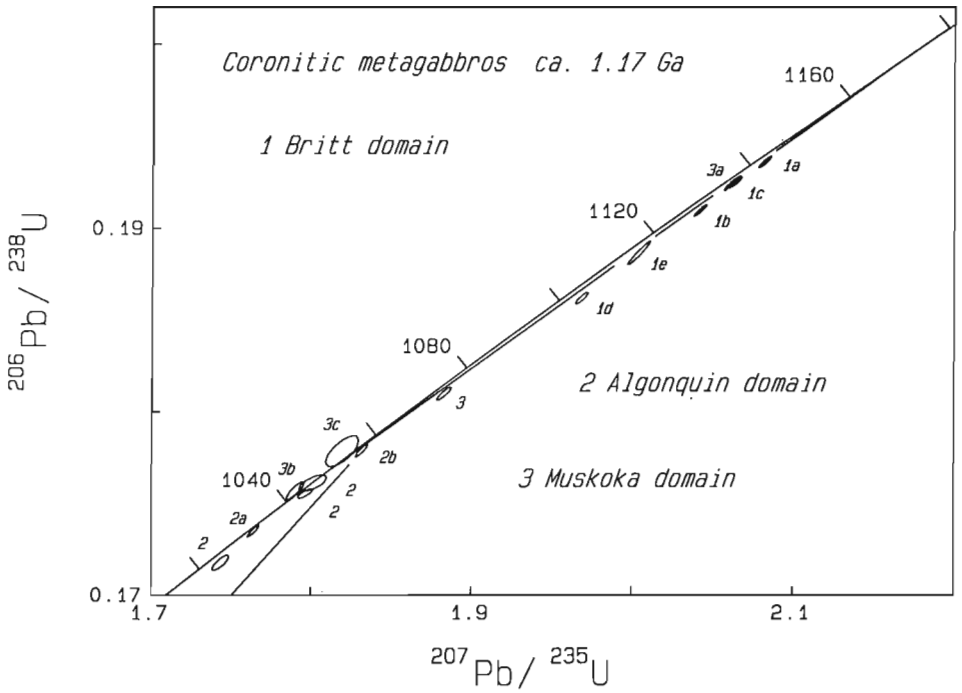

Figure 2. Concordia diagram with isotopic ratios of baddeleyite and metamorphic zircon from three coronitic metagabbros from: 1, Parry Sound domain; 2, Algonquin domain; and 3, Seguin subdomain of Muskoka domain. Error ellipses of baddeleyite data points are filled. Numbers and letters identifying data points correspond to those of Table 1. Also shown are data points for ovoid zircon from samples 2 and 3, as well as coronitic metagabbro 84DMSA-11d from Algonquin domain previously published in Davidson and van Breemen (1988). These data points are identified by "2" and "3", indicating that samples came from the either Algonquin or Muskoka domain.

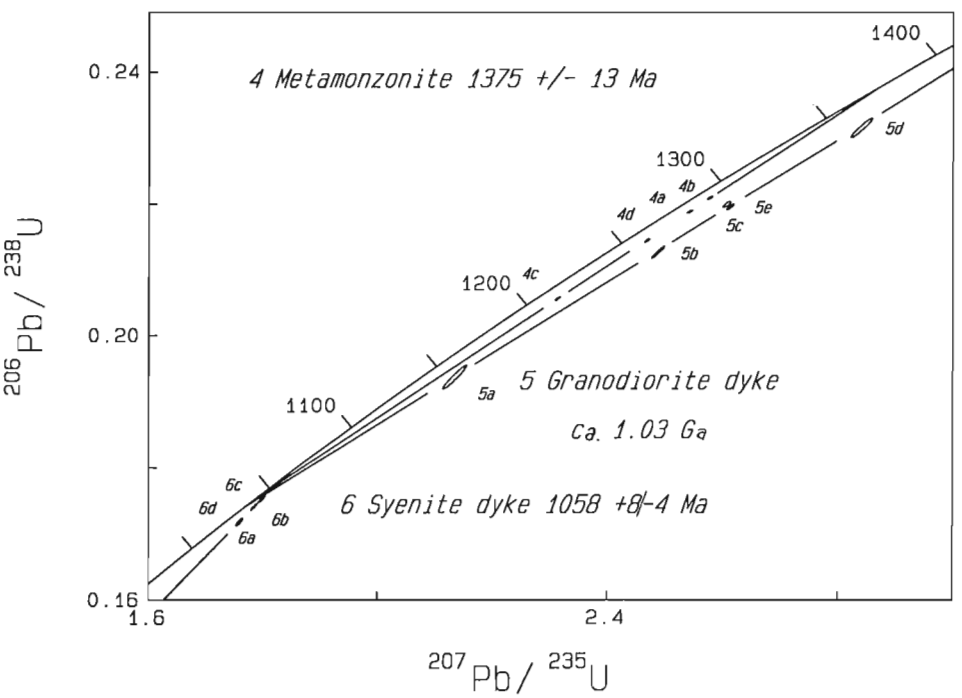

Figure 3. Concordia diagram with isotopic ratios of zircon from: 4, metamonzonite in granulite facies, Algonquin domain; 5, hypersthene-bearing granodiorite dyke, Algonquin domain; and 6, clinopyroxene syenite dyke, boundary between Seguin and Rosseau subdomains. Numbers and letters identifying data points correspond to those of Table 1.

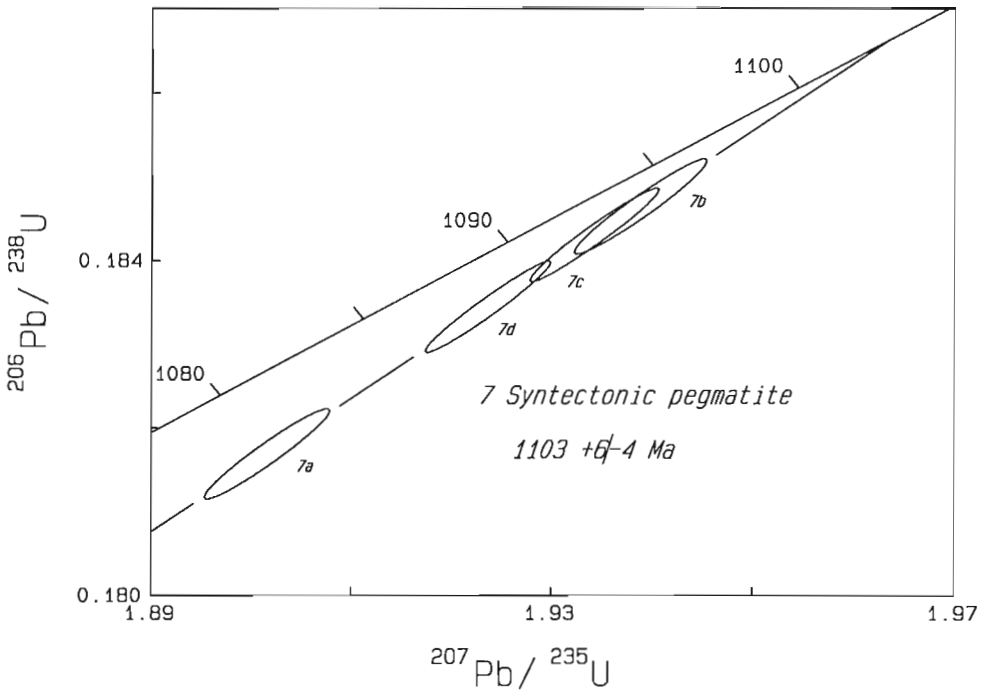

Figure 4. Concordia diagram with isotopic ratios of zircon from 7, syntectonic pegmatite, boundary between Moon River subdomain of Muskoka domain and Parry Sound domain. Numbers and letters identifying data points correspond to those of Table 1.

Orthogneiss, metamonzonite in granulite facies (sample 4; 85DM-115)

Sample 4 is from an orthogneiss unit that is conformable with the local north-northwest-trending foliation. The rock is uniform, olive-buff, very fine and even grained, and is free from bands or lenses of darker material. This orthogneiss unit from eastern Algonquin domain is part of the gneiss assemblage that hosts coronitic gabbro specimens 84DMSA-11d and 85DM-165 described in Davidson and van Breemen (1988).

The zircons recovered from sample 4 range from prismatic, simple subhedral shapes commonly featuring sharp corners to more ovoid multifaceted shapes. They could not be etched with HF acid. Two coarse fractions (4a, 4b) of the prismatic type were picked, assuming that these consist largely of the igneous precursor. Two finer fractions (4c, 4d) were picked in the belief that these may have a metamophic rim component. U contents are low (80-95 ppm). On a concordia plot, the four fractions are aligned with upper and lower intercept ages of 1375 +13/ -12 Ma and 1043 +22/ -23 Ma (MSWD = 2.03). These ages are interpreted in terms of igneous crystallization and metamorphism respectively, although the lower intercept age may be a composite of more than one effect.

Preservation of pre-1.3 Ga igneous ages confirms the argument that younger metamorphic ages for zircon rims around baddeleyite are metamorphic and not cooling ages. In Davidson and van Breemen (1988), this argument was based on the zircon isotopic systematics of an orthogneiss from a different subdomain of Algonquin domain, 50 km to the southwest. The orthogneiss collected for the present study is in the same subdomain and separated by only 5 km from coronite samples 2 and 3, thus providing a more solid foundation for the above argument.

Hypersthene-bearing granodiorite dyke (sample 5; 85DMSD-62h)

A sample was collected in the southwestern part of Algonquin domain from a pale buff-green, fine-grained hypersthene granodiorite dyke that cuts cleanly across the foliation of a coronitic olivine metagabbro body and includes fragments of it. Although this metagabbro has not been dated, it is similar in every respect to the other metagabbros of the 1170 Ma suite. The granodiorite locally intrudes the margin of the metagabbro body, but was not observed to cut the neighbouring layered quartzofeldspathic granulites.

The zircons from sample 5 range from subhedral prisms to entirely equant, multifaceted grains. The different morphologies show little range in U concentration. There is, however, a considerable scatter with an imperfect alignment of data points corresponding to upper and lower intercept ages of 1523 +91/ -63 Ma and 1034 +73/ -96 Ma and a MSWD of 8.7 (York, 1969). The oldest ^{207}Pb-^{206}Pb age of 1404 Ma corresponds to the fraction of most equidimensional grains and the youngest ^{207}Pb-^{206}Pb age of 1196 Ma to the most prismatic. Samples 5c and 5e with almost identical U-Pb isotopic ages consist of prismatic and round grains respectively, with the latter indicating a slightly older age. A regression line through prismatic fractions 5a, 5b, and 5c yields upper and lower intercepts of ca. 1500 and 1050 Ma.

The data are interpreted in terms of intrusion of the dyke at about 1050 Ma with a large inheritance of older zircons of at least two ages, one being younger than 1500 Ma and the other equidimensional variety older than 1500 Ma. It has not been established whether the older age is of igneous or sedimentary origin. The intrusive granodiorite may have been derived by local melting of the country rock at the margin of the metagabbro body during granulite-facies regional metamorphism.

Clinopyroxene syenite dyke (sample 6; 86DM-10b)

Sample 6 from the margin of level 3 near the southeastern end of Rosseau subdomain is from one of several greenish-buff clinopyroxene syenite dykes that cut a well-reacted coronitic olivine metagabbro. This metagabbro has not been dated, but is identical to other bodies of the 1170 Ma suite.

Zircons from sample 6 are not of good quality, containing cracks and inclusions. They are generally prismatic (finer fractions 6b, 6c, and 6d), but a coarse fraction (6a) is stubby to equidimensional. U concentrations are consistently high for all four fractions (900-1300 ppm). A regression (York, 1969) analysis yielded an upper intercept age of 1058 +8/ -4 Ma with a lower intercept age of ca. 270 Ma and a MSWD of 3.1. The data provide a minimum age of 1054 Ma for the metamorphism of the coronite intruded by the syenite dyke.

Syntectonic pegmatite, Horseshoe Lake (sample 7)

A mildly internally deformed boudinaged pegmatite **(Fig. 5)** was sampled for U-Pb zircon dating from the shear zone bounding Moon River subdomain (level 3) and Parry Sound domain (level 2). The pegmatite is a cross-cutting but rotated 'climbing' pegmatite, which according to the criteria of Hanmer (1984) has been interpreted in terms of emplacement into the shear zone during movement of the hanging wall over the foot wall. The strong foliation of the shear zone is cut by the pegmatite, which itself contains the same fabric as its sheared country rock, a straight-layered tectonite with rotated mafic boudins. Emplacement thus occurred at a late stage of the shearing that resulted from northwest overthrusting of the Moon River subdomain (level 3) over Parry Sound domain (level 2).

Zircons from sample 7 are mainly long prismatic and subhedral to euhedral. Cracks abound, and many crystals were apparently very coarse but have been broken into irregular fragments. Three fractions were picked from these broken fragments (7b, 7c, 7d), and one from the prismatic crystals (7a). The latter had an extremely high U content of 5400 ppm, whereas the fragments had U contents of ca. 1600 ppm. All four fractions are nearly concordant and collinear, yielding an upper intercept age of 1103 +6/ -4 Ma and a lower intercept of ca. 500 Ma with a MSWD of 0.04. This age is interpreted to date emplacement of this syntectonic pegmatite.

Figure 5. Boudinaged but cross-cutting 'climbing' pegmatite (sample 7), Horseshoe Lake, southwest road cut.

DISCUSSION

The data sets presented in this report are of a fragmented nature but provide support for other geochronological studies (van Breemen et al., 1986; Davidson and van Breemen, 1988; L. Nadeau and O. van Breemen, manuscript in preparation). The 1375 +13/ -12 Ma upper intercept age for the granulite-facies metamonzonite (sample 4) is best interpreted as dating igneous crystallization. This age corresponds to the younger of two igneous phases encountered in the Central Gneiss Belt (CGB) (van Breemen and Davidson, 1988), which in turn is within the 1400-1340 Ma range of magmatic activity in the western granite rhyolite province of the midcontinent (Bickford et al., 1986). The older 1450-1480 Ma magmatism of the eastern province may be represented by the inherited zircons of the hypersthene granodiorite dyke (sample 5).

U-Pb data on the baddeleyite from the coronite in the Parry Sound shear zone (sample 1) indicate that the 1170 Ma basic magmatism extended into Britt domain northwest of the Parry Sound shear zone, supporting inferences drawn from field observations and geochemical data (Davidson and Grant, 1986). (It is noted, however, that the coronitic olivine metagabbro suite is absent from the interior of Parry Sound domain).

The 1058 +8/ -4 Ma age for the clinopyroxene syenite dyke (sample 6) should be a minimum age not only for the metamorphism of the coronitic metagabbro, which it intrudes, but also for the emplacement of deck 3 (Seguin) over deck 1 (Rosseau). According to the model of Culshaw et al. (1983), this event saw the emplacement of deck 3 (both the Seguin and the Moon River subdomains) against the Parry Sound domain. A late stage of this movement has now also been dated at 1103 +6/ -4 Ma, the age of a late syntectonic pegmatite (sample 7). This age is intermediate between the 1159 +5/ -4 Ma age of a late stage of shear in the Parry Sound shear zone and movement along the Central Metasedimentary Belt boundary thrust zone at 1060 ± 6 Ma

and continuing at 1029 +14/ ±-4 Ma (van Breemen and Hanmer, 1986). These new data thus provide further evidence for a southeastward younging of at least the final stages of thrusting between the Parry Sound shear zone and the Central Metasedimentary Belt thrust zone.

The 1043 +22/ -23 Ma lower intercept age for the granulite facies metamonzonite (sample 4) appears to be consistent with the ca. 1047 ± 5 Ma age previously obtained from zircon from a nearby coronitic metagabbro (87DM-11d). With one exception (sample 3; point 3, Fig. 3), U-Pb ages for zircons from metagabbros in the southeastern part of the CGB range from 1060 Ma to 1030 Ma (Fig. 2); this range coincides with ages obtained so far for late-stage thrusting along the Central Metasedimentary Belt boundary thrust zone (van Breemen and Hanmer, 1986).

The range of lower intercept ages is, however, younger than late thrust movements in the same region, which postdate granulite-facies metamorphism. The oldest syntectonic pegmatite in Algonquin domain, near Huntsville, which cuts the local granulite facies metamorphic fabric, was dated at 1080 ± 3 Ma (L. Nadeau and O. van Breemen, manuscript in preparation). In view of the latter information, the previously published 1080 Ma ^{207}Pb-^{206}Pb age for ovoid zircon from the coronitic gabbro in the Seguin domain (point 3, Fig. 3) may be reinterpreted as being entirely of metamorphic origin. Given the clear evidence for the preservation of older igneous U-Pb ages in coarse (ca. 100 micron) grains from metamonzonite (sample 4) and from one other granulite-facies meta-igneous rock in the region (van Breemen et al., 1986), it is unlikely that a significant proportion of radiogenic Pb was lost from zircon crystals larger than 50 microns either by solid-state diffusion or by lattice recrystallization during metamorphism. However, Davidson and van Breemen (1988) suggested that fine polycrystalline zircon aggregates forming around baddeleyite may recrystallize into coarser zircon grains. The new data are consistent with this interpretation, indicating that the ca. 100 micron-sized ovoid multifaceted zircon crystals in the coronitic metagabbros are the end product of a recrystallizing process at high temperatures. This recrystallization of fine to coarse zircon coincided with continued compressional movement along the Central Metasedimentary Belt boundary thrust zone.

The above scenario is also consistent with the isotopic evidence from the mantles of the fine zircon surrounding baddeleyite in the coronitic metagabbro (sample 1) from the northwestern edge of the Parry Sound shear zone, which clearly have not continued to recrystallize during the 1060 - 1030 Ma interval. However, the question as to when granulite-facies metamorphism began after 1170 Ma is more subtle and at present is undated.

Finally it is noteworthy that the 1103 +6/ -4 Ma age for the syntectonic pegmatite, which is related to the compressive overthrusting within the CGB, is contemporaneous with the Keweenawan rift volcanism dated between 1109 Ma and 1094 Ma (Davis and Sutcliffe, 1985; Paces and Davis, 1988). Other dated compressive events in the southwestern Grenville Structural Province, however, are outside this range.

ACKNOWLEDGEMENTS

The manuscript has benefitted from a critical review by L. Nadeau. We thank W.D. Loveridge, K. Santowski, J. MacRae, and J.C. Bisson for their contributions in generating the age determinations.

REFERENCES

Bickford, M.E., Van Schmus, W.R., and Zietz, I.
1986: Proterozoic history of the midcontinental region of North America; Geology, v. 14, p. 492-496.

Culshaw, N.G., Davidson, A., and Nadeau, L.
1983: Structural subdivisions of the Grenville Province in the Parry Sound - Algonquin region, Ontario; in Current Research, Part B; Geological Survey of Canada, Paper 83-1B, p. 243-252.

Davidson, A.
1984: Tectonic boundaries within the Grenville Province of the Canadian Shield; Journal of Geodynamics v. 1, p. 433-444.

Davidson, A., and Grant, S.M.
1986: Reconnaissance geology of western and central Algonquin Park and detailed study of coronitic olivine metagabbro, Central Gneiss Belt, Grenville Province of Ontario; in Current Research, Part B; Geological Survey of Canada, Paper 86-1B, p.837-848.

Davidson, A., and van Breemen, O.
1988: Baddeleyite-zircon relationships in coronitic metagabbro, Grenville Province, Ontario: implications for geochronology; Contributions to Mineralogy and Petrology, v. 100, p. 291-299.

Davis, D.W., and Sutcliffe, R.H.,
1985: U-Pb ages from the Nipigon plate and northern Lake Superior; Geological Society of America Bulletin, v. 96, p. 1572-1579.

Hanmer, S.K.
1984: The potential use of planar and elliptical structures as indicators of strain regime and kinematics of tectonic flow; in Current Research, Part B; Geological Survey of Canada, Paper 84-1B, p. 133-142.

Paces, J.B., and Davis, D.W.
1988: Implications of high precision U-Pb age dates on zircons from Portage Lake volcanic basalts on midcontinent rift subsidence rates, lava flow repose periods and magma production rates; in Proceedings and Abstracts; 34th Annual Institute on Lake Superior Geology, Marquette, Michigan, p. 85-86.

van Breemen, O., and Davidson, A.
1988: Northeast extension of Proterozoic terranes of midcontinental North America; Geological Society of America Bulletin, v. 100, p. 630-638.

van Breemen, O., and Hanmer, S.
1986: Zircon morphology and U-Pb geochronology in active shear zones: studies on syntectonic intrusions along the northwest boundary of the Central Metasedimentary Belt, Grenville Province, Ontario; in Current Research, Part B, Geological Survey of Canada, Paper 86-1B, p. 775-784.

van Breemen, O., Davidson, A., Loveridge, W.D., and Sullivan, R.W.

1986: U-Pb zircon geochronology of Grenville tectonites, granulites and igneous precursors, Parry Sound, Ontario; in The Grenville Province, ed. J.M. Moore, A. Davidson, and A.J. Baer; Geological Association of Canada, Special Paper 31, p. 191-207.

Parrish, R.R., Roddick, J.C., Loveridge, W.D., and Sullivan, R.W.

1987: Uranium-lead analytical techniques at the geochronology laboratory, Geological Survey of Canada; in Radiogenic Age and Isotopic Studies: Report 1; Geological Survey of Canada, Paper 87-2, p. 3-7.

Roddick, J.C.

1987: Generalized numerical error analysis with applications to geochronology and thermodynamics; Isotope Geoscience, v. 66, p. 2129-2135.

Wynne-Edwards, H.R.

1972: The Grenville Province; in Variations in Tectonic Styles in Canada, ed. R.A. Price and R.J.W. Douglas; Geological Association of Canada, Special Paper 11, p. 263-334.

York, D.

1969: Least squares fitting of a straight line with correlated errors; Earth and Planetary Science Letters, v. 5, p. 320-324.

U-Pb geochronology of Silurian granites, Miramichi Terrane, New Brunswick[1]

Mary Lou Bevier[2] and Joseph B. Whalen[2]

Bevier, M.L., and Whalen, J.B., U-Pb geochronology of Silurian granites, Miramichi Terrane, New Brunswick; in Radiogenic age and isotopic studies: Report 3, Geological Survey of Canada, Paper 89-2, p. 93-100, 1990.

Abstract

Granitic plutons emplaced during the Acadian orogeny are abundant in the Miramichi Terrane of New Brunswick. Previous workers have generally assigned Devonian ages to these plutons. Seven new U-Pb ages for Acadian granitic rocks from the Miramichi Terrane are presented, which indicate that more than 90% of the felsic plutonism in this region is Silurian and not Devonian as previously thought.

Résumé

Des plutons granitiques mis en place au cours de l'orogène acadien sont abondants dans le terrane de Miramichi du Nouveau-Brunswick. Les premiers géologues ont généralement attribué à ces plutons des âges dévoniens. Dans le présent document, on trouve sept des nouveaux âges obtenus par la méthode U-Pb pour des roches granitiques de l'Acadien provenant du terrane de Miramichi; ces âges indiquent que plus de 90 % du plutonisme felsique dans cette région est d'origine silurienne et non pas dévonienne.

INTRODUCTION

The purpose of this paper is to present the analytical data for U-Pb ages of seven Silurian and Devonian granitic intrusions from the Miramichi Terrane, New Brunswick (Fig. 1). Rb-Sr and K-Ar age determinations on samples from additional plutons in the same area are reported in Whalen and Theriault (1990). The geological setting of these plutons is described in Bevier and Whalen (1990), and these data constrain the tectonic interpretations presented therein.

Sample locations are given in Table 1. The granitic rocks intrude metavolcanic and metasedimentary rocks of the Cambro-Ordovician Tetagouche Group and, in part, a suite of deformed Ordovician granitic plutons (Fig. 1)(Whalen, 1987). Modal analyses of the samples are presented in Table 2. The Pokiok batholith and North Pole Stream pluton were previously dated as Devonian by Rb-Sr and K-Ar methods (McCutcheon et al., 1981; Fyffe, 1982), and the Mount Elizabeth complex was considered to be the same age based on similar rock types and lack of deformation. These plutons are mostly undeformed and unmetamorphosed, except adjacent to major faults. Because of their geological relationships and scattered Devonian mineral ages these plutons have long been regarded as Acadian intrusions (Fyffe et al., 1981).

ANALYTICAL TECHNIQUES

Zircon and other datable minerals were concentrated from 25 kg of each rock sample, and individual zircon populations were separated initially on the basis of grain size and magnetic susceptibility and subsequently by crystal habit. Grains selected for analysis were hand picked using a binocular microscope to isolate the most euhedral, optically homogeneous, fracture-free and inclusion-free grains. All zircon and sphene fractions were abraded to remove potentially altered outer parts of the grains (Krogh, 1982).

1 Contribution to the Canada-New Brunswick Mineral Development Agreement, 1984-1989.
2 Geological Survey of Canada, 601 Booth Street, Ottawa, Ontario K1A 0E8

Table 1. Sample locations* and descriptions.

U-Pb sample number	Map Sheet	East	North	Batholith/Suite	Pluton or Phase	Sample Description
WXNB-707	21J/15	888	064	North Pole Stream	granite (SNg)	mg-cg granite, rare larger Kfs
WXNB-710	21O/8	893	477	Mount Elizabeth complex	granite (SEpg)	mg eq bt granite
WXNB-711	21O/7	829	518	Mount Elizabeth complex	Alkaline Suite (SEag)	cg bt granite
WXNB-701	21G/14	277	903	Pokiok batholith	Hartfield	cg slightly fol bt granodiorite
WXNB-700	21G/14	368	922	Pokiok batholith	Hawkshaw	mg Kfs porph (2-5 cm) bt granite
WXNB-724	21G/14	192	695	Pokiok batholith	Skiff Lake	cg eq bt-musc tonalite
WXNB-723	21G/14	393	943	Pokiok batholith	Allandale	mg eq bt-musc granodiorite

*NTS map sheet and UTM Zone 19 grid locations are given for the samples. Note: Letters in parentheses are the intrusive map units of Whalen (1988). Abbreviations: bt - biotite, musc - muscovite, Kfs - K feldspar, cg - coarse-grained, mg - medium grained, eq - equigranular, porph - porphyritic, fol - foliated.

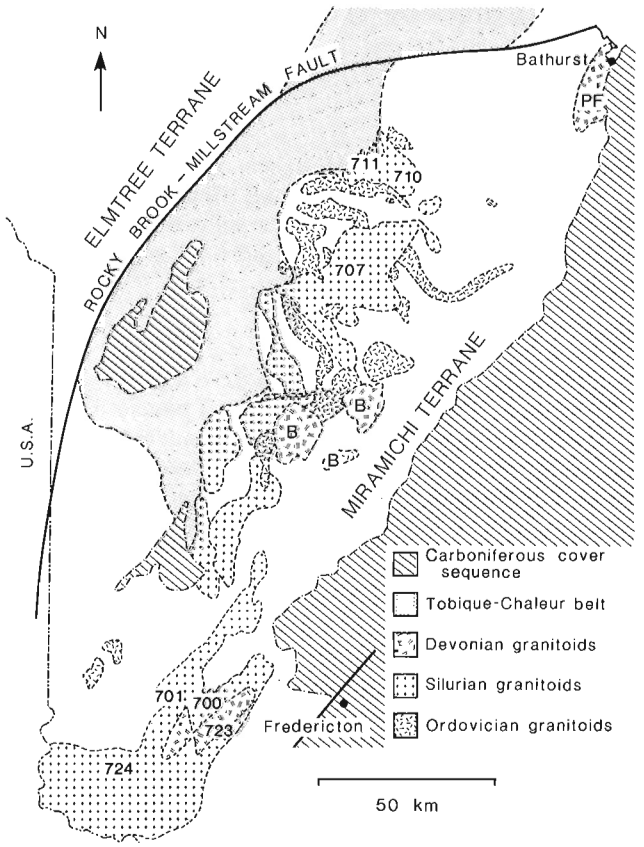

Figure 1. Map of major Paleozoic plutons in the Miramichi Terrane (Fyffe and Fricker, 1987), New Brunswick, showing the locations of samples analyzed for this study. Unpatterned area of Miramichi Terrane represents Cambro-Ordovician rocks of the Tetagouche Group. Sample numbers are keyed to the tables. (Sample prefixes are omitted from the diagram for clarity). PF = Pabineau Falls pluton; B = Burnthill suite of plutons. The distribution of Silurian plutons is based on this paper and Whalen and Theriault (1990).

Several fractions of zircon as well as monazite or sphene or xenotime (if present) were analyzed from each sample. Procedures for dissolution, separation of Pb and U, and purification techniques employing a $^{205}Pb/^{233-235}U$ spike were the same as those detailed in Parrish et al. (1987). Total procedural blanks for Pb ranged from 9 to 44 pg (average 20 pg; n=32) for zircon, monazite, and xenotime, and were 36 pg for three sphene analyses. U blanks averaged

Table 2. Modes (volume %) for Miramichi granitoid samples.

U-P sample no.: WXNB	-707	-710	-711	-701	-700	-724	-723
Quartz	31.8	29.7	26.3	26.7	27.5	31.3	29.9
Plagioclase	29.2	34.8	8.0	50.0	38.3	42.3	41.9
K feldspar	32.0	29.4	60.9	11.3	22.6	1.8	19.5
Amphibole	-			tr	-	-	-
Biotite	7.0	5.5	4.4	10.5	10.8	23.5	5.5
Muscovite	-	0.2	-	-	-	tr	3.2
Opaques	tr	tr	0.2	-	0.4	0.1	tr
Sphene	-	-	-	0.8	0.3	-	-
Allanite	-	-	0.2	0.1	-	-	-
Apatite	tr	0.2	-	0.3	tr	0.7	tr
Zircon	tr	0.2	tr	tr	0.1	0.2	tr
Monazite	tr	tr	-	-	-	-	tr
Xenotime	-	-	-	-	-	tr	-
Fluorite	-	tr	-	-	-	-	-
Epidote	-	-	-	0.1	-	-	-

Note: Each mode represents a combination of point counts on a stained 12 by 20 cm slab (1000 points) and a thin section (1000 points).

3 pg for zircon, monazite, and xenotime analyses and 5 pg for sphene analyses. Isotopic analyses were carried out on a Finnigan MAT 261 solid-source mass spectrometer equipped with multiple collectors, secondary electron multiplier, and operating software designed for simultaneous measurement of all five Pb isotopes (Parrish et al., 1987). Discordia line intercepts and associated errors were calculated using a modified York technique (York, 1969) as detailed in Parrish et al. (1987). Errors were propogated numerically (Roddick, 1987) and are quoted at the 2σ level, with $^{207}Pb/^{235}U$ and $^{206}Pb/^{238}U$ errors averaging 0.27 and 0.20%, respectively, for zircon, monazite, and xenotime analyses, and 1.11 and 0.28%, respectively, for sphene analyses. All age determinations were calculated using the decay constants of Steiger and Jäger (1977), and sphene analyses were corrected with measured common Pb from feldspars in the same granitic samples (Bevier, 1987).

A number of analyses generated in this study fall on or near concordia. We consider an analysis to be concordant when there is a substantial overlap of the 2σ error envelope with concordia. For such analyses, the errors we assign to the crystallization age is the 2σ error of the $^{206}Pb-^{238}U$ age. For monazite analyses that plot above concordia due to excess ^{206}Pb (Schärer, 1984), and in the absence of Th and U corrections, the $^{207}Pb-^{235}U$ age is taken to be the crystallization age of the monazite. The geological time scale of Palmer (1983) is used throughout this paper.

RESULTS

The U-Pb analytical data are given in Table 3. In three of the seven samples at least one fraction of zircon or sphene gave a concordant result. In three samples containing monazite, duplicate ^{207}Pb-^{235}U ages agree within error, the points being slightly above concordia. In most samples the zircon ± sphene ± xenotime fractions display either simple Pb loss systematics or a combination of Pb loss and an inherited component. In many samples, xenocrystic zircons were recognized by their morphology and specifically excluded from analysis.

Sample WXNB-707 is a biotite granite with minor K feldspar megacrysts from the North Pole Stream pluton. Zircons from WXNB-707 are pale yellow with very good clarity and about 5% clear tubular or spherical inclusions. Two morphological populations of zircon are present, euhedral acicular grains with length:breadth (l:b) of 10:1 and multifaceted prismatic grains (l:b=2:1). Monazites are yellow, euhedral prisms that have excellent clarity.

Three analyses of zircons of different magnetic susceptibility and grain morphology are all discordant in a pattern that suggests small degrees of Pb loss (Fig. 2). Duplicate

Table 3. U-Pb analytical data.

Mineral fraction	Weight (mg)	U (ppm)	Pb* (ppm)	Measured $^{206}Pb/^{204}Pb$	$^{208}Pb^*$ (%)	Isotopic ratios $^{206}Pb^*/^{238}U$	$^{207}Pb^*/^{235}U$	Age,Ma $^{207}Pb^*/^{206}Pb^*$
WXNB-707 North Pole Stream granite								
A. N +149 Mu A	0.1119	315.2	21.50	3974	12.6	0.06569	0.50049	422.7±1.8
B. N +105-149 Ac A	0.1500	329.9	22.95	3969	12.9	0.06678	0.50884	422.9+1.7
C. W +105-149 Ac A	0.1009	419.7	28.96	4760	13.3	0.06590	0.50160	420.4±1.8
D. Monazite +149 S	0.0120	1877.9	1378.0	2135	91.7	0.06690	0.50742	(416.7±0.7)
E. Monazite +149 S	0.0210	1658.2	988.1	3097	89.7	0.06691	0.50765	(416.9±0.7)
WXNB-710 Mount Elizabeth biotite granite								
F. N +74-149 A	0.0174	584.2	36.10	1503	8.2	0.06666	0.50623	415.5±3.6
G. M +105 F A	0.0483	2669.8	166.8	2147	6.2	0.06461	0.49168	420.1±3.3
H. M +105 Ac A	0.1247	3098.6	188.0	4586	6.5	0.06254	0.47503	415.7±1.9
I. Monazite +149 S	0.0083	1204.5	1204.0	1286	93.9	0.06712	0.50935	(418.0±1.1)
J. Monazite +149 S	0.0046	2323.1	1742.0	1392	91.8	0.06694	0.50816	(417.2±0.8)
WXNB-711 Mount Elizabeth alkaline granite								
K. N+149 A	0.1315	200.6	13.68	1285	11.7	0.06634	0.50525	421.8±4.9
L. W +149 A	0.1657	423.0	29.09	1745	12.1	0.06657	0.50690	421.2±3.9
M. N +44-62 A	0.2075	777.6	53.51	8991	12.0	0.06667	0.51196	440.1±1.9
WXNB-701 granodiorite, Hartfield phase, Pokiok batholith								
N. N +149 Ac A	0.1064	1157.3	74.25	5217	7.1	0.06565	0.50044	423.9±1.8
O. W +149 Ac A	0.2085	1104.4	69.94	5458	7.3	0.06471	0.49144	415.5±1.8
P. M +149 Ac A	0.1254	1515.1	97.20	11270	8.3	0.06487	0.49311	417.6±1.4
Q. Sphene +149 A	0.2980	134.0	12.05	289	32.8	0.06644	0.50434	414.3±9.7
R. Sphene +149 A	0.1490	241.1	19.02	352	24.1	0.06587	0.50136	420.5±7.8
WXNB-700 granite, Hawkshaw phase, Pokiok batholith								
S. N +105-149 F A	0.0312	1496.1	91.89	1681	7.9	0.06239	0.47137	403.7±3.6
T. N +105-149 Ac A	0.0830	979.2	62.50	6930	9.0	0.06405	0.48450	406.5±1.5
U. N +105-149 F,E A	0.0845	1190.8	75.09	2684	8.0	0.06392	0.48363	407.1±2.6
V. W +105-149 F A	0.0556	1576.5	98.69	3594	9.8	0.06222	0.47062	406.4±2.1
W. Sphene +149 A	0.0950	131.2	9.30	75	15.6	0.06589	0.50105	418.4±34
WXNB-724 tonalite, Skiff Lake phase, Pokiok batholith								
X. N +149 Ac A	0.0790	174.8	11.48	2520	11.8	0.06510	0.49359	411.8±3.4
Y. N +149 Mu A	0.0269	150.9	17.84	1407	15.3	0.11105	1.28607	1292.4±2.9
Z. W +149 Ac A	0.0500	154.6	10.44	1639	15.1	0.06507	0.49257	408.1±2.7
AA. M +149 Ac A	0.0466	165.5	10.86	1873	11.4	0.06527	0.49426	409.2±2.2
BB. Xenotime +177 S	0.0325	2028.8	125.4	1716	5.4	0.06488	0.49150	409.9±3.5
CC. Xenotime +177 S	0.0120	4690.6	303.6	5826	10.4	0.06493	0.49168	409.1±1.5
WXNB-723 granodiorite, Allandale phase, Pokiok batholith								
DD. N +105 A	0.0513	978.5	60.01	2807	4.5	0.06457	0.49350	429.6±2.5
EE. W +105 A	0.0871	1614.5	94.70	4025	3.9	0.06218	0.47000	404.9±2.0
FF. M +105 Ac A	0.0873	1454.6	85.61	2803	5.6	0.06125	0.46332	406.6±2.6
GG. Monazite +149 S	0.0252	772.7	400.3	2511	88.5	0.06518	0.49054	(405.3±1.0)
HH. Monazite +149	0.0343	1429.2	756.0	2255	88.9	0.06442	0.48549	(401.8±0.8)
II. Monazite +149 S	0.0188	2300.4	863.8	2397	84.3	0.06445	0.48606	(402.2±0.8)

*radiogenic Pb, blank corrected. Errors are $\pm 2\sigma / \sqrt{n}$. N = non-magnetic at <1° side tilt, 1.7 amps on Frantz magnetic separator; W= weakly magnetic at <2°, >1°, 1.7 amps; M = magnetic at <5°, 1 amp, and >2°, 1.7 amps; V= very magnetic at >5°, 1 amp; A = abraded; S = single grains; F = flat tablets; Mu = multifaceted; Ac = acicular; E = elongate. Sphene analyses are corrected using measured common Pb in feldspar from the same sample (Bevier, 1987). Ages cited in parentheses for monazites are ^{207}Pb-^{235}U ages.

single crystal monazite ^{207}Pb-^{235}U ages of 417 ± 1 Ma, however, confirm a Silurian age for this sample. Because the ^{207}Pb-^{206}Pb ages of all zircon analyses are greater than 417 Ma, these zircons must be characterized by some inheritance.

Sample WXNB-710 is an equigranular biotite granite from the most volumetrically dominant phase of the Mount Elizabeth complex (Whalen, 1987). Zircons from this sample are pale yellow to pale brown, euhedral, and have good to fair clarity owing to a high percentage of cloudy fractures. Flat, pseudo-hexagonal tablets, elongate grains (l:b=4:1 to 7:1), and simple forms (prism + dipyramid) with l:b=2:1 to 3:1 are present. Monazites are present as subhedral prisms with very good clarity.

Duplicate single monazite grains yield ^{207}Pb-^{235}U ages of 418 ± 1 Ma (Fig. 3). One zircon analysis (fraction F) is analytically concordant at 416 ± 1 Ma, whereas two other zircon analyses show minor Pb loss. Although the 2σ error envelopes for the concordant zircon fraction and the monazite fractions overlap slightly they are not in exact agreement. Therefore we assign an average age of 417 ± 2 Ma to the sample.

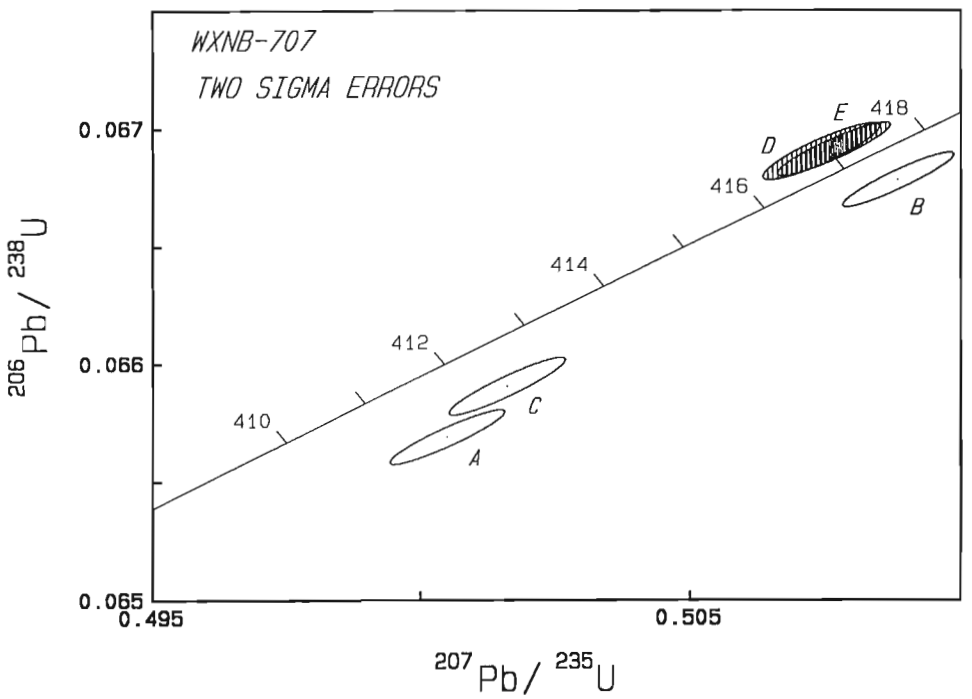

Figure 2. U-Pb concordia plot for zircons (open ellipses) and monazites (shaded ellipses) from the North Pole Stream granite.

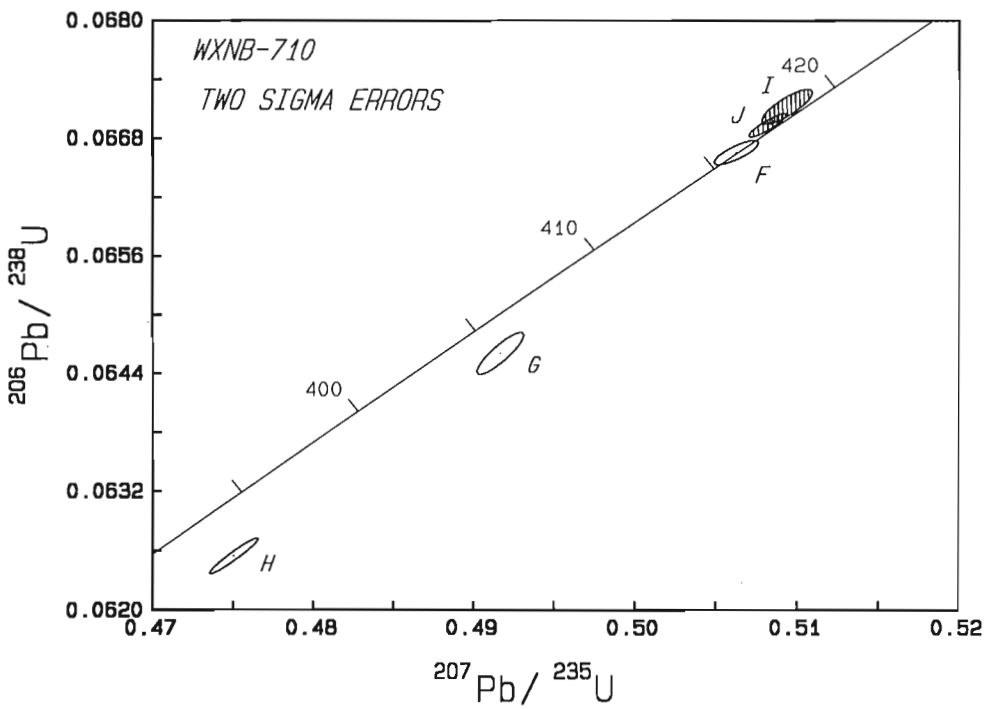

Figure 3. U-Pb concordia plot for zircons (open ellipses) and monazites (shaded ellipses) from the Mount Elizabeth biotite granite.

Sample WXNB-711 is a medium-grained alkaline granite from the northwest lobe of the Mount Elizabeth complex. It contains biotite pseudomorphs after amphibole and possibly fayalite. Zircons from this sample are pale yellow, euhedral simple prisms with dipyramidal terminations (l:b=1.5:1 to 2.5:1). No cores are visible, and cross-fractures are rare except in fraction L.

Zircon analyses from the Mount Elizabeth alkaline granite, however, are not concordant and show evidence for an inherited xenocrystic component (Fig. 4). The lower intercept of a regression line through the data with concordia (414 ± 1 Ma) is interpreted as a minimum age for the intrusion and the upper intercept (ca. 2.7 Ga) gives an average age for the inherited component. Given the possibility of Pb loss, it is unlikely that the emplacement age is significantly older than the ^{207}Pb–^{206}Pb age of the most concordant zircon fraction (421 ± 4 Ma). Therefore, the best estimate of the age of emplacement of the Mount Elizabeth alkaline granite is 414 +11/-1 Ma.

New ages are presented for four phases of the Pokiok batholith (Lutes, 1987). Sample WXNB-701 is a slightly foliated biotite granodiorite from the Hartfield phase of the Pokiok batholith. All zircons in this sample are euhedral and acicular (l:b=4:1 to 10:1). Clear, colourless cores are visible in many grains, and the euhedral overgrowths are strongly zoned. Many grains, especially in the more magnetic fractions, are cloudy because of the presence of numerous fractures. The sphenes are red-brown, euhedral grains with excellent clarity and rare small black inclusions, possibly ilmenite.

Three zircon analyses yield ^{207}Pb-^{206}Pb ages of 416 to 424 Ma and form a linear array (MSWD=0.36) sub-parallel to concordia with lower and upper intercepts of 383 +10/-32 Ma and 592 +131/-104 Ma, respectively (Fig. 5). The calculated upper intercept age is geologically unreasonable, as this pluton intruded Cambro-Ordovician rocks of the Tetagouche Group. The presence of zircon grains with clear cores and obvious overgrowths, as well as the range of ^{207}Pb-^{206}Pb ages of all zircon fractions, both suggest that many of the zircons contain a xenocrystic component that may be only slightly older than the age of the sample. Two fractions of sphene were analyzed in an attempt to resolve the crystallization age of the rock. Sphene fraction Q is concordant at 415 ± 1 Ma and provides the best estimate of a crystallization age for the sample. The sphene age is regarded as a minimum crystallization age for the sample because of the lower closure temperature for the U-Pb system in sphene relative to that in zircon (Ghent et al., 1988).

Sample WXNB-700 is a K-feldspar megacrystic biotite granite from the Hawkshaw phase of the Pokiok batholith. Zircon morphologies in this sample vary widely and include flat, pseudo-hexagonal tablets, elongate flat tablets, acicular grains (l:b=4:1 to 7:1), and multifaceted prismatic grains with l:b=2:1. Sphenes are red-brown, subhedral grains with excellent clarity.

Several fractions of flat or acicular grains of zircon were isolated for analysis. Fractions S, T, U, and V define a discordia line that has an upper intercept with concordia of 407 ± 3 Ma (MSWD=0.97) (Fig. 6). One fraction of sphene intersects concordia at 411 ± 1 Ma. This age represents the

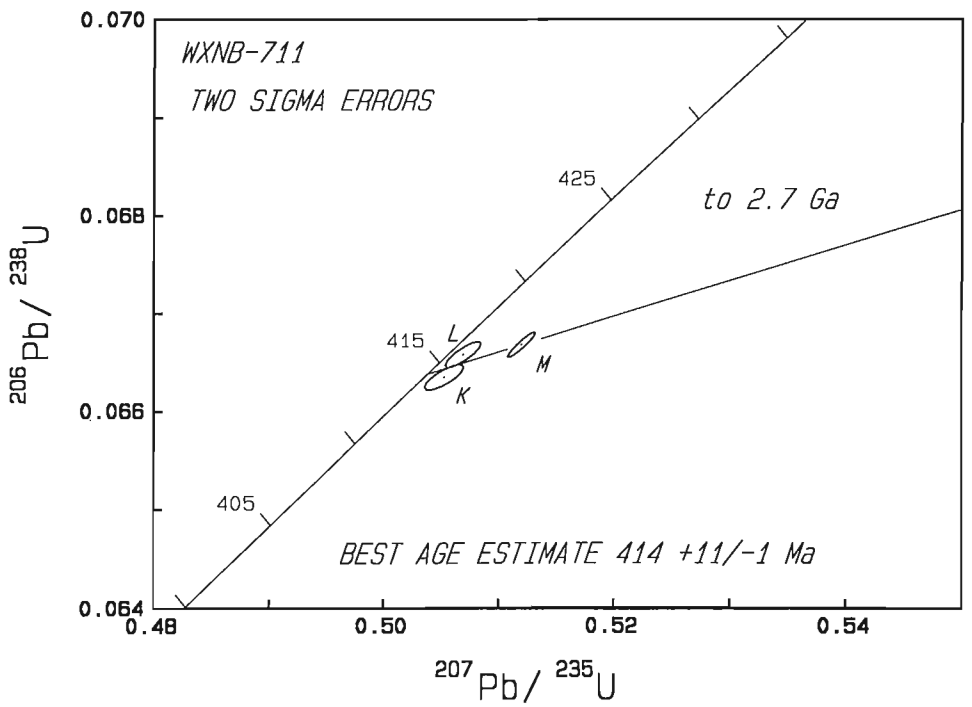

Figure 4. U-Pb concordia plot for zircons from the Mount Elizabeth alkaline granite.

time at which the pluton cooled through the closure temperature for the U-Pb system in sphene and is probably close to the crystallization age of the pluton. The four zircon fractions yield ^{207}Pb-^{206}Pb ages all less than 411 Ma and their discordance is probably due to post-crystallization Pb loss.

Sample WXNB-724 is a biotite-muscovite tonalite from the Skiff Lake phase of the Pokiok batholith. Pale yellow, euhedral acicular grains (l:b=4:1 to 10:1) with excellent clarity and rare inclusions dominate the zircon population in this rock, although multifaceted prisms with multifaceted dipyramids are also common; in these latter grains some of the dipyramids are overgrowths. Xenotime, magnetic at <0.5 amps on a Frantz magnetic separator and confirmed by x-ray diffraction, is present as yellow, euhedral orthorhombic dipyramids with rare prismatic forms and excellent clarity.

All fractions of zircon and xenotime exhibit discordance because of slight Pb loss (Fig. 7). The most concordant analysis, AA, has a ^{207}Pb-^{206}Pb age of 409 ± 2 Ma, and we interpret this as the best estimate of the crystallization age of the sample. One fraction of multifaceted grains (Y; not plotted in Fig. 7) is highly discordant but has a ^{207}Pb-^{206}Pb age of 1.3 Ga, confirming that the multifaceted grains are xenocrystic.

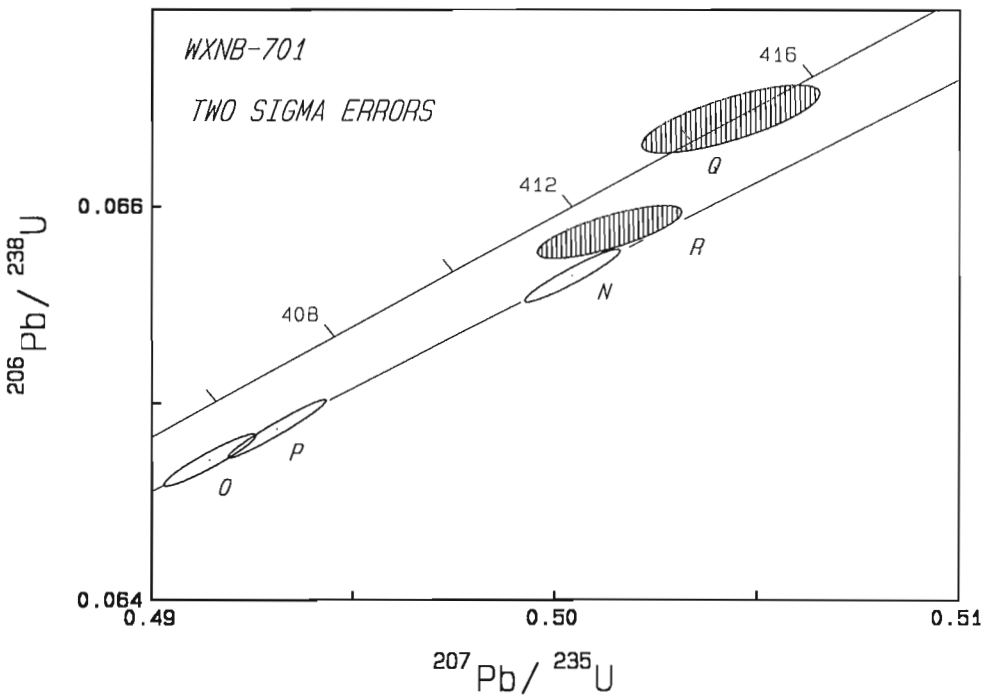

Figure 5. U-Pb concordia plot for zircons (open ellipses) and sphenes (shaded ellipses) from a granodiorite from the Hartfield phase of the Pokiok batholith.

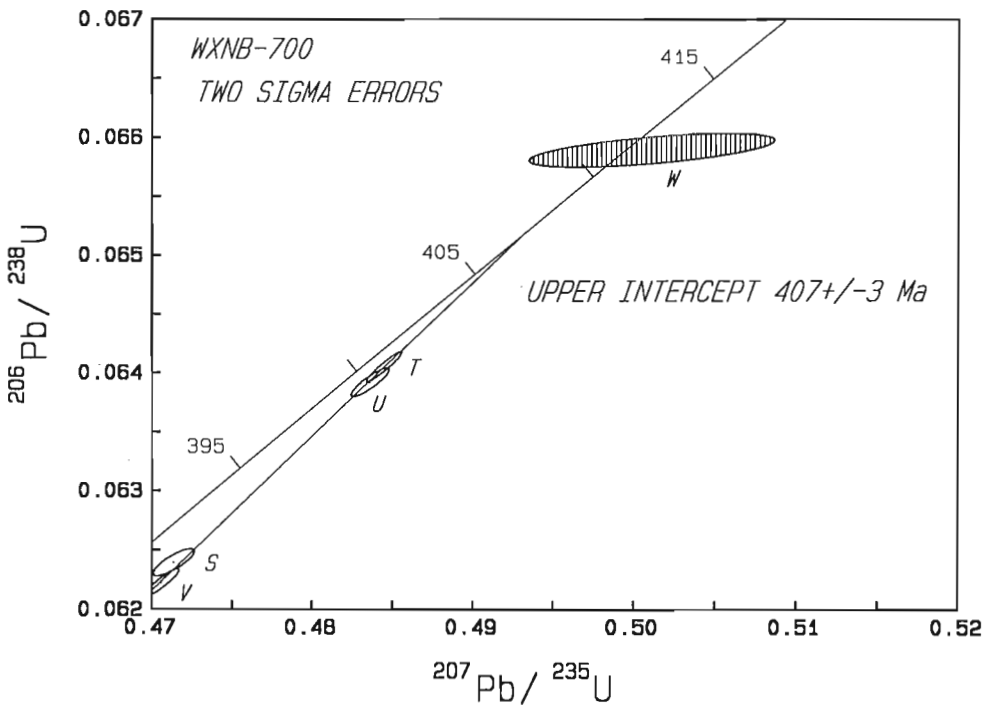

Figure 6. U-Pb concordia plot for zircons (open ellipses) and sphenes (shaded ellipses) from the Hawkshaw granite, Pokiok batholith.

Sample WXNB-723 is a fine-grained, equigranular muscovite granodiorite from the Allandale phase of the Pokiok batholith. The zircon population includes pale beige euhedral prisms (l:b=2:1 to 3:1) with multifaceted tips, some of which are definitely younger overgrowths. In general the cores of these grains have very good clarity but contain rare large, cloudy fracture zones. Also present are pale yellow-brown elongate prisms (l:b=3:1 to 5:1) with only fair to good clarity owing to a high number of cloudy fractures. Monazites are yellow, euhedral prisms with excellent to good clarity and contain rare black specks, possibly ilmenite.

Three fractions of zircons yield discordant analyses and do not form a linear array; these analyses have ^{207}Pb-^{206}Pb ages of 405-430 Ma (Fig. 8). These data suggest variable mixing between an older, inherited zircon component and igneous overgrowths, with subsequent Pb loss. Duplicate monazite analyses with ^{207}Pb-^{235}U ages of 402 ± 1 Ma provide an age for this sample, which is the only Devonian intrusion sampled for this study, according to the time scale of Palmer (1983). Another single monazite analysis, fraction GG, gives a slightly older ^{207}Pb-^{235}U age. The simplest explanation for this discrepancy is analytical error owing to incomplete dissolution of the sample.

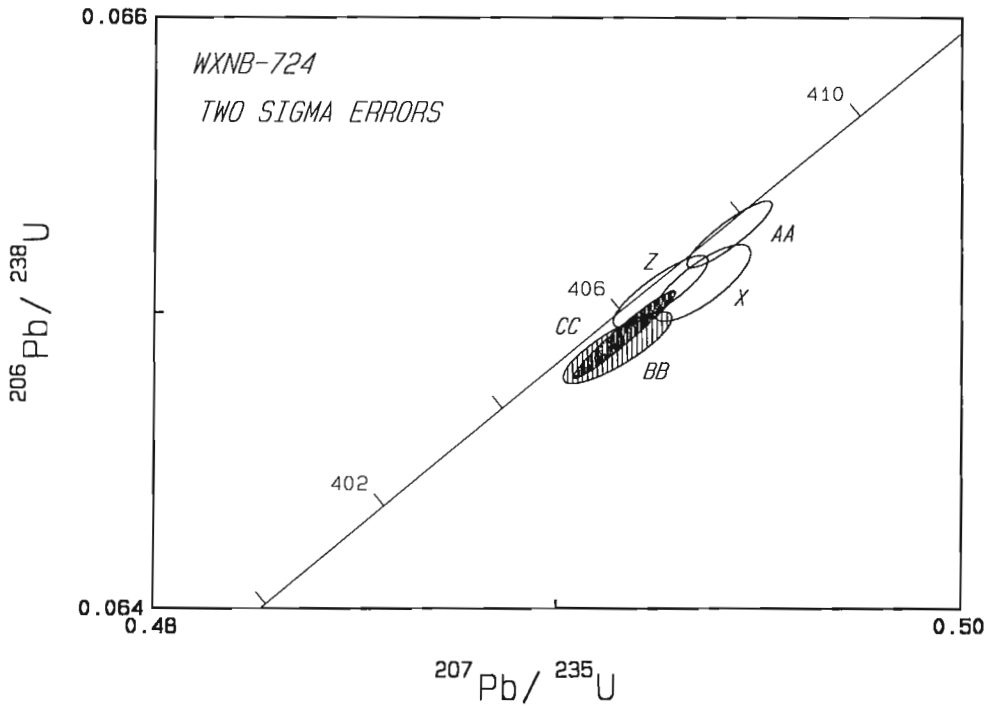

Figure 7. U-Pb concordia plot for zircons (open ellipses) and xenotimes (shaded ellipses) from a tonalite from the Skiff Lake phase of the Pokiok batholith. Fraction Y, which has a ^{207}Pb–^{206}Pb age of 1.3 Ga, plots off the diagram.

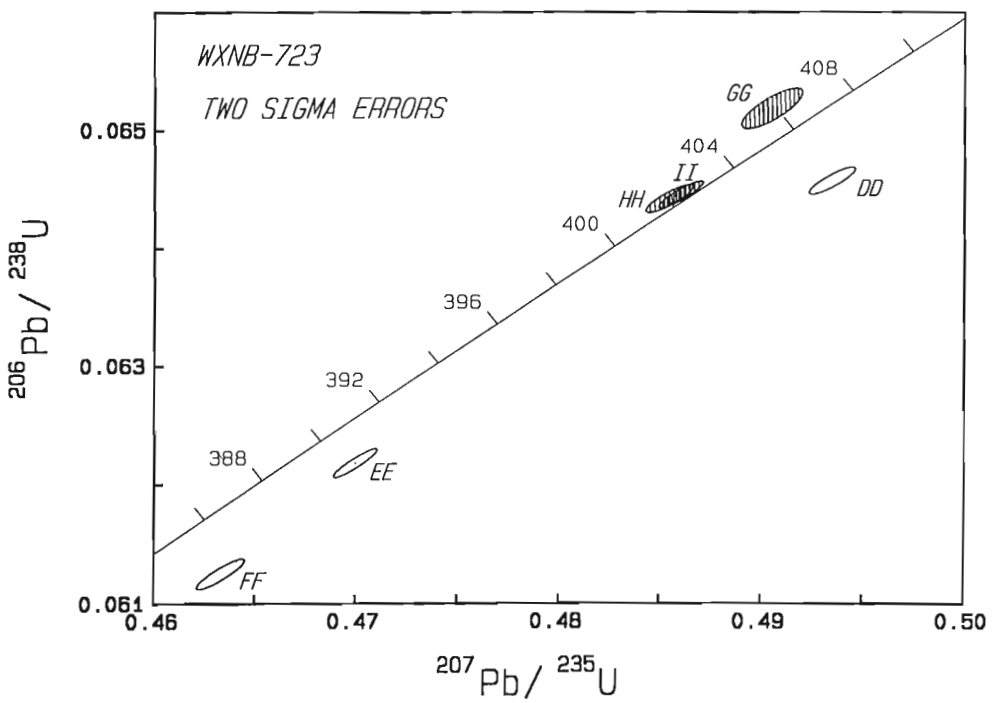

Figure 8. U-Pb concordia plot for zircons (open ellipses) and monazites (shaded ellipses) from a granodiorite from the Allandale phase of the Pokiok batholith.

SUMMARY

The new ages presented here and in Whalen and Theriault (1990) demonstrate that Devonian granites, previously considered abundant within Miramichi terrane, are volumetrically minor, whereas Silurian granites comprise more than 90% of the exposed undeformed plutonic rocks. Only a few intrusions (Fig. 1), such as the Pabineau Falls granite (Bevier, 1988), Allandale granite phase of the Pokiok batholith (this paper), and the Burnthill suite (Taylor and others, 1987), yield definite Devonian ages. These new U-Pb ages require significant revisions of the timing of Acadian orogenesis in New Brunswick.

ACKNOWLEDGMENTS

We thank the technical staff of the Geochronology Section for their help in generating the data. A critical review by Randy Parrish greatly improved the final version of the manuscript.

REFERENCES

Bevier, M.L.
1987: Pb isotopic ratios of Paleozoic granitoids from the Miramichi terrane, New Brunswick, and implications for the nature and age of the basement rocks; in Radiogenic Age and Isotopic Studies: Report 1; Geological Survey of Canada, Paper 87-2, p. 43-50.
1988: U-Pb geochronologic studies of igneous rocks in New Brunswick; in Thirteenth Annual Review of Activities, ed. S.A. Abbott; New Brunswick Department of Natural Resources and Energy, Minerals and Energy Division, Information Circular 88-2, p. 134-140.

Bevier, M.L., and Whalen, J.B.
1990: Tectonic significance of Silurian magmatism in the Canadian Appalachians; Geology, v. 18, p. 411-414.

Fyffe, L.R.
1982: Geology, Woodstock (sheet 21J); New Brunswick Department of Natural Resources, Map NR-4, scale 1:250 000.

Fyffe, L.R., and Fricker, A.
1987: Tectonostratigraphic terrane analysis of New Brunswick; Maritime Sediments and Atlantic Geology, v. 23, p. 113-122.

Fyffe, L.R., Pajari, G.E., and Cherry, M.E.
1981: The Acadian plutonic rocks of New Brunswick; Maritime Sediments and Atlantic Geology, v. 17, p. 23-36.

Ghent, E.D., Stout, M.Z., and Parrish, R.R.
1988: Determination of metamorphic pressure-temperature-time (P-T-t) paths; in Short Course on Heat, Metamorphism, and Tectonics, ed. E.G. Nisbet and C.M.R. Fowler; Mineralogical Association of Canada, Short Course Handbook, v. 14, p. 155-188.

Krogh, T.E.
1982: Improved accuracy of U-Pb ages by the creation of more concordant systems using an air abrasion technique; Geochimica et Cosmochimica Acta, v. 46, p. 637-649.

Lutes, G.G.
1987: Geology and geochemistry of the Pokiok batholith, New Brunswick; New Brunswick Department of Natural Resources and Energy, Report of Investigation 22, 55p.

McCutcheon, S., Lutes, G., Gauthier, G., and Brooks, C.
1981: The Pokiok batholith: a contaminated Acadian intrusion with an anomalous Rb/Sr age; Canadian Journal of Earth Sciences, v. 18, p. 910-918.

Palmer, A.R.
1983: The Decade of North American Geology, 1983 geologic time scale; Geology, v. 11, p. 503-504.

Parrish, R.R., Roddick, J.C., Loveridge, W.D., and Sullivan, R.W.
1987: Uranium-lead techniques at the geochronology laboratory, Geological Survey of Canada; in Radiogenic Age and Isotopic Studies: Report 1; Geological Survey of Canada, Paper 87-2, p. 3-7.

Roddick, J.C.
1987: Generalized numerical error analysis with applications to geochronology and thermodynamics; Geochimica et Cosmochimica Acta, v. 51, p. 2129-2135.

Schärer, U.
1984: The effect of initial ^{230}Th equilibrium on young U-Pb ages: The Makalu case, Himalaya; Earth and Planetary Science Letters, v. 67, p. 191-204.

Steiger, R.H. and Jäger, H.
1977: Subcommision on geochronology: convention on the use of decay constants in geo- and cosmochronology; Earth and Planetary Science Letters, v. 36, p. 359-362.

Taylor, R.P., Lux, D.R., MacLellan, H.E., and Hubacher, F.
1987: Age and genesis of granite-related W-Sn-Mo mineral deposits, Burnthill, New Brunswick, Canada; Economic Geology, v. 82, p. 2187-2198.

Whalen, J.B.
1987: Geology of a northern portion of the Central Plutonic Belt, New Brunswick; in Current Research, Part A; Geological Survey of Canada, Paper 87-1A, p. 209-217.
1988: Geology of a northern portion of the Central Plutonic Belt, New Brunswick - 1:50 000 map with marginal notes; Geological Survey of Canada, Open File 1908.

Whalen, J.B. and Theriault, R.J.
1990: K-Ar and Rb-Sr geochronology of granites, Miramichi Terrane, New Brunswick; in Radiogenic Age and Isotopic Studies: Report 3; Geological Survey of Canada, Paper 89-2, p. 101-107.

York, D.
1969: Least squares fitting of a straight line with correlated errors; Earth and Planetary Science Letters, v. 5, p. 320-324.

K-Ar and Rb-Sr geochronology of granites, Miramichi Terrane, New Brunswick[1]

Joseph B. Whalen[2] and Reginald Theriault[2]

Whalen, J.B. and Theriault, R., K-Ar and Rb-Sr geochronology of granites, Miramichi Terrane, New Brunswick; in Radiogenic Age and Isotopic Studies: Report 3, Geological Survey of Canada, Paper 89-2 p. 101-107, 1990.

Abstract

K-Ar and Rb-Sr muscovite and biotite isotopic ages are reported on samples from the North Pole Stream granite suite, the Lost Lake, Juniper Barrens, and Nashwaak granites, and the Pokiok batholith (Skiff Lake, Hawkshaw and Allandale phases), Miramichi terrane, New Brunswick. These ages, together with U-Pb ages, indicate that many major intrusive units in this terrane, previously thought to be Devonian, are actually of Silurian age. Some of these intrusions were probably emplaced at a high level in the crust and cooled rapidly, while others were intruded at a deeper level and cooled more slowly. Also, one composite intrusion has undergone thermal overprinting. Our preliminary conclusions on variations in intrusion level and cooling histories require further more detailed work.

Résumé

On donne les âges isotopiques obtenus par les méthodes K-Ar et Rb-Sr appliquées à la muscovite et à la biotite prélevées dans des échantillons provenant de la série granitique de North Pole Stream, des granites de Lost Lake, de Juniper Barrens et de Nashwaak ainsi que du batholithe de Pokiok (phases de Skiff Lake, de Hawkshaw et d'Allandale), du terrane de Miramichi au Nouveau-Brunswick. Ces âges, ainsi que les âges obtenus par la méthode U-Pb, indiquent qu'un grand nombre d'unités intrusives importantes situées dans ce terrane, que l'on avait jusqu'ici considéré d'âge dévonien, sont en réalité d'âge silurien. Certaines de ces intrusions ont probablement été mises en place haut dans la croûte et se sont refroidies rapidement, alors que d'autres l'ont été en profondeur et se sont donc refroidies plus lentement. En outre, une intrusion composée a subi une surimpression thermique. Les conclusions préliminaires des auteurs sur les variations des niveaux d'intrusion et des refroidissements nécessitent des travaux plus détaillés.

INTRODUCTION

The geology of New Brunswick has been subdivided, from west to southeast, into five pre-Middle Paleozoic tectonostratigraphic terranes: Elmtree, Miramichi, St. Croix, Mascarene, and Avalonian terranes (Fyffe and Fricker, 1987). Miramichi terrane, which lies south of the Rocky Brook - Millstream fault (Fig. 1), is correlated with the Gander terrane in Newfoundland. Earlier workers subdivided plutonic rocks in this belt into older deformed granites and younger undeformed granites, which were considered to be of Ordovician and Devonian age, respectively (Fyffe et al., 1981). Recent U-Pb dating studies (Bevier, 1988; Bevier and Whalen, 1990) have found the deformed granites to be of middle Ordovician age and most of the undeformed granites to be of Silurian age (see Fig. 1).

This K-Ar and Rb-Sr geochronological study was undertaken to augment and extend granite U-Pb ages from Miramichi terrane (Bevier and Whalen, 1990a) to other plutonic units and also to obtain preliminary information on the thermal history of this plutonic belt.

1 Contribution to the Canada - New Brunswick Mineral Development Agreement, 1984-1989
2 Geological Survey of Canada, 601 Booth Street, Ottawa, Ontario K1A OE8

GENERAL GEOLOGY

The locations of the dated granitic intrusions are given in Figure 1. A brief outline of previous work and important geological features of these intrusions is given below, in a north-to-south order.

North Pole Stream granite suite

This is one of the largest granitic intrusions in Miramichi terrane, portions of which were included in a number of different map sheets produced by earlier workers. This body was remapped by Whalen (1987, 1988, 1990), and renamed the North Pole Stream granite suite (NPSGS). It includes a number of phases, the most voluminous of which is a medium- to coarse-grained light grey to pink biotite granite. Intruding this main phase in the western part of the body are a number of fine- to medium-grained muscovite-biotite granite intrusions, which are interpreted as high-level or roof-zone phases of the suite. Samples for dating were collected from the three largest of these intrusions. One sample (WXNB-136), from a body named the Squaw Lake granodiorite (Fyffe and Pronk, 1985), has been grouped with the NPSGS as it is lithologically and geochemically similar to the sample (WXNB-122) from an intrusion within the NPSGS.

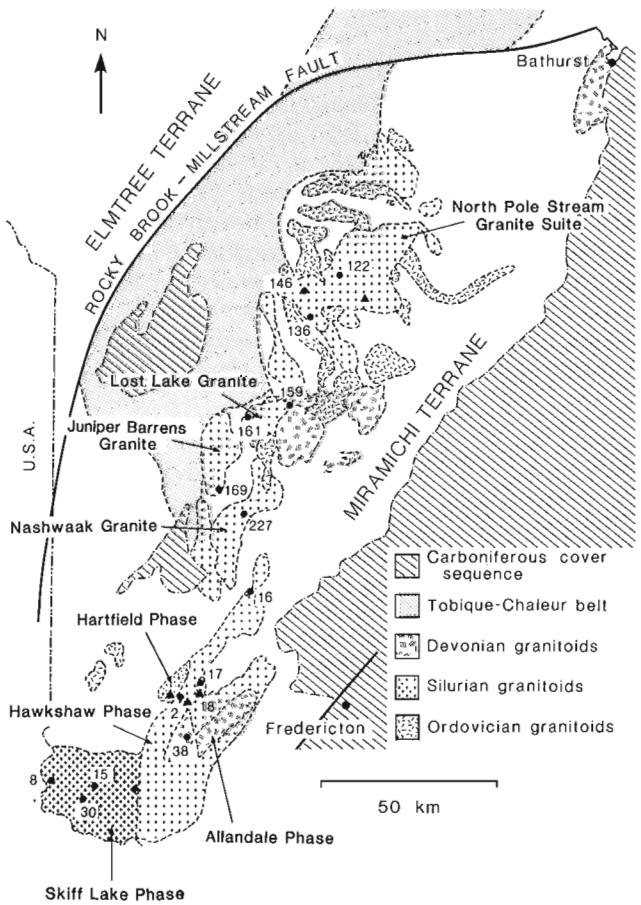

Figure 1. Simplified geologic map of Miramichi terrane granites; plutons or phases discussed in the text are labelled; K-Ar and Rb-Sr sample localities (solid circles), numbered as in Table 1, and U-Pb sample localities (unlabelled solid triangles) discussed by Bevier and Whalen (1990) are shown.

A ten-point whole-rock Rb-Sr isochron from the eastern part the suite gave an age of 387±7 Ma with an initial $^{87}Sr/^{86}Sr$ ratio of 0.703 (Fyffe, 1982). Bevier and Whalen (1990a) report a U-Pb monazite age of 417±1 Ma from the main biotite granite phase of the NPSGS.

Lost Lake granite

Poole (1963) divided the granites in this area of central New Brunswick into an older deformed and recrystallized granite assemblage of presumed Late Ordovician or Early Silurian age and a group of undeformed younger granites, which were thought to be of Devonian age. Crouse (1981) and St. Peter (1981) subdivided Poole's older granites into three types, one of which, the Lost Lake granite, was thought to be of Devonian age. These authors subdivided the Lost Lake granite into two subtypes; a grey to pink, massive to weakly foliated, equigranular biotite granite to granodiorite (their map unit Df2a); and pink, equigranular to subporphyritic, biotite-muscovite granite (their map unit Df2b).

In response to the work of Crouse, Poole (1980) undertook a Rb-Sr study to determine the magmatic crystallization age of his older granites. He obtained a Rb-Sr whole-rock errochron age of 444±72 Ma, with an initial ratio of 0.707 for four samples from the Lost Lake granite. Using a sample with a high $^{87}Rb/^{86}Sr$ ratio, he regressed an isochron to the 0.707 initial ratio and obtained a model age of 412±12 Ma. He also obtained a Rb-Sr muscovite whole-rock age of 424±24 Ma from a Lost Lake granite sample. Additional K-Ar biotite (394±18 Ma) and muscovite (363±16 Ma) ages from the Lost Lake granite were reported by Wanless et al. (1973).

Nashwaak Granite

Parts of this granite have been mapped by Crouse (1981) and St. Peter (1981). An older part of the intrusion consists of grey to pink, medium-grained, biotite and hornblende-biotite granite and granodiorite. The younger part of the intrusion, which we have dated (sample WXNB227 in Table 1), consists of fine- to medium-grained, muscovite-biotite granite with minor biotite-muscovite granite.

Juniper Barren Granite

This granite was mapped and named by Crouse (1981), who described it as being mainly a light grey to pink, medium- to coarse-grained biotite granite. The intrusion also includes minor muscovite-biotite and biotite-muscovite granite, garnetiferous aplite, and pegmatite. The dated sample (WXNB-169) is a biotite-muscovite rich tonalite (Table 1) containing common metasedimentary inclusions. This sample, collected from the margin of the Juniper Barren granite, may be from a "contaminated" contact zone or envelope of this intrusion. Though no isotopic dating has been previously performed on this intrusion, based on its unfoliated character, St. Peter (1981) suggested that it was a late Acadian pluton of Devonian age.

Table 1. Sample locations, rock type and modes for dated Miramichi Terrane granites.

Phase	Skiff Lake			Hawshaw			Allandale			North Pole Stream			Lost Lake		Jun B	Nash
WXNB-:	8	13	30	2	17	16	18	38	122	136	146	159	161	169	227
NTS Sheet	21G/13	21G/13	21G/12	21G/14	21J/3	21J/6	21G/14	21G/14	21O/2	21J/15	21O/2	21J/10	21J/11	21J/11	21J/6
Easting	962	092	034	313	370	518	393	344	778	660	613	604	468	409	489
Northing	688	671	640	898	966	238	943	799	177	030	091	752	750	529	433
Rock Type	G	G	G	KG	KG	G	GD	GD	GD	G	G	GD	GD	T	G
Quartz	52.0	33.0	32.1	24.0	27.8	35.5	29.9	33.9	23.7	32.8	23.7	21.9	31.5	39.2	33.7
Plagioclase	12.0	31.9	29.9	34.1	33.9	35.2	41.9	29.8	55.9	22.9	29.7	53.1	42.5	31.4	30.2
Kfeldspar	3.6	26.0	28.6	25.6	28.9	24.0	19.5	27.5	8.9	34.6	34.8	16.3	4.7	1.2	25.6
Biotite	15.4	4.8	3.8	15.4	7.6	3.8	5.5	6.8	7.6	5.9	6.7	8.3	18.5	19.4	5.2
Muscovite	7.8	4.3	5.4	-	1.3	1.3	3.2	1.0	3.9	2.6	4.9	tr	1.7	7.5	4.7
Opaques	0.4	tr	tr	0.5	0.3	tr	tr	tr	tr	0.4	0.1	0.1	0.8	0.2	tr
Apatite	0.1	tr	0.2	0.5	0.3	0.2	tr	0.4	0.1	0.2	0.1	0.3	0.1	tr	-
Zircon	tr	tr	tr	tr	tr	tr	tr	0.2	-	tr	tr	tr	tr	0.1	0.1
Fluorite	-	-	-	-	-	-	-	-	-	-	tr	-	-	-	4.6
Cordierite	8.6	-	-	-	-	-	-	0.4	-	0.7	-	-	-	1.0	-
Sillimanite	-	-	-	-	-	-	-	-	-	-	-	-	-	0.1	-
Tourmaline	-	-	-	-	-	-	-	-	-	-	-	-	-	tr	-
Topaz	-	-	-	-	-	-	-	-	-	-	-	-	-	-	0.6
Epidote	-	-	-	-	-	-	-	-	-	-	-	-	0.3	-	-

Sample locations in NTS map sheet and UTM Zone 19 northing and easting grid locations.
Abbreviations: Jun B = Juniper Barrens; Nash = Nashwaak; tr = trace; G = granite; KG = K-feldspar porphyritic granite; GD = granodiorite; T = tonalite.
* mode of host granite to dated pegmatitic pod WX84-15
Each mode (volume %) represents a combination of point counts on a stained 12 by 20 cm slab (1000 points) and a thin section (1000 points).

Pokiok batholith

Lutes (1987) described the geology of the various components of the Pokiok batholith and also summarizes earlier work, including geochronological studies. The summary that follows is derived mainly from Lutes (1987) and from field work by the senior author.

The Pokiok batholith can be subdivided into four main components, which are from oldest to youngest, the Hartfield, Skiff Lake, Hawkshaw, and Allandale phases. Both of the last two components are composite. The Hartfield phase consists of medium- to coarse-grained equigranular biotite-hornblende tonalite and granodiorite. The Skiff Lake phase consists mainly of coarse-grained grey biotite-muscovite K-feldspar porphyritic granite but also includes some fine- to medium-grained muscovite-biotite granite with associated muscovite-bearing pegmatite. The Hawkshaw phase consists mainly of coarse-grained, pink K-feldspar porphyritic biotite granite cut by various fine- to medium-grained, equigranular, muscovite-biotite granite bodies, which have been called the Allandale phase.

Wanless et al. (1972) reported K-Ar ages of 362±16 and 348±16 Ma on the Hawkshaw phase. Rb-Sr whole-rock isochron ages by McCutcheon et al.(1981) from this batholith include:
(1) a 27 point age of 431±9 Ma with an initial ratio of 0.706 for all of the data from the Pokiok batholith;
(2) a 11-point age of 432±11 Ma and initial ratio of 0.705 for the Hawkshaw phase;
(3) a 10-point age of 389±20 Ma and initial ratio of 0.708 for the Skiff Lake biotite granite phases; and
(4) a 6-point age of 453±13 Ma and initial ratio of 0.703 for the Skiff Lake two-mica granite phases.
The 431±9 Ma age was interpreted by McCutcheon et al. (1981) as being 40 Ma older than the actual age of intrusion. U-Pb ages from this batholth reported by Bevier and Whalen (1990a) are: Hartfield phase (sphene - 415±1 Ma); Skiff Lake phase (zircon -409±2 Ma); Hawkshaw phase (sphene - 411±1 Ma); Allandale phase (monazite - 402±1 Ma). These results indicate that significant age gaps exist between the Hartfield phase, the Skiff Lake plus Hawkshaw phases, and the Allandale phases. Grouping of the finer grained muscovite-biotite granite phases in the Hawkshaw part of the batholith with the K-feldspar porphyritic biotite granite, as has been done by Lutes (1987), may not be appropriate. These phases are apparently significantly younger. A similar relationship may exist between the main Skiff Lake granite phase and similar two-mica granites in the Skiff Lake part of the batholith. All of these finer grained two-mica granite phases in the Pokiok batholith may be cogenetic younger intrusions which should be grouped together and called the Allandale phase. Further U-Pb dating is required to substantiate such a suggestion.

ANALYTICAL TECHNIQUES

Analytical techniques used in this study are have been described by other authors; K-Ar (Hunt and Roddick, 1987), ^{40}Ar-^{39}Ar (Roddick, 1990), and Rb-Sr (Theriault, 1990).

RESULTS AND INTERPRETATION

Locations of dated samples are indicated in Figure 1 and given as NTS coordinates along with modal data in Table 1. K-Ar and Rb-Sr data are tabulated in Table 2.

North Pole Stream granite suite

Based on intrusive relationships, dated muscovite-bearing phases of the NPSGS are younger than the main biotite granite phase. However, K-Ar ages and one Rb-Sr age (WXNB-136) indicate that these phases are not significantly younger than the U-Pb monazite age (418±1 Ma) obtained from the main biotite granite phase (Fig. 2). The whole suite was emplaced in the Late Silurian Epoch, not during the Devonian Period, as previously indicated by the whole-rock Rb-Sr isochron (Fyffe, 1982).

Table 2. K-Ar and Rb-Sr mineral ages for Miramichi terrane granites.

NB*	Phase	Miner.	K (wt.%)	Rad.Ar*10^{-7} % (cm^3/g)	Atm Ar	Rb (ppm)	Sr (ppm)	$^{87}Rb/^{86}Sr$	$^{87}Sr/^{86}Sr$	±2 SE	$(^{87}Sr/^{86}Sr)_i$	K-Ar Ages	Rb-Sr (Ma) ± 2se
8	Skiff Lake	Musc	8.00	1352	1.7	243.4	27.36	26.12	0.85988	0.00002	0.708	389±6	408±4
		Biot	7.55	1277	1.0	-	-	-	-	-	-	390±5	-
15	Skiff Lake	Musc		see Table 3		-	-	-	-	-	-	394±4	-
30	Skiff Lake?	Musc	8.48	1600	2.3	-	-	-	-	-	-	430±5	-
17	Hawkshaw	Musc	8.69	1478	8.0	678.7	16.05	131.11	1.43614	0.00010	0.705	392±6	392±4
16	Allandale	Musc	8.86	1515	1.7	618.9	95.51	209.80	1.87823	0.00134	0.705	394±6	393±4
18	Allandale	Musc	8.76	1440	2.0	795.4	14.66	172.03	1.68291	0.00066	0.705	380±5	399±4
		Biot	7.01	1210	12.0	-	-	-	-	-	-	397±6	-
38	Allandale	Musc	8.07	1322	3.4	-	-	-	-	-	-	379±6	-
122	North Pole Stream	Musc	8.62	1560	1.4	748.3	6.56	400.50	2.88231	0.00015	0.703	414±5	382±4
136	North Pole Stream	Musc	8.66	1572	1.1	794.7	8.00	343.69	2.71279	0.00014	0.703	416±5	411±4
146	North Pole Stream	Biot	-	-	-	624.0	15.31	126.17	1.42365	0.00005	0.703	-	401±4
159	Lost Lake	Musc	8.76	1562	0.7	350.2	18.80	55.55	1.02525	0.00003	0.707	408±7	402±4
161	Lost Lake	Musc	8.85	1551	1.1	358.6	11.36	96.21	1.25153	0.00007	0.707	402±5	398±4
169	Juniper Barren	Musc	8.23	1518	1.7	213.0	27.72	22.53	0.84494	0.00005	0.706	421±6	433±4
227	Nashwaak	Musc	8.60	1437	0.8	609.7	8.07	250.85	2.21386	0.00011	0.706	386±5	422±4

Initial $^{87}Sr/^{86}Sr$ ratios from sources referenced in text or assumed.
Abbreviations: musc = muscovite; biot = biotite; se = standard error.

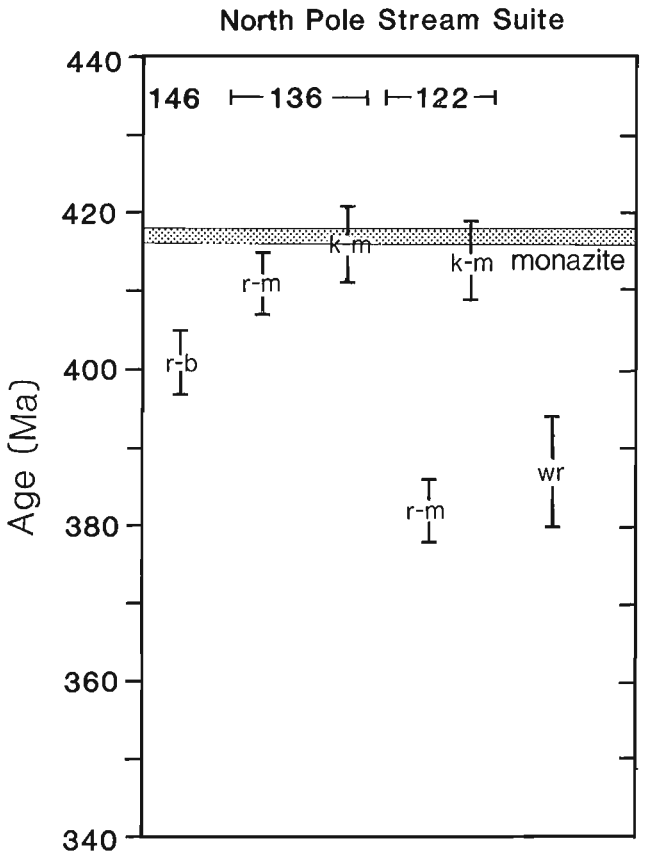

Figure 2. Diagrammatic presentation of isotopic ages from the North Pole stream granite suite. Ages from Table 2 and others referenced in the text are plotted together with error bars (2 sigma); sample numbers given along top of figure. Abbreviations: r = Rb-Sr mineral age; wr = whole-rock Rb-Sr isochron age; patterned band = U-Pb age with 2 sigma errors; k = K-Ar age; b = biotite; m = muscovite.

Overlap of the K-Ar and U-Pb ages suggests that emplacement of all of these phases was at a fairly high level (1.5-2.5 km?) and was followed by rapid cooling; this is an interpretation that is supported by the presence of miarolitic cavities in the muscovite-bearing granite phases. These results support the suggestion of Whalen (1988) that muscovite-bearing phases represented a high-level, possible roof-zone portion of the NPSGS. The biotite granite sample dated by the U-Pb technique is from a deeper level (3-4 km?) of the intrusion and could have been above the closing temperature of monazite at the time of emplacement and solidification of the muscovite-bearing phases in the roof of the intrusion. If so, then K-Ar and Rb-Sr mineral ages from the U-Pb sample could prove to be younger than the ages obtained from the muscovite-bearing phases. The younger whole-rock Rb-Sr age of Fyffe (1982) can be interpreted as supporting the suggestion that in deeper level portions of the intrusion the Rb-Sr system remained open longer than near the roof zone.

Lost Lake Granite

In this study, we dated one sample from each of the subunits of the Lost Lake granite, as defined by Crouse (1981), unit Df2a (WXNB159) and unit Df2b (WXNB161). Both K-Ar and Rb-Sr muscovite ages from these samples are identical within standard errors, with an average age of 403 Ma. All ages, except for a K-Ar muscovite age of Poole (1980), but including his Rb-Sr whole-rock age, overlap in the range 400-415 Ma (see Fig. 3). The age data can be interpreted in at least two ways: (1) The granite was intruded at a high level in the crust and cooled quickly. This would explain the tight clustering of ages as recording a crystallization age. As the granite has been variably deformed, this interpretation would seem unlikely. (2) Deformation and recrystallization of the Lost Lake granite has completely reset muscovite, both for the Rb-Sr and K-Ar systems. The age we obtained from this granite (about 403 Ma) would thus record a deformation event and the actual intrusion of the granite is probably >403 Ma. As significant age differences were obtained in this study between the K-Ar and Rb-Sr systems for apparently undeformed granites, the second interpretation would seem the most reasonable. A U-Pb age is required to obtain the actual intrusion age of the Lost Lake granite.

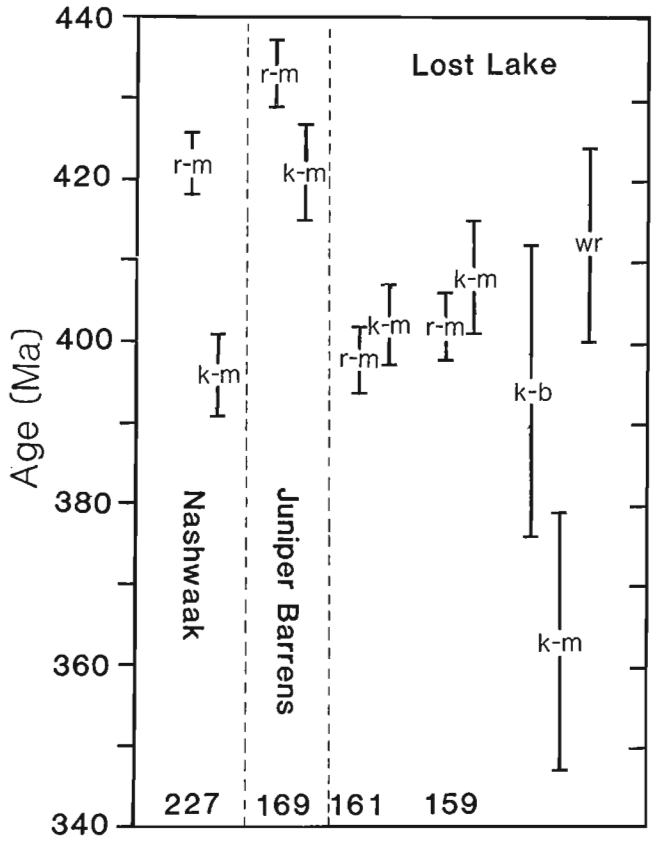

Figure 3. Diagrammatic presentation of isotopic ages from the Lost Lake, Juniper Barrens, and Nashwaak granites. Presentation and abbreviations as in Figure 2.

Nashwaak Granite

A minimum age gap of 16 Ma exists between Rb-Sr (422±4 Ma) and K-Ar (396±5 Ma) muscovite ages (Fig. 3) obtained from the Nashwaak granite, an age gap that can be interpreted as reflecting a cooling history after emplacement of the granite in the Early Silurian Epoch. This large age gap helps substantiate our suggestion that the ages from the Lost Lake granite have been completely reset, for that granite and the Nashwaak granite are not separated by a very great distance, and exhibit features suggesting a similar level of intrusion.

Table 3. ^{40}Ar-^{39}Ar analytical results for muscovite sample WX85-15.

TEMP. (°C)	^{36}Ar	^{37}Ar ($\times10^{-9}$ cm^3 STP)	^{38}Ar	^{39}Ar	^{40}Ar	APPARENT AGE ±2se		^{39}Ar (%)
WX85-15 Musc						(1.21 MG)		
700	0.042	0.024	0.002	0.122	19.66	401.1	11.4	0.5
800	0.039	0.053	0.004	0.268	27.47	399.8	3.6	1.0
900	0.034	0.168	0.009	6.945	420.12	394.6	.5	26.0
1000	0.010	0.224	0.026	12.479	737.59	393.4	1.1	46.6
1050	0.002	0.057	0.002	2.164	128.45	394.9	2.1	8.1
1100	0.001	0.027	0.002	1.234	73.29	394.8	1.5	4.6
1150	0.001	0.031	0.002	1.673	99.23	395.1	2.3	6.3
1200	0.004	0.042	0.002	1.572	94.27	395.1	1.6	5.9
1250	0.003	0.007	0.000	0.271	16.78	393.6	5.8	1.0
1300	0.001	0.001	−0.000	0.027	1.71	363.9	32.3	0.1
1600	0.001	0.016	0.000	0.007	0.58	276.14	15.8	0.0
TOTAL	0.14	0.05	0.65	26.76	1619.2	394.2	4.3	
Conc./g.	12.3	57.99	4.37	2387.23	144438.			

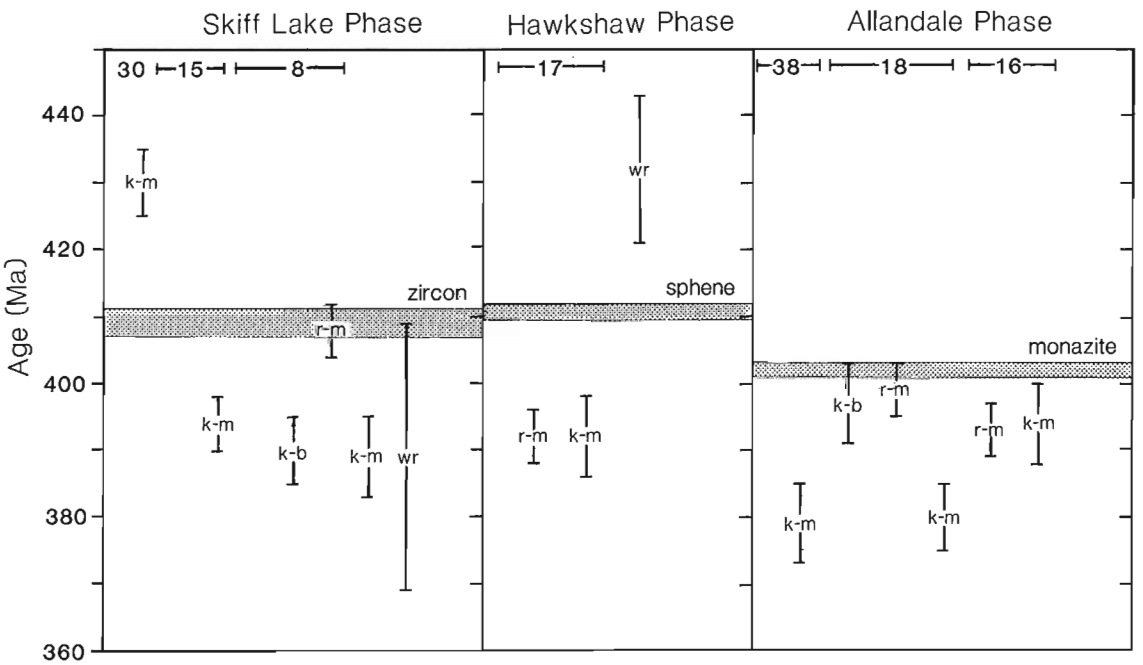

Figure 4. Diagrammatic presentation of isotopic ages from phases of the Pokiok batholith. Presentation and abbreviations as in Figure 2.

Juniper Barrens granite

One muscovite separate from one sample gave a Late Silurian K-Ar age of 421±6 and an Early Silurian Rb-Sr age of 433±4 Ma. The data (Fig. 4) suggest an Early Silurian intrusion age for the Juniper Barren granite, rather than the Devonian age suggsted by St. Peter (1981).

Pokiok batholith

New mineral ages of this study (Table 2), Rb-Sr whole-rock data of McCutcheon et al. (1981) and U-Pb data of Bevier and Whalen (1990) from various components of the Pokiok batholith are presented in Figure 4. We have not dated any samples from the Hartfield phase of the Pokiok batholith in this study.

(i) Skiff Lake phase

New mineral ages are presented in Table 2 for three samples, for one of which (WXNB-8) muscovite was dated by both Rb-Sr and K-Ar methods (Fig. 4). A coarse-grained muscovite from a pegmatitic pod in geochemical sample WXNB-15 was dated by the ^{40}Ar-^{39}Ar technique (see Table 3). The age spectra for this muscovite is flat, with an apparent age of 394±4 Ma (Fig. 5). Though one of the Rb-Sr muscovite ages (WXNB-8) overlaps with the U-Pb zircon age (409±2 Ma), most of the K-Ar ages are younger and similar to the whole-rock Rb-Sr age. Our data suggest that it took a minimum of 9 Ma and a mean time of 18 Ma for the Skiff Lake phase to cool from ≤600°C to 350°C.

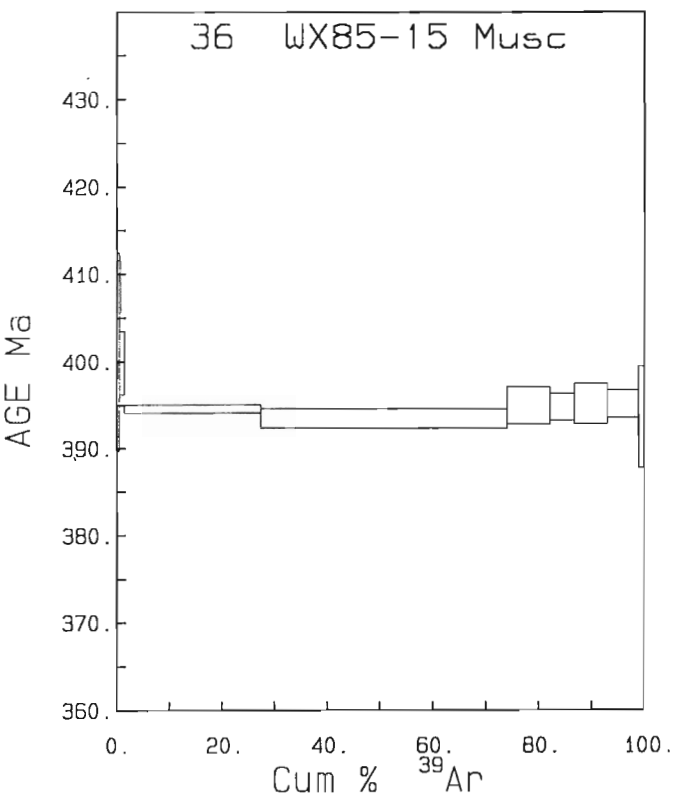

Figure 5. Age versus cumulative percent ^{39}Ar plot for muscovite sample WX85-15.

(ii) Hawkshaw phase

K-Ar and Rb-Sr muscovite ages from one sample overlap at 392 Ma and are significantly younger than the U-Pb age (411±1 Ma). The whole-rock Rb-Sr isochron age (432±11 Ma) exhibits no overlap with the other ages from this phase. Our data can be interpreted as indicating that it took a minimum of 5 Ma and a mean time of 17 Ma for the Hawkshaw phase to cool from ≤600 to 350°C.

(iii) Allandale phase

Sample WXNB-18 K-Ar biotite and Rb-Sr muscovite ages overlap with the U-Pb monazite age (402±1 Ma), whereas other mineral ages are slightly to significantly younger. The overlap of some of the mineral ages with the U-Pb age suggests rapid cooling of much of this phase in ≤1 (minumum) to ≤4 (average) Ma. The fine-grained to patchy medium-grained texture of this phase is compatible with it cooling more rapidly than other phases of the Pokiok batholith.

Although our K-Ar and Rb-Sr mineral ages from the Pokiok batholith overlap, the U-Pb age of Bevier and Whalen (1990a) from the Allandale phase is younger than the other phases. The concordance of our mineral ages can be interpreted in two main ways:
(1) Resetting of mineral ages (other than U-Pb) from the other phases by the Allandale phase; ie., apparent "cooling ages" are really reset ages;
(2) The Allandale phase was emplaced during or just preceeding rapid uplift and erosion of the Pokiok batholith, ie., the cooling history from the other phases is real.

CONCLUSIONS

Our K-Ar and Rb-Sr mineral dating, together with U-Pb dating (Bevier and Whalen, 1990a), have indicated that major intrusive units in Miramichi terrane, previously considered to be Devonian, are actually of Silurian age. The large-scale implications of this major Silurian magmatic event are discussed in Bevier and Whalen (1990). This study has provided preliminary information on variations in levels of intrusion and cooling histories in Miramichi terrane granites. Some granites were apparently intruded at a high level in the crust and cooled rapidly (North Pole Stream suite, Allandale phase of Pokiok batholith), while others were emplaced at a deeper level and cooled more slowly (Nashwaak, Juniper Barrens, Skiff Lake, and Hawkshaw phases of Pokiok batholith). Also, this work has indicated that one composite intrusion (Lost Lake granite) exhibits evidence of major thermal overprinting and resetting of the Rb-Sr and K-Ar isotopic systems. More detailed and extensive work is required to properly substantiate our results on Miramichi terrane granites.

REFERENCES

Bevier, M.L.

1988: U-Pb geochronologic studies of igneous rocks in New Brunswick; *in* Thirteenth Annual Review of Activities, ed. S.A. Abbott; New Brunswick Department of Natural Ressources and Energy, Minerals and Energy Division, Information Circular 88-2, p.134-140.

1990a: U-Pb geochronology of Silurian granites, Miramichi terrane, New Brunswick; *in* Rediogenic Age and Isotopic Studies: Report 3; Geological Survey of Canada, Paper 89-2 (this publication).

Bevier, M.L. and Whalen, J.B.

1990b: Tectonic significance of Silurian magmatism in the Canadian Appalachians; Geology V. 18.

Crouse, G.W.

1981: Geology of parts of Burnthill, Clearwater and McKiel Brooks map-areas K-14, K-15, and K-16 (Parts of 21J/15 and 21J/10). New Brunswick Department of Natural Resources, Mineral Resources Branch, Map Report 81-5.

Fyffe, L.R.

1982: Geology in the vicinity of the 1982 Miramichi earthquake, Northumberland County, New Brunswick. New Brunswick Department of Natural Resources, Mineral Resources Division, Open File 82-27, 37p.

Fyffe, L.R. and Fricker, A.

1987: Tectonostratigraphic terrane analysis of New Brunswick. Maritime Sediments and Atlantic Geology, V.23, p. 113-122.

Fyffe. L.R., Pajari, G.E., and Cherry, M.E.

1981: The Acadian plutonic rocks of New Brunswick; Maritime Sediments and Atlantic Geology, v. 17, p. 23-36.

Fyffe, L.R. and Pronk, A.G.

1985: Bedrock and surficial geology - rock and till geochemistry in the Trousers Lake area, Victoria County, New Brunswick, New Brunswick Department of Natural Resources, Mineral Resources Branch, Report of Investigation No. 20, 74p.

Hunt, P.A. and Roddick, J.C.

1987: A compilation of K-Ar ages; in Radiogenic Age and Isotopic Studies: Report 1; Geological Survey of Canada, Paper 87-2, p.143-205.

Lutes, G.G.

1987: Geology and geochemistry of the Pokiok Batholith, New Brunswick, New Brunswick Department of Natural Resources, Mineral Resources Branch, Report of Investigation No. 22, 74p.

McCutcheon, S., Lutes, G., Gauthier, G., and Brooks, C.

1981: The Pokiok batholith: a contaminated Acadian intrusion with an anomalous Rb/Sr age. Canadian Journal of Earth Science, 18, p.910-918.

Poole, W.H.

1963: Geology of Hayesville, New Brunswick. Geological Survey of Canada, Map 6-1963.

1980: Rb-Sr ages of the "Sugar" granite and Lost Lake granite, Miramichi Anticlinorium, Hayesville map area, New Brunswick. in Current Research, Part C; Geological Survey of Canada, Paper 80-1C, p.174-180.

Roddick, J.C.

1990: ^{40}Ar–^{39}Ar evidence for the age of the New Quebec crater, northern Quebec in Radiogenic Age and Isotopic Studies: Report 3; Geolical Survey of Canada, Paper 89-2 (this publication).

St. Peter, C.

1981: Geology of North Branch Southwest Miramichi River map-areas J-14, J-15, J-16 (Parts of 21J/11E, 21J/14E). New Brunswick Department of Natural Resources, Mineral Resources Branch, Map Report 80-1.

Theriault, R.J.

1990: Methods for Rb-Sr and Sm-Nd isotopic analyses at the geochronology laboratory, Geological Survey of Canada; in Radiogenic Age and Isotopic Studies: Report 3; Geological Survey of Canada, Paper 89-2, (this publication).

Wanless, R.K., Stevens, R.D., Lachance, G.R., and Delabio, R.N.

1972: Age determinations and geological studies, K-Ar isotopic ages, report 10, Geological Survey of Canada, Paper 71-2, p. 68-72.

1973: Age determinations and geological studies, K-Ar isotopic ages, report 11, Geological Survey of Canada, Paper 73-2, p. 78-90.

Whalen, J.B.

1987: Geology of a northern portion of the Central Plutonic Belt, New Brunswick. in Current Research, Part A; Geological Survey of Canada, Paper 87-1A, p. 209-217.

1988: Geology of a northern portion of the Central Plutonic Belt, New Brunswick - 1:50 000 map with marginal notes; Geological Survey of Canada, Open File 1908.

1990: Geology of a northern portion of the Central Plutonic Belt, New Brunswick - 1:100 000 map with marginal notes. Geological Survey of Canada, Map 1751A.

Age of a metarhyolite from the Tetagouche Group, Bathurst, New Brunswick, from U-Pb isochron analyses of zircons enriched in common Pb[1]

R.W. Sullivan[2] and C.R. van Staal[2]

Sullivan, R.W. and van Staal, C.R., Age of a metarhyolite from the Tetagouche Group, Bathurst, New Brunswick, from U-Pb isochron analyses of zircons enriched in common Pb; in Radiogenic Age and Isotopic Studies: Report 3, Geological Survey of Canada, Paper 89-2, p. 109-117, 1990.

Abstract

A U-Pb zircon age of 466.0 ± 5.3 Ma is reported for a metarhyolite of the Tetagouche Group volcanics in the northern Miramichi Highlands, New Brunswick. The surface morphology of the zircons indicates rapid growth followed by strong magmatic resorption. The zircons contain up to 75 % common lead originating from inclusions. U-Pb isochron regressions were used to determine the initial common lead composition associated with the inclusions, and thereby permit a relatively small error to be assigned to what was originally a highly imprecise data set.

Résumé

On a établi au moyen de la méthode U-Pb appliquée au zircon un âge de 466 ± 5,3 Ma pour une métarhyolite des roches volcaniques du groupe de Tétagouche provenant de la partie nord des hautes terres de Miramichi, au Nouveau-Brunswick. La morphologie de surface des cristaux de zircon indique une croissance rapide suivie d'une forte résorption magmatique. Le zircon renferme jusqu'à 75% de plomb provenant d'inclusions. On a utilisé des régressions de l'isochrone du système U-Pb pour déterminer la composition initiale du plomb associé à ces inclusions et, par conséquent, pour réduire considérablement le niveau d'erreur de ce qui était, à l'origine, un ensemble de données très imprécis.

INTRODUCTION

This paper reports a U-Pb zircon age determination for a spherulitic metarhyolite of the Flat Landing Brook Formation of the Middle Ordovician Tetagouche Group in northern New Brunswick (Helmstaedt, 1971; Skinner, 1974; van Staal and Fyffe, in preparation). The zircons in the rhyolite are peculiar in that they have a high common lead content and display very irregular surface features with numerous inclusions of various types and compositions. These inclusions, as will be discussed below, are probably the source of the high common lead content. U-Pb and Pb-Pb isochron regressions were employed to determine the initial common lead ratios and to estimate the crystallization age of the sample.

GEOLOGICAL SETTING

The volcanic-dominated Tetagouche Group underlies much of the Miramichi Highlands (Fyffe, 1982) in central and northern New Brunswick. It is host to numerous base-metal massive sulphide deposits, including the giant Brunswick No. 12 deposit. A large number of the massive sulphide deposits are hosted by, or closely associated with felsic metavolcanic rocks of the Flat Landing Brook and Nepisiguit Falls Formations (van Staal and Fyffe, in preparation). The latter two formations together comprise a huge volume of rocks (Davies, 1979), which cover an area in the order of 1000 km^2. Such large volumes of felsic volcanic extrusive rocks are found only associated with very large calderas (e.g., Yellowstone) or volcanic depressions such as Tobe in Sumatra. It is not surprising, therefore, that these rocks are generally interpreted to represent the deposits of one or more Ordovician calderas (Davies, 1966; Harley, 1979).

1 Contribution to the Canada - New Brunswick Mineral Development Agreement, 1984-1989. Project carried by the Geological Survey of Canada, Continental Geoscience Division.

2 Geological Survey of Canada, 601 Booth Steet, Ottawa, Ontario K1A 0E8

The Flat Landing Brook Formation consists mainly of aphyric or feldspar-phyric silicic volcanic rocks, ranging from rhyolite to dacite in composition (Whitehead and Goodfellow, 1978; Winchester and van Staal, 1988). These volcanic rocks include tuffs and lavas, which experienced varying degrees of deformation and alteration (van Staal and Williams, 1984; van Staal, 1986). The lavas are locally flow banded, and in places spherulitic and vesicular textures are preserved. The rhyolites are locally interleaved with agglomerate, bedded ash and lapilli tuff, and a jasperitic iron formation. The association of ellipsoidal bodies of massive rhyolite with agglomerate, tuff, and iron formation suggests that the rhyolite may in part represent intrusive domes.

The deformation of the Tetagouche Group is polyphase, although the strain is typically unevenly distributed. Strongly deformed volcanic rocks are characterized by well developed foliations defined by phyllosilicates, whereas the phyllosilicate content is generally low in weakly deformed volcanic rocks. The degree of sericite, chlorite, and biotite alteration of the volcanic rocks and the preservation of primary features is, therefore, generally a function of strain (van Staal, 1986, 1987).

The Flat Landing Brook Formation is stratigraphically overlain by shaly and sandy phyllites of the Boucher Brook Formation, which yielded Caradocian graptolites and conodonts in its upper part (Nowlan, 1981; J. Riva in van Staal et al., 1988). It is underlain by calcareous sediments of the Vallee Lourdes Formation (van Staal et al., 1988), which have middle Arenigian to early Llanvirnian brachiopods and conodonts (Nowlan, 1981; Neuman, 1984). The Flat Landing Brook Formation is thus older than the Caradoc Series and younger than the Arenig Series.

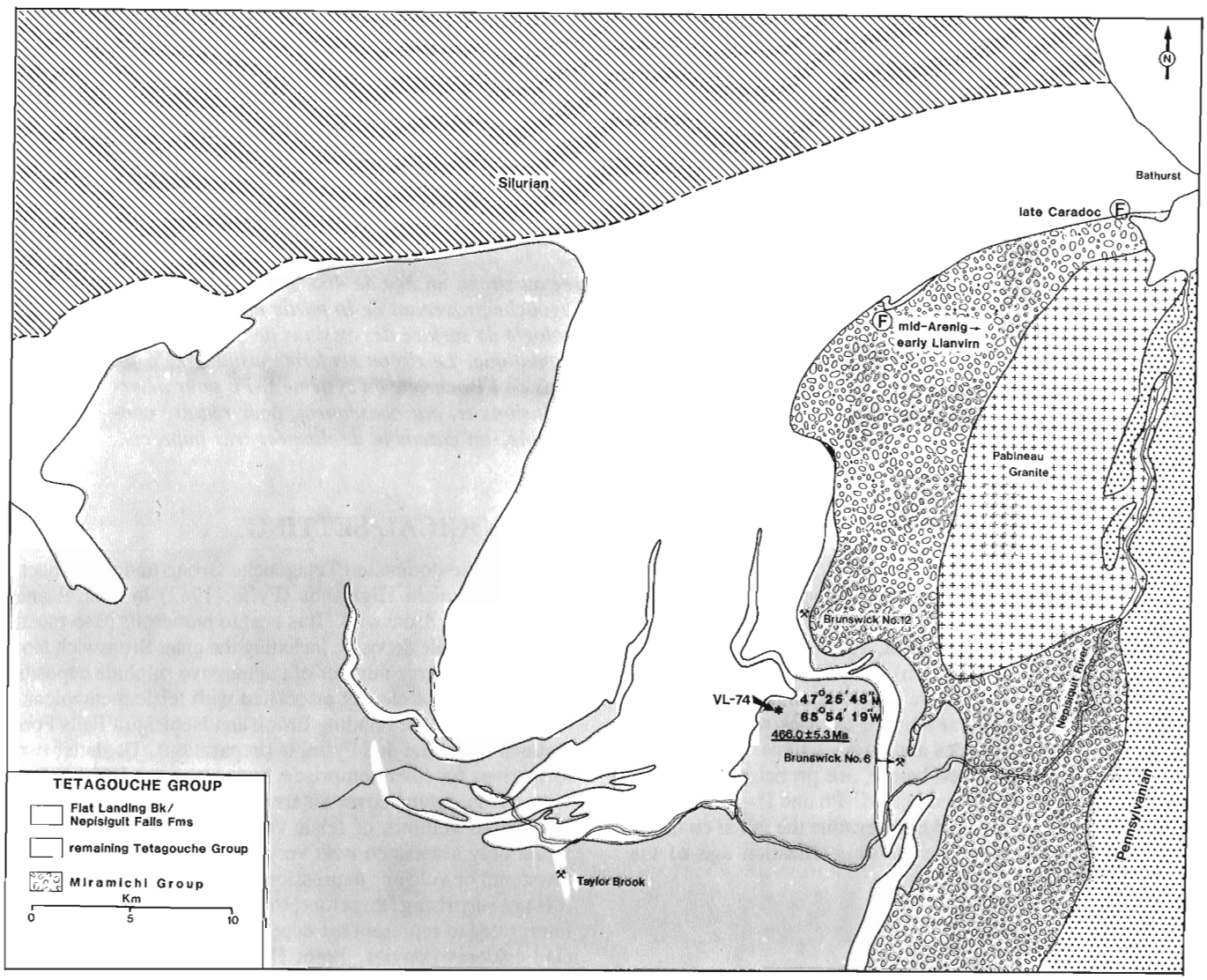

Figure 1. Simplified geological map of the Bathurst area in northern New Brunswick showing location of analysed sample VL-74. Massive sulphide deposits and fossil locations mentioned in the text are also shown. Lithostratigraphy simplified after van Staal and Fyffe (in preparation).

SAMPLE LOCATION AND DESCRIPTION

The sample selected for U-Pb analysis is a spherulitic, aphyric rhyolite, which was sampled close to the contact with the stratigraphically overlying metasediments of the Boucher Brook Formation approximately 5 km southwest of the Brunswick No. 12 mine (Fig. 1). The U-Pb zircon age determination thus provides information concerning the end of felsic volcanic activity and the age of the lower part of the Boucher Brook Formation.

The degree of internal strain of the rhyolite is low because the spherulites remained almost spherical and a foliation of muscovite and chlorite is poorly developed. Alteration to phyllosilicates is moderate; muscovite and biotite do not constitute more than 15 to 20 (vol.) % of the rock and the remainder is mainly made up of a microcrystalline matrix of feldspar and quartz. Nevertheless, whole-rock analysis (J. Winchester, pers. comm., 1988) shows that the rhyolite has an anomalously high K_2O/Na_2O ratio, suggesting at least some alkali metasomatism.

ZIRCON DESCRIPTION AND INTERPRETATION

The zircon population consists of euhedral to anhedral crystals, L:B=3:1, with a generally rounded habit and distinct, irregular, smoothly corroded surfaces (Fig. 2). These irregular surfaces cause a 'shimmering' optical effect when viewed in alcohol under a binocular microscope. In addition, 'ridges' that are now the edges of these zircons (Fig. 2) cause another optical effect, which can be confused for a distinct over-

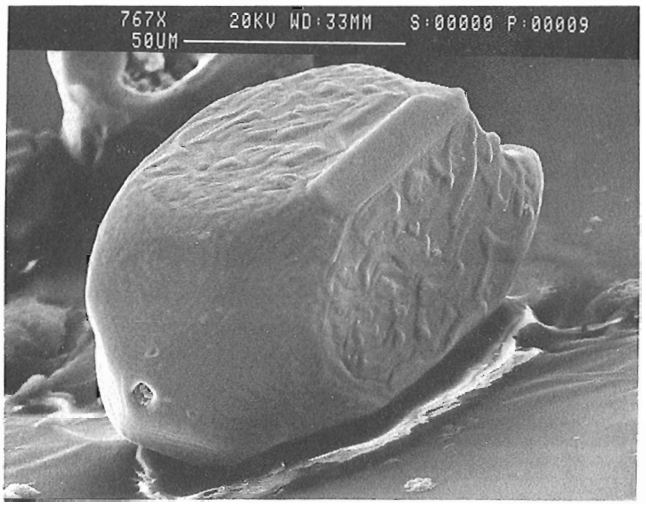

Figure 2. SEM photomicrograph with sketch of a zircon showing irregular ropey, and smoothly corroded surfaces. These probably reflect partial magmatic resorption prior to or during extrusion. Corrosion is perhaps controlled by local compositional reactivity or, as may be the case here, by the crystal structure. What is now an edge-ridge was perhaps a (110) surface originally. EDX analysis of the inclusion in the tip of the zircon indicated non-zircon mineral or rock material. The scale bar indicates 50 microns.

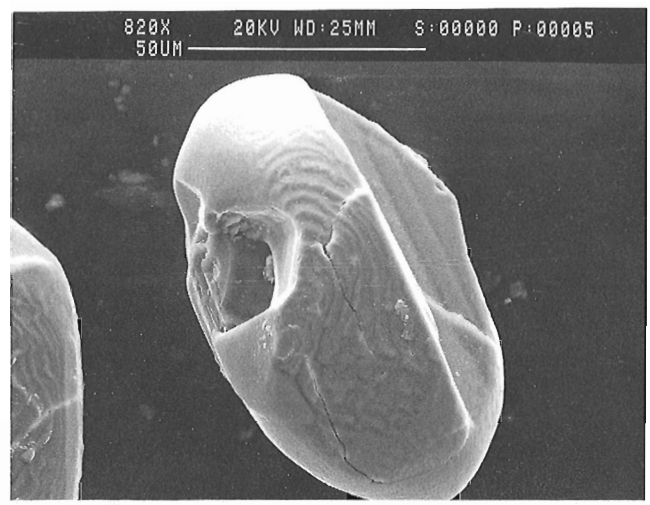

Figure 3. This SEM photo and sketch shows a ropy surface and a large angular surface cavity, which are resorption features. A linear 'trough' or terrace with a 90° cross section, in this example parallel to the c-axis, is a prominant feature. This is perhaps an artifact of rapid constrained crystallization of two neighbouring but different minerals.

growth. These edge-ridges, as discussed below, are resorption features and represent original zircon that was more resistant to corrosion. It is not known whether these ridges were originally (110) crystal faces or corners. Although a few crystals are internally featureless the majority have inclusions of various shapes and types. Fine euhedral zoning often defines a central domain, but zoning is generally absent in the outer domain. A few twin and triplet terminations are also present. Petrographic and scanning electron microscope (SEM) examination of grain mounts, and energy dispersive x-ray (EDX) analysis of polished grain mounts were used to characterize surface and internal features.

Many zircons display large angular surface cavities and linear troughs with 90° cross sections (Figs. 3,4). These, plus the distinctly corroded appearance of the prism faces, appear to be indicative of rapid crystal growth, impingment with other crystals, and magmatic resorption.

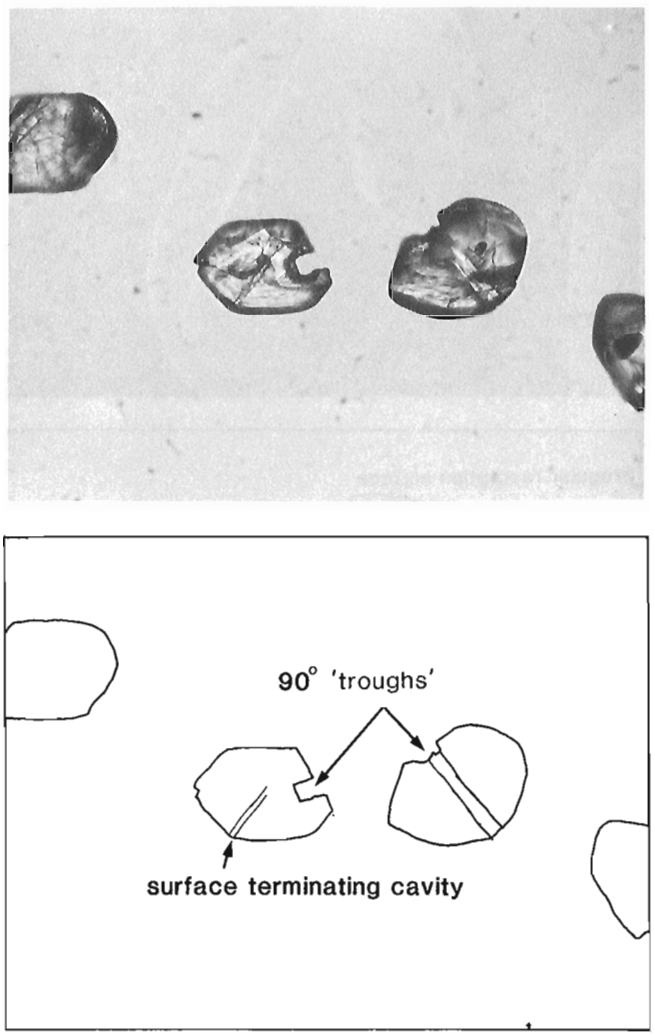

Figure 4. Petrographic microscope photomicrograph and sketch of fine (approx. 50 microns) zircon grains in Canada balsam showing distinct 90° cavities. This feature was also visible in thin section, but its origin is uncertain. A tunnel-like resorption cavity is also visible.

There are at least four types of inclusions:

(i) acicular, parallel, and oblique to the c-axis, with major Ca and P (apatite). These appear to be mostly internal (Fig. 5).
(ii) round inclusions of pure silica (quartz), also internal.
(iii) dumbbell-shaped inclusions of variable amounts (major to minor) of Si,K,Al,Ca,Fe, and Mg, indicating rock material (Fig. 6).
(iv) dumbbell or rounded inclusions (tunnel-like cavities), some very large, which are now 'empty' but presumably were originally filled with fluid. The latter two types of inclusions often terminate at the surface of the zircon. Many zircons broke apart during abrasion, presumably because of these deep cavities.

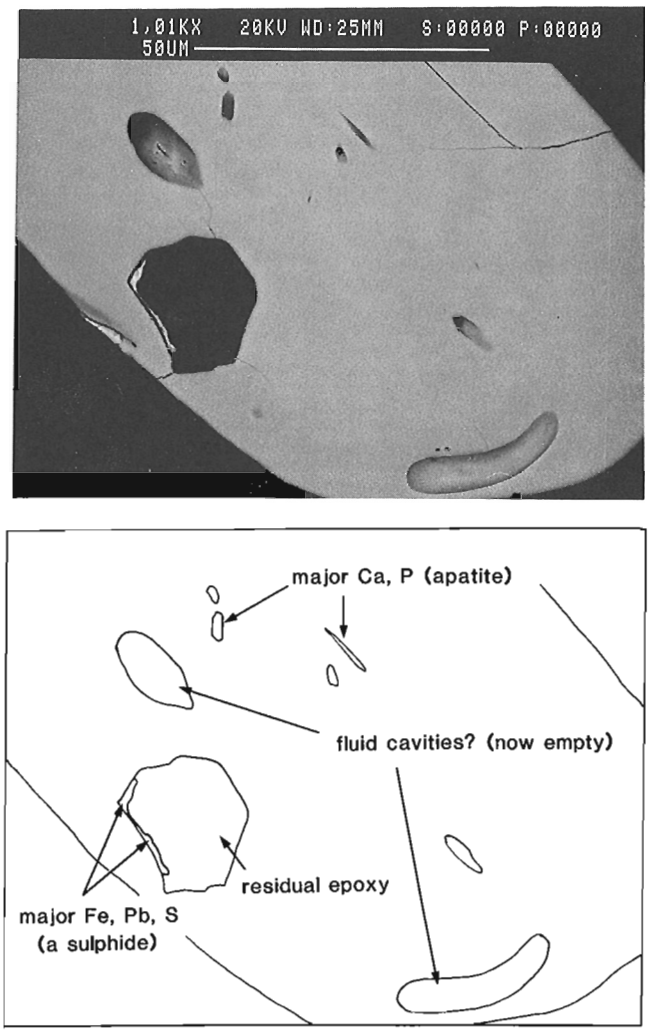

Figure 5. SEM photomicrograph with sketch of a polished zircon grain. EDX analyses indicates acicular apatite inclusions, and what appears to be a sulphide inclusion. EDX detected only Zr and Si in the rounded features, indicating that these were fluid cavities that are now 'empty'. The large black opaque has a high organic content, indicating it is residual epoxy. Residual grinding compound (Al, Si) was also detected in the zircon. These residues from the slide preparation are further evidence of original deep cavities in the zircon. Except for the apatite all of the features pictured here were depressions.

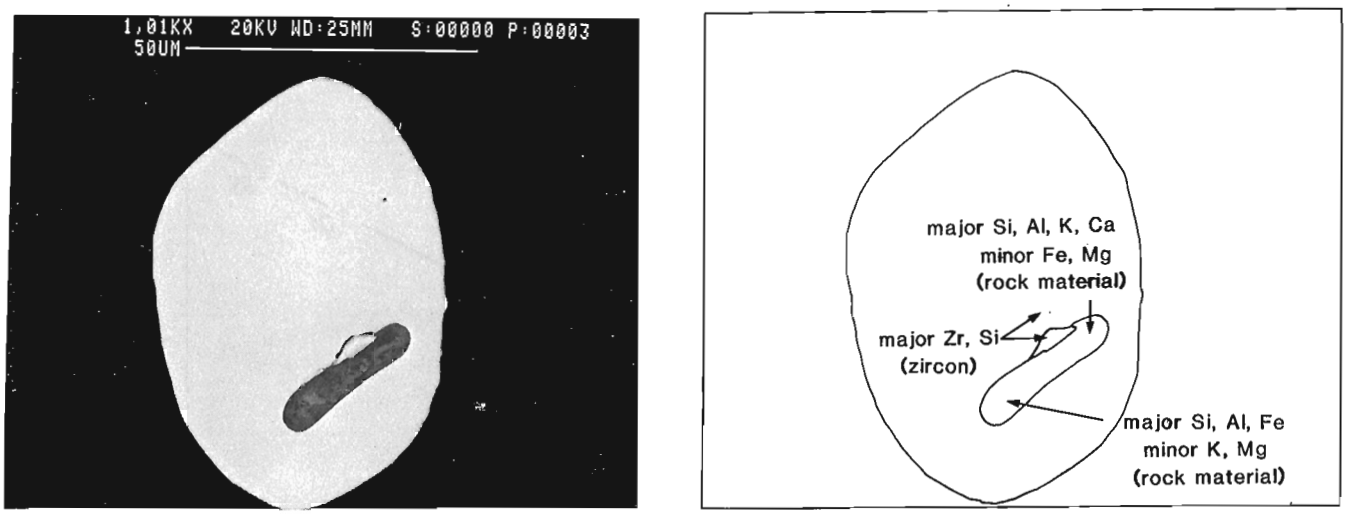

Figure 6. Photomicrograph with sketch showing a large dumbbell inclusion apparently totally inside the zircon. The EDX analyses indicate variable composition, but similar to feldspar. In another polished mount (not shown) a single spherical inclusion of pure Si was found, indicating quartz. Scale bar indicates 50 microns.

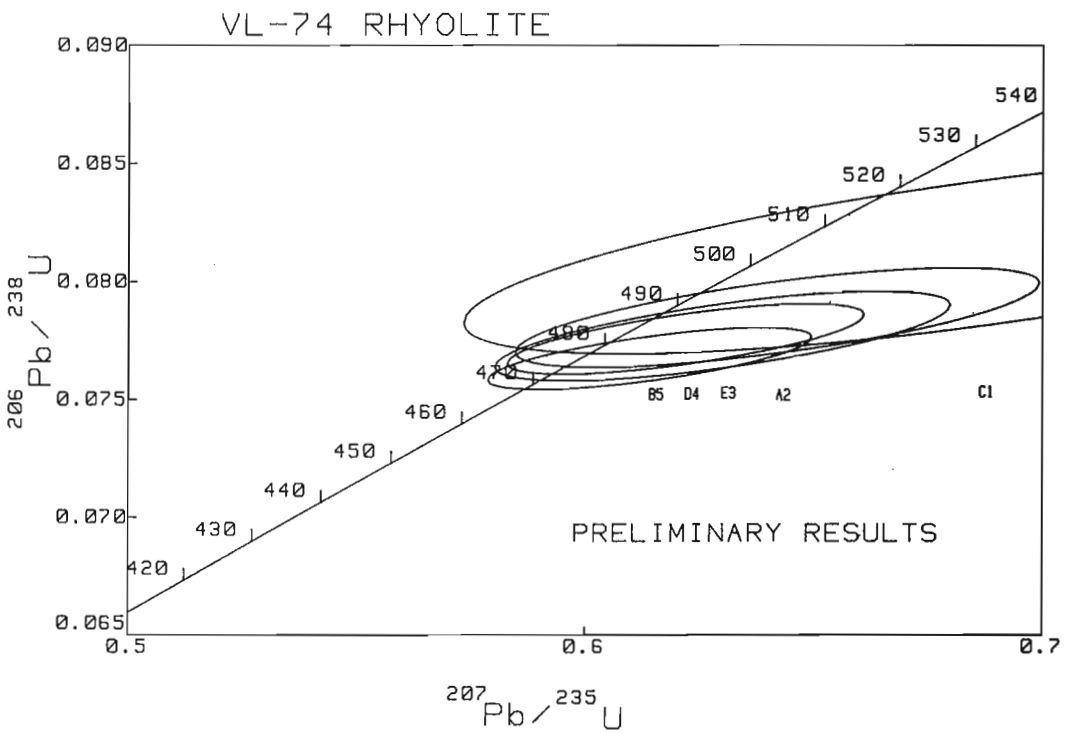

Figure 7. U-Pb concordia diagram of the original data, with 475 Ma common Pb correction, displays a pattern similar to results involving inheritance. This pattern is false, however, for the discordance is directly correlated to the amount of common Pb, Table 1 B, indicating an incorrect common Pb composition. The common Pb originates primarily from inclusions in the zircon fractions.

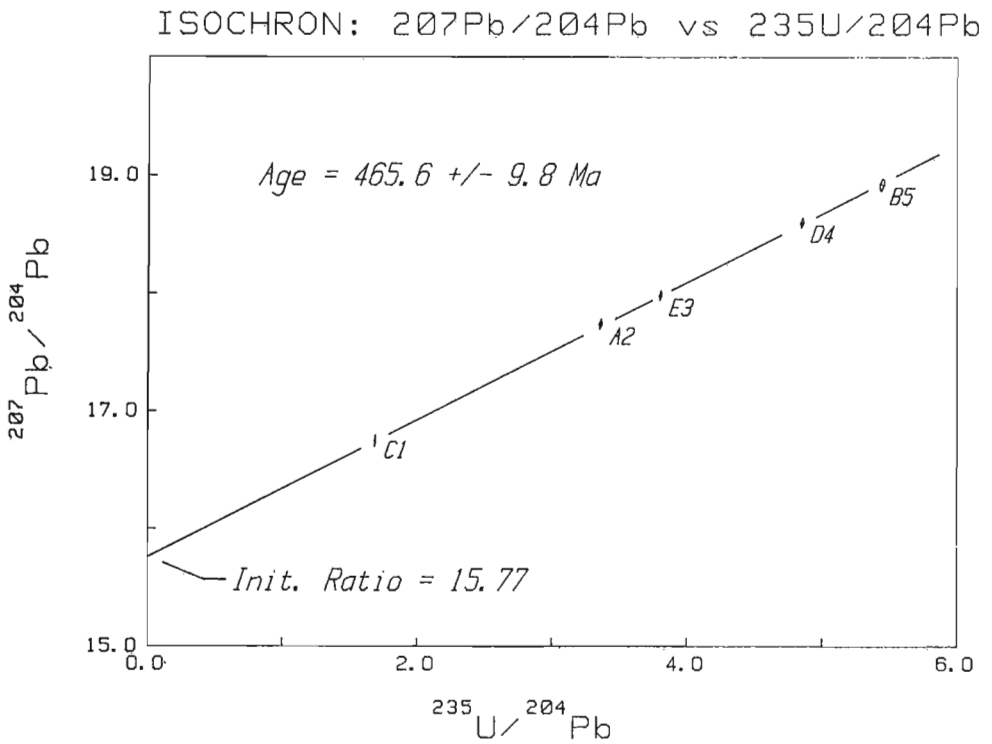

Figure 8. U-Pb isochron plot was used to generate an age and a relatively low error estimate (MSWD = 0.37) for the initial $^{207}Pb/^{204}Pb$, which was then used to recalculate the original data.

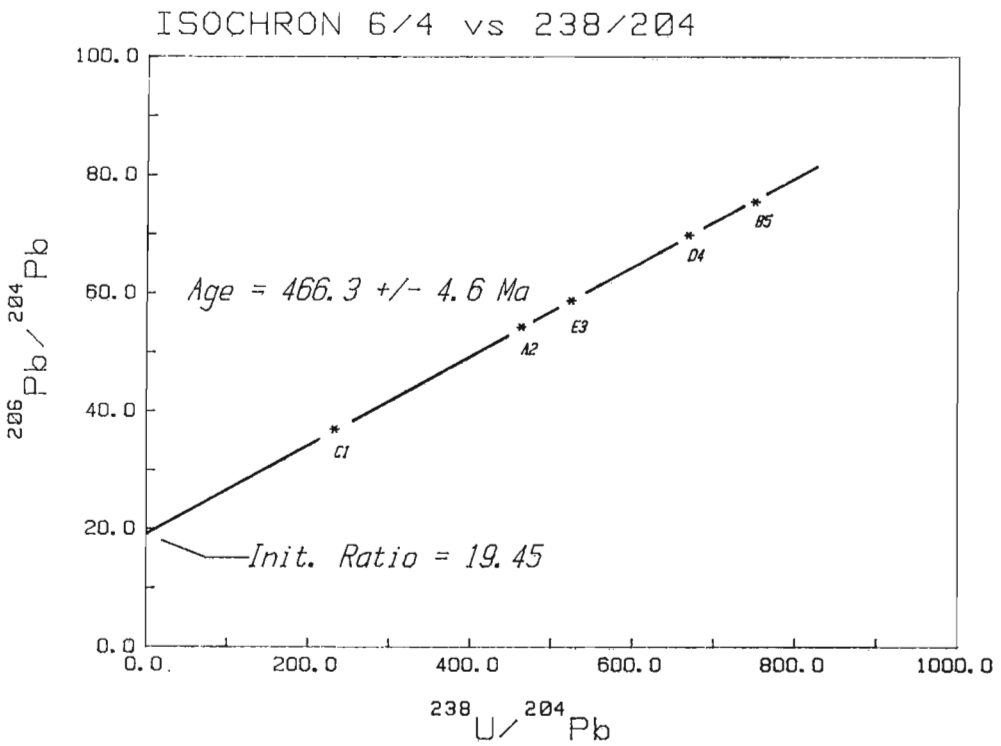

Figure 9. U-Pb isochron plot was used to generate an age and a relatively low error estimate (MSWD = 12.93) for the initial $^{206}Pb/^{204}Pb$, which was then used to recalculate the original data.

EDX analysis also detected Y,Dy, and Er from a tiny crystal inside a zircon, indicating a rare earth element (REE) mineral, possibly xenotime. Small sulphide crystals were also detected.

We interpret the features described above to indicate rapid crytallization of zircon followed by strong magmatic resorption. Resorbed surfaces such as these are not uncommon within zircons from plutonic rocks; in this case the magma was apparently quenched rapidly after eruption, before new igneous zircon overgrowths could form. Rapid crystallization of the magma is consistent with the spherulitic and felsitic textures preserved in the rhyolite.

The inclusions are thought to be the source of the high common lead content (49 to 75%) that was present in the analyzed zircon.

ANALYTICAL RESULTS

U-Pb analytical techniques follow those described in Parrish et al. (1987). The zircons were carefully selected by hand picking to obtain the best fractions possible and were abraded prior to dissoluton. Procedural blanks were typically 3 pg and 20 pg for U and Pb, respectively. All quoted age errors are at the two sigma level.

Table 1. A: U-Pb model ages, with errors, using the calculated common Pb ratios B: Measured $^{206}Pb/^{204}Pb$ and % common lead from each fraction.

	MODEL AGES (Ma)					
	C1	A2	E3	D4	B5	
A:	465.7	467.1	465.7	468.5	464.3	206/238
	± 9.9	± 5.0	± 4.5	± 4.5	± 3.2	
	462.	467.7	465.3	466.9	463.9	207/235
	± 30.	± 14.4	± 12.8	± 9.9	± 9.1	
	444.	471.	463.	459.	462.	207/206
	± 161.	± 73.	± 65.	± 50.	± 46.	
B:	36.84	54.06	58.62	69.71	75.20	6/4meas
	74.5	61.5	57.5	52.0	49.0	%cmPb

Table 2. Isochron ages and initial Pb ratios.

Regression	MSWD	Age Ma ± error	Initial Pb Ratio ± % 1 SE
206/204 vs 238/204	12.93	466.3 ± 4.6	19.45 ± 0.97
207/204 vs 235/204	0.37	465.6 ± 9.8	15.77 ± 0.20
207/204 vs 206/204	0.13	464.0 ± 53.0	---------

Normal data reduction using Stacey and Kramers (1975) model Pb composition at 475 Ma for the common Pb component in the zircon resulted in a very imprecise data set. The high errors were due to the high common lead content and the relatively high errors (approx. 2.7 and 0.6% standard error of the mean (SE) for $^6/_4$ and $^7/_4$) assigned to the model Pb composition. A U-Pb concordia plot of these data displayed a pattern similar to results involving inheritance (Fig. 7). This apparent inheritance pattern is false, however, for the discordance is directly correlated to the amount of common lead found in the zircon fractions (Table 1, B), indicating an incorrect common Pb composition used for the correction.

To investigate the common Pb composition the original blank and spike corrected analytical data, representing the total Pb (including the common Pb) were regressed and plotted to produce U-Pb isochron ages and initial Pb ratios, namely: $^{207}Pb/^{204}Pb$ vs $^{235}U/^{204}Pb$ and $^{206}Pb/^{204}Pb$ vs $^{238}U/^{204}Pb$ (Figs. 8,9). This procedure resulted in a better estimate of the composition, and lower errors (0.97 and 0.20% 1 SE. for $^6/_4$ and $^7/_4$) for the common Pb. In addition data were regressed and plotted on a Pb-Pb plot generating a Pb-Pb age, but not shown here. These three isochron ages are listed in Table 2. The errors and correlation coefficients required for these regressions were calculated by the procedure of Roddick (1987); the regressions were by the method of York (1969).

Finally the analytical results were recalculated using the improved estimate for the common Pb (Table 3). This resulted in concordant ages within smaller, concentric error elipses (Table 1, A) and concordia diagram (Fig. 10).

The best estimate for the age of the rhyolite is taken from the average of the two U-Pb isochron ages, with the error estimated graphicallly from the intersection of the error ellipses with concordia (ignoring data C1), namely 466.0 ± 5.3 Ma.

DISCUSSION

Scanning electron microscopic examination of the zircons from this metarhyolite showed irregular surface features and cavities that appear to reflect partial resorption of primary zircon phenocrysts prior to or during extrusion. The 90° cross-section feature is problematic but probably resulted from simultaneous rapid crystallization of dissimilar neighbouring minerals (e.g., zircon and apatite) in a restricted environment. These 'troughs' and the large angular cavities are the imprints of previously impinging crystals.

Table 3. U-Pb isotopic data for zircon from Tetagouche Group volcanics, New Brunswick.

Sample and fraction[4]	Weight (mg)	U (ppm)	Pb* (ppm)	Measured[1] $^{206}Pb/^{204}Pb$	Isotopic abundances[2] (^{206}Pb=100) ^{204}Pb	^{207}Pb	^{208}Pb	Isotopic ratios[3] $^{206}Pb/^{238}U$	$^{207}Pb/^{235}U$	Age,Ma $^{207}Pb/^{206}Pb$
1. Spherulitic rhyolite: VL-74 (47° 25' 48" N 65° 54' 19" W)										
C1, -74+62, NM, A	0.1898	329.5	28.9	36.8	2.7127	45.427	119.530	0.074922	0.576328	444.0
A2, +105, NM, A	0.0770	373.8	32.8	54.1	1.8440	32.709	90.825	0.075151	0.585091	470.7
E3, -105+74, NM, A	0.2310	378.8	32.9	58.6	1.7033	30.633	85.425	0.074910	0.581240	463.2
D4, -62, NM, A	0.2460	408.5	36.1	69.7	1.4319	26.640	77.482	0.075383	0.583756	458.8
B5, -105+74, M, A	0.1260	383.0	33.2	75.2	1.3250	25.075	72.952	0.074686	0.579050	461.5

NOTES: *radiogenic Pb; [1]corrected for fractionation and spike; [2]corrected for Pb blank; [3]corrected for U,Pb blank and calculated common Pb; [4]size in microns; A abraded; NM, M relative non-magnetic, magnetic separation

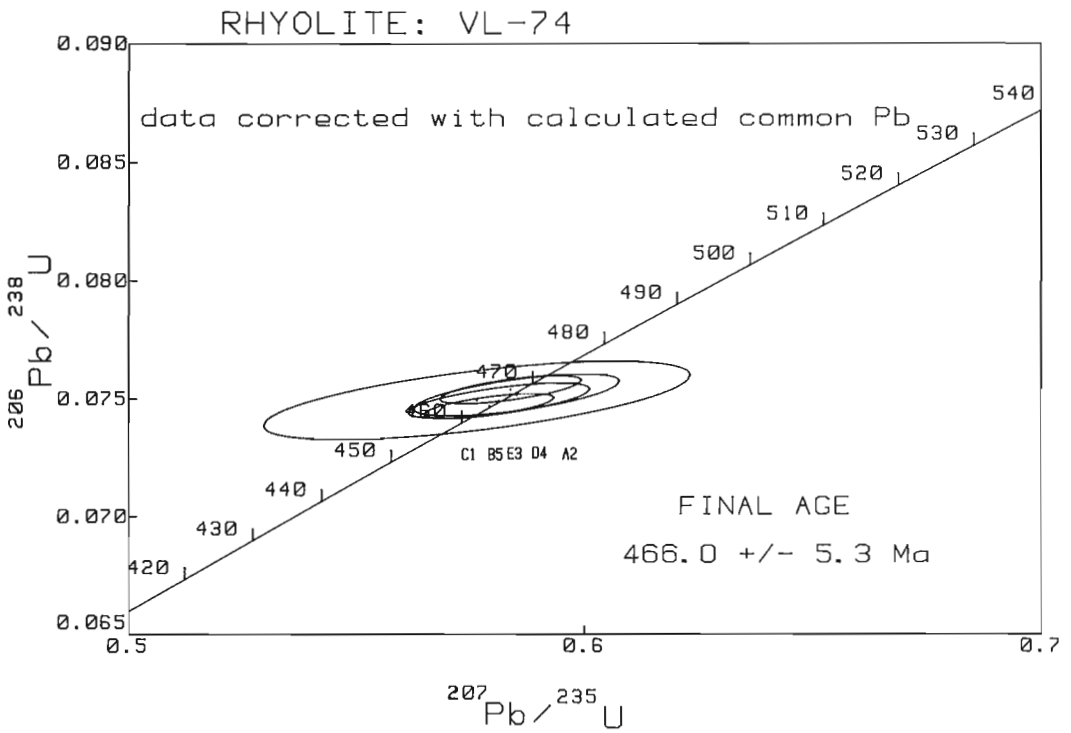

Figure 10. U-Pb concordia diagram of recalculated data using the better estimate for the common Pb composition generated from the U-Pb isochrons. The data are much improved (compare with Fig. 7). The age of the rhyolite is taken from the average of the two isochron ages, with errors estimated graphically from the intersection of the error ellipses with concordia (ignoring C1).

Energy Dispersive X-ray analyses of polished zircon grain mounts detected various types and compositions of inclusions that are considered to be the primary source of the high common Pb content. Some of the inclusions, such as apatite and quartz, were probably incorporated into the zircon during rapid crystallization, whereas other inclusions may be rock material filling resorption cavities. An imprecise data set was significantly improved by applying a better estimate for the common Pb composition.

GEOLOGICAL IMPLICATIONS

The U-Pb zircon age of 466 ± 5.3 Ma for the top of the Flat Landing Brook Formation falls in the late Llanvirnian of the time scale of Snelling (1985) and around the Llanvirnian/Llandeilian boundary in the time scales of Harland et al. (1982), Palmer (1983), and of Haq and van Eysinga (1987).

This age indicates that extrusion of the large volume of dacitic to rhyolitic volcanic rocks took place mainly in Llanvirnian and/or early Llandeilan times, taking into account the time constraints given by fossil ages in the underlying rocks (see above). Furthermore, the stratigraphically lower part of the Boucher Brook Formation may extend into the Llandeilan Series.

Poorly preserved, deformed pelecypods found in tuffaceous sediments enclosed by the Flat Landing Brook Formation near the Taylor Brook massive sulphide deposit (Fig. 1) were tentatively interpreted by J. Pojeta Jr.(written comm., 1988) to belong to the genus *Orthonota*, which is known to have an Early to Middle Devonian age range. However this age determination is in direct conflict with the Ordovician fossils found in the Tetagouche Group and the zircon age reported in this paper. We, therefore, think that either the poor state of preservation of the pelecypods did not allow correct identification, or these clams represent unique fauna that possibly occurred around hydrothermal vents associated with the formation of the Taylor Brook massive sulphide deposit, and as such may have been misassigned to the Devonian Period.

ACKNOWLEDGMENTS

We are grateful to Chris Roddick for his invaluable assistance in data reduction and for useful suggestions, and to Jim Mortensen and Randy Parrish for their critical review of the paper. Dave Walker is thanked for providing the SEM photomicrographs and EDX analyses. Dale Loveridge and Klaus Santowski are also thanked for the mass analyses.

REFERENCES

Davies, J.L.

1966: Geology of the Bathurst-Newcastle area, N.B.; in Guidebook, Geology of parts of Atlantic Provinces, ed. W.H. Poole; Annual meeting, Geological Association of Canada and Mineralogical Association of Canada, Halifax, N.S., p. 33-43.

1979: Geological map of northern New Brunswick. New Brunswick Department of Natural Resources, Mineral Resources Branch, Map NR-3.

Fyffe, L.R.

1982: Taconian and Acadian structural trends in central and northern New Brunswick; in Major Structural Zones and Faults of the Northern Appalachians, ed. P. St-Julien and J. Beland; Geological Association of Canada, Special Paper 24, p. 117-129.

Haq, B.U. and van Eysinga, W.B.

1987: Geological time table, 4th edition; Elsevier, Amsterdam.

Harland, W.B., Cox, A.V., Llewellyn, P.G., Pickton, C.G.A., Smith, A.G., and Walters, R.

1982: A geologic time scale; Cambridge University Press, Cambridge, UK.

Harley, D.N.

1979: A mineralized Ordovician resurgent caldera complex in the Bathurst-Newcastle mining district, New Brunswick, Canada; Economic Geology, v. 74, p. 786-796.

Helmstaedt, H.

1971: Structural geology of Portage Lakes area, Bathurst-Newcastle District, New Brunswick; Geological Survey of Canada, Paper 70-28, 52p.

Neuman, R.B.

1984: Geology and paleobiology of islands in the Ordovician Iapetus Ocean: review and implications; Geological Society of America, Bulletin, v. 94, p. 1188-1201.

Nowlan, G.S.

1981: Some Ordovician conodont faunules from the Miramichi Anticlinorium, New Brunswick; Geological Survey of Canada, Bulletin 345, 35p.

Palmer, A.R.

1983: The decade of North American geology, geologic time scale; Geology, v. 11, p. 503-508.

Parrish, R.R., Roddick, J.C., Loveridge, W.D., and Sullivan, R.W.,

1987: Uranium-lead analytical techniques at the Geological Survey of Canada; in Radiogenic Age and Isotopic Studies: Report 1; Geological Survey of Canada, Paper 87-2, p. 3-7.

Roddick, J.C.

1987: Generalized numerical error analysis with applications to geochronology and thermodynamics; Geochimica et Cosmochimica Acta, v. 51, p. 2129-2135.

Skinner, R.

1974: Geology of Tetagouche Lakes, Bathurst and Nepisiquit Falls map areas, New Brunswick; Geological Survey of Canada, Memoir 371, 133p.

Snelling, N.J.

1985: An interim time scale; in The Chronology of the Geological Record, ed. N.J. Snelling; British Geological Survey, Memoir No. 10, p. 261-265.

Stacey, J.S. and Kramers, J.D.

1975: Approximation of terrestrial lead isotope evolution by a two-stage model; Earth and Planetary Science Letters, v. 26, p. 207-221.

van Staal, C.R.

1986: Preliminary results of structural investigations in the Bathurst Camp of northern New Brunswick; in Current Research, Part A; Geological Survey of Canada, Paper 86-1A, p. 193-204.

1987: Tectonic setting of the Tetagouche Group in northern New Brunswick: implications for plate tectonic models of the northern Appalachians; Canadian Journal of Earth Sciences, v. 24, p. 1329-1351.

van Staal, C.R. and Fyffe, L.R.

in preparation: The New Brunswick Dunnage Zone; in Geology of the Appalachian Orogen in Canada and Greenland, H. Williams and E.R.W. Neale (co-ordinators); Decade of North American Geology, Vol. F-1, Geology of Canada No. 6.

van Staal, C.R. and Williams, P.F.

1984: Structure, origin and concentration of the Brunswick No. 12 and No. 6 orebodies; Economic Geology, v. 79, p. 1669-1692.

van Staal, C.R., Winchester, J., and Cullen, R.

1988: Evidence for D1-related thrusting and folding in the Bathurst-Millstream River area, New Brunswick; in Current Research Part B; Geological Survey of Canada, Paper 88-1B, p. 135-148.

Whitehead, R.E.S. and Goodfellow, W.D.

1978: Geochemistry of volcanic rocks from the Tetagouche Group, Bathurst, New Brunswick, Canada; Canadian Journal of Earth Sciences, v. 15, p. 207-219.

Winchester, J.A. and van Staal, C.R.

1988: Middle Ordovician volcanicity in northern New Brunswick: geochemistry and probable tectonic setting; in Geological Association of Canada/ Mineralogical Association of Canada/ Canadian Society of Petroleum Geologists, Joint Annual Meeting, St. John's, Newfoundland, 1988, Program with Abstracts, v. 13, p. A135.

York, D.

1969: Least squares fitting of a straight line with correlated errors; Earth and Planetary Science Letters, v. 5, p. 320-324.

U-Pb zircon ages of plagiogranite and gabbro from the ophiolitic Deveraux Formation, Fournier Group, northeastern New Brunswick[1]

R.W. Sullivan[2], C.R. van Staal[2], and J.P. Langton[2]

Sullivan, R.W., van Staal, C.R., and Langton, J.P., U-Pb zircon ages of plagiogranite and gabbro from the ophiolitic Deveraux Formation, Fournier Group, northeastern New Brunswick; in Radiogenic Age and Isotopic Studies: Report 3, Geological Survey of Canada, Paper 89-2, p. 119-122, 1990.

Abstract

Two concordant U-Pb zircon ages are reported for the ophiolitic Deveraux Formation in the Dunnage Zone of northeastern New Brunswick. Zircons from a coarse-grained gabbro preserved in a low-strain pod in mylonitic gabbroic gneisses give a revised age of 463.9 ± 1.0 Ma. Zircons from a plagiogranite that intrudes the sheared and metamorphosed gabbro give an age of 459.6 ± 1.0 Ma. The data suggest that the ophiolitic Deveraux Formation is Middle Ordovician, coeval with or slightly younger than felsic and mafic magmatism in the Tetagouche Group in the neighbouring Miramichi Highlands. The approximate 4 Ma difference in age between the gabbro and the plagiogranite is consistent with field relationships and is considered to be real and due to an off-axis formation of the plagiogranite.

Résumé

On signale deux âges concordants obtenus par la méthode U-Pb appliquée au zircon pour la formation ophiolitique de Deveraux qui se trouve dans la zone de Dunnage, dans la partie nord-est du Nouveau-Brunswick. Des cristaux de zircon provenant d'un gabbro grossier conservé dans une lentille à faible déformation logée dans des gneiss mylonitiques et gabbroïques, donnent un âge révisé de 463,9 ± 1 Ma. Du zircon provenant d'un plagiogranite qui pénètre le gabbro cisaillé et métamorphisé donne un âge de 459,6 ± 1 Ma. Ces données semblent indiquer que la formation ophiolitique de Deveraux date de l'Ordovicien moyen, et est contemporaine du magmatisme felsique et mafique du groupe de Tétagouche au voisinage des hautes terres de Miramichi, ou que sa mise en place date d'une période légèrement plus récente que ce magmatisme. La différence d'âge, de l'ordre de 4 Ma, entre le gabbro et le plagiogranite correspond aux relations sur le terrain. On la considère réelle; elle aurait comme origine une formation en dehors de l'axe du plagiogranite.

INTRODUCTION

This paper reports two new U-Pb ages for a plagiogranite and a gabbro of the ophiolitic Deveraux Formation of the Fournier Group in the Belledune Subzone of the New Brunswick Dunnage Zone (Fig. 1). The Belledune Subzone forms part of a new tectonostratigraphic subzonal division of the Dunnage Zone (referred to as Elmtree Terrane in our previous paper, van Staal et al., 1988) introduced by van Staal and Fyffe (in press), which replaces the formerly existing nomenclature for terrane and zone (Williams, 1978; Fyffe, 1987; Fyffe and Flicker, 1987).

The new ages serve 1) to revise a preliminary U-Pb zircon age of 461 ± 3 Ma for the gabbro (van Staal et al., 1988), based on additional zircon fractions, one of which gave a very low error concordant result, and 2) to test whether there is a measurable age difference between the gabbro and the plagiogranite. The plagiogranite cuts through already sheared and metamorphosed gabbro (amphibolite facies), but was itself also weakly deformed during the shearing, suggesting it intruded syntectonically (see van Staal et al., 1988). The plagiogranite consists of sericitized plagioclase, quartz, chlorite pseudomorphs after biotite, epidote, some white mica, and prehnite.

1 Contribution to the Canada - New Brunswick Mineral Development Agreement, 1984-1989. Project carried by the Geological Survey of Canada, Continental Geoscience Division.

2 Geological Survey of Canada, 601 Booth Street, Ottawa, Ontario K1A 0E8

More information concerning the geological setting, sample descriptions, and relevant literature references are given in van Staal et al. (1988).

ANALYTICAL RESULTS

U-Pb analytical techniques follow those for zircon described in Parrish et al. (1987). Zircons were carefully selected by hand picking and were strongly abraded. Total procedural blanks were typically 3 and 11 pg of U and Pb respectively. Analytical data are presented in Table 1 and displayed in Figure 2. Errors are at the 2 sigma level and were calculated using numerical error propagation (Roddick, 1987).

Zircons from the gabbro, ranging in size from +149 to -74 μ are clear, anhedral, and pale pink or straw coloured. They appear equidimensional and blocky, but when turned on their sides display a more typical prismatic zircon habit. Eleven fractions were analyzed, (1 to 22 grains) yielding only six relatively low error results, including two ages, which are concordant within 2 sigma error and are essentially duplicates (JJ, HH, Fig. 2). The JJ result, however, is sligtly better at 463.9 ± 1.0 Ma, and this concordant age is taken as the age of the gabbro. There is a slight scatter in fraction DD, the reason for which is uncertain, but it may imply a slight inheritance. Fraction KK (not plotted) was selected to test for possible inheritance, but it has high uranium and suffers from severe lead loss. The $^{207}Pb/^{206}Pb$ age of KK, however, is consistent with the concordant JJ result. Fractions AA and CC in this report are the same as fractions A and C reported previously (van Staal et al., 1988) and are included here only for continuity between reports. They are now ignored in favour of the new superior data.

Zircons from the plagiogranite are generally clear, colourless, and euhedral but with a somewhat rounded appearance. Some crystals are multifaceted 'gems'. A few zircons have sharp nippled terminations, and a few twins were seen. Five zircon fractions were analyzed yielding a linear trend when plotted on a concordia diagram (Fig. 2). This discordance is interpreted to result from simple surface correlated lead loss. Fraction E is concordant at 459.6 ± 1.0 Ma, which is taken as the age of the plagiogranite.

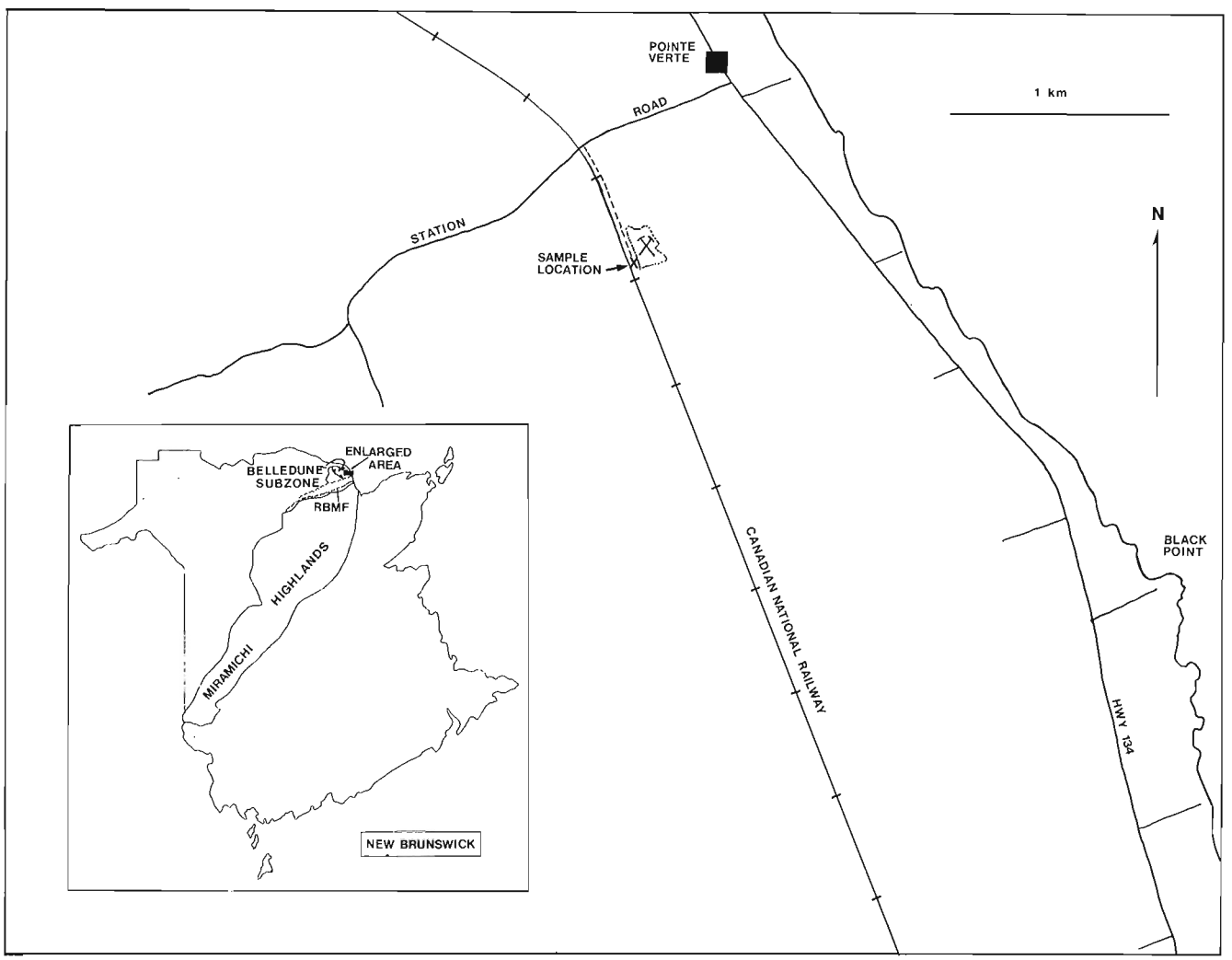

Figure 1. Sample location map. Sample site is located at 47° 50' 36" N, 65° 46' 00" W. RBMF is the Rocky Brook-Millstream fault system.

DISCUSSION

The U-Pb zircon age of 463.9 ± 1.0 Ma for the Deveraux gabbro, which is interpreted as the formation age of the ophiolite, falls in the late Llanvirnian of the time scale of Snelling (1985) or in the Llandeilian of the time scales of Harland et al. (1982), Palmer (1983), and Haq and van Eysinga (1987). The U-Pb zircon age of 459.6 ± 1.0 Ma for the plagiogranite falls in the Llandeilian of all the above-mentioned time scales.

Because these rocks are ophiolitic, a more appropriate mantle type Pb isotopic composition for the common lead correction was applied, namely 17.35 ± 1.0% 1 standard error of the mean (SE) for $^{206}Pb/^{204}Pb$ and 15.43 ± 0.5% 1 SE. for $^{207}Pb/^{204}Pb$. These ratios were calculated by interpolating to a 465 Ma model age (version II, Table VI, of Zartman and Doe 1981). The approximate 4 Ma age difference between the gabbro and the plagiogranite is consistent with field relationships.

Table 1. U-Pb zircon isotopic data: Ophiolitic Deveraux Formation, Fournier Group, New Brunswick.

Sample and fraction[4]	Weight (mg)	U (ppm)	Pb* (ppm)	Measured[1] $^{206}Pb/^{204}Pb$	Isotopic abundances[2] (^{206}Pb=100) ^{204}Pb	^{207}Pb	^{208}Pb	Isotopic ratios[3] $^{206}Pb/^{238}U$	$^{207}Pb/^{235}U$	Age,Ma ^{207}Pb-^{206}Pb
1. Coarse gabbro: JPG (47° 50' 36" N, 65° 46' 00" W)										
AA +149, 1 XL, A	0.0192	71.1	5.75	436	0.08201	6.855	23.411	0.074444	0.582054	480.1
CC +149, 6 XL, A	0.0678	31.8	2.54	676	0.05231	6.362	21.417	0.074176	0.573298	454.6
DD +149, 20 XL, A	0.2127	33.8	2.74	1604	0.02449	5.998	21.276	0.074656	0.581005	469.9
HH -149, 20 XL, A	0.0699	20.9	1.67	483	0.05458	6.419	20.680	0.074644	0.579419	464.2
JJ -149, 22 XL, A	0.0903	66.1	5.30	1492	0.02852	6.045	20.304	0.074627	0.579622	465.4
KK 15 poor XLs, A	0.0485	231.1	18.69	2642	0.01689	5.867	22.712	0.073511	0.569904	461.4
2. Plagiogranite: VL-632 (47° 50' 36" N, 65° 46' 00" W)										
A -74+62, A	0.0537	345.4	28.3	3072	0.01396	5.812	25.150	0.072936	0.564169	456.3
B -105+74, A	0.0751	233.7	19.6	4198	0.00428	5.680	26.630	0.073599	0.570099	459.5
C -149+105, A	0.1050	221.9	18.0	4445	0.00766	5.731	23.314	0.073012	0.565803	460.4
D +149, A	0.0688	196.0	16.3	3544	0.00278	5.665	25.765	0.073578	0.570612	462.1
E -149+105, A	0.1235	189.0	15.8	7775	0.00461	5.684	25.990	0.073914	0.572500	459.3

NOTES: *radiogenic Pb; [1]corrected for fractionation and spike; [2]corrected for Pb blank; [3]corrected for U,Pb blank and mantle type assumed common Pb composition, $^{206}Pb/^{204}Pb$=17.35, $^{207}Pb/^{204}Pb$=15.43 (see text); [4]size in microns; analytical errors are reflected in the 2 sigma error ellipses on the concordia plot; A=abraded.

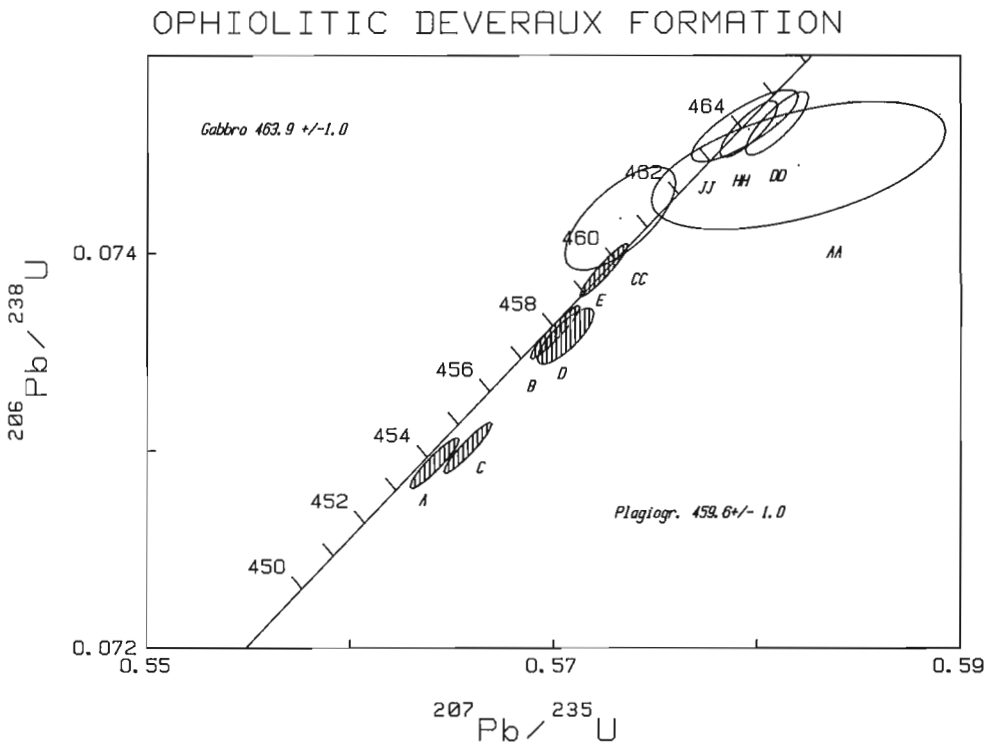

Figure 2. U-Pb concordia plot for zircon from a coarse-grained gabbro (open ellipses) and from a plagiogranite (shaded ellipses) from the ophiolitic Deveraux Formation. Ages are in Ma. Errors are shown at the two sigma level.

Because the data for the two ages are concordant within analytical error and their errors do not overlap (JJ, E, Fig. 2) we believe the approximate 4 Ma age difference between the gabbro and the plagiogranite is real. This supports the suggestion made earlier by Flagler and Spray (1988); van Staal et al. (1988), that based on the spatial and age relationship between narrow zones of highly strained amphibolite and plagiogranite dykes, the plagiogranite was generated off-axis during active transform shearing in oceanic crust. The shearing along the transform fault transformed part of the gabbro into high-grade amphibolites and may have juxtaposed a hot spreading centre next to cold oceanic crust, inducing generation of the plagiogranite melt.

ACKNOWLEDGMENTS

We are grateful to Randy Parrish for his critical review of this paper and to Jim Mortensen for helpful discussions. Dale Loveridge and Klaus Santowski are thanked for providing the mass analyses, as is Herb Helmstaedt for his discussions and assistance in the field.

REFERENCES

Flagler, P.A. and Spray, J.G.
1988: Metamorphism in shear zones within the Fournier oceanic fragment; in Geological Association of Canada/ Mineralogical Association of Canada/ Canadian Society of Petroleum Geologists, Joint Annual Meeting, St. John's, Newfoundland, 1988, Program with abstracts, v. 13, p. A39.

Fyffe, L.R.
1987: Stratigraphy and tectonics of the Miramichi and Elmtree terranes in the Bathurst area, northeastern New Brunswick; Geological Society of America, Centennial Field Guide - Northeastern section, p. 389-393.

Fyffe, L.R. and Fricker,A.
1987: Tectonostratigraphic terrane analysis of New Brunswick; Maritime Sediments and Atlantic Geology, v. 23, p. 113-122.

Haq, B.U. and van Eysinga, W.B.
1987: Geological Time Table, 4th edition; Elsevier, Amsterdam.

Harland, W.B., Cox, A.V., Llewellyn,P.G., Pickton, C.G.A., Smith, A.G., and Walters, R.
1982: A Geologic Time Scale; Cambridge University Press, Cambridge, U.K.

Palmer, A.R.
1983: The Decade of North American geology, geologic time scale; Geology, v. 11, p. 503-508.

Parrish, R.R., Roddick, J.C., Loveridge, W.D., and Sullivan, R.W.,
1987: Uranium-lead analytical techniques at the Geological Survey of Canada; in Radiogenic Age and Isotopic Studies: Report 1; Geological Survey of Canada, Paper 87-2, p. 3-7.

Roddick, J.C.
1987: Generalized numerical error analysis with applications to geochronology and thermodynamics; Geochimica et Cosmochimica Acta, v. 51, p. 2129-2135.

Snelling, N.J.
1985: An interim time scale; in The Chronology of the Geological Record, ed. N.J. Snelling; British Geological Survey, Memoir No. 10, p. 261-265.

van Staal, C.R. and Fyffe, L.R.
in preparation: The New Brunswick Dunnage Zone; in Geology of the Appalachian Orogen in Canada and Greenland, H. Williams and E.R.W. Neale (co-ordinators); Decade of North American Geology, Vol. F-1, Geology of Canada No. 6.

van Staal, C.R., Langton, J.P., and Sullivan, R.W.,
1988: A U-Pb zircon age for the ophiolitic Deveraux Formation, Elmtree Terrane, northeastern New Brunswick; in Radiogenic Age and Isotopic Studies: Report 2; Geological Survey of Canada, Paper 88-2, p. 37-40.

Williams, H.
1978: Tectonic lithofacies map of the Appalachian orogen; Memorial University of Newfoundland, St. John's, Nfld., Map 1.

Zartman, R.E. and Doe, B,R.
1981: Plumbotectonics-the model; Tectonophysics, v. 75, p. 135-162.

Reconnaissance geochronology of Baffin Island, N.W.T.

G.D. Jackson[1], P.A. Hunt[1], W.D. Loveridge[1], and R.R. Parrish[1]

Jackson, G.D., Hunt, P.A., Loveridge, W.D., and Parrish, R.R., Reconnaissance geochronology of Baffin Island, N.W.T.; in Radiogenic Age and Isotopic Studies: Report 3, Geological Survey of Canada, Paper 89-2, p. 123-148, 1990.

Abstract

U-Pb zircon and monazite ages and whole-rock Rb-Sr data, from a number of widely separated localities, suggest that Baffin Island can be subdivided into a northern region dominated by Archean protoliths, and a southern region, the Baffin Orogen, characterized by intense Aphebian high-grade metamorphism and plutonism.

Southern region:
In the Iqaluit area pink monzogranite that intrudes monzocharnockite rocks is dated at 1857 +21/-6 Ma (U-Pb zircon). A Rb-Sr whole-rock isochron age of 1877 ± 45 Ma on mixed lithologies from the same location is in general agreement with the U-Pb age.

In central Baffin Island emplacement of a charnockitic pluton intrusive into the Piling Group is dated at ca. 1850 Ma by U-Pb on zircon. A Rb-Sr whole-rock isochron of 1730 ± 49 Ma, initial $^{87}Sr/^{86}Sr = 0.7149 \pm 0.0034$, indicates Sr isotopic re-equilibration subsequent to emplacement. U-Pb dates of zircon and monazite from a large monzocharnockitic pluton 120 km to the south document inherited zircon and a minimum age for its emplacement at 1854 Ma (monazite).

Northern region:
In the Mary River area, north-central Baffin Island,
dacite from the Mary River Group is dated at 2718 +5/-3 Ma (zircon). A pluton in the intrusive sequence yields a zircon age of 2709 +4/-3 Ma, whereas foliated tonalite representing basement to the group is 2851 +20/-17 Ma.

U-Pb zircon studies on two components of a migmatite near Cambridge Fiord, and on a small monzogranite body west of Navy Board Inlet, indicate complex mineral systematics, and suggest Aphebian melting of Archean protoliths followed by formation of Aphebian igneous zircon.

Rb-Sr data for migmatite components at Admiralty Inlet suggest a minimum age of about 2300 Ma for granulite metamorphism. Rb-Sr results for the Nauyat volcanic rocks are difficult to interpret. Both sets of data indicate complex whole-rock systematics.

Résumé

Des âges obtenus par la méthode U-Pb appliquée au zircon et à la monazite et des âges obtenus par la méthode Rb-Sr appliquée à la roche totale, provenant d'un certain nombre de localités très espacées, semblent indiquer que l'île de Baffin peut être divisée en une région nord dominée par des protolites de l'Archéen et une région sud, l'orogène de Baffin, caractérisée par un degré de métamorphisme élevé et un plutonisme intenses remontant à l'Alphébien.

Région sud
Dans le secteur d'Igaluit, le monzogranite rose qui pénètre des roches monzocharnockitiques a un âge de 1857 ± 21/ −6 Ma (méthode U-Pb appliquée au zircon). Un âge Rb-Sr isochrone de la roche totale établi à 1877 ± 45 Ma et obtenu de différentes lithologies provenant du même endroit, correspond de façon générale avec l'âge U-Pb.

1 Geological Survey of Canada, 601 Booth Street, Ottawa, Ontario K1A 0E8

Dans la partie centrale de l'île de Baffin, la mise en place d'un pluton charnockitique dans le groupe de Piling a été daté à environ 1850 Ma au moyen de la méthode U-Pb appliquée au zircon. Un âge Rb-Sr isochrone de la roche totale établi à 1730 ± Ma, avec un rapport de strontium originel ($^{87}Sr/^{86}Sr$) égal à 0,7149± 0,0034, indique qu'il y a eu un nouvel équilibre isotopique ultérieur à la mise en place. Des âges obtenus par la méthode U-Pb appliquée au zircon et à la monazite provenant d'un grand pluton monzocharnockitique situé à 120 km au sud, témoignent de la présence d'un zircon hérité dont la mise en place remonte à au moins 1854 Ma (monazite).

Région nord

Dans la région de la rivière Mary, la partie centre-nord de l'île de Baffin, une dacite provenant du groupe de Mary River a un âge de 2718 + 5/−3 Ma (zircon). Un pluton, appartenant à la séquence intrusive, fournit un âge de 2709 + 4/−3 Ma à partir du zircon alors qu'une tonalit foliée qui représente le socle de ce groupe a un âge de 2851 + 20/−17 Ma.

Des études réalisées à l'aide de la méthode U-Pb appliquée au zircon de deux composantes d'une migmatite située près du fjord Cambridge et d'un petit massif de monzogranite situé à l'ouest de l'inlet Navy Board, établissent une classification et une taxonomie minérales complexes, et laissent supposer une fusion d'âge aphébien de roches mères de l'Archéen suivie de la formation d'un zircon igné de l'Aphébien.

Des données Rb-Sr pour des composantes de migmatite dans l'inlet Admiralty semblent indiquer un âge minimum d'environ 2300 Ma pour un métamorphisme à faciès des granulites. Les résultats Rb-Sr pour les roches volcaniques de Nauyat sont difficiles à interpréter. Les deux ensembles de données indiquent une classification et une taxonomie complexes pour la roche totale.

INTRODUCTION

Topical and reconnaissance geological and geochronological studies on Baffin Island have been carried out by the Geological Survey of Canada over a period of more than two decades. Geochronological work related to the mapping by the senior author includes Rb-Sr, K-Ar, and U-Pb studies, some of which have only recently been completed. In order to make this data base available, this paper brings together Rb-Sr and U-Pb data for several areas of Baffin Island, in an attempt to provide a geochronological framework for future more detailed studies.

Three U-Pb zircon and monazite ages and two Rb-Sr isochrons are presented here that bear on the age of plutonism and metamorphism related to the Cumberland batholithic complex of Southern Baffin Island. Three other zircon ages from north-central Baffin Island date the Mary River Group, its basement, and a slightly younger granitic pluton. U-Pb zircon data are also presented for two components of a migmatite from the eastern part of northern Baffin Island. Results for Borden Basin on northwestern Baffin Island include U-Pb zircon and Rb-Sr whole-rock data for the basement to the Neohelikian (Middle Proterozoic) Bylot Supergroup and Rb-Sr whole-rock data for the basalt flows in the Nauyat Formation at the base of the supergroup. Selected K-Ar ages are discussed briefly.

The paper presents a summary of the geological framework of the island, followed by sections on the study areas, arranged from south to north. Terminology for charnockites of Baffin Island is defined in Jackson (manuscrit in preparation). Analytical proceedures are presented in Appendix 1.

Geological Framework

Most of Baffin Island consists of Archean and Aphebian (Lower Proteerozoic) metamorphic and igneous rocks, with metamorphic grade chiefly of upper amphibolite to granulite facies, but locally as low as subgreenschist facies (Jackson and Morgan, 1978).

Geologically Baffin Island can be divided into two main blocks. The northern block contains Archean basement and supracrustal, and plutonic sequences, which were deformed, metamorphosed, and intruded by Aphebian plutons. The southern part of the island, termed the Baffin Orogen, contains the huge Aphebian Cumberland Batholithic Complex and adjacent Aphebian supracrustal sequences and fold belts, with an uncertain amount of Archean basement rocks.

The oldest rocks throughout Baffin Island occur in a deformed granitic basement complex that in northern Baffin Island (Fig. 1) is composed mostly of nebulitic migmatitic granitic gneisses and deformed and metamorphosed granite-granodiorite plutons. These ancient rocks were migmatized and intruded by mafic dyke swarms before the Archean Mary River Group was deposited. Most of the northern half of Baffin Island (Figs. 1, 2) lies in the northeast-trending, late Archean, Committee Fold Belt (Jackson and Taylor, 1972; Jackson, manuscript in preparation). It is defined by the Mary River Group, a greenstone assemblage (Jackson, 1966) that was deposited nonconformably on the basement complex, probably in a continental island-arc environment (Jackson, manuscript in preparation). This was followed in the late Archean by intrusion of porphyritic monzogranite, migmatization and deformation, and probably local granulite-facies metamorphism.

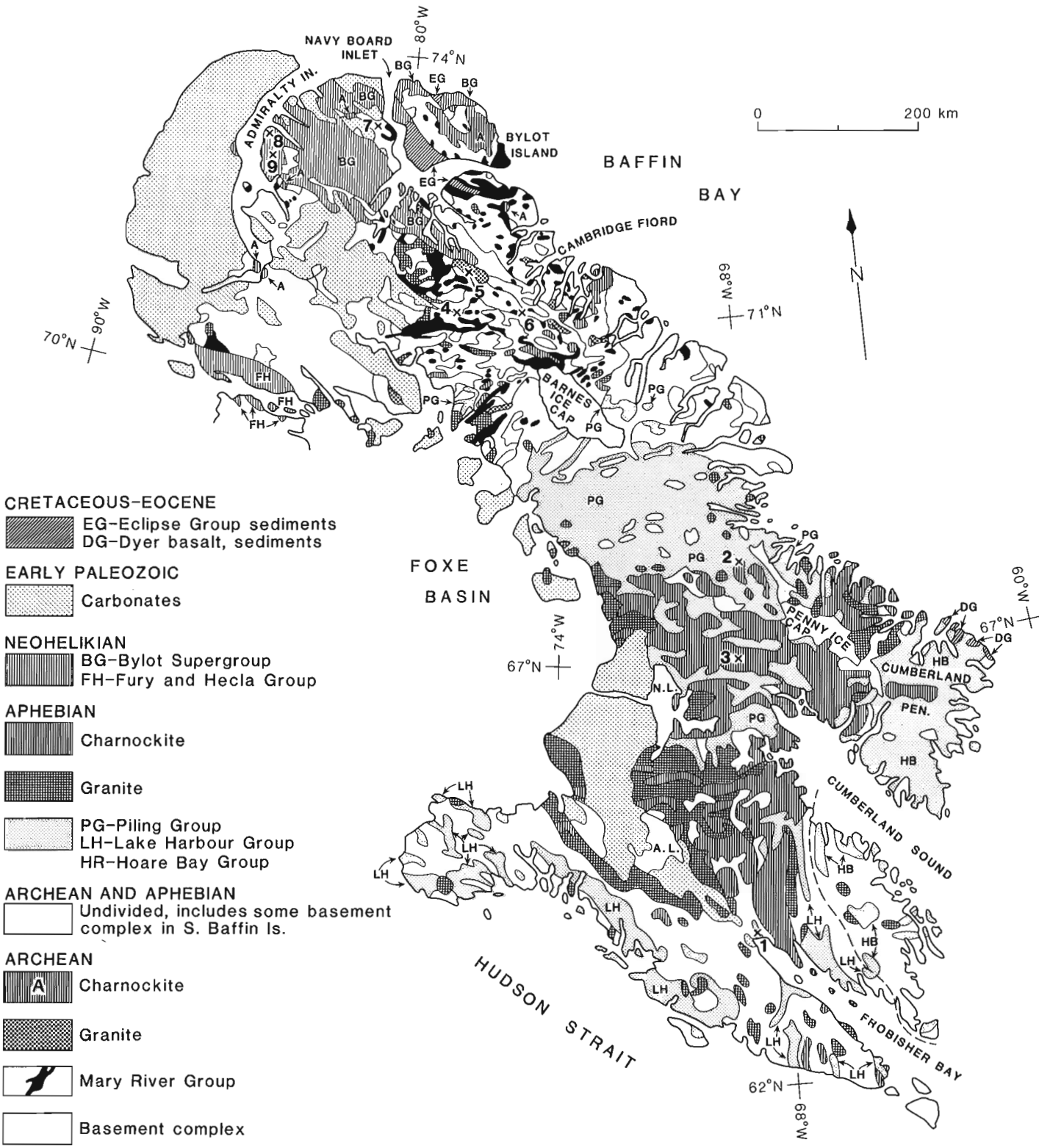

Figure 1. Geology of Baffin Island: 1- Iqaluit, 2- West of Nudlung Fiord, 3- north-central Cumberland Batholithic Complex, 4- Mary River Group dacite, and basement tonalite, 5- late Archean quartz monzodiorte in Mary River region, 6- nebulitic migmatite at head of Cambridge Fiord, 7- monzogranite west of Navy Board Inlet, 8- crystalline complex east of Admiralty Inlet, 9- Nauyat plateau basalt.

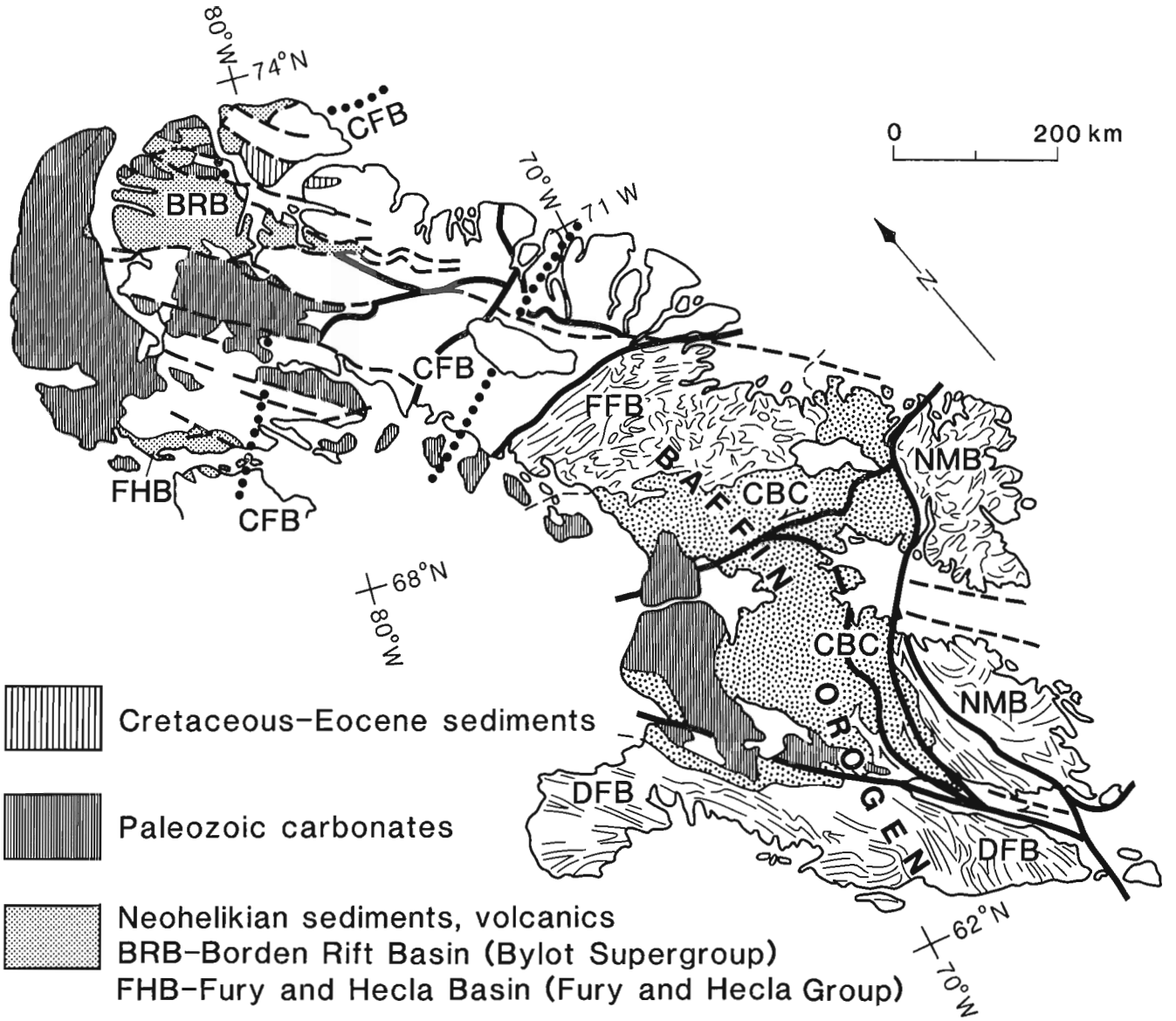

Figure 2. Some tectonic features of Baffin Island.

Aphebian granitic plutons were emplaced into northern Baffin Island and late Aphebian regional metamorphism produced a northeast-trending belt of granulite and monzocharnockite plutons across the island. Aphebian regional deformation affected most of eastern Baffin Island, forming southwest-directed nappes and ductile thrust zones in the northeastern coastal region (Jackson, manuscript in preparation).

The late Aphebian (ca. 1.85 Ga) Baffin Orogen includes all of southern Baffin Island (Jackson, manuscript in preparation; Hoffman, in press) and extends into western Greenland, Melville Peninsula, and northern Quebec and Labrador. On Baffin Island the orogen comprises a batholithic complex, and three supracrustal components that may be coeval (Jackson, manuscript in preparation). The huge triangular-shaped Cumberland batholithic complex forms the core of the orogen, and is composed of anastomosing late Aphebian (1.90-1.85 Ga) monzogranite-monzocharnockite plutons interspersed with lenses and inclusions of bordering supracrustals and old basement. Granulite-facies rocks are most abundant south of the complex.

The Cumberland batholithic complex is bordered by three deformed Aphebian supracrustal sequences. The Piling Group defines the Foxe Fold Belt north of the batholith; the Lake Harbour Group defines the Dorset Fold Belt to the south, and the Hoare Bay Group defines the Nagsuggtoqidian Mobile Belt, southeast of the batholith. All of these contain metagreywacke and metapelite sequences with iron-formation and metamorphosed mafic and/or ultramafic rocks, and variable amounts of quartzite and marble. The late Aphebian was characterized on most of Baffin Island by granitic and charnockitic plutonism, deformation of supracrustal sequences, and metamorphism to mainly amphibolite- granulite grade.

Epeirogenic uplift and erosion followed the late Aphebian orogenesis. By Neohelikian time, block faulting and rifting led to deposition of strata nonconformably on the gneissic terrain of northwestern Baffin Island. The Bylot Supergroup of Borden Rift Basin contains a lower clastic (Eqalulik), middle carbonate platform (Uluksan), and an upper clastic (Nunatsiaq) group. Deposition of the lower and upper groups was in response to rifting during opening of the Poseidon Ocean to the northwest (Jackson and Iannelli, 1981). Some of the lower Supergroup strata are in subgreenschist facies. The Fury and Hecla Group to the south is correlative with the lower part of the Bylot Supergroup.

Post-metamorphic northwest-trending faults occur throughout Baffin Island. Movement along some of them is at least as old as Neohelikian and along others is as young as Recent (Jackson and Morgan, 1978). At least three generations of late Precambrian diabase dykes have been emplaced along and parallel to these faults.

Cumberland Batholithic Complex

Iqaluit (Southern) Area

Geological Setting

Iqaluit lies in the centre of a large region mapped on a reconnaissance scale by Blackadar (1967). The general area about Iqaluit and Frobisher Bay is underlain chiefly by quartz feldspar gneiss (Blackadar's unit 3) in which mafic minerals are of minor importance, but commonly include hypersthene. Metamorphic grade is upper amphibolite to granulite facies, and at least some of the upper-amphibolite-grade rocks are retrograded granulites. Jackson and Morgan (1978; in Fraser et al., 1978) considered Blackadar's unit 3 and part of unit 4 to be part of the metamorphic Archean complex that is basement to the Aphebian, Lake Harbour Group (Jackson and Taylor, 1972). This inferred basement was remetamorphosed up to granulite grade with the Lake Harbour Group. Pink monzogranitic (Blackadar, 1967 - unit 13) - monzocharnockitic (*ibid*; unit 14) rocks, forming the southern part of the Cumberland batholithic complex, occur north and northwest of Iqaluit (Jackson and Taylor, 1972; Henderson et al., 1980). The southern extension of these lies several kilometres to the east of Iqaluit and dies out to the southeast in Frobisher Bay. The monzocharnockite is considered by Jackson and Morgan (1978) to be chiefly the metamorphosed equivalent of the monzogranite. Patches of gneiss with vague nebulitic structures (basement?) in the monzocharnockite suggest that more of the area mapped as monzocharnockite may be recrystallized Archean gneisses than is presently recognized. In addition to the quartz-feldspar gneiss, marble, sillimanite-biotite paragneiss, lit-par-lit migmatite, and metamorphosed felsic and mafic intrusions are common in the immediate vicinity of Iqaluit. The paragneisses are considered to belong to the Lake Harbour Group (Jackson and Taylor, 1972).

An area adjacent to the Frobisher Inn at Iqaluit was levelled by blasting several years ago in preparation for the construction of the building complex now attached to the Inn. A remnant knob of fresh bedrock just northeast of the hotel contains several rock types and was sampled for U-Pb zircon and whole rock Rb-Sr age determination. This locality includes minor paragneisses amongst various granitic rocks akin to the Cumberland batholitic complex previously described.

Most of the knob is composed of two types of layered granitoid rocks: grey-green, greasy, massive to foliated on a small scale, and sheared rocks of monzocharnockite composition, and pink, massive, medium-grained to pegmatitic monzogranite with clinopyroxene and local hypersthene. The latter intrudes the other rocks and occurs also in discordant dykes up to 1 m thick. Minor pyribolite, paragneiss, and metamorphosed grey pegmatite are also present.

U-Pb Zircon (Sample JD70-1B)

Pink monzogranite was collected from this locality for U-Pb age determination. The age for this intrusive granite would be a minimum age for the associated gneisses. The monzogranite is similar to the large granite body to the north and probably belongs to same episode of granite emplacement, and thus should be of similar age.

The pink monzogranite (sample 1B, Table A1, Appendix 2) is inequigranular, slightly porphyritic, and massive to foliated with palimpsest structure. The quartz and feldspars have interlocking sutured contacts. Oligoclase (An_{18-22}) and microcline are very slightly altered, contain minor brown

dusting and few tiny grains of carbonate and muscovite. The microcline is perthitic, and exsolution perthite predominates over vein perthite. Some hornblende seems to be in equilibrium with clinopyroxene, but most of the hornblende either rims the clinopyroxene or replaces it along cleavages (uralite).

The zircons recovered from this sample are pristine, euhedral, stubby grains with sharp terminations and an aspect ratio of about 2:1. Under transmitted light the zircons show distinct zoning and inclusions at the centre of each grain. These inclusions, observed in more detail in a polished and etched section (Fig. 3), were analyzed and reported to be fragments of quartz, feldspar, or zircon.

Six zircon fractions were analyzed (Table 1). They plot slightly below concordia in a cluster (Fig. 4) that forms a line with a Davis (1982) calculated upper intercept of 1857 +21/-6 Ma, a lower intercept of 1472 Ma, and a probability of fit of 62%. We interpret the upper intercept as the approximate age of emplacement and crystallization of the monzogranite, and a minimum age for the rocks the monzogranite intrudes.

Table 1. U-Pb zircon and monazite data.

Fraction,[1] Size	Weight (mg)	U (ppm)	Pb^2 (ppm)	$^{206}Pb/^{204}Pb$[3]	Pb_c[4] (pg)	^{208}Pb[2] (%)	$^{206}Pb/^{238}U \pm$SEM%[5]	$^{207}Pb/^{235}U \pm$SEM%[5]	$^{207}Pb/^{206}Pb \pm$SEM%[5]	$^{207}Pb/^{206}Pb$ age, error (Ma)[6]
Iqaluit Hybrid Granulite (JD70-1B)										
A 149 NM0 abr	0.0493	285.0	113.3	13430	22	20.6	0.32947 (.08)	5.1188 (.10)	0.11268 (.03)	1843.1 (1.0)
B 149 Mag0 abr	0.0415	246.7	97.8	4588	47	20.3	0.32977 (.09)	5.1239 (.10)	0.11269 (.03)	1843.3 (1.1)
C 74 NM0 abr	0.0153	266.7	106.5	1647	52	20.8	0.32981 (.09)	5.1230 (.11)	0.11266 (.04)	1842.7 (1.6)
D +74 Mag0 abr	0.0115	201.0	83.8	2350	20	24.0	0.33080 (.09)	5.1486 (.11)	0.11288 (.04)	1846.3 (1.3)
E +149 NM0 abr	0.0475	765.6	267.4	18610	40	10.9	0.32552 (.08)	5.0160 (.10)	0.11176 (.03)	1828.2 (1.0)
F +105 NM0 abr	0.0208	228.6	92.9	3504	28	22.4	0.32902 (.09)	5.0994 (.10)	0.11241 (.04)	1838.7 (1.3)
West of Nudlung Fiord Charnockite (JDC168/22-70)										
A Monazite	0.0146	1092.7	4553.0	9019	37	92.4	0.32824 (.09)	5.0704 (.10)	0.11204 (.03)	1832.7 (1.2)
B Monazite	0.0075	1594.0	6865.0	7840	32	92.7	0.32731 (.09)	5.0524 (.10)	0.11196 (.03)	1831.4 (1.0)
A +74 NM0 abr 3:1	0.0210	1886.5	596.2	1600	499	4.4	0.31617 (.09)	4.8516 (.13)	0.11129 (.07)	1820.6 (2.5)
B +74 NM0 abr 2:1	0.0445	1542.0	485.3	3832	356	4.6	0.31433 (.09)	4.8054 (.11)	0.11088 (.04)	1813.8 (1.4)
C +74 NM0 abr 1:1	0.0140	821.9	259.3	7571	30	3.6	0.31825 (.09)	4.8818 (.10)	0.11125 (.03)	1820.0 (1.1)
D -74+62 NM0 abr	0.0090	1955.2	586.1	2487	136	3.8	0.30253 (.08)	4.5483 (.10)	0.10904 (.05)	1783.4 (1.7)
North Central Cumberland Batholithic Complex Monzocharnockite (JDM355-68)										
A Monazite	0.0088	521.3	9237.0	2348	41	98.2	0.33306 (.11)	5.2053 (.13)	0.11335 (.05)	1853.8 (1.9)
A +149 NM0 abr	0.0430	508.9	181.7	6925	67	9.1	0.33769 (.09)	5.4873 (.10)	0.11785 (.03)	1923.9 (1.1)
B -149+93 NM0 abr	0.0398	566.9	203.8	11210	43	3.0	0.33582 (.09)	5.3890 (.10)	0.11639 (.03)	1901.5 (1.0)
C -93 NM0 abr	0.0106	465.6	173.1	1257	85	13.1	0.33660 (.09)	5.3544 (.12)	0.11537 (.06)	1885.7 (2.3)
D +149 NM0 abr	0.0240	539.1	186.9	13610	20	6.8	0.33653 (.08)	5.3606 (.10)	0.11553 (.03)	1888.1 (1.0)
Mary River Group Dacite (JD100/12-68)										
A +74 NM2 abr	0.0484	229.0	140.5	5686	63	14.0	0.51368 (.09)	13.2034 (.10)	0.18642 (.03)	2710.8 (1.0)
B -74 NM2 abr	0.0251	278.8	169.3	6780	33	14.4	0.50794 (.09)	13.0137 (.10)	0.18582 (.03)	2705.5 (1.0)
C +74 Mag2 abr	0.1148	233.5	141.6	15000	57	14.0	0.50976 (.08)	13.0716 (.10)	0.18598 (.03)	2706.9 (1.0)
D -74+62 Mag2	0.0576	117.4	71.0	4771	45	14.2	0.50526 (.09)	12.9422 (.10)	0.18578 (.03)	2705.1 (1.1)
Mary River Region Monzogranite (JD138/1-68)										
A +105 NM0 abr	0.0790	149.6	93.6	7361	52	16.3	0.51128 (.09)	13.0732 (.10)	0.18545 (.03)	2702.2 (1.0)
B -105+74 NM0 abr	0.0480	122.5	76.4	864	224	15.9	0.51376 (.09)	13.1365 (.13)	0.18544 (.08)	2702.2 (2.7)
C -74+62 NM0 abr	0.0423	169.2	103.5	5144	44	15.5	0.50688 (.09)	12.9321 (.10)	0.18504 (.03)	2698.5 (1.0)
D -74+62 NM0 abr	0.0389	178.1	108.3	3919	56	15.4	0.50416 (.08)	12.8532 (.10)	0.18490 (.03)	2697.3 (1.1)
Mary River Group Basement Trondhjemite-Tonalite (JDC56/1-68)										
A -105+74 NM0 abr	0.0109	136.0	75.6	2373	19	10.1	0.48717 (.11)	12.4298 (.13)	0.18505 (.03)	2698.6 (1.1)
B -105+74 NM0 abr	0.0148	331.1	184.6	3727	41	9.6	0.48891 (.01)	12.6076 (.11)	0.18703 (.03)	2716.2 (1.1)
C -74+62 NM0 abr	0.0291	257.2	140.3	2770	82	9.8	0.47686 (.09)	12.0136 (.10)	0.18272 (.04)	2677.7 (1.2)
D -74+62 NM0 abr	0.0323	316.9	166.0	7797	38	9.9	0.46303 (.09)	11.5174 (.10)	0.18040 (.03)	2656.6 (1.0)
E -105+74 NM0 abr	0.0250	236.4	148.8	6218	32	11.9	0.53719 (.09)	14.7562 (.10)	0.19923 (.03)	2819.9 (0.9)
F -105+74 NM0 abr	0.0344	318.1	179.9	7823	44	10.4	0.49540 (.08)	12.8772 (.10)	0.18852 (.03)	2729.3 (0.9)
G -105+74 NM0 abr	0.0144	237.7	143.8	2663	43	11.0	0.52335 (.09)	14.0988 (.10)	0.19538 (.03)	2788.0 (1.0)
Borden Rift Basin Monzogranite (JD79-84)										
A +74 NM+1 abr	0.0085	140.7	47.7	423	51	22.0	0.27764 (.18)	4.0609 (.31)	0.10608 (.20)	1733.2 (7.2)
B -74+62 Mag+1 abr	0.0235	289.8	111.7	1699	80	21.3	0.31538 (.09)	5.0679 (.11)	0.11655 (.05)	1903.9 (1.9)
C -62 Mag+1 abr	0.0185	372.1	149.5	2123	68	20.0	0.33247 (.09)	5.6622 (.11)	0.12352 (.05)	2007.7 (1.8)
D +74 Mag+2 abr	0.0260	302.8	114.7	1195	128	22.9	0.30488 (.09)	4.7005 (.14)	0.11182 (.08)	1829.2 (2.9)
E +74 Mag+1 abr	0.0087	128.0	52.5	431	58	18.5	0.34256 (.15)	6.3108 (.24)	0.13361 (.16)	2146.0 (5.5)
Cambridge Fiord Migmatite-Anatectite Amphibolite Phase (JDD218Z-68)										
A +149 NM+1 abr	0.0407	454.9	208.1	3400	142	10.5	0.41201 (.09)	8.7356 (.10)	0.15377 (.03)	2388.3 (1.2)
B -149+105 NM+1 abr	0.0430	273.1	177.8	5075	73	22.7	0.49495 (.08)	12.2708 (.10)	0.17981 (.03)	2651.1 (1.0)
C -105+74 NM+1 abr	0.0385	212.5	125.1	6404	38	18.2	0.47579 (.09)	11.4898 (.10)	0.17514 (.03)	2607.4 (1.0)
D -74 NM+1 abr	0.0418	208.6	117.6	4488	57	16.6	0.46460 (.09)	11.1395 (.10)	0.17390 (.03)	2595.5 (1.0)
Leucocratic Phase (JDD218X-68)										
A +74 NM0 abr	0.0149	1226.6	432.9	3332	121	3.5	0.34940 (.09)	6.4068 (.10)	0.13299 (.04)	2137.8 (1.4)
B +74 NM0 abr	0.0052	680.6	268.3	2296	37	7.1	0.37310 (.10)	7.2522 (.12)	0.14098 (.04)	2239.2 (1.4)
C -74 NM0 abr	0.0067	1258.9	514.2	3965	53	4.3	0.39612 (.09)	8.0591 (.10)	0.14756 (.03)	2317.8 (1.1)

Notes: [1]sizes (-74+62) refer to length aspect of zircons in microns (i.e., through 74 micron sieve but not the 62 micron sieve); abr=abraded, NM1=non-magnetic cut with frantz at 1 degree side slope, Mag0=magnetic cut with frantz at 0 degree side slope; [2]radiogenic Pb; [3]measured ratio, corrected for spike and fractionation; [4]total common Pb in analysis corrected for fractionation and spike; [5]corrected for blank Pb and U, common Pb, errors quoted are one sigma in percent; [6]corrected for blank and common Pb, errors are two sigma in Ma; for analytical details see Appendix 1.

Rb-Sr Whole Rock

Seven samples for Rb-Sr whole-rock study were also collected from the above locality and include the following (Table A1). Sample 1F is from one of the paragneiss bands. Sample 1H may represent Blackadar's unit 14 (monzocharnockite) and sample 1I his unit 3, but both could be in either unit. The greasy grey pegmatite (sample 1C) intrudes the rocks represented by samples 1F, 1H, and 1I and the pyribolite, but not the pink massive monzogranite (sample 1B). Sample 1E is from the foliated margin to the massive pink granite layer (= sample 1B) and sample 1D is a variety of the same rock.

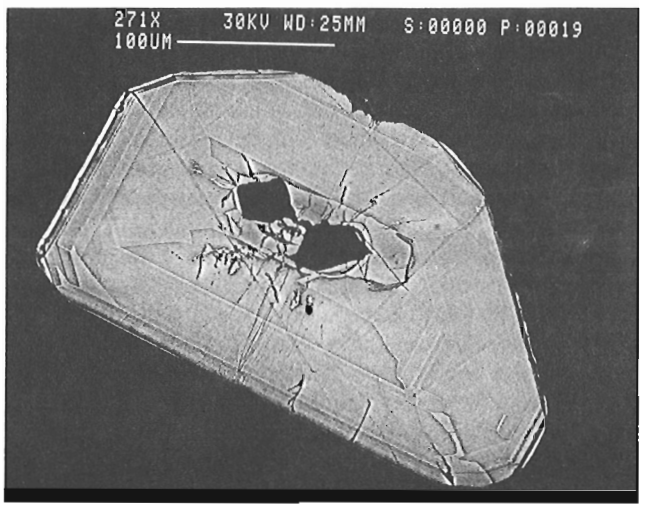

Figure 3. Electron microscope photomicrograph of a polished and etched zircon grain from the Iqaluit hybrid granulite. The polished grain shows distinct igneous zoning. The centre black inclusions are quartz and feldspar fragments.

The results of Rb-Sr analyses of the seven whole-rock samples are presented in Table 2 and displayed in an isochron plot (Fig. 5). Five of seven points are collinear (MSWD=0.41), yielding an isochron age of 1877 ± 45 Ma and initial $^{87}Sr/^{86}Sr = 0.7047 \pm 0.0028$. Data point 1F (paragneiss) falls above the isochron, possibly because of the sedimentary origin of the paragneiss. Point 1B falls slightly below the isochron.

The U-Pb age of ca. 1.86 Ga for the pink monzogranite was measured on zircon from Rb-Sr sample 1B. This age is in agreement with the Rb-Sr isochron age within analytical uncertainty but sample 1B (model age 1812 Ma) falls below the Rb-Sr isochron. Since samples 1E and 1D, both of which yield points on the isochron, represent other phases of the same rock as sample 1B, it is probable that point 1B falls below the isochron owing to minor isotopic and elemental re-equilibration specific to that sample.

Samples 1E, 1B, and 1D are tentatively considered to represent the massive pink monzogranite of Blackadar's (1967) unit 13, whereas 1H, 1I, and 1C could represent phases of the green-grey monzocharnockite (unit 14) or the quartz-feldspar gneiss (unit 3). Any difference in age between these units appears to be small with regard to the uncertainties in the Rb-Sr results.

K-Ar

K-Ar ages on biotite and hornblende from Frobisher Bay are summarized in Table 3. The relatively recent, more reliable analyses (post-1968) yield dates near 1.7 Ga, presumably reflecting cooling through mineral closure temperatures. Dates obtained before 1968 are considered to be less precise, and hornblende from pyribolite (GSC 78-122) may suffer from excess argon in a probable hornblende-clinopyroxene mineral mixture.

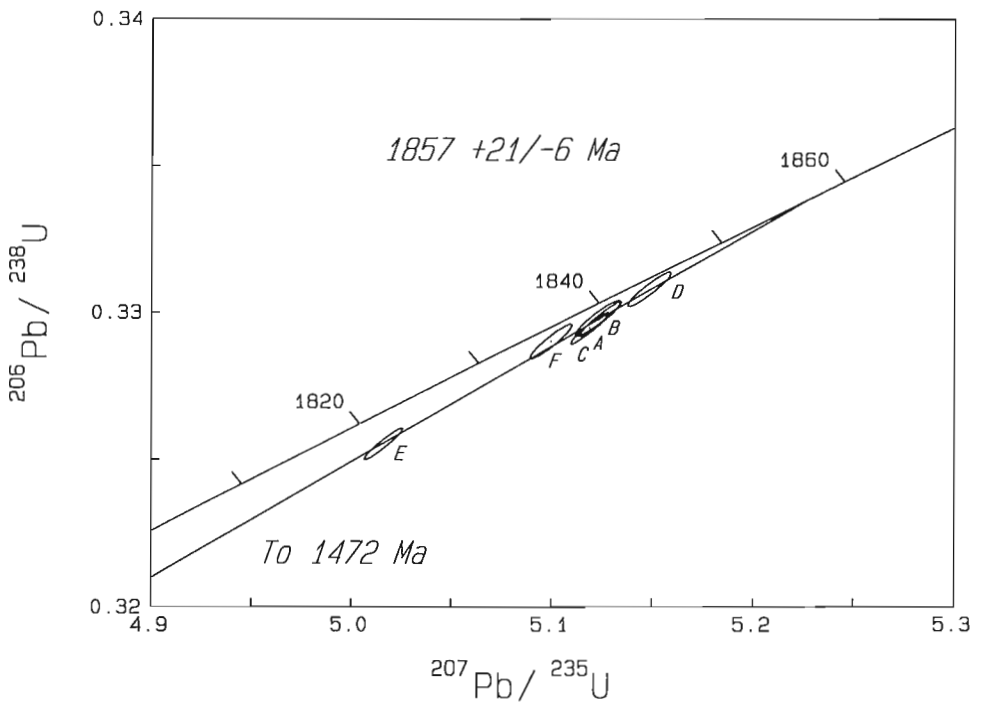

Figure 4. Concordia diagram showing the results of U-Pb analyses of zircon fractions from the Iqaluit hybrid granulite (JD70-1B). See Table 1 for data.

Northern and North-Central Areas (Cumberland Batholith Complex)

Geological Setting

A 60-100 km-wide migmatite zone separates the Piling Group of central Baffin Island from the Cumberland batholithic complex to the south, which is composed chiefly of anastomosing monzocharnockite and monzogranite plutons up to 150 km long (Blackadar, 1967; Henderson, 1985; Henderson and Tippett, 1980; Henderson et al., 1979, 1980; Jackson, 1971; Jackson and Morgan, 1978; Jackson and Taylor, 1972; Morgan et al., 1975, 1976; Tippett, 1980). Granulite-facies paragneiss, migmatite, and older Archean nebulitic granitic rocks are minor components within the batholith complex and are intruded by dykes, sills, and stocks of monzocharnockite. They also surround the complex except, apparently, to the west, where charnockite grades into granite (Blackadar, 1967; Fraser et al., 1978; Jackson and Morgan, 1978).

Intrusive rocks range from hypersthene syenite and minor alkali feldspar charnockite to hypersthene trondhjemite, minor hypersthene tonalite, and rare norite and andesine anorthosite. The monzocharnockite and monzogranite are texturally and chemically similar, the monzocharnockites being deficient in hydrous minerals. These rocks are massive to locally foliated, fine to coarse grained or pegmatitic, and commonly contain feldspar phenocrysts (up to 10 cm long). Mafic minerals consist commonly of biotite or biotite + hypersthene, although hornblende, garnet, and clinopyroxene also occur. Sillimanite and cordierite occur in a few areas.

Jackson and Morgan (1978) concluded that the monzocharnockite-monzogranite plutons that intrude the Piling Group were formed in part by the reworking and recrystallization of older rocks and emplaced both diapirically and as sheet-like and mushroom-shaped bodies (see also Kranck, 1972). Metamorphism continued after deformation had largely ceased. However, deformed isograds have been reported from some areas (Tippett, 1980; Henderson and Tippett, 1980).

The migmatite belt, between the Piling Group to the north and the batholithic complex to the south, swings southeast to the north end of the Penny Ice Cap in the eastern part of Baffin Island. Most of the migmatite belt comprises anatectic migmatites derived from the Piling Group and remnants of relatively unmigmatized Piling strata. Figure 6 shows the geology of part of this belt and the locality of one group of samples dated in this study. Metagreywacke and metapelite predominate, while marble, calc-silicates, amphibolite, and meta-ultramafite are common. Thin quartzite, meta-arkose, and iron-formation have been traced southward discontinuously as far as northern Cumberland Peninsula. Parts of the belt are composed of supracrustal strata and granite-charnockite intrusions alternating in layers up to several hundred metres thick. Some of these tabular intrusions have been isoclinally folded and boudined on a large scale (Fig. 6). Many scattered irregularly shaped monzocharnockite-monzogranite bodies up to 25 km across intrude the other rocks (except the Hadrynian diabases - Fig. 1) in the migmatite belt. Nebulitic granitic migmatites and intrusions are abundant locally and resemble the gneissic complex that is basement to the north side of the Piling Group. These nebulitic rocks are intruded by monzocharnockite and are considered here to be Archean in age.

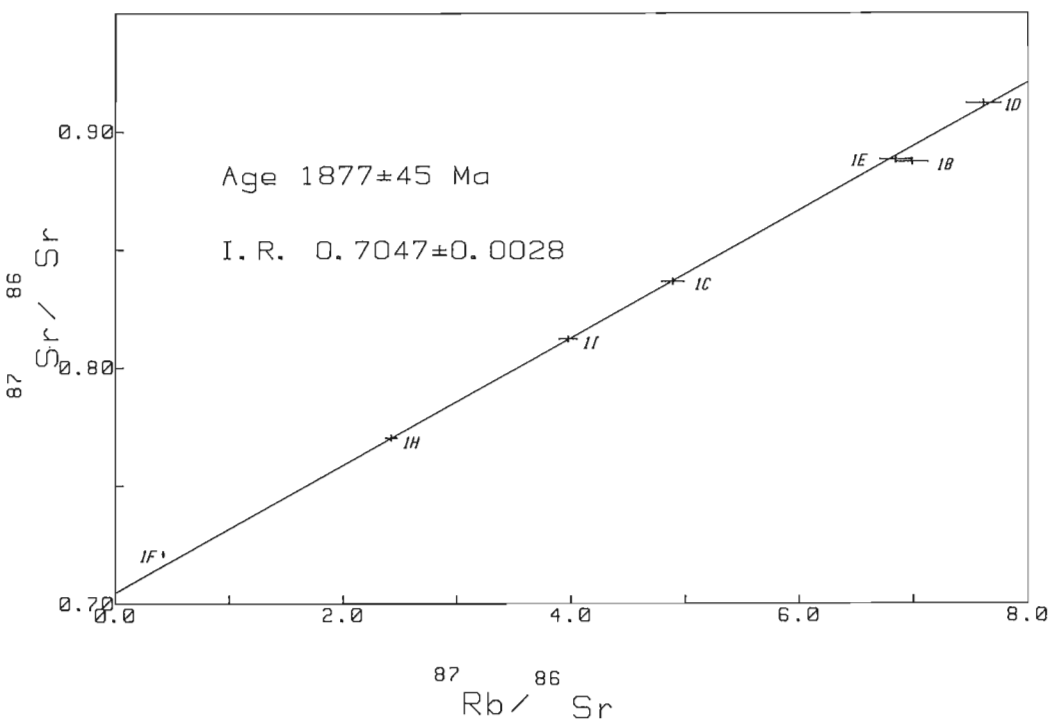

Figure 5. Rb-Sr whole-rock isochron, Iqaluit hybrid granulite. Points 1F and 1B are not included in data regression. See Table 2 for data.

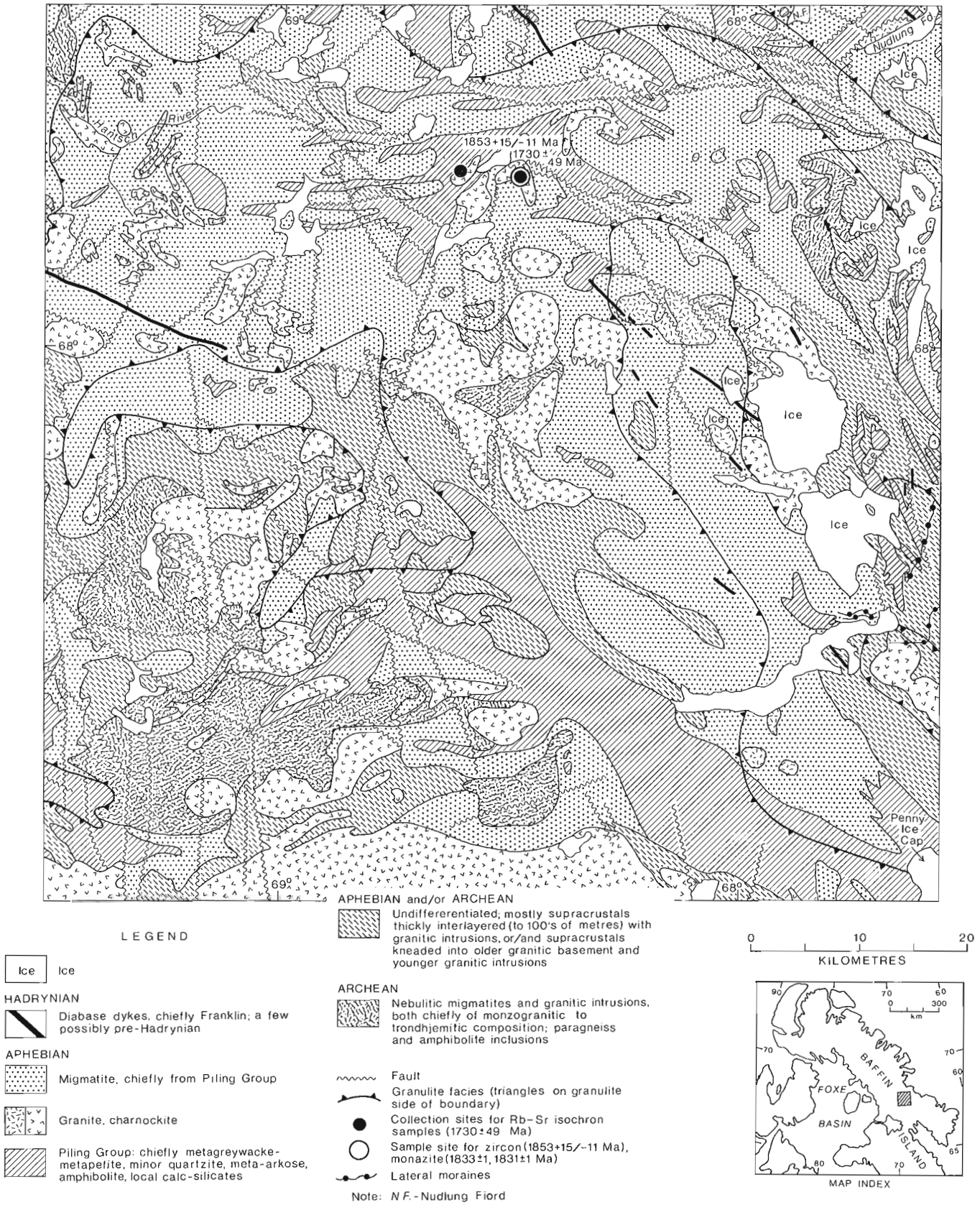

Figure 6. Map of the geology in part of the migmatite belt along the north side of the Cumberland batholithic complex, and showing sample locations west of Nudlung Fiord (Tables 1, A2, A5). The large pluton along the south edge of the map is part of the complex. The central part, about 50 km south of the south edge of the map, was sampled (JDM355-68: Tables 1 and A5).

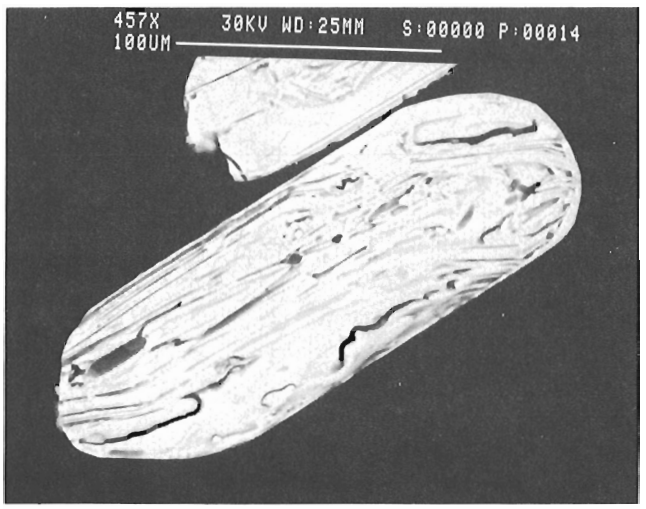

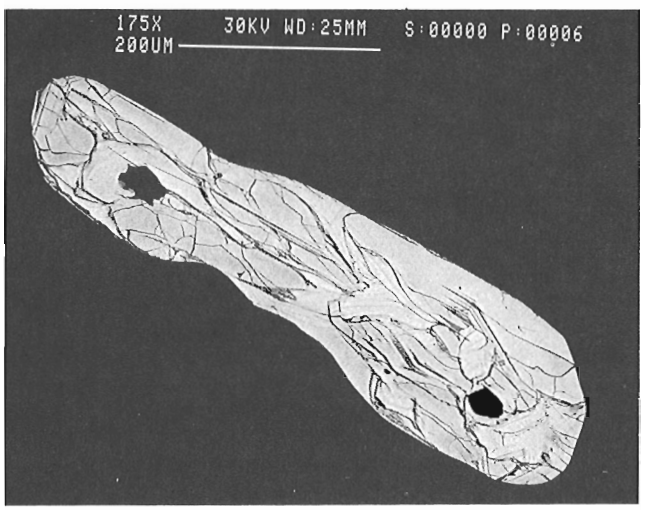

Figure 7. a. Electron microscope photomicrograph of a polished and etched zircon grain from the charnockite west of Nudlung Fiord. Grain shows non-uniform and highly contorted zoning pattern. b. Electron microscope photomicrograph of a polished and etched zircon grain from the north-central Cumberland batholithic complex monzocharnockite. Grain shows a complex internal structure with remnant zoning that is non-uniform and contorted. Grain boundary shows resorption and regrowth.

Geochronology West of Nudlung Fiord (North Area)

Seven samples for whole-rock Rb-Sr and U-Pb zircon and monazite age determinations were collected from two small plutons that intrude the Piling Group on the northern side of the migmatite belt (Fig. 6). Rock types, sample numbers, and locations are listed in Table A2 (Appendix 2). The plutons range in composition from alkali feldspar charnockite to monzocharnockite (hyperthene monzogranite). Sample 166/3 is from a small body of medium-grained, equigranular, noritic andesine (An $_{38\text{-}47}$) anorthosite in the southeastern part of the eastern pluton. It contains 14% hypersthene and 1% orange-brown biotite. Sample 168/22, an alkalifeldspar charnockite, was selected for U-Pb and Rb-Sr dating.

In general the charnockite plutons are light grey and massive to faintly foliated, with the foliation attributed to flow banding. Locally, primary layers up to 6 m thick consist of intergradational medium- and coarse-grained zones with slight differences in mafic (biotite ± hypersthene) content. Orthoclase phenocrysts up to 3 cm long are common. Common accessory minerals are apatite, monazite, zircon, ilmenite, pyrite, pyrrhotite, garnet, fluorite, chlorite, magnetite, hematite-goethite, leucoxene, prehnite, and blue-green hornblende. Occasional pale sphene is associated chiefly with the opaques, and clay minerals are retrograde products.

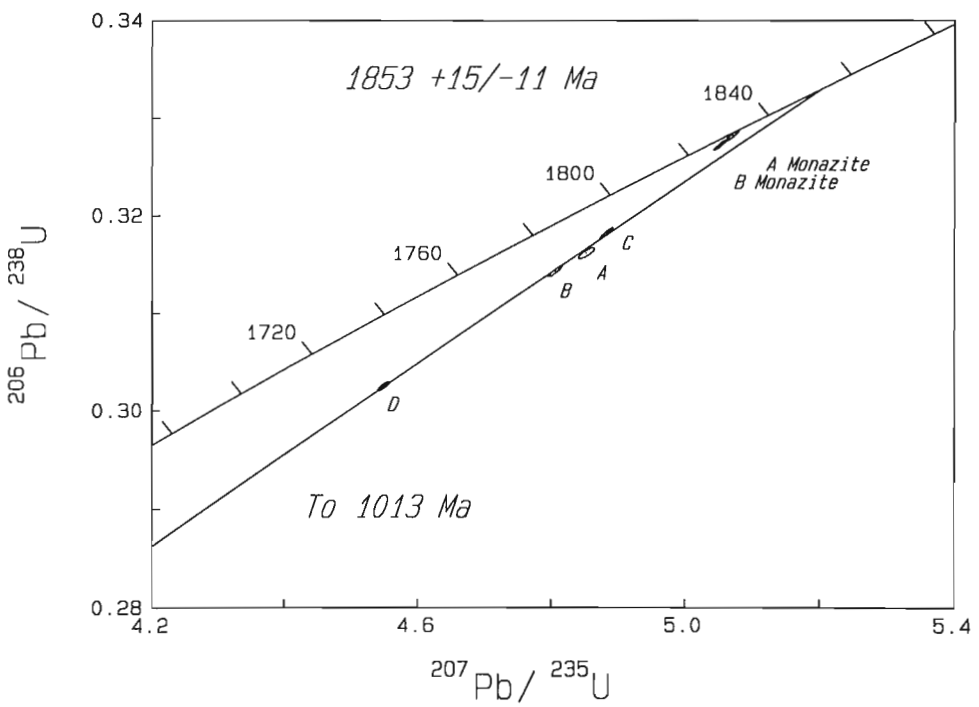

Figure 8. Concordia diagram showing the results of U-Pb analyses of zircon fractions from the charnockite west of Nudlung Fiord (JDC168/22-70). See Table 1 for data.

The plutons are intruded by aplite and pegmatite dykes. Micro-shearing, fracturing parallel to foliation, recrystallization along grain boundaries, and retrogression of hypersthene to biotite occurred during emplacement of the plutons and before the rocks had cooled significantly.

U-Pb zircon and monazite ages (JDC168/22-70)

This charnockite sample, selected for U-Pb zircon and monazite age determination, should give the emplacement age of the granite (charnockite) magma.

The igneous zircons are generally euhedral to subhedral with rounded terminations and an aspect ratio of 3:1. The grains are fractured and have abundant inclusions but show no evidence of inherited cores. Polished and etched grains reveal strong zoning that is non-uniform and highly contorted (Fig. 7a); the interpretation of these textures is uncertain. The four fractions analyzed were strongly abraded but are still fairly discordant (Fig. 8). A modified York (Parrish et al. 1987) regression gives an upper intercept of 1853 +15/-11 Ma, and a lower intercept of 1013 Ma, with a MSWD of 8. The zircon age of 1853 Ma is considered to be the approximate age of emplacement for this charnockite.

Two slightly discordant monazite fractions have $^{207}Pb/^{206}Pb$ ages of 1832.7 ± 1.2 Ma and 1831.4 ± 1.0 Ma. These can be interpreted as minimum crystallization ages, since the high Th contents of the monazites (^{208}Pb is 92% of the radiogenic Pb) suggest that $^{207}Pb/^{206}Pb$ ages could be low owing to the presence of excess ^{206}Pb (see Analytical Considerations, Appendix 1). Alternatively, they could be the age of cooling below monazite closure temperature, at 1832 Ma.

Rb-Sr whole rock

The results of Rb-Sr analyses on seven whole-rock samples are presented in Table 2 and displayed on an isochron diagram (Fig. 9). Data points for samples 166/2, 168/2, 168/4, 169/1, and 169/2 are collinear and the data points for samples 166/3 and 168/22 fall above the line. A regression of the five collinear results yields a Rb-Sr isochron age of 1730 ± 49 Ma, initial $^{87}Sr/^{86}Sr$ of 0.7149 ± 0.0034, and a MSWD of 0.36.

Discussion

The U-Pb zircon age from the same locality as Rb-Sr sample 168/22 is about 120 Ma older than the Rb-Sr isochron age but is in agreement with the model age for sample 168/22 if an initial $^{87}Sr/^{86}Sr$ of ca. 0.7075 is employed. Since the Rb-Sr isochron includes samples from both the eastern and western intrusions, and the $^{87}Sr/^{86}Sr$ is unusually high at 0.7149+/-0.0034, it is probable that the isochron is a combination of regional isotopic homogenization of Sr at, or shortly after, the culmination of granulite metamorphism that was superimposed on isotopically inhomogeneous rocks.

Table 2. Rb-Sr isotopic data.

Sample no.	Rb (ppm)	Sr (ppm)	$^{87}Rb/^{86}Sr$	$^{87}Sr/^{86}Sr$	Uncertainty $^{87}Sr/^{86}Sr$
Frobisher Bay Hybrid Granulite					0.07%
1B	180.8	74.83	6.985	0.8870	
1C	160.6	94.95	4.890	0.8365	
1D	120.0	45.60	7.608	0.9118	
1E	128.6	54.34	6.842	0.8880	
1F	12.87	87.76	0.424	0.7211	
1H	86.09	102.50	2.428	0.7703	
1I	90.28	65.66	3.975	0.8123	
Charnockites West of Nudlung Fiord					0.07%
166/2	253.1	147.3	4.968	0.8378	
166/3	13.68	531.5	0.0744	0.7210	
168/2	240.1	147.4	4.709	0.8329	
168/4	214.5	206.5	3.003	0.7894	
168/22	309.4	121.0	7.393	0.9047	
169/1	327.8	146.4	6.473	0.8766	
169/2	354.3	116.3	8.807	0.9330	
Crystalline complex, junction of Admiralty Inlet and Adams Sound					0.007%
A2	141.6	330.2	1.240	0.74546	
A5	99.27	271.4	1.058	0.73839	
A7	122.4	281.0	1.259	0.74534	
A8	112.1	305.6	1.061	0.73833	
B2	84.90	496.5	0.4944	0.72075	
B4	103.2	424.9	0.7022	0.72639	
B5	85.06	488.1	0.5038	0.72077	
C2	188.7	665.3	0.8200	0.72107	
C3	119.9	646.6	0.5361	0.71646	
C4	178.2	914.7	0.5632	0.71695	
C6	93.06	927.6	0.2900	0.71044	
D1	99.80	535.6	0.5387	0.72124	
D5	37.07	370.2	0.2895	0.71297	
E	129.8	371.5	1.010	0.73787	
Nauyat Formation Basalt					0.03%
3	40.29	57.73	2.018	0.7375	
3A	35.51	81.75	1.256	0.7272	
5/1	10.24	19.94	1.485	0.7367	
5/2	31.30	21.33	4.242	0.7644	
5/3	39.19	48.44	2.339	0.7398	
6	17.56	35.64	1.424	0.7341	
7/2	54.79	145.0	1.092	0.7325	
7/4	18.99	82.36	0.6666	0.7223	
7/6	0.415	42.08	0.0285	0.7128	
9	9.64	102.2	0.2728	0.7165	
26	9.35	39.15	0.6904	0.7276	
75A	24.00	34.66	2.002	0.7371	
75D	54.53	64.93	2.428	0.7520	

Table 3. K-Ar mineral ages in Frobisher Bay area.

Publication no.	Age (Ma)	Material	Rock Type	Locality
GSC 61-52 (1)	1740±90	biotite	pegmatite	62°58'N 69°52'W
GSC 66-68 (2)	1555±50	biotite	mafic lens in granite	65°06'N 68°02'W
GSC 66-69 (2)	1540±50	biotite	granite	64°10'N 68°14'W
GSC 66-70 (2)	1500±50	biotite	granite gneiss	62°39'N 65°17'W
GSC 73-73 (3)	1696±42	biotite	biotite gneiss	64°49'N 66°34'W
GSC 78-122 (4)	1839±52	hornblende	pyribolite	64°29'N 66°44'W
GSC 78-123 (4)	1670±52	hornblende	amphibolite	63°26'N 64°42'W
GSC 89-133 (5)	1722±41	hornblende	meta-ultrabasic	62°49'N 65°26'W

References: (1) Lowden et al. (1963); (2) Wanless et al. (1968); (3) Wanless et al. (1974); (4) Wanless et al. (1979); (5) Hunt and Roddick (1990)

K-Ar and Rb-Sr dates on biotite, hornblende, and muscovite from rocks in the migmatite belt and the monzocharnockite Cumberland batholith complex (Table 4) are in the range of 1.6-1.7 Ga. This pattern suggests a period of prolonged slow cooling between 1.8 and 1.6 Ga.

Geochronology, North-Central Area

U-Pb Zircon and Monazite (JDM355-68)

A sample of a monzocharnockite from the central part of the Cumberland batholithic complex, midway between Nettilling Lake and the north end of Penny Ice Cap, was collected for age determination.

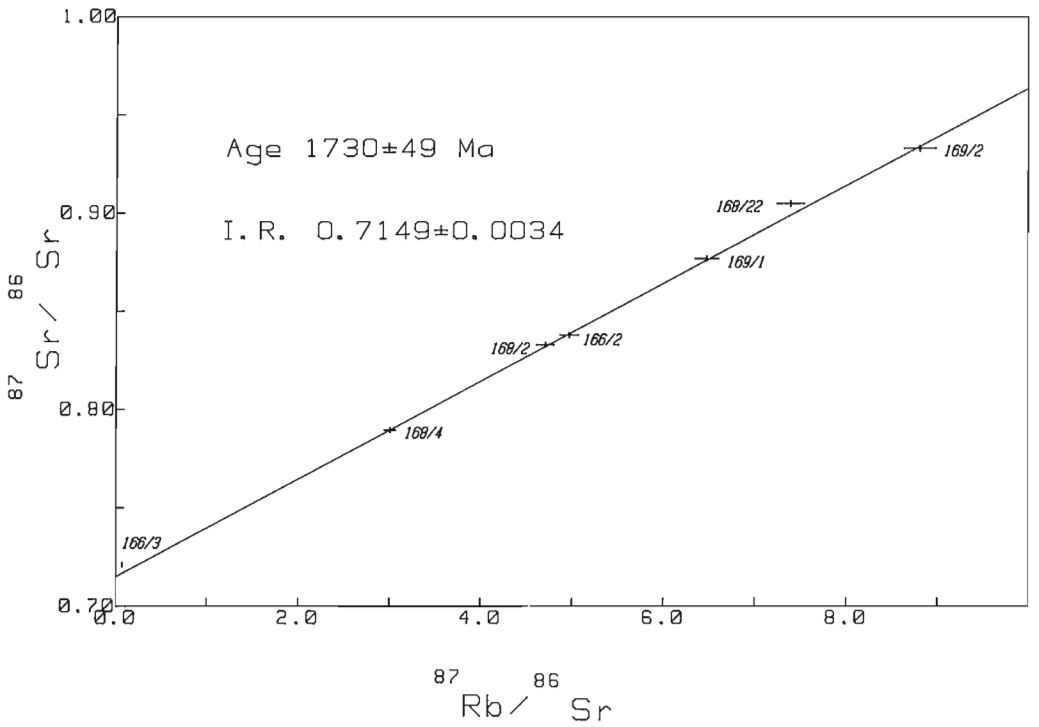

Figure 9. Rb-Sr whole-rock isochron charnockitic rocks west of Nudlung Fiord. Points 166/3 and 168/22 are not included in the data regression. See Table 2 for data.

Table 4. Some ages previously determined for rocks in the migmatite belt and Cumberland Batholithic Complex.

Publication no.	Age (Ma)	Material	Rock type	Method	Locality
(1)	1895+47/-21	zircon	charnockite	U-Pb	68°04'04''N; 66°53'28''W
(2)	1870±20	zircon	charnockite	U-Pb	66°05'N; 65°45'W
GSC 66-68 (3)	1555±55	biotite	granodiorite	K-Ar	65°06'N; 68°02'W
GSC 70-60 (4)	1680±55	pegmatite	muscovite	K-Ar	68°36'N; 73°16'W
GSC 70-61 (4)	1735±55	biotite	metasilstone	K-Ar	68°36'N; 73°16'W
GSC 76-172 (5)	1603±40	biotite	granite	K-Ar	65°58'N; 69°21'W
GSC 76-173 (5)	1678±49	hornblende	granite	K-Ar	65°58'N; 69°21'W
GSC 81-117 (6)	1688±24	biotite	charnockite	K-Ar	68°04'04''N; 66°53'28''W
GSC 81-118 (6)	1685±24	biotite	charnockite	K-Ar	68°04'04''N; 66°53'28''W
GSC 81-119 (6)	1727±24	biotite	charnockite	K-Ar	68°04'04''N; 66°53'28''W
GSC 81-130 (6)	1639±41	biotite	granitoid gneiss	K-Ar	6827'N;7206'W
GSC 81-134 (6)	1646±40	biotite	monzogranite	K-Ar	68°13'N; 72°23'W
GSC 81-139 (6)	1723±50	hornblende	monzocharnockite	K-Ar	66°32'N; 66°05'W
GSC 81-140 (6)	1743±50	hornblende	amphibolite	K-Ar	65°47'N; 64°22'W
GSC 87-134 (7)	1640±23	muscovite	pegmatite	K-Ar	68°37'23''N; 70°54'42''W
GSC 87-134 (7)	1592	muscovite	pegmatite	Rb-Sr	68°37'23''N; 70°54'42''W
GSC 87-135 (7)	1617±22	muscovite	pegmatite	K-Ar	68°37'23''N; 70°54'42''W
GSC 87-135 (7)	1633	muscovite	pegmatite	Rb-Sr	68°37'23''N; 70°54'42''W

References: (1) Henderson (1985); (2) Pidgeon and Howie (1975); (3) Wanless et al. (1968); (4) Wanless et al. (1972); (5) Wanless et al. (1978); (6) Stevens et al. (1982); (7) Hunt and Roddick (1987).

The monzocharnockite (hypersthene monzogranite) has a resinous yellow-brown colour, is generally massive, and contains feldspar phenocrysts up to 10 cm long in a medium-grained equigranular matrix. The grains are fractured but not crushed. Small discontinuous folia of mafic minerals impart a weak foliation to the rock locally. Orthoclase is perthitic (5-10%) and contains rare plagioclase veinlets. Plagioclase (An_{33}) is antiperthitic and is associated with minor myrmekite. The mafic component (7%) is chiefly hypersthene with minor brown biotite and opaque minerals (magnetite, pyrite, hematite-limonite, leucoxene).

Zircons are quite coarse in grain size, with an aspect ratio of 3:1. They are euhedral to subhedral with rounded terminations, highly fractured, and have abundant inclusions. Polished and etched mounts of zircon grains reveal a complex internal structure (Fig. 7b). Differential melting seems to have occurred in some grains, and all show resorption and renewed growth.

The four fractions analyzed are discordant and form a scattered non-linear array (Fig. 10). A concordant monazite from this sample has a $^{207}Pb/^{206}Pb$ model age of 1854 $\pm$ 2 Ma. The scattered array of zircon points is attributed to inheritance of an older crustal component followed by minor subsequent Pb loss. The textures described above are consistent with the U-Pb systematics and suggest that the zircons are composite. The rock was probably derived from melting of an older protolith. The 1854 Ma monazite age is a minimum for the major melting event and the emplacement of the charnockite. Monazites are Th-rich (radiogenic Pb is 98% ^{208}Pb), and consequently the $^{207}Pb/^{206}Pb$ ages may be reduced because of the effect of excess ^{206}Pb (see Analytical Considerations). The zircon data suggest that the age of the charnockites is not likely to exceed ca. 1.9-1.95 Ga.

Mary River Region

Geological Setting

A complex composed chiefly of nebulitic granitic migmatites, foliated granitic plutons, and minor, locally massive granitic intrusions underlies the Mary River Group in north-central Baffin Island (Crawford, 1973; Gross, 1966; Jackson, 1966, 1978a, 1978b; Jackson and Morgan, 1978; Jackson et al., 1978a, 1987b; Jackson and Taylor, 1972; Morgan et al., 1975, 1976). Compositions range from monzogranite to quartz diorite. The rocks are white to light grey and pink, fine to coarse grained, and are commonly megacrystic (potash feldspar, plagioclase, quartz). The rocks have been recrystallized, and the metamorphic grade ranges from greenschist to granulite. Contacts between the three major rock types (nebulitic-banded, foliated, massive) are gradational to sharp and discordant, with the more massive rocks generally the youngest. Bands, boudins, and schlieren of paragneisses, and metamorphosed felsic to mafic extrusive and intrusive rocks are scattered throughout most of the complex, and locally are abundant. Meta-ultramafic rocks are rare.

Metamorphosed blastoporphyritic (quartz, plagioclase) rhyolites-dacites, chiefly metapyroclastic rocks, have been recognized in the basement complex at several localities such as west of Mary River No. 1 Iron Deposit (37G; Jackson, 1966, 1978b; Jackson et al., 1978a). Metamorphosed shallow feldsparphyric monzogranite-granodiorite intrusions, quartzofeldspathic metasediments, and minor amphibolite are commonly associated with the felsic metavolcanics. Locally, metamorphosed felsic and mafic dykes intrude the complex but not the overlying Mary River Group (Jackson, 1966). Coarse conglomerate lenses in the lower part of the

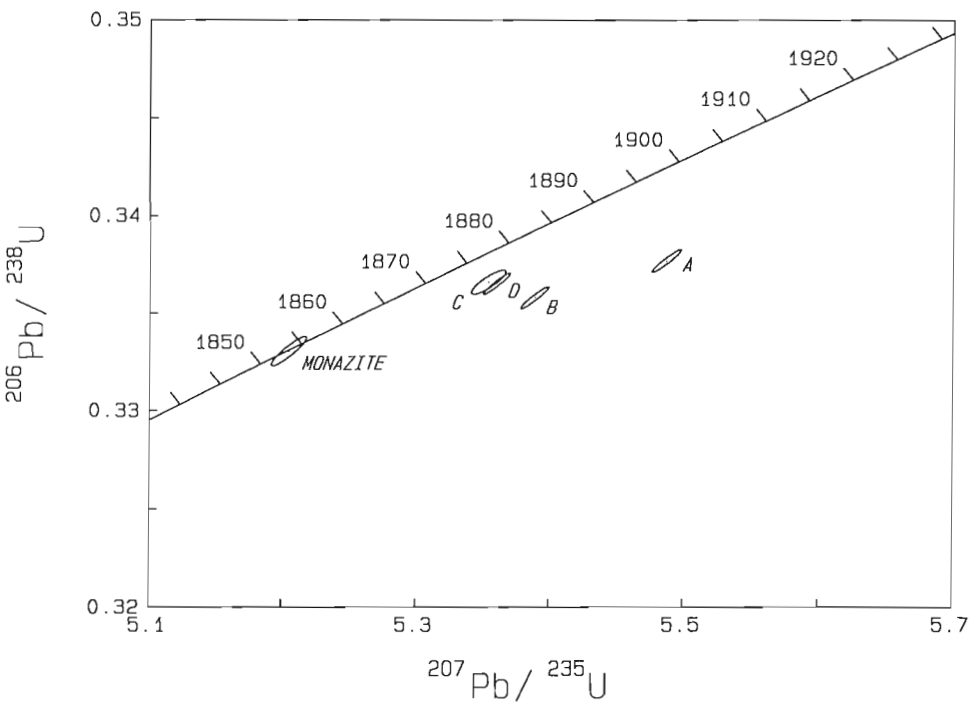

Figure 10. Concordia diagram showing the results of U-Pb analyses of zircon fractions from the charnockite (JDM355-68) from the Cumberland batholithic complex. See text for discussion and Table 1 for data.

Mary River Group also suggest the presence of an unconformity between it and the underlying complex (Crawford, 1973; Jackson, 1966, 1978b). Locally the contact may be marked by a metamorphosed regolith, or may be gradational.

The Mary River Group is a metamorphosed (greenschist to granulite) and intensely deformed assemblage composed chiefly of felsic to mafic metavolcanics, metapelites, and metagreywackes. Quartzite, metamorphosed iron formation, ultramafic rocks, and anorthositic and gabbroic intrusions are commonly an integral part of the assemblage, which is a typical Archean greenstone sequence.

Mary River Group rocks are abundant in a large arcuate belt (NTS 36C-G, 47H) that extends northeast from the west coast of Baffin Island (Eqe Bay) to the north end of the Barnes Ice Cap. There the belt swings northwestward and extends to the Mary River area (Jackson and Taylor, 1972; Jackson and Morgan, 1978) and the heads of Milne Inlet and Tay Sound. Within and adjacent to this belt the Mary River Group crops out in numerous narrow, lenticular, separated and interconnected, en echelon bodies up to 65 km long.

The Mary River Group and its basement are intruded by at least two suites of granitic intrusions. Rb-Sr investigations in the vicinity of No. 4 Iron Deposit, 80 km to the west of the present area (Jackson, 1978b), indicate an Archean age for the basement gneisses and a late Archean- early Aphebian age for the Mary River Group (although variable re-equilibration of the Rb-Sr systems of most samples analyzed made even these broad conclusions somewhat tenuous). K-Ar ages on biotite and muscovite presented in the above study ranged from 1750 to 1610 Ma and were interpreted as reflecting cooling through mineral closure temperatures for Ar in the waning stages of the Hudsonian Orogeny.

U-Pb Zircon

Mary River Group Dacite (JD100/12-68)

A sample of dacite representative of the Mary River Group was collected for zircon dating. The dacite is associated with iron formation, quartzite, schist, metabasalt, and meta-ultramafic rocks.

The dacite is light grey, finely foliated, fine grained, and has quartz and a few plagioclase phenocrysts up to 2 mm in diameter. Nearly half of the dacite is plagioclase (oligoclase?). Quartz and greenish-brown biotite are abundant, and microcline and muscovite are minor components.

Zircons from the dacite are euhedral and have sharp terminations. The aspect ratio ranges from 3:1 to 2:1 for the finer fractions. The grains are strongly zoned with frequent inclusions and fractures, but cores were not observed. All fractions were heavily abraded.

The four zircon fractions analyzed are 2.8 to 4.9% discordant (Fig. 11). A Davis (1982) regression analysis yields an upper intercept of 2718 +5/-3 Ma, a lower intercept of 807 Ma and a probability of fit of 13%. The upper intercept age of 2718 Ma is interpreted as the time of eruption and crystallization of the dacite.

Quartz syenite-leucomonzodiorite (JD138/1-68)

This sample, collected for U-Pb age measurement on zircon, is part of a southwest-trending granitic pluton in northeastern NTS 37G, approximately 50 km north of the dacite and trondhjemite sample locations. It is not associated with the Mary River Group directly, but similar smaller plutons do intrude the Mary River Group in other areas. The pluton

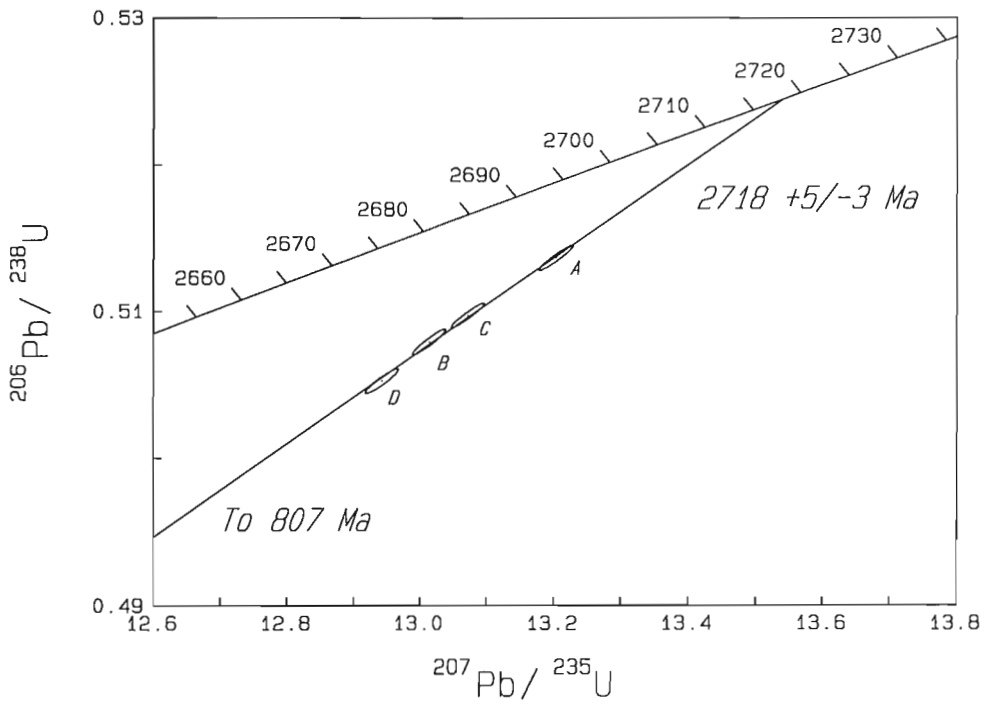

Figure 11. Concordia diagram showing the results of U-Pb analyses of zircon fractions from the Mary River Group dacite (JD100/12-68). See Table 1 for data.

is mostly pink to pinkish grey, coarse grained, and ranges from quartz monzonite through to granodiorite. The dated sample is a quartz-poor leucomonzodiorite-quartz monzodiorite. It contains about 55% plagioclase (An $_{25-32}$), and both orthoclase and microcline may be present (total 25%). Green biotite and chlorite are minor components.

Zircons recovered are generally euhedral with sharp terminations. Fraction D represents a separate population of flat subhedral grains with rounded terminations and an aspect ratio of 2:1.

Data points for the four fractions analyzed are collinear (Fig. 12) and range from 2.1 to 4.59% discordant. A Davis (1982) regression analysis yields an upper intercept of 2709 +4/-3 Ma, a lower intercept of 730 Ma, and a probability of fit of 48%. This tightly constrained age is interpreted as the age of emplacement of the 50 km long pluton.

Foliated trondhjemite-tonalite (JDC56/1-68)

This sample, collected for U-Pb age measurement on zircon, is believed to be basement to the Mary River Group. It was collected just north of a small, east-trending synclinal lens of Mary River Group strata 2 km south of a similar parallel synclinal lens. At least one shear zone occurs between the two lenses. The rock is light grey, fairly homogeneous, equigranular, granoblastic, and fine to medium grained. About two-thirds of the rock is oligoclase (An $_{25-28}$), and quartz is next in abundance. Minor amounts of olive-green biotite, microcline, and myrmekite are accompanied by accessory olive-green hornblende, sphene, apatite, zircon, allanite, magnetite, and clay minerals.

The zircons recovered are euhedral with slightly rounded terminations and an aspect ratio of 2:1. The crystals are slightly cloudy, have abundant inclusions and fractures, but show no visible cores.

Data points representing the seven zircon fractions analyzed form a somewhat scattered, linear trend (Fig. 13). A modified York (1969) regression analysis of all seven fractions yields an upper intercept age of 2851 +20/-17 Ma, a lower intercept of 1711 Ma, and a MSWD of 40.

This 2851 Ma upper intercept is considered to approximate the time of emplacement for the rock, which is one component of the basement complex to the Mary River Group.

Migmatite at Cambridge Fiord (JDD218X-68 and JDD218Z-68)

Geological Setting

An extremely inhomogenous migmatite about the head of Cambridge Fiord ranges from banded gneiss to anatectite and nebulite. The oldest component is a dark grey quartz diorite gneiss and amphibolite; the youngest is pale pinkish grey to white monzogranite (Fig. 14). Samples of both end members (amphibolite, syenogranite) were collected from the same locality for U-Pb zircon age determinations. Biotite and hornblende are the major mafic minerals, whereas plagioclase (An $_{24-30}$) microcline, and quartz are the main felsic minerals in both rocks.

U-Pb Zircon

Zircons separated from the amphibolite phase were anhedral, with rounded terminations, and had little or no zoning.

Four analyzed zircon fractions form a scattered linear trend (Fig. 15). A modified York (1969) regression analysis of all four points yields an upper intercept age of 2734 +59/-45 Ma, a lower intercept of 1800 Ma, and a MSWD = 163. Regression of the three least discordant points

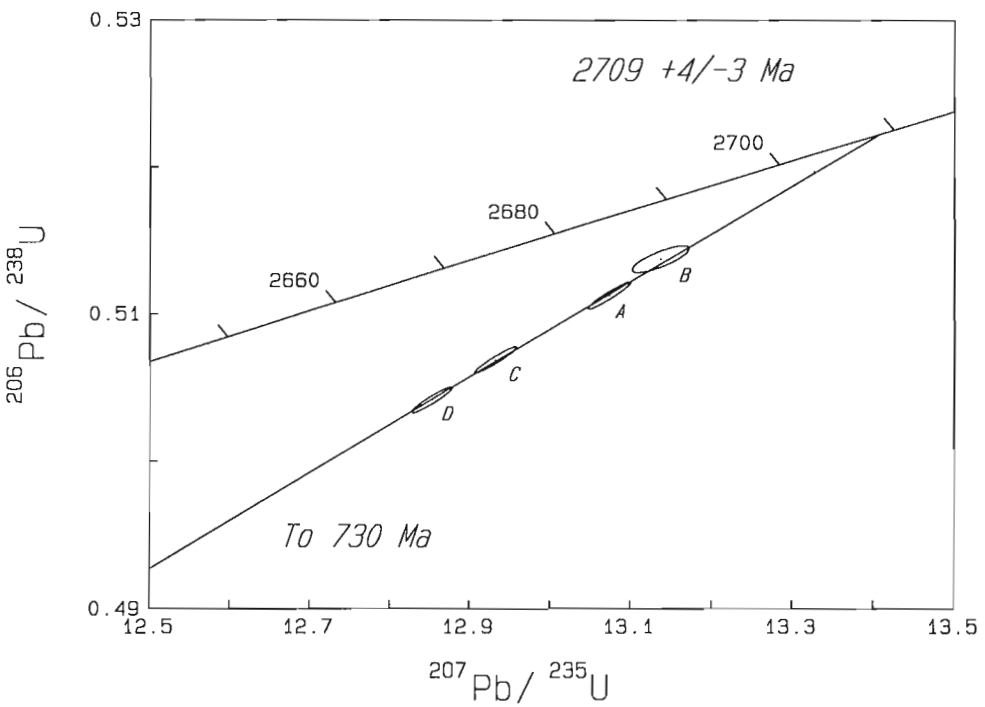

Figure 12. Concordia diagram showing the results of U-Pb analyses of zircon fractions from quartz monzodiorite (JD138/1-68) in the Mary River region. See Table 1 for data.

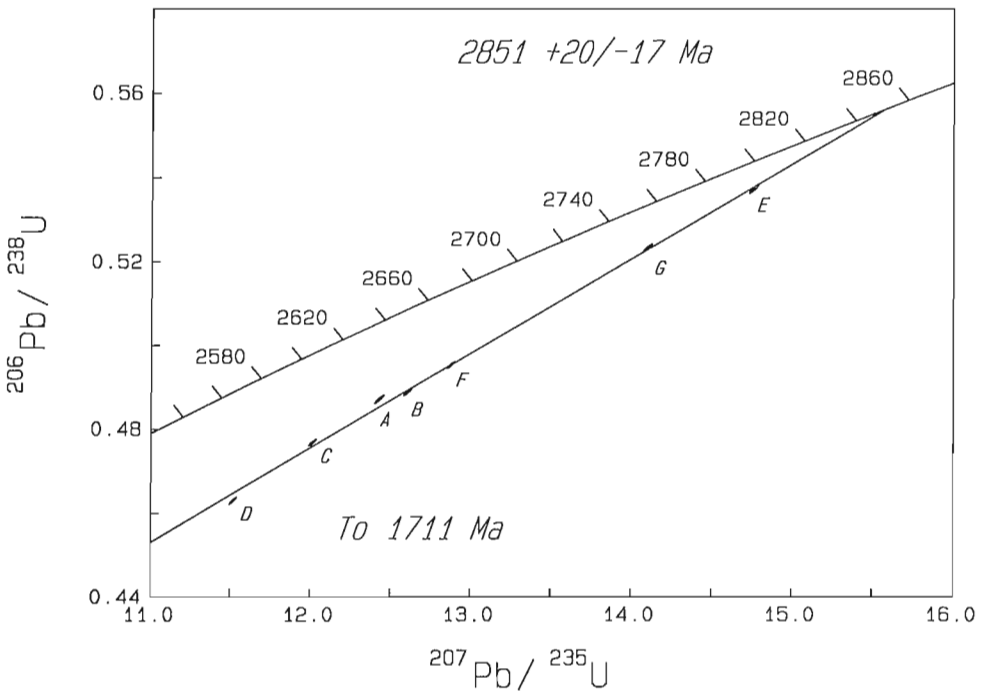

Figure 13. Concordia diagram showing the results of U-Pb analyses of zircon fractions from the Mary River region basement tonalitic gneiss (JDC56/1-68). See Table 1 for data.

Figure 14. Nebulitic migmatite at the site sampled for zircons near the head of Cambridge Fiord. The major components are amphibolite and granite. Note the fold axes, agmatite, and partial ingestion of mafic rock by the granite. Most mineral lineations and fold axes in the area are subhorizontal and trend east-southeast. Note the pencil for scale. Geological Survey of Canada photo 185407 by S.L. Blusson.

yields upper and lower intercept age of 2688 +57/-31 Ma and 1495 Ma respectively (MSWD=95). Neither result yields a precise age for crystallization of zircon in the amphibolite, but both demonstrate an Archean age for this protholith.

Zircons separated from the leucocratic phase are euhedral in shape, with an aspect ratio of 3:1, cloudy, heavily zoned, and have distinct cores. Fraction A comprises tips of whole grains that were broken off prior to abrasion. Fractions B and C were grains where cores were generally avoided during picking.

A Davis (1982) regression of the three fractions gives an upper intercept of 2522 +11/-10 Ma, a lower intercept of 1525 Ma, and a probability of fit of 43% (Fig. 16). The points are 40 to 60% discordant, with Fraction A, the abraded tips, the most discordant. We interpret these data as representing a mixture of Proterozoic igneous zircon and older Archean xenocrysts or cores.

These data suggest Proterozoic melting of an Archean protolith and igneous zircon growth in the felsic melt.

U-Pb ZIRCON AND Rb-Sr 'ISOCHRON' AGES IN BORDEN RIFT BASIN, NORTHWESTERN BAFFIN ISLAND (NTS 48B/7-10,15,16; NTS 48D/2)

Geological Setting

The Precambrian rocks adjacent to and within the Neohelikian Borden Rift Basin, on Borden Peninsula, northwestern Baffin Island, contain three easily differentiated major geological units:

Archean-Aphebian crystalline complex,

Neohelikian Bylot Supergroup, and

Helikian-Hadrynian diabase dykes.

These rocks have been described and interpreted by several writers (Blackadar, 1970; Christie and Fahrig, 1983; Fahrig et al., 1971, 1981; Galley, 1978; Geldsetzer, 1973; Jackson and Iannelli, 1981; Jackson et al., 1985; Jackson and Sangster, 1987; Jackson and Taylor, 1972; Lemon and Blackadar, 1963; Olson, 1984; Trettin, 1969). The crystalline complex is composed mostly of felsic to intermediate (and some mafic) banded migmatites of anatectic origin. Preserved remnants indicate the rocks were mostly pelite- and metagreywacke-type metasediments, and felsic to mafic

metavolcanic rocks. Minor quartz-rich to arkosic metasandstones, and local calc-silicate paragneisses and iron formation are also present. Irregularly shaped pods of white and pink granitic rocks probably represent neosome derived locally during anatexis.

The migmatites and supracrustal remnants are intruded by a large variety of intersecting dykes and sills of several ages, which locally make up most of the bedrock. They include aplite, pegmatite, granite-granodiorite, and intermediate to mafic types. Several small metabasite and metaultramafic plutons are scattered through the complex. A coarse-grained to pegmatitic, layered and differentiated, 600 m-thick, metamorphosed mafic-ultramafic intrusion occurs on the west side of Navy Board Inlet. Small concordant and discordant granitic plutons are of at least two ages and range up to 1000 + m across. The earlier intrusions are chiefly foliated granite-granodiorite and charnockitic metamorphic equivalents. Younger massive granite-granodiorite intrusions have also, locally at least, undergone granulite metamorphism.

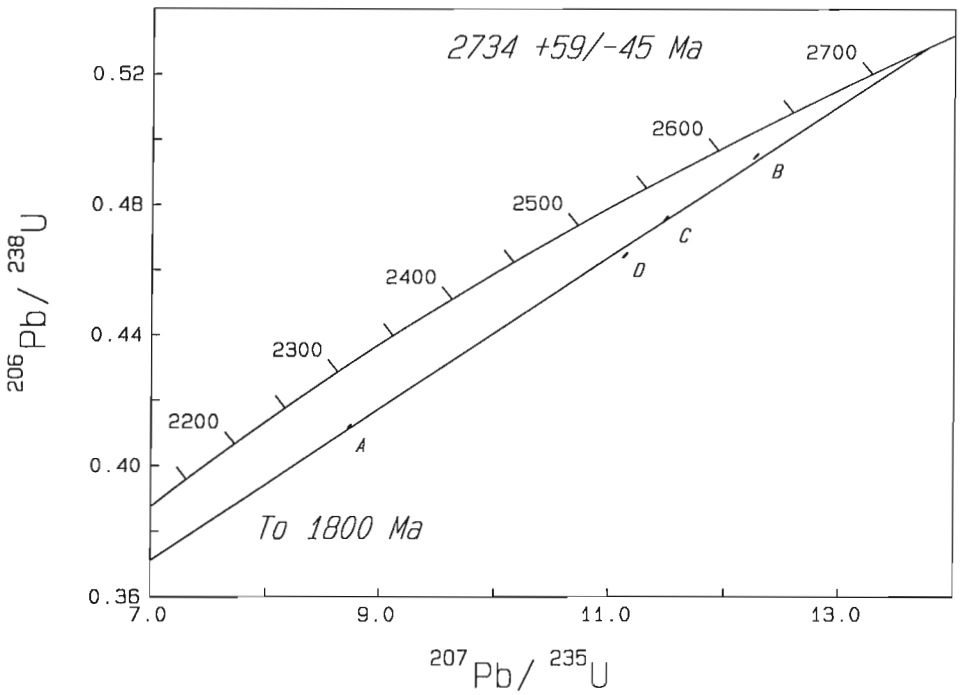

Figure 15. Concordia diagram showing the results of U-Pb analyses of zircon fractions from the amphibolite phase of the Cambridge Fiord migmatite-anatectite. See text for discussion and Table 1 for data.

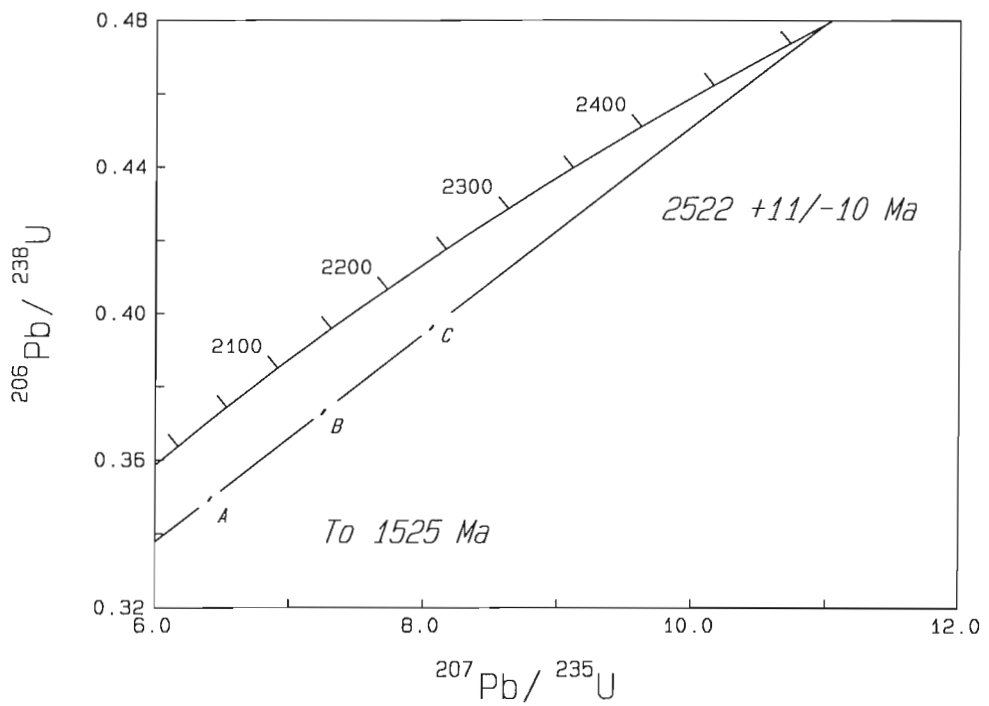

Figure 16. Concordia diagram showing the results of U-Pb analyses of zircon fractions from the leucocratic phases of the Cambridge Fiord migmatite-anatectite. See text for discussion and Table 1 for data.

Table 5. Some K-Ar age determinations for gneisses on Borden Peninsula and adjacent areas.

Publication no.	Age (Ma)	Material	Rock type	Locality
GSC 62-85 (1)	1590±90	biotite	banded migmatite	72°17'N; 86°08'W
GSC 64-31 (2)	1730±55	biotite	biotite-quartz-feldspar gneiss	73°00'N; 81°00'W
GSC 70-52 (3)	1660±52	phlogopite	metabasite-meta-ultramafite	73°15'N; 78°06'W
GSC 70-53 (3)	1685±53	biotite	quartz-feldspar biotite-garnet gneiss	72°42'10"N; 77°58'15"W
GSC 70-58 (3)	1690±55	biotite	banded migmatite	72°16'N; 74°57'W
GSC 70-58 (3)	1660±55	biotite	banded migmatite	72°16'N; 74°57'W
GSC 73-68 (4)	1710±52	biotite	metabasite	72°58'N; 77°17'W

References: (1) Leech et al. (1963); (2) Wanless et. al. (1966); (3) Wanless et al. (1972); (4) Wanless et al. (1974).

Upper-amphibolite-facies regional metamorphism predominates in the gneiss complex and in some places has been superimposed on earlier amphibolite-facies rocks (Fraser et al., 1978; Jackson and Morgan, 1978). Granulite-facies rocks occur locally and, on Borden Peninsula, may be more abundant adjacent to Borden Rift Basin than away from it. In some places the Neohelikian Bylot Supergroup was deposited on granulite.

Some K-Ar age determinations on biotite and phlogopite from gneisses on Borden Peninsula are presented in Table 5.

The Neohelikian Bylot Supergroup of Borden Rift Basin is separated from the underlying gneiss complex by a nonconformity, and contains several thousand metres of strata that have been separated into three groups (Jackson and Iannelli, 1981; Jackson et al., 1985). The lower, Eqalulik Group contains fluvial to shallow marine quartzarenites, plateau basalts (Nauyat Formation), marginal sandstone-shale delta fan complexes, and subtidal marine shales. The middle, Uluksan Group consists of shelf carbonates, subtidal shale, marginal gypsiferous sabkha deposits, and a lead-zinc replacement deposit. The upper, Nunatsiaq Group contains coeval alluvial fan conglomerates, submarine fan sandstones and shales, platformal biohermal carbonates, and fluvial and marine shelf quartzarenites. At least the lower part of the Bylot Supergroup has been regionally metamorphosed to subgreenschist facies.

Northwest-trending Hadrynian dykes of at least two ages (Christie and Fahrig, 1983) intrude the older rocks. Some paleomagnetic data presented in Fahrig et al. (1971) indicate a few Mackenzie dykes may also be present (Fahrig, 1987; Fahrig and Jones, 1967; LeCheminant and Heaman, 1989). Precambrian rocks in northern and southern Baffin Island are overlain unconformably by Phanerozoic strata.

Monzogranite rocks west of Navy Board Inlet (JD79-84)

Upper-amphibolite-facies, banded, white, black and grey, lit-par-lit migmatite and mixed gneisses occur south of the Hartz Mountain Fault Zone just west of Navy Board Inlet. These representatives of the Archean-Aphebian crystalline complex are intruded by white pegmatite and granitic dykes, monzogranite bodies, and amphibolite dykes. Locally these various rocks are in the granulite facies.

A sample of a pink monzogranite intrusion, 50 m in diameter, was collected for U-Pb zircon age determination (sample JD79-84). The slightly porphyritic monzogranite contains about equal amounts of quartz, fresh microcline, and altered (clay, sericite) plagioclase (An $_{18\text{-}22}$), and

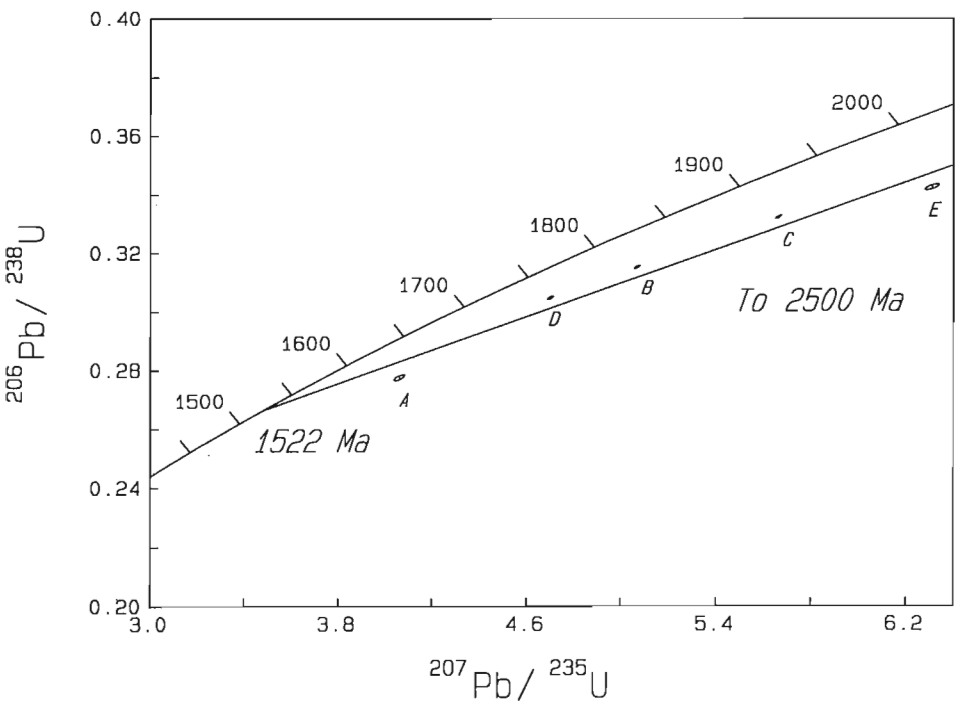

Figure 17. Concordia diagram showing the results of U-Pb analyses of zircon fractions from the Borden Rift Basin monzogranite (JD79-84). See text for discussion and Table 1 for data.

10-15% mafic minerals and minor myrmekite, oxides, sphene, apatite, and zircon. Traces of uralite suggest this rock might be a retrograded granulite. Biotite is partly altered to chlorite. Field evidence indicates that this granite is the youngest rock in this part of the gneissic complex.

U-Pb Zircon

The zircons from this sample are generally euhedral sharp terminations, and a aspect ratio of 3:1. All grains show fractures with abundant inclusions. Zircons with distinct cores were abundant; attempts were made to exclude them from the final selection for analysis.

Results of U-Pb analyses yielded a very scattered array of data. A modified York (1969) regression on all five points yields a lower intercept age of 1522 Ma and a upper intercept age of 2500 Ma (Fig. 17). The fractions plot nearer the lower, 1522 Ma intercept. We interpret this array as indicating a mixture of Proterozoic magmatic zircons with a large amount of either Archean cores or xenocrysts followed considerably later by post-crystallization Pb loss. These problems preclude estimating the age of this rock more precisely. Our tentative interpretation is that the rock is at least 1600 Ma old, and probably younger than 1800-1850 Ma.

Small horst, junction of Admiralty Inlet and Adams Sound

A small east-trending horst (2 km x 10 km) of the crystalline complex occurs on the east side of Admiralty Inlet about 5 km south of the mouth of Adams Sound. It is typical of the crystalline complex and is surrounded by Eqalulik Group strata, chiefly Nauyat Formation. At the locality sampled (Table A3, Appendix 2), the crystalline complex is composed chiefly of fairly homogeneous foliated to nebulitic granitoid augen gneiss (unit 2), which locally grades into banded migmatite. Four lithologic units have been differentiated (Table A3). Schlieren of metamorphosed greywacke-type sediments and/or acid-intermediate volcanic rocks (unit 3) in the augen gneiss are intruded by metamorphosed diorite-gabbro dykes (unit 4). Massive to foliated granitoid dykes (unit 1) intrude units 2, 3, and possibly 4. Metamorphic grade is upper amphibolite to granulite, with some retrograde minerals present.

Rb-Sr Whole Rock

Each of the above four units was sampled for Rb-Sr dating. Results are presented in Table 2 and displayed on an isochron diagram (Fig. 18). Regression analyses of selected data sets are summarized in Table 6.

The data points for the 10 samples from units 1, 2, and 3 form a linear array with MSWD 5.6, age 2321 ± 76 Ma, and initial $^{87}Sr/^{86}Sr$ of 0.7035 ± 0.0007 (Fig. 18). Since regression of data from each of units 1, 2, and 3 does not separately provide consistent or unambiguous isochron ages for these units, we interpret these results as indicating:

1) either the complex was emplaced at about 2300 Ma with variable crustal components modifying the inital $^{87}Sr/^{86}Sr$ of each sample, or

2) the emplacement age of the complex is somewhat older, perhaps Archean, and the Rb-Sr systems were reset at approximately 2300 Ma, possibly by the granulite metamorphism. Field relations indicate that the latter is the more likely alternative.

Results of Rb-Sr measurements on the four dyke samples may be subdivided into two sets of three collinear data points

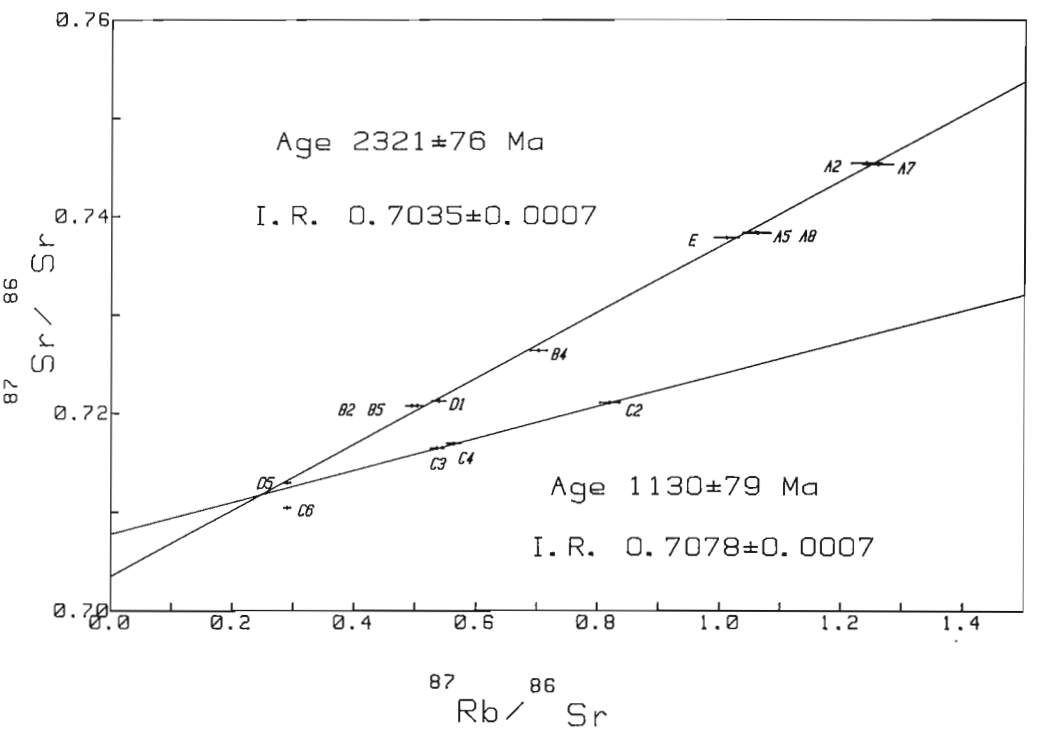

Figure 18. Rb-Sr isochron diagram, crystalline complex east of Admiralty Inlet. Unit 1, data points D1, D5, granitoid dykes; unit 2, data points A2, A5, A8, A7, and E, augen gneiss; unit 3, data points B2, B5, B4, metavolcanics; unit 4, data points C3, C2, C4, C6, metamorphosed diorite-gabbro dykes. See Table 2 for data.

(unit 4, Table 6). Although the age results are ambiguous, both age-initial $^{87}Sr/^{86}Sr$ pairs yield younger ages for unit 4 than for units 1-3; these apparently younger ages probably result from metamorphic retrogression.

Nauyat volcanics rocks, south Adams Sound

The Nauyat Formation is the lowermost formation of the Neohelikian Bylot Supergroup, has an average thickness of nearly 240 m east of Admiralty Inlet, and may attain 430 m south of Adams Sound. Two conformable members have been recognized (Jackson and Iannelli, 1981): a lower quartzarenite member and an upper basalt member with up to seven flows. All flows are fine grained, have subophitic to intersertal textures and most are dark green-grey. Most flows are amygdaloidal (with amygdules up to 10 cm in size) in their upper parts and some are amygdaloidal throughout. Columnar joints, vesicles, and local flow banding are common, but pillows and volcanic breccia or pyroclastic lenses are rare.

The major primary minerals in the basalt flows include calcic plagioclase (An_{30-75}) augite, olivine, and titanomagnetite (Galley, 1978). In thin sections the basalts are seen to be highly altered, with albitized plagioclase and chlorite-rich pseudomorphs after olivine. Secondary mineral assemblages are typical for pumpellyite-prehnite facies metamorphism.

Rb-Sr whole rock

Rb and Sr measurements were conducted on 14 samples of Nauyat plateau basalt (Table A4, Appendix 2). Results are presented in Table 2 and depicted on an isochron diagram (Fig. 19). The data points are bounded by two reference isochrons, age 982 Ma, initial $^{87}Sr/^{86}Sr$ of 0.7179, and age 819 Ma, initial $^{87}Sr/^{86}Sr$ of 0.7125. K-Ar data on 17 whole-rock samples from the Nauyat volcanics cover a somewhat greater range: 762 ± 26 to 1221 ± 31 Ma (Jackson and Iannelli, 1981). Neither the Rb-Sr nor the K-Ar age results are interpreted as indicating the time span of basalt extrusion; they are instead regarded as artifacts of the most recent isotopic and/or elemental re-equilibrations.

Table 6. Regression analyses of selected data sets, crystalline complex, junction of Admiralty Inlet and Adams Sound.

Unit(s)	Sample numbers	Age(Ma)	Initial $^{87}Sr/^{86}Sr$	*MSWD
1,2,3	A2,A5,A7,A8,E, B2,B4,B5,D1,D5	2321±76	0.7035±0.0007	5.6
4	C3,C4,C6	1678±69	0.7035±0.0004	0.7
4	C2,C3,C4	1130±79	0.7078±0.0007	0.1

* Mean square of weighted deviates. As discussed by Brooks et al. 1972, a MSWD of ca. 2.5 or greater indicates scatterin linear data in excess of analytical uncertainty.

Paleomagnetic data (Fahrig et al., 1981) indicate that the Nauyat volcanic rocks are a Mackenzie igneous event (1.27 Ga, e.g. LeCheminant and Heaman, 1989), and chemical data, for the basalt flows (Galley et al., 1983; Jackson and Iannelli, 1981) are similar to those for other Mackenzie events. LeCheminant and Heaman (1989) have dated Mackenzie dykes at 1267 ± 2 Ma and the Muskox intrusion, cut by Mackenzie dykes, at 1270 ± 4 Ma. Assuming the paleomagnetic correlation is valid, the Nauyat volcanic rocks were probably extruded at about this time.

The Nauyat volcanic rocks have undergone subgreenschist metamorphism but the Hadrynian-aged Franklin (750 Ma) and Borden (950 Ma) diabase dykes have not (Jackson and Morgan, 1978; Christie and Fahrig, 1983).

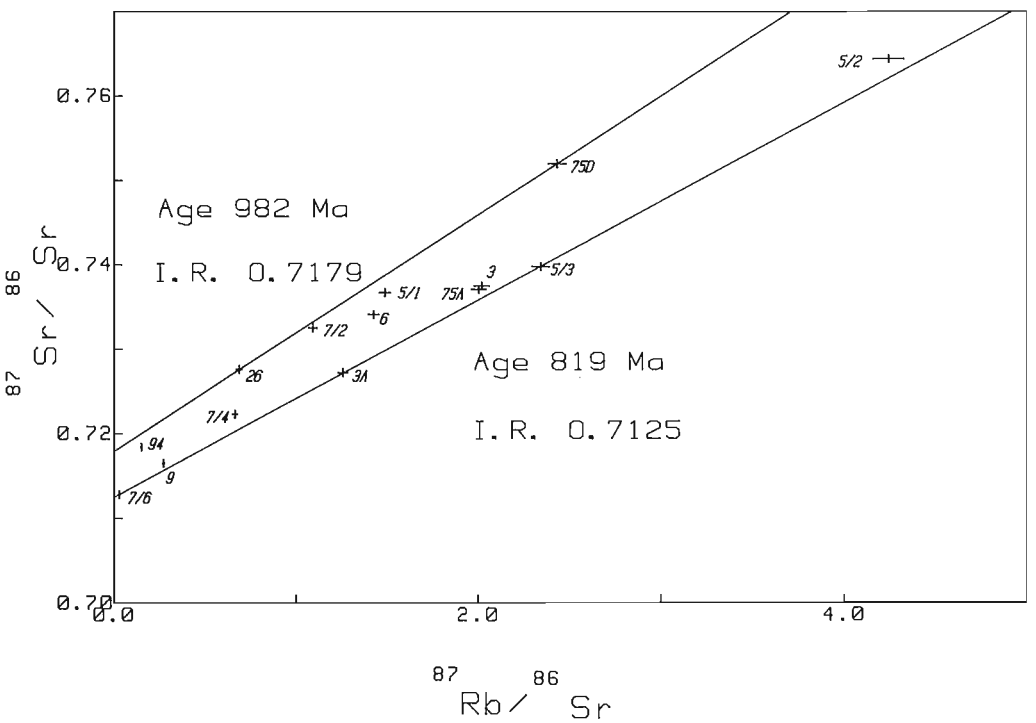

Figure 19. Rb-Sr data, plateau basalt, Nauyat volcanics. Reference isochrons shown were chosen to delimit the boundaries of the Rb-Sr data. See Table 2 for data.

Therefore the subgreenschist metamorphism is considered to be older than the dykes and may have caused the scattering of Rb-Sr and K-Ar ages for Nauyat flows. According to Galley et al. (1983) and Jackson and Iannelli (1984) the metamorphism may be related to the closing of the Poseidon Ocean, possibly at about 1000 Ma.

SUMMARY AND DISCUSSION

In southern Baffin Island, the charnockitic Cumberland batholithic complex of ca. 1.85 Ga forms the core of the Baffin Orogen (Fig. 2). Granulite-grade metamorphism and related plutonism are widespread. U-Pb zircon, Pb-Pb monazite, and Rb-Sr whole-rock ages are reported here for three localities in and adjacent to this batholith (Fig. 1):

(a) In Iqaluit, near the south end of the batholithic complex, a zircon age of 1857 + 12/-6 Ma was determined for a monzogranite. A Rb-Sr age of 1877 ± 45 Ma was determined for mixed lithologies, including the monzocharnockite, with a $^{87}Sr/^{86}Sr_o = 0.7046 \pm 0.0019$.

(b) In the north-central batholithic complex scattered U-Pb results for zircon from a monzocharnockite suggest an age between 1.85 and 1.95 Ga. Monazite from the same sample gave a U-Pb age of 1854 ± 2 Ma.

(c) From west of Nudlung Fiord, two small adjacent charnockite plutons on the northern edge of the batholithic complex were sampled for U-Pb and Rb-Sr age determination. The alkali feldspar charnockite gave a zircon age of 1853 +15/-11 Ma and a monazite age of 1832 ± 2 Ma. This latter age probably dates the cooling of the rock below the monazite closure temperature. A Rb-Sr composite whole-rock age for the two charnockite plutons gave 1730 ± 49 Ma ($^{87}Sr/^{86}Sr_o = 0.7149 \pm 0.0034$).

The zircon ages indicate that the Cumberland batholithic complex is about 1.85 Ga or slightly older. These dates are roughly similar to the ca. 1.87-1.90 Ga dates reported by Henderson (1985) and Pidgeon and Howie (1975). Zircon inheritance has been documented within some of the samples dated, reflecting an older crustal source. Sm-Nd analyses and preliminary Nd model ages obtained for samples from the Cumberland batholithic complex and older gneisses, including basement gneisses, range chiefly from 3.3 to 2.3 Ga (E. Hegner, pers. comm. 1989), corroborating the presence of an older crustal component.

Preliminary Nd model ages for northern Baffin Island are at least 2.8 Ga (E. Hegner, pers. comm. 1989).

Zircon from foliated trondhjemite-tonalite from basement to the Mary River Group, southeast of the Mary River area in northern Baffin Island, yielded an age of 2851 +20/-17 Ma. Zircon from Mary River Group dacite, collected about 10 km northeast of the locality of the dated tonalitic basement gave 2718 +5/-3 Ma. A marginally younger age of 2709 +4/-3 Ma was obtained for zircon from a monzogranite pluton about 50 km north of the dacite. It may be representative of later intrusions of Archean age in northern Baffin Island.

Samples of the oldest and youngest components in nebulitic migmatite near the head of Cambridge Fiord were studied using U-Pb zircon dating. These samples have complex U-Pb systematics and do not yield unambiguous dates. However, they are interpreted as indicating early Proterozoic melting and igneous zircon growth, with a protolith of late Archean age.

Rb-Sr and U-Pb age studies in three areas of the Borden Rift Basin, northwestern Baffin Island, generally have yielded imprecise and ambiguous results. In one study, Rb-Sr analyses were made of four components in the Archean-Aphebian high-grade basement gneiss complex exposed in a small horst along the east coast of Admiralty Inlet. Data for three of the components indicate an age of about 2300 Ma, the significance of which is unclear. Younger age results for metamorphosed dykes are probably the result of a later disturbance of the Rb-Sr system during metamorphic retrogression. In the second area, a small irregular monzogranite pluton, possibly an anatectite, intrudes a heterogenous basement complex just west of Navy Board Inlet. U-Pb analysis of zircon from the monzogranite yields a very scattered array, indicating late Aphebian melting with abundant older zircon inheritance of probable Archean age. In the third area, new Rb-Sr and previously published K-Ar measurements on Nauyat plateau basalts from the Borden Rift Basin fail to provide an unequivocal age, although none indicates an age older than Neohelikian. Published paleomagnetic and chemical data suggest the Nauyat volcanic rocks represent a 1.27 Ga (Mackenzie) igneous event.

Previously published K-Ar mineral (muscovite, biotite, hornblende) dates from Baffin Island generally span the range from 1.6 to 1.7 Ga. They indicate regional cooling and closure of isotopic systems well after the culmination of plutonism and metamorphism, dated in southern Baffin Island at about 1.85 Ga.

The U-Pb, Rb-Sr, and K-Ar results presented or summarized in this paper provide a reconnaissance geochronological framework for future geological and geochronological studies on Baffin Island.

ACKNOWLEDGMENTS

We particularly thank Klaus Santowski for performing the mass spectrometry and J.C. Bisson and J.L. MacRae for U-Pb chemistry. Tom Frisch read the manuscript critically and made many improvements.

REFERENCES

Blackadar, R.G.

1967: Geological reconnaissance southern Baffin Island, District of Franklin; Geological Survey of Canada, Paper 66-47, 32p.

1970: Precambrian geology, northwestern Baffin Island, District of Franklin; Geological Survey of Canada, Bulletin 191, 89p.

Brooks, C., Hart, S.R. and Wendt, I.

1972: Realistic use of two-error regression treatments as applied to rubidium-strontium data; Reviews of Geophysics and Space Physics, v. 10, p. 551-557.

Christie, K.W. and Fahrig, W.F.
1983: Paleomagnetism of the Borden dykes of Baffin Island and its bearing on the Grenville Loop; Canadian Journal of Earth Sciences, v. 20, p. 275-289.

Crawford, W.J.P.
1973: Metamorphic iron formations of Eqe Bay and adjacent parts of northern Baffin Island; unpublished Ph.D. thesis, University of Washington, 101p.

Davis, D.
1982: Optimum linear regression and error estimation applied to U-Pb data; Canadian Journal of Earth Sciences, v. 29, p. 2141-2149.

Fahrig, W.F.
1987: The tectonic settings of continental mafic dyke swams: failed arm and early passive margin, in Mafic Dykes Swans, ed. H.C. Halls and W.F. Fahrig, Geological Association of Canada, Special Paper 34, p. 331-348.

Fahrig, W.F. and Jones, D.L.
1969: Paleomagnetic evidence for the extent of Mackenzie igneous events; Canadian Journal of Earth Sciences, v. 6, p. 679-688.

Fahrig, W.F., Christie, K.W., and Jones, D.L.
1981: Paleomagnetism of the Bylot Basins: Evidence for Mackenzie continental tensional tectonics; in Proterozoic Basins of Canada, ed. F.H.A. Campbell; Geological Survey of Canada, Paper 81-10, Report 17, p. 303-312.

Fahrig, W.F., Irving, E., and Jackson, G.D.
1971: Paleomagnetism of the Franklin diabases; Canadian Journal of Earth Sciences, v. 8, p. 455-467.

Fraser, J.A., Heywood, W.W., and Mazurski, M.
1978: Metamorphic map of the Canadian Shield; Geological Survey of Canada, Map 1475A (1:3 500 000).

Galley, A.
1978: The petrology and chemistry of the Nauyat Formation volcanics, Borden Peninsula, Northwestern Baffin Island; unpublished B.Sc. thesis, Carleton University, 53 p.

Galley, A.G., Jackson, G.D., Iannelli, T.R.
1983: Neohelikian subaerial basalts with ocean-floor-type chemistry, northwestern Baffin Island; Geological Association of Canada, Program with Abstracts, v. 8, p. A25.

Geldsetzer, H.
1973: The tectono-sedimentary development of an algal-dominated Helikian succession on northern Baffin Island, N.W.T.; in Proceedings of the Symposium on the Geology of the Canadian Arctic, ed. J.D. Aitken and D.J. Glass; Geological Association of Canada Saskatoon, May 1973, p. 99-126.

Gross, G.A.
1966: The origin of high-grade iron deposits of Baffin Island, Northwest Territories; Canadian Mining Journal, v. 87, p. 111-114.

Henderson, J.R.
1985: Ekalugad Fiord-Home Bay, District of Franklin, Northwest Territories; Geological Survey of Canada, Map 1606A, 1:250 000.

Henderson, J.R., Jackson, G.D., and Morgan, W.C.
1980: The Cumberland Sound Metamorphic Culmination: a major tectonic element of the Hudsonian orogen in northeast Canada and west Greenland; Geological Association of Canada - Mineralogical Association of Canada, Program with Abstracts, v. 5, p. 59.

Henderson, J.R., Shaw, D., Mazurski, M., Henderson, M., Green, R., and Brisbin, D.
1979: Geology of part of Foxe Fold Belt, central Baffin Island, District of Franklin; in Current Research, Part A; Geological Survey of Canada, Paper 79-1A, p. 95-99.

Henderson, J.R. and Tippett, C.R.
1980: Foxe Fold Belt in western Baffin Island, District of Franklin; in Current Research, Part A; Geological Survey of Canada, Paper 80-1A, p. 147- 152.

Hoffman, P.F.
in press: Subdivision on the Churchill Province and extent of the Trans-Hudson Orogen; in The Early Proterozoic Trans-Hudson orogen; lithotectonic correlations and evolution; ed. J.F. Lewry and M.R. Stauffer; Geological Association of Canada, Special Paper.

Hunt, P.A. and Roddick, J.C.
1987: A compilation of K-Ar Ages, Report 17; in Radiogenic Age and Isotopic studies, Report 1; Geological Survey of Canada, Paper 87-2, p. 143-204.

1990: A compilation of K-Ar Ages, Report 19; in Radiogenic Age and Isotopic studies, Report 3; Geological Survey of Canada, Paper 89-2 (this publication).

Jackson, G.D.
1966: Geology and mineral possibilities of the Mary River region, northern Baffin Island; Canadian Mining Journal, v. 87, p. 57-61.

1971: Operation Penny Highlands, south-central Baffin Island; in Report of Activities, Part A; Geological Survey of Canada, Paper 71-1A, p. 138-140.

1978a: McBeth Gneiss Dome and associated Piling Group, central Baffin Island, District of Franklin; in Rubidium-Strontium Isotopic Age Studies, Report 2; ed. R.K. Wanless and W.D. Loveridge; Geological Survey of Canada, Paper 77-14, p. 13-17.

1978b: Basement gneisses and the Mary River Group, No. 4 Deposit area, northwest Baffin Island, District of Franklin; in Rubidium-Strontium Isotopic Age Studies, Report 2; ed. R.K. Wanless and W.D. Loveridge; Geological Survey of Canada, Paper 77- 14, p. 18-24.

Jackson, G.D. and Iannelli, T.R.
1981: Rift-related cyclic sedimentation in the Neohelikian Borden Basin, northern Baffin Island; in Proterozoic Basins of Canada, ed. F.H.A. Campbell; Geological Survey of Canada, Paper 81-10, p. 269- 302.

Jackson, G.D. and Iannelli, T.R.
1984: Borden Basin, N.W. Baffin Island: Mid-Proterozoic rifting and possible ocean opening; in Geological Association of Canada, Program with Abstracts, v. 9, p. 76.

Jackson, G.D., Iannelli, T.R., Knight, R.D., and Lebel, D.
1985: Neohelikian Bylot Supergroup of Borden Rift Basin, northwestern Baffin Island, District of Franklin; in Current Research, Part A; Geological Survey of Canada, Paper 85-1A, p. 639-649.

Jackson, G.D., Morgan, W.C., and Davidson, A.
1978a: Geology, Icebound Lake, District of Franklin; Geological Survey of Canada, Map 1451A, with expanded legend, 1:250 000.

Jackson, G.D., Morgan, W.C., and Davidson, A.
1978b: Geology, Buchan Gulf-Scott Inlet, District of Franklin; Geological Survey of Canada, Map 1449A, with expanded legend, 1:250 000.

Jackson, G.D. and Morgan, W.C.
1978: Precambrian metamorphism on Baffin and Bylot Islands; in Metamorphism in the Canadian Shield, J.A. Fraser and W.W. Heywood; Geological Survey of Canada, Paper 78-10, p. 249- 267.

Jackson, G.D. and Sangster, D.F.
1987: Geology and resource potential of a proposed national park, Bylot Island and northwest Baffin Island, Northwest Territories; Geological Survey of Canada, Paper 87-17, 31p, map at scale 1:250 000.

Jackson, G.D. and Taylor, F.C.
1972: Correlation of major Aphebian rock units in the northeastern Canadian Shield; Canadian Journal of Earth Sciences, v. 9, p. 1650-1669.

Kranck, E.H.
1972: Remark about the tectonics of the gneisses of central Baffin Island and the rise of the infrastructure. Bulletin Geological Society of Finland, v. 44, p. 111-112.

Lecheminant, A.N., and Heaman, L.M
1989: Mackenzie igneous events, Canada: Middle Proteoozoic hotspot magnetism associated with ocean opening; Earth and Planetery Science Letters, v. 96, p. 38-48.

Leech, G.B., Lowdon, J.A., Stockwell, C.H., and Wanless, R.K.
1963: Age Determinations and Geological Studies: Report 4; Geological Survey of Canada, Paper 63-17, 111p.

Lemon, R.R.H. and Blackadar, R.G.
1963: Admiralty Inlet area, Baffin Island, District of Franklin; Geological Survey of Canada, Memoir 328, 84p.

Lowdon, J.A., Stockwell, C.H., Tipper, H.W., and Wanless, R.K.
1963: Age determinations and geological studies; Geological Survey of Canada, Paper 62-17, 140p.

Morgan, W.C., Bourne, J., Herd, R.K., Pickett, J.W., and Tippett, C.R.
1975: Geology of the Foxe Fold Belt, Baffin Island, District of Franklin; in Report of Activities, Part A; Geological Survey of Canada, Paper 75-1A, p. 343- 347.

Morgan, W.C., Okulitch, A.V., and Thompson, P.H.
1976: Stratigraphy, structure, and metamorphism of the west half of the Foxe Fold Belt, Baffin Island; in Report of Activities, Part A; Geological Survey of Canada, Paper 76-1A, p. 387-391.

Olson, R.A.
1984: Genesis of paleokarst and strata-bound zinc-lead sulphide deposits in a Proterozoic dolostone, northern Baffin Island, Canada; Economic Geology, v. 79, p. 1059-1103.

Parrish, R.R., Roddick, J.C., Loveridge, W.D., and Sullivan, R.W.
1987: Uranium-lead analytical techniques at the Geochronology Laboratory, Geological Survey of Canada; in Radiogenic Age and Isotopic Studies: Report 1; Geological Survey of Canada, Paper 87-2, p. 3-7.

Pidgeon, R.T. and Howie, R.A.
1975: U-Pb age of zircon from a charnockitic granulite from Pangnitung on the east coast of Baffin Island; Canadian Journal of Earth Sciences, v. 12, p. 1046-1047.

Schärer, U.
1984: The effect of initial ^{230}Th equilibrium on young U-Pb ages: the Makalu case, Himalaya; Earth and Planetary Science Letters, v. 67, p. 191-204.

Stevens, R.D., Delabio, R.N., and Lachance, G.R.
1982: Age determinations and geological studies, K-Ar isotopic ages, Report 16; Geological Survey of Canada, Paper 82-2, 56p.

Tippett, C.R.
1980: A geological cross-section through the southern margin of the Foxe Fold Belt, Baffin Island, Arctic Canada, and its relevance to the tectonic evolution of the northwestern Churchill Province; Ph.D. thesis, Queen's University, Kingston, 409p.

Trettin, H.P.
1969: Lower Paleozoic sediments of northwestern Baffin Island, District of Franklin; Geological Survey of Canada, Bulletin 157, 70p.

Wanless, R.K. and Loveridge, W.D.
1972: Rubidium-strontium isochron age studies, Report 1; Geological Survey of Canada, Paper 72-23, p. 67-69.

1978: Rubidium-strontium isotope age studies, Report 2 (Canadian Shield); Geological Survey of Canada, Paper 74-2, p. 67-68.

Wanless, R.K., Stevens R.D., Lachance, G.R., and Delabio, R.N.
1972: Age determinations and geological studies, K-Ar isotopic age, Report 10; Geological Survey of Canada, Paper 71-2, 96p.

1974: Age determinations and geological studies, K-Ar sotopic age, Report 12; Geological Survey of Canada, Paper 74-2, p. 23-24.

1978: Age determinations and geological studies, K-Ar isotopic ages, Report 13; Geological Survey of Canada, Paper 77-2, 60p.

1979: Age determinations and geological studies, K-Ar isotopic ages, Report 14; Geological Survey of Canada, Paper 79-2, 60p.

Wanless, R.K., Stevens R.D., Lachance, G.R., and Edmonds, C.M.
1968: Age determinations and geological studies, K-Ar isotopic ages, Report 8: Geological Survey of Canada, Paper 67-2A, 141p.

Wanless, R.K., Stevens, R.D., Lachance, G.R., and Rimsaite, J.Y.H.
1966: Age determinations and geological studies, K-Ar isotopic ages, Report 6; Geological Survey of Canada, Paper 65-17, p. 29.

York, D.
1969: Least squares fitting of a straight line with correlated errors; Earth and Planetary Science Letters, v. 5, p. 320-324.

APPENDIX 1

Analytical Considerations

Results of U-Pb analysis on zircon and monazite, and Rb-Sr analyses on whole-rock samples are presented in Tables 1 and 2.

U-Pb

U-Pb analyses on zircon and monazite were carried out between 1987 and 1989, and their analytical techniques were described by Parrish et al., 1987. Analytical uncertainties are presented in Table 1. A table of locations is presented for zircon samples in the appendix (Table A5, Appendix 2).

The U-Pb studies on zircon presented in this report do not generally yield simple collinear arrays of data. Therefore the model of a single period of Pb loss affecting an otherwise undisturbed U-Pb system cannot necessarily be applied, and the age estimates are dependent on the interpretation of the observed systematics. When the samples are believed to have corresponded to this simple behaviour, ages and uncertainties based on fitting a chord to three or more data points have been calculated in the following manner:

1) If the array of data points is collinear or if the array contains a data point less than 5% discordant, the method of Davis (1982) is used.

2) If neither of these conditions apply, a method based on that of York (1969) as modified by Parrish et al. (1987) is used.

Most monazite analyses presented in this study are essentially concordant; despite this, the interpretation of their ages is not without complexity. Scherer (1984) has shown that the U decay series are not always in equilibrium in zircon, xenotime, and monazite at the time of formation of these minerals, relative to the rock in which they occur. In particular, 230Th, a member of the ^{238}U–^{206}Pb decay chain, is preferentially concentrated in monazite at the time of formation, owing to the affinity of monazite for Th. The decay of the ^{230}Th produces excess ^{206}Pb which distorts the measured U-Pb age pattern, causing ^{238}U–^{206}Pb ages to be anomalously high (1-3 Ma excess being typical) and ^{207}Pb–^{206}Pb ages to be low, but by amounts that depend on the degree of Th/U fractionation and the mineral's age. Therefore ^{207}Pb–^{206}Pb ages of concordant monazite should be considered minimum ages of crystallization. Alternatively, some could represent cooling below monazite's closure temperature, and may give an accurate age of that event, since prior to this cooling excess ^{206}Pb would have diffused out of the monazite during open system behaviour.

Rb-Sr

Rb-Sr analyses of whole-rock samples were carried out between 1975 and 1981. General techniques for the extraction and analysis of Rb and Sr from rocks and minerals are described in Wanless and Loveridge (1972), with the following exception: use of a more highly enriched (99.89%) ^{84}Sr tracer allowed determination of sample $^{87}Sr/^{86}Sr$ ratios directly from isotope dilution analyses, eliminating the requirement for separate Sr isotopic composition analyses.

Techniques for the mass spectrometric analysis of Rb and Sr between 1975 and 1978 are described in Wanless and Loveridge (1978) (applicable to Frobisher Bay hybrid granulite and charnockites of south-central Baffin Island). Nauyat Formation basalt samples were analyzed on a rebuilt and improved 10-inch radius mass spectrometer in 1979-80. Selection and switching of the magnetic field was automated in 1980; Rb-Sr measurements on the samples from the crystalline complex, junction of Admiralty Inlet and Adams Sound, were obtained in the automated mode.

In the measurement of Rb-Sr results one sigma analytical uncertainties are estimated at: Rb ppm, 1%; Sr ppm, 0.5%; $^{87}Rb/^{86}Sr$, 1%; $^{87}Sr/^{86}Sr$, as indicated in Table 2. Tables of sample locations and lithologies are presented in Appendix 2.

APPENDIX 2

Table of rock types and localities for Rb-Sr and U-Pb samples.

Table A1. Samples of Iqaluit hybrid granulite (NTS 25N/10-NE corner Frobisher Inn), used for Rb-Sr and U-Pb zircon age determinations (63°44'56"N, 68°30'46"W).

Sample No. (this paper)	Field No.	Rock type
1B	JD70-1B	Pink massive to foliated, medium- to coarse-grained monzogranite with minor clinopyroxene, hornblende, magnetite, hypersthene, apatite, and traces of biotite, chlorite, pyrite, pyrrhotite, myrmekite.
1C	JD70-1C	Greasy grey massive biotite pegmatite.
1D	JD70-1D	Pink with black mafic laminae, foliated fine- to medium-grained contaminated monzogranite, with minor clinopyroxene, hornblende, biotite, magnetite, graphite.
1E	JD70-1E	Pale pinkish grey fine-grained, finely foliated monzogranite with minor magnetite, hornblende, clinopyroxene.
1F	JD70-1F	Mottled pale and dark grey fine-grained, foliated quartz-plagioclase paragneiss, with hornblende and pyroxene.
1H	JD70-1H	Massive to faintly foliated and banded greasy green-grey fine-grained rocks of monzogranite (= monzocharnockite) composition with minor hypersthene, magnetite, biotite, clinopyroxene?, hornblende?.
1I	JD70-1I	Finely foliated sheared homogeneous greasy green-grey fine- to medium-grained quartz-plagioclase-potash feldspar gneiss of monzocharnockite composition; with minor biotite, hornblende, magnetite, hypersthene?.
Note: U-Pb zircon study on same rock as Rb-Sr sample 1B		

Table A2. Samples of Monzocharnockite west of Nudlung Fiord (NTS 27B/1), used for Rb-Sr and U-Pb zircon and monazite age determinations.

Sample No. (this paper)	Field No.	Rock type	Locality
166/2	JDE166/2-70	syenocharnockite	68°8'42"N; 68°27'59"W
166/3	JDE166/3-70	noritic andesine anorthosite	68°8'42"N; 68°27'59"W
168/2	JDC168/2-70	alkali-feldspar charnockite	68°8'58"N; 68°29'00"W
168/4	JDC168/4-70	syenocharnockite	68°8'57"N; 68°30'10"W
168/22	JDC168/22-70	alkali-feldspar charnockite	68°8'58"N; 68°29'00"W
169/1	JDC169/1-70	syenocharnockite	68°9'01"N; 68°36'15"W
169/2	JDC169/2-70	syenocharnockite	68°9'01"N; 68°36'15"W
Notes: U-Pb zircon study on same rock as Rb-Sr sample 168/22. Samples 169/1 and 169/2 are from the western intrusion. The others are from the eastern intrusion (Fig. 6).			

Table A3. Rb-Sr samples of crystalline complex, junction of Admiralty Inlet, Adams Sound (72°54'18"N; 85°38'41"W).

Sample No. (this paper)	Sample No. Field	Unit	Description
D-1	77 JDW-72D-1	1	Fine-grained foliated monzogranite
D-5	77 JDW-72D-5	1	Medium-grained foliated monzocharnockite
A-2	77 JDW-72A-2	2	Fine-medium grained nebulitic granite-granodiorite augen gneiss, less than 10% mafic
A-5	77 JDW-77A-5	2	Fine-medium grained nebulitic granite-granodiorite augen gneiss, less than 10% mafic
A-8	77 JDW-77A-8	2	Fine-medium grained nebulitic granite-granodiorite augen gneiss, less than 10% mafic
A-7	77 JDW-77A-7	2	Fine-medium grained nebulitic granite-granodiorite augen gneiss, 10-15% mafic
E	77 JDW-77E	2	Fine-medium grained nebulitic granite-granodiorite augen gneiss, 15-20% mafic
B-2	77 JDW-77B-2	3	Fine-grained biotite-hornblende-plagioclase gneiss, more hornblende than biotite, little to no quartz
B-4	77 JDW-77B-4	3	Fine-grained biotite-hornblende-plagioclase gneiss, more hornblende than biotite, minor quartz
B-5	77 JDW-77B-5	3	Fine-grained hornblende-biotite-plagioclase gneiss, more biotite than hornblende, moderate to minor quartz
C-2	77 JDW-77C-2	4	Metabasite dyke; major andesine with minor hornblende, anthophyllite, little magnetite
C-6	77 JDW-77C-6	4	Metabasite dyke; major andesine with minor hornblende, anthophyllite, little magnetite
C-3 77	JDW-77C-3	4	Metabasite dyke; major hornblende with minor andesine, little anthophyllite, no magnetite
C-4 77	JDW-77C-4	4	Meta-ultramafic dyke; chiefly hornblende, anthophyllite, biotite, no plagioclase

Table A4. Samples of Nauyat Formation basalt for whole-rock Rb-Sr age determinations (48BNE).

Sample No. (this paper)	Field		Description	Locality
26	77 JDI-26		massive, large amygdules	72°49'07"N; 85°36'40"W
7/6	78 JDG-7/6	a	massive, amygdules to 5 mm	72°48'04"N; 85°34'30"W
7/4	77 JDG-7/4	a	massive, red-green, amygdules to 3 m	72°48'04"N; 85°34'30"W
3A	77 JDG-3A	a	massive	72°48'04"N; 85°34'30"W
3	77 JDG-3	a	massive	72°48'04"N; 85°34'30"W
7/2	77 JDG-7/2	a	massive, amygdules to 1 mm	72°48'04"N; 85°34'30"W
5/3	77 JDG-5/3	a	massive, large amygdules	72°48'04"N; 85°34'09"W
5/2	77 JDG-5/2	a	massive, amygdules to 1 mm	72°48'04"N; 85°34'09"W
75D	77 JDI-75D/1		massive	72°40'00"N; 85°25'42"W
75A	77 JDI-75A/1		massive, large amygdules	72°40'07"N; 85°25'43"W
5/1	77 JDG-5/1	a,c	massive	72°48'04"N; 85°34'09"W
9	77 JDG-9	a,b	massive	72°48'N; 85°34'W
6	77 JDG-6	a,b	massive	72°48'N; 85°34'W
94	77 JDI-94	b	massive, large amygdules	72°49'19"N; 85°31'17"W

Notes: Samples listed in approximate ascending stratigraphic order except for samples marked "b". a- samples all from same stratigraphic section; b- stratigraphic position uncertain. c- from lower member, all others from upper member.

Table A5. Sample localities, U-Pb studies on zircon.

Field No.	Latitude	Longitude	Locality
JD70-1B	63°44'56"N	68°30'46"W	Iqaluit
JDC168/22-70	68°8'58"N	68°29'00"W	West Nudlung Fiord
JDM355-68	67°3'58"N	68°33'34"W	North-central Cumberland Batholithic Complex
JD100/12-68	71°6'15"N	77°24'16"'W	Mary River region
JD138/1-68	71°32'18"N	77°29'48"W	Mary River region
JDC56/1-68	71°1'43"N	77°31'43"W	Mary River region
JD79-84	73°19'41"N	81°20'26"W	Navy Board Inlet
JDD218X(Z)-68	71°8'52"N	75°24'43"W	Head of Cambridge Fiord

U-Pb age constraint on the Wager shear zone, District of Keewatin, N.W.T.

J.R. Henderson[1] and J.C. Roddick[1]

Henderson J.R. and Roddick, J.C., U-Pb age constraint on the Wager shear zone, District of Keewatin, N.W.T.; in Radiogenic Age and Isotopic Studies: Report 3, Geological Survey of Canada, Paper 89-2, p. 149-152, 1990.

Abstract

A U-Pb age of 1808 ± 2 Ma for a calc-alkaline granite deformed by the Wager shear zone provides a maximum limit to the time of shearing. This is the youngest pluton yet dated in a calc-alkaline intrusive suite extending northeast from the shear zone to the Foxe belt.

Résumé

L'âge U-Pb de 1808 ± 2 Ma d'un granite calco-alcalin deformé dans la zone de cisaillement de Wager fournit une limite maximum pour l'âge de la déformation. Le pluton fait partie d'un suite intrusive calco-alcaline mise en place entre la zone de cisaillement de Wager et la ceinture de Foxe; c'est le plus jeune pluton de cette suite daté jusqu'à prèsent.

INTRODUCTION

The Wager shear zone is a major east-west transcurrent ductile shear zone, which can be traced for about 300 km along the northwest shore of Hudson Bay (Fig. 1; Henderson et al., 1986). This shear zone cuts a granitic pluton, which is part of a calc-alkaline granitoid suite that intrudes early Proterozoic supracrustal gneisses (quartzite, pelitic gneiss, marble, and calc-silicate gneiss) comprising the Hudsonian-age Foxe belt. Two components of the granitoid suite collected about 50 km north of the shear zone were previously dated by U-Pb zircon at 1823 ± 3 Ma and 1826 +4/-3 Ma (LeCheminant et al., 1987). These ages provide indirect evidence that the shear zone is younger than 1.82 Ga. The minimum age limit of the shear zone is constrained by mafic dykes of the 1267 Ma Mackenzie swarm (LeCheminant and Heaman, 1989). To better define the age of the Wager shear zone the calc-alkaline granite that it cuts (Fig. 2), the 'Base Camp Granite', was dated using U-Pb geochronological methods.

The 'Base Camp Granite' is located at the southwestern corner of Wager Bay. It is considered to be a component of the calc-alkaline suite, as it is compositionally similar to the granitoids to the northwest. The granite is structurally isotropic except where it is mylonitized by the shear zone forming its southern margin (Fig. 2). The dated sample was collected from undeformed, medium-grained, hypidiomorphic-granular granite located on the northern septa of the main body, west of Paliak Islands (Fig. 3) at 65° 25' N and 89° 10' W.

U-Pb GEOCHRONOLOGY

About 0.5 g of zircon was concentrated from 30 kg of sample 5-HSA-94-2. The zircon population consists of euhedral to subhedral grains with length to width dimensions from 1:1 to 6:1. There are two zircon types; about 50% of the population are pale pink grains with euhedral zoning. The colour is the result of many small fractures throughout the grains. The remaining grains are clear, unzoned grains, some with spherical to elongate fluid inclusions. This two-fold division is present in all grain sizes, ranging from 150 to about 20 μm, though the smaller grains are dominated by the clear type. No visible cores are present in the grains. Grains selected for U-Pb analysis were concentrated from non-magnetic clear grains, sieved into three different grain sizes (Table 1).

1 Geological Suvey of Canada, 601 Booth Street, Ottawa, Ontario K1A 0E8

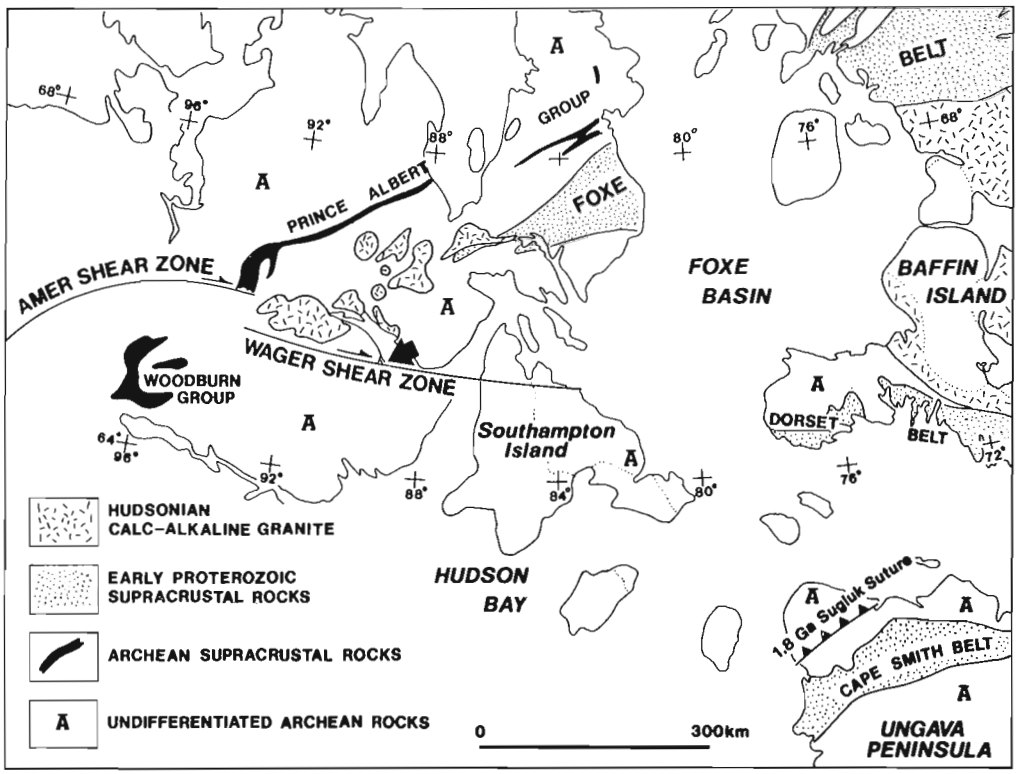

Figure 1. Location map and regional geological setting of the 'Base Camp Granite' at the southwestern corner of Wager Bay (see arrow).

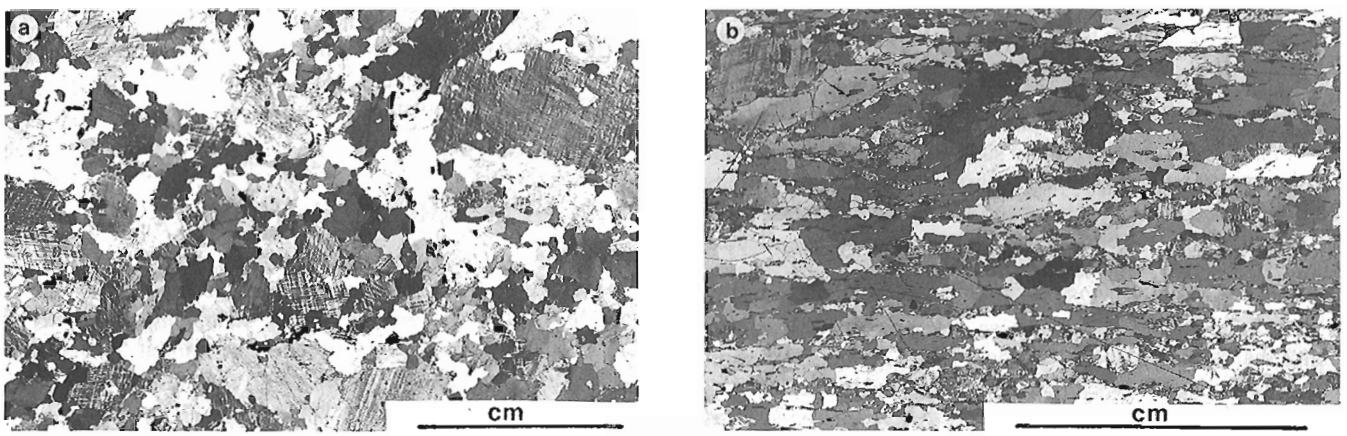

Figure 2. Photomicrographs of the 'Base Camp Granite' (Crossed nicols). (a) Primary hypidiomorphic-granular fabric (GSC 209589-L). (b) Secondary mylonitic fabric in a specimen from the southern margin (thin section cut parallel to lineation and perpendicular to foliation). Foliation trace is defined by oriented small recrystallized feldspar inclusions within larger quartz grains, as well as ribbon-shaped quartz aggregates (GSC 204589-C). From Fig. 5 in Henderson and Broome, 1990.

Table 1. U-Pb zircon data - Base Camp Granite (5-HSA-2; lat. 65° 25' N, long. 89° 10' W).

Fraction size	Wt. mg	U ppm	Pb* ppm	$^{206}Pb^{b}/^{204}Pb$	Pb^{c} pg	^{208}Pb %	$^{206}Pb/^{238}U$	$^{207}Pb/^{235}U$	Corr.[d] Coeff.	$^{207}Pb/^{206}Pb$	$^{207}Pb/^{206}Pb$ Age (Ma)
>105 NM Abr	.039	320	106	3856	64	8.8	.3169 ±.14%	4.837 ±.15%	.9771	.11070 ±.03%	1810.9 ±1.1
−105+74 NM Abr	.032	137	48	1125	77	12.6	.3230 ±.25%	4.921 ±.26%	.9755	.11051 ±.06%	1807.9 ±2.1
−74+62 NM Abr	.066	198	69	1290	195	12.2	.3208 ±.10%	4.896 ±.14%	.8585	.11069 ±.07%	1810.8 ±2.6
−74+62 NM	.061	187	64	1157	187	12.2	.3163 ±.17%	4.811 ±.20%	.9178	.11032 ±.08%	1804.7 ±2.9

Errors are 1 std. error of mean in % except $^{207}Pb/^{206}Pb$ age errors, which are 2 std. errors in Ma.
Pb* = Radiogenic Pb; NM = Non-magnetic; Abr = Abraded; b = Corrected for fractionation and spike Pb; c = Total common Pb in analysis in picograms; d = Correlation Coefficient of errors in $^{206}Pb/^{238}U$ and $^{207}Pb/^{235}U$.

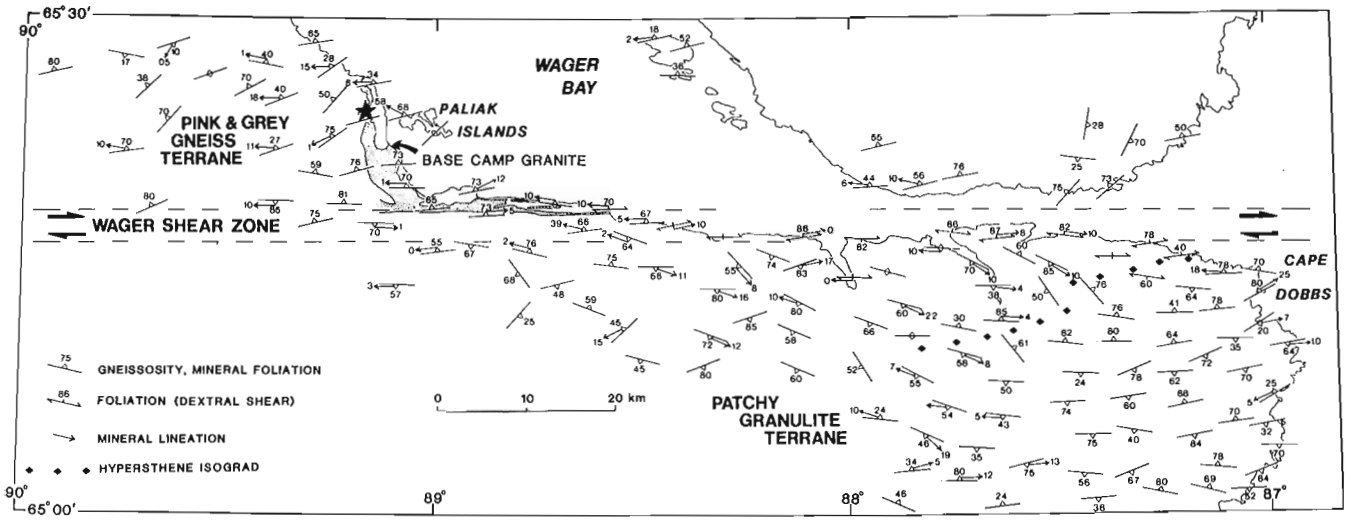

Figure 3. Structural geology of the region around Wager Bay. Three structural fabric domains are shown on the map: (1) pink and grey gneiss terrane, (2) Wager shear zone, and (3) patchy granulite terrane. The locality for the dated sample is shown by the star near the northern extent of the 'Base Camp Granite'.

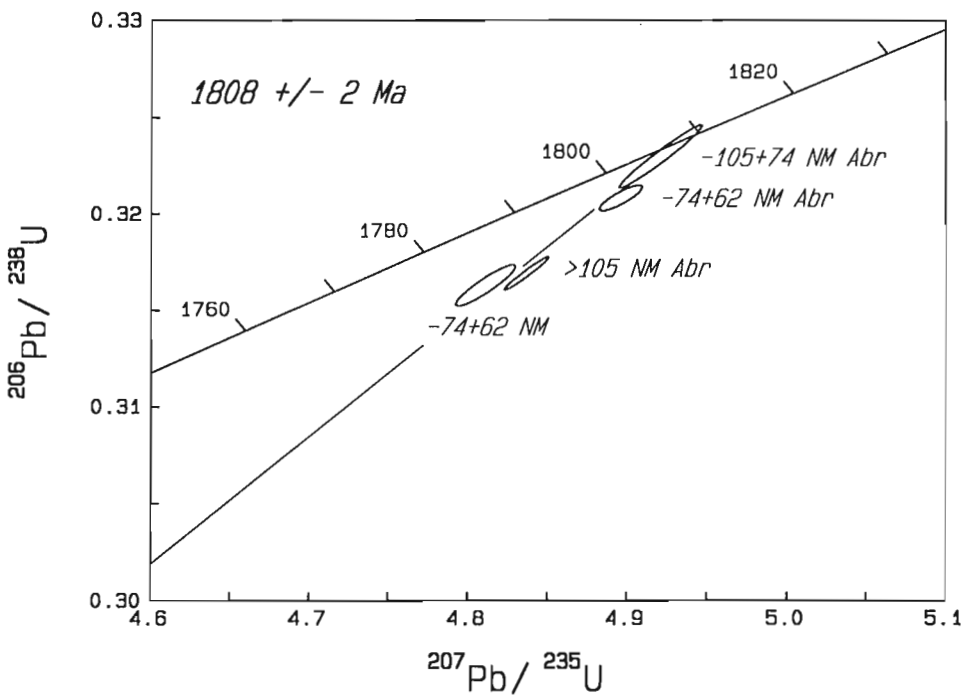

Figure 4. Concordia plot of zircon fractions from the 'Base Camp Granite'.

Four fractions of zircon were analyzed following the procedures outlined in Parrish et al. (1987). Three of the fractions were abraded to remove potentially altered outer parts of the grains (Krogh, 1982). Blanks were 44 pg Pb and 21 pg U. The analyses are tabulated in Table 1 and plotted in Fig. 4. The data form a roughly linear array, with one fraction lying on concordia at 1808 $\pm$ 2 Ma. The other fractions extend down a recent Pb loss line, which extrapolates to a lower intercept age of about 0 Ma. Most fractions contain $\leq$200 ppm U; wheras the coarsest fraction ($>$105 μm) contains 320 ppm U and is located to the right of the other fractions. It may contain a minor older, inherited, cryptic zircon component with a higher U concentration. The only fraction not abraded is the most discordant. The one fraction on concordia best defines the intrusive age of the granite at 1808 $\pm$ 2 Ma, as defined by its $^{207}Pb/^{206}Pb$ age.

CONCLUSION

The 'Base Camp Granite' is deformed on its southern margin by the Wager shear zone. Thus, the U-Pb zircon age of 1808 $\pm$ 2 Ma interpreted as the date of emplacement of the granite also provides a maximum age for the Wager shear zone. It is the youngest pluton yet dated in the calc-alkaline suite of the area.

REFERENCES

Henderson, J.R. and Broome, J.
1990: Geometry and kinematics of the Wager shear zone interpreted from structural fabrics and magnetic data; Canadian Journal of Earth Sciences, in press.

Henderson, J.R., LeCheminant, A.N., Jefferson, C.W., Coe, K. and Henderson, M.N.
1986: Preliminary account of the geology around Wager Bay, District of Keewatin; in Current Research, Part A, Geological Survey of Canada Paper 86-1A, p. 159-176.

Krogh, T.E.
1982: Improved accuracy of U-Pb ages by the creation of more concordant systems using an air abrasion technique; Geochimica et Cosmochimica Acta, v.46, p. 637-649.

LeCheminant, A.N., and Heaman L.M.
1989: Mackenzie igneous events, Canada: Middle Proterozoic hotspot magmatism associated with ocean opening; Earth and Planetary Science Letters, V. 96 p. 38-48.

LeCheminant, A.N., Roddick, J.C., Tessier, A.C. and Bethune, K.M.
1987: Geology and U-Pb ages of early Proterozoic calc-alkaline plutons northwest of Wager Bay, District of Keewatin; in Current Research, Part A; Geological Survey of Canada Paper 87-1A, p. 773-782.

Parrish, R.R., Roddick, J.C., Loveridge, D.W. and Sullivan, R.W.
1987: Uranium-lead analytical techniques at the geochronology laboratory, Geological Survey of Canada; in Radiogenic Age and Isotopic Studies: Report 1; Geological Survey of Canada, Paper 87-2, p. 3-7.

A COMPILATION OF K-AR AGES REPORT 19

P.A. Hunt[1] and J.C. Roddick[1]

Hunt, P.A. and Roddick, J.C., A compilation of K-Ar ages, Report 20; in Radiogenic Age and Isotopic Studies: Report 3, Geological Survey of Canada, Paper 89-2, p. 153-190, 1990.

Abstract

One hundred and thirty-five potassium-argon age determinations carried out by the Geological Survey of Canada are reported. Each age determination is accompanied by a description of the rock and mineral concentrate used; brief interpretative comments regarding the geological significance of each age are also provided where possible. The experimental procedures employed are described in brief outline. An index of all Geological Survey of Canada K-Ar age determinations published in this format has been prepared using NTS quadrangles as the primary reference.

Résumé

Les auteurs présentent 135 datations au potassium-argon effectuées par la Commission géologique du Canada. Chaqe datation est accompagnée d'une description de la roche ou du concentré mineral utilisé ainsi que d'une brève inérprétation touchant l'aspect géologique. Les méthodes expériéntales qui ont servi aux datations sont aussi résumées. De plus, à l'aide de quadrilatères du SRCN, un index de toutes les datations au potassium-argon a été publié par la Commission géologique du Canada.

INTRODUCTION

This compilation of K-Ar ages determined in the Geochronological Laboratories of the Geological Survey of Canada is the latest in a series of reports, the last of which was published in 1988 (Hunt and Roddick, Paper 88-2). In this new contribution one hundred and thirty-five determinations are reported. The format of this compilation is similar to the previous reports with data ordered by province or territory and subdivided by map sheet number. In addition to the GSC numbers, laboratory numbers (K-Ar xxxx) are also included for internal reference.

Experimental Procedures

The data compiled here represent analysis over a period of time from 1986 to 1988. Potassium was analyzed by atomic absorption spectrometry on duplicate dissolutions of the samples. Argon extractions were carried out using an RF vacuum furnace with a multi-sample loading system capable of holding six samples. The extraction system is on-line to a modified A.E.I. MS-10 with a 0.18 Tesla magnet. An atmospheric Ar aliquot system is also incorporated to provide routine monitoring of mass spectrometer mass discrimination. While computer acquisition and processing of data has been in operation since 1978, complete computer control of the mass spectrometer was initiated in 1986. Further details are given in Roddick and Souther (1987). Decay constants recommended by Steiger and Jäger (1977) are used in the age calculations.

1 Geological Survey of Canada, 601 Booth Street, Ottawa, Ontario K1A 0E8

The complete series of reports including the present one is as follows:

Determinations

GSC Paper 60-17,	Report 1	59-1 to 59-98
GSC Paper 61-17,	Report 2	60-1 to 60-152
GSC Paper 62-17,	Report 3	61-1 to 61-204
GSC Paper 63-17,	Report 4	62-1 to 62-190
GSC Paper 64-17,	Report 5	63-1 to 63-184
GSC Paper 65-17,	Report 6	64-1 to 64-165
GSC Paper 66-17,	Report 7	65-1 to 65-153
GSC Paper 67-2A,	Report 8	66-1 to 66-176
GSC Paper 69-2A,	Report 9	67-1 to 67-146
GSC Paper 71-2,	Report 10	70-1 to 70-156
GSC Paper 73-2,	Report 11	72-1 to 72-163
GSC Paper 74-2,	Report 12	73-1 to 73-198
GSC Paper 77-2,	Report 13	76-1 to 76-248
GSC Paper 79-2,	Report 14	78-1 to 78-230
GSC Paper 81-2,	Report 15	80-1 to 80-208
GSC Paper 82-2,	Report 16	81-1 to 81-226
GSC Paper 87-2,	Report 17	87-1 to 87-245
GSC Paper 88-2,	Report 18	88-1 to 88-105
GSC Paper 89-2,	Report 19	89-1 to 89-135

REFERENCES

Hunt, P.A. and Roddick, J.C.
1988: A compilation of K-Ar ages, Report 18; in Radiogenic Age and Isotopic Studies: Report 2; Geological Survey of Canada, Paper 88-2, p. 127-153.

Roddick, J.C. and Souther, J.G.
1987: Geochronology of Neogene Volcanic Rocks in the northern Garibaldi Belt, B.C.; in Radiogenic Age and Isotopic studies: Report 1; Geological Survey of Canada, Paper 87-2, p. 25-32.

Steiger, R.H. and Jäger, E.
1977: Subcommission on Geochronology: Convention on the use of decay constants in Geo- and Cosmo-chronology; Earth and Planetary Science Letters, v. 36, p. 359-362.

BRITISH COLUMBIA
(GSC 89-1 to GSC 89-97)

GSC 89-1 Biotite
62 ± 1 Ma

K-Ar 3883 Wt % K = 5.776
Rad. Ar = 1.426 x 10^{-5} cm^3/g
% Atmos. Ar = 17.1

(104 M) From a granite.
Roadcut on Skagway Road close to Tutshi River canyon, 2 km east-northeast of Log Cabin, Skagway map area, B.C. 59°46'11''N, 134°55'56''W. Sample 380-DGA-82-2, collected and interpreted by C.J. Dodds.

The sample is a light pinkish-grey, weakly foliated, coarse-grained, porphyritic hornblende biotite granite. Dark brown, subhedral biotite (6%) and bluish-green, anhedral hornblende (4%) constitute the bulk of the mafic minerals. Both minerals are erratically chloritized and occur mainly as clotted intergrowths. Felsic minerals comprise slightly saussuritized, subhedral, zoned plagioclase; cloudy, subhedral to anhedral and megacrystic microcline; and strained anhedral quartz. Accessories include opaque ore(s), sphene, allanite(?), and zircon.

The rock is a grab sample from a roughly delineated, distinctive megacrystic granite pluton outcropping near Tutshi River. The body forms part of the northeast extremity of the Coast Plutonic Complex.

This biotite K-Ar age compares favourably with biotite and hornblende K-Ar ages of 63.3 and 66.5 Ma respectively, obtained from the pluton by Barker et al. (1986). However, that study also provided two U-Pb zircon ages of 72.4 and 71.6 Ma and suggested that the K-Ar dates from the pluton may record either thermal resetting or post-emplacement uplift.

GSC 89-2 Biotite
54 ± 1 Ma

K-Ar 3886 Wt % K = 6.872
Rad. Ar = 1.469 x 10^{-5} cm^3/g
% Atmos. Ar = 18.1

(104 M) From a granite.
Newly blasted roadcut on Skagway Road near north end of Summit Lake, 5 km due southwest of Fraser, Skagway map area, B.C. 59°40'44''N, 135°05'48''W. Sample 393-DGA-82-1, collected and interpreted by C.J. Dodds.

The sample is a fresh, light pinkish creamy-grey, homogeneous, medium-grained, leucocratic, hornblende biotite granite. Mafic minerals are dominantly clotted, slightly chloritized, subhedral, dark brown biotite (3%) and rare, unaltered, subhedral, bluish-green hornblende. Felsic minerals comprise cloudy, anhedral orthoclase, variably saussuritized, complexly zoned, subhedral plagioclase, and smoky grey quartz. Accessories are of opaque ore(s), zircon and epidote.

The rock is a grab sample from a crudely outlined, apparently homogeneous, distinctive granite pluton underlying the Summit Lake area. The intrusion lies within the northern part of the Coast Plutonic Complex. Sharp cross-cutting contacts with host granitic rocks indicate the body to be among the younger plutons in the area, and local miarolitic cavities suggest a shallow emplacement.

The Eocene K-Ar age from this biotite separate closely agrees with the 52 Ma K-Ar biotite age and the nearly concordant 53 Ma U-Pb zircon age obtained from this pluton by Barker et al. (1986). Plutons similar in lithology, setting, and age to this body occur fairly widely in adjoining parts of the Coast Belt and constitute the Eocene suite of Morrison et al. (1979).

REFERENCES

Barker, F., Arth, J.G., and Stern, T.W.
1986: Evolution of the Coast batholith along the Skagway Traverse, Alaska and British Columbia; American Mineralogist, v. 71, p. 632-643.

Morrison, G.W., Godwin, C.I., and Armstrong, R.L.
1979: Interpretation of isotopic ages and $^{87}Sr/^{86}Sr$ initial ratios for plutonic rocks in the Whitehorse map area, Yukon; Canadian Journal of Earth Sciences, v. 16, p. 1988-1997.

GSC 89-3 Biotite
103 ± 2 Ma

K-Ar 3805 Wt % K = 7.554
Rad. Ar = 3.125 x 10^{-5} cm^3/g
% Atmos. Ar = 12.3

(104 P) From a granite.
See GSC 89-6 for sample location and discussion.

GSC 89-4 Biotite
103 ± 3 Ma

K-Ar 3803 Wt % K = 7.559
Rad. Ar = 3.108 x 10^{-5} cm^3/g
% Atmos. Ar = 21.6

(104 P) From a granite.
See GSC 89-5 for sample location and GSC 89-6 for discussion.

GSC 89-5 Hornblende
110 ± 3 Ma

K-Ar 3804 Wt % K = 0.749
Rad. Ar = 3.303 x 10^{-6} cm^3/g
% Atmos. Ar = 20.3

(104 P) From a granite.
From quarry on west side of Highway 37 and Dease River, north end of Pinetree Lake. 59°02'00''N, 129°46'30''W. Sample GAH-85-353B, collected and interpreted by H. Gabrielse.

See GSC 89-6 for discussion.

GSC 89-6 Muscovite
100 ± 2 Ma

K-Ar 3806 Wt % K = 5.990
Rad. Ar = 2.399 x 10^{-5} cm^3/g
% Atmos. Ar = 12.7

(104 P) From a granite.
Roadcut on west side of Highway 37 and Dease River near north end of Pinetree Lake. 59°01'00''N, 129°47'30''W. Sample GAH-85-354, collected and interpreted by H. Gabrielse.

The granite sampled for age determination is typical of a two-mica phase of the Cassiar Batholith, the largest mid-Cretaceous pluton in the Omineca Belt. Another phase is characterized by biotite and hornblende (see GSC 89-4, 89-5) whereas some leucocratic lithologies contain only biotite as the mafic mineral. The K-Ar ages are in agreement with those obtained elsewhere along the length of the pluton.

GSC 89-7 Biotite
116 ± 3 Ma

K-Ar 3946 Wt % K = 6.777
Rad. Ar = 3.153 x 10^{-5} cm^3/g
% Atmos. Ar = 20.4

(104 J) From a quartz monzodiorite.
On south bank of deep easterly trending gorge about 1.5 km north of Canyon Creek west of Dease River. 58°54'15''N, 130°03'20''W. Sample GA85-10, collected and interpreted by H. Gabrielse.

This sample represents one phase of a granitic complex assigned to the terrane Quesnellia. The complex includes hornblende diorite to granodiorite intruded by pink weathering rocks containing more abundant K-feldspar. The larger homogeneous bodies of pink weathering rocks approach granite in composition and locally have mid-Cretaceous K-Ar ages. It is not known whether the discordant ages obtained from GSC 89-7 and 89-8 are the result of partial resetting of older systems or approximate a time of intrusion. To the southeast in Cry Lake map area similar ages have been obtained on rocks of the same composition with the oldest ages on hornblende between 150 and 160 Ma.

GSC 89-8 Hornblende
128 ± 3 Ma

K-Ar 3947 Wt % K = 0.679
Rad. Ar = 3.51 x 10^{-6} cm^3/g
% Atmos. Ar = 16.8

(104 J) From a quartz monzodiorite.
See GSC 89-7 for sample location and discussion.

GSC 89-9 Biotite
122 ± 3 Ma

K-Ar 3807 Wt % K = 7.358
Rad. Ar = 3.612 x 10^{-5} cm^3/g
% Atmos. Ar = 13.7

(104 J) From a schist.
About 2.5 km northeast of the cairn on Northwest Mountain, west of Dease River. 58°57'30''N, 130°03'00''W. Sample GA-85-7b, collected and interpreted by H. Gabrielse.

The schist is part of a regionally metamorphosed sequence of calcareous, siliceous sediments considered to be part of the autochthon (Ancestral North America) upon which the Terrane Quesnellia was emplaced. The discordant ages for GSC 89-9 and 89-10 fall into the same range as do ages for associated granitic rocks in Quesnellia. The oldest age obtained on the schist similar to this sample is 158.3 ± 2.4 Ma but collected farther northeast on biotite.

GSC 89-10 Muscovite
138 ± 2 Ma

K-Ar 3808 Wt % K = 5.546
Rad. Ar = 3.089 x 10^{-5} cm^3/g
% Atmos. Ar = 13.2

(104 J) From a schist.
See GSC 89-9 for sample location and discussion.

GSC 89-11 Biotite
49.1 ± 1.4 Ma

K-Ar 3404 Wt % K = 7.24
Rad. Ar = 140.1 x 10^{-7} cm^3/g
% Atmos. Ar = 12.1

(93 F/16) From granitoid gneiss.
Road cut about 7 km south of the west end of Sinkut Lake, Intermontane Belt, B.C. 53°50.7'N, 124°01.9'W. Sample 80-TD-110AG, collected by H.W. Tipper and interpreted by G.J. Woodsworth. Published as GSC 87-213 without interpretation.

The sample is from a body of granitoid gneiss in a region for which there is no modern geological information. The gneissic nature of the rock and the Eocene date suggest that the body may be a core complex similar to that described by Friedman (1988) in the Tatla Lake area, some 200 km to the south. The Tatla Lake complex also gives Eocene biotite dates (e.g. GSC 78-60) and much of the complex has a mylonitic or gneissic fabric. Tentatively, the 49 Ma date from the Sinkut Lake body reflects the time of unroofing of a core complex during widespread Eocene extension, rather than the age of intrusion.

REFERENCE

Friedman, R.M.
1988: Geology and geochronology of the Eocene Tatla Lake metamorphic core complex, western edge of the Intermontane Belt, British Columbia; unpublished Ph.D. thesis, University of British Columbia, 348p.

GSC 89-12 Biotite
50 ± 2 Ma

K-Ar 3881 Wt % K = 6.558
Rad. Ar = 1.291 x 10^{-5} cm^3/g
% Atmos. Ar = 20.6

(93 E/2) From a porpyritic biotite granodiorite.
About 3.5 km south of the south end of Pondosy Lake, B.C. 53°07.96'N, 126°54.71'W. Sample WV-1003, collected and interpreted by G.J. Woodsworth.

The sample is from a high level granodiorite body at the west edge of the Intermontane Belt. The pluton intrudes volcanic rocks of both the Lower Cretaceous Gambier Group(?) and Upper Cretaceous Kasalka Group. The 50 Ma date agrees with others obtained from similar plutons in the area and indicates an Eocene age of emplacement.

GSC 89-13 Hornblende
82 ± 2 Ma

K-Ar 3888 Wt % K = 0.595
Rad. Ar = 19.48 x 10^{-6} cm^3/g
% Atmos. Ar = 15.0

(92 M/10) From a tonalite.
See GSC 89-14 for description and interpretation.

GSC 89-14 Biotite
85 ± 1 Ma

K-Ar 3887 Wt % K = 7.872
Rad. Ar = 2.677 x 10^{-5} cm^3/g
% Atmos. Ar = 6.6

(92 M/10) From a tonalite.
About 21 km southwest of First Narrows on Owikeno Lake, Coast Mountains, B.C. 51°32.70'N, 126°55.79'W. Sample RD-82-42090, collected and interpreted by G.J. Woodsworth.

The sample is unfoliated biotite-hornblende tonalite containing about 15% mafic minerals, 20% quartz, and 2% K-feldspar (as megacrysts), 63% plagioclase, minor sphene. The sample is from a large, poorly mapped body in the central Coast Plutonic Complex. The date is a 'spot' age in an area of little geochronological control; a unique interpretation of the dates is not possible at present.

GSC 89-15 Hornblende
77 ± 1 Ma

K-Ar 3890 Wt % K = 0.944
Rad. Ar = 2.873 x 10^{-6} cm^3/g
% Atmos. Ar = 9.4

(92 M/15) From a tonalite.
See GSC 89-16 for description and interpretation.

GSC 89-16 Biotite
67 ± 1 Ma

K-Ar 3889 Wt % K = 7.370
Rad. Ar = 1.956 x 10^{-5} cm^3/g
% Atmos. Ar = 12.5

(92 M/15) From a tonalite.
From about 15 km west of the head of South Bentick Arm, Coast Mountains, B.C. 51°59.7'N, 126°53.6'W. Sample RD-82-12026, collected by J.A. Roddick and interpreted by G.J. Woodsworth.

The sample is fresh, weakly foliated hornblende > biotite tonalite containing about 25% mafic minerals, 10% quartz, 5% K-feldspar, 60% plagioclase, and minor sphene and epidote. Hornblende is concentrated in schlieren-like layers. The sample is from a large, poorly mapped body in the west-central Coast Plutonic Complex. The date is a 'spot' age in an area of little geochronological control and unique interpretation of the dates is not possible at this time. However, the discordance between the biotite and hornblende dates suggests a complex history.

GSC 89-17 Biotite
82 ± 2 Ma

K-Ar 3885 Wt % K = 7.698
Rad. Ar = 2.522 x 10^{-5}
% Atmos. Ar = 2.1

(92 J/10) From a granitoid gneiss.
Ridge crest about 3.5 km west-northwest of Mt. Taillefer, eastern margin of Coast Belt, B.C. 50°38.6'N, 122°41.5'W. Sample WVR-84-124, collected and interpreted by G.J. Woodsworth and M.E. Rusmore.

The sample is from the centre of a roughly circular body of biotite quartz diorite. For sample description see Rusmore, 1985.

REFERENCE

Rusmore, M.E.
1985: Geology and tectonic significance of the Upper Triassic Cadwallader Group and its bounding faults, southwestern British Columbia; unpublished Ph.D. thesis, University of Washington, 234 p.

GSC 89-18 Hornblende
164 ± 3 Ma

K-Ar 3977 Wt % K = 0.262
Rad. Ar 17.44 x 10^{-7} cm^3/g
% Atmos. Ar = 22.0

(103 B) From a biotite-hornblende quartz monzodiorite.
West coast of the northernmost of the Bischof Islands, at sea level, 1 km east of Richardson Point, 2.6 km southwest of Sedgwick Point (NTS 103 B/12E), south of Lyell Island, Queen Charlotte Islands, British Columbia, 52°34'47''N, 131°34'09''W (UTM zone 9, N5828400, E325925); see Anderson (1988), Anderson and Greig (1989), and Anderson and Reichenbach (1989). Sample AT-87-122-1, collected and interpreted by R.G. Anderson.

The sample is typical of the foliated, fairly fresh, inclusion-bearing, equigranular, medium-grained, biotite (chlorite)-hornblende quartz monzodiorite of the intermediate phases in the Burnaby Island plutonic suite. The phase crosscuts the Upper Triassic Karmutsen Formation volcanic rocks and is crosscut by aphanitic green andesite dykes.

For interpretation see GSC 89-20.

GSC 89-19 Hornblende
166 ± 3 Ma

K-Ar 3979 Wt % K = 0.521
Rad. Ar = 35.23 x 10^{-7} cm^3/g
% Atmos. Ar = 38.0

(103 B) From a biotite-hornblende gabbro or diorite.
Southeast end of Sac Bay, at sea level, off De La Beche Inlet, 3.5 km west-by-southwest of De La Beche Island, 5.6 km southwest of Darwin Point (NTS 103 B/12E), central Moresby Island, Queen Charlotte Islands, British Columbia, 52°31'56''N, 131°40 25''W (UTM zone 9, N5823375, E318650); see Anderson (1988), Anderson and Greig (1989), and Anderson and Reichenbach (1989). Sample AT-87-115-1, collected and interpreted by R.G. Anderson.

The sample is typical of massive, inclusion-poor, equigranular to seriate, medium- to coarse-grained (poikiloblastic) biotite-hornblende gabbro or diorite, the most mafic and earliest phase of the eastern part of the San Christoval pluton (San Christoval plutonic suite). The pluton intrudes the Upper Triassic Karmutsen Formation and the mafic phase is intruded by the quartz diorite phase.

For interpretation see GSC 89-20.

GSC 89-20 Hornblende
43.7 ± 1.1 Ma

K-Ar 3980 Wt % K = 0.511
Rad. Ar 8.783 x 10^{-7} cm^3/g
% Atmos. Ar = 34.0

(103 B) From a plagioclase-hornblende-biotite porphyry dyke.
Peninsula south of Carpenter Bay, at sea level, north of Benjamin Point, 2 km south of Langtry Island (NTS 103 B/3,), southeastern Moresby Island, Queen Charlotte Islands, British Columbia, 53°12'51''N, 131°00'14''W (UTM zone 9, N5786550, E363100); see Anderson (1988), Anderson and Greig (1989), and Anderson and Reichenbach (1989). Sample AT-87-7-3, collected and interpreted by R.G. Anderson.

The sample is from north-trending plagioclase-hornblende-biotite porphyry dykes that intrude rusty black argillite of Lower Jurassic Sandilands Formation of Upper Triassic-Lower Jurassic Kunga Group. Dykes are part of extensive Carpenter Bay dyke swarm and considered coeval and cogenetic with the Carpenter Bay plutons of the Tertiary Kano plutonic suite

INTERPRETATION OF QUEEN CHARLOTTE ISLAND K-AR RESULTS (GSC 89-18, 19, 20)

The geological settings for the two Jurassic plutonic suites and the Tertiary Kano plutonic suite in Queen Charlotte Islands is outlined in Anderson (1988) and Anderson and Greig (1989). New K-Ar isotopic age data for samples collected in 1987 are reviewed below and in more detail in Anderson and Reichenbach (1989).

Nearly identical K-Ar dates for San Christoval plutonic suite (SCPS; 166 ± 3 Ma) and Burnaby Island plutonic suite (BIPS; 164 ± 3 Ma) hornblendes are slightly older than earlier determinations (145-160 Ma) for the suites (see Young, 1981 for compilation) and emphasize the contemporaneity of the two suites (Fig. 1). A latest Middle to earliest Late Jurassic (Callovian-Oxfordian) isotopic age for BIPS is consistent with its Bajocian to Early Cretaceous stratigraphic age (Anderson and Greig, 1989). Zircon U-Pb geochronometry in progress indicates slightly older isotopic ages for the suites but confirms their contemporaneity (I. Reichenbach, unpub. data).

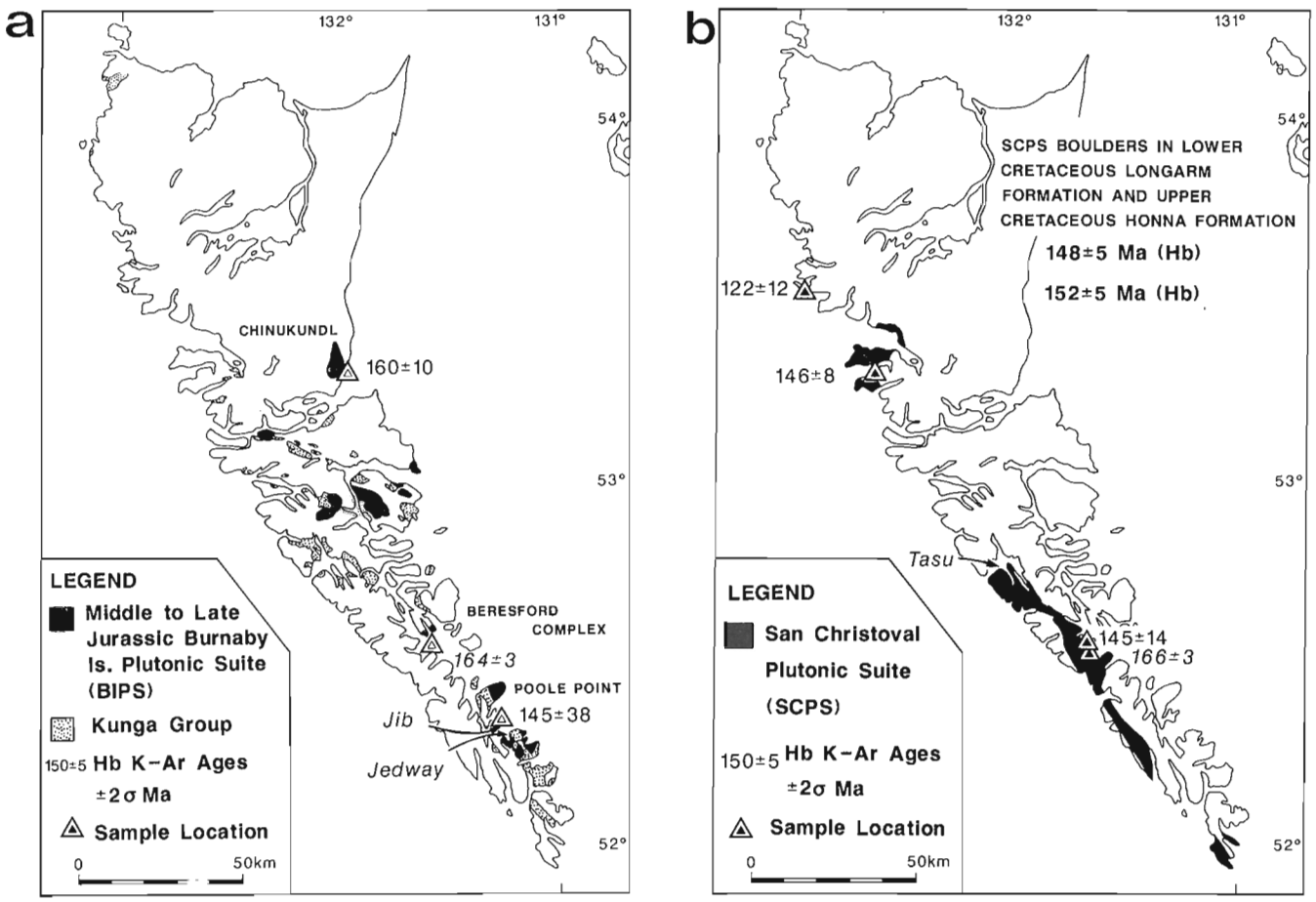

Figure 1. Distribution of Middle to Late Jurassic (a, b) and Tertiary plutonic suites in Queen Charlotte Islands and isotopic ages from Anderson and Reichenbach (1989). New K-Ar dates are shown in italic lettering. Sources for earlier determinations and U-Pb dates are given in Anderson and Reichenbach (1989).

The latest Middle Eocene isotopic age for hornblende from the Carpenter Bay porphyritic dyke (43.7 ± 1.1 Ma) is slightly older than but compares closely with K-Ar ages from the Pocket Inlet pluton (39-40 ± 2 Ma; Young, 1981). The northerly trends of the dykes (e.g. Souther, 1988; Souther and Bakker, 1988) are mimicked by orientation of interphase contacts in Carpenter Bay plutons, which host the dykes. Zircon geochronometry for the Carpenter Bay plutons indicates a slightly older age than the K-Ar date for the dyke, in accord with intrusive relations.

Similar extensional tectonic conditions apparently prevailed through pluton emplacement to the later period of dyke intrusion. Late Eocene (40-44 Ma) extension in southeastern Queen Charlotte Islands is reflected in bimodal plutonism in Pocket Inlet pluton (Anderson and Greig, 1989) and in widespread dyke formation (and coeval plutonism) in and south of Carpenter Bay, southeastern Lyell Island and eastern Faraday Island. Eocene extension-related magmatism may herald the opening of the Queen Charlotte basin.

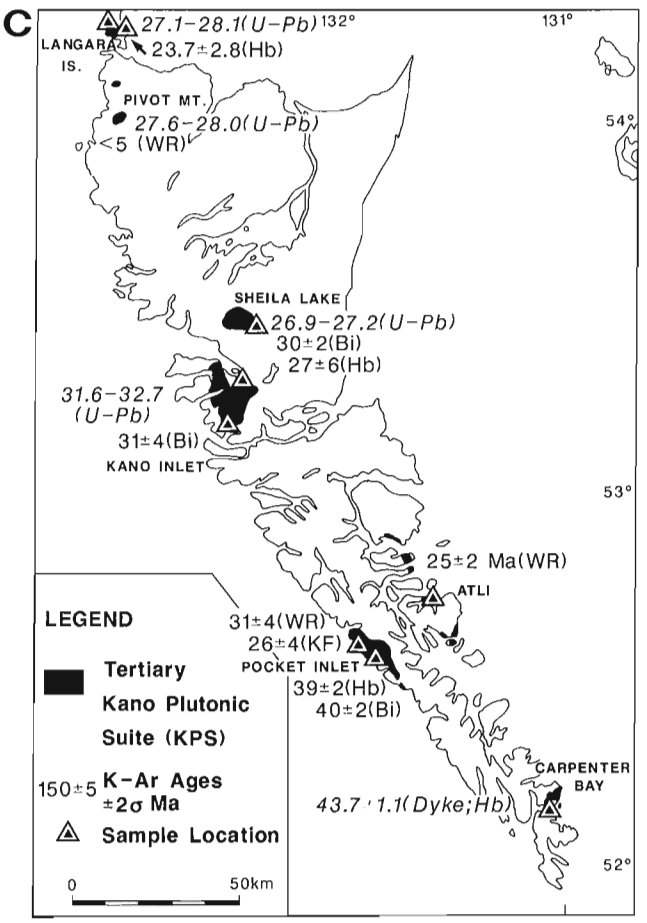

Figure 1. Continued

REFERENCES

Anderson, R.G.
1988: Jurassic and Cretaceous-Tertiary plutonic rocks on the Queen Charlotte Islands, British Columbia; in Current Research, Part E; Geological Survey of Canada, Paper 88-1E, p. 213-216.

Anderson, R.G. and Greig, C.J.
1989: Jurassic and Tertiary plutonism in the Queen Charlotte Islands, British Columbia; in Current Research, Part H; Geological Survey of Canada, Paper 89-1H, p. 95-104.

Anderson, R.G. and Reichenbach, I.
1989: A note on the geochronometry of Late Jurassic and Tertiary plutonism in the Queen Charlotte Islands, British Columbia; in Current Research, Part H; Geological Survey of Canada, Paper 89-1H, p. 105-112.

Souther, J.G.
1988: Implications for hydrocarbon exploration of dyke emplacement in the Queen Charlotte Islands, British Columbia; in Current Research, Part E; Geological Survey of Canada, Paper 88-1E, p. 241-245.

Souther, J.G. and Bakker, E.
1988: Petrography and chemistry of dykes in the Queen Charlotte Islands, British Columbia; Geological Survey of Canada, Open File 1833.

Young, I.F.
1981: Geological development of the western margin of the Queen Charlotte basin, British Columbia; unpublished M.S.C. thesis, University of British Columbia.

K-Ar AGE DETERMINATIONS OF MICAS AND HORNBLENDES IN THE NORTHERN MONASHEE MOUNTAINS, SOUTHEASTERN BRITISH COLUMBIA

Introduction

Potassium-argon age determinations have been made on muscovites, biotites, and hornblendes from three areas in the northern Monashee Mountains of southeastern British Columbia, and the data are summarized in subsequent entries in this report (see table 1). These data were collected as part of a larger study on the cooling and uplift history of the northern Monashee Mountains, a high-grade metamorphic terrane contained within the southern Omineca Crystalline Belt of British Columbia. The results of this study may be found in Sevigny et al. (1990). The K-Ar ages reported here are interpreted as cooling ages from a Middle Cretaceous (?100 Ma) amphibolite-facies metamoprhic event.

Geologic Setting

The northern Monashee Mountains are underlain by late Proterozoic metasediments and metabasalts of the Horsethief Creek Group. Metamorphism was largely coeval with large-scale refolding of an earlier nappe structure, producing a northeast-verging stack of tight to isoclinal second-phase folds (Sevigny and Simony 1989). Muscovites, biotites, and hornblendes crystallized during this event. These minerals

Table 1. K-Ar age determination of micas and hornblendes in the Northern Monashee mountains, southeastern British Columbia.

GSC #	Smpl. #	Lith ; Min	Grid Ref.	K(wt%)	(cc/gm x 10^{-7})	(%)	Age (Ma)
89-21	JS-85-028	Pel ; Bt	708672	6.92	153.2	89.0	56.1 ± 1.0
89-22	JS-85-032	Amph ; Hb	697668	0.412	14.22	81.0	86.7 ± 2.9
89-23	JS-85-038	Amph ; Hb	721687	0.773	22.39	85.0	73.0 ± 2.1
89-24	JS-85-090	Amph ; Hb	675665	0.593	17.01	85.0	72.3 ± 1.5
89-25	JS-85-098	Gran ; Bt	670662	6.77	147.4	82.0	55.2 ± 0.9
89-26	JS-85-098	Gran ; Mus	670662	8.67	171.0	68.0	50.1 ± 0.9
89-27	JS-85-102	Amph ; Hb	667656	1.16	34.51	93.8	74.7 ± 1.9
89-28	JS-85-121	Pel ; Bt	665655	7.44	159.6	91.8	54.4 ± 1.1
89-29	JS-85-123	Gran ; Bt	672683	6.10	122.1	86.0	50.8 ± 0.9
89-30	JS-85-123	Gran ; Mu	672683	8.80	176.3	67.0	50.8 ± 0.7
89-31	JS-85-128	Gran ; Bt	665663	7.12	143.3	90.3	51.1 ± 1.8
89-32	JS-85-128	Gran ; Mu	665663	8.69	179.5	86.0	52.4 ± 1.1
	Howard Ridge Transect						
89-33	JS-85-129	Pel ; Bt	730072	7.14	154.0	90.2	54.7 ± 1.2
89-34	JS-85-129	Pel ; Mu	730072	6.30	114.4	20.0	46.1 ± 1.5
89-35	JS-85-131	Amph ; Hb	753068	0.481	41.62	87.0	209.9 ± 6.0
89-36	JS-85-132	Pel ; Mu	753068	6.73	139.3	73.0	52.5 ± 1.4
89-37	JS-85-132	Pel ; Bt	753068	7.27	164.0	92.4	57.2 ± 1.1
89-38	JS-85-141	Pel ; Mu	794064	6.71	149.9	75.0	56.6 ± 1.2
89-39	JS-85-141	Pel ; Bt	794064	7.07	167.5	92.6	60.0 ± 1.3
89-40	JS-85-143	Amph ; Hb	720070	1.35	73.51	93.5	73.5 ± 1.9
	Mica Creek Transect						
89-41	JS-85-013	Pel ; Bt	927690	7.22	159.0	73.0	55.8 ± 1.2
89-42	JS-85-014	Amph ; Hb	926617	0.671	22.0	74.0	82.4 ± 2.3
89-43	JS-85-015	Amph ; Hb	927590	1.20	34.12	88.0	71.8 ± 2.5
89-44	JS-85-017S	Pel ; Bt	956722	7.29	161.2	87.0	56.0 ± 0.8

Lith = lithology: Pel = metapelite, Amph = amphibolite, and Gran = granite.
Min = mineral dated: Bt = biotite, Mus = muscovite, and Hb = hornblende.
Uncertainty in the age is reported at two sigma deviation.

define a regionally developed axial planar foliation. Mineral separates have been obtained from granites, schists, and amphibolites. The field relations, mineralogy, and age of these lithologies are discussed briefly below.

Granites

Peraluminous granites (samples JS-85-98, JS-85-123, JS-85-128) occur as sills, dykes,and sheeted-bodies that cut the regional, phase-two foliation and lithologic contacts. The granites contain garnet-muscovite-biotite-plagioclase-potassium feldspar-quartz. U-Pb dating of zircon and monazite gives an age of 63 Ma (Sevigny et al., 1989).

Amphibolites

Amphibolites (samples JS-85-14A, -15, -32, -38, -90, -102, -131, -143) occur as: sills(?) up to 100 m thick, boudins of variable size interpreted to represent transposed basalt dykes, and thin layers (1-10 cm) of tuffaceous origin interlayered with metasedimentary rocks (Sevigny, 1987). The amphibolites contain hornblende + plagioclase ± quartz ± sphene ± biotite ± garnet ± ilmenite (Sevigny, 1988).

Schists

Kyanite- and/or sillimanite-bearing schists containing garnet + biotite + quartz + plagioclase ± muscovite ± potassium feldspar ± ilmenite ± rutile ± graphite (samples JS-85-13, -17S, -28, -121, -129, -132, -141) comprise much of the lower most part of the Horsethief Creek Group. These schists are interlayered with amphibolite and have been intruded by 63 Ma peraluminous granite.

Summary

Hornblende, muscovite, and biotite K-Ar ages from the northern Monashee Mountains are: 76.3 ± 5.8 (n=7), 51.4 ± 3.5 (n=6), and 55.1 ± 2.7 (n=10) (mean and one sigma deviation) (Sevigny et al., 1990). Biotites probably have excess argon because they are older than the muscovites. We interpret the hornblende and muscotvite K-Ar ages as reflecting cooling below about 500°C and 350°C, respectively.

REFERENCES

Sevigny, J.H.

1987: Field and stratigraphic relations of amphibolites in the Late Proterozoic Horsethief Creek Group, northern Adams River area, British Columbia; in Current Research, Part A; Geological Survey of Canada, Paper 87-1A, p. 751-756.

1988: Geochemistry of Late Proterozoic amphibolites and ultramafic rocks, southeastern Canadian Cordillera; Canadian Journal of Earth Sciences, v. 25, p. 1323-1327.

Sevigny, J.H. and Simony, P.S.

1989: Geometric relationship between the Scrip Nappe and metamorphic isograds in the northern Adams River area, Monashee Mountains, British Columbia; Canadian Journal of Earth Sciences (in press).

Sevigny, J.H., Parrish, R.R., and Ghent, E.D.

1989: Petrogenesis of peraluminous granites, Monashee Mountains, southeastern Canadian Cordillera; Journal of Petrology, v. 30, p. 557-581.

Sevigny, J.H., Parrish, R.R., Donelick, R., and Ghent, E.D.

1990: Tectonic evolution of the northern Monashee Mountains: constraints on the timing of metamorphism and tectonic denudation of the southern Omineca Crystalline Belt; Geology, v.18, p. 103-106.

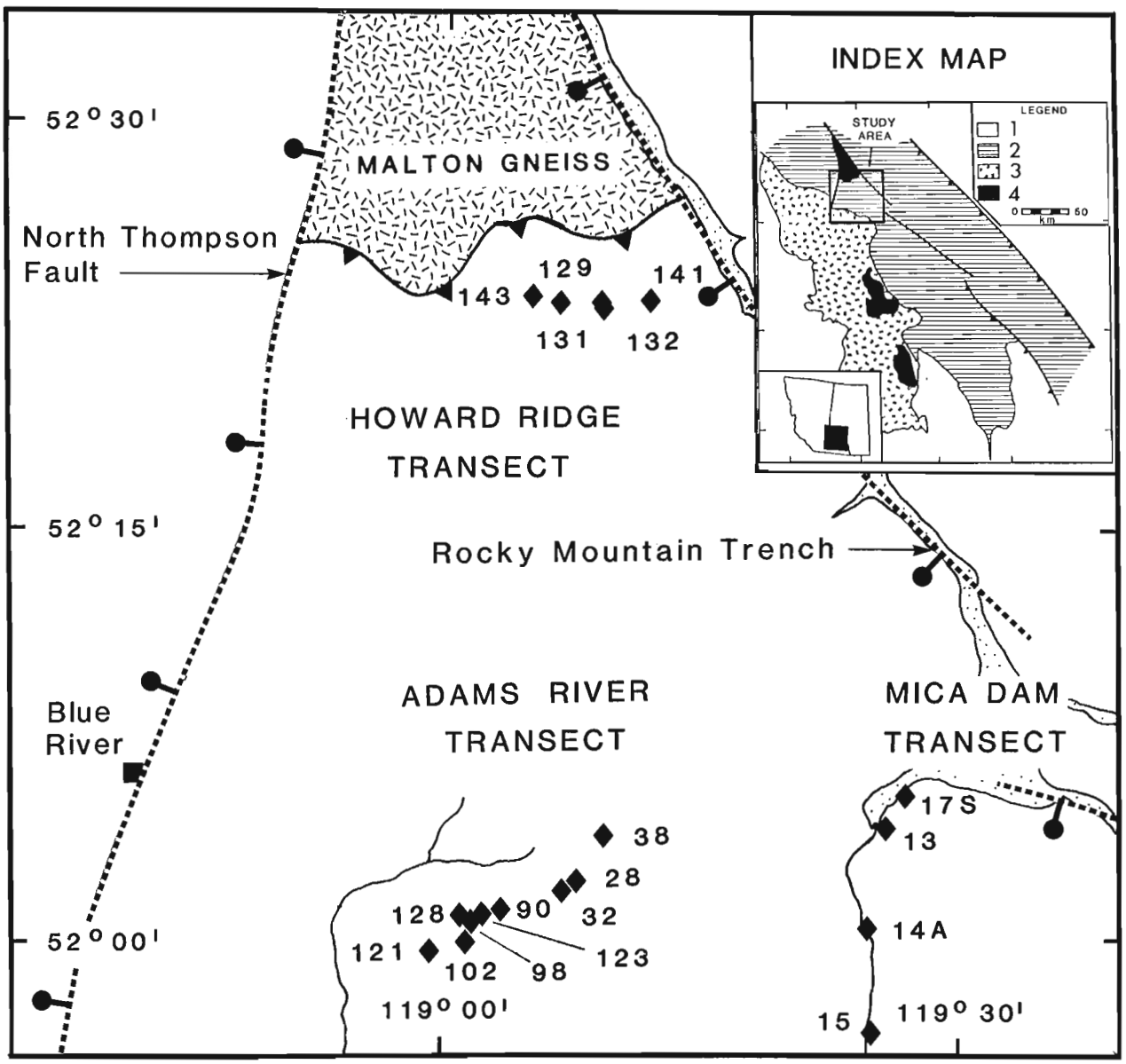

Figure 2. Geological map of the northern Monashee Mountains showing sample location for Adams River, Howard Creek, and Mica Dam transects, and the location of bounding normal faults. Index map: 1 = undifferentiated, 2 = Windermere Supergroup and Lower Paleozoic rocks, 3 = high-grade gneiss of the Shuswap Complex, 4 = basement gneiss.

GSC 89-21 Biotite
56 ± 1 Ma

K-Ar 3863 Wt % K = 6.923
Rad. Ar = 1.532 x 10^{-5} cm^3/g
% Atmos. Ar = 11.2

(83 D) From a schist.
On forest boundary, in col on north-wertheast-west-southwest ridge, B.C., 52°02'30''N, 118°51'45''W. Sample JS-85-28. Collected and interpreted by J. Sevigny.

GSC 89-22 Hornblende
87 ± 3 Ma

K-Ar 3862 Wt % K = 0.412
Rad. Ar = 1.422 x 10^{-6} cm^3/g
% Atmos. Ar = 18.8

(83 D) From an amphibolite.
Elevation 7060ft, on small knob south of icefield on north-northeast-west-southwest ridge, head of south fork of Soards Ck, B.C., 52°02'20''N, 118°52'20''W. Sample JS-85-32. Collected and interpreted by J. Sevigny.

GSC 89-23 Hornblende
73 ± 2 Ma

K-Ar 3861 Wt % K = 0.773
Rad. Ar = 2.239 x 10^{-6} cm^3/g
% Atmos. Ar=15.3

(83 D) From an amphibolite.
Head of the south fork of the Adams River at an elevation of 6520ft, B.C. 50°03'30''N, 118°01'05''W. Sample JS-85-38. collected and interpreted by J. Sevigny.

GSC 89-24 Hornblende
72 ± 2 Ma

K-Ar 3860 Wt % K = 0.593
Rad. Ar = 1.701 x 10^{-6} cm^3/g
% Atmos. Ar = 15.1

(83 D) From an amphibolite.
Elevation 7560ft, first knob on northeast-southwest ridge northeast of col, B.C. 52°02'15''N, 118°55'30''W. Sample JS-85-90. Collected and interpreted by J. Sevigny.

GSC 89-25 Biotite
55 ± 1 Ma

K-Ar 3829 Wt % K = 6.770
Rad. Ar = 1.474 x 10^{-5} cm^3/g
% Atmos. Ar = 18.0

(83 D) From a granite.
In center of small col on northeast-southwest ridge, B.C. 52°02'00''N, 118°56'00''W. Sample JS-85-98. Collected and interpreted by J. Sevigny.

GSC 89-26 Muscovite
50 ± 1 Ma

K-Ar 3828 Wt % K = 8.666
Rad. Ar = 1.71 x 10^{-5} cm^3/g
% Atmos. Ar = 32.0

(83 D) From a granite.
In center of small col on northesat-southwest ridge, B.C.; 52°02'00''N, 118°56'00''W. Sample JS-85-98. Collected and interpreted by J. Sevigny.

GSC 89-27 Hornblende
75 ± 2 Ma

K-Ar 3859 Wt % K = 1.164
Rad. Ar = 3.451 x 10^{-6} cm^3/g
% Atmos. Ar = 6.2

(83 D) From an amphibolite.
Elevation 7500ft, north of icefield and adjacent to north-mortheast ridge, B.C. 52°01'40''N; 118°56'30''W. Sample JS-85-102. Collected and interpreted by J. Sevigny.

GSC 89-28 Biotite
54 ± 1 Ma

K-Ar 3858 Wt % K = 7.436
Rad. Ar = 1.596 x 10^{-5} cm^3/g
% Atmos. Ar = 8.2

(83 D) From a schist.
Upper semi-pelite-amphibolite unit, 100 m below main marble, B.C. 52°01'40''N, 118°56'30''W. Sample JS-85-121. Collected and interpreted by J. Sevigny.

GSC 89-29 Biotite
51 ± 1 Ma

K-Ar 3827 Wt % K = 6.102
Rad. Ar = 1.221 x 10^{-5} cm^3/g
% Atmos. Ar = 13.5

(83 D) From a granite.
On northeast side of small col on northeast-southwest ridge, B.C. 52°02'00''N, 118°56'00''W. Sample JS-85-123. Collected and interpreted by J. Sevigny.

GSC 89-30 Muscovite
51 ± 1 Ma

K-Ar 3826 Wt % K = 8.802
Rad. Ar = 1.763 x 10^{-5} cm^3/g
% Atmos. Ar = 33.0

(83 D) From a granite.
On northeast side of small col on northeast-southwest ridge, B.C. 52°02'00''N, 118°56'00''W. Sample JS-85-123. Collected and interpreted by J. Sevigny.

GSC 89-31 Biotite
51 ± 2 Ma

K-Ar 3857 Wt % K = 7.119
Rad. Ar = 1.433 x 10^{-5} cm^3/g
% Atmos. Ar = 9.7

(83 D) From a granite.
Elevation 6100ft, west of col in northeast-southwest ridge, B.C. 52°02'00''N, 118°56'40''W. Sample JS-85-128. Collected and interpreted by J. Sevigny.

GSC 89-32 Muscovite
52 ± 1 Ma

K-Ar 3856 Wt % K = 8.687
Rad. Ar = 1.795 x 10^{-5} cm^3/g
% Atmos. Ar = 14.2

(83 D) From a granite.
Elevation 6100ft, west of col in northeast-southwest ridge, B.C. 52°02'00''N, 118°56'40''W. Sample JS-85-128. Collected and interpreted by J. Sevigny.

GSC 89-33 Biotite
55 ± 1 Ma

K-Ar 8771 Wt % K = 7.135
Rad. Ar = 1.54 x 10^{-5} cm^3/g
% Atmos. Ar = 9.8

(83 D) From a schist.
Elevation 7560ft, on knob north of north fork of Howard Creek on east-west ridge, B.C. 50°24'30''N, 118°51'35''W. Sample JS-85-129. Collected and interpreted by J. Sevigny.

GSC 89-34 Muscovite
46 ± 1 Ma

K-Ar 3870 Wt % K = 6.297
Rad. Ar = 1.144 x 10^{-5} cm^3/g
% Atmos. Ar = 80.5

(83 D) From a schist.
Elevation 7560ft, on knob north of north fork of Howard Creek on east-west ridge, B.C. 50°24'30''N, 118°51'35''W. Sample JS-85-129. Collected by J. Sevigny.

GSC 89-35 Hornblende
210 ± 6 Ma

K-Ar 3869 Wt % K = 0.481
Rad. Ar = 4.162 x 10^{-6} cm^3/g
% Atmos. Ar = 13.1

(83 D) From an amphibolite.
Elevation 7100ft, on east-west ridge to the east side of a small knob, B.C. 52°24'10''N, 118°49'50''W. Sample JS-85-131. Collected and interpreted by J. Sevigny.

GSC 89-36 Muscovite
53 ± 1 Ma

K-Ar 3867 Wt % K = 6.729
Rad. Ar = 1.393 x 10^{-5} cm^3/g
% Atmos. Ar = 27.2

(83 D) From a schist.
Elevation 7100ft, on east-west ridge to the east side of small knob, B.C. 52°24'10''N, 118°49'50''W. Sample JS-85-132. Collected and interpreted by J. Sevigny.

GSC 89-37 Biotite
57 ± 1 Ma

K-Ar 3868 Wt % K = 7.265
Rad. Ar = 1.64 x 10^{-5} cm^3/g
% Atmos. Ar = 7.6

(83 D) From a schist.
Elevation 7100ft, on east-west ridge to the east of small knob, B.C. 52°24'10''N, 118°49'50''W. Sample JS-85-132. Collected and interpreted by J. Sevigny.

GSC 89-38 Muscovite
57 ± 1 Ma

K-Ar 3865 Wt % K = 6.709
Rad. Ar = 1.499 x 10^{-5} cm^3/g
% Atmos. Ar = 24.7

(83 D) From a schist.
Elevation 6590ft, on the east end of Howard Ridge, B.C. 52°24'00''N, 118°46'00''W. Sample JS-85-141. Collected and interpreted by J. Sevigny.

GSC 89-39 Biotite
60 ± 1 Ma

K-Ar 3866 Wt % K = 7.065
Rad. Ar = 1.675 x 10^{-5} cm^3/g
% Atmos. Ar = 7.4

(83 D) From a schist.
Elevation 6590ft, on the east end of Howard Ridge, B.C. 52°24'00''N, 118°46'00''W. Sample JS-85-141. Collected and interpreted by J. Sevigny.

GSC 89-40 Hornblende
74 ± 2 Ma

K-Ar 3864 Wt % K = 1.346
Rad. Ar = 3.925 x 10^{-6} cm^3/g
% Atmos. Ar = 6.5

(83 D) From an amphibolite.
Howard Ridge area, elevation 8040ft, adjacent to icefield, B.C. 52°25'25''N, 118°52'30''W. Sample JS-85-143. Collected and interpreted by J. Sevigny.

GSC 89-41 Biotite
56 ± 1 Ma

K-Ar 3872 Wt % K = 7.223
Rad. Ar = 1.59 x 10^{-5} cm^3/g
% Atmos. Ar = 27.3

(83 D) From a schist.
1.6 km south of Mica Dam on the road, B.C. 52°05'50''N, 118°34'00''W. Sample JS-85-13. Collected and interpreted by J. Sevigny.

GSC 89-42 Hornblende
82 ± 2 Ma

K-Ar 3873 Wt % K = 0.671
Rad. Ar = 2.2 x 10^{-6} cm^3/g
% Atmos. Ar = 26.4

(83 D) From an amphibolite.
8.0 km north of Birch Creek, 1.7 km south of Mica townsite, B.C. 51°59'50''N, 118°33'48''W. Sample JS-85-14. Collected and interpreted by J. Sevigny.

GSC 89-43 Hornblende
72 ± 2 Ma

K-Ar 2874 Wt % K = 1.199
Rad. Ar = 3.412 x 10^{-6} cm^3/g
% Atmos. Ar = 11.5

(83 D) From an amphibolite.
5.3 km north of Birch Creek on the road, B.C. 51°58'20''N, 118°33'50''W. Sample JS-85-15. Collected and interpreted by J. Sevigny.

GSC 89-44 Biotite
56 ± 1 Ma

K-Ar 3875 Wt % K = 7.289
Rad. Ar = 1.612 x 10^{-5} cm^3/g
% Atmos. Ar = 13.0

(83 D) From a schist.
On the road at the Potlatch Creek/McNaughton Lake locality, B.C. 52°05'40''N, 118°31'30''W. Sample JS-85-17S. Collected and interpreted by J. Sevigny.

GSC 89-45 Biotite
49 ± 1 Ma

K-Ar 3893 Wt % K = 7.564
Rad. Ar = 1.449 x 10^{-5} cm^3/g
% Atmos. Ar = 2.2

(82 E) From a Dacite.
CP abandoned railway near Highway 33 and Devil Creek, B.C. 49°42'35''N, 119°06'50''W. Sample MBX-4. Collected and interpreted by Marc Bardoux.

Sample was taken from a dacitic dyke cutting through deformed coarse-grained granodiorite. The dyke contains biotite and hornblende phenocrysts in an aphanitic matrix and resembles a rhyodacitic unit occurring in large outliers 5 km north of this locality. Bardoux and Irving (in press) correlated both rocks with the Marama Formation of Church (1973). The undeformed texture of the dyke suggests that regional deformation associated with the Okanagan Valley Fault had ceased 49 Ma ago.

REFERENCE

Church, B.N.
1973: Geology of the White Lake Basin; British Columbia Department of Mines and Petroleum Resources, Bulletin 61, 120p.

Bardoux, M., and Irving, E.
1989: Paleomagnetism of Eocene rocks of the Kelowna and Castlegar area, British Columbia: studies and determining paleo-horizontal; Canadian Journal of Earth Sciences, v. 26, 829-844.

GSC 89-46 Biotite
159 ± 2 Ma

K-Ar 3894 Wt % K = 7.742
Rad. Ar = 4.999 x 10^{-5} cm^3/g
% Atmos. Ar = 2.1

(82 E) From a biotite granodiorite.
Highway 33 near Arlington Lakes, B.C. 49°37'52''N, 119°03'30''W. Sample MXB-39-83. Collected and interpreted by Marc Bardoux.

Sample was taken from an undeformed coarse-grained biotite granodiorite interlayered with gneisses. Biotite in the granodiorite rarely exceeds 10% of the modal composition and occurs either as small aggregates or individual crystals with ragged boundaries. Textures of the granitic assemblage show an important degree of dynamic recrystallization formed in a tectonized environment. This age is interpreted as a crystallization age and is similar to crystallization ages of other plutonic bodies (Similkameen and Okanagan complex) occurring on the west side of Okanagan Lake (Tempelman-Kluit and Parkinson, 1985).

REFERENCE

Tempelman-Kluit, D., and Parkinson, D.
1985: Extension across the Eocene Okanagan crustal shear in British Columbia; Geology, v. 14, p. 318-321.

GSC 89-47 Biotite
50 ± 1 Ma

K-Ar 3895 Wt % K = 6.929
Rad. Ar = 1.378 x 10^{-5} cm^3/g
% Atmos. Ar = 5.0

(82 E) From a rhyodacitic porphyry.
Trépanier Creek, south of Mount Law, B.C. 49°48'15''N, 119°44'35''W. Sample MBX-1. Collected and interpreted by Marc Bardoux.

Sample was taken from a quartz-biotite-orthoclase rhomb porphyry at the base of an Eocene volcanic pile, which is unconformably overlying a granodiorite of Mesozoic age. The unit is local and contains up to 50% subhedral phenocrysts in an aphanitic matrix. Similar hypabyssal rocks occur in the south near Shingle Creek and Beaverdell (Little, 1961). This date is interpreted as a crystallization age. It is 2 Ma older than another date (47.7 ± 1.4 Ma) obtained by Church (1981) from altered biotites in a layered rhyolitic lava located stratigraphically above the present sample, 500 m east of the present location.

REFERENCES

Little, H.W.
1961: Kettle River (west half), B.C.; Geological Survey of Canada, Map 15-1961.

Church, B.N.
1981: Geology of the Kelowna Tertiary outlier; British Columbia Ministry of Mines and Petroleum Resources, Preliminary map 35.

GSC 89-48 Biotite
54 ± 2 Ma

K-Ar 3896 Wt % K = 6.685
Rad. Ar = 1.414 x 10^{-5} cm^3/g
% Atmos. Ar = 5.5

(82 E) From a trachyandesite.
Logging road west of McCullough Creek, B.C. 49°54'30''N, 119°36'56''W. Sample MBX-2. Collected and interpreted by M. Bardoux.

Sample was taken from a porphyritic trachyandesite cutting through a Mesozoic hornblende granitoid body (GSC 89-52). Unit is correlated with the Kitley Lake Member of the Marron Formation (Church, 1973) and contains up to 15% plagioclase and biotite phenocrysts. This age is slightly older than three other ages obtained from biotite fractions in similar rocks (53 ± 2 Ma) by Church (1981, 1982) in the Kelowna outlier and White Lake basin near Penticton. The data are interpreted as a crystallization age.

REFERENCES

Church, B.N.
1973: Geology of the White Lake basin; British Columbia Department of Mines and Petroleum Resources, Bulletin 61, 120p.

1981: Geology of the Kelowna Tertiary outlier; British Columbia Ministry of Mines and Petroleum Resources, Revised Preliminary Map 45.

1982: Geology of the Penticton Tertiary outlier; British Columbia Ministry of Mines and PetroleumResources, Preliminary map 35.

GSC 89-49 Hornblende
44 ± 1 Ma

K-Ar 3897 Wt % K = 1.065
Rad. Ar = 1.849 x 10^{-6} cm^3/g
% Atmos. Ar = 74.7

(82 E) From an amphibolite.
CP abandoned railway near the headwaters of Hydraulic Creek, B.C. 49°48'15''N, 119°14'50''W. Sample MBX-48-85. Collected and interpreted by M. Bardoux.

Same unit as GSC 89-52. This age is 4 Ma younger than the biotite age of the same unit and likewise indicates an Eocene thermal event.

GSC 89-50 Biotite
48 ± 1 Ma

K-Ar 3900 Wt % K = 7.522
Rad. Ar = 1.412 x 10^{-5} cm^3/g
% Atmos. Ar = 18.0

(82 E) From an amphibolite.
CP abandoned railway near the headwaters of Hydraulic Creek, B.C. 49°48'15''N, 119°14'50''W. Sample MBX-48-85. Collected and interpreted by M. Bardoux.

Sample was taken from a coarse-grained amphibolite in a paragneissic section correlated with the Vaseaux Formation (Bostock, 1941; Christie, 1965). The rock is coarse grained with 60% subhedral hornblende slightly chloritized and 20% biotite. The date implies that high-grade gneisses of this area were thermally reheated and rapidly cooled during the Eocene Epock.

REFERENCES

Bostock,H.S.
1941: Okanagan Falls, British Columbia. Geological Survey of Canada, Map 341 A.

Christie, J.S.
1965: Geology of the Vaseaux Lake area; unpublished Ph.D. thesis, University of British Columbia, 136p.

GSC 89-51 Hornblende
51 ± 1 Ma

K-Ar 3899 Wt % K = 0.993
Rad. Ar = 2.011 x 10^{-6} cm^3/g
% Atmos. Ar = 58.2

(82 E) From a paragneiss.
Lakeshore road, 2 km before entrance gate to Okanagan Mountain Provincial Park, B.C. 49°46'35''N, 119°34'15''W. Sample MBX-229. Collected and interpreted by Marc Bardoux.

Sample was taken from a medium-grained hornblende-rich layer within a mylonitized paragneiss section interlayered with calc-silicate rocks. The sampled section is correlated with the Vaseaux Formation of (Bostock, 1941). The rock is intensely deformed and chloritized. The date agrees with the general characteristic that high-grade rocks of the Okanagan gneiss complex were reheated in Eocene time.

REFERENCE

Bostock, H.S.
1941: Okanagan Falls, British Columbia. Geological Survey of Canada, Map 341 A.

GSC 89-52 Hornblende
157 ± 2 Ma

K-Ar 3998 Wt % K = 0.765
Rad. Ar = 4.883 x 10^{-6} cm^3/g
% Atmos. Ar = 25.0

(82 E) From a biotite granodiorite.
Headwaters of McCullough Creek, B.C. 49°56'35''N, 119°36'55''W. Sample MBX-32-85. Collected and interpreted by M. Bardoux, 1985.

Sample was taken from biotite granodiorite unconformably overlain by Eocene trachyandesites. This age agrees with several other crystallization ages of other granitic bodies west of Okanagan Lake (Tempelman-Kluit and Parkinson, 1985) and suggests that this unit was not reheated above 300°C since its emplacement. The age of this intrusive body also agrees with that of sample GSC 89-46 (dated 159 ± 2 Ma) suggesting a comagmatic origin for several plutonic bodies adjacent to the Okanagan Valley.

REFERENCE

Tempelman-Kluit, D. and Parkinson, D.
1985: Extension across the Eocene Okanagan crustal shear in British Columbia; Geology, v. 14, p. 318-321.

GSC 89-53 Hornblende
55 ± 1 Ma

K-Ar 3901 Wt % K = 1.184
Rad. Ar = 2.579 x 10^{-6} cm^3/g
% Atmos. Ar = 14.3

(82 E) From a hornblende orthogneiss.
Kelowna quarry, B.C. 49°49'35''N, 119°21'52''W. Sample MX-133. Collected and interpreted by M. Bardoux.

Sample was taken from a chloritized mylonitic hornblende orthogneiss located at high structural levels in the Okanagan gneiss complex near an Eocene volcanic outlier. The rock is medium to fine grained with unannealed strain fabrics. Hornblende forms less than 5% of the modal composition and is anhedral and partly retrograded to chlorite. The sampled unit is interpreted as a strained equivalent of Mesozoic granitoids. This Eocene date agrees with the presence of a regional thermal event overprinting high-grade rocks of south-central British Columbia.

GSC 89-54 Hornblende
51 ± 1 Ma

K-Ar 3902 Wt % K = 0.779
Rad. Ar = 1.575 x 10^{-6} cm^3/g
% Atmos. Ar. = 22.1

(82 E) From an amphibolite.
Siemalt Speedway near Highway 33, B.C. 49°46'08''N, 119°07'07''W. Sample MBX-5. Collected and interpreted by M. Bardoux.

This date agrees with a similar hornblende age of 54.4 ± 2 Ma obtained by Medford (1975) from an altered paragneiss located 1 km north of the present locality. Same interpretation as for GSC 89-55.

REFERENCE

Medford, G.A.
1975: Geology of Okanagan Mountain; unpublished Ph.D. thesis, University of British Columbia, 126p.

GSC 89-55 Biotite
49 ± 1 Ma

K-Ar 3903 Wt % K = 7.636
Rad. Ar = 1.482 x 10^{-5} cm^3/g
% Atmos. Ar = 4.3

(82 E) From an amphibolite.
Siemalt Speedway near Highway 33, B.C. 49°46'08''N, 119°07'07''W. Sample MBX-5. Collected and interpreted by M. Bardoux.

Sample was taken from massive amphibolite interlayered with well banded orthogneiss and overlain unconformably by Eocene dacitic lava flows and conglomerate. The rock is coarse grained, with euhedral hornblende containing pyroxene cores. Unit was interpreted as equivalent to Vaseaux Formation (Bostock, 1941). This date is slightly younger than the hornblende date on the same sample (GSC 89-54) and confirms that a major thermal event was overprinted in Eocene time on rocks of the Okanagan gneiss complex. The 2 Ma difference between hornblende and biotite ages of the same sample suggest a very rapid cooling rate in the order of 100°C/Ma.

REFERENCE

Bostock, H.S.
1941: Okanagan Falls, British Columbia; Geological Survey of Canada, Map 341 A.

VALHALLA COMPLEX

The following eleven K-Ar dates on hornblende and biotite come mostly from Valhalla Complex or its immediately overlying metaplutonic rocks above the Valkyr shear zone, B.C: GSC 89-56, 57, 58, 59, 60, 61, 62, 63, 64, 65, 66.

In general, as outlined by Parrish et al. (1988) and Carr et al. (1987), hornblendes from foliated to gneissic metaplutonic rocks of Valhalla Complex are 56-60 Ma old, reflecting cooling during uplift and tectonic denudation. Similarly, biotite K-Ar ages are close to 50 Ma, somewhat younger because of its lower closure temperature. Three cross-cutting bodies (GSC 89-62, 89-61, 89-58) are somewhat younger and place upper limits to the age of uplift and cooling of the complex.

Two samples, from Grand Forks Complex (GSC 89-66) and beneath Columbia River Fault near Burton (GSC 87-56), are in similar structural positions to rocks of Valhalla Complex, and their hornblende ages are similarly about 60-65 Ma.

REFERENCES

Parrish, R.R., Carr, S.D. and Parinson, D.L.
1988: Eocene extensional tectonics and geochronology of the southern Omineca Belt, British Columbia and Washington; Tectonics, v. 7, p. 181-212.

Carr, S.D., R. Parrish, and R.L. Brown
1987: Eocene structural development of the Valhalla Complex, southeastern British Columbia; Tectonics, v. 6, p. 175-196.

GSC 89-56 Hornblende
107 ± 2 Ma

K-Ar 3811 Wt % K = 0.495
Rad. Ar = 2.127 x 10^{-6} cm^3/g
% Atmos. Ar = 25.5

(82 F) From a hornblende-biotite quartz diorite.
Roadcut on Sullivan Creek logging road at 3000ft elevation, 3 km southwest of Genelle, B.C. UTM Zone 11 u, 446150E, 5449250N. Sample PCA-27-85. Collected and interpreted by R.R. Parrish.

This is part of the foliated base of the Middle Jurassic Mackie Pluton. The sample occurs in the upper part of the zone of strain proximal to the Valkyr shear zone, which separates the Mackie pluton (and other related Jurassic plutons of the Nelson suite) from the underlying gneisses of Valhalla Complex. The hornblende age, like that of GSC 89-65, reflects substantial, but incomplete degassing of Jurassic hornblende in Paleocene-Eocene time, during development of the Valhalla Complex.

GSC 89-57 Hornblende
65 ± 1 Ma

K-Ar 3812 Wt % K = 1.113
Rad. Ar = 2.855 x 10^{-6} cm^3/g
% Atmos. Ar = 22.2

(82 F) From a hornblende- K-feldspar megacrystic quartz monzonite.
Along roadcut of logging road 1.8 km east of Burton, elevation 1950ft, B.C. UTM Zone 11u, 438900E, 5537300N. Sample PCA-264-85. Collected and interpreted by R.R. Parrish

This K-feldspar megacrystic quartz monzonite is slightly to moderately foliated and lies in the footwall of the southernmost part of the Columbia River normal fault. It displays east-directed kinematic indicators consistent with its fabric development being related to the Columbia River fault. It is part of the Caribou Creek Stock and is identical in lithology to the Whatshan batholith. A preliminary U-Pb zircon age is ca. 79 Ma, and the 65 ± 1 Ma hornblende K-Ar age reflects partial degassing during the Eocene Epock.

GSC 89-58 Hornblende
45 ± 1 Ma

K-Ar 3813 Wt % K = 0.838
Rad. Ar = 1.489 x 10^{-6} cm^3/g
% Atmos. Ar = 20.9

(82 F) From a granite.
On ridge between Blueberry and Chinas Creeks, elevation 1920 m, B.C. UTM Zone 11u, 444700E, 5456100N. Sample PCA-ST-85-1. Collected by D. Halwas and P. Simony and interpreted by R.R. Parrish.

The published U-Pb zircon age of this undeformed, cross-cutting granite is 47 Ma. The intrusion cuts the Valkyr shear zone and places constraints on the youngest age of displacement in it. The hornblende is nearly concordant with the zircon age, suggesting rapid cooling following crystallization.

GSC 89-59 Hornblende
56 ± 1 Ma

K-Ar 3814 Wt % K = 1.039
Rad. Ar = 2.292 x 10^{-6} cm^3/g
% Atmos. Ar = 24.8

(82 F) From a hornblende leucosyenite.
Outcrop at 4650ft in cleared logged area near drainage divide of Robson Ridge, 13.5 km west. of Castlegar, B.C. UTM Zone 11u, 438300E, 5462250N. Sample PCA-34A-85. Collected and interpreted by R.R. Parrish.

The sample is a hornblende ± clinopyroxene ± biotite leucocratic syenite or syenodiorite near the trace of the Valkyr shear zone. The 56 Ma K-Ar age is probably a cooling age, and a minimum for crystallization. The hornblende age is similar to others in Valhalla Complex.

GSC 89-60 Hornblende
71 ± 1 Ma

K-Ar 3815 Wt % K = 1.056
Rad. Ar = 2.974 x 10^{-6} cm^3/g
% Atmos. Ar = 15.5

(82 F) From a megacrystic granodiorite.
Roadcut along logging road near switchback at 3800-3850ft on north side of Blueberry Creek, 12 km west-southwest of Castlegar, B.C. UTM Zone 11u 440550E, 5460850N. Sample PCA-9—85-CG. Collected and interpreted by R.R. Parrish.

The sample is a slightly to moderately foliated hornblende-biotite K-feldspar megacrystic granodiorite of the Kinnaird (formerly Castlegar) gneiss. The preliminary U-Pb age of this rock, based on zircons, suggests it is ca. 110 Ma old; its 71 Ma age reflects either near-complex degassing in the Paleocene-Eocene time or cooling through hornblende closure temperatures at ca. 70 Ma. Its young age is similar to other hornblendes of Valhalla Complex.

GSC 89-61 Muscovite
51 ± 1

K-Ar 3832 Wt % K = 8.336
Rad. Ar = 1.671 x 10^{-5} cm^3/g
% Atmos. Ar = 10.7

(82 F) From a muscovite pegmatite.
Elevation 2256 m, on ridge west of Upper Norns Creek, 6.5 km north of Ladybird Mtn., B.C., UTM Zone 11u, 441300E, 5481200N. Sample PCA-83-85. Collected and interpreted by R.R. Parrish

The rock is a cross-cutting pegmatite of the Ladybird granite suite and has a U-Pb zircon and monazite age of ca. 56 Ma. The rock cuts fabric development in the Valkyr shear zone; the 51 ± 1 Ma age reflects cooling below the muscovite closure temperature of about 350°C.

GSC 89-62 Biotite
48 ± 2 Ma

K-Ar 3833 Wt % K = 6.922
Rad. Ar = 1.315 x 10^{-5} cm^3/g
% Atmos. Ar = 4.1

(82 F) From a lamprophyric dyke.
Roadcut along highway 6, about 6 km north of Slocan, 1 km east of bridge over Memphis Creek, elevation 2300ft, B.C. UTM Zone 11u, 467500E, 5518500N. Sample PCA-LDYKE-85. Collected and interpreted by R.R. Parrish.

The biotite from this lamprophyric dyke is an igneous mineral, and the 48 ± 2 Ma probably reflects the age of emplacement and rapid cooling. The dyke cross-cuts the foliation in ca. 58 Ma Ladybird granite on the east side of Valhalla Complex beneath the Slocan Lake normal fault.

GSC 89-63 Hornblende
56 ± 2 Ma

K-Ar 3834 Wt % K = 1.086
Rad. Ar = 2.392 x 10^{-6} cm^3/g
% Atmos. Ar = 12.1

(82 F) From a hornblende-biotite quartz monzonite.
Outcrop on powerline road, elevation 5600ft, west of Koch Creek, B.C., UTM Zone 11u, 430330E, 5507500N. Sample PCA-104-85. Collected and interpreted by R.R. Parrish.

This hornblende age of 56 ± 2 and biotite age of 52 ± 2 Ma (GCS 89-64) are interpreted as cooling ages of an older granitic pluton. These ages are similar to all others within Valhalla Complex where hornblende ages are 58-60 Ma and biotites are ~50 Ma.

GSC 89-64 Biotite
52 ± 2 Ma

K-Ar 3948 Wt % K = 7.230
Rad. Ar = 1.48 x 10^{-5} cm^3/g
% Atmos. Ar = 7.0

(82 F) see GSC 89-63 for location rock type, and interpretation.

GSC 89-65 Hornblende
107 ± 4 Ma

K-Ar 3835 Wt % K = 0.728
Rad. Ar = 3.124 x 10^{-6} cm^3/g
% Atmos. Ar = 11.0

(82 F) From a hornblende quartz diorite.
Roadcut along logging road in upper Ladybird Creek drainage, elevation 5000ft, B.C. UTM Zone 11u, 436150E, 5478050N. Sample PCA-64-85. Collected and interpreted by R.R. Parrish.

The sample is a slightly foliated to massive hornblende quartz diorite structurally above and west of the trace of Valkyr shear zone, an Eocene ductile normal fault. A preliminary U-Pb zircon age of this same sample is in excess of 190 Ma, and the 107 ± 4 Ma K-Ar age is interpreted to reflect substantial but incomplete degassing of Jurassic hornblende during Eocene thermal events associated with development of Valhalla Complex.

GSC 89-66 Hornblende
60 ± 1 Ma

K-Ar 3836 Wt % K = 1.189
Rad. Ar = 2.833 x 10^{-6} cm^3/g
% Atmos. Ar = 15.7

(82 E) From a hornblende syenite gneiss. Roadcut at 550 m elevation, 1 km northwest along road from prominent slag piles, 2.5 km north of Grand Forks, B.C., UTM Zone 11u, 393600E, 543400N. Sample PCA-237-85. Collected and interpreted by R.R. Parrish.

The sample is a foliated to gneissic hornblende syenite that is a folded tabular unit within the Grand Forks complex. A preliminary zircon U-Pb age on this body is Middle Jurassic, and its 60 ± 1 Ma K-Ar age reflects cooling, a pattern similar to all units of the Valhalla Complex.

GSC 89-67 Biotite
55 ± 3 Ma

K-Ar 3837 Wt % K = 6.751
Rad. Ar = 1.47 x 10^{-5} cm^3/g
% Atmos. Ar = 5.5

(82 M) From a granodiorite. Near head of Seymour River, in saddle of ridge due east of small lake, B.C. UTM Zone 11u, 363700E, 5716700N. Sample PCA-M47-85. Collected by R.L. Brown and J.M. Journeay and interpreted by R.R. Parrish.

The sample is a strongly foliated ca. 360 Ma (preliminary U-Pb zircon) granodioritic gneiss laced with abundant leucocratic granitic and pegmatitic dykes. The K-Ar ages for hornblende and biotite, (GSC 89-67, 68) both ca. 55 Ma, reflect total degassing or quenching during the Eocene Epoch as a result of intrusion of Eocene granitic rocks, uplift and tectonic denudation, or both.

GSC 89-68 Hornblende
55 ± 2 Ma

K-Ar 3838 Wt % K = 1.109
Rad. Ar = 2.415 x 10^{-6} cm^3/g
% Atmos. Ar = 14.9

(82 M) See GSC 89-67 for location rock type, and interpretation.

GSC 89-69 Hornblende
185 ± 3 Ma

K-Ar 3831 Wt % K = 1.338
Rad. Ar = 1.013 x 10^{-5} cm^3/g
% Atmos. Ar = 5.9

(82 N) From a hornblende-biotite granodiorite. Southeast ridge of Mount Graham, west of Tangier River, Golden (Rogers Pass) map-area, B.C. 51°10'N, 17°53'W. Sample WB-127-W-9. Collected and interpreted by J.O. Wheeler.

This sample was taken from the Fang Stock, emplaced after the main deformation of the lower Paleozoic Lardeau Group. As reported in GSC Paper 63-17 it yielded a K-Ar date of 172 Ma (new constant).

This sample was rerun yielding a K-Ar date of 185 ± 3 Ma, which appears to be too old for two reasons. First, farther south in Kootenay Arc the youngest rocks involved in the deformation before emplacement of Middle Jurassic intrusions are of Toarcian age (Parrish and Wheeler, 1983). According to the DNAG time-scale (Palmer, 1983) the end of the Toarican was at 187 Ma. Thus an age of 185 Ma for the Fang stock leaves little time for the deformation of Toarcian and older rocks in Kootenay Arc. Second, the Fang stock has also yielded a U-Pb zircon age of 167 Ma (R.L. Brown, pers. comm., 1989). It appears, therefore, that the K-Ar of 185 ± 3 Ma is too old and that the sample probably contains excess argon.

REFERENCES

Palmer, A.R.
1983: Decade of North American Geology, 1983, Geologic Time Scale; Geology, v. 11, p. 503-504.

Parrish, R.R. and Wheeler, J.O.
1983: A U-Pb zircon age from the Kuskanax batholith, southeastern British Columbia; Canadian Journal of Earth Sciences, v. 20, p. 1751-1756.

GSC 89-70 Hornblende
86 ± 3 Ma

K-Ar 3907 Wt % K = 0.271
Rad. Ar = 9.239 x 10^{-7} cm^3/g
% Atmos. Ar = 33.4

(92 H/7) From a hornblende feldspar porphyry. On a ridge elevation 6100ft, running northeast from summit of Snass Mountain; bearing N067° and 3.5 km from summit. B.C. 49°17'10''N, 120°55'30''W. Sample MV-86-354. Collected and interpreted by J.W.H. Monger.

This is one of a swarm of similar dykes, that intrude sandstone and shale of the mid- to lower Upper Cretaceous Pasayten Group. The date is considered to be the age of emplacement. The dykes make up about 20% of the total outcrop in this area, and thus record considerable extension. Since the dyke swarm parallels the trend of the major Pasayten Fault, which lies to the east, it is possible that normal movement on the fault took palce at about the time of emplacement. GSC 89-71 is a lithologically similar dyke.

GSC 89-71 Hornblende
85 ± 1 Ma

K-Ar 3908 Wt % K = 0.341
Rad. Ar = 1.151 x 10^{-6} cm^3/g
% Atmos. Ar = 33.1

(92 H/6) From a hornblende feldspar porphyry. On road up Vuitch Creek, 1.1 km west of crossing of Sutter Creek; elevation 4050ft. B.C. Dyke in mid- to Upper Cretaceous Pasayten Group; date is emplacement age. 49°25'20''N, 121°00'40''W. Sample MV-86-0284. Collected and interpreted by J.W.H. Monger.

For interpretation see GSC 89-70.

GSC 89-72 Muscovite
103 ± 2 Ma

K-Ar 3909 Wt % K = 8.701
Rad. Ar = 3.577 x 10^{-5} cm^3/g
% Atmos. Ar = 13.6

(92 H/11) From a granite.
On Coquihalla highway, approximately 1 km south of crossing of Falls Creek, B.C. 49°36'05''N, 121°04'05''W. Sample MV-85-881A. Collected and interpreted by J.W.H. Monger. Muscovite-biotite granite typical of western part of Eagle Plutonic Complex. The date represents a cooling age.

GSC 89-73 Hornblende
25 ± 1 Ma

K-Ar 3913 Wt % K = 0.409
Rad. Ar = 3.943 x 10^{-7} cm^3/g
% Atmos. Ar = 49.5

(92 H/12) From a hornblende biotite granodorite.
From lakeshore, east side of Harrison Lake, and due east of Doctors Point across lake, B.C. 49°39'50''N, 121°57'50''W. Sample MV-85-492. Collected and interpreted by J.W.H. Monger.

Date represents a crystallization date. Body is elongated in a northeast direction; this elongation is probably structurally controlled and is shown by other Chilliwack Plutonic Suite intrusions.

GSC 89-74 Biotite
48 ± 1 Ma

K-Ar 3914 Wt % K = 7.212
Rad. Ar = 1.354 x 10^{-5} cm^3/g
% Atmos. Ar = 13.9

(92 H/11) From a granodiorite.
From a logging road in headwaters of Anderson River, 1 km west of Zupjok Peak, B.C; 49°37'10''N, 121°10'25''W. Sample MVM-85-136. Collected and interpreted by J.W.H. Monger. Hornblende biotite granodiorite from central part of Needle Peak pluton. Concordant biotite and hornblende dates are probably close to crystallization age of the pluton.

GSC 89-75 Hornblende
48 ± 1 Ma

K-Ar 3915 Wt % K = 0.751
Rad. Ar = 1.427 x 10^{-6} cm^3/g
% Atmos. Ar = 19.1

(92 H/11) For rock type, location. and interpretation see GSC 89-74. Sample MVM-85-136. Collected and interpreted by J.W.H. Monger.

GSC 89-76 Biotite
80 ± 1 Ma

K-Ar 3911 Wt % K = 7.472
Rad. Ar = 2.369 x 10^{-5} cm^3/g
% Atmos. Ar = 16.4

(92 H/12) From a biotite granodiorite.
Spuzzum Creek logging road, approx. 9 km northwest of confluence of Spuzzum and Urquhart creeks, and 7.5 km due east of 6220ft peak, B.C. 49°44'N, 121°36'10''W. Sample MV-85-654. Collected and interpreted by J.W.H. Monger.

Specimen comes from near northern limit of Spuzzum batholith, just south of its gradational contact with Scuzzy quartz monzonite. Date is possibly fairly close to age of recrystallization and is typical of K-Ar dates from this part of Coast Belt (see GSC 89-77).

GSC 89-77 Biotite
79 ± 2 Ma

K-Ar 3912 Wt % K = 7.496
Rad. Ar = 2.354 x 10^{-5} cm^3/g
% Atmos. Ar = 9.5

(92 H/13) From a biotite granodiorite.
On ridge top, elevation 5300ft due south of cirque lake; 8.2 km northeast of summit of Cairn Needle, B.C. 49°52'10''N, 121°49'30''W. Sample MV-85-636. Collected by J.W.H. Monger.

see GSC 89-76 for interpretation.

GSC 89-78 Hornblende
137 ± 3 Ma

K-Ar 3905 Wt % K = 0.798
Rad. Ar = 4.432 x 10^{-6}
% Atmos. Ar = 8.1

(92 H/14) From a biotite granodiorite.
Logging road, north side of Spius Creek, 3.6 km above confluence with Maka Creek; elevation 2800ft, B.C. 49°46'05''N, 121°6'20''W. Sample MV-86-118. Collected and interpreted by J.W.H. Monger.

This slightly foliated rock is from the eastern part of the Eagle Plutonic Complex. U-Pb dates from this unit cluster around 150 Ma (C. Greig, UBC, pers. comm.,1989) and the date may reflect resetting during Early Cretaceous intrusion of rocks in western/central parts of the complex (see GSC 89-79).

GSC 89-79 Biotite
108 ± 1 Ma

K-Ar 3906 Wt % K = 7.420
Rad. Ar = 3.205 x 10^{-5} cm^3/g
% Atmos. Ar = 5.7

(92 H/14) From a biotite granodiorite.
On a power line road north of Utzlius Creek, 4.5 km east-southeast of 6012' peak. 49°52'10''N, 121°11'50''W. Sample MV-86-119. Collected and interpreted by J.W.H. Monger.

Sample from central part of Eagle Plutonic Complex; date is similar to others from western parts of the complex (see GSC 89-72), reported by C. Greig (UBC, pers. comm. 1989), although the lithology is closer to that of rocks of the eastern part (see GSC 89-78).

GSC 89-80 Biotite
53 ± 1 Ma

K-Ar 3904 Wt % K = 7.362
Rad. Ar = 1.533 x 10^{-5} cm^3/g
% Atmos. Ar = 15.7

(92 H/16) From a biotite quartz feldspar porphyry.
From an old logging road, 1 km northeast of confluence of Siwash and Galena Creeks, elevation 4500ft, B.C. 49°47'25''N, 120°19'10''W. Sample MV-86-117. Collected and interpreted by J.W.H. Monger.

Small intrusion cutting Osprey Lake batholith; intrusion is part of "Otter intrusions" of Rice (1947); the date is probably close to a crystallization age (cf. GSC 89-81)

REFERENCE

Rice, H.M.A.
1947: Geology and mineral deposits of the Princeton map-area, British Columbia; Geological Survey of Canada, Memoir 243, 136p.

GSC 89-81 Biotite
53 ± 1 Ma

K-Ar 3910 Wt % K = 7.469
Rad. Ar = 1.563 x 10^{-5} cm^3/g
% Atmos. Ar = 13.4

(92 H/16) From a biotite quartz feldspar porphyry.
On logging road where it crosses ridge 1.6 km west-southwest of summit of Mount Kathleen, B.C. 49°45'30''N, 120°04'55''W. Sample MV-86-99. Collected and interpreted by J.W.H. Monger.

Forms a small body emplaced in Early Jurassic granodiorite of the Pennask batholith. It is probably one of the Otter intrusions of Rice (1947) (see reference listed under GSC 89-80).

GSC 89-82 Whole Rock
0.760 ± .033 Ma

K-Ar 3850 Wt % K = 1.041
Rad. Ar = 3.075 x 10^{-8} cm^3/g
% Atmos. Ar = 83.3

(92 J/13) From a Basalt.
Intrusive basalt from the summit ridge of Tuber Hill volcano, American high Cascades, B.C. Sample SE070386. Collected and interpreted by J.G. Souther.

Tuber Hill, on the Bridge River upland, is a small composite volcano about 2 km across that still retains much of its original morphology. The lower part of the pile consists of hyaloclastite and pillow lava, formed during an initial subglacial stage of activity. The hyaloclastite is overlain by subaerial columnar flows deposited soon after the edifice was free of glacial meltwater. Moderate erosion has exposed a tabular intrusive body, clearly part of the main feeder system, along the crest of the summit ridge.

This is one of five samples from the area that have been dated. The age is older than expected from the erosional state of Tubor Hill and comparison with ages of more dissected but younger volcanos nearby (see GSC 89-83, 89-86). It may contain some excess argon. Despite this potential problem it is clear that the ages of the volcanic rocks of the Bridge River upland are within or younger than the 0.59 to 0.97 Ma range of ages previously reported by Lawrence et al. (1984) for volcanic rocks from the Salal Creek area. These data suggest that volcanism in the northern Garibaldi Belt, from north of Meager Mountain, was concentrated during a relatively short interval between 400 and 970 ka.

See Roddick and Souther (1987) for details of sample preparation and further interpretation of these samples.

REFERENCES

Lawrence, R.B., Armstrong, R.L. and Berman, R.G.
1984: Garibaldi Group volcanic rocks of the Salal Creek area, southwestern British Columbia; alkaline lavas on the fringe of the predominantly calc-alkaline Garibaldi (Cascade) volcanic arc; Journal of Volcanology and Geothermal Research, v. 21, no. 3/4, p. 255-276.

Roddick, J.C. and Souther, J.G.
1987: Geochronology of Neogene volcanic rocks in the northern Garibaldi Belt, British Columbia; in Radiogenic Age and Isotopic Studies: Report 1; Geological Survey of Canada, Paper 87-2, p. 21-24.

GSC 89-83 Whole Rock
0.598 ± .015 Ma

K-Ar 3854 Wt % K = 0.981
Rad. Ar = 2.279 x 10^{-8} cm^3/g
% Atmos. Ar = 78.8

(92 J/13) From a basalt.
From a pahoehoe tow near the top of the hyaloclastite succession of Tuber Hill volcano, B.C. Sample SE060186. Collected and interpreted by J.G. Souther.

Details as for GSC 89-82.

GSC 89-84 Whole Rock
0.731 ± .027 Ma

K-Ar 3851 Wt % K = 0.998
Rad. Ar = 2.836 x 10^{-8} cm^3/g
% Atmos. Ar = 89.9

(92 J/13) From a basalt.
From a thick flow of columnar basalt near the top of the upper subaerial succession of Tuber Hill volcano, B.C. Sample SE0780586. Collected and interpreted by J.G. Souther.

Details as for GSC 89-82.

GSC 89-85 Whole Rock
0.374 ± .023 Ma

K-Ar 3852 Wt % K = 0.419
Rad. Ar = 6.098 x 10^{-9} cm^3/g
% Atmos. Ar = 93.9

(92 J/13) From a basalt.
From a columnar basalt succession forming a median ridge in the upper part of the Nichols Creek valley, B.C. Sample SE210686. Collected and interpreted by J.G. Souther.

This age is considered to reflect the extrusive age of the basalt flow. See GSC 89-82 for further details.

GSC 89-86 Whole Rock
0.755 ± .018 Ma

K-Ar 3853 Wt % K = 1.051
Rad. Ar = 3.074 x 10^{-8} cm^3/g
% Atmos. Ar = 76.1

(92 J/13) From a basalt.
From the side of Sham Hill volcanic neck, B.C. Sample SE040486. Collected and interpreted by J.G. Souther.

Sham Hill is a steep-sided volcanic neck, about 300 m across at the base, which rises more than 60 m above the southern edge of Bridge River upland. Its bare, glaciated surface is strewn with glacial erratics and no vestiges remain of any associated flows or pyroclastic deposits. Based on its state of erosion this neck appears to be older than Tuber Hill, a nearby volcano dated at 600-750 ka (see GSC 89-82 for further details). The age of this sample is considered to reflect the maximum age of the neck, as some excess argon could be present.

GSC 89-87 Muscovite
85 ± 2 Ma

K-Ar 3816 Wt % K = 7.624
Rad. Ar = 2.583 x 10^{-5} cm^3/g
Atmos. Ar = 11.8

(93 G) From a quartz monzonite.
Approximately 700 m west of the lake at the head of Knutson Creek, Quesnel Lake map area, British Columbia, 52°30'53''N, 119°40'45''W. Sample SCB-84-606. Collected and described by L.C. Struik.

The muscovite is from a 10 m wide foliated, light grey dyke. It has 8% biotite and is cut by a 1 m wide shear zone approximately parallel to the contact. The host rocks are Kazu Group quartzite and schist, which may contain garnet, biotite, chlorite, muscovite, or quartz. The muscovite defines the foliation and may date some of the latest deformation and metamorphism.

GSC 89-88 Biotite
227 ± 4 Ma

K-Ar 3884 Wt % K = 7.01
Rad. Ar = 659.8 x 10^{-7} cm^3/g
% Atmos. Ar. = 3.0

(93 H/15) From a quartz monzonite.
Road-cut of the Maeford Lake Forest Road, central British Columbia. The exact location of the sample site is uncertain because of conflicting records, but the site is certainly along the road east of the pass at the head of the Little River and west of the sharp bend in the road at elevation 4000ft. UTM N5855525 E643955 zone 10. 52°49'56''N, 121°51'47''W. Sample SCB-H83-1. Collected by D. Humer and interpreted by L.C. Struik.

The sample is from the Little River stock, which appears to be confined to the hanging wall of the Little River Fault. The stock intrudes the Hadrynian and lower Paleozoic Cariboo Group, and has little structural fabric. The stock was considered to be Jurassic from lithological and textural comparisons with other plutons of the area, and the Late Triassic age is a surprise.

GSC 89-89 Hornblende
142 ± 2 Ma

K-Ar 3882 Wt % K = 0.464
Rad. Ar = 2.674 x 10^{-6} cm^3/g
% Atmos. Ar = 14.4

(104 N/6) From a granite.
Location is an island on east side of Atlin Lake west of Pike Bay, B.C. 59°19'40''N, 133°15'00'W. Sample 84TD6. Collected and interpreted by H.W. Tipper.

Material is a granite boulder in an Inklin Formation conglomerate that is no older than Early Pliensbachian and no younger than Early Bajocian. Preferred age of the conglomerate is Early Pliensbachian. Age of the granite source is unknown but is probably Late Triassic or older.

The age determination of 142 ± 2 Ma suggests resetting since an Early Cretaceous age as suggested here is impossible.

GSC 89-90 Biotite
78 ± 2 Ma

K-Ar 3809 Wt % K = 7.366
Rad. Ar = 2.276 x 10^{-5} cm^3/g
% Atmos. Ar = 5.4

(92 H/12) From a granodiorite.
South side of Hornet Creek; 4.3 km east-northeast of confluence of Clear Creek and Big Silver Creek, B.C. 49°38'38''N 121°46'38''W. Sample MV-85-444. Collected and interpreted by J.W. Monger.

Poorly foliated, lineated gneissic biotite hornblende granodiorite.

Age date is discordant and older than 55 ± 3 Ma from same rock. Sample lies within strongly deformed chert, pelite, amphibolite, and ultramafic rocks of Cogburn Group in a region where mid- to early Late Cretaceous K-Ar dates are typical. The dates bear some resemblance to the discordant K-Ar dates of (Bi) 39 Ma/(Hb) 54 Ma on the Bear Creek stock, 15 km to south (GSC 88-16, 88-17; MV-85-124).

GSC 89-91 Hornblende
55 ± 3 Ma

K-Ar 3810 Wt % K = 0.681
Rad. Ar = 1.484 x 10^{-6} cm^3/g
% Atmos. Ar = 45.9

(92 H/12) From a granodiorite.
For location and interpretation see GSC 89-90. Sample MV-85-444. Collected and interpreted by J.W. Monger.

GSC 89-92 Biotite
19.3 ± 0.4 Ma

K-Ar 3950 Wt % K = 7.081
Rad. Ar = 5.334 x 10^{-6} cm^3/g
% Atmos. Ar = 35.7

(92 H/5) From a biotite hornblende granodiorite.
North bank of Harrison River, 2.7 km west-southwest of Whippoorwill Point, southwest end of Harrison Lake, B.C. 49°18'04''N 121°50'02''W. Sample MV-85-526. Collected and interpreted by J.W.H. Monger.

Sample is lithologically fairly typical of much of the Chilliwack batholith to SE and east; biotite age is slightly younger than typical Oligocene dates from that batholith, and more closely resembles numbers from the Miocene Mount Barr batholith, although Hb date (24 ± 1 Ma) is typical of Chilliwack Batholith. Interpreted as reset rate.

GSC 89-93 Hornblende
24 ± 1 Ma

K-Ar 3957 Wt % K = 0.337
Rad. Ar = 3.192 x 10^{-7} cm^3/g
% Atmos. Ar = 79.1

(92 H/5) From a biotite hornblende granodiorite.
For location and interpretation see GSC 89-92. Sample MV-85-526. Collected and interpreted by J.W.H. Monger.

GSC 89-94 Biotite
78 ± 1 Ma

K-Ar 3951 Wt % K = 6.783
Rad. Ar = 2.092 x 10^{-5} cm^3/g
% Atmos. Ar = 42.9

(92 H/12) From a biotite hornblende quartz diorite.
From logging road running north of Cogburn Creek; elevation 2800ft, azimuth 209° from Mount Urquhart at distance of 7 km, B.C. 49°22'48''N, 121°38'35''W. Sample MV-85-211. Collected and interpreted by J.W.H. Monger.

Sample fairly typical of much of the Spuzzum batholith; age discordant but close to ca. 90-100 Ma dates from typical Spuzzum. Hornblende pair published GSC 88-15 age = 120.4 ± 2.6 Ma.

GSC 89-95 Biotite
160 ± 3 Ma

K-Ar 3952 Wt % K = 6.076
Rad. Ar = 3.94 x 10^{-5} cm^3/g
% Atmos. Ar = 5.1

(92 H/5) From a biotite quartz monzonite.
From logging road running on west side of Elbow Lake, at bend about 0.8 km from south end, B.C. 49°16'03''N, 121°57'33''W. Sample MV-85-558. Collected and interpreted by J.W.H. Monger.

Date probably close to cooling age of intrusion, as it is comparable to a ca. 160 Ma U-Pb date from small felsic intrusions in Jurassic Harrison Lake volcanics above the head of Vaughan Creek, 13 km to north-northeast, which were determined for the writer at UBC laboratory by P. van der Heyden. Similar granitic rocks (extending to north and northwest of this locality), appear to intrude the little-metamorphosed Jurassic volcanic sequence on their eastern margin.

GSC 89-96 Hornblende
103 ± 3 Ma

K-Ar 3953 Wt % K = 0.260
Rad. Ar = 1.068 x 10^{-6} cm^3/g
Atmos. Ar = 77.5

(92 H/12) From a biotite hornblende granodiorite.
From old logging road above south side of Urquhart Creek, 5 km northeast of Mount Urquhart, B.C. 49°39'40''N, 121°35'45''W. Sample MV-85-652. Collected and interpreted by J.W.H. Monger.

Date probably close to cooling age of intrusion; possibly very slight excess argon. It is within northern part of Spuzzum Batholith, and the date falls close to the 90-100 Ma range typical of that pluton.

GSC 89-97 Muscovite
63 ± 3 Ma

K-Ar 3876 Wt % K = 8.277
Rad. Ar = 2.053 x 10^{-5} cm^3/g
% Atmos. Ar = 11.9

(104 O) From a granite.
North side of northeast-trending ridge, 19 km east of Jennings Lakes, British Columbia, 59°39'27''N, 130°20'44''W. Sample SYA86-34. Collected and interpreted by W.D.Sinclair.

The sample is a leucocratic, medium-grained muscovite granite that consists of approximately 30% quartz, 30% K-feldspar, 30% albite, and 10% muscovite. Apatite, fluorite, and magnetite are prominent accessory minerals. In thin section, the muscovite is clear, colourless, and inclusion-free.

The muscovite age of 63 ± 3 Ma confirms the early Tertiary age of this pluton determined previously as 60 ± 3 Ma* (GSC 67-1). Although its geological contacts were not observed, this pluton lies within the western margin of the mid-Cretaceous Cassiar Batholith, which it has apparently intruded. This intrusion is part of a suite of early Tertiary, fluorine-rich intrusions in the northern Cordillera, many of which are associated with tin-tungsten and silver-lead-zinc deposits and occurrences.

*Age recalculated according to the constants of Steiger and Jäger (1977).

REFERENCE

Steiger, R.H. and Jäger, E.
1977: Subcommission on Geochronology: Convention on the use of decay constants in Geo- and Cosmochronology; Earth and Planetary Science Letters, v. 36, p. 359-362.

YUKON
(GSC 89-98 to GSC 89-107)

GSC 89-98 Biotite
94 ± 2 Ma

K-Ar 3840 Wt % K = 6.664
Rad. Ar = 2.491 x 10^{-5} cm^3/g
% Atmos. Ar = 2.3

(105 K/9) From mid-Cretaceous South Fork volcanic suite.
63 km north-northeast of Ross River, Tay River map area, Yukon 62°31.32'N, 132°3.28'W (UTM zone 8, N6935600, E651590); Sample GGA-85-17A2, collected and interpreted by S.P. Gordey.

The sample is a quartz-biotite-feldspar-hornblende crystal tuff. The stratigraphic position within the volcanic pile is not established. The rock is fresh and the age is interpreted as the age of eruption. The sample was dated to better establish the age range of the South Fork Volcanic suite.

GSC 89-99 Biotite
100 ± 2 Ma

K-Ar 3841 Wt % K = 6.582
Rad. Ar = 2.638 x 10^{-5} cm^3/g
% Atmos. Ar = 3.7

(105 K/9) From mid-Cretaceous South Fork volcanic suite.
2.0 km northeast of peak 7018 ft (2142 m), Tay River map area, Yukon, 62°32.81'N, 132°19.49'W (UTM zone 8, N6937750, E637580); Sample GGA-83-26A, collected and interpreted by S.P. Gordey.

The sample is a quartz-biotite-hornblende-feldspar crystal tuff. The stratigraphic position within the volcanic pile is not established. The rock is fresh, and the age is interpreted as the age of eruption. The sample was dated to better establish the age range of the South Fork volcanic suite.

GSC 89-100 Biotite
101 ± 2 Ma

K-Ar 3842 Wt % K = 4.722
Rad. Ar = 1.898 x 10^{-5} cm^3/g
% Atmos. Ar = 5.9

(105 J/12) From mid-Cretaceous South Fork volcanic suite.
68 km northeast of Ross River, Sheldon Lake map area, Yukon, 62°30.81'N, 131°44.15'W (UTM zone 9, N6934175, E359150); Sample GGA-85-49A1, collected and interpreted by S.P. Gordey.

For interpretation see GSC 89-99.

GSC 89-101 Biotite
98 ± 2 Ma

K-Ar 3843 Wt % K = 6.836
Rad. Ar = 2.665 x 10^{-5} cm^3/g
% Atmos. Ar = 5.4

(105 K/8) From mid-Cretaceous South Fork volcanic suite.
5.5 km southeast of peak 7018 ft (2142 m), Tay River map area, Yukon, 62°29.8'N, 132°17.23'W (UTM zone 8, N6932250, E639750); Sample GGA-85-69D1, collected and interpreted by S.P. Gordey.

The sample is a quartz-biotite-feldspar-hornblende-pyroxene crystal tuff. The stratigraphic position within the volcanic pile is not established. The rock is fresh, and the age is interpreted as the age of eruption. The sample was dated to better establish the age range of the South Fork volcanic suite.

GSC 89-102 Biotite
100 ± 2 Ma

K-Ar 3839 Wt % K = 6.338
Rad. Ar = 2.527 x 10^{-5} cm^3/g
% Atmos. Ar = 3.6

(105 J/4) From mid-Cretaceous South Fork volcanic suite.
25 km east-northeast of Ross River, Yukon Sheldon Lake map area, 62°3.90'N, 131°58.66'W (UTM zone 9, N6884790, E344399); Sample GGA-85-21B1, collected and interpreted by S.P. Gordey.

The sample is a quartz-biotite-feldspar crystal tuff. The stratigraphic position within the volcanic pile is not established. The rock is fresh, and the age is interpreted as the age of eruption. The sample was dated to better establish the age range of the South Fork volcanic suite.

GSC 89-103 Biotite
96 ± 2 Ma

K-Ar 3891 Wt % K = 6.838
Rad. Ar = 2.617 x 10^{-5} cm^3/g
% Atmos. Ar = 1.6

(105 K/15) From a mid-Cretaceous South Fork volcanic suite.
17.3 km west-southwest of confluence of Riddel and South Macmillan rivers, Tay River map area, Yukon, 62°48.03'N, 132°44.66'W (UTM zone 8, N6965175, E615025); Sample GGA-83-24B, collected and interpreted by S.P. Gordey.

The sample is a quartz-feldspar-biotite-hornblende crystal tuff. The stratigraphic position within the volcanic pile is not established. The rock is fresh, and the age is interpreted as the age of eruption. The sample was dated to better establish the age range of the South Fork volcanic suite. Hornblende from the same sample, GSC 89-104, gave a date of 102 ± 2 Ma.

GSC 89-104 Hornblende
102 ± 2 Ma

K-Ar 3892 Wt % K = 0.679
Rad. Ar = 2.779 x 10^{-6} cm^3/g
% Atmos. Ar = 5.9

(105 K/15) From mid-Cretaceous South Fork volcanic suite.
17.3 km west-southwest of confluence of Riddel and South Macmillan rivers, Tay River map area, Yukon, 62°48.03'N, 132°44.66'W (UTM zone 8, N6965175, E615025); Sample GGA-83-24B, collected and interpreted by S.P. Gordey.

The sample is a quartz-feldspar-biotite-hornblende crystal tuff. The stratigraphic position within the volcanic pile is not established. The rock is fresh, and the age is interpreted as the age of eruption. The sample was dated to better establish the age range of the South Fork volcanic suite. A biotite date from the same sample, GSC 89-103 is 96 ± 2 Ma.

GSC 89-105 Hornblende
113 ± 2 Ma

K-Ar 3945 Wt % K = 1.34
Rad. Ar = 60.73 x 10^{-7} cm^3/g
% Atmos. Ar = 12.0

(116B/7) From hornblende alkali-feldspar megacrystic syenite of Mt. Brenner pluton.
3.5 km west of «Lower Syenite Lake», north of Tombstone River and east of Chandindu River, Dawson map area, west-central Yukon; 64°28'09''N, 138°47'25''W (UTM zone 7, N7150950, E605750); see Anderson (1987). Sample AT-87-25-2, collected and interpreted by R.G. Anderson.

The sample is typical of seriate to porphyritic, medium- to coarse-grained, alkali-feldspar megacrystic hornblende-alkali-feldspar syenite of Lambert's (1966) ''monzonite porphyry'' unit. The phase predates undated aplite intrusions and postdates hornblende clinopyroxenite and augite-biotite monzonite phases in the Mount Brenner pluton (Anderson, 1987).

The Early Cretaceous K-Ar isotopic age for the penultimate phase of the Mount Brenner pluton is anomalously old compared to published K-Ar ages for the Tombstone suite (84 ± 13 Ma* (K-Ar, hornblende) and 95 ± 5 Ma* (K-Ar, biotite; Wanless et al., 1968, p. 54; Tempelman-Kluit, 1970, p. 41 and 98). The age is older than mid-Cretaceous Rb-Sr isotopic ages (M.L. Bevier and D. Eaton, unpub. data) for the suite and for a sample of an early phase from the Mt. Brenner pluton. U-Pb isotopic analyses are underway on sphene and zircon from Tombstone, Antimony, Mt. Brenner, and Deadman plutons to resolve the discordant K-Ar isotopic ages.

REFERENCES

Anderson, R.G.
1987: Plutonic rocks in the Dawson map area (116B and C), Yukon Territory; in Current Research, Part A, Geological Survey of Canada, Paper 87-1A; p. 689-697

Lambert, M.R.
1966: Geology of the Mount Brenner stock near Dawson City, Yukon Territory; unpublished M.Sc. thesis, University of British Columbia, Vancouver, 64p.

Steiger, R.H. and Jäger, E.
1977: Subcommission on Geochronology: Convention on the use of decay constants in Geo- and Cosmochronology; Earth and Planetary Science Letters, v. 36, p. 359-362

* Age recalculated according to the constants of Steiger and Jager (1977).

Tempelman-Kluit, D.J.
1970: Stratigraphy and structure of the "Keno Hill Quartzite" in Tombstone River-Upper Klondike River map-areas, Yukon Territory (116 B/7, B/8); Geological Survey of Canada, Bulletin 180, 102p.

Wanless, R.K., Stevens, R.D., Lachance, G.R., and Edmonds, C.M.
1968: Age determinations and geological studies, K-Ar isotopic ages, Report 8; Geological Survey of Canada, Paper 67-2, Part A, 141p.

GSC 89-106 Biotite
78 ± 2 Ma

K-Ar 3800 Wt % K = 6.833
Rad. Ar = 2.116 x 10^{-5} cm^3/g
% Atmos. Ar = 5.1

(105 B) From a mafic dyke.
Near top of northeast-trending ridge, 9.5 km south of Meister Lakes and 19 km north-northwest of Rancheria, Yukon. 60°14'N, 130°23'W. Sample 38-1A. Collected and interpreted by G.W. Lowey.

The biotite is from a mafic dyke that consists of approximately 10% biotite phenocrysts and 5% augite phenocrysts in a fine-grained to aphanitic matrix of augite, plagioclase, magnetite, and trace amounts of apatite. In thin section, biotite forms subhedral grains with about 10% inclusions of pyroxene, magnetite, and minor carbonate.

The date obtained from the biotite (78 ± 2 Ma) is comparable to those from other mafic and felsic intrusions in the Cassiar-Rancheria area and helps document a Late Cretaceous period of intrusion and related mineralization. The dyke from which this sample was obtained parallels a prominent set of joints trending east-west, which, suggests that these joints are at least Late Cretaceous in age.

GSC 89-107 Whole Rock
105 ± 4 Ma

K-Ar 3877 Wt % K = 2.045
Rad. Ar = 8.599 x 10^{-6} cm^3/g
% Atmos. Ar = 4.0

(105 L) From a hornfels.
North side of east-trending ridge, 20 km east of east end of Little Salmon Lake and 3.3 km north of the Campbell Highway, Yukon. 62°11'58'N, 134°09'23'W. Sample SYA86-64A-1. Collected and interpreted by W.D. Sinclair.

The sample is a fine-grained hornfels that consists of about 30% muscovite, 20% biotite, 40% feldspar, and 10% quartz; minor amounts of epidote and fluorite are also present. The hornfels is associated with garnet-diopside-magnetite skarn that contains varied amounts of sphalerite, galena, chalcopyrite, pyrite, pyrrhotite, and scheelite (Green, 1965, p. 38-40). Both the skarn and hornfels are related to a small stock or sill of quartz-feldspar porphyry.

The 105 ± 4 Ma date obtained from the hornfels represents the age of intrusion of the quartz-feldspar porphyry and formation of the related skarn and hornfels. The date suggests that the quartz-feldspar porphyry may be related to granitic rocks of the nearby Glenlyon batholith, which have not been dated radiometrically but are considered by Campbell (1967) to be mid-Cretaceous in age. The age is consistent with other mid-Cretaceous intrusions and related skarn deposits in the northern Canadian Cordillera (Sinclair, 1986).

REFERENCES

Campbell, R.B.
1967: Geology of Glenlyon map-area, Yukon Territory; Geological Survey of Canada, Memoir 352, 92p.

Green, L.H.
1965: The mineral industry of Yukon Territory and southwestern District of Mackenzie, 1964; Geological Survey of Canada, Paper 65-19, 94p.

Sinclair, W.D.
1986: Molybdenum, tungsten and tin deposits and associated granitoid intrusions in the northern Canadian Cordillera and adjacent parts of Alaska; in Mineral Deposits of Northern Cordillera, ed. J.A. Morin; The Canadian Institute of Mining and Metallurgy, Special Volume 37, p. 216-233.

DISTRICT OF MACKENZIE
(GSC 89-108 to GSC 89-109)

GSC 89-108 Hornblende
1822 ± 14 Ma

K-Ar 3962 Wt % K=1.237
Rad. Ar = 1.515 x 10^{-4} cm^3/g
% Atmos. Ar = 0.4

(75 J/8) From a quartz syenite.
Southern part of Lynx Lake, where Thelon River originates; from southern part of a large island along an esker. 62°19'30'N; 106°02'30'W; District of Mackenzie, N.W.T. Sample GFA-85-197. Collected and interpreted by S.S. Gandhi.

An intrusive sheet of quartz syenite occurs in the gneissic domain of Lynx Lake containing abundant garnetiferous quartzo-feldspathic rocks (Gandhi, 1986; Davidson and Gandhi, 1989). The intrusion is exposed along an arcuate zone over 50 km long and up to 4 km wide, at the crest of a 15 km wide antiform plunging gently to the southwest. It has sharp contacts with the gneissic rocks, at low angle to their foliation and layering. Pegmatitic dykes and pods related to the intrusion occur near the contacts.

The intrusion varies in composition from monzonite through quartz syenite to granite, and in texture from medium to coarse grained, and is massive to crudely lineated due to streaky aggregates of mafic minerals. Potash feldspar predominates over plagioclase, and hornblende is generally more abundant than biotite. Quartz makes up to 15% of the rock. Accessory minerals are magnetite, apatite, zircon, and fluorite, and rarely garnet at the contacts.

The K-Ar date of 1822 ± 14 Ma is interpreted as close to the time of emplacement of this gently deformed but little metamorphosed intrusion. It post-dates the intense Hudsonian deformation and high-grade metamorphism of the gneisses, which are believed to be derived from Aphebian platform-shelf sediments (Wright, 1967; Gandhi, 1986; Davidson and Gandhi, 1989). The older granitic rocks in the region are represented by a gneissic granite sample located 25 km south of the quartz syenite sample and dated at *2035 Ma by the K-Ar method (GSC 59-27, Lowdon, 1960; Wright, 1967). The southern margin of the quartz syenite intrusion is close to the northeast-trending Howard Lake shear zone that includes some mylonitized rocks (Gandhi, 1986).

Pegmatitic offshoots of the intrusion south of the margin in the gneisses are in some places affected by shearing related to this shear/mylonite zone. A biotite-rich amphibolitic sheared gneiss sample from this zone, located 20 km southwest of the quartz syenite sample, yielded a K-Ar date of *1672 Ma (GSC 59-28, Lowdon, 1960; Wright, 1967). This date was regarded as too young in relation to the date on the gneissic granite, which is interpreted as younger than the paragneiss-amphibolite (Lowdon, 1960, p. 14-15), but it can be explained now by resetting of the K-Ar isotopic equilibrium in the paragneiss-amphibolite owing to movements along the Howard Lake shear zone that post-date the quartz syenite intrusion mentioned above.

REFERENCES

Davidson, G.I. and Gandhi, S.S.
1989: Unconformity-related U-Au mineralization in the middle Proterozoic Thelon sandstone, Boomerang Lake prospect, Northwest Territories, Canada; Economic Geology, v. 84, p. 143-157.

Gandhi, S.S.
1986: Garnetifeorus gneisses and a quartz syenite intrusive sheet at Lynx Lake, Northwest Territories; in Current Research, Part B; Geological Survey of Canada, Paper 86-1B, p. 853-857.

Lowdon, J.A.
1960: Age determinations by the Geological Survey of Canada, Report 1 - isotopic ages; Geological Survey of Canada, Paper 60-17, 51p.

Steiger, R.H. and Jäger, E.
1977: Subcommission on Geochronology: Convention on the use of decay constants in Geo - and Cosmochronology; Earth and Planetory Science Letters, v. 36, p. 359-362.

Wright, G.M.
1967: Geology of the southeastern barren ground, parts of the Districts of Mackenzie and Keewatin (Operations Keewatin, Baker, Thelon); Geological Survey of Canada Memoir 350, 91p.

GSC 89-109 Biotite
2482 ± 22 Ma

K-Ar 3965 Wt % K = 7.312
Rad. Ar = 1.516 x 10^{-3} cm^3/g
% Atmos. Ar = .2

(75 K/15) From a biotite-apatite rich pegmatitic aggregate in paragneiss.
12 km northeast of McLeod Bay in the east arm of Great Slave Lake, and 25 km north-northeast of Reliance. 62°55'21'N; 108°54'25'W; District of Mackenzie, NWT. Sample GFA-83-298. Collected and interpreted by S.S. Gandhi.

The sample is from the McLeod Bay Northeast 1 uranium showing discovered in 1983 by S.S. Gandhi and S.M. Roscoe during the course of mineral resource assessment of a proposed national park in the east arm of Great Slave Lake and Artillery Lake region (Roscoe et al., 1987, p. 60). The rock is from an area of layered gneiss, which is intruded by, and in places grades into, granitic and pegmatitic lenses, pods, dykes, and small bodies. The gneiss is variable in composition and in attitude of layering. Biotite-rich quartzofeldspathic gneiss is the dominant variety. Some amphibolitic zones are present in it. These various rocks are grouped together under 'gneissic complex' unit 3, of probable Archean age, on the Geological Survey of Canada Map 1123A (Stockwell et al., 1968). It is in the southeastern part of the Slave Structural Province near the Thelon Front.

The sample is coarse grained, and contains more than 50% potash feldspar (microcline and perthite), approximately 20% sodic plagioclase, 10% quartz (including myrmekite), 7% biotite, 2% muscovite, and an unusually large amount of fluorapatite close to 10% of the rock). Spectrometric determination revealed 98 ppm U, 1.3 ppm Th, and 9.3% K. Other minerals present are oxides, zircon, sphene, uraninite, and alteration products, mainly fibrous amphibole and chlorite. Fluorapatite tends to form aggregates with biotite interstitial to coarse feldspars, but it also occurs as disseminated crystals elsewhere in the rock.

The date obtained on the sample confirms an Archean age of the gneiss and reflects the timing of late Archean metamorphism, migmatization, and granitic intrusions in this part of the Slave Province. The nearest other Archean rock dated is a granodiorite located 16 km to the south near Reliance, from the east end of Charlton Bay, and it yielded a K-Ar date of *2538 ± 71 Ma (GSC 63-81, Wanless et al., 1965; Reinhardt, 1969). The gneissic complex is regarded as derived largely from metasediments (Wright, 1952; Stockwell et al., 1968). The unusual apatite-rich character

* Age recalculated according to the constants of Steiger and Jager (1977).

* Age recalculated according to the constants of Steiger and Jager (1977).

of the sample and its location within 1 km north-northeast of a large circular aeromagnetic anomaly, some 30 km in diameter, suggested the possibility of an alkaline intrusive complex in this little-studied region, similar to the anorogenic Aphebian alkaline intrusive complex at Blachford Lake, located 200 km west-southwest of Reliance and marked by a similar magnetic high (Davidson, 1978; Roscoe et al. 1987, p. 9 and 60). A U-Pb zircon date on an older alkaline granite phase of the complex is 2175 ± 7 Ma and on a younger peralkaline syenite is 2094 ± 10 Ma (Bowring et al., 1984). The K-Ar date reported here shows that the biotite-apatite aggregate is some 300 million years older than the Blachford complex. The cause of the Reliance magnetic high, however, is not certain. A more detailed airborne magnetic radiometric and electromagnetic survey carried out during 1988 in the Reliance area, confirmed the circular magnetic anomaly and detected a zone of high radioactivity over the 'gneissic complex' (Geological Survey of Canada, 1989). A ground follow-up program is planned for the 1989 summer.

REFERENCES

Bowring, S.A., van Schmus, W.R., and Hoffman, P.F.
1984: U-Pb zircon ages from Athapuscow aulacogen, East Arm of Great Slave Lake, N.W.T., Canada; Canadian Journal of Earth Sciences, v. 21, p. 1315-1324.

Davidson, A.
1978: The Blachford Lake Intrusive Suite; an Aphebian alkaline plutonic complex in the Slave Province, Northwest Territories; in Current Research, Part A; Geological Survey of Canada, Paper 78-1A, p. 119-127.

Geological Survey of Canada
1989: Airborne Geophysical Survey, Fort Reliance area, Northwest Territories; Parts of NTS 75 K/10, 11, 14 and 15; Gamma Ray Spectrometer, VLF and Magnetometer survey; Open File 1981.

Reinhardt, E.W.
1969: Geology of the Precambrian rocks of Thubun Lakes map-area in relationship to the McDonald Fault system, District of Mackenzie; Geological Survey of Canada, Paper 69-21, 29p.

Roscoe, S.M., Gandhi, S.S., Charbonneau, B.W., Maurice, Y.T., and Gibb, R.A.
1987: Mineral resource assessment of the area in the East Arm (Great Slave Lake) and Artillery Lake region, N.W.T., proposed as a National park; Geological Survey of Canada Open File 1434, 92 p.

Steiger, R.H. and Jäger, E.
1977: Subcommission on Geochronology: Convention on the use of decay constants in Geo - and Cosmochronology; Earth and Planetory Science Letters, v. 36, p. 359-362.

Stockwell, C.H., Henderson, J.F., Brown, I.C., Wright, G.M., and Barnes, F.Q.
1968: Geological Map: Reliance, District of Mackenzie; scale 1:253,440, NTS 75 K; Geological Survey of Canada, Map 1123A.

Wanless, R.K., Stevens, R.D., Lachance, G.R., and Rimsaite, R.Y.H.
1965: Age determinations and geological studies, Part 1 - Isotopic Ages, Report 5; Geological Survey of Canada, Paper 64-17, 126p.

Wright, G.M.
1952: Second preliminary map, Reliance, District of Mackenzie, Northwest Territories; Geological Survey of Canada, Paper 57-26.

DISTRICT OF KEEWATIN
(GSC 89-110)

GSC 89-110 Hornblende
1780 ± 20 Ma

K-Ar 3830 Wt % K = 0.804
Rad. Ar = 9.488×10^{-5} cm^3/g
% Atmos. Ar = 0.7

(56 E/15) From a coarse-grained amphibolite. The contact of a metamorphosed ultramafic body with well-layered biotite granodiorite gneiss. The meta-ultramafic rock is a boudin-like body enclosed within ductilely deformed gneisses of the Amer mylonite zone. UTM, Zone 15, 429000E, 7317450N; 65°58'26"N, 94°33'42"W. District of Keewatin, N.W.T., Sample 86LAA-T303-1. Collected and interpreted by A.N. LeCheminant.

The Amer mylonite zone is a major northeast-trending structural break that contains tectonites showing both ductile and brittle deformation textures. There are at least two periods of movement along the zone and previously determined K-Ar ages suggest the latest brittle displacements are as young as 1.7 Ga (Tella, 1984). This 1.78 Ga age is interpreted as a cooling age that postdates the main ductile deformation. The mylonite zone is cut by a 1.79 Ga granite in the Amer Lake area in the southwest. Ductile deformation fabrics within the mylonite zone are truncated by the granite, although late brittle dextral transcurrent movements offset the granite.

REFERENCE

Tella, S.
1984: Geology of the Amer Lake (NTS 66H), Deep Rose Lake (NTS 66 G), and parts of the Pelly Lake (NTS 66 F) map areas, District of Keewatin, NWT.; Geological Survey of Canada, Open File 1043.

MANITOBA
(GSC 89-111)

GSC 89-111 Biotite
1727 ± 17 Ma

K-Ar 3944 Wt % K = 7.493
Rad. Ar = 8.431 x 10^{-4} cm^3/g
% Atmos. Ar = 1.6

(63 K/16) From a granodiorite.
East shore of File Lake, Manitoba. 54°53'N, 100°18W. Sample Ham Lake. Collected and interpreted by T. Gordon.

The Ham Lake pluton (Bailes, 1980, 1986) is a 6.5 by 18 km, north-northeast trending batholith on the east shore of File Lake in the Flin Flon volcanic belt. It is massive to gneissic, medium to coarse grained, and composed of granodiorite, leucotonalite, and tonalite. Amisk Group xenoliths are abundant on its eastern margin. Its emplacement postdates the earliest folding episode (D1 of Bailes, 1980), but predates the second deformation (D2) and the main episode of regional metamorphism. The sample is a pink-weathering, coarse-grained, biotite-hornblende granodiorite. Accessory minerals include apatite, sphene, and zircon.

An imprecise U-Pb zircon age of 1830 +27/-19 Ma has been obtained from this sample (Gordon, 1988; Gordon et al., in press). The range in the zircon age spans the 1835 to 1860 Ma time interval of widespread plutonism during the Trans-Hudson Orogen.

The K-Ar biotite age is interpreted as the time at which the pluton cooled through 280°C (Harrison and McDougall, 1980). Within error, this age is identical to four other K-Ar biotite ages obtained on a transect extending from File Lake 100 km north to the core of the Kisseynew sedimentary gneiss belt (Gordon, 1989; Hunt and Roddick, in press). These data indicate that, along the transect, i) the present erosion surface had a depth of approximately 10 km at ca. 1710 Ma., and ii) it has not experienced significant tilting during subsequent erosional unroofing.

REFERENCES

Bailes, A.H.
1980: Geology of the File Lake Area, Manitoba Department of Energy and Mines, Mineral Resources Division, Geological Report 78-1, 134p.

1986: Chisel-Morgan Lakes Project; Manitoba Energy and Mines, Minerals Division, Report of Field Activities 1986, p. 70-76.

Gordon, T.M.
1988: Geochronology in the Churchill Province; Manitoba Energy and Mines, Minerals Division, Report of Field Activities 1988, p. 170-172.

1989: Thermal evolution of the Kisseynew sedimentary gneiss belt, Manitoba: Metamorphism at an Early Proterozoic accretionary margin: in Evolution of Metamorphic Belts, eds. J.S. Daly, R.A. Cliff, and B.W.D. Yardley; Geological Society Special Publication 42, p. 233-243.

Gordon, T.M., Hunt, P.A., Bailes, A.H., and E.C. Syme
in press: U-Pb ages from the Flin Flon and Kisseynew belts, Manitoba: Chronology of Early Proterozoic crust formation, in The Early Proterozoic Trans-Hudson Orogen, ed. J.F. Lewry and M.R. Stauffer; Geological Association of Canada Special Paper.

Harrison, T.M. and McDougall, I.
1980: Investigations of an intrusive contact, northwest Nelson, New Zealand – I. thermal, chronological, and isotopic constraints; Geochimica et Cosmochimica Acta, v. 44, p. 1985-2003.

Hunt, P.A. and Roddick, J.C.
1988: A compilation of K-Ar ages, Report 18; in Radiogenic Age and Isotopic Studies: Report 2; Geological Survey of Canada, Paper 88-2, p. 127-155.

QUEBEC
(GSC 89-112)

GSC 89-112 Hornblende
987 ± 17 Ma

K-Ar 3949 Wt % K = 1.064
Rad. Ar = 5.432 × 10^5 cm^3/g
% Atmos. Ar = 7.3

(31 L/11) From a mafic dyke in granitic body.
2.8 km north of town of Timiskaming along highway 101, Quebec. 40°44'N, 79°04'30''W. Sample RT-87-4B. Collected and interpreted by R. Theriault.

The archean signature is not present in this mafic dyke 30 km south of the Grenville Front.

GSC 89-113 Whole Rock
361 ± 9 Ma

K-Ar 3878 Wt % K = 3.910
Rad. Ar = 6.069×10^{-5} cm^3/g
% Atmos. Ar = 0.9

(21 G) From a hornfels.
Mount Pleasant, 1000 m north-northwest of fire tower; Billiton Canada drill hole LNZ-3 at 329 m, N.B. 45°26'21'N, 66°49'05'W. Sample SYA86-81. Collected and interpreted by W.D. Sinclair.

The sample is a of medium to dark brown, fine-grained hornfels consisting of 60% biotite, 25% quartz, and 15% feldspar; minor amounts of epidote are also present. In thin section, biotite forms randomly oriented, subhedral grains with no obvious chlorite alteration.

The hornfels is from one of two units of sedimentary breccia that are interbedded with felsic ash-flow tuffs. The two sedimentary breccia units consist mainly of slate or argillite fragments in a fine-grained matrix of similar material and represent talus or other colluvial deposits derived from nearby metasedimentary rocks that formed the southwest wall of the Mount Pleasant caldera. The breccias and associated volcanic rocks are part of the intracaldera sequence of the Upper Devonian Piskahegan Group, recently dated as late Famennian (McGregor and McCutcheon, 1988).

At Mount Pleasant, the breccias have been metamorphosed to biotite hornfels by underlying granitic intrusions (Sinclair et al., 1988). The date obtained from the hornfels (361 ± 9 Ma) should represent the age of emplacement of these intrusions and is consistent with preliminary $^{40}Ar/^{39}Ar$ data that indicated an age of about 360 Ma (D.A. Archibald, pers. comm., 1985). This would indicate that the granitic intrusions are comparable in age to the volcanic rocks of the Piskahegan Group in the Mount Pleasant caldera and may be related. Previous K-Ar and Rb-Sr isotopic studies (Kooiman et al., 1986) indicated a younger age of 340 to 330 Ma for the Mount Pleasant intrusions. Several stages of intrusion and mineralization are present at Mount Pleasant, however, and the younger age may reflect either a later stage of intrusion or postmagmatic hydrothermal alteration. More accurate and precise dating of the granitic rocks and related alteration and mineralization are necessary to resolve this discrepancy.

REFERENCES

Kooiman, G.J.A., McLeod, M.J., and Sinclair, W.D.
1986: Porphyry tungsten-molybdenum orebodies, polymetallic veins and replacement bodies, and tin-bearing greisen zones in the Fire Tower Zone, Mount Pleasant, New Brunswick; Economic Geology, v. 81, p. 1356-1373.

McGregor, D.C. and McCutcheon, S.R.
1988: Implications of spore evidence for Late Devonian age of the Piskahegan Group, southwestern New Brunswick; Canadian Journal of Earth Sciences, v. 25, p. 1349-1364.

Sinclair, W.D., Kooiman, G.J.A., and Martin, D.A.
1988: Geological setting of granites and related tin deposits in the North Zone, Mount Pleasant, New Brunswick; in Current Research, Part B; Geological Survey of Canada, Paper 88-1B, p. 201-208.

GSC 89-114 Biotite
390 ± 5 Ma

K-Ar 3818 Wt % K = 7.545
Rad. Ar = 1.277×10^{-4} cm^3/g
% Atmos. Ar = 1.0

(21 G/13) Skiff Lake granite phase of Pokiok batholith, south-central New Brunswick; UTM Zone 19T, 9620E, 6880N. Sample WXNB-8. Collected and interpreted by J.B. Whalen.

Granite samples for various intrusions of the central plutonic belt of New Brunswick. Location map and interpretation of results given in Whalen and Theriault (this volume).

GSC 89-115 Muscovite
389 ± 6 Ma

K-Ar 3919 Wt % K = 8.003
Rad. Ar = 1.352×10^{-4} cm^3/g
% Atmos. Ar = 1.7

(21 G/13) For sample location, rock type, and interpretation see GSC 89-114. Sample WXNB-8.

GSC 89-116 Muscovite
430 ± 5 Ma

K-Ar 3924 Wt % K = 8.483
Rad. Ar = 1.64 10^{-4} cm^3/g
% Atmos. Ar = 2.3

(21 G/12) From a medium-grained granite phase of Pokiok batholith, south-central New Brunswick, UTM Zone 19T, O34-OE, 6400N. Sample WXNB-30. Collected and interpreted by J.B. Whalen.

For interpretation and references see GSC 89-114.

GSC 89-117 Muscovite
379 ± 6 Ma

K-Ar 3925 Wt % K = 8.066
Rad. Ar = 1.322 4 10^{-4} cm^3/g
% Atmos. Ar = 3.4

(21 G/14) Annadale granite phase of the Pokiok batholith, south-central New Brunswick, UTM Zone 19T, 3440E, 7990N. Sample WXNB-38. Collected and interpreted by J.B. Whalen.

For interpretation and references see GSC 89-114.

GSC 89-118 Biotite
397 ± 6 Ma

K-Ar 3922 Wt % K = 7.007
Rad. Ar = 1.21 × 10^{-4} cm^3/g
% Atmos. Ar = 11.5

(21 G/14) Annadale granite phase of Pokiok batholith, south-central New Brunswick, UTM Zone 19T, 3930E, 9430N. Sample WXNB-18. Collected and interpreted by J.B. Whalen.

For interpretation and references see GSC 89-114.

GSC 89-119 Muscovite
380 ± 5 Ma

K-Ar 3923 Wt % K = 8.764
Rad. Ar = 1.44 × 10^{-4} cm^3/g
% Atmos. Ar = 2.0

(21 G/14) For rock type, location, and interpretation see GSC 89-114. Sample WXNB-18. Collected and interpreted by J.B. Whalen.

GSC 89-120 Muscovite
392 ± 6 Ma

K-Ar 3921 Wt % K = 8.690
Rad. Ar = 1.478 × 10^{-4} cm^3/g
% Atmos. Ar = 8.0

(21 J/3) Hawkshaw K-feldspar porphyritic granite phase of Pokiok batholith, south-central New Brunswick, UTM Zone 19T, 3700E, 9660N. Sample WXNB-17. Collected and interpreted by J.B. Whalen.

For interpretation and references see GSC 89-114.

GSC 89-121 Muscovite
385 ± 5 Ma

K-Ar 3932 Wt % K = 8.603
Rad. Ar = 1.437 × 10^{-4} cm^3/g
% Atmos. Ar = 0.8

(21 J/6) Coarse-grained Nashwaak granite. South of Highway 107, central New Brunswick, UTM Zone 19T, 4887E, 4325N. Sample WXNB-227. Collected and interpreted by J.B. Whalen.

For interpretation and refernces see GSC 89-114.

GSC 89-122 Muscovite
394 ± 6 Ma

K-Ar 3920 Wt % K = 8.862
Rad. Ar = 1.5125 × 10^{-4} cm^3/g
% Atmos. Ar = 1.7

(21 J/6) Annadale granite phase of Pokiok batholith, south-central New Brunswick, UTM Zone 19T, 5180E, 2380N. Sample WXNB-16. Collected and interpreted by J.B. Whalen.

For interpretation and references see GSC 89-114.

GSC 89-123 Muscovite
408 ± 7 Ma

K-Ar 3929 Wt % K = 8.764
Rad. Ar = 1.562 × 10^{-4} cm^3/g
% Atmos. Ar = 0.7

(21 J/10) Medium-grained, Lost Lake granodiorite between Highways 107 and 108, central New Brunswick, UTM Zone 19T, 6040E, 7520N. Sample WXNB-159. Collected and interpreted by J.B. Whalen.

For interpretation and references see GSC 89-114.

GSC 89-124 Muscovite
421 ± 6 Ma

K-Ar 3931 Wt % K = 8.233
Rad. Ar = 1.518 × 10^{-4} cm^3/g
% Atmos. Ar = 1.7

(21 J/11) Medium-grained, Juniper Barren granite on Highway 107, central New Brunswick, UTM Zone, 19t, 4090E, 5290N. Sample WXNB-169. Collected and interpreted by J.B. Whalen.

For interpretation and references see GSC 89-114.

GSC 89-125 Muscovite
402 ± 5 Ma

K-Ar 3930 Wt % K = 8.854
Rad. Ar = 1.551 × 10^{-4} cm^3/g
% Atmos. Ar = 1.1

(21 J/11) Coarse-grained, Lost Lake granodiorite between Highways 107 and 108, central New Brunswick, UTM Zone 19T, 4680E, 7500N. Sample WXNB-161. Collected and interpreted by J.B. Whalen.

For interpretation and references see GSC 89-114.

GSC 89-126 Muscovite
416 ± 5 Ma

K-Ar 3927 Wt % K = 8.656
Rad. Ar = 1.572 x 10^{-4} cm^3/g
% Atmos. Ar = 1.1

(21 J/15) Squaw Lake granite, east of Squaw Lake, central New Brunswick, UTM Zone 19T, 6600E, 0300N. Sample WXNB-136.Collected and interpreted by J.B. Whalen.

For interpretation and references see GSC 89-114.

GSC 89-127 Muscovite
414 ± 5 Ma

K-Ar 3926 Wt % K = 8.620
Rad. Ar = 1.56 x 10^{-4} cm^3/g
% Atmos. Ar = 1.4

(21 O/2) Medium-grained granodiorite of the North Pole Stream granite suite, central New Brunswick, UTM Zone 19T, 7780E, 1770N. Sample WXNB-122. Collected and interpreted by J.B. Whalen.

For interpretation and references see GSC 89-114.

NEWFOUNDLAND
(GSC 89-128 to GSC 89-130)

GSC 89-128 Hornblende
448 ± 28 Ma

K-Ar 3708 Wt % K = 0.298
Rad. Ar = 5.889 x 10^{-6} cm^3/g
% Atmos. Ar = 6.2

(12 A/5) From a metagabbro.
Northwest of Cormacks Lake, Southwestern Newfoundland, 40°20'30''N,57°58'W. Sample 78-HPA-057-3. Collected and interpreted by R.K. Herd.

Metagabbro/amphibolite from the Cormacks Lake complex. Interlayered and interfolded with layered granitic gneisses and paragneiss. The age is consistent with other cooling ages from this region.

GSC 89-129 Hornblende
416 ± 37 Ma

K-Ar 3709 Wt % K = 0.280
Rad. Ar = 5.085 x 10^{-6} cm^3/g
% Atmos. Ar = 9.9

(12 A/5) From an amphibolite.
Northwest of Cormacks Lake, Southwestern Newfoundland, 48°18'N,57°57'W. Sample 78-HPAD-114-3. Collected by G.R. Dunning and interpreted by R.K. Herd.

Coarse-grained amphibolite layer in mixed mafic rocks and paragneiss, possible calc-silicates, of the Cormacks Lake complex. The age is consistent with other cooling ages from this region.

GSC 89-130 Hornblende
449 ± 32 Ma

K-Ar 3710 Wt % K = 0.141
Rad. Ar = 2.797 x 10^{-6} cm^3/g
% Atmos. Ar = 12.7

(12 A/5) From an amphibolite.
Northwest of Cormacks Lake, Southwestern Newfoundland, 48°21'N,57°57'W. Sample 78-HPAD-070-2. Collected by G.R. Dunning and interpreted by R.K. Herd.

Medium-grained amphibolite in coarse-grained orthogneiss, layered and foliated consistently with the surrounding Cormacks Lake complex. The age is consistent with other cooling ages from this region.

OFFSHORE WEST COAST
(GSC 89-131 to GSC 89-132)

GSC 89-131 Whole rock
26.3 ± 1.5 Ma

K-Ar 3995 Wt% K = 0.676
Rad. Ar = 6.97 x 10^{-7} cm^3/g
% Atmos. Ar = 52.0

Altered basalt from Patton Seamount, Patton Seamount Group, Northeast Pacific. The sample was dredged from the northwestern flank of the seamount during an ODP site survey cruise PAR87-11. The dredge line is located between 54°05.88'N, 149°27.31'W and 54°06.77'N, 149°25.56'W. Sample PGC-87-11-D2-A1. Collected and interpreted by B.D. Bornhold and B. Blaise.

The age of 26.3 ± 1.5 Ma is the second age obtained from this very large plateau. Despite the altered nature of the sample, the age agrees with the age obtained from Murray seamount, the southernmost seamount of the plateau, 25.7 Ma.

Patton Seamount Group, part of the volcanoes and volcanic ridges in the Gulf of Alaska are subparallel with other volcanic lineaments in the Central Pacific plate are probably related to motion of the Pacific plate over stationary hotspots near the Gorda-Juan de Fuca-Explorer spreading system. The predicted northwestward age progression along these hotspot tracks is not well documented (Duncan and Clague, 1985). The volcano migration rates determined for these lineaments form an especially strong constraint on the location of the rotation pole for Pacific plate motion over the hotspot network during Oligocene to present time.

The age will help to establish the time span over which the volcanic basement developed and to define better the maximum anticipated age for the plateau sediments. The average sedimentation rate would be approximatively 1-1.5 cm/ka based on the seismic coverage available.

REFERENCE

Duncan, R.A. and Clague, D.A.
1985: Pacific plate motion recorded by linear volcanic chains; in The Ocean Basins and Margins, Vol. 7A, The Pacific Ocean, ed. A.E.M. Naim, F.G. Stenli, and S. Uyeda; Plenum Press, New-York, p. 89-122.

GSC 89-132 Whole rock
18.8 ± 0.73 Ma

K-Ar 3996 Wt% K = 0.742
Rad. Ar = 5.45 x 10^{-7} cm^3/g
% Atmos. Ar = 87.0

Altered basalt from Cowie Seamount, Patton Seamount Group, Northeast Pacific. The sample was dredged from the southern flank of the seamount during an ODP site survey cruise, PAR87-11. The dredge line is located between 54°34.65'N, 150°19.06'W and 54°35.20'N, 150°20.05'W. Sample PGC-87-11-D3-A2. Collected and interpreted by B.D. Bornhold and B. Blaise.

Based on sample GSC 89-131 age of 26.3 ± 1.5 Ma and another date at 25.7 Ma from this plateau, the age of 18.8 ± 0.73 Ma does not agree with the general age of the plateau. The presence of 87% atmospheric argon probably reflects the altered nature of the basalt. For these reasons this date cannot be taken into account in the historical reconstruction of the seamount.

OUTSIDE CANADA
(GSC 89-133 to GSC 89-135)

GSC 89-133 Hornblende
1722 ± 41 Ma

K-Ar 3935 Wt % K = 0.314
Rad. Ar = 3.516 x 10^{-5} cm^3/g
% Atmos. Ar = 0.9

(25 I/14) From a ultrabasic amphibolite.
From the Countess of Warwich Mine, Kodlunan I., Northwest Territories. A steeply dipping mafic sill in aluminous gneisses of amphibolite to granulite grade. Sample K 9 D; 62°48'N, 65°26'W. Collected and interpreted by D.D. Hogarth.

The age reflects last cooling from high-grade metamorphic conditions during the Hudsonian Orogeny. See GSC 89-134 for further information.

GSC 89-134 Hornblende
1810 ± 29 Ma

K-Ar 3933 Wt % K = 0.134
Rad. Ar = 1.622 x 10^{-5} cm^3/g
% Atmos. Ar = 2.4

( ) From a hornblendite.
From a beach below Fort Dún-an-Óir on the west side of Smerwich Harbour, County Kerry, Ireland. Sample S-5. Collected and interpreted by D.D. Hogarth.

The sample and GSC 89-135 are two cobbles from a beach on the shore of southern Ireland. They are believed to have been derived from the cargo of a ship wrecked and beached in Smerwich Harbour in 1578. This cargo was supposedly gold ore collected by Martin Frobisher from localities in southeastern Baffin Island. The ages of the two samples are consistent with ages from southeastern Baffin Is. (see GSC 89-133) but much older than typical ages of less than 600 Ma from Ireland. See Hogarth and Roddick (1989) for further details and interpretation.

REFERENCE

Hogarth, D.D. and Roddick, J.C.
1989: Discovery of Martin Frobisher's Baffin Island "ore" in Ireland; Canadian Journal of Earth Sciences, v. 26, p. 1053-1060.

GSC 89-135 Hornblende
1881 ± 30 Ma

K-Ar 3934 Wt % K = 0.122
Rad. Ar = 1.571 x 10^{-5} cm^3/g
% Atmos. Ar = 2.2

From a hornblendite.
Sample S-4. Collected and interpreted by D.D. Hogarth.

For interpretation see GSC 89-134.

APPENDIX

The numbers listed below refer to the individual sample determination numbers, e.g. (GSC) 62-189, published in the Geological Survey of Canada age reports listed below:

	Determinations
GSC Paper 60-17, Report 1	59-1 to 59- 98
GSC Paper 61-17, Report 2	60-1 to 60-152
GSC Paper 62-17, Report 3	61-1 to 61-204
GSC Paper 63-17, Report 4	62-1 to 62-190
GSC Paper 64-17, Report 5	63-1 to 63-184
GSC Paper 65-17, Report 6	64-1 to 64-165
GSC Paper 66-17, Report 7	65-1 to 65-153
GSC Paper 67-2A, Report 8	66-1 to 66-176
GSC Paper 69-2A, Report 9	67-1 to 67-146
GSC Paper 71- 2, Report 10	70-1 to 70-156
GSC Paper 73-2, Report 11	72-1 to 72-163
GSC Paper 74-2, Report 12	73-1 to 73-198
GSC Paper 77-2, Report 13	76-1 to 76-248
GSC Paper 79-2, Report 14	78-1 to 78-230
GSC Paper 81-2, Report 15	80-1 to 80-208
GSC Paper 82-2, Report 16	81-1 to 81-226
GSC Paper 87-2, Report 17	87-1 to 87-245
GSC Paper 88-2, Report 18	88-1 to 88-105
GSC Paper 89-2, Report 19	89-1 to 89-135

GSC Age Determinations Listed by N.T.S. Co-ordinates

1-M	62-189, 190; 63-136, 137; 66-170, 171; 70-145, 146, 147, 152
1-N	65-150; 70-156
2-C	70-155
2-D	59-94, 95, 96, 97, 98; 60-151, 152; 63-182; 65-142, 143; 66-172; 70-153, 154
2-E	62-187, 188; 63-168, 169, 170, 171, 183, 184; 64-159; 65-144, 145, 146, 147, 148, 149; 67-144; 70-151; 78-229, 230
2-F	70-148; 80-206
2-L	72-158, 159
2-M	66-173; 73-192, 193, 194
3-D	63-161
10-N	72-163
11-D	70-122, 123
11-E	66-156, 157, 158; 70-124, 125; 78-209; 87-14
11-F	62-168, 169; 78-211; 80-200; 87-14
11-J	78-212
11-K	6-159, 160, 161; 78-210; 80-199
11-L	65-133, 134, 135; 66-163; 70-128, 129, 130; 72-124, 125, 126; 76-231, 232, 233, 234, 235, 236, 237, 238, 239
11-N	78-206, 207, 208; 81-206, 207
11-O	61-202; 63-162; 65-138, 139, 140, 141; 66-168
11-P	67-143
12-A	67-142; 70-120, 121; 72-160, 161; 73-197, 198; 81-212, 213, 214, 215, 216, 217
12-A/5	89-128, 129, 130
12-B	60-147; 61-199; 62-186; 63-166, 167; 81-218, 219
12-E	65-129; 66-153; 70-102, 103, 104, 105; 72-95
12-H	60-148; 61-203, 204; 70-143, 144, 149
12-I	60-149; 61-200, 201; 64-158; 66-169; 70-150; 72-153, 154, 155, 156, 157; 73-195, 196
12-L	60-133, 134, 143
12-M	78-202, 203, 204, 205
12-O	60-135
12-P	73-191
13-C	66-167; 67-138
13-D	60-132
13-E	64-160; 70-133; 80-201
13-F	60-145; 67-136, 137
13-H	60-146; 67-141
13-I	70-138, 142; 72-140, 150
13-J	70-134, 135, 136, 137; 72-139; 78-228; 87-1, 2, 3, 4, 5
13-K	60-144; 61-196; 62-183, 184, 185; 63-178, 179; 72-141, 142, 143; 73-168, 169; 76-241, 242, 244, 247, 248; 81-208, 209, 211
13-L	61-197; 62-177; 63-148, 163, 177; 64-157; 65-151; 73-163, 164, 167; 76-240, 245
13-M	63-174; 64-162; 70-131, 132; 73-174; 76-243
13-M/3	87-19
13-M/6	87-6
13-M/11	87-7
13-M/14	87-8
13-N	62-178; 63-172; 73-176, 177, 178, 179, 183, 184; 76-246; 81-210
13-N/6	87-9
13-N/9	87-10
13-O	62-179, 180, 181, 182; 67-133, 134, 135; 70-140, 141; 72-144, 145, 146, 147, 148, 149, 151, 152; 73-180, 181, 185, 186, 187, 188, 189, 190
13-0/13	87-11
14-C	72-138; 73-182
14-D	60-143; 63-175; 65-122, 152; 73-166
14-D/3	87-12
14-E	61-195; 62-172; 63-181; 64-164; 65-153; 66-166; 72-134; 73-165, 172
14-F	62-171; 63-180; 64-163; 72-135, 136, 137
14-L	63-173, 176; 64-165; 67-130, 131, 132, 140; 73-171, 175; 78-213, 214, 215, 216, 217, 218, 219, 220, 221, 222, 223, 224, 225, 226, 227
14-M	67-129; 72-133; 73-170, 173
15-M	76-174, 175
20-I	72-162
20-P	61-194; 62-167
21-A	59-93; 62-163, 164, 165, 166; 65-132; 66-155
21-B	61-193; 62-161, 162
21-E	59-89, 90, 91; 60-117, 118; 64-132; 66-142; 72-103, 104, 105
21-G	60-136; 62-159; 63-155; 66-154; 67-128; 70-108, 109, 110; 72-111, 112, 113, 114, 115, 116, 117, 118, 119, 120, 121, 122, 123; 80-198; 87-15, 16, 17; 89-113
21-G/12	89-116
21-G/13	89-114, 115
21-G/14	89-117, 118, 119
21-H	62-160; 64-156; 65-131; 72-127, 128, 129, 130
21-I	64-154; 70-127
21-J	61-187, 188, 189, 190, 191, 192; 62-155, 156, 157, 158; 63-156, 157, 158, 159; 65-130; 70-111, 115, 116, 117, 118, 119; 72-107, 108, 109, 110
21-J/3	89-120
21-J/6	89-121, 122
21-J/10	89-123

Other publications containing geochronological data generated by the Geochronology Section of the Geological Survey of Canada

Copeland, P., Parrish, R. R., and Harrison, T. M.
1988: Identification of inherited radiogenic Pb in monazite and its implications for U-Pb systematics; Nature, v. 333, p. 760-763.

This paper, for the first time, documents inheritance in monazite, a mineral increasingly used in U-Pb geochronology. The paper also presents data from a leucogranite from southern Tibet (China) that is 21 Ma old, placing constraints on the age of a north Himalayan normal fault.

Davidson, A. and van Breemen, O.
1988: Baddeleyite-zircon relationships in coronitic metagabbro, Grenville Province, Ontario: implications for geochronology; Contributions to Mineralogy and Petrology, v. 100, p. 291-299.

In a number of coronitic metagabbros from the Central Gneiss Belt of the Grenville Structural Province of Ontario it was found that single baddeleyite crystals with radiating columnar coronas of polycrystalline zircon, in places with outer rims of garnet, are analogous to the coronas around olivine and ilmenite. Both zirconium minerals have been dated by the U-Pb isotopic method at three widely separated localities. In each case baddeleyite records an igneous crystallization age of ca. 1170 Ma, 125 Ma older than the ca. 1045 Ma age of the zircons, which is interpreted as the age of metamorphism.

Hogarth, D.D. and Roddick, J.C.
1989: Discovery of Martin Frobisher's Baffin Island 'ore' in Ireland; Canadian Journal of Earth Sciences, 26: p.1053-1060.

This paper presents petrological, geochemical, and age data to document the discovery in Ireland of rock transported by Frobisher, in 1578, from Baffin Island. It was deposited on the Irish coast during the wreck of one of his ships.

Loveridge, W.D., Eade, K.E. and Sullivan, R.W.
1988: Geochronological studies of Precambrian rocks from the southern District of Keewatin; Geological Survey of Canada, Paper 88-18.

A summary of geology and the results of U-Pb, Rb-Sr and K-Ar studies are presented for three regions in the southern part of the District of Keewatin, Northwest Territories: Angikuni-Yathkyed lakes area, Edehon-Hyde lakes area, and Kasba gneiss area. U-Pb measurements on zircon from basement rocks yield Archean ages; in a limited area east of Kasba lake the basement gneiss is early Archean, ca. 3270 Ma.

Roddick, J.C.
1988: K-Ar dating of basalts from site 647, ODP Leg 105; in Proceedings of the Ocean Drilling Program, Final Reports (Part B), Ed. S.P. Srivastava, M. Arthur, and others; College Station, Texas, v. 105: 885-887.

This study presents age and microprobe data showing that very minor alteration has had a major effect on the K-Ar ages of ocean floor basalts, rendering the ages unreliable. It also Highlights problems often ignored in dating basaltic rocks.

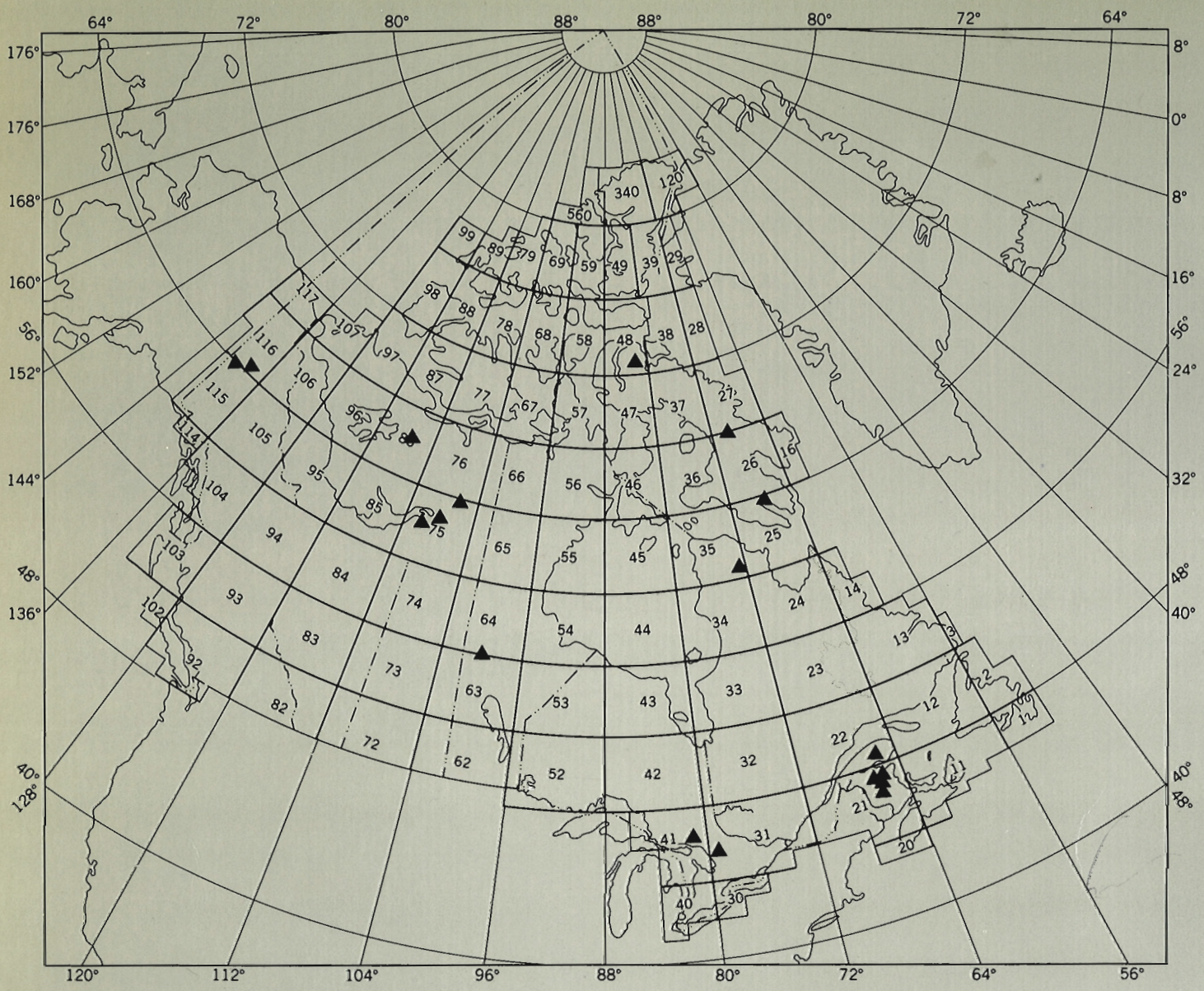
64° 72° 80° 88° 88° 80° 72° 64°
176° 176° 168° 160° 56° 152° 144° 48° 136° 40° 128°
8° 0° 8° 16° 56° 24° 32° 48° 40° 48°
120° 112° 104° 96° 88° 80° 72° 64° 56°